Universität Rostock Traditio et Innovatio

Selektionsbedingte und bewegungsabhängige Adaptationen in der Langzeit-Selektionslinie DUhTP und ihre Eignung als Modell für metabolische Flexibilität

Kumulative Habilitationsschrift

zur

Erlangung des akademischen Grades

doctor rerum naturalium habilitata (Dr. rer. nat. habil.)

der Mathematisch-Naturwissenschaftlichen Fakultät

der Universität Rostock

vorgelegt von

Julia Brenmoehl

Rostock, 08.05.2024

https://doi.org/10.18453/rosdok_id00004849

Gutachter:

Prof. Dr. Tom Goldammer (Universität Rostock, Agrar- und Umweltwissenschaftliche Fakultät; FBN Dummerstorf)

Prof. Dr. med. Wilhelm Bloch (Deutsche Sporthochschule Köln, Institut für Kreislaufforschung und Sportmedizin)

Prof. Dr. Inna Sokolova (Universität Rostock, Institut für Biowissenschaften)

Datum der Einreichung: 08.05.2024

Probevorlesung: 24.04.2025

Kolloquium: 08.05.2025

für meinen Daddy

Inhalt

Abkürzungsverzeichnis

ACC	Acetyl-CoA Carboxylase 1
ACSS2	*acyl-CoA synthetase short chain family member 2*
ACTH	adrenokortikotrophes Hormon
AKT	Proteinkinase B
ATP	Adenosintriphosphat
bzw.	beziehungsweise
CD36	Thrombozytenglykoprotein 4
Cidea	Lipidtransferase
Cycs	Cytochrom C
CytB	Cytochrom B
DUC	Dummerstorfer Kontrolle
DUhTP	Dummerstorfer Langzeitselektionslinie (paternal auf hohe Laufleistung selektiert)
FNDC5/Fndc5	*fibronectin type III domain-containing protein 5*
FSH	follikelstimulierendes Hormon
Fzt:DU	Dummerstorfer Auszuchtlinie
GDH	Glutamatdehydrogenase
GH	*growth hormone*
GLUT	Glukosetransporter
IGF	*insulin-like growth factor*
IGFBP	IGF-Bindungsproteine
kDa	Kilo-Dalton
LCAD	Langketten-Acyl-CoA-Dehydrogenase
LH	luteinisierende Hormon
m	Meter
MAPK	*mitogen-activated protein kinase*
MCT1	*monocarboxylate transporter isoform 1*
Mef2c	*myocyte enhancer factor 2C*
Mfn1	Mitofusin 1

min	Minute
MPC1/2	*mitochondrial pyruvate carrier* 1, 2
mTOR1/2	*mammalian target of rapamycin*
mTORC1/2	mTOR-Komplex 1/2
Myl4	*myosin light chain 4*
Myod	*myoblast determination protein 1*, Myogener Faktor 3
NAD+/NADH	oxidiertes/reduziertes Nicotinamidadenindinucleotid
ND-1	*NADH-ubiquinone oxidoreductase chain 1*
NDUFA9	*NADH dehydrogenase [ubiquinone] 1 alpha subcomplex subunit 9*
NRF	*nuclear respiratory factor*
Opa1	*Dynamin-like 120 kDa protein, form S1*
PAPPA	*pregnancy-associated plasma protein A*
PEPCK	Phosphoenolpyruvat-Carboxykinase
PGC1α/Ppargc1a	*peroxisome proliferator-activated receptor -γ coactivator 1-α*
Pou1f1	*pituitary-specific positive transcription factor 1*
PPAR	*peroxisome proliferator-activated receptor*
QTL	*quantitative trait locus*
s	Sekunde
SB	Semi-Barriere
Sirt3	Sirtuin 3
SPF	spezifiziert pathogenfrei
Tbx1	*T-box transcription factor 1*; Browningmarker
Tcf1	*T cell factor 1*; Marker für weißes Fettgewebe
TFAM/Tfam	mitochondrialer Transkriptionsfaktor
TSH	schilddrüsenstimulierendes Hormon
usw.	und so weiter
VO_2max	maximale Sauerstoffaufnahme

1. Einleitung

Sport beziehungsweise sportliche Betätigung bringt nicht nur Spaß, sondern ist vor allem der Gesundheit dienlich. Dabei kann körperliche Betätigung vor allem Stoffwechsel-assoziierte Erkrankungen verbessern aber auch vorbeugend wirken [1]. Physische Inaktivität hingegen kann zu Erkrankungen des Bewegungsapparates (Sarkopenie, Osteoporose, Osteoarthritis), des Stoffwechsels (Typ II Diabetes, metabolisches Syndrom), des Herz-Kreislauf-Systems (Bluthockdruck, koronare Herzerkrankung, Schlaganfall, periphere Gefäßerkrankung), zu Krebs und Übergewicht führen [1]. In Deutschland waren laut dem RKI 2019/2020 53 % der Erwachsenen übergewichtig, davon 19 % fettleibig [2].

Übergewicht ist auf ein Energieungleichgewicht zurückzuführen, bei dem die Energieaufnahme den Energieverbrauch übersteigt und so zu einer Speicherung „überschüssiger Energie“ führt [3]. Regelmäßige körperliche Aktivität bewirkt eine Erhöhung des Energieverbrauchs, einerseits während der körperlichen Ertüchtigung aber auch durch einen insgesamt höheren Grundumsatz bedingt durch den trainingsbedingten Muskelzuwachs. Wenn der Energieverbrauch die Energieaufnahme übersteigt, werden die Energiereserven mobilisiert und das Körpergewicht reduziert.

Gemäß einer wissenschaftlichen Stellungnahme des *Cardiac Rehabilitation/Secondary Prevention Program* von 2007 verringern 150 Minuten regelmäßige, mäßig intensive körperliche Betätigung pro Woche nicht nur das Körpergewicht, sondern auch das Risiko von Herz-Kreislauf-Erkrankungen, Diabetes, Darm- und Brustkrebs [4]. Gleiches bewirkt laut dieser Stellungnahme dreimal 20 Minuten intensives Ausdauertraining bzw. zweimaliges Krafttraining pro Woche.

Entscheidend für die gesundheitlichen Auswirkungen bzw. die Gewichtsabnahme ist demnach nicht die Art der körperlichen Aktivität, sondern viel mehr, dass regelmäßige Bewegung stattfindet, bei der der Körper durch einen erhöhten Energieverbrauch einen „Energiemangel erfährt“, welcher durch Energiereserven gedeckt wird.

1.1 Energiestoffwechsel der Bewegung

Die für die Muskelkontraktionen notwendige Energie wird in Form von ATP abhängig von der Art und Dauer der Bewegung und verschiedenen Faktoren wie Umwelteinflüsse, Alter, Ernährung, Geschlecht usw. bereitgestellt [5]. Während die Skelettmuskulatur die eigentliche Bewegung realisiert, liefern Leber, Fettgewebe aber auch die Muskulatur Energieäquivalente (Glukose, Fettsäuren), die über das Blutsystem transportiert und am Zielort zur ATP-Produktion und somit zu den Muskelkontraktionen

beitragen. Die Energiebereitstellung beruht auf der gleichzeitigen Beteiligung von phosphagenen, glykolytischen und oxidativen Energieströmen [6]. Dauer und Intensität der Bewegung bestimmen die vorherrschenden Energieflüsse [5,6].

Freies ATP und Phosphokreatin stehen dem Muskel sofort zur Verfügung, ihre Vorräte sind aber schnell erschöpft [6,7]. Nach dem Phosphokreatinabbau dominiert die ATP-Bildung aus der anaeroben Glykolyse [5,8], die unabhängig von Sauerstoff und Mitochondrien ist. Nach dreißig bis sechzig Sekunden körperlicher Anstrengung überwiegen die oxidativen (aeroben) Energieströme, zunächst die Glukose-, später die Fettsäureoxidation [6,9]. ATP-Moleküle werden durch mitochondriale oxidative Phosphorylierung unter Verwendung von Sauerstoff in oxidativen Muskelfasern mit einer hohen Anzahl von Mitochondrien erzeugt.

Sowohl anaerobe als auch der aerobe glykolytische Stoffwechselprozesse werden durch Kohlenhydrate angetrieben. Die Ausgangssubstanz kann zirkulierende Glukose oder das in den Muskelfasern gespeicherte Glukosereservoir Glykogen sein. Letzteres liegt in Form einzelner Glykogenpartikel innerhalb der Fasern vor; i) direkt unter dem Sarkolemma, ii) zwischen den Myofibrillen auf der Höhe des I-Bandes in der Nähe der Mitochondrien und des Sakroplasmatischen Retikulums (intermyofibrillar) und iii) in der Myofibrille nahe der Z-Linie (intramyofibrillar) [10]. In trainierten Muskeln wird eine erhöhte Akkumulation von intramyofibrillarem und subsarcolemmalem Glykogen mit einer verbesserten Ausdauerleistungsfähigkeit und eine erhöhte intermyofibrillare Glykogenmenge hingegen mit einer verbesserten Kontraktionsgeschwindigkeit in Verbindung gebracht [11]. Durch wiederholtes Training wird Glykogen (Speicherglukose) vermehrt im Muskel angereichert [12].

Glukose aus der Zirkulation stammt aus der Nahrung oder aus der Leber, wo es aus dem dort gespeicherten Glykogen gebildet wird [13]. Während das Muskelglykogen ausschließlich für Muskelkontraktionen mobilisiert wird, dient das in der Leber gespeicherte Glykogen in erster Linie für die Aufrechterhaltung des Blutzuckerpiegels sowie für die Versorgung von Gehirn und Erythrozyten aber auch anderen Geweben. Der Auf- bzw. Abbau des Leberglykogens steht unter der hormonellen Kontrolle von Glucagon und Insulin. Glukose wird vom Muskel über induzierbare (GLUT4) und konstitutive Glukosetransporter (GLUT1) aus dem Blut aufgenommen [14]. Wiederholte Muskelkontraktionen führen zu einem Anstieg des Glukosetransports in den Muskel, worauf der sinkende Blutzuckerspiegel durch Abbau des Leberglykogens wieder stabilisiert wird [13]. Die Erschöpfung in Folge einer längeren, anstrengenden körperlichen Betätigung ist deshalb abhängig vom totalen Verbrauch des Muskelglykogens oder einer Hypoglykämie (Unterzuckerung), ausgelöst durch Entleerung des Leber-Glykogenspeichers [15].

Bei der anaeroben Glykolyse werden Glukose und Glykogen zu Pyruvat und durch die Laktatdehydrogenase weiter zu Laktat abgebaut, wobei pro Glukose-Molekül zwei ATP-Moleküle für Muskelkontraktionen entstehen. Bei der Bildung von Laktat wird der Cofaktor NAD+ regeneriert, der in ausreichend hohen intrazellulären Konzentrationen für die vorangegangenen Reaktionen der Glykolyse vorhanden sein muss. Laktat wird entsprechend des Zell-Zell-Shuttle-Konzeptes [16,17] in glykolytischen Fasern produziert [18], im Symport mit Protonen exportiert [19] und dient vorrangig den oxidativen Muskelfasern als primäres Substrat [20,21]. In glykolytischen Fasern verbleibendes Laktat wird höchstwahrscheinlich in Glykogen umgewandelt, vor allem nach der Bewegungseinheit [22].
Ob zelluläres Laktat exportiert oder importiert wird, ist konzentrations- oder protonenabhängig. Die Laktatbildungsrate und der anschließende zelluläre Export steigen zu Beginn der Muskelkontraktion [23]. Die Laktataufnahme erfolgt, wenn Laktat in der Zelle verstoffwechselt wurde und die Laktatabbaurate die Laktatproduktionsrate übersteigt [24]. Somit spiegelt der Laktatspiegel im Blut das Gleichgewicht zwischen Laktatproduktion und -abbau wider.

Die Belastungsintensität an der oberen Grenze des Gleichgewichts zwischen Laktatproduktion und Laktatabbau wird als Laktatschwelle bezeichnet. Ausdauersportler nutzen diesen Wert, um die individuelle Belastungsintensität während des Ausdauertrainings zu beurteilen oder um zu bestimmen, bei welcher Intensität der oxidative Stoffwechsel ausreicht, um den Gesamtenergiebedarf eines Organismus zu decken [25,26].

In oxidativen Muskelfasern wird Laktat zu Pyruvat umgewandelt und über Pyruvat-Carrier (*mitochondrial pyruvate carrier* MPC1/2) in die Mitochondrien transportiert [27]. Alternativ kann Laktat entsprechend des intrazellulären Laktat-Shuttle-Konzeptes [16,17] direkt über MCT1 (*monocarboxylate transporter isoform 1*) in die Mitochondrien transportiert werden [28,29] und dort von der mitochondrialen Laktatdehydrogenase in Pyruvat umgewandelt werden. In den Mitochondrien findet dann unter oxidativen Bedingungen die ATP-Produktion durch Substratkettenphosphorylierung (Citratzyklus) und oxidative Phosphorylierung (Atmungskette) statt, wodurch ein vollständiger Abbau zu CO_2 und H_2O sowie 38 ATP-Molekülen (im Vergleich zu 32 ATP beim Transport von NADH aus der Glykolyse über den Malat-Aspartat-Shuttle) erzielt wird.

Quantitativ gesehen werden die meisten ATP-Moleküle bei der Oxidation von Fettsäuren erzeugt, abhängig von der Länge der Fettsäure (z.B. Stearinsäure (C18) 120 ATP-Moleküle). Die Fettsäuren stammen aus der Mobilisierung peripherer Fettdepots, wo sie nach Sezernierung aus dem Fettgewebe an Albumin gebunden und von dort über das Blut in verschiedene Organe und Gewebe verteilt werden. Der Transport in die Muskelzelle erfolgt zum einen durch Diffusion der Fettsäuren beziehungsweise wird durch induzierbaren Fettsäuretransporter CD36 zusammen mit Fettsäure-bindenden Proteinen

(FABP) oder dem Fettsäure-Transportprotein FATP erleichtert [30,31]. Im Zytosol der Muskelzellen werden die Fettsäuren aktiviert (Veresterung mit Coenzym A) und dann durch die Carnitin-O-Palmitoyl-transferase 1/2 in die Mitochondrien transloziert, wo sie in verschiedenen katabolischen Prozessen (β-Oxidation, Citratzyklus, Atmungskette) zur ATP-Gewinnung abgebaut werden.

Die Speicherung der Fettsäuren im Fettgewebe erfolgt als Triglyzeride in den Fettvakuolen der Adipozyten. Adipozyten von weißem Fettgewebe (Speicherfett) sind gekennzeichnet durch eine große Fettvakuole (*lipid droplet*), welche die gesamte Zelle einnimmt, einen an den Rand gedrängten Zellkern sowie wenige Mitochondrien [32]. Die Mitochondrien in den weißen Fettzellen spielen unter anderem eine Rolle bei der *de novo* Lipogenese, also bei der Bildung von Triglyzeriden [33,34], obwohl die Fettsäuren hauptsächlich in der Leber aus Glukose gebildet werden [35]. Zwar findet die Synthese von Fettsäuren und Triglyceriden im Zytosol statt, aber die Mitochondrien liefern wichtige Zwischenprodukte wie Acetyl-CoA [36]. Eine ganz andere Funktion erfüllen die Mitochondrien des braunen Fettgewebes. Sie enthalten UCP1 (*uncoupling protein 1* oder auch Thermogenin genannt), welches den bei der oxidativen Phosphorylierung erzeugten Protonengradient entkoppelt, so die ATP-Synthese aussetzt und zu einer Energiefreisetzung in Form von Wärme führt [37], und welches vor allem bei Winterschlaf und Winterruhe haltenden Tieren sowie Säuglingen eine Rolle spielt. Beiges Fett, weißes Fettgewebe mit Charakteristika von braunem Fett, wie mehr Mitochondrien, mehrere kleinere Fettvakuolen, exprimiert ebenfalls UCP1 und kann deshalb ebenfalls thermogenetisch aktiv werden und Substrate abbauen ohne ATP zu synthetisieren. Die Transformation von weißem in beiges Fettgewebe kann zum Beispiel durch Kälteexposition ausgelöst [38], aber auch durch intensives Training erzielt werden [39]. Trainingsinduzierte Erhöhung der UCP1-Konzentrationen im weißen Fettgewebe und damit die Umwandlung von weißen in beige Adipozyten setzt die Expression von PGC1α (*peroxisome proliferator-activated receptor (PPAR)-γ coactivator 1-α)* voraus [39]. PGC1α-Knockout-Mäuse zeigen, dass PGC1α für die belastungsabhängige Regulierung der UCP1-Expression in weißem Fettgewebe erforderlich ist, aber nicht für die basale UCP1-Expression [39].

PGC1α wird allgemein als Auslöser von mitochondrialer Biogenese, der Erhöhung von mitochondrialer Masse, angesehen [40]. Es ist ein transkriptioneller Coaktivator, der die Transkription von Genen reguliert, die für den Energiestoffwechsel von Bedeutung sind. PGC1α interagiert mit verschiedenen Transkriptionsfaktoren (*nuclear respiratory factors* (NRF)1, 2; PPAR-α, -δ; PPAR-γ und weitere), die wiederum an einer Vielzahl biologischer Reaktionen, wie mitochondriale Biogenese, Fettsäureoxidation, UCP1-Induktion sowie Differenzierung von braunen Fettzellen, beteiligt sind [41]. Auch die Expression von PGC1α kann durch körperliche Aktivität und Kälteexposition in Fett- wie Muskelgewebe erhöht werden [42-46]. Die Menge an PGC1α im Muskel beeinflusst die Anzahl und

Funktion der Mitochondrien, die Anzahl der oxidativen Typ-I-Muskelfasern sowie die Ausdauerleistung, wie in PGC1α-transgenen [47] und –Knockout-Modellen [48] gezeigt werden konnte. Mäuse mit muskelspezifischem PGC1α-Knockout weisen beispielsweise eine verminderte Expression von Stoffwechselgenen, eine erhöhte Anzahl glykolytischer Fasern (Muskelfaserswitch) sowie eine verringerte körperliche Aktivität auf [48], während PGC1α-transgene Tiere mehr oxidative Muskelfasern aufweisen und vermehrt mitochondriale Proteine (Cytochrome) exprimieren [47].

Die Dauer und die Intensität der körperlichen Aktivitäten bestimmen auf Muskelebene die Substratquelle (Glukose, Fettsäuren) für die Energieproduktion [5,49,50]. Kontinuierliche Aktivität mit einer Arbeitsbelastung von 30 % maximaler Sauerstoffaufnahme (VO_2max) wie Radfahren führt zur Substratverwertung von Glukose und freien Fettsäuren, wobei in den ersten 90 Minuten die Glukoseoxidation überwiegt und danach die Fettsäureoxidation [51]. Allgemein ist bei Ausdauerbelastungen niedriger und mittlerer Intensität die Fettsäureoxidation erhöht, wobei die maximale Fettoxidation bei 64 % VO_2max stattfindet [52]. Bei einer Belastung über 80 % VO_2max nimmt die Fettsäureoxidation ab und die Nutzung von Plasmaglukose und Muskelglykogen überwiegt [50]. Auch bei Marathonläufen dominiert die Kohlenhydratoxidation, wobei ein Zusammenhang zwischen der Laufgeschwindigkeit und der Kohlenhydratoxidationsrate zu beobachten ist [53]. Bei einer hohen Geschwindigkeit ist die Oxidationsrate höher, während bei einer niedrigeren Geschwindigkeit die Dauer der Kohlenhydratoxidation länger anhält.

Die physiologische Anpassungsfähigkeit, auf die beim Sport steigenden Energieanforderungen und die Verfügbarkeit von Brennstoffen angemessen auf der Ebene der Substraterkennung, des Transports, der Verwertung und Speicherung zu reagieren, ist ein Hinweis für eine hohe metabolische Flexibilität [54,55]. Allgemein bezeichnet die metabolische Flexibilität die Leichtig- und Schnelligkeit, je nach Brennstoffverfügbarkeit, frei zwischen oxidativen Brennstoffen zu wechseln [56]. Das bedeutet beispielsweise bei gesunden schlanken Individuuen, dass eine kohlenhydratreiche Nahrungszufuhr zu einem geringen Anstieg des Blutinsulinspiegels und zu einer starken Verlagerung von der Fettsäure- zur Glukoseoxidation bei konstant gehaltenem Blutzuckerspiegel führt [57] oder der Verzehr einer fettreichen Diät die Fettsäureoxidation auf Kosten von Glukose erhöht [58]. Nach dem Essen (postprandial) oxidieren die Mitochondrien eine Mischung aus Fett und Kohlenhydraten und in Folge von Fasten (postabsorptiv) hauptsächlich Fette [57]. Dabei wird der Fettsäurefluss im postprandialen Kreislauf durch das Fettgewebe und der Glukosefluss durch die Leber und in geringerem Maße die Skelettmuskulatur reguliert [59]. Metabolisch unflexible Probanden zeigen eine gestörte Brennstoffumschaltung, welches eine anhaltende Oxidation aller drei Hauptbrennstoffe (Fette, Kohlenhydrate und Aminosäuren) und damit verbunden eine mitochondriale Überlastung bewirkt, die

mit Stoffwechselstörungen wie Fettleibigkeit, Insulinresistenz und Typ-2-Diabetes in Verbindung gebracht wird [57,60].

Um den enormen Anstieg des Energiebedarfs bei körperlicher Aktivität mit der Brennstoffverfügbarkeit und dem Stoffwechsel effizient zu koordinieren, ist ebenfalls eine gewisse metabolische Flexibilität von Nöten. Freizeitsportler weisen eine geringere metabolische Flexibilität sowie ineffiziente anaerobe Beiträge (glykolytische und phosphagene Systeme) und damit geringere energetische Leistung als Athleten auf, was auf deren mitochondriale Funktion und kardiovaskuläre Fitness zurückzuführen ist [61]. Eine Ernährungsumstellung auf eine *lowCarb-highFat*-Diät für sechs Wochen resultiert bei Freizeitausdauerathleten in einem höheren Anteil der aus der Fettoxidation gewonnenen Energie selbst bei hohen Trainingsintensitäten (VO_2 max > 70%) als bei Athleten, die einer *highCarb-lowFat*-Ernährung folgten. Dies spricht für eine höhere metabolische Flexibilität durch die *lowCarb-highFat*-Diät und stellt die Glukoseabhängigkeit bei hochintensivem Ausdauersport in Frage [62].

Verbunden mit der beim regelmäßigen Sport zunehmenden Energieanforderung steigt bei metabolisch flexiblen Individuuen in Abhängigkeit von den jeweiligen verfügbaren Brennstoffen deren Oxidation sowie auch die Transkription von Genen, die die Kohlenhydrat- oder Fettoxidation in der Skelettmuskulatur regulieren. Transkriptionsfaktoren, wie PGC1α [63] oder Transkriptionsfaktor EB (TFEB) [64] spielen dabei eine wichtige Rolle. Induziert durch regelmäßiges Training reguliert PGC1α direkt oder indirekt mit weiteren Transkriptionsfaktoren zellkern- und mitochondrienkodierte Gene, die für kontraktile und metabolische Anpassungen im Skelettmuskel erforderlich sind [54,65]. So werden zum Beispiel über NRFs die Transkription von Genen aktiviert, die für Proteine der oxidativen Phosphorylierung, oder via PPARs, die für Enzyme kodieren, welche am Lipidtransport und -oxidation beteiligt sind [66]. TFEB erhöht ebenfalls die Nrf2-Expression, aber auch die von Tfam- und Ppara, Pparg und Ppard und somit den Lipidstoffwechsel sowie die mitochondriale Biogenese im Muskel [64]. Dies geschieht PGC1α unabhängig, obgleich die Expression und Aktivierung von TFEB bewegungs- und PGC1α abhängig sind [64,67]. Des Weiteren steuert TFEB die Expression von Genen wie GLUT1 und 4 und Hexokinase I/II, die an der Glukoseaufnahme und –verstoffwechslung beteiligt sind, sowie über die Glykogensynthase die Glykogenproduktion und -akkumulation, um die Energieproduktion während des Trainings sicherzustellen [64]. Da TFEB den zellulären Glukosehaushalt, die Insulinsensitivität, die Lipidoxidation und die mitochondriale Biogenese direkt beeinflusst, wird er, genauso wie PGC1α [63], als entscheidender Faktor für die metabolische Flexibilität bei körperlicher Aktivität angesehen [64].

1.2 Modelle für die Untersuchung von Bewegung

Obgleich viele Untersuchungen hinsichtlich des Einflusses von Sport direkt am Menschen durchgeführt werden können, sowohl nicht invasiv (Speichel, Puls, nicht kalorimetrisch) als auch invasiv (Blutuntersuchungen, Gewebeproben/Biopsien), bieten sich Tiermodelle an, um umfassendere Analysen, wie die Wechselwirkung von Geweben oder Kontraktionsmessungen am isolierten Muskel, vorzunehmen. Nager als Modelltiere sind in der medizinischen Forschung weit verbreitet und werden für verschiedene Fragestellungen eingesetzt.

Um den Einfluss von körperlicher Aktivität zu untersuchen, kann auf verschiedene Inzucht- oder Auszuchtlinien von Mäusen oder Ratten zurückgegriffen werden, denen man ein Laufrad, Laufband, Schwimmbecken oder eine Leiter zur Verfügung stellt. Für Fragen hinsichtlich physischer Leistung sind der Trainingszustand und die genetische Veranlagung wichtig [68,69], so dass Modelle mit spezifischer Leistungsfähigkeit verwendet werden. Ein Modell stellt zum Beispiel das auf "hohe Laufradaktivität" Langzeit-gezüchtete Mausmodell dar, welches von der Gruppe um T. Garland entwickelt wurde. Dieses wurde durch Selektion auf erhöhtes freiwilliges "Laufradverhalten" etabliert, ermittelt durch einen sechstägigen Laufradzugang [70]. Ein anderes Modell, ein Rattenmodell, beruht auf Selektion auf hohe bzw. niedrige Laufleistung auf einem Laufband, wobei die Trainingslaufleistung über 8 Wochen ermittelt und Weibchen und Männchen des oberen 10. Perzentil bzw. des unteren 10. Perzentil als Gründereltern der nächsten Generation ausgewählt wurden [71,72].

Beide Modelle beruhen auf genetisch heterogene Auszuchtstämme, die durch direktes, vorheriges Training [70] oder durch Training der Elterntiere [72] generiert wurden. Um die genetischen Effekte zu untersuchen, die mit einer angeborenen extremen körperlichen Leistung als "Langstreckenläufer" verbunden sind, dient die Dummerstorfer Mauslinie mit hoher Laufbandleistung (DUhTP) [73,74]. Dieses Mausmodell wurde ohne Trainingseinfluss entwickelt.

In Dummerstorf wurden in den späten 70er und frühen 80er Jahren verschiedene Mausmodelle durch Langzeitselektion auf ein bestimmtes Merkmal etabliert. Ausgangspunkt aller Linien bildete eine eigens generierte Auszuchtlinie Fzt:DU, die durch das Kreuzen von vier Inzucht- (CBA/Bln, AB/Bln, C57BL/Bln und XVII/Bln) und vier Auszuchtlinien (NMRI orig., Han:NMRI, CFW und CF1) beginnend in den späten 70er Jahren erzeugt wurde [75] (Abbildung 1). Die erhaltene Mauslinie Fzt:DU zeichnete sich durch eine hohe genetische Vielfalt aus, die sich visuell in unterschiedlichen Fellfarben widerspiegelte. Ausgehend von dieser Auszuchtlinie wurden vier Mal pro Jahr bis zu 200 Paare pro Generation zufällig, bei gleichzeitiger Inzuchtvermeidung, verpaart und als nicht-ingezüchtete Kontrolllinie DUC (Dummerstorfer Kontrolle) gehalten. Bis in die frühen 80er Jahre wurden verschiedene

Langzeitselektionslinien, ebenfalls unter Vermeidung der Inzucht, etabliert, mit deren Hilfe die Forschungsschwerpunkte der Landwirtschaft zu jener Zeit untersucht werden sollten. Neben Mausmodellen mit maximalem Muskelansatz, schnellem Wachstum und hoher Nachkommenszahl mit hohem Geburtsgewicht, wurde auch ein Tiermodell DUhTP (*Dummerstorf high treadmill performance mouse line* bzw. DUhLB – Dummerstorfer Mausmodell mit hoher Laufleistung) generiert, welches besonders robust, widerstandsfähig und wenig stressanfällig sein sollte.

Das Modell DUhTP wurde seit 1982 durch paternale Selektion auf hohe Laufbandleistung generiert (Abbildung 1). Dafür wurden die Männchen nach der Anpaarung, ungefähr im Alter von 77 Tagen, auf ein computergesteuertes Laufband gesetzt und durch einen einmaligen Submaximaltest die besten Läufer ermittelt. Die Nachkommen der besten Läufer wurden dann als Elterntiere der nächsten Generation bestimmt. Je Generation wurden 60-100 Verpaarungen mit geringstmöglichem Inzuchtgrad durchgeführt. Die Selektionsschärfe, also der Anteil der Tiere mit dem besten Selektionsmerkmal, die für die nächste Generation ausgewählt wurden, betrug 40-45 %.

Die Bedingungen für den Submaximallauftest wurden 1995 von Ulla Renne und Lutz Bünger festgelegt und lösten den bis zur 50. Generation angewandten Maximallauftest [76] auf Weisung der Tierschutzkommission des Landes MV ab. Dabei wurde nicht nur das Laufprogramm angepasst, sondern vor allem auch die Verweildauer auf der Stimulierungseinrichtung auf 2x 1,2 s verkürzt, so dass die Tiere den Versuchsabbruch jederzeit vor der Erschöpfungsphase provozieren konnten.

Der Submaximallauftest wurde wie folgt durchgeführt: Die Mäuse liefen initial 30 m mit einer Geschwindigkeit von 15 m/min (≙ 120 s), bevor eine Laufpause von 1 min folgte. Danach wurde das Band wieder gestartet und es folgte eine Strecke von 15 m bei 15 m/min (≙ 60 s). Danach wurde die Geschwindigkeit nach jeweils 50 m schrittweise auf 22 m/min (≙ 136 s), 26 m/min (≙ 115 s), 30 m/min (≙ 100 s), 34 m/min (≙ 88 s) und 36 m/min (≙ 83 s) erhöht bis die Höchstgeschwindigkeit von 38 m/min erreicht wurde.

Nach 90 Generationen konnten bei den DUhTP-Männchen eine Laufperformance von 3778 ± 591 m beobachtet werden [77], was einem Selektionserfolg von +249 % entsprach. Die zurückgelegte Laufstrecke der Kontrollmäuse betrug im Durchschnitt 1003 ± 172 m und war somit um das etwa 3,8-fache geringer als bei den DUhTP-Mäusen, die deshalb auch als Marathonmäuse bezeichnet werden. Vierzig Generationen später lag die durchschnittliche Laufstrecke der DUhTP-Mäuse bei etwa 5414 ± 238 m (Selektionserfolg +400 %) und die der Kontrollmäuse bei 1705 ± 145 m (DUC) [78].

Seit 2012 ist die Linie von einer semi-Barriere Haltung zu einer speziell pathogen-freien (SPF) Haltung durch Embryotransfer umgesiedelt worden. Nach 35 Jahren mit vier Generationen pro Jahr, also 140

Generationen, wird die Linie DUhTP als Erhaltungslinie, ohne weitere Selektion aber unter Vermeidung von Inzucht, fortgeführt.

Da die Laufleistung der Väter im Zuge der Selektion erst nach der Anpaarung ermittelt wurde und die ausgewählten Nachkommen zur Verpaarung nie auf dem Laufband gewesen sind oder ein Laufrad zur Verfügung hatten, wurde hier durch Selektion ein genetisches Modell geschaffen, welches sich durch hohes Laufvermögen ohne vorheriges Training auszeichnet.

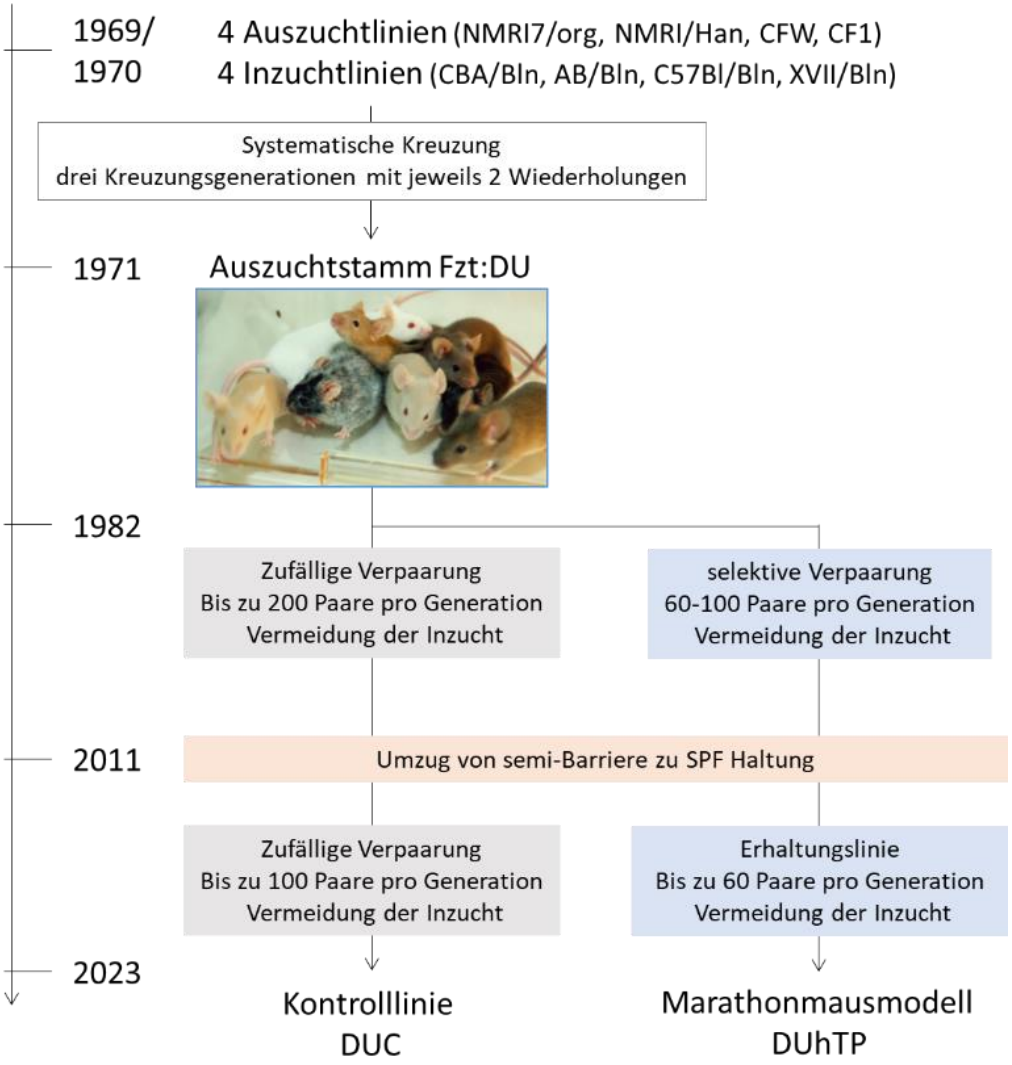

Abbildung 1: Darstellung des zeitlichen Verlaufs der Etablierung der Kontrolllinie DUC und der Selektionslinie DUhTP aus dem Auszuchtstamm Fzt:DU.

1.3 Struktur und Fragestellung der Arbeit

Die hier vorliegende kumulative Habilitationsschrift beschäftigt sich mit dem Mausmodell DUhTP. Das ursprünglich für nutztierrelevante Fragestellungen hinsichtlich Widerstandsfähigkeit und Robustheit entwickelte Modell hat im Laufe der jahrelangen Selektion Anpassungen erfahren, die unter anderem zu einem Stoffwechseltyp mit hoher metabolischer Flexibilität geführt hat. Die vorliegende Schrift setzt sich aus neun Arbeiten zusammen, die einerseits das genetische Modell charakterisieren (Teil 1), sowie den Einfluss von freiwilliger Bewegung im Laufrad (Teil 2) als auch die Auswirkungen von gezieltem Laufbandtraining (Teil 3) untersuchen. Dabei werden die Ergebnisse immer im Vergleich zur Kontrolllinie (DUC) betrachtet, welche die ursprüngliche Auszuchtlinie (Fzt:DU) repräsentiert.

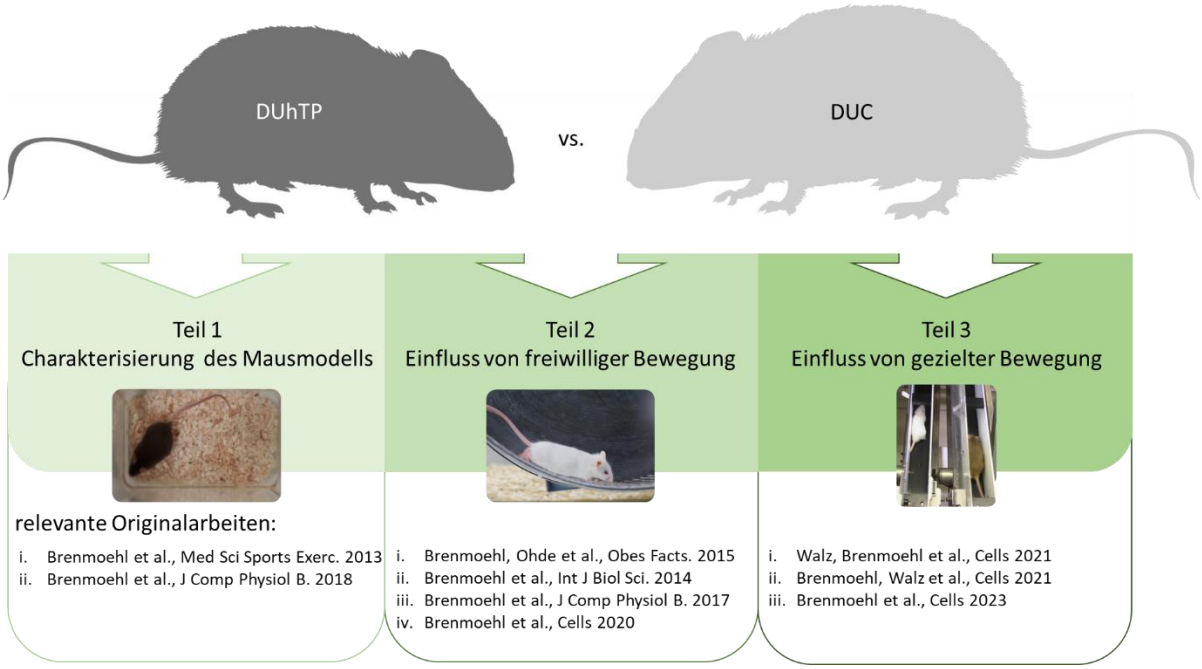

Abbildung 2: Struktur der Habilitationsschrift und Zuordnung der relevanten Publikationen

Übergeordnetes Ziel dieser Untersuchungen war es, die Mechanismen zu identifizieren, die einerseits die außerordentliche Laufleistung der DUhTP-Mäuse und andererseits die effiziente Energiebereitstellung / Substratbereitstellung ermöglichen.

2. Zusammenfassungen der thematisch relevanten Publikationen

2.1 Charakterisierung des Marathon-Mausmodells

i) Metabolische Anpassungen in der Leber von Marathonmäusen

Die körperliche Leistungsfähigkeit hängt vom Trainingszustand und der genetischen Veranlagung ab [68,69,79] und ist eng mit dem Energiestoffwechsel verbunden. Die Leber als zentrales Stoffwechselorgan nimmt eine wichtige Rolle im Kohlenhydrat- und Lipidstoffwechsel ein. In der Leber wird die Umschaltung des Stoffwechsels zwischen dem satten, wenn Substrate wie Glukose im Überfluss vorliegen, und dem nüchternen Zustand streng kontrolliert [80]. Wenn Kohlenhydrate im Überfluss vorhanden sind, wandelt die Leber Glukose in Glykogen und Fettsäuren um. Während des Fastens oder körperlicher Betätigung werden diese Substrate (Glukose und Fettsäuren) von der Leber in den Blutkreislauf abgegeben und von Muskel-, Fett- und anderen extrahepatischen Geweben verstoffwechselt. Der hepatische Stoffwechsel wird auf genomischer Ebene durch zahlreiche Transkriptionsfaktoren und Koregulatoren, wie beispielsweise PPAR delta oder Sirtuin 1, gesteuert, wodurch die Gluconeogenese, β-Oxidation und Lipogenese in der Leber dynamisch reguliert werden, um den systemischen Stoffwechselbedarf zu decken. Es wurde daher untersucht, ob die Marathonmaus aufgrund jahrelanger Selektion auf hohe Laufbandaktivität spezifische Anpassungen im Leberstoffwechsel mit veränderter Expression von PPAR delta und Sirtuin 1 erfahren hat.

Unsere Untersuchungen zeigen, dass untrainierte DUhTP-Männchen neben einem höheren Laufvermögen (3,8-fach) im Vergleich zu den untrainierten Kontrolltieren, auch Unterschiede in der Körperzusammensetzung sowie im Stoffwechsel aufwiesen. Im Alter von 49 Tagen war das Körpergewicht der DUhTP- im Vergleich zu DUC-Mäusen zwar nicht verschieden, aber die fettfreie Körpermasse reduziert und periphere Fettdepots vermehrt zu finden. Erhöhte Triglyzerid- und Cholesterollevel im Serum und höhere Triglyzeridlevel in der Leber ließen den Rückschluss zu, dass der Fettstoffwechsel in der Marathonmaus eine wichtigere Rolle einnimmt als in der Kontrolllinie. Bestätigt werden konnte dies durch eine Gaschromatografie-Massenspektrometrie-Analyse mit Leberextrakten beider Linien im Alter von 49 Tagen, mit deren Hilfe verschiedene Fettstoffwechselmetaboliten in der DUhTP-Linie vermehrt detektiert werden konnten. Allerdings konnten auch gehäuft Metaboliten des Glukosestoffwechsels wie Glukose, Glukose-6-Phosphat, Glukose-1-Phosphat oder Hexose-6-Phosphat beobachtet werden, was auf Glykolyse aber auch auf den Glykogenstoffwechsel hindeutet. Hepatisches Speicherglykogen wurde in der Marathonmaus um 75 % höher nachgewiesen als in Kontrollmäusen. Demnach lag die Vermutung nahe, dass vermehrt

Kohlenhydrate und Lipide in der Leber akkumuliert werden. Da auch erhöhte hepatische mRNA-Level der Enzyme PEPCK, GDH, ACSS2 und ACC gezeigt werden konnten, ist von metabolischen Anpassungen in der Leber auszugehen, die sich während des Selektionsprozesses genetisch manifestiert haben. Höhere Genexpressionsraten von Ppard sowie höhere Sirtuin 1 Proteinlevel in der Leber der DUhTP-Mäuse deuteten zudem auf eine gesteigerte hepatische Lipogenese im Vergleich zu den Kontrollmäusen hin, so dass wir postulierten, dass die Akkumulation von Fett für die Energiebereitstellung unter Belastung von Bedeutung ist.

ii) Differentielle Merkmalsreaktion auf Haltungsbedingungen bei Mäusen

Die Körpermasse und die Körperzusammensetzung sind das Resultat des Verhältnisses von Energieaufnahme und -abgabe und werden durch endogene (genetische Voraussetzungen, Hormone) und exogene Faktoren (Umwelteinflüsse, Ernährung, körperliche Aktivität) reguliert. Eine hygienische Umstellung von der Semi-Barriere (SB) auf eine neue SPF (*specified pathogen-free*)-Barriere-Einheit führte bei den Marathonmäusen und der Kontrolllinie zu unterschiedlichen Reaktionen auf die neue Umgebung, unter anderem zu einer partiellen Umkehrung des Phänotyps, weshalb die in beiden Mauseinrichtungen erhobenen Daten beider Linien (DUC und DUhTP) miteinander verglichen wurden.

Nur die Kontrolllinie DUC war nach der Neuetablierung der Linie in der SPF-Haltung durch eine höhere Körpergröße sowie ein erhöhtes Körpergewicht im Alter von 21 und 42 Tagen gekennzeichnet als in der SB-Haltung. Zwar war das Geburtsgewicht der DUhTP-Mäuse deutlich höher als das der DUC-Mäuse und als in der SB-Haltung, jedoch nahmen die Kontrolltiere wesentlich besser und schneller zu als die DUhTP-Nachkommen. Im Alter von 70 Tagen wiesen die SPF-Kontrolltiere höhere Körpergewichte, mehr Muskelmasse, Subkutanfett und höhere Serumtriglyzeridwerte verglichen mit der SB-Haltung auf. Die SPF-DUhTP-Tiere waren nur wenig schwerer als die SB-DUhTP-Tiere und wiesen sogar geringere Epididymalfettmassen und Serumtriglyzeridlevel auf. Somit unterschieden sich die beiden Linien phänotypisch enorm nach dem Umzug in die SPF-Haltung. Als Ursache konnte die neue Haltung trotz eines besseren Gesundheitsstatus ausgeschlossen werden, da nur die DUC-Mäuse durch deutlich höhere Körpergewichte und Serumtriglyzeridlevel gekennzeichnet waren. Auch der unterschiedlichen Kryotransfer beider Linien in die SPF-Haltung konnte als Ursache ausgeschlossen werden, da in der Literatur nur von Effekten im Erwachsenenalter [81], jedoch nicht auf deren Nachkommen berichtet wurde [82]. Nach 15 Generationen wurden konstant höhere Körpergewichte in allen Altersstufen der DUC beobachtet als in der vorherigen SB-Haltung. Da in der SB- und in der SPF-Anlage unterschiedliche Futtermittel verwendet wurden, wurden die Auswirkungen der beiden kommerziellen Futtermittel auf das Körpergewicht unter identischen Haltungsbedingungen untersucht. Das vorherige Futter aus der SB-Haltung bewirkte eine Gewichtsreduktion der DUC-Tiere

sowie eine Verringerung der Serumtriglyzeridlevel. In den DUhTP-Mäusen resultierte das SB-Futter in keiner Gewichtsveränderung, jedoch in einer Erhöhung der Triglyzeridkonzentrationen im Blut. Somit legen die Daten nahe, dass vor allem das neue Futter für die phänotypischen Veränderungen, vor allem in der Linie DUC, verantwortlich ist und dass die Gabe des vorherigen Futters eine teilweise (Rück)Umkehr der Phänotypen bewirken kann.

2.2 Einfluss von moderater freiwilliger Bewegung

i) Dynamik der Fettmasse bei DUhTP-Mäusen

Der positive Einfluss von Bewegung auf die Gesundheit ist wohl bekannt. Jedoch sind die Auswirkungen auf Körpergewichtsreduktion oder Körperzusammensetzung meist mit hohem Leistungsaufkommen verbunden. Außerdem spielen verschiedene Faktoren wie Geschlecht, Alter, Trainingsstatus und vor allem der Stoffwechseltyp eine große Rolle [5]. Gleiches Training kann bei zwei Individuen zu einem unterschiedlichen Erfolg führen [68,79]. Auch in unseren Studien mit den Marathon- bzw. Kontrollmäusen konnten unterschiedliche Auswirkungen auf den Phänotyp der Tiere beobachtet werden.

Unsere Ergebnisse zeigen, dass sich DUhTP-Mäuse zwar freiwillig nicht ausgiebiger bewegten als die Kontrolllinie aber dafür mehr peripheres Depotfett mobilisierten, vor allem das Subkutanfett. Eine Analyse dieses Fettgewebes ergab eine hohe Proteinexpression von Fett-synthetisierenden und -degradierenden Enzymen, sowohl im sedentären Zustand als auch nach freiwilliger körperlicher Aktivität. Zudem konnten im Subkutanfett der aktiven DUhTP-Mäuse mehr PGC1α, TFAM, SIRT3, ND-1 and NDUFA9 Proteinlevel sowie allgemein eine erhöhte mitochondriale Masse detektiert werden als bei sedentären DUhTP-Tieren oder aktiven Kontrollmäusen. Die Ergebnisse lassen darauf schließen, dass sich die DUhTP-Linie während der Langzeitselektion eine Reihe von Energiestoffwechsel relevanten Anpassungen erworben hat, um den hohen Energiebedarf bei körperlicher Aktivität zu decken, welche den Mäusen die Fähigkeit verleiht, vorhandene Fettmasse auch bei vergleichsweise leichter körperlicher Betätigung zu mobilisieren. Da eine erhöhte mitochondriale Masse sowie mehr mitochondriale Proteine im Subkutanfettgewebe der DUhTP-Mäuse gefunden wurden, spekulierten wir, dass eine Fettzell-Bräunung stattgefunden hat. Beweise für die trainingsinduzierte mitochondriale Biogenese in subkutanem Fett bei Mäusen wurden schon zuvor geliefert [83]. Somit weist das Subkutanfett „beige“ Fettzellen auf, die aus weißen Adipozyten entstanden sind und Eigenschaften von braunen Adipozyten aufweisen.

ii) Irisin in der Skelettmuskulatur und im Serum von Mäusen nach Bewegung

Der Induktor (Auslöser) der „Fettzell-Bräunung“ im weißen Fettgewebe ist PGC1α [40]. In Mäusen, die PGC1α überexprimieren, ist zudem die Expression des Transmembranproteins *fibronectin type III domain-containing protein 5* (Fndc5) erhöht. FNDC5 besteht unter anderem aus dem Signalpeptid Irisin, einem Zytokin, welches aus dem Muskel nach akuter Kontraktion oder aus dem Fett unabhängig von körperlicher Betätigung proteolytisch freigesetzt werden soll [84,85]. Da wir zuvor (siehe 2.2i [86]) bereits vermuteten, dass die DUhTP-Mäuse eine stärkere Bräunung des Subkutanfettes aufweisen und durch Bewegung diese Fettzellbräunung gesteigert werden kann, wurde die Expression von PGC1α im Muskelgewebe von sedentären (inaktiven) sowie im Laufrad bzw. auf dem Laufband aktiven DUhTP-Mäusen überprüft. Verschiedene mRNA Transkripte (Ppargc1a1-4) von PGC1α sind bekannt, wobei laut Ruas et al. bei Ausdauertraining Ppargc1a1 und bei akuter Belastung (Krafttraining) Ppargc1a4 stärker exprimiert werden [44].

Unsere Untersuchungen an Marathonmäusen zeigen, dass Irisin im Serum, Oberschenkel- (*Quadricep femoris*) und Unterschenkelgewebe (*Soleus*, *Extensor digitorum longus*, *Gastrocnemius* Muskel) von sedentären und körperlich aktiven Mäusen nachweisbar war, jedoch in erhöhten Konzentrationen nur im Serum und im Oberschenkelmuskel unmittelbar nach einmaligem Submaximallauf auf dem Laufband detektiert werden konnte. Interessanterweise fanden sich keine Unterschiede in der Expression von Fndc5 mRNA sowie FNDC5 Protein zwischen den Bewegungsgruppen, weder im Oberschenkel- noch im Unterschenkelgewebe. Ppargc1a4 Transkripte waren in den Oberschenkel- bzw. Unterschenkelmuskeln in der Laufbandgruppe höher als in der Kontrollgruppe exprimiert, wobei die mRNA-Häufigkeit mit der Laufleistung korrelierte. Zudem konnten im Oberschenkelgewebe von chronisch aktiven Mäusen (Laufrad) mehr Ppargc1a1 Transkripte nachgewiesen werden. Da während der akuten Belastung (Laufband) unveränderte Fndc5 mRNA- und Proteinexpression im Muskel zu beobachten und dennoch hohe Irisinwerte im Serum nachweisbar waren, stellten wir die Hypothese auf, dass einerseits die schnelle Induktion von Ppargc1a mRNA während der Belastung einen Prozess der Wiederherstellung des Muskelirisins und seines Vorläufers Fndc5 einleiten könnte, und dass andererseits die Spaltung und Sekretion von Irisin bei Mäusen ein kontinuierlicher physiologischer Prozess ist. In diesen Überlegungen haben wir jedoch außen vorgelassen, dass Irisin auch direkt im Fettgewebe produziert wird und demnach nicht nur als Myokin sondern auch als Adipomyokin betrachtet werden muss [85].

iii) Bräunung des subkutanen Fetts und höhere Oberflächentemperatur bei DUhTP-Mäusen

Eine Reihe von Studien haben gezeigt, dass die Zugabe von exogenem Irisin oder Irisin-Vorläufern (FNDC5) die Bräunung weißer Fettzellen bei Nagetieren [84,87] induziert. Auch in menschlichen weißen Fettzellen konnte vereinzelt die Bräunung der Fettzellen nach Irisin-Behandlung [88-90] und die Induktion von zellulärer Thermogenese in reifen menschlichen weißen Fettzellen gezeigt werden [90]. Im Vorversuch (siehe 2.2.ii [91]) wurden freiwillig im Laufrad und einmalig auf dem Laufband aktive DUhTP-Mäuse untersucht und höhere Level an Irisin explizit im Serum der akut aktiven Mäuse (Laufband) detektiert. Da keine Kontrollmäuse in diese Untersuchungen involviert waren und nur Muskelproben analysiert wurden, wurden nun weitere Untersuchungen mit freiwillig aktiven DUhTP- und DUC-Tieren durchgeführt.

Die FNDC5 Expression unterschied sich weder im Muskel- noch im Subkutanfettgewebe zwischen beiden Linien. Irisin konnte in größeren Konzentrationen im Serum und im Subkutanfett der DUhTP-Mäuse im Vergleich zu den Kontrollen nachgewiesen werden. Unterschiede zwischen sedentären und moderat körperlich aktiven DUhTP-Mäusen waren im Muskelgewebe, wie im Vorversuch [91], und im Subkutanfett nicht zu beobachten. Jedoch konnte ein auffälliger Browning-Phänotyp im DUhTP-Mausmodell aufgrund erhöhter Genexpression von „Browningmarkern“ (Ucp1, Tbx1) und verringerter Expression des Markers für weißes Fettgewebe Tcf1 identifiziert werden. Zudem konnte durch das Verwenden einer Infrarotkamera eine erhöhte Thermogenese im Marathon-Mausmodell visualisiert werden, die sich durch eine allgemein um 1°C höhere Oberflächentemperatur im Bereich des braunen Fettgewebes im Vergleich zu den Kontrollen auszeichnete. Mit diesen Ergebnissen schlossen wir darauf, dass aufgrund der jahrelangen Selektion die DUhTP-Mäuse von Geburt an energetische und metabolische Anpassungen aufweisen und auch unter sedentären Bedingungen eine Bräunung der Fettzellen zeigen, die andere Modelle erst nach langem und wiederholtem Training, wie beispielsweise von Stanford et al. [45] gezeigt, aufweisen. Wir schlugen deshalb das Mausmodell DUhTP als ein einzigartiges polygenes Modell für die Analyse des Mechanismus der Bräunung von Fettzellen ohne vorangestelltes Training, Kälteexposition oder Kalorienrestriktion vor.

In den letzten Jahren sind zahlreiche widersprüchliche Publikationen zu FNDC5 und Irisin erschienen. Zwar gibt es keinen Zweifel an der Existenz beider, jedoch sind die Detektionsmethoden sowie die Größe und die Konzentrationen der detektierten Proteine strittig (ausführlich diskutiert in verschiedenen Übersichtsarbeiten [92-95]). Für humanes FNDC5 wurde lange ein mutiertes ATA Startcodon diskutiert, welches jedoch kaum eine Translation des humanen FNDC5 Proteins zur Folge hat (1%), und in anderen Spezies (Affe, Maus, Ratte) nicht konserviert ist [96]. Ganz neue Untersuchungen belegen die Existenz eines Startcodons ATG upstream vor dem Fndc5 Gen [97], was

jedoch zu einem anderen Molekulargewicht (34 kDa) führt [97] als ursprünglich gedacht (25 kDa) und auch von uns nachgewiesen. Für die Detektion von Irisin gibt es ebenfalls widersprüchliche Angaben der Größe, aber auch der Konzentrationen im Blut. Wir setzten explizit auf den Einsatz von Antikörpern im Western Blot und wiesen eine Proteingröße von ca 12 kDa nach, welche der Größe von nicht glykosyliertem Irisin entspricht [93]. Bedingt durch die Verwendung von anderen Antikörpern zeigten andere Arbeiten auch Proteinbandengrößen, welche größer als das vorausgesagte Molekulargewicht von Irisin sind [94,98]. Des Weiteren verwendeten viele Autoren ELISA-Kits, welche neben den eigentlichen Proteinen auch falsch-positive Ergebnisse detektieren und deshalb Konzentrationen von teilweise über 1000 ng/ml gemessen wurden [99]. Die bessere und genauere Methode scheint die Massenspektroskopie zu sein. Mit dieser Methode wurden basale Irisinkonzentrationen von 0,3 ng/ml in Mausplasma detektiert [100], welche sich stark von ELISA-basierten Konzentrationen von 917 ng/ml [99] unterscheiden und mit Western Blots nicht detektierbar wären [93]. Diese „nicht sichtbaren" Banden wiederum bzw. die Proteinbanden mit verschiedenen Molekulargewichtsgrößen, abhängig vom verwendeten Antikörper [94], sind verantwortlich für die Diskussion der Existenz von Irisin, welche bis zu einer Grundsatzdiskussion der Funktion von Irisin für das Browning, besonders im Menschen, reicht [94,95,101]. Viele publizierten Ergebnisse, vor allem mit rekombinantem Irisin, gründen daher nicht auf physiologischen oder pharmakologischen Konzentrationen [93].

iv) Analyse der aktivitätsabhängigen Expression von Energiestoffwechsel-Transkripten im subkutanen Fett von Marathonmäusen

Die selektions- und aktivitätsvermittelte Erhöhung der mitochondrialen Masse im Subkutanfettgewebe der Marathonmäuse führt zu einer Umwandlung in beiges Fettgewebe und damit zur Beeinflussung der Funktion des ursprünglich weißen Fettgewebes und spricht für eine Verbesserung des systemischen Stoffwechsels durch höheren Energieverbrauch [102]. Um zu überprüfen, ob diese aktivitätsvermittelten Effekte längerfristig anhalten, wurde eine Cross-Over-Studie mit der Marathon- und Kontrolllinie über sechs Wochen durchgeführt, bei der die Tiere ein Laufrad im Käfig für die gesamte Zeit, die ersten drei Wochen, die letzten drei Wochen oder gar nicht zur Verfügung hatten.

Die Studie zeigt die größten Effekte auf die Körperzusammensetzung hinsichtlich der Fettdepots (subkutanes, viszerales, Nieren- sowie braunes Fettgewebe) in der Linie DUhTP in den Gruppen, welche bis zum Schluss körperlich aktiv waren. Dabei machte es keinen Unterschied, ob die Tiere drei oder sechs Wochen aktiv waren. Eine Reduktion der Serumtriglyzeridwerte konnte nur bei durchgängig aktiven DUhTP-Männchen beobachtet werden. Tiere, die nur die ersten drei Wochen körperlich aktiv

waren, ähnelten denen, welche die gesamten sechs Wochen inaktiv waren. Lediglich die Reduktion des braunen Fettgewebes blieb bestehen, sowohl in den DUhTP- als auch in den Kontrollmäusen. Eine Untersuchung der Transkripte, die für „Browningmarker"-Gene (Ucp1, Tbx1, Cidea), mitochondriale DNA, Transkriptionsfaktoren für mitochondriale Gene sowie Gene der Atmungskette kodierten, zeigten keine Effekte, die unmittelbar auf das Bewegungsprogramm zurückgeführt werden konnte. Es waren lediglich für die Expression von Browningmarkern Selektioneffekte zu beobachten, das heißt, dass sie unabhängig vom Trainingsprogramm in den DUhTP-Mäusen höher war als in den DUC Mäusen. In den Bewegungsgruppen der DUhTP-Mäuse konnten positive Korrelationen zwischen Ppargc1a, dem Impulsgeber der „Fettzell-Bräunung" [84], und dem mitochondrialen Transkriptionsfaktor (Tfam) sowie mitochondrialen Genen (Cyc, CytB, Mfn1 und Opa1) ermittelt werden, welche in den Kontrollen nicht vorhanden waren. Zusätzlich dazu unterschieden sich die Expressionen von Dynamin1, Mitofusin1 und Mitofusin 2 in den verschiedenen Bewegungsgruppen der DUhTP-Linie. Dabei wiesen vor allem die kurzzeitig aktiven Mäuse geringere Expressionslevel als inaktive DUhTP-Mäuse auf. Somit schlussfolgerten wir, dass nur im subkutanen Fett von Marathonmäusen auf der Ebene der Genexpression der mitochondriale Energiestoffwechsel durch freiwillige körperliche Aktivität aktiviert werden kann, nicht aber in unselektierten Kontrollen.

2.3 Einfluss von gezielter, erzwungener Bewegung

Da die DUhTP-Mäuse ihr Laufpotential nicht ausschöpfen, wenn sie sich freiwillig bewegen, wurde ein Trainingsprotokoll konzipiert, das dem Laufvermögen beider Linien gerecht wird und eine vergleichbare Bewegungs- bzw. Trainingsintensität von Mäusen der Linien DUhTP und DUC schafft. Dafür wurden die Submaximaltestläufe beider Linien, die zur Selektion der Linie DUhTP erhoben wurden, herangezogen. Die tägliche Trainingsdauer für die DUhTP-Mäuse wurde auf 30 min festgesetzt, was durchschnittlich der 23%igen Submaximallaufleistung der Linie entspricht, und die Trainingsdauer der Kontrollmäuse entsprechend berechnet und auf 15 min angesetzt. Das Trainingsprogramm beinhaltete für beide Linien einen Fünf-Tage-Trainingsplan mit zweitägiger Pause. Die Laufgeschwindigkeit wurde wöchentlich erhöht und die maximale Geschwindigkeit in der Linie DUhTP von 0,5 m/s in der letzten Trainingswoche angewandt, während die Tiere der Linie DUC bei bis zu einer Geschwindigkeit von 0,42 m/s trainiert wurden. Als Kontrollen dienten Tiere, die keinem Training unterzogen wurden. Unmittelbar nach dem letzten Lauf am 70. Lebenstag erfolgte die Sektion der Mäuse.

Um vor allem Aussagen zum Crosstalk einzelner Organe aufgrund von Training holistisch beleuchten zu können, wurden aus zentralem (Hypophyse) und peripherem Gewebe (Leber, Subkutanfett und Oberschenkelmuskulatur) RNA isoliert und Transkriptomanalysen durchgeführt.

i) Anpassungen des Protein- und Energiestoffwechsels in der Hypophyse nach dreiwöchigem Lauftraining von Mäusen

Als adaptive Reaktion auf körperliche Aktivität und Sport ist das Zusammenspiel von zentralem und peripherem Gewebe von großer Bedeutung. Regulatoren bei diesem Crosstalk sind unter anderem Hormone. Die Hypophyse produziert das Wachstumshormon (GH), Fortpflanzungshormone wie das luteinisierende Hormon (LH) und das follikelstimulierende Hormon (FSH), das adrenokortikotrophe Hormon (ACTH) oder das schilddrüsenstimulierende Hormon (TSH) und reguliert so das Wachstum, die Entwicklung der Fortpflanzung, die Stressreaktion und den Energiestoffwechsel. Adaptive und positive Auswirkungen von körperlicher Aktivität werden durch die Hypophyse vermittelt und betreffen die Hypophysen-Gonadal- [103], Hypophysen-Nebennieren- [104] und Hypophysen-Schilddrüsen-Hormonachsen [105,106], je nach experimentbedingter Bewegungsart. Beim Menschen wurde eine erhöhte GH-Sekretion nach Krafttraining beobachtet [107]. In Ratten führte akute Bewegung ebenfalls zu einer Erhöhung der GH-Konzentration im Schlachtblut, wobei ein vorangegangenes Training die Konzentration noch zusätzlich erhöhte [108]. Somit reagiert die Hypophyse sehr empfindlich auf die Auswirkungen körperlicher Aktivität. Um zu ermitteln, ob körperliche Aktivität auch organweite molekulare Pfade in der Hypophyse induziert, die nicht direkt mit bestimmten Hormonachsen oder bestimmten Zelltypen in Verbindung stehen, wurden die Hypophysen-Transkriptomdaten unserer Mauslinien verwendet, um zu prüfen, ob die genetisch manifestierten molekularen Signalwege in der Hypophyse von Marathonmäusen auch durch dreiwöchiges Training in unselektierten Kontrollmäusen (DUC) hergeleitet werden können.

Die Ergebnisse der Studie zeigen interessanterweise nur in der Kontrolllinie Auswirkung des Trainings auf die Regulierung molekularer Signalwege in der Hypophyse, nicht aber in DUhTP-Mäusen. Dabei wurden hauptsächlich Stoffwechselwege durch das Training induziert, welche an der Proteintranslation und dem Energiestoffwechsel beteiligt sind. Da diese Unterschiede auch zwischen trainierten DUC- und DUhTP-Mäusen bestanden, aber nicht zwischen untrainierten Tieren beider Linien, vermuteten wir eine erhöhte Proteinsynthese und eine höhere Energieversorgung in der Hypophyse von DUC-Mäusen als Reaktion auf das Training. Somit sahen wir durch unsere Ergebnisse die Beobachtungen der anderen Arbeitsgruppen hinsichtlich der adaptiven Auswirkungen von körperlicher Aktivität zumindest in der Linie DUC bestätigt. Konkret vermuteten wir die microRNA miR-124, welche im Rahmen der Studie identifiziert wurde, als neuen möglichen Mechanismus. Da auch bei Ratten die miR-124 Expression durch Training reduziert wird [109] und sich miR-124 in unmittelbarer Nachbarschaft zu einer QTL-Region befindet, die mit Trainingsreaktionen bei Mäusen assoziiert ist [110],

sahen wir uns bestätigt die miR-124, welche auf den AKT/mTOR-Signalweg abzielt, als Kandidat für weitere Studien im Mausmodell DUC zu betrachten.

ii) Zentrale Unterdrückung der GH/IGF-Achse und Aufhebung der trainingsbedingten mTORC1/2-Aktivierung im Muskel von Marathonmäusen

Über die Hypothalamus-Hypophysen-Hormonachse, auch als somatotrope Achse bezeichnet, wird die Synthese und Ausschüttung von Wachstumshormon (*growth hormone* (GH) / Somatotropin) stimuliert. GH wird pulsatil ausgeschüttet, wobei die Freisetzung verschiedenen Faktoren wie Pubertät, Hunger, körperlicher Belastung, Angst, Stress und Wach-Schlaf-Rhythmus unterliegt [111]. Es steuert primär Wachstumsprozesse während der Kindheit und der Adoleszenz, ist allerdings selbst nach Abschluss des Längenwachstums aktiv und beeinflusst den Eiweiß-, den Fett- und den Kohlenhydratstoffwechsel [112]. Eine GH-Ausschüttung durch körperliche Aktivität konnte bereits 1963 in Menschen nachgewiesen werden [113]. Das GH/IGF (*insulin-like growth factor*)-System ist aufgrund der positiven Auswirkungen auf das Muskelwachstum bei Ausdauertraining von großem Interesse, da IGF1 einen Teil der wachstumsfördernden Wirkungen von zirkulierendem GH vermittelt [114]. Um die Kontrolle der Genexpression und die Anpassung an die körperliche Leistungsfähigkeit in unseren Tiermodellen zu untersuchen und mit dem außergewöhnlichen Laufvermögen der Marathonmäuse in Zusammenhang zu bringen, wurde die Genexpression des GH/IGF-Systems und die damit verbundenen Signalkaskaden in der Hypophyse und im Muskel von trainierten und inaktiven DUhTP-und DUC-Mäusen analysiert.

Die Ergebnisse zeigen eine verringerte Pou1f1- (GH-Transkriptionsfaktor) und Gh-mRNA-Expression in der Hypophyse von Marathonmäusen, welche mit verringerten IGF1-Serumkonzentrationen und koordinierter verringerten Expression mehrerer Komponenten des IGF-Systems und der mTORC1- und -2-Signalwege im Oberschenkelmuskel der DUhTP-Mäuse korrelierten. Die IGF-Bindungsprotein-Transkripte Igfbp3, 4, 6 und 7 im Muskel von trainierten DUhTP-Mäusen waren stärker exprimiert als in trainierten Kontrolltieren, genauso wie Stanniocalcin 2, der Inhibitor der Protease PAPPA (*pregnancy-associated plasma protein A*) und damit der Inhibitor der Freisetzung von bioaktivem IGF1. Die auf mRNA-Expressionsebene nachgewiesene reduzierte Expression hormonabhängiger Signalwege in den trainierten DUhTP-Mäusen ging mit einer verminderten Aktivierung von AKT und somit mTORC2 [115] sowie einer geringeren Aktivierung von S6K und somit mTORC1 [116] in diesen Tieren im Vergleich zu den trainierten DUC-Mäusen einher. Da bei Kontrollmäusen eine Aktivierung von mTORC1 (S6K) und mTORC2 (Akt) nach Training beobachtet wurde, schlossen wir darauf, dass die zentrale Herunterregulierung der somatotropen Achse und die lokale Herunterregulierung der hormonabhängigen mTORC-Aktivität in den Marathonmäusen Anpassungen infolge der Langzeit-

Selektion auf hohe Laufleistung darstellen. Daraus ergab sich die Schlussfolgerung, dass die somatotrope Achse für eine verbesserte Ausdauerleistung nicht erforderlich ist bzw. für die Etablierung extremer Ausdauerleistung auf dem Laufband sogar unterdrückt werden muss.

iii) Modellierung der Stoffwechselwege im Muskel von Marathonmäusen

Die Energiebereitstellung während körperlicher Bewegung ist ATP-abhängig und seine Verfügbarkeit entscheidend für die kontraktile Aktivität der Skelettmuskulatur. Dabei wird ATP nicht nur für den Myofilament-Querbrücken-Zyklus (Myosin-ATPase) benötigt, sondern auch für Schlüsselenzyme, die Erregbarkeit der Membranen (Na+/K+ ATPase) sowie die Kalziumverarbeitung im sarkoplasmatischen Retikulum (Ca2+ATPase) [5]. Die dafür benötigten ATP-Moleküle stammen entweder aus der Phosphorylierung auf Substratebene (anaerob), welche Phosphokreatin und die Glykolyse, bei der hauptsächlich Glykogen zu Laktat verstoffwechselt wird, mit einschließt, oder aus der oxidativen Phosphorylierung von Kohlenhydraten und Fett (aerob), welche Signalwege wie die β-Oxidation, den Citratzyklus und die Atmungskette beinhaltet, die zum vollständigen Abbau zu CO_2 und H_2O führen [5,117,118]. Da die anaeroben Prozesse eine bessere Leistung (ATP-Produktionsrate), aber eine geringere Kapazität (insgesamt produziertes ATP) haben als die aeroben, dominieren die Phosphokreatin- und Laktatbildung bei kurzen, hochintensiven Belastungen und die aeroben Prozesse bei längerer Belastung [119]. Hier erzielt die Oxidation von Kohlenhydraten eine höhere Leistung und die der Fette eine höhere Kapazität. Unsere bisherigen Ergebnisse zu den selektionsbedingten Anpassungen in den Marathonmäusen rückten muskelwachstumsbedingte Anpassungen in den Hintergrund und stoffwechselbedingte in den Vordergrund. Deshalb wurden die Transkriptomdaten des Muskels im Zusammenhang mit dem Energiestoffwechsel betrachtet, um selektionsbedingte Anpassungen im kohlenhydrat- und lipidbasierten Energiestoffwechsel zu identifizieren und diese mit erhöhten Lipidumsatz im subkutanen Fettgewebe der Marathonmäuse in Verbindung zu bringen.

Die Beobachtungen, dass muskelwachstumsbedingte Anpassungen in der Langzeitselektionslinie DUhTP marginal sind, konnten durch histologische Untersuchungen des Muskelgewebes bestätigt werden, da kaum Unterschiede in den Muskelfasertypen beider Linien zu finden waren. Erst nach dem Training waren Veränderungen hinsichtlich des Muskelquerschnittes (kleiner), der Muskelfaseranzahl pro mm² (größer), der Anzahl der Mitochondrienreichen Fasern pro mm² (höher) und der Größe der mitochondrienarmen (weißen) Fasern (kleiner) zwischen beiden Linien zu beobachten. Zusätzlich konnte gezeigt werden, dass Enzym-Transkripte der Glykolyse, des Citratzyklus, der β-Oxidation und der Atmungskette vermehrt im Muskelgewebe von DUhTP-Mäusen vergleichend zu Kontrollmäusen exprimiert waren und durch dreiwöchiges Training noch weiter gesteigert werden konnten. Der Glykogenabbau war hingegen in inaktiven und trainierten Marathonmäusen herunterreguliert. Im Blut

der trainierten Tiere konnte mehr Glukose und Laktat in den DUC-Tieren und dafür mehr zirkulierende Lipide in den DUhTP-Mäusen detektiert werden. Da im Muskel der trainierten DUhTP-Mäuse mehr Glykogen, eine geringere Laktatdehydrogenase-Aktivität und eine gesteigerte Pyruvatdehydrogenase-Aktivität nachgewiesen werden konnte, stellten wir eine Hypothese zum Mechanismus der Energiebereitstellung in der Marathonmaus auf, der sich durch die Langzeitselektion muskulär manifestiert hat und die überragende Laufleistung des Tiermodells erklären kann. Als entscheidenden Faktor sahen wir die verminderte Aktivität der Laktatdehydrogenase, da dies eine erhöhte Laktatproduktion während des Ausdauertrainings verhindert und damit eine Laktat-vermittelte Lipolyse-Inhibition aussetzt und selektiv periphere Energie aus den Fettdepots bereitstellt [120,121]. Dieser Mechanismus verleiht der Marathonmaus zusammen mit weiteren Faktoren wie PGC1α [63] und TFEB [64], die durch Training höher als in Kontrollmäusen exprimiert sind, regulatorisch eine größere metabolische Flexibilität, um bei hochintensiven Belastungen gleichzeitig Glukose und Fettsäuren oxidativ zu verwerten.

3. Publikationsübergreifende Diskussion und Fazit

Übergeordnetes Ziel dieser Untersuchungen war es, Mechanismen zu identifizieren, die an der außerordentlichen Laufleistung der Marathonmäuse (DUhTP) und an der effizienten Substratbereitstellung / Energiebereitstellung beteiligt sein könnten. Dafür wurden zunächst DUhTP-Mäuse charakterisiert und mit der nicht selektierten Kontrolllinie DUC, die durch Zufallsverpaarung aus der gemeinsamen ursprünglichen Linie (Fzt:DU) hervorgegangen ist, verglichen. Wir konnten zeigen, dass sich aufgrund der jahrelangen paternalen Selektion Anpassungen in der Linie DUhTP manifestiert hatten. Da das Mausmodell nicht wie andere Modelle [70-72] durch vorheriges Training generiert wurde, sondern das einmalige hohe Ausdauerlaufvermögen der Väter nach der Anpaarung das Selektionsmerkmal zur Etablierung der Mauslinie DUhTP war, sind diese Anpassungen als genetisch fixiert zu betrachten. Interessanterweise unterscheidet sich das Langzeitselektionsmodell vom Kontrollmausmodell nicht durch strukturelle Anpassungen im Muskelgewebe *(2.3iii),* sondern durch metabolische Veränderungen im Muskel- *(2.3iii)*, Leber- *(2.1i)* und Subkutanfettgewebe *(2.2i, iii, iv)*. Wir konnten zeigen, dass die Muskeln der DUhTP-Mäuse ein stärkeres oxidatives Stoffwechselpotenzial besitzen als die Kontrollmäuse und dass sowohl in der Leber als auch im Subkutanfett der Lipidstoffwechsel dominiert und vermehrt Fette akkumuliert werden. Ohne einen physischen Reiz sind sowohl fettsynthetisierende als auch fettabbauende Enzyme im Subkutanfett von Marathonmäusen vermehrt exprimiert *(2.2i)*.

Allgemein ist das Subkutanfettgewebe der Marathonmäuse reich an Mitochondrien. Eine Bräunung des Fettes, begründet durch den Hämanteil (Komplex III, IV) in den Mitochondrien, ist schon mit bloßem Auge erkennbar sowie auf RNA- und Proteinebene nachweisbar und indiziert die Existenz von beigen Fettzellen im Subkutanfett der Tiere. Sowohl PGC1α als auch Irisin, welche mitochondriale Biogenese und damit Bräunung des Fettgewebes auslösen [40,84], sind vermehrt im Subkutanfettgewebe zu beobachten *(2.2iii).* Unsere Ergebnisse lassen den Schluss zu, dass aufgrund der jahrelangen Selektion beige Fettzellen im Subkutanfett der Marathonmaus vorhanden sind. Dies liegt darin begründet, dass vermehrt bräunungsauslösende Faktoren im Subkutanfett der Marathonmäuse gebildet werden (PGC1α, Irisin, UCP1), ohne einen äußeren Reiz.

Andere Studien zeigen vergleichbare Effekte erst nach Kälteexposition oder wiederholter körperlicher Aktivität [45,46]. Eine Kälteexposition kann dabei nicht völlig ausklammert werden, da die Tiere in unserer Maushaltung bei einer Temperatur von ca. 22,5 °C gehalten werden, einer Temperatur, die nicht thermoneutral (28-30 °C) ist. Bei Raumtemperaturen von 20 bzw. 22 °C muss man davon ausgehen, dass den Mäusen kalt ist und dass zusätzliche Energie aufgewendet werden muss, um die

Körpertemperatur konstant zu halten [102]. Allerdings werden beide Linien bei dieser niedrigeren Temperatur gehalten und nur die Linie DUhTP weist den beigen Fettphänotyp auf.

Infolge eines physischen Reizes (freiwillige Laufradbewegung, gezieltes Laufbandtraining) werden gespeicherte Lipide in den Fettdepots in der Linie DUhTP effizienter mobilisiert als in der Kontrolllinie DUC. Selbst wenn sich die Marathonmäuse freiwillig ähnlich oder weniger bewegen als die Kontrollmäuse, werden periphere Fettdepots stärker mobilisiert *(2.2i).* Bei DUhTP-Mäusen sind eine Reihe von energiestoffwechselrelevanten Anpassungen im Subkutanfett (erhöhte Werte von LCAD, PGC1α, TFAM, NDUFA9 und SIRT3 sowie mitochondriale Biogenese) beteiligt, um den hohen Energiebedarf bei körperlicher Aktivität zu decken und vorhandene Fettmasse auch bei vergleichsweise leichter körperlicher Betätigung für die Energiebereitstellung zu nutzen. Aber auch das Zusammenspiel zwischen zentralem und peripherem Gewebe ist von großer Bedeutung. Während die Skelettmuskulatur die eigentliche Bewegung realisiert, liefern Leber, Fettgewebe aber auch die Muskulatur Energieäquivalente, welche über das Blutsystem transportiert und am Zielort zur ATP-Produktion und somit zu den Muskelkontraktionen beitragen. Als Botenstoffe könnte unter anderem Irisin fungieren, welches aus dem Muskelgewebe in Folge von körperlicher Bewegung sezerniert und im Fettgewebe für die Umwandlung von lipidspeichernden weißen Adipozyten in energieverbrennende beigefarbene Adipozyten und somit für eine verbesserte Stoffwechselkontrolle durch die Induzierung von UCP1 im Fettgewebe verantwortlich sein soll. In DUhTP-Mäusen sind Irisin und auch UCP1 vermehrt nachzuweisen und deren Level können durch wiederholtes Training gesteigert werden *(2.2ii)*. Allerdings sei zu erwähnen, dass die Ergebnisse zu den Auswirkungen von körperlicher Betätigung auf zirkulierendes Irisin und damit verbunden auf das Fettzellbrowning nach wie vor umstritten sind (siehe Anmerkungen unter *2.2iii)*.

Als weiteres Signalmolekül kann Laktat verstanden werden [24], dessen Bildung durch die Laktatdehydrogenase katalysiert wird und in der Zirkulation als energiereiche Verbindung für oxidative Muskelfasern [20] oder andere laktatverbrauchende Organe wie Herz, Gehirn, Leber, Nieren und Fettgewebe [122] dient. Mit Hilfe der holistischen Transkriptomdaten aus Gewebe von trainierten und inaktiven DUhTP- und DUC-Mäusen konnte demonstriert werden, dass das wiederholte Training mit hoher Geschwindigkeit bei den Kontrollmäusen eher zu wachstumsfördernden Veränderungen wie die Steigerung der Proteinsynthese in der Hypophyse *(2.3i)* und des Muskelwachstums (höhere Aktivität von MAPK und Akt *(2.3ii)*, Transkripterhöhung von Muskelentwicklung und –differenzierung relevanten Faktoren Mef2c, Myod, Myl4 *(2.3iii)*) führt als bei den Marathonmäusen. Aufgrund der relativ hohen Trainingslaufgeschwindigkeit dominiert bei den DUC-Mäusen der anaerobe Stoffwechsel (höhere Laktatwerte, gesteigerte Laktatdehydrogenase- und Kreatinkinase-Aktivität), während bei den

DUhTP-Tieren der oxidative Stoffwechsel überwiegt *(2.3iii)*. Es konnte keine Erhöhung der Laktatkonzentrationen in den trainierten DUhTP-Mäusen, stattdessen aber vermehrt Lipidderivate im Blut feststellt werden, was wir mit der inhibierenden Wirkung von Laktat [121] auf die Lipolyse der peripheren Fettdepots erklären. In den Marathonmäusen ist aufgrund des wiederholten Trainings die Aktivität der Laktatdehydrogenase reduziert, wodurch die Laktatlevel im Blut nicht steigen und die Lipolyse nicht inhibiert wird. Als Konsequenz werden Fette mobilisiert, um im Muskel der Energiegewinnung zu dienen, was durch die erhöhten Plasma-Lipidkonzentrationen und erhöhte Transkriptlevel von Enzymen der β-Oxidation und Citratzyklus belegt werden kann. Da auch Transkripte der Glykolyse vermehrt exprimiert werden und die Aktivität der Pyruvatdehydrogenase erhöht ist, kann von einer gleichzeitigen oxidativen Verwertung von Glukose und Fettsäuren trotz der hohen Trainingsgeschwindigkeit ausgegangen werden, wodurch sowohl eine hohe ATP-Produktionsleistung (Glukoseoxidation) als auch eine hohe Kapazität (β-Oxidation) erzielt werden [119]. Daher kommen wir zu dem Schluss, dass durch die Regulation der Laktatdehydrogenase, aber auch PGC1α [63] und Pyruvatdehydrogenase, das Marathon-Mausmodell über eine hohe metabolische Flexibilität verfügt, welche Substrate effizient nutzt, um die außerordentliche Laufleistung der Marathonmäuse und die damit verbundene Energiebereitstellung zu ermöglichen. Damit ist das Marathon-Mausmodell für Forschungen hinsichtlich eines flexiblen und effizienten Energiestoffwechsels prädestiniert, welches Aufschluss darüber geben kann, wie gezielt der oxidative Stoffwechsel auf Ebene der Substraterkennung (hohe Enzymkonzentrationen im Muskel und Subkutanfettgewebe katalysieren sowohl katabole als auch anabole Stoffwechselwege), des Transports (Aufnahme von Substraten (Fette und Kohlenhydrate) in die Zellen bzw. Mitochondrien der Zelle), der Verwertung (hohe energetische Leistung durch oxidative Beiträge (Citratzyklus, β-Oxidation, Atmungskette)) und Speicherung (metabolisch aktive periphere Fettdepots mit hohem Gehalt an Mitochondrien, hepatische und muskuläre Glykogenspeicher) gesteuert werden kann und dabei die Gewebe (Muskel, Gehirn, Leber, Fett) im Crosstalk stehen.

4. Literaturverzeichnis

1. Vuori, I. Physical inactivity is a cause and physical activity is a remedy for major public health problems. *Kinesiology* **36**, 123-153 (2004).
2. RKI. Gesundheit in Deutschland aktuell. Vol. 2023 (2019/2020).
3. Hill, J.O., Wyatt, H.R. & Peters, J.C. Energy balance and obesity. *Circulation* **126**, 126-132 (2012).
4. Balady, G.J.*, et al.* Core Components of Cardiac Rehabilitation/Secondary Prevention Programs: 2007 Update. *Circulation* **115**, 2675-2682 (2007).
5. Hargreaves, M. & Spriet, L.L. Skeletal muscle energy metabolism during exercise. *Nat Metab* **2**, 817-828 (2020).
6. Spencer, M.R. & Gastin, P.B. Energy system contribution during 200- to 1500-m running in highly trained athletes. *Med Sci Sports Exerc* **33**, 157-162 (2001).
7. Soderlund, K. & Hultman, E. ATP and phosphocreatine changes in single human muscle fibers after intense electrical stimulation. *Am J Physiol* **261**, E737-741 (1991).
8. Parolin, M.L.*, et al.* Regulation of skeletal muscle glycogen phosphorylase and PDH during maximal intermittent exercise. *Am J Physiol* **277**, E890-900 (1999).
9. Medbo, J.I. & Tabata, I. Relative importance of aerobic and anaerobic energy release during short-lasting exhausting bicycle exercise. *J Appl Physiol (1985)* **67**, 1881-1886 (1989).
10. Ørtenblad, N., Westerblad, H. & Nielsen, J. Muscle glycogen stores and fatigue. *The Journal of Physiology* **591**, 4405-4413 (2013).
11. Nielsen, J. & Ørtenblad, N. Physiological aspects of the subcellular localization of glycogen in skeletal muscle. *Applied Physiology, Nutrition, and Metabolism* **38**, 91-99 (2013).
12. Hickner, R.C.*, et al.* Muscle glycogen accumulation after endurance exercise in trained and untrained individuals. *Journal of Applied Physiology* **83**, 897-903 (1997).
13. Roach, P.J. Glycogen and its Metabolism. *Current Molecular Medicine* **2**, 101-120 (2002).
14. Ryder, J.W., Chibalin, A.V. & Zierath, J.R. Intracellular mechanisms underlying increases in glucose uptake in response to insulin or exercise in skeletal muscle. *Acta Physiol Scand* **171**, 249-257 (2001).
15. Holloszy, J.O., Kohrt, W.M. & Hansen, P.A. The regulation of carbohydrate and fat metabolism during and after exercise. *Front Biosci* **3**, D1011-1027 (1998).
16. Brooks, G.A. Cell-cell and intracellular lactate shuttles. *J Physiol* **587**, 5591-5600 (2009).
17. Brooks, G.A. Lactate shuttles in nature. *Biochem Soc Trans* **30**, 258-264 (2002).
18. Brooks, G.A. Lactate:Glycolytic End Product and Oxidative Substrate During Sustained Exercise in Mammals — The "Lactate Shuttle". in *Circulation, Respiration, and Metabolism* (ed. Gilles, R.) 208-218 (Springer Berlin Heidelberg, Berlin, Heidelberg, 1985).
19. Adijanto, J. & Philp, N.J. The SLC16A family of monocarboxylate transporters (MCTs)--physiology and function in cellular metabolism, pH homeostasis, and fluid transport. *Curr Top Membr* **70**, 275-311 (2012).
20. Kitaoka, Y., Hoshino, D. & Hatta, H. Monocarboxylate transporter and lactate metabolism. *The Journal of Physical Fitness and Sports Medicine* **1**, 247-252 (2012).
21. GLADDEN, L.B. Muscle as a consumer of lactate. *Medicine & Science in Sports & Exercise* **32**, 764-771 (2000).
22. Pascoe, D.D. & Gladden, L.B. Muscle Glycogen Resynthesis after Short Term, High Intensity Exercise and Resistance Exercise. *Sports Medicine* **21**, 98-118 (1996).
23. Stanley, W.C.*, et al.* Lactate extraction during net lactate release in legs of humans during exercise. *J Appl Physiol (1985)* **60**, 1116-1120 (1986).
24. Brooks, G.A. The Science and Translation of Lactate Shuttle Theory. *Cell Metab* **27**, 757-785 (2018).

25. Faude, O., Kindermann, W. & Meyer, T. Lactate threshold concepts: how valid are they? *Sports Med* **39**, 469-490 (2009).
26. Svedahl, K. & MacIntosh, B.R. Anaerobic threshold: the concept and methods of measurement. *Can J Appl Physiol* **28**, 299-323 (2003).
27. Herzig, S.*, et al.* Identification and functional expression of the mitochondrial pyruvate carrier. *Science* **337**, 93-96 (2012).
28. Dubouchaud, H., Butterfield, G.E., Wolfel, E.E., Bergman, B.C. & Brooks, G.A. Endurance training, expression, and physiology of LDH, MCT1, and MCT4 in human skeletal muscle. *Am J Physiol Endocrinol Metab* **278**, E571-579 (2000).
29. Jacobs, R.A., Meinild, A.-K., Nordsborg, N.B. & Lundby, C. Lactate oxidation in human skeletal muscle mitochondria. *American Journal of Physiology-Endocrinology and Metabolism* **304**, E686-E694 (2013).
30. Koonen, D.P., Glatz, J.F., Bonen, A. & Luiken, J.J. Long-chain fatty acid uptake and FAT/CD36 translocation in heart and skeletal muscle. *Biochim Biophys Acta* **1736**, 163-180 (2005).
31. Chen, Y., Zhang, J., Cui, W. & Silverstein, R.L. CD36, a signaling receptor and fatty acid transporter that regulates immune cell metabolism and fate. *Journal of Experimental Medicine* **219**(2022).
32. Cinti, S. The Adipose Tissue. in *Adipose Tissue and Adipokines in Health and Disease*, Vol. I (ed. Fantuzzi, G.M., T.) 3-19 (Humana Press, 2007).
33. Forner, F.*, et al.* Proteome Differences between Brown and White Fat Mitochondria Reveal Specialized Metabolic Functions. *Cell Metabolism* **10**, 324-335 (2009).
34. Nascimento, C.M.O.d., Ribeiro, E.B. & Oyama, L.M. Metabolism and secretory function of white adipose tissue: effect of dietary fat. *Anais da Academia Brasileira de Ciências* **81**(2009).
35. Denechaud, P.D., Girard, J. & Postic, C. Carbohydrate responsive element binding protein and lipid homeostasis. *Curr Opin Lipidol* **19**, 301-306 (2008).
36. Cedikova, M.*, et al.* Mitochondria in White, Brown, and Beige Adipocytes. *Stem Cells International* **2016**, 6067349 (2016).
37. Matthias, A.*, et al.* Thermogenic responses in brown fat cells are fully UCP1-dependent. UCP2 or UCP3 do not substitute for UCP1 in adrenergically or fatty scid-induced thermogenesis. *J Biol Chem* **275**, 25073-25081 (2000).
38. Murano, I., Barbatelli, G., Giordano, A. & Cinti, S. Noradrenergic parenchymal nerve fiber branching after cold acclimatisation correlates with brown adipocyte density in mouse adipose organ. *J Anat* **214**, 171-178 (2009).
39. Ringholm, S.*, et al.* PGC-1alpha is required for exercise- and exercise training-induced UCP1 up-regulation in mouse white adipose tissue. *PLoS. One* **8**, e64123 (2013).
40. Wu, Z.*, et al.* Mechanisms controlling mitochondrial biogenesis and respiration through the thermogenic coactivator PGC-1. *Cell* **98**, 115-124 (1999).
41. Liang, H. & Ward, W.F. PGC-1alpha: a key regulator of energy metabolism. *Adv Physiol Educ* **30**, 145-151 (2006).
42. Sutherland, L.N., Bomhof, M.R., Capozzi, L.C., Basaraba, S.A. & Wright, D.C. Exercise and adrenaline increase PGC-1{alpha} mRNA expression in rat adipose tissue. *J Physiol* **587**, 1607-1617 (2009).
43. Baar, K.*, et al.* Adaptations of skeletal muscle to exercise: rapid increase in the transcriptional coactivator PGC-1. *The FASEB Journal* **16**, 1879-1886 (2002).
44. Ruas, J.L.*, et al.* A PGC-1alpha isoform induced by resistance training regulates skeletal muscle hypertrophy. *Cell* **151**, 1319-1331 (2012).
45. Stanford, K.I., Middelbeek, R.J. & Goodyear, L.J. Exercise Effects on White Adipose Tissue: Beiging and Metabolic Adaptations. *Diabetes* **64**, 2361-2368 (2015).
46. Chung, N., Park, J. & Lim, K. The effects of exercise and cold exposure on mitochondrial biogenesis in skeletal muscle and white adipose tissue. *J Exerc Nutrition Biochem* **21**, 39-47 (2017).

47. Lin, J.*, et al.* Transcriptional co-activator PGC-1 alpha drives the formation of slow-twitch muscle fibres. *Nature* **418**, 797-801 (2002).
48. Handschin, C.*, et al.* Skeletal muscle fiber-type switching, exercise intolerance, and myopathy in PGC-1alpha muscle-specific knock-out animals. *J Biol Chem* **282**, 30014-30021 (2007).
49. Kruszynska, Y.T., Ciaraldi, T.P. & Henry, R.R. Regulation of Glucose Metabolism in Skeletal Muscle. in *Comprehensive Physiology* 579-607.
50. Jeukendrup, A.E. Regulation of fat metabolism in skeletal muscle. *Ann N Y Acad Sci* **967**, 217-235 (2002).
51. Ahlborg, G., Felig, P., Hagenfeldt, L., Hendler, R. & Wahren, J. Substrate Turnover during Prolonged Exercise in Man: SPLANCHNIC AND LEG METABOLISM OF GLUCOSE, FREE FATTY ACIDS, AND AMINO ACIDS. *The Journal of Clinical Investigation* **53**, 1080-1090 (1974).
52. Achten, J., Gleeson, M. & Jeukendrup, A.E. Determination of the exercise intensity that elicits maximal fat oxidation. *Medicine & Science in Sports & Exercise* **34**(2002).
53. O'Brien, M.J., Viguie, C.A., Mazzeo, R.S. & Brooks, G.A. Carbohydrate dependence during marathon running. *Med Sci Sports Exerc* **25**, 1009-1017 (1993).
54. Smith, R.L., Soeters, M.R., Wüst, R.C.I. & Houtkooper, R.H. Metabolic Flexibility as an Adaptation to Energy Resources and Requirements in Health and Disease. *Endocrine Reviews* **39**, 489-517 (2018).
55. Goodpaster, B.H. & Sparks, L.M. Metabolic Flexibility in Health and Disease. *Cell Metab* **25**, 1027-1036 (2017).
56. Palmer, B.F. & Clegg, D.J. Metabolic Flexibility and Its Impact on Health Outcomes. *Mayo Clinic Proceedings* **97**, 761-776 (2022).
57. Muoio, Deborah M. Metabolic Inflexibility: When Mitochondrial Indecision Leads to Metabolic Gridlock. *Cell* **159**, 1253-1262 (2014).
58. Obre, E. & Rossignol, R. Emerging concepts in bioenergetics and cancer research: metabolic flexibility, coupling, symbiosis, switch, oxidative tumors, metabolic remodeling, signaling and bioenergetic therapy. *Int J Biochem Cell Biol* **59**, 167-181 (2015).
59. Frayn, K.N. Adipose tissue as a buffer for daily lipid flux. *Diabetologia* **45**, 1201-1210 (2002).
60. Prior, S.J., Ryan, A.S., Stevenson, T.G. & Goldberg, A.P. Metabolic inflexibility during submaximal aerobic exercise is associated with glucose intolerance in obese older adults. *Obesity* **22**, 451-457 (2014).
61. Yang, W.-H., Park, J.-H., Park, S.-Y. & Park, Y. Energetic contributions including gender differences and metabolic flexibility in the general population and athletes. *Metabolites* **12**, 965 (2022).
62. Prins, P.*, et al.* High fat diet improves metabolic flexibility during progressive exercise to exhaustion (VO2max testing) and during 5km running time trials. *Biology of Sport* **40**, 465-475 (2023).
63. Storlien, L., Oakes, N.D. & Kelley, D.E. Metabolic flexibility. *Proceedings of the Nutrition Society* **63**, 363-368 (2004).
64. Mansueto, G.*, et al.* Transcription Factor EB Controls Metabolic Flexibility during Exercise. *Cell Metabolism* **25**, 182-196 (2017).
65. Lira, V.A., Benton, C.R., Yan, Z. & Bonen, A. PGC-1α regulation by exercise training and its influences on muscle function and insulin sensitivity. *American Journal of Physiology-Endocrinology and Metabolism* **299**, E145-E161 (2010).
66. Perry, C.G.R.*, et al.* Repeated transient mRNA bursts precede increases in transcriptional and mitochondrial proteins during training in human skeletal muscle. *The Journal of Physiology* **588**, 4795-4810 (2010).
67. Erlich, A.T., Brownlee, D.M., Beyfuss, K. & Hood, D.A. Exercise induces TFEB expression and activity in skeletal muscle in a PGC-1α-dependent manner. *Am J Physiol Cell Physiol* **314**, C62-c72 (2018).

68. Massett, M.P. & Berk, B.C. Strain-dependent differences in responses to exercise training in inbred and hybrid mice. *Am J Physiol Regul Integr Comp Physiol* **288**, R1006-1013 (2005).
69. Houle-Leroy, P., Garland, T., Jr., Swallow, J.G. & Guderley, H. Effects of voluntary activity and genetic selection on muscle metabolic capacities in house mice Mus domesticus. *J Appl Physiol (1985)* **89**, 1608-1616 (2000).
70. Swallow, J.G., Carter, P.A. & Garland, T., Jr. Artificial selection for increased wheel-running behavior in house mice. *Behav Genet* **28**, 227-237 (1998).
71. Koch, L.G., Pollott, G.E. & Britton, S.L. Selectively bred rat model system for low and high response to exercise training. *Physiol Genomics* **45**, 606-614 (2013).
72. Koch, L.G. & Britton, S.L. Divergent selection for aerobic capacity in rats as a model for complex disease. *Integrative and Comparative Biology* **45**, 405-415 (2005).
73. Falkenberg, H., Langhammer, M. & Renne, U. Comparison of biochemical blood traits after long-term selection on high or low locomotory activity in mice. *Arch. Anim. Breed.* **43**, 513-522 (2000).
74. Petkov, S., Brenmoehl, J., Langhammer, M., Hoeflich, A. & Röntgen, M. Myogenic Precursor Cells Show Faster Activation and Enhanced Differentiation in a Male Mouse Model Selected for Advanced Endurance Exercise Performance. *Cells* **11**(2022).
75. Dietl, G., Langhammer, M. & Renne, U. Model simulations for genetic random drift in the outbred strain Fzt : DU. *Archiv Fur Tierzucht-Archives of Animal Breeding* **47**, 595-604 (2004).
76. Renne, U., Bunger, L. & Schuler, L. Experimentelle Untersuchungen an Labormäusen zur Selektions auf Belastbarkeit - Belastbarkeitskonzept und Versuchsdurchführung. *Arch. Tierz. Berlin* **27**, 453-463 (1984).
77. Brenmoehl, J*., et al.* Metabolic adaptations in the liver of born long-distance running mice. *Med Sci Sports Exerc* **45**, 841-850 (2013).
78. Brenmoehl, J*., et al.* Partial phenotype conversion and differential trait response to conditions of husbandry in mice. *J Comp Physiol B* **188**, 527-539 (2018).
79. Avila, J.J., Kim, S.K. & Massett, M.P. Differences in Exercise Capacity and Responses to Training in 24 Inbred Mouse Strains. *Frontiers in Physiology* **8**(2017).
80. Rui, L. Energy metabolism in the liver. *Compr Physiol* **4**, 177-197 (2014).
81. Dulioust, E*., et al.* Long-term effects of embryo freezing in mice. *Proc Natl Acad Sci U S A* **92**, 589-593 (1995).
82. Wennerholm, U.B*., et al.* Postnatal growth and health in children born after cryopreservation as embryos. *Lancet* **351**, 1085-1090 (1998).
83. Trevellin, E*., et al.* Exercise training induces mitochondrial biogenesis and glucose uptake in subcutaneous adipose tissue through eNOS-dependent mechanisms. *Diabetes* **63**, 2800-2811 (2014).
84. Boström, P*., et al.* A PGC1-α-dependent myokine that drives brown-fat-like development of white fat and thermogenesis. *Nature* **481**, 463-468 (2012).
85. Roca-Rivada, A*., et al.* FNDC5/Irisin Is Not Only a Myokine but Also an Adipokine. *PLOS ONE* **8**, e60563 (2013).
86. Brenmoehl, J*., et al.* Dynamics of Fat Mass in DUhTP Mice Selected for Running Performance - Fat Mobilization in a Walk. *Obes Facts* **8**, 373-385 (2015).
87. Zhang, Y*., et al.* Irisin stimulates browning of white adipocytes through mitogen-activated protein kinase p38 MAP kinase and ERK MAP kinase signaling. *Diabetes* **63**, 514-525 (2014).
88. Huh, J.Y., Dincer, F., Mesfum, E. & Mantzoros, C.S. Irisin stimulates muscle growth-related genes and regulates adipocyte differentiation and metabolism in humans. *Int J Obes (Lond)* **38**, 1538-1544 (2014).
89. Lee, P*., et al.* Irisin and FGF21 are cold-induced endocrine activators of brown fat function in humans. *Cell Metab* **19**, 302-309 (2014).

90. Zhang, Y.*, et al.* Irisin exerts dual effects on browning and adipogenesis of human white adipocytes. *American Journal of Physiology-Endocrinology and Metabolism* **311**, E530-E541 (2016).
91. Brenmoehl, J.*, et al.* Irisin is elevated in skeletal muscle and serum of mice immediately after acute exercise. *Int J Biol Sci* **10**, 338-349 (2014).
92. Dinas, P.C.*, et al.* Effects of physical activity on the link between PGC-1a and FNDC5 in muscle, circulating Irisin and UCP1 of white adipocytes in humans: A systematic review. *F1000Res* **6**, 286 (2017).
93. Maak, S., Norheim, F., Drevon, C.A. & Erickson, H.P. Progress and Challenges in the Biology of FNDC5 and Irisin. *Endocrine Reviews* **42**, 436-456 (2021).
94. Albrecht, E.*, et al.* Irisin - a myth rather than an exercise-inducible myokine. *Sci Rep* **5**, 8889 (2015).
95. Erickson, H.P. Irisin and FNDC5 in retrospect. *Adipocyte* **2**, 289-293 (2013).
96. Raschke, S.*, et al.* Evidence against a beneficial effect of irisin in humans. *PLoS One* **8**, e73680 (2013).
97. Witmer, N.H., Linzer, C.R. & Boudreau, R.L. Fndc5 is translated from an upstream ATG start codon and cleaved to produce irisin myokine precursor protein in humans and mice. *Cell Metab* (2024).
98. Lee, P.*, et al.* Irisin and FGF21 Are Cold-Induced Endocrine Activators of Brown Fat Function in Humans. *Cell Metabolism* **19**, 302-309 (2014).
99. Stengel, A.*, et al.* Circulating levels of irisin in patients with anorexia nervosa and different stages of obesity – Correlation with body mass index. *Peptides* **39**, 125-130 (2013).
100. Kim, H.*, et al.* Irisin Mediates Effects on Bone and Fat via αV Integrin Receptors. *Cell* **175**, 1756-1768.e1717 (2018).
101. Elsen, M., Raschke, S. & Eckel, J. Browning of white fat: does irisin play a role in humans? *J Endocrinol* **222**, R25-38 (2014).
102. Harms, M. & Seale, P. Brown and beige fat: development, function and therapeutic potential. *Nature Medicine* **19**, 1252-1263 (2013).
103. Khajehnasiri, N., Khazali, H. & Sheikhzadeh, F. Various responses of male pituitary-gonadal axis to different intensities of long-term exercise: Role of expression of KNDYrelated genes. *J Biosci* **43**, 569-574 (2018).
104. Sze, Y., Gill, A.C. & Brunton, P.J. Sex-dependent changes in neuroactive steroid concentrations in the rat brain following acute swim stress. *J Neuroendocrinol* **30**, e12644 (2018).
105. Uribe, R.M.*, et al.* Voluntary exercise adapts the hypothalamus-pituitary-thyroid axis in male rats. *Endocrinology* **155**, 2020-2030 (2014).
106. Fortunato, R.S.*, et al.* The effect of acute exercise session on thyroid hormone economy in rats. *Journal of Endocrinology* **198**, 347-353 (2008).
107. Sutton, J. & Lazarus, L. Growth hormone in exercise: comparison of physiological and pharmacological stimuli. *J Appl Physiol* **41**, 523-527 (1976).
108. Kraemer, W.J.*, et al.* Resistance exercise induces region-specific adaptations in anterior pituitary gland structure and function in rats. *Journal of Applied Physiology* **115**, 1641-1647 (2013).
109. Ma, Z., Qi, J., Meng, S., Wen, B. & Zhang, J. Swimming exercise training-induced left ventricular hypertrophy involves microRNAs and synergistic regulation of the PI3K/AKT/mTOR signaling pathway. *Eur J Appl Physiol* **113**, 2473-2486 (2013).
110. Massett, M.P., Fan, R. & Berk, B.C. Quantitative trait loci for exercise training responses in FVB/NJ and C57BL/6J mice. *Physiol Genomics* **40**, 15-22 (2009).
111. Müller, E.E., Locatelli, V. & Cocchi, D. Neuroendocrine Control of Growth Hormone Secretion. *Physiological Reviews* **79**, 511-607 (1999).
112. Møller, N. & Jørgensen, J.O.L. Effects of Growth Hormone on Glucose, Lipid, and Protein Metabolism in Human Subjects. *Endocrine Reviews* **30**, 152-177 (2009).

113. Roth, J., Glick, S.M., Yalow, R.S. & Berson, S.A. Secretion of human growth hormone: physiologic and experimental modification. *Metabolism* **12**, 577-579 (1963).
114. Velloso, C.P. Regulation of muscle mass by growth hormone and IGF-I. *British Journal of Pharmacology* **154**, 557-568 (2008).
115. Hresko, R.C. & Mueckler, M. mTOR.RICTOR is the Ser473 kinase for Akt/protein kinase B in 3T3-L1 adipocytes. *J Biol Chem* **280**, 40406-40416 (2005).
116. Magnuson, B., Ekim, B. & Fingar, D.C. Regulation and function of ribosomal protein S6 kinase (S6K) within mTOR signalling networks. *Biochem J* **441**, 1-21 (2012).
117. Hawley, J.A., Hargreaves, M., Joyner, M.J. & Zierath, J.R. Integrative biology of exercise. *Cell* **159**, 738-749 (2014).
118. Parolin, M.L.*, et al.* Regulation of skeletal muscle glycogen phosphorylase and PDH during maximal intermittent exercise. *American Journal of Physiology-Endocrinology and Metabolism* **277**, E890-E900 (1999).
119. Sahlin, K., Tonkonogi, M. & Soderlund, K. Energy supply and muscle fatigue in humans. *Acta Physiol Scand* **162**, 261-266 (1998).
120. Ahmed, K.*, et al.* An autocrine lactate loop mediates insulin-dependent inhibition of lipolysis through GPR81. *Cell Metab* **11**, 311-319 (2010).
121. Liu, C.*, et al.* Lactate inhibits lipolysis in fat cells through activation of an orphan G-protein-coupled receptor, GPR81. *J Biol Chem* **284**, 2811-2822 (2009).
122. Brooks, G.A. Lactate as a fulcrum of metabolism. *Redox Biol* **35**, 101454 (2020).

5. Anhang - Originalarbeiten in Erstautorenschaft für die kumulative Habilitationsschrift

5.1 Publikationen zum Marathon-Mausmodell

i) **Brenmoehl, J.**, Walz, C., Renne, U., Ponsuksili, S; Wolf, C., Langhammer, M., Schwerin, M., Hoeflich, A. (2013). Metabolic adaptations in the liver of born long-distance running mice. *Med Sci Sports Exerc., 45:841-50. doi: 10.1249/MSS.0b013e31827e0fca.*

Geleisteter Eigenanteil: Labortätigkeiten (Western Blots, quantitative real-time (qRT-)PCR), Auswertung und Darstellung der Daten sowie Schreiben des Manuskriptes (Teile).

ii) **Brenmoehl, J.**, Walz, C., Spitschak, M., Wirthgen, E., Walz, M., Langhammer, M., Tuchscherer, A., Naumann, R., Hoeflich, A. (2018). Partial phenotype conversion and differential trait response to conditions of husbandry in mice. *J Comp Physiol B., 188:527-539. doi: 10.1007/s00360-017-1138-x.*

Geleisteter Eigenanteil: Projekt- und Tierversuchsplanung, Phänotypische Erhebungen (Sektion, Gewebeentnahme und -wiegung), Auswerten und Darstellung der Daten sowie Schreiben des Manuskriptes.

Metabolic Adaptations in the Liver of Born Long-Distance Running Mice

JULIA BRENMOEHL[1], CHRISTINA WALZ[1], ULLA RENNE[1], SIRILUCK PONSUKSILI[2], CAROLA WOLF[3], MARTINA LANGHAMMER[1], MANFRED SCHWERIN[2,4], and ANDREAS HOEFLICH[1]

[1]*Research Unit of Genetics and Biometry, Leibniz-Institute for Farm Animal Biology, Dummerstorf, GERMANY;*
[2]*Research Group Functional Genomics, Leibniz-Institute for Farm Animal Biology, Dummerstorf, GERMANY;*
[3]*State Offices for Agriculture, Food Safety and Fishery Mecklenburg–Vorpommern, Rostock, GERMANY; and*
[4]*Institute of Farm Animal Sciences and Technology, University of Rostock, Rostock, GERMANY*

ABSTRACT

BRENMOEHL, J., C. WALZ, U. RENNE, S. PONSUKSILI, C. WOLF, M. LANGHAMMER, M. SCHWERIN, and A. HOEFLICH. Metabolic Adaptations in the Liver of Born Long-Distance Running Mice. *Med. Sci. Sports Exerc.*, Vol. 45, No. 5, pp. 841–850, 2013. **Purpose**: Long-distance runners have increased needs of energy supply. To unravel genetically based mechanisms required for efficient energy supply, we have analyzed hepatic metabolism of mice characterized by the inborn capacity to perform as long-distance runners. **Methods**: The mouse model had been established by phenotypic selection for high treadmill performance for 90 generations and was characterized by approximately 3.8-fold higher running capacities (Dummerstorf high Treadmill Performance mouse line [DUhTP]) compared with unselected and also untrained controls (Dummerstorf Control mouse line [DUC]). From 7-wk-old male mice, serum and liver samples were collected and analyzed for messenger RNA, protein, and metabolite levels, respectively. **Results**: In livers from DUhTP mice, we identified significantly higher messenger RNA transcript levels of peroxisome proliferator–activated receptor delta and higher protein levels of sirtuin-1, acetyl-CoA-synthetase, acetyl-CoA-carboxylase, phosphoenolpyruvate carboxykinase, and glutamate-dehydrogenase, suggesting higher gluconeogenesis and lipogenesis in DUhTP mice. In fact, higher hepatic levels of glycogen and triglycerides as well as higher concentrations of carbohydrate, fatty acid, and cholesterol metabolites were found in DUhTP mice. In parallel, in DUhTP mice, which did not have access to running wheels, a marked hyperlipidemia (cholesterol = 160% ± 8%, triglycerides = 174% ± 14% of controls, respectively), and abdominal obesity (DUhTP = 0.396 ± 0.019 g, DUC = 0.291 ± 0.019 g) were found. **Conclusions**: From our data, we conclude that the physiological basis of genetically fixed higher endurance-running performance in DUhTP marathon mouse is related to increased hepatic gluconeogenesis and lipogenesis. Expression of sirtuin 1 as well as of gluconeogenic and lipogenic key enzymes may be related to peroxisome proliferator–activated receptor delta. Metabolic adaptations presented in our study represent inborn features of superior endurance-running performance. **Key Words:** PPAR DELTA, SIRTUIN 1, LIVER, METABOLISM, GLUCONEOGENESIS, LIPOGENESIS

BASIC SCIENCES

Physical fitness is dependent on the state of training and genetic predisposition (21,32). Both genetic and physiological factors involved in physical performance had been studied in long-term selected mouse lines bred for "high running wheel activity" (49). This model had been established by selection for increased voluntary "running wheel behavior," including a 6-d period of access to running wheels using Hsd:ICR mice. To address the genetic effects associated with inborn extreme physical performance as a "long-distance runner," we have established the Dummerstorf high Treadmill Performance mouse line (DUhTP) mouse model by phenotype selection for high treadmill performance for 90 generations using a singular submaximal endurance test on day 70 of life (13). This mouse model was developed in the absence of running wheels.

Physical fitness is intricately related to energy metabolism, and an important source of energy for working muscles during endurance exercise is constituted by endogenous triglycerides (35). In fact, a recent contribution in the field has identified higher lipid oxidation particularly in one "high running mouse line" characterized by 50% reduction in hindlimb muscle mass and a markedly elevated capacity of muscles for the uptake and transport of fatty acid (54). As evolutionary highly conserved tools of energy metabolism and supply, the family of peroxisome proliferator–activated receptor (PPAR) has important functions for lipid mobilization, transport, and catabolism (2,56). To date, three family members (PPAR alpha, delta, and gamma) have been identified with established or suggested functions in liver, muscle, or adipose tissues (2). Wang et al. (55) postulated a central role of PPAR delta in promotion of endurance exercise. Furthermore, PPAR delta directly or indirectly regulates fatty acid metabolism (53) and cholesterol efflux (37). In addition to the effects on lipid metabolism, gene expression of *Ppard* in the liver as effectors

Address for correspondence: Prof. Dr. Manfred Schwerin, Leibniz-Institute for Farm Animal Biology, Dummerstorf Wilhelm-Stahl-Allee 2 18196, Dummerstorf, Germany; E-mail: schwerin@fbn-dummerstorf.de.
Submitted for publication February 2012.
Accepted for publication November 2012.

0195-9131/13/4505-0841/0
MEDICINE & SCIENCE IN SPORTS & EXERCISE®

DOI: 10.1249/MSS.0b013e31827e0fca

of stress and metabolic adaptation were determined. As one of the direct targets of PPAR delta (36), also sirtuin 1 has been assessed in the liver from DUhTP mice. Interestingly, sirtuin 1 represents an evolutionary conserved NAD^+ deacetylase and has also been considered as a potent effector of metabolism (6). We thus have asked if altered PPAR delta and sirtuin 1 expression correlates with specific adaptations of liver metabolism in DUhTP mice. Expression of PPAR and sirtuins in the liver is discussed in the context of metabolic adaptions and expression of metabolic key enzymes in the liver.

MATERIALS AND METHODS

Animals and Treadmill Performance

Genetic background of animals and selection procedure. *In vivo* experiments were approved by an institutional review board. All procedures adhered to the American College of Sports Medicine animal care standards. The Dummerstorf mouse lines were originally derived by systematic crossbreeding of four inbred (CBA/Bln, AB/Bln, C57BL/Bln, and XVII/Bln) and four outbred (NMRI orig., Han:NMRI, CFW, and CF1) lines (10,45). From this genetic pool (FztDU), the mouse line DUhTP used in the present study has been generated by selection for 90 generations for high treadmill performance (13). The control line Dummerstorf Control mouse line (DUC) had been established from the same base population by random breeding. Both mouse lines were kept in the absence of running wheels. The experimental design of the long-term selected mouse line DUhTP and the related control line DUC is shown in Table 1. Before the running experiments started, 80 matings were performed. These families were used for phenotype selection and thus for the establishment of the following generation depending on the results from the running experiment later. By this strategy, a direct effect of physical performance itself on breeding performance was excluded. In each generation, the selection trait high treadmill performance was measured in 70-d-old male mice. The offspring of males with the highest running performance on the treadmill was chosen for further selection, applying a selection intensity of 44% in DUhTP mice (Table 1). Therefore, on the basis of paternal performance progeny, 35 families originating from 80 crossings were used for further mating minimizing inbreeding. To enhance the speed of the selection process, male mice were chosen because reproduction is faster in males than that in females. The endurance fitness was recorded as running distance in meters on a treadmill. The treadmill performance was determined by a singular submaximal test with a start speed of 12 $m \cdot min^{-1}$ and a final speed of 38 $m \cdot min^{-1}$. As soon as the first 30 m were accomplished, the speed was increased to 22 $m \cdot min^{-1}$. Then, after 50 m, respectively, the speed was further increased to 26, 30, 34, and 38 $m \cdot min^{-1}$. Test termination was a function of the run discontinuity. The test stop depends on remaining the mice on the stimulating equipment of the treadmill. Because of technical problems with the treadmill, the selection trait could not be measured in the generation number 36, 38–46, and 79, respectively. In that time, random mating without any selection procedure was performed in both mouse lines. Thus, in the entire period of selection experiment, 79 generations received the selection. The result of selection is a mouse population with a 3.8-fold and significantly higher running capacity compared with the mean treadmill performance in the control line. The selection trait is characterized by a high variability among the individuals per generation and the mean running performance in the different generations too. For that reason, a genetic plateau is not yet reached, and the selection response could be described with a linear slope (Fig. 1).

Husbandry

The animals were housed in Makrolon-cages Type II (EBECO, Castrop-Rauxel, Germany) in a semibarrier system under environmentally controlled conditions with a 12-h light–12-h dark cycle (room temperature = 22.5°C ± 0.2°C, humidity = 50%–60%). Fresh tap water and fixed formula food for laboratory mice was supplied *ad libitum* (Altromin® 1314 : protein, 22.5%; fat, 5%; raw fiber, 4.5%; ash, 6.5%; germ reduced by heat during the production process; Altromin GmbH, Lage, Germany). Food consumption was monitored as described previously (9) during 50 d in 3- to 10-wk mice of both genetic groups (n = 20). Analysis of physical activity was assessed by including running wheels (d = 33.4 cm) equipped with wheel counters (Tecniplast, Hohenpeisenberg, Germany) in their home cages for a period of 3 wk in 7- to 10-wk male DUhTP mice and controls. Total lean body mass

TABLE 1. Experimental design and selection response in mice long-term selected for high treadmill performance (DUhTP) and in unselected controls.

Mouse Lines	DUhTP	DUC
Length of the experiment (gen)	0–90	0–90
Selection trait	High treadmill performance at day 70	None
Selection procedure	Paternal performance test	Random mating
Litter size standardization at birth	4M, 4F	4M, 4F
Pairs/generation with mating ratio (1M/1F)	60–100	60–100
Effective population size in gen 0	200	200
Successful matings (%)	87.2	89.8
Selection intensity (%)	44.0	41.1
Running performance at gen 0 (m)	1082 ± 107	1229 ± 187
Running performance at gen 90 (m)	3778 ± 591*	1003 ± 172
Selection response at gen 90 (%)	+249	−18

Values are presented as mean ± SE. DUhTP gen 0, n = 92; DUhTP gen 90, n = 75; DUC gen 0, n = 50; DUC gen 90, n = 90. gen, generation; M, male; F, female.
*$P < 0.0001$ if compared with DUC.

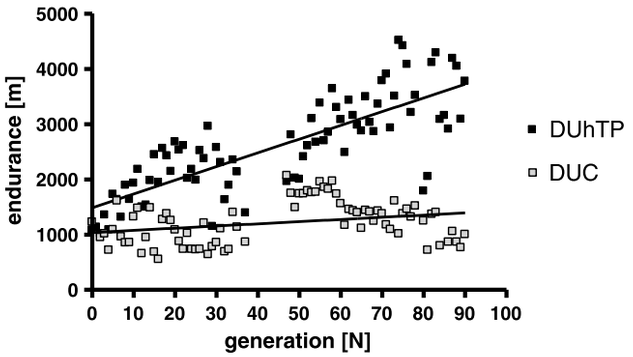

FIGURE 1—Selection response for endurance-running distance in DUhTP mice and in nonselected controls (DUC). After a period of 90 generations, long-term selection for high treadmill performance resulted in a nearly 3.8-fold higher and linear development of endurance-running distance in line DUhTP compared with line DUC. Values are presented as the mean per generation and the linear functions $y = 1487.3 + 24.83x$ for the line DUhTP and $y = 1037.2 + 3.95x$ for the control line DUC describe the selection response of the endurance fitness.

was quantified by dual energy x-ray absorptiometry (Lunar PIXImus II; GE Medical Systems, Solingen, Germany).

In this experiment, the endurance fitness was measured in 49-d-old juvenile male mice (n = 10) by use of a "computer controlled treadmill." For the analyses, overnight fasted animals were killed AM by decapitation (10 animals per line and group), and serum or plasma samples were prepared according to standard procedures. Total livers were flash frozen, grinded in liquid nitrogen to a homogenous powder, and stored in liquid nitrogen for subsequent analysis.

Analysis of Serum Parameters

Mice were deprived of food for 12–14 h (overnight), with free access to water. Blood samples were drawn from the head artery after decapitation. For the test, the Ascensia ELITE® Blood Glucose Monitoring System and the blood glucose test strips from Bayer Vital GmbH were used. Glucose levels were expressed as milligrams per deciliter. Plasma samples, collected in lithium–heparin-coated tubes, were assessed for their levels of total protein, triglycerides, and cholesterol by using an automated analyzer (Roche Cobas Mira Plus; Axonlab AG, Reichenbach, Germany). All plasma parameters were determined by the employment of commercial kits (total protein: No. LT-TP 0503; triglycerides: No. LT-TR 0015; total cholesterol: No. LT-CH 0031; Labor + Technik Eberhard Lehmann, Berlin, Germany). Insulin concentrations in serum were determined using the competitive rat insulin ^{125}I radioimmunoassay (SRI-13K; Linco Research, Inc., St. Charles, MO) with purified rat insulin as a standard. A standard curve was generated ranging from 0.02 to 1.0 ng·mL^{-1}. The intra- and interassay coefficients of variation were 4.8% and 9.2%, respectively.

Quantitative Reverse Transcriptase Polymerase Chain Reaction

The expression of PPAR alpha and delta messenger RNA transcripts was determined in liver samples from 10 animals per group. Liver samples were homogenized in 1 mL TRI reagent using syringes and needles (21G × 1½ in.) according to the manufacturer's instructions. After DNase treatment, RNA was quantified and integrity was verified by tris-acetate-EDTA electrophoresis. Reverse transcription was performed in 100 ng·μL^{-1} of total RNA using random hexamers and oligo (dT) primers and Superscript III reverse transcriptase (Invitrogen, Karlsruhe, Germany). For gene-specific polymerase chain reaction (PCR), 2 ng reverse-transcribed RNA were used in reaction mixtures containing 5 μM forward and reverse primers and IQ SYBR Green Supermix (BioRad, Munich, Germany), according to the manufacturer's instructions. Compared with other housekeeping genes (β-actin, GAPDH, SDHA, and serpin a), HPRT1 was characterized by almost identical cycle threshold values in both genetic groups (DUC = 24.98 ± 0.43, DUhTP = 25.09 ± 0.43, n = 10). Thus, expression of PPAR alpha (NM_011144) and delta messenger RNA (NM_011145) was normalized by using Hprt1 (NM_013556). Templates were amplified after 5 min at 95°C by 40 cycles of the following program: 15 s at 95°C for denaturation, 30 s for annealing, and 30 s at 72°C for extension. On the basis of the melting curve analysis from the PCR products, a high-temperature fluorescence acquisition point was determined and included in the amplification cycle program for 10 s. For all assays, a standard curve, which was generated by amplifying serial dilutions of specific PCR products, was analyzed using the iCycler IQ real-time detection apparatus software (BioRad) to determine assay efficiency and correlation coefficient.

Preparation of Nuclear and Cytosolic Extracts and Western Immunoblotting

Liver samples were homogenized in extraction buffer (Cell Signaling Technology, New England Biolabs, Frankfurt, Germany) using the Precellys (Bertin Technology, Peqlab, Erlangen, Germany). For the preparation of cytoplasmic, mitochondrial, or nuclear fractions, liver samples were homogenized in sucrose buffer (0.3 M Sucrose, 5 mM MOPS, 1 mM ethyleneglycotetraacetic acid, pH 7.4) and centrifuged at 1000g for 10 min at 4°C. Nuclei, present in the pellet, were lysed in extraction buffer and treated in ultrasonic water bath to reduce DNA-mediated viscosity. The presence of high amounts of DNA was confirmed by agarose gel electrophoresis. Supernatants, containing cytosolic proteins were achieved by centrifugation at 12,000g for 60 min at 4°C. In the obtained pellet, the mitochondria were accumulated. The amounts of protein were quantified using the bicinchonic acid method as described previously (20). Twenty micrograms of total protein were loaded and separated on 12% sodium dodecyl sulfate–polyacrylamide gel electrophoresis gels and transferred to polyvinylidenfluorid membranes (Roth, Karlsruhe, Germany). To verify equal loading and protein transfer, membranes were stained with Coomassie blue according to standard procedures. Membranes were blocked (5% dry milk and 1% Tween 20 in Tris-buffered saline) and incubated with primary antibodies overnight at 4°C. We analyzed the expression of

phosphoenolpyruvate carboxykinase (PEPCK) (sc-32879; rabbit polyclonal antibody; Santa Cruz, Heidelberg, Germany), glutamate dehydrogenase (GDH) (sc-160382, rabbit polyclonal antibody; Santa Cruz), liver-specific phosphofructokinase (sc-130226; rabbit polyclonal antibody; Santa Cruz), acetyl-CoA-carboxylase (ACC) (#3662; rabbit polyclonal antibody, Cell Signaling Technology), acetyl-CoA-synthase 1 (ACSS2) (sc-85258; rabbit polyclonal antibody; Santa Cruz), and sirtuin 1 (sc-15404; rabbit polyclonal antibody; Santa Cruz). After washing the membranes, horseradish peroxidase–conjugated secondary antibodies (Cell Signaling Technology) were incubated for 1 h. Protein detection was achieved by enhanced chemiluminescence (ECL Advance Western Blotting Detection Kit; GE Healthcare, VWR, Darmstadt, Germany) using Kodak Image Station 4000 MM (Raytest, Straubenhardt, Germany). After exposure, the antibody was stripped from the membrane (2% SDS, 100 mM 2-mercaptoethanol in 62.5 mM Tris, pH 6.7) for 1 h at 70°C.

Analysis of Liver Metabolites by GC-MS

Samples (50 mg) of total liver grinded in liquid nitrogen were extracted in 1 mL chloroform/methanol/water (1:2.5:1) and centrifuged at 14,000*g* by 10 min at 4°C. Supernatants were dried and derivatized by an incubation in 10 μL methoxyamin (40 mg·mL^{-1} Pyridin) for 90 min at 30°C after an incubation in 90 μL 2,2,2-trifluoro-*N*-methyl-*N*-(trimethylsilyl) acetamid for 30 min at 30°C. Metabolites were quantified by gas chromatography-mass spectrometry (GC-MS) using the GCxGC PEGASUS® III (Leco) TOFMS (16,41). The split-injection started with a volume of 1 μL at 230°C. Gas chromatography was performed at temperatures of initially 85°C and 360°C at the end of the analysis applying an increase of 15°C·min^{-1}. Detectable mass spectra, which ranged between *m/z* 85 and 500, were analyzed by Leco's ChromaTOF software and included background normalization. For peak identification, we used alignment of a metabolite library (Wiley, Palisade Corporation und http://www.mpimp-golm.mpg.de/mms-library/index-e.html). Metabolite peaks were quantified with target ion traces (16,27,44) (http://csbdb.mpimp-golm.mpg.de).

Analysis of Liver Glycogen and Triglycerides

Glycogen content was quantified in the livers from 7-wk-old male DUC and DUhTP mice (n = 4 per group) using the Starch kit (#10207748035, charge number 11849700; Boehringer Mannheim/R-Biopharm, Germany) according to the manufacturer's instructions. Triglyceride content was quantified in liver extracts from 7-old male DUC (n = 7) and DUhTP (n = 8) mice by using the LT-TR 0015 triglyceride kit (Labor + Technik Eberhard Lehmann).

Statistical Analysis

Data analysis was performed using the general linear model (PROC GLM, SAS 2007). For all data, the model included line (selected DUhTP vs control mice DUC) as a fixed effect. Statistical significance was accepted at $P < 0.05$. Data are expressed as LS mean ± SE type III (mean ± SE). Statistically significant differences are indicated by the presence of different letters in figures and tables. Pearson product–moment correlation coefficient (r) was calculated between cholesterol and triglyceride level in plasma and PPAR delta expression in liver. All P values in our study were corrected for multiplicity using the false discovery rate estimating approach developed by Benjamini and Hochberg (4).

RESULTS

Endurance fitness of untrained mice after long-term selection for high treadmill performance. Long-term selection for high treadmill performance for a period of 90 generations in DUhTP mice resulted in a more than five-fold increased endurance capacity when compared with unselected control mice (DUC mice) in untrained 49-d-old male animals. Although DUC mice accomplished 246 ± 21 m until the experimental settings defined termination of the run, DUhTP mice were able to manage a distance of 1317 ± 175 m under the same experimental conditions ($P < 0.001$).

Table 2 shows phenotypic traits in the different mouse lines. No significant differences in total body mass were found. By contrast, lean mass was reduced in DUhTP mice if

TABLE 2. Phenotypical traits of long-term selected male mice, selected for high treadmill performance (DUhTP) and unselected controls (DUC) at an age of 49 d.

	n	DUhTP	DUC	*P*
Body mass (g)	20	30.3 ± 0.4	31.1 ± 0.4	0.1840
Lean body mass (g)	10	18.2 ± 1.6	20.1 ± 1.1	0.0186
Musculus rectus femoris (g)	20	0.38 ± 0.01	0.39 ± 0.01	0.1483
Liver mass (g)	20	1.85 ± 0.03	1.96 ± 0.03	0.0254
Epididymal fat mass (g)	20	0.41 ± 0.02	0.29 ± 0.02	0.0012
Subcutaneous fat mass (g)	10	0.25 ± 0.07	0.15 ± 0.03	0.0060
Renal fat mass (g)	10	0.08 ± 0.02	0.05 ± 0.01	0.0027
Brown fat mass (g)	10	0.08 ± 0.01	0.06 ± 0.03	0.0186
Food consumption (g·d^{-1})	20	4.2 ± 0.7	4.09 ± 1.15	0.2998
Running wheel activity (rev·d^{-1})	>18	4431 ± 2067	4835 ± 2260	0.5862
Glucose (g·L^{-1})	10	101.9 ± 16.6	113.4 ± 13.5	0.1472
Insulin (ng·mL^{-1})	10	0.70 ± 0.28	0.64 ± 0.13	0.4929
Total protein (g·L^{-1})	10	58.2 ± 3.4	58.6 ± 7.9	0.9080
Serum triglycerides (g·100 mL^{-1})	10	3.5 ± 0.3	2.0 ± 0.3	0.0217
Serum cholesterol (mmol·L^{-1})	10	4.8 ± 0.3	3.0 ± 0.2	0.00025
Liver triglycerides (mg·g^{-1})	>6	13.1 ± 1.6	6.2 ± 0.3	5.5×10^{-8}

Total body lean mass was analyzed by dual energy x-ray absorptiometry. Food consumption was assessed in 3- to 10-wk mice for a period of 50 d in both genotypes. Physical activity was studied in the presence of running wheels for a period of 3 wk in 7- to 10-wk male mice of both lines. Values are presented as mean ± SE.

compared with controls. Although lean mass reductions were not correlated with lower weights of an isolated muscle (musculus quadriceps femoris), which were similar in both groups, significantly reduced liver weights ($P < 0.05$) were present in DUhTP mice at an age of 49 d. All fat depots (epididymal, subcutaneous, brown, and renal fat mass) assessed in DUhTP were significantly increased when compared with DUC mice ($P < 0.05$; Table 2). "Running wheel activity" and food consumption were comparable in both genetic groups. No significant differences were found for blood glucose or for the protein concentrations between both genetic groups. In correspondence, insulin concentrations were similar in DUC and DUhTP mice. In DUhTP animals, plasma triglyceride and cholesterol concentrations as well as the levels of liver triglycerides were significantly higher compared with DUC mice ($P < 0.05$).

Metabolic control in the liver. PPAR represent evolutionary conserved sensors of lipid concentrations and known effectors of energy metabolism. Thus, we have quantified expression of *Ppara* and *Ppard* genes in DUhTP und DUC mice by quantitative reverse transcriptase PCR. In contrast to PPAR alpha, PPAR delta transcript levels were significantly higher in livers from DUhTP mice (7.5E + 03 ± 7.0E + 02 copy numbers) in comparison with DUC mice (3.3E + 03 ± 7.4E + 02 copy numbers; $P < 0.00005$). Notably, gene expression of *Ppard* in the liver correlated with the lipid concentrations from blood samples ($N = 39$) in our mouse lines (for cholesterol: $r = 0.53$, $P < 0.001$; for triglycerides: $r = 0.60$, $P < 0.001$). Also sirtuin 1 protein levels in crude hepatic lysates were almost twofold higher ($P < 0.01$) in DUhTP mice if compared with controls (Fig. 2). This increase was exclusively due to higher levels of sirtuin 1 in the cytosol (twofold increase; $P < 0.01$), whereas nuclear sirtuin 1 was unaffected in both groups.

Expression of selected metabolic key enzymes in the liver. Livers from DUhTP mice had more than twofold increased levels of PEPCK (Fig. 3A; $P < 0.05$), whereas protein levels of phosphofructokinase were similar in both genotypes (data not shown). Also higher protein levels of GDH (Fig. 3B) were found in liver extracts from DUhTP mice (163%; $P < 0.01$). Protein levels of acetyl-CoA synthetase 1 (ACSS2) were higher by 45% ($P < 0.01$) in livers from DUhTP mice (Fig. 3C). In addition, protein levels of acetyl-CoA carboxylase (Fig. 3D) were more than twofold higher in livers from DUhTP mice ($P < 0.00001$).

Analysis of liver metabolites. In total liver extracts, several metabolites have been quantified by GC-MS (Table 3). Notably, glucose and different hexose-monophosphates including activated hexose, ribose, and ribulose were significantly higher in liver extracts from DUhTP mice, suggesting higher glucose production and glucose phosphorylation. In parallel, we have found higher hepatic glycogen content in DUhTP (3.15% ± 0.4%) mice versus controls (1.81% ± 1.04%), representing an increase by 75% ($P < 0.05$) in DUhTP mice. In addition, steroid and fatty acid metabolites (methylcholesterol and dodecanol) were elevated in liver extracts from DUhTP mice. The relative amounts of dodecanol in DUhTP mice were 337% compared with DUC mice, which

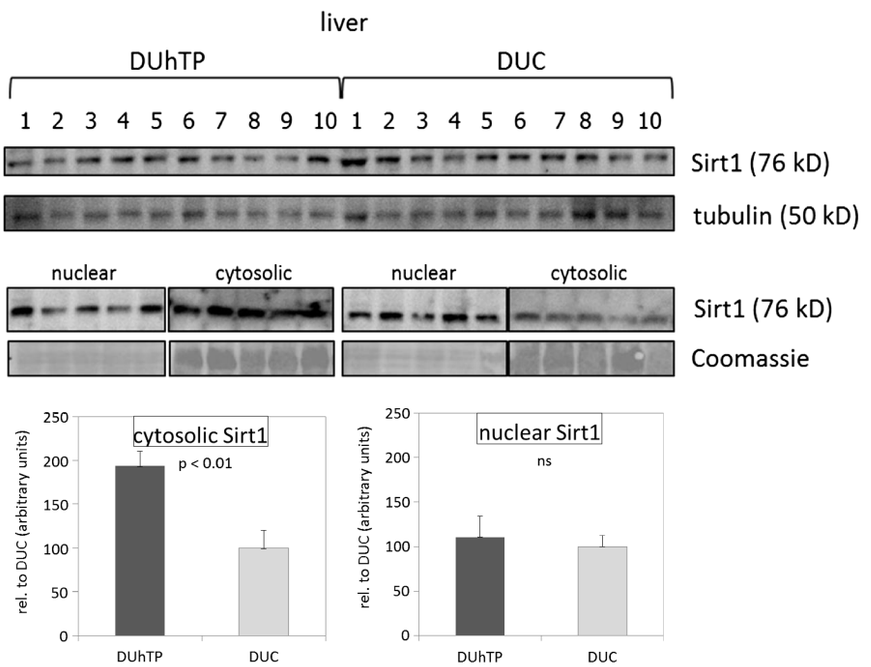

FIGURE 2—Expression of sirtuin 1 in the liver of 7-wk-old male DUhTP and DUC mice. Assessment of subcellular sirtuin 1 localization revealed higher amounts in the cytosolic fraction. The analysis was performed by Western blotting. Protein expression was quantified by densitometry and normalized for the Coomassie blue signal. Data are presented as mean and SE and are expressed relative to the expression level of the unselected control DUC. Significant differences as indicated.

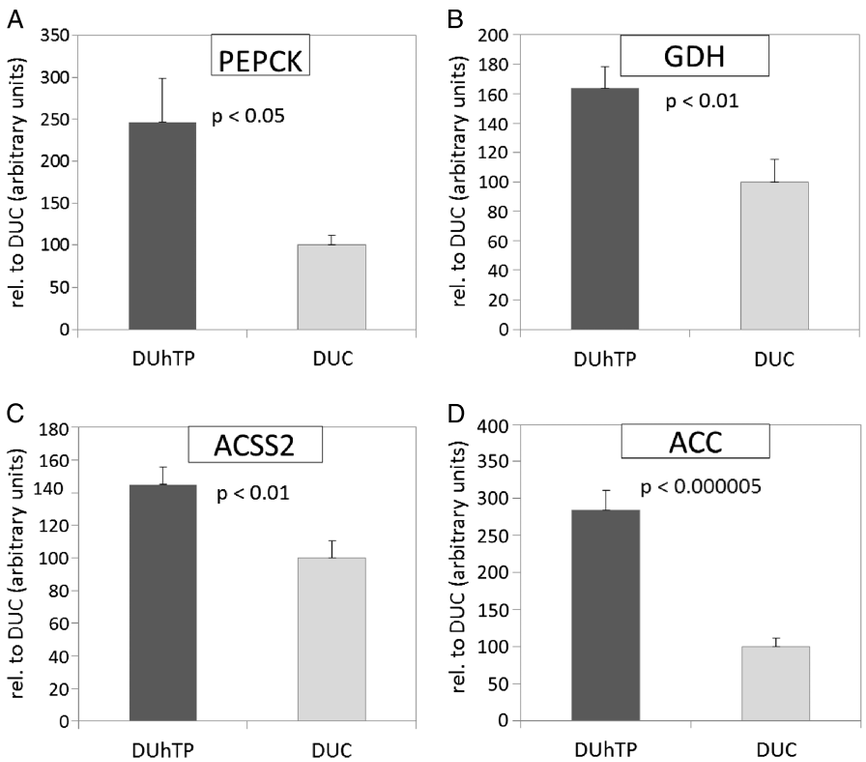

FIGURE 3—Expression of PEPCK (A), GDH (B), ACSS2 (C), and ACC (D) in the liver from 7-wk-old male DUhTP and DUC mice. The analysis was performed by Western blotting. Protein expression was quantified by densitometry and normalized for the Coomassie blue signal. Data are presented as mean and SE and are expressed relative to the expression level of the unselected control DUC that have been set to 100%. Significant differences are indicated. PEPCK, phosphoenolpyruvate carboxykinase; GDH, glutamate dehydrogenase; ACSS, acetyl-coenzyme A synthetase; ACC, acetyl-coenzyme A carboxylase.

represented the highest numerical change if compared with other metabolites. An increased rate of lipid synthesis may further be concluded from higher levels of myo-inositol derivatives.

DISCUSSION

Long-term selected mouse models represent a useful tool of functional genome analysis because they can be used to test the physiological relevance of existing hypotheses. Their unique potential moreover is because they display the complex genetic and physiological basis underlying specific traits (5,21,26,32). Here we used a genetic model established by phenotypic long-term selection for high treadmill endurance and investigated potential physiological mechanisms responsible for outstanding physical fitness to identify potential mechanisms of adapted energy metabolism. However, results from phenotype-derived mouse models clearly have caveats because associations may be spurious particularly in unreplicated mouse lines (19). This limitation also cannot be circumvented by choosing a relatively complex genetic background in DUhTP contributed by eight genetically different mouse lines or by inflating the dimensions of the selection experiment including 60–100 families in our model. However, if confirmed by other, for example, transgenic models, a particular degree of physiological relevance may be connected with findings from phenotype-selected models.

The treadmill endurance performance of 7-wk-old DUhTP mice differed by approximately fivefold if compared with unselected DUC mice. Although total body mass was unaffected by the genotype, lean mass and liver mass were reduced in 49-d DUhTP mice. In other rodent models selected for increased "running wheel activity" (49,50) or higher endurance capacity (25), reduced body mass and lower body fat has been observed. Thus, it may well be that higher accretion of body fat in abdominal and subcutaneous fat depots has masked the effect of trait selection on body weight in DUhTP mice. Furthermore, the difference in body fat may be because voluntary activity was not different in DUhTP mice.

The massive increases of body fat may be discussed with respect to the high demands of energy during endurance exercise and can be explained only by the physical state of inactivity because of the absence of running wheels. Although this hypothesis needs to be tested in the future, abdominal and subcutaneous obesity plastically visualize the marked phenotype of increased hepatic lipid synthesis as discussed further in the following paragraphs. It is known that the energy content present in endogenous carbohydrates may not be sufficient, for example, in "long-distance runners" and that the balance between carbohydrate and fat metabolism is required to prevent the depletion of glycogen

TABLE 3. Liver metabolites in DUhTP mice and controls (DUC).

	DUhTP		DUC		
Metabolite	**LS mean ± SE**	***n***	**LS mean ± SE**	***n***	***t*-test**
Carbohydrate metabolism					
Fructose 1,6-bisphosphate	260 ± 87	18	353 ± 170	17	0.03
Gluconic acid	143 ± 47	17	89 ± 20	10	0.003
Glucose	3914 ± 914	15	3173 ± 1324	14	0.055
Glucose-6-phosphate	7176 ± 2121	19	3563 ± 2067	20	0.003
Glucose-1-phosphate	1322 ± 377	19	682 ± 375	20	0.003
Glucuronic acid	2306 ± 460	19	1449 ± 386	20	0.0001
Glyceric acid 3-phosphate	355 ± 87	18	750 ± 394	20	0.003
Hexose 6-phosphate	1757 ± 607	19	743 ± 485	20	0.0001
Mannose	2222 ± 707	19	4377 ± 2104	20	0.0015
Ribose	1976 ± 630	17	3771 ± 2961	20	0.03
Ribose 5-phosphate	828 ± 496	19	519 ± 404	20	0.02
Ribulose 5-phosphate	343 ± 84	16	222 ± 143	16	0.008
Threonic acid	994 ± 188	19	758 ± 261	20	0.025
alpha-Ketoglutaric acid	48 ± 15	15	63 ± 20	15	0.055
Lipid metabolism					
alpha-Glycerol-phosphate	2737 ± 505	18	1956 ± 569	20	0.018
Dihydrostigmasterol	1349 ± 580	19	897 ± 407	20	0.055
Dodecanol	1842 ± 983	19	557 ± 655	19	0.001
Ethanolamine	1756 ± 501	19	2897 ± 1347	20	0.001
Methylcholesterol	1273 ± 611	19	596 ± 227	20	0.008
Myo-inositol-phosphate	2380 ± 1101	19	1699 ± 512	20	0.018
Myo-inositol-phosphate-1-glyceride	237 ± 53	19	190 ± 24	20	0.018
Butyric acid 2-hydroxy	2167 ± 618	19	2894 ± 653	20	0.044
Amino acid metabolism					
Adipic acid 2-amino	585 ± 182	19	1464 ± 1174	20	0.0036
Alanine	557 ± 346	19	1076 ± 442	20	0.0035
Histidine	12,732 ± 5430	18	17,248 ± 6169	20	0.055
Leucine	3093 ± 906	11	2632 ± 687	19	0.055
Oxoproline	194,878 ± 32,642	19	168,600 ± 32,256	20	0.031
Nucleic acid metabolism					
Uric acid	1433 ± 372	19	732 ± 311	20	0.0037

Hepatic extracts were analyzed by GC-MS as described in the Materials and Methods section.

stores (39). With the progressive consumption of glycogen during physical exercise, endogenous fat is getting more relevant for energy supply (43). Thus, besides glycogen, fat metabolism also needs to be reflected in a functional context with endurance capacity in DUhTP mice. As discussed earlier, fat depots were increased in DUhTP mice, which correlated with higher plasma concentrations of triglycerides and cholesterol in DUhTP versus DUC. Although higher levels of plasma cholesterol are found in response to endurance exercise in human athletes (8,12), higher plasma triglycerides have been described in birds during migratory flight (24) or in trained race horses (29). Thus, hyperlipidemia in DUhTP mice may be due to higher fat mass but at least partially may also be seen in a functional context with higher endurance capacity. Interestingly, in "high running Garland mice," higher lipid oxidation rates and specific adaptations for lipid metabolism in the isolated muscle have been provided very recently (54). If greater reliance on lipids is present under conditions of higher physical activity or endurance training, which further had been suggested in race horses (29), it is necessary to study potential mechanisms of lipid supply in the respective context. First of all, it is important to note that the higher abdominal fat mass and hyperlipidemia were not due to an excessive eating behavior because food consumption was similar in both genetic groups between 3 and 10 wk of age. Moreover, in our system, those metabolic adaptations are not due to differential activity patterns because the mice were caged in the absence of running wheels and did not display altered "running wheel activity" if tested. Thus, we assume that metabolic adaptations have contributed to the phenotype of hyperlipidemia and obesity of DUhTP mice. Similar to DUhTP mice also in human subjects, serum cholesterol concentrations are determined by genetic factors (1). When lipid metabolism is to be concerned, the PPAR family of ligand-activated transcription factors involved in the regulation of energy balance has to be reflected (1,51), particularly because PPAR family members are involved in hepatic fatty acid synthesis as well as in energy expenditure (47). The liver as the central organ of metabolic control is capable in uptake, synthesis, and secretion of lipids like cholesterol or fatty acids. The activation of PPAR delta in the liver increased lipogenesis (30) and glucose flux through the pentose phosphate pathway (PPP) (40). Several phosphorylated hexose derivatives, including glucose, ribose, and ribulose phosphate, were present at higher abundance in liver extracts from DUhTP mice, indicating higher activity of the PPP in the liver of DUhTP mice (23). According to this assumption, the lower levels of ribose and glyceric acid 3-phosphate can also be modeled as both molecules fuel the PPP (23). Although glucose levels were unaffected by the genotype in the circulation, total hepatic glucose levels (free and phosphorylated) were markedly increased, which may be due to the

increases of PEPCK, which is required for gluconeogenesis in the liver. By contrast, the lower levels of fructose 1,6-bisphosphate in the liver was discussed in the context with reduced glycolysis (11). Most obviously, phosphorylated hexoses, particularly glucose metabolites, are found at higher abundance in DUhTP mice. Both glucose-1-phosphate and glucose-6-phosphate are indicative of an active glycogen metabolism (15) as confirmed also by higher absolute glycogen levels in the liver of DUhTP mice. The concentrations of hepatic glycogen in DUC (1.8%) and DUhTP (2.15%) mice are in the upper range of those from the Garland mice (0.5%–5.2%) as provided by Gomes et al. (17). Although in the later model no effect was found in four replicated mouse lines, DUhTP mice were characterized by moderately increased hepatic glycogen concentrations. The reason for this discrepancy is unclear; however, it may be related to the different selection strategy: while the Garland mice have been developed by selection for voluntary physical activity, the DUhTP model was selected for physical performance as delivered in a singular "long-distance run." Nevertheless, the Garland mice were also characterized by increased endurance capacity, which was increased by up to 35% (33). Because endurance exercise was the primary selection trait in DUhTP, endurance capacity was increased to a much higher extent and amounted up to 500% in this model. It is well known that carbohydrates may be a limiting factor in endurance exercise (7) and that hepatic and muscle glycogen depots fuel physical performance particularly during more intense exercise (39). Thus, both reasons may indicate higher hepatic glycogen levels as part of a more complex adaption to endurance exercise in our model. Also oxidation products of glucose were found at higher concentrations in the liver of DUhTP mice. Interestingly, those products are not only indicative of a higher glucose metabolism but can be discussed in a context with higher endurance fitness. In rats, application of glucuronic acid increased endurance fitness and prevented fatigue (52).

In addition and in line with the higher levels of ribose 5- and ribulose 5-phosphate, glucose-6-phosphate also may fuel the PPP, which generates energy equivalents required for lipid synthesis. In fact, in the liver of DUhTP mice, an increase of lipid metabolism might be indicated by distinct levels of steroid metabolites (methylcholesterol and dihydrostigmasterol), intermediates of fatty acids (dodecanol), and phospholipids (myo-inositol derivatives, α-glycerol-phosphate, and ethanolamine). In rats, the liver metabolome was studied under conditions of endurance training or exhaustive exercise (22). Although endurance training was associated with glycogen synthesis, exhaustive exercise caused glycogen depletion and lipolysis. Thus, in DUhTP mice, increased glycogen and lipid metabolism may be interpreted as an adaption toward improved endurance exercise. Interestingly, an adverse effect of lipids on insulin sensitivity is not present in trained athletes, characterized by an increased oxidative capacity (38). Thus, hyperlipidemia in DUhTP may not to be interpreted as a harmful adaptation only. However, the effects of hyperlipidemia, for example, on the cardiovascular system or lifespan of DUhTP mice need to be addressed in subsequent studies. The interpretation of results from the liver metabolomic investigation is in line with hyperlipidemia and obesity on one hand but also in line with expression of lipogenic key enzymes on the other. Interestingly, PPAR delta has been shown to increase lipogenesis via an increase of ACC expression in the liver (28,30). The coincidence of higher PPAR delta and ACC levels in the liver from DUhTP mice corresponds to the findings of Liu et al. (30) and indicates higher lipogenesis in DUhTP mice if compared with DUC mice. For the effects of PPAR delta on lipogenesis, distinct sirtuin family members may be also relevant (36). Recently, PPAR delta has been demonstrated to increase sirtuin 1 (3). Thus, higher expression levels of sirtuin 1 may be due to higher PPAR delta levels in the liver of DUhTP mice. Because sirtuin 1 represents a well-accepted effector of body energy expenditure (18) and lipogenesis, which directly activates ACSS2 by deacetylation (6), PPAR delta potentially affects lipogenesis in the liver by direct and indirect effects via sirtuin 1. It is important to note that the capacity of sirtuin 1 to increase acetyl-CoA via ACSS2 is dependent on its presence in the cytosol (34). In fact, predominantly cytosolic sirtuin 1 was increased in the liver of DUhTP mice. This was not expected because the nucleus has been mentioned as the primary location of sirtuin 1.

We do not have hints of a distinct effect on amino acid metabolism in the liver because proteinogenic amino acids (alanine, histidine, and leucine) were decreased or elevated in the liver of DUhTP mice. Notably, alanine represents an important precursor of gluconeogenesis in the liver (14). Thus, the severe reductions of alanine in the liver of DUhTP mice could be due to higher gluconeogenesis. Because muscles represent the main source of alanine in the glucose-alanine cycle (14), reduced lean mass of DUhTP mice, at least in part, may be explained. However, also this hypothesis needs to be studied in more detail in subsequent studies. An increase of oxoproline, as a derivative of glutamic acid, is linked with defects of glutathione biosynthesis (48). The mild increase of oxoproline may thus point to altered glutathione biosynthesis in the liver of DUhTP mice. Altered glutathione production further might be related to lower 2-hydroxybutyric acid (31) in DUhTP mice. Also from the severe reductions of 2-amino adipic acid, an established biomarker of carbonyl oxidation (46), altered oxidative capacity may have developed in DUhTP mice. Altered oxidative capacity is certainly relevant in a context of higher lipid metabolism in the liver (42).

In summary, the "marathon mouse" model DUhTP represents a model of outstanding physical fitness, which had acquired high performance endurance capacities for a period of 90 generations of selective breeding. We have demonstrated that the model is characterized by increased fat mass and hyperlipidemia. On the basis of differential dynamics of gene expression of distinct PPAR members in the liver, we assume that DUhTP mice have acquired highly efficient mechanisms of energy metabolism, providing an increased energy supply

for fuel consuming tissues. In the absence of running wheels, the energy is stored in adipose tissues, resulting in hyperlipidemia and obesity. Hepatic metabolism of DUhTP mice is characterized by higher lipid and carbohydrate metabolism, which could feed the higher demands of energy indicated by higher levels of lipogenic metabolites. Results from the metabolite analysis can be correlated with higher levels of gluconeogenic and lipogenic key enzymes as detected in the liver. In our model, elevated sirtuin 1 expression, as a genetic trait, may drive the hepatic metabolism toward higher production of fuels to provide for the increased demands of energy as required during the performance of exhaustive exercise.

The authors thank Mandy Sawitzky, Barbara Bachnick, Sabine Hinrichs, and Nicole Gentz for technical assistance. They are particularly grateful to Prof. Oliver Fiehn and Aenne Eckhard, MPIMP Golm, for the GC-MS analysis. The help of Dr. Dirk Repsilber with the statistical analysis is highly appreciated. This study was supported by the Deutsche Forschungsgemeinschaft (DFG Schw 466/17-1 and DFG HO 2003/6-1).

Results of the present study do not constitute endorsement by the American College of Sports Medicine.

All authors declare no conflict of interest.

REFERENCES

1. Aberle J, Hopfer I, Beil FU, Seedorf U. Association of the T+294C polymorphism in PPAR delta with low HDL cholesterol and coronary heart disease risk in women. *Int J Med Sci*. 2006;3(3):108–11.
2. Ahmed W, Ziouzenkova O, Brown J, et al. PPARs and their metabolic modulation: new mechanisms for transcriptional regulation? *J Intern Med*. 2007;262(2):184–98.
3. Bai P, Canto C, Brunyanszki A, et al. PARP-2 regulates SIRT1 expression and whole-body energy expenditure. *Cell Metab*. 2011; 13(4):450–60.
4. Benjamini Y, Hochberg Y. Controlling the false discovery rate: a practical and powerful approach to multiple testing. *J R Stat Soc B*. 1995;57:289–300.
5. Bunger L, Lewis RM, Rothschild MF, Blasco A, Renne U, Simm G. Relationships between quantitative and reproductive fitness traits in animals. *Philos Trans R Soc Lond B Biol Sci*. 2005; 360(1459):1489–1502.
6. Canto C, Auwerx J. Targeting sirtuin 1 to improve metabolism: all you need is NAD+? *Pharmacol Rev*. 2011;64(1):166–87.
7. Carter J, Jeukendrup AE, Mundel T, Jones DA. Carbohydrate supplementation improves moderate and high-intensity exercise in the heat. *Pflugers Arch*. 2003;446(2):211–9.
8. Couillard C, Despres JP, Lamarche B, et al. Effects of endurance exercise training on plasma HDL cholesterol levels depend on levels of triglycerides: evidence from men of the Health, Risk Factors, Exercise Training and Genetics (HERITAGE) Family Study. *Arterioscler Thromb Vasc Biol*. 2001;21(7):1226–32.
9. Diehl D, Hessel E, Oesterle D, et al. IGFBP-2 overexpression reduces the appearance of dysplastic aberrant crypt foci and inhibits growth of adenomas in chemically induced colorectal carcinogenesis. *Int J Cancer*. 2009;124(9):2220–5.
10. Dietl G, Langhammer M, Renne U. Model simulations for genetic random drift in the outbred strain Fzt:DU. *Arch Tierz*. 2004;47: 595–604.
11. Dohm GL, Kasperek GJ, Barakat HA. Time course of changes in gluconeogenic enzyme activities during exercise and recovery. *Am J Physiol*. 1985;249(1 Pt 1):E6–11.
12. Durstine JL, Haskell WL. Effects of exercise training on plasma lipids and lipoproteins. *Exerc Sports Sci Rev*. 1994;22:477–521.
13. Falkenberg H, Langhammer M, Renne U. Comparison of biochemical blood traits after long-term selection on high or low locomotory activity in mice. *Arch Tierz*. 2000;43:513–22.
14. Felig P. Amino acid metabolism in man. *Annu Rev Biochem*. 1975;44:933–55.
15. Ferrer JC, Favre C, Gomis RR, et al. Control of glycogen deposition. *FEBS Lett*. 2003;546(1):127–32.
16. Fiehn O, Kind T. Metabolite profiling in blood plasma. *Methods Mol Biol*. 2007;358:3–17.
17. Gomes FR, Rezende EL, Malisch JL, et al. Glycogen storage and muscle glucose transporters (GLUT-4) of mice selectively bred for high voluntary wheel running. *J Exp Biol*. 2009;212(Pt 2):238–48.
18. Hallows WC, Lee S, Denu JM. Sirtuins deacetylate and activate mammalian acetyl-CoA synthetases. *Proc Natl Acad Sci U S A*. 2006;103(27):10230–5.
19. Henderson ND. Spurious associations in unreplicated selected lines. *Behav Genet*. 1997;27(2):145–54.
20. Hoeflich A, Nedbal S, Blum WF, et al. Growth inhibition in giant growth hormone transgenic mice by overexpression of insulin-like growth factor-binding protein-2. *Endocrinology*. 2001;142(5): 1889–98.
21. Houle-Leroy P, Garland T Jr, Swallow JG, Guderley H. Effects of voluntary activity and genetic selection on muscle metabolic capacities in house mice *Mus domesticus*. *J Appl Physiol*. 2000;89(4): 1608–16.
22. Huang CC, Lin WT, Hsu FL, Tsai PW, Hou CC. Metabolomics investigation of exercise-modulated changes in metabolism in rat liver after exhaustive and endurance exercises. *Eur J Appl Physiol*. 2010;108(3):557–66.
23. Huck JH, Struys EA, Verhoeven NM, Jakobs C, van der Knaap MS. Profiling of pentose phosphate pathway intermediates in blood spots by tandem mass spectrometry: application to transaldolase deficiency. *Clin Chem*. 2003;49(8):1375–80.
24. Jenni-Eiermann S, Jenni L, Kvist A, Lindstrom A, Piersma T, Visser GH. Fuel use and metabolic response to endurance exercise: a wind tunnel study of a long-distance migrant shorebird. *J Exp Biol*. 2002;205(Pt 16):2453–60.
25. Koch LG, Britton SL. Artificial selection for intrinsic aerobic endurance running capacity in rats. *Physiol Genomics*. 2001;5(1):45–52.
26. Koch LG, Britton SL. Divergent selection for aerobic capacity in rats as a model for complex disease. *Integr Comp Biol*. 2005;45(3): 405–15.
27. Kopka J, Schauer N, Krueger S, et al. GMD@CSB.DB: the Golm Metabolome Database. *Bioinformatics*. 2005;21(8):1635–8.
28. Lee CH, Olson P, Hevener A, et al. PPARdelta regulates glucose metabolism and insulin sensitivity. *Proc Natl Acad Sci U S A*. 2006;103(9):3444–9.
29. Li G, Lee P, Mori N, Yamamoto I, Arai T. Long term intensive exercise training leads to a higher plasma malate/lactate dehydrogenase (M/L) ratio and increased level of lipid mobilization in horses. *Vet Res Commun*. 2012;36(2):149–55.
30. Liu S, Hatano B, Zhao M, et al. Role of peroxisome proliferator–activated receptor {delta}/{beta} in hepatic metabolic regulation. *J Biol Chem*. 2011;286(2):1237–47.
31. Lord RS, Bralley JA. Clinical applications of urinary organic acids. Part I: detoxification markers. *Altern Med Rev*. 2008;13(3):205–15.
32. Massett MP, Berk BC. Strain-dependent differences in responses to exercise training in inbred and hybrid mice. *Am J Physiol Regul Integr Comp Physiol*. 2005;288(4):R1006–13.
33. Meek TH, Lonquich BP, Hannon RM, Garland T Jr. Endurance capacity of mice selectively bred for high voluntary wheel running. *J Exp Biol*. 2009;212(18):2908–17.

34. Michishita E, Park JY, Burneskis JM, Barrett JC, Horikawa I. Evolutionarily conserved and nonconserved cellular localizations and functions of human SIRT proteins. *Mol Biol Cell*. 2005;16(10): 4623–35.
35. Mittendorfer B, Klein S. Physiological factors that regulate the use of endogenous fat and carbohydrate fuels during endurance exercise. *Nutr Res Rev*. 2003;16(1):97–108.
36. Okazaki M, Iwasaki Y, Nishiyama M, et al. PPARbeta/delta regulates the human SIRT1 gene transcription via Sp1. *Endocr J*. 2010;57(5):403–13.
37. Oliver WR Jr, Shenk JL, Snaith MR, et al. A selective peroxisome proliferator–activated receptor delta agonist promotes reverse cholesterol transport. *Proc Natl Acad Sci U S A*. 2001;98(9):5306–11.
38. Phielix E, Meex R, Ouwens DM, et al. High oxidative capacity due to chronic exercise training attenuates lipid-induced insulin resistance. *Diabetes*. 2012;61(10):2472–8.
39. Rapoport BI. Metabolic factors limiting performance in marathon runners. *PLoS Comput Biol*. 2010;6(10):e1000960.
40. Reilly SM, Lee CH. PPAR delta as a therapeutic target in metabolic disease. *FEBS Lett*. 2008;582(1):26–31.
41. Roessner U, Wagner C, Kopka J, Trethewey RN, Willmitzer L. Technical advance: simultaneous analysis of metabolites in potato tuber by gas chromatography-mass spectrometry. *Plant J*. 2000; 23(1):131–42.
42. Rolo AP, Teodoro JS, Palmeira CM. Role of oxidative stress in the pathogenesis of nonalcoholic steatohepatitis. *Free Radic Biol Med*. 2012;52(1):59–69.
43. Romijn JA, Coyle EF, Sidossis LS, et al. Regulation of endogenous fat and carbohydrate metabolism in relation to exercise intensity and duration. *Am J Physiol*. 1993;265(3 Pt 1):E380–91.
44. Schauer N, Steinhauser D, Strelkov S, et al. GC-MS libraries for the rapid identification of metabolites in complex biological samples. *FEBS Lett*. 2005;579(6):1332–7.
45. Schüler L. Selection for fertility in mice: the selection plateau and how to overcome it. *Theor Appl Genet*. 1985;70:72–9.
46. Sell DR, Strauch CM, Shen W, Monnier VM. 2-Aminoadipic acid is a marker of protein carbonyl oxidation in the aging human skin: effects of diabetes, renal failure and sepsis. *Biochem J*. 2007;404(2):269–77.
47. Seo YS, Kim JH, Jo NY, et al. PPAR agonists treatment is effective in a nonalcoholic fatty liver disease animal model by modulating fatty-acid metabolic enzymes. *J Gastroenterol Hepatol*. 2008;23(1): 102–109.
48. Shi ZZ, Habib GM, Rhead WJ, et al. Mutations in the glutathione synthetase gene cause 5-oxoprolinuria. *Nat Genet*. 1996;14(3):361–5.
49. Swallow JG, Carter PA, Garland T Jr. Artificial selection for increased wheel-running behavior in house mice. *Behav Genet*. 1998;28(3):227–37.
50. Swallow JG, Koteja P, Carter PA, Garland T. Artificial selection for increased wheel-running activity in house mice results in decreased body mass at maturity. *J Exp Biol*. 1999;202(Pt 18):2513–20.
51. Takahashi S, Tanaka T, Sakai J. New therapeutic target for metabolic syndrome: PPARdelta. *Endocr J*. 2007;54(3):347–57.
52. Tamura S, Tsutsumi S, Ito H, Nakai K, Masuda M. Effects of glucuronolactone and the other carbohydrates on the biochemical changes produced in the living body of rats by hard exercise. *Jpn J Pharmacol*. 1968;18(1):30–8.
53. Tanaka T, Yamamoto J, Iwasaki S, et al. Activation of peroxisome proliferator–activated receptor delta induces fatty acid beta-oxidation in skeletal muscle and attenuates metabolic syndrome. *Proc Natl Acad Sci U S A*. 2003;100(26):15924–9.
54. Templeman NM, Schutz H, Garland T Jr, McClelland GB. Do mice bred selectively for high locomotor activity have a greater reliance on lipids to power submaximal aerobic exercise? *Am J Physiol Regul Integr Comp Physiol*. 2012;303(1):R101–11.
55. Wang YX, Zhang CL, Yu RT, et al. Regulation of muscle fiber type and running endurance by PPARdelta. *PLoS Biol*. 2004; 2(10, e294):1532–9.
56. Zhang P, O'Loughlin L, Brindley DN, Reue K. Regulation of lipin-1 gene expression by glucocorticoids during adipogenesis. *J Lipid Res*. 2008;49(7):1519–28.

Journal of Comparative Physiology B (2018) 188:527–539
https://doi.org/10.1007/s00360-017-1138-x

ORIGINAL PAPER

Partial phenotype conversion and differential trait response to conditions of husbandry in mice

Julia Brenmoehl[1] · Christina Walz[1] · Marion Spitschak[1] · Elisa Wirthgen[1] · Michael Walz[1] · Martina Langhammer[2] · Armin Tuchscherer[2] · Ronald Naumann[3] · Andreas Hoeflich[1]

Received: 24 May 2017 / Revised: 22 November 2017 / Accepted: 27 November 2017 / Published online: 6 December 2017

Abstract

Functional genome analysis usually is performed on the level of genotype–phenotype interaction. However, phenotypes also depend on the relations between genomes and environment. In our experimental system, we observed differential response to environmental factors defined by different conditions of husbandry in a semi-barrier unit or in a SPF (specific pathogen free) barrier unit, which resulted in partial reversal of phenotypes previously observed under semi-barrier conditions. To provide an update of basic phenotypes in unselected and randomly mated controls (DUC) and long-term selected DUhTP (Dummerstorf high treadmill performance) mice in the SPF facility, we compared growth parameters, reproductive performance, the accretion of muscle and fat mass, physical activity, and running performance as well as food intake in all experimental groups. For selected parameters, the comparative analysis spans more than 30 generations. In DUC mice, under SPF conditions a more than threefold ($P < 0.0001$) higher subcutaneous fat mass, higher muscle mass by about 25% ($P < 0.0001$), but lower epididymal fat mass in DUhTP mice by about 20% ($P < 0.0001$) were observed. In SPF husbandry, body weight increased to a stronger extent in adult DUC mice ($\approx 20\%$; $P < 0.0001$) than in DUhTP mice ($\approx 8\%$; $P = 0.001$). The concentrations of IGF-1 and IGFBPs in the serum as well as the liver weights were similar in all experimental groups, indicating growth effects independent of the somatotropic axis. Under SPF conditions the litter size at birth increased in DUC mice ($P < 0.001$) but not in DUhTP mice. The differential effect of husbandry on body weights at day 21 and concentrations of triglycerides in the serum of our model were due to the different diets used in the semi-barrier and in the SPF facility. Our results demonstrate differential trait response to environmental factors resulting in partial phenotype conversion in our experimental system. The existence of conditional phenotypes as a result of genotype–environment interactions points to the importance of environmental factors in functional genome analysis.

Keywords Semi-barrier husbandry · SPF husbandry · Body weight · Non-inbred mouse line · Standard chow · Phenotype conversion

Introduction

Since 1983 in Dummerstorf a high treadmill performance mouse model (DUhTP) had been established for the analysis of energy metabolism applying long term phenotype selection for high treadmill performance (Dietl et al. 2004). Selection was performed in the absence of running wheels within the home cage to exclude self-training effects within the selection response. The dimension of the selection experiment is remarkable, because selection period took more than 30 years and included up to 100 families per generation. The initial population of the Dummerstorf outbred mouse lines was a systematic crossbred of four inbred and four outbred founder mouse strains starting in the 1970s (Falkenberg

Communicated by G. Heldmaier.

✉ Andreas Hoeflich
hoeflich@fbn-dummerstorf.de

[1] Institute for Genome Biology, Leibniz-Institute for Farm Animal Biology (FBN), Wilhelm-Stahl-Allee 2, 18196 Dummerstorf, Germany

[2] Institute Biometry and Genetics, Leibniz-Institute for Farm Animal Biology (FBN), Wilhelm-Stahl-Allee 2, 18196 Dummerstorf, Germany

[3] Max Planck Institute of Molecular Cell Biology and Genetics, Pfotenhauerstraße 108, 01307 Dresden, Germany

et al. 2000). Both the unselected and randomly mated control line (DUC) and the DUhTP originate from this genetic founder pool. Trait selection in DUhTP was based on a singular submaximal endurance exercise test on a treadmill at day 70 of life (Falkenberg et al. 2000). Without previous training, DUhTP mice cover fourfold increased distances if compared to DUC mice (Brenmoehl et al. 2013). Interestingly, subcutaneous adipose tissue of DUhTP mice is characterized by elevated concentrations of metabolic enzymes for lipid synthesis (fatty acid synthase, acetyl-CoA carboxylase) but also for lipid hydrolysis (hormone-sensitive lipase) or oxidation (long-chain acyl dehydrogenase), respectively, as well as elevated levels of mitochondrial proteins arguing for high mitochondrial biogenesis (Brenmoehl et al. 2015). In response to moderate voluntary physical activity over a period of 3 weeks in running wheels, concentrations of inducer of mitochondrial biogenesis are further increased resulting in efficient fat mobilization in DUhTP mice (Brenmoehl et al. 2015). Recently, we identified genetic linkage of fat cell browning and metabolic health, because young male DUhTP mice are characterized by increased tolerance against oral glucose (Brenmoehl et al. 2016). Under semi-barrier conditions, sedentary DUhTP mice are characterized by increased accumulation of body fat compared to DUC mice (Brenmoehl et al. 2015). After hygienic reorganization of both lines from the semi-barrier to a new SPF barrier unit, we observed differential responses for the new environment resulting in the partial reversal of phenotype, which prompted us to compare isolated phenotypes observed in both mouse facilities. Because we used different diets in the semi-barrier and in the SPF facility, we also assessed the effects of both commercial diets on body weight under identical husbandry conditions.

Materials and methods

Animals and husbandry

All in vivo experiments were performed in accordance with national and international animal protection guidelines [German Animal Welfare Act (TierSchG)] and were approved by our internal institutional review board. The study was conducted at the mouse animal facility of the Leibniz Institute for Farm Animal Biology in Dummerstorf, Germany. We used a non-inbred mouse line that has been generated by selection over 130 generations for high treadmill performance (DUhTP) (Falkenberg et al. 2000) and the control mice (DUC) that had been generated from the identical base population without phenotype selection (Dietl et al. 2004). Body weights were simultaneously considered from animals between generations 103 and 137 (DUhTP; each $n > 23$) and between 147 and 182 (DUC; each $n > 87$). For both lines, littermates were registered for every generation and standardized to a number of eight pups per female in the semi barrier unit and to ten pups per mother immediately after birth in the SPF unit. Animals were housed in Makrolon-cages Type II (EBECO, Castrop-Rauxel, Germany) in a semi-barrier system like described recently (Brenmoehl et al. 2013). In the SPF barrier unit, the mice were kept in polysulfone cages of 267 × 207 × 140 mm (H-Temp PSU, Type II, Eurostandard Tecniplast, Germany). Hygiene management and health monitoring in SPF husbandry were performed according to the recommendations of the FELASA (Mahler Convenor et al. 2014). In both conditions of mouse husbandry, environmental conditions were defined by a 12-h light–dark cycle (room temperature 22.5 ± 0.2 °C, humidity 40–60%) and the animals had free access to pellet concentration and water. Semi-barrier animals received food #1314 from Altromin (Lage, Germany). Mice in SPF conditions were fed with autoclaved Ssniff® M-Z food (Ssniff-Spezialdiäten GmbH, Soest, Germany; Table 1). For the resettlement of the new SPF mouse facility in Dummerstorf, by vitrification cryopreserved embryos from individual DUC mice were transferred into pseudopregnant Crl:CD1(ICR) fosters in an existing SPF facility (Max Planck Institute of Molecular Cell Biology and Genetics, Dresden, Germany). New generated DUC_{SPF} mice of generation 150 were then imported to the empty SPF facility in Dummerstorf and expanded as the initial base population. After verification of the SPF status in the new barrier unit (Gesellschaft für innovative Mikroökologie mbH, Michendorf, Germany), fresh recovered embryos from $DUhTP_{SB}$ and DUC_{SB} mice were fresh-transferred to pseudopregnant CD1 foster females and DUC_{SPF} mice.

Voluntary physical activity and food consumption in both mouse lines were recorded at an age of 49–70 days using running wheels ($d = 33.4$ cm; Tecniplast, Hohenpeißenberg, Germany). In the same period, food consumption was monitored in animals of DUhTP (semi-barrier: generation 105; SPF: generation 128 and 135) and DUC mice (semi-barrier: generation 149; SPF: generation 173 and 180). For

Table 1 Composition of used food

	Altromin #1314	Ssniff M-Z
Dry matter	89.0%	88.0%
Crude protein	22.5%	22.0%
Crude fat	5.0%	4.5%
Crude fiber	4.5%	3.9%
Crude ash	6.5%	6.7%
Nitrogen-free extracts	50.5%	50%
Metabolized energy	2988 kcal/kg	3272 kcal/kg
Calories from protein	27%	36%
Calories from fat	13%	11%
Calories from carbohydrates	60%	53%

the examination of body composition of DUhTP and DUC mice, data from generation 93, 95, 105, 118 ($DUhTP_{SB}$), 137,149,162 (DUC_{SB}), 121–124 ($DUhTP_{SPF}$) and 166–167 (DUC_{SPF}) were used. Body length determination was performed at day 42 with mice of generation 100 ($DUhTP_{SB}$), 144 (DUC_{SB}), 137 ($DUhTP_{SPF}$) and 182 (DUC_{SPF}). All mice were killed at day 70 of age via decapitation for blood sampling and tissues (liver, Musculus rectus femoris, epididymal fat, and isolated subcutaneous fat (generation 105, 121–124, 149, 167)) were weighted, snap-frozen in liquid nitrogen, and stored at − 70 °C for subsequent analysis. Serum was stored at − 20 °C. For the longitudinal analysis of body mass after weaning, we analyzed animals of generation 134 ($DUhTP_{SPF}$) and 179 (DUC_{SPF}). We included 30 (DUC_{SPF}) and 15 ($DUhTP_{SPF}$) standardized litters ($n = 10$), respectively. Furthermore, 30 males and 16 females of $DUhTP_{SPF}$ in generation 135 and DUC_{SPF} mice in generation 180 were divided and afterwards kept for two generations as an own subpopulation without selection procedure (marked as generation 135*–137* and 180*–182*, respectively). Mice in the parallel husbandry were kept in individually ventilated cages (GM500 Mouse IVC Green Line, Tecniplast, Germany) and received either "semi-barrier food" from Altromin or "autoclaved SPF-food" from Ssniff and were analyzed for body masses and food consumption.

Analysis of the IGF system

Serum concentrations of IGF-1 were analyzed using the specific ELISA for mouse and rat IGF-1 (E25, Mediagnost, Reutlingen, Germany) according to the manufacturer's instruction. The sensitivity of the assay system was < 0.029 ng/ml and the analytical range for recombinant IGF-1 was 0.5–18 ng/ml. The intra- and inter-assay coefficients of variation (CV%) were 4.2–5.9 and 5.3–6.7%, respectively.

Serum IGFBP-2, -3, and -4 were analyzed by quantitative Western ligand blot analysis as described previously (Wirthgen et al. 2016). Briefly, serum samples were diluted 1:20, boiled in sample buffer (312.5 mM Tris at pH 6.8, 50% (w/v) glycerol, 5 mM EDTA, 1% (w/v) SDS, and 0.02% bromophenol blue) for 5 min. Proteins were separated by 12% SDS-PAGE followed by the transfer onto a polyvinylidene fluoride membrane (Millipore, Bedford, USA). The blots were blocked and then incubated with biotin-labeled human IGF-2 (1:500; BioIGF2-10; ibt-systems, Binzwangen, Germany). The IGF-binding proteins were detected by enhanced chemiluminescence using LuminataTM Forte (Millipore, Bedford, USA). Bands were visualized on KODAK Image Station 4000MM (Molecular Imaging Systems, Carestream Health, Inc., New Haven, USA) and quantified using Gelanalyzer2010a software. Signal intensities were corrected for background and quantified using human recombinant standards (IGFBP-2 to -4, R&D Systems, Wiesbaden-Nordenstadt, Germany) diluted in artificial serum matrix (Biopanda, County Down, United Kingdom) as calibrators on each blot. The calculation of the IGFBP concentrations in plasma was performed using GraphPad Prism6 software and corrected for dilution and volume/lane of each sample. The analytical range for each IGFBP was 150–15000 ng/ml.

Analysis of serum triglycerides

Triglycerides (TG) were assayed in serum samples using a commercial kit (No. LT-TR 0015; Labor & Technik Eberhard Lehmann, Berlin, Germany).

Statistical analysis

Data analysis was performed using SAS software (Version 9.4 for Windows, SAS Institute Inc., Cary, NC, USA). Descriptive statistics and tests for normality were calculated with the UNIVARIATE procedure of Base SAS software (SAS Institute Inc. 2013. Base SAS® 9.4 Procedures Guide, Second Edition. Cary,NC: SAS Institute Inc.). Data considered as approximately normal were analyzed by ANOVA using the MIXED procedure of SAS/STAT software (SAS Institute Inc. 2013. SAS/STAT® 13.1 User's Guide. Cary, NC: SAS Institute Inc.). The ANOVA model for the 70d data contained the fixed factors line (levels: DUC, DUhTP), group (levels SB, SPF) and the interaction line × group. Homogeneity of covariance parameters across groups was tested for all ANOVA models. In addition, least-squares means (LSM) and their standard errors (SE) were computed for each fixed effect in the models, and all pairwise differences of LS-means were tested by the Tukey–Kramer procedure. Effects and differences were considered significant if $P < 0.05$.

Results

Body mass as a function of animal husbandry

The mouse models DUC and DUhTP were established under semi-barrier conditions starting in the early 1970s and 1980s, respectively. In 2012, all mouse lines were transferred from the semi-barrier unit to the newly built mouse facility with standardized environmental and working procedures defined by the SPF status. Longitudinal analysis of body mass in DUC and DUhTP mice revealed positive effects of SPF husbandry only in DUC but not in DUhTP mice (Fig. 1). At an age of 21 days, DUC_{SPF} mice were heavier by 36.4% ($P < 0.0001$) if compared to DUC mice in the semi-barrier (Fig. 1a). Also, at an age of 42 days, DUC_{SPF} mice were characterized by elevated body mass if compared to

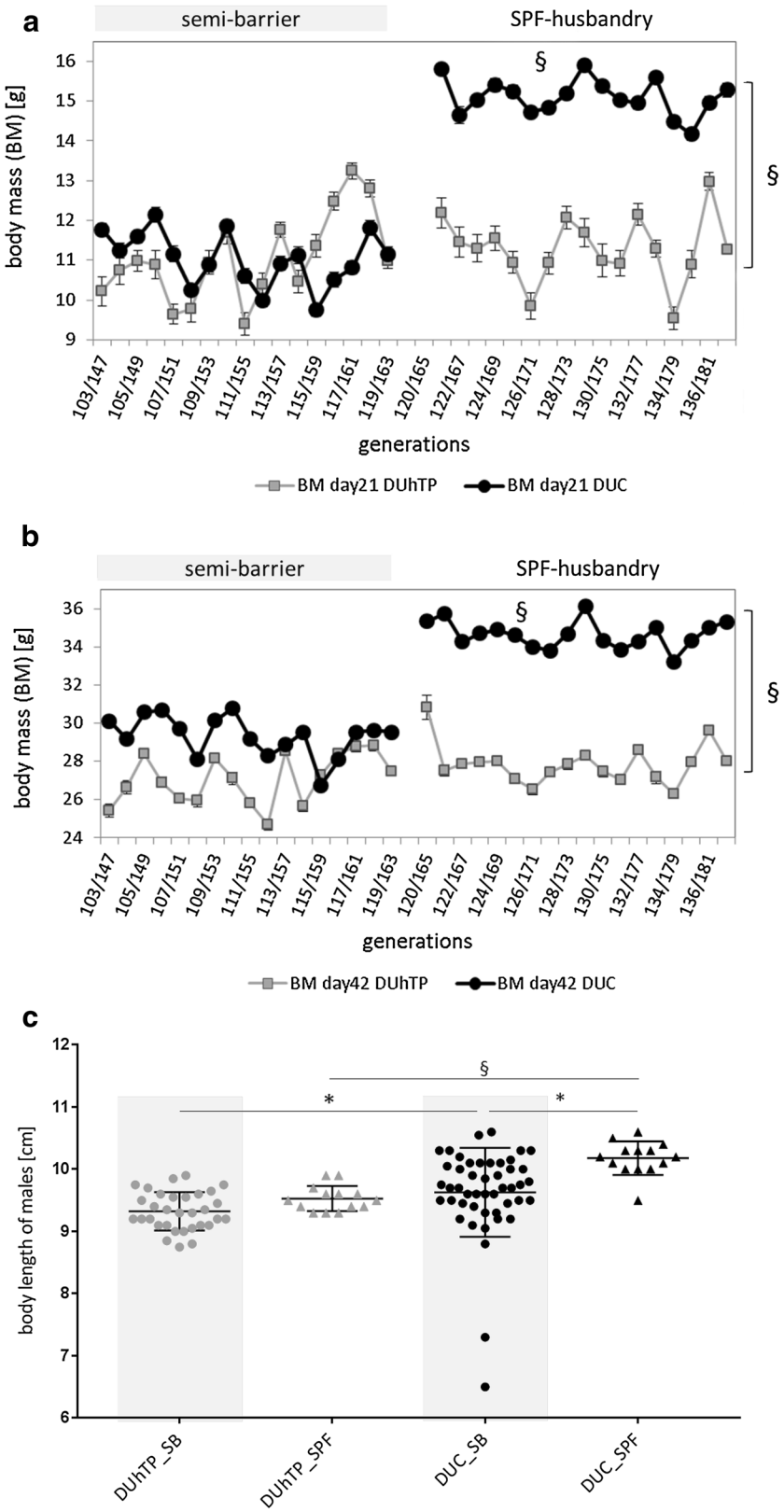

Fig. 1 Body mass and body length of male DUhTP (grey data points) and DUC mice (black data points) kept under semi-barrier or SPF conditions. Body mass is presented for an age of 21 days (**a**) and 42 days after birth (**b**). Body lengths were recorded at day 42 in both mouse lines (**c**). Animals were kept in semi-barrier (dots) and SPF husbandry (triangles), respectively. Data are presented as means ± SE (*$P < 0.05$, § $P < 0.0001$)

DUC mice kept in the semi-barrier (+ 18%; $P < 0.0001$; Fig. 1b). By contrast, both conditions of husbandry did not impact on body mass of DUhTP mice at an age of 21 or 42 days. Under SPF conditions, DUC mice also were significantly taller than mice of the same line in SB husbandry (10.18 ± 0.072 versus 9.63 ± 0.104 cm, $P < 0.01$) while the

body lengths of DUhTP mice were similar in both facilities (Fig. 1c). Consequently, body lengths differed between both mouse lines in SPF husbandry by more almost 7% ($P < 0.0001$). Under semi-barrier conditions, DUhTP mice were smaller by only 3% ($P < 0.05$).

At birth, SPF conditions increased body weights in both mouse lines (DUC + 3.3%; DUhTP + 6.9%; both $P < 0.0001$; Fig. 2a). The body weights of DUhTP mice were higher at birth if compared to DUC mice (BM0 in DUhTP 1.95 g ± 0.03; BM0 in DUC 1.81 g ± 0.02; $P < 0.0001$; Fig. 2a). Interestingly, litter size was significantly increased by SPF husbandry exclusively in DUC mice (DUC + 1.07 littermate, $P < 0.0001$; Fig. 2b), which further increased the difference of litter size between DUC_{SPF} and $DUhTP_{SPF}$ mice (+ 13.7%, $P < 0.0001$).

Postnatal weight gain

Longitudinal assessment of body mass in SPF husbandry revealed higher body weights in DUC_{SPF} versus $DUhTP_{SPF}$ mice shortly between days 6 and 21 after birth (Fig. 3a). DUC_{SPF} offspring has significantly increased level of postnatal weight gain immediately after birth prolonging the whole suckling period. In fact, postnatal weight gain from birth to day 21 identified significantly higher mass accretion in DUC_{SPF} offspring if compared to $DUhTP_{SPF}$ mice (Fig. 3b).

Differential effects of animal husbandry on organ weights

At an age of 70 days under semi-barrier conditions, body and liver weights were higher in DUC_{SB} mice ($P < 0.01$), whereas epididymal and subcutaneous fat depots revealed decrease weights ($P < 0.001$) if compared to $DUhTP_{SB}$ mice (Table 2). Under SPF conditions, higher body and liver weights also were observed in DUC_{SPF} mice ($P < 0.001$). However, the increases of body weights in DUC_{SPF} mice were much higher if compared to semi-barrier husbandry ($P < 0.0001$). In DUC mice, maintained under SPF conditions a more than threefold increase of subcutaneous fat

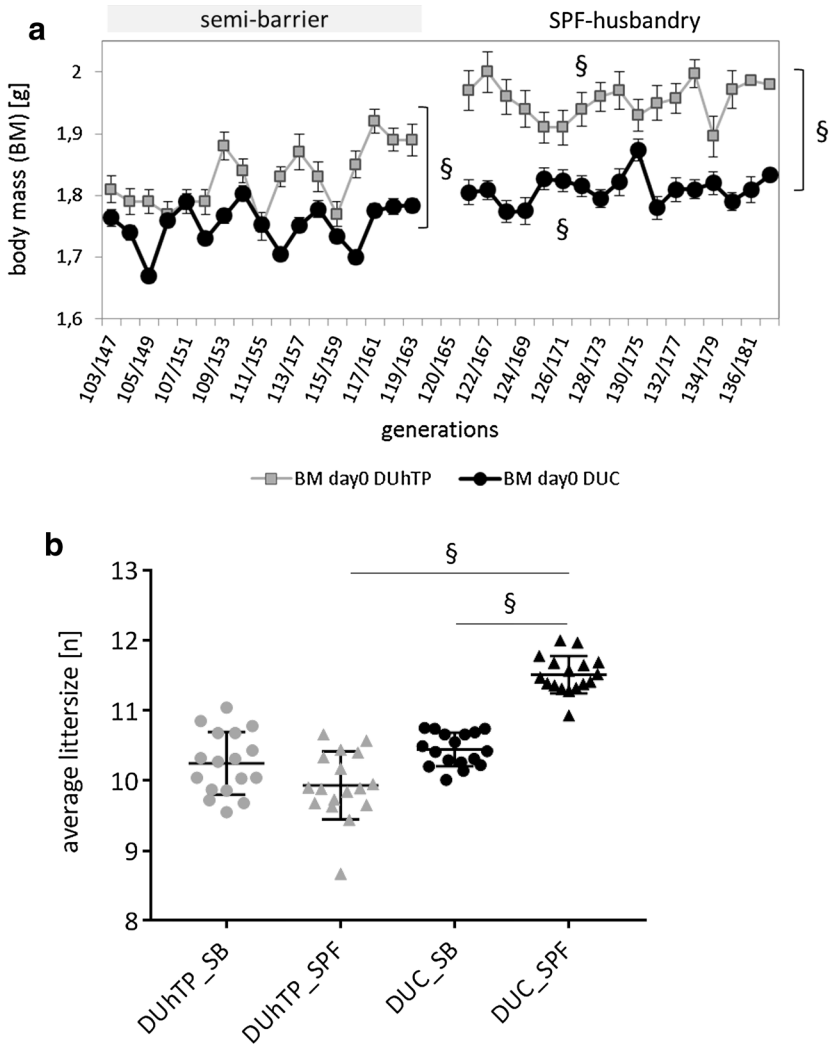

Fig. 2 Birth weight (**a**) and litter size (**b**) in DUhTP (grey data points) and DUC mice (black data points) kept under semi-barrier or SPF conditions. Data are presented as means ± SE (§ $P < 0.0001$)

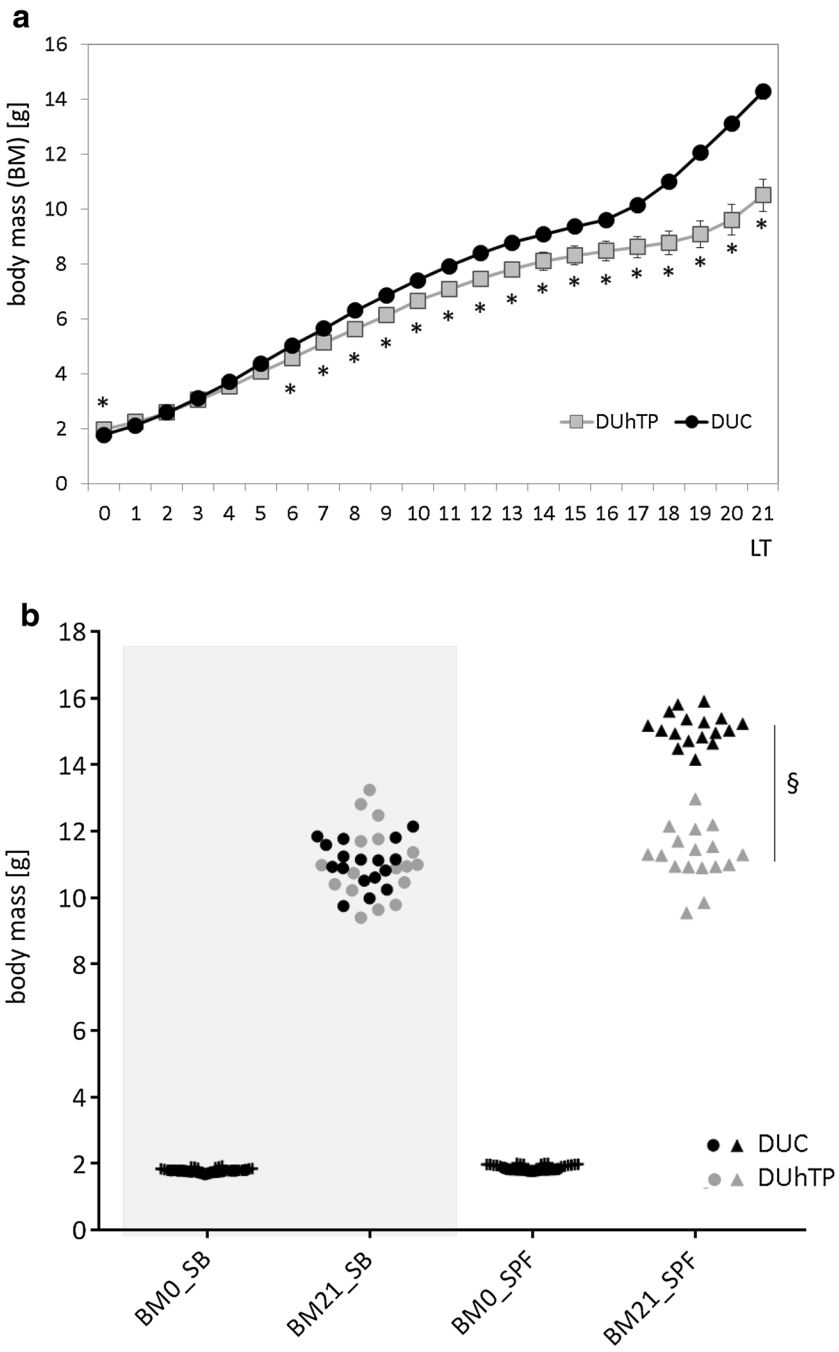

Fig. 3 Postnatal weight gain in DUhTP (grey data points) and DUC mice (black data points) kept under SPF conditions (**a**) and effect of animal husbandry on postnatal weight gain (**b**) in both mouse lines. For the comparison of weight gain, animals of individual generations were kept in semi-barrier (dots) and SPF husbandry (triangle), respectively. One data point represents one generation. Body mass of litter size-standardized pups ($n = 10$) between day 0 and 21 after birth was determined in DUC ($n = 30$, generation 134) and DUhTP ($n = 15$, generation 179) littermates. Data are presented as means ± SE (* $P < 0.05$, § $P < 0.0001$)

mass was observed if compared to semi-barrier husbandry ($P < 0.0001$). In $DUhTP_{SPF}$, an increase of subcutaneous fat by only 25% was found if kept under SPF conditions (not significant). The increase of epididymal fat by about 30% only has borderline significance ($P = 0.067$). By contrast, in $DUhTP_{SPF}$ mice epididymal fat mass was decreased if kept under SPF conditions (− 30%; $P < 0.0001$). Thus, DUhTP mice, characterized by higher fat mass under semi-barrier conditions ($P < 0.001$), have lower fat mass under SPF conditions ($P < 0.001$) if compared to DUC_{SPF} mice.

Generally, while control mice DUC_{SB} in semi-barrier husbandry were characterized by decreased epididymal and subcutaneous fat in contrast to $DUhTP_{SB}$ mice, they show now higher fat masses than $DUhTP_{SPF}$ mice.

In response to SPF husbandry, concentrations of serum TG were decreased in DUhTP ($P < 0.0005$; Fig. 4) and increased in DUC mice ($P < 0.05$). In SB conditions, DUhTP mice were characterized by higher TG level when compared to controls ($P < 0.05$) while under SPF conditions DUC mice had higher TG concentrations than DUhTP mice ($P < 0.0001$).

Table 2 Overview of body masses and tissue weights of 70 day old male DUhTP and DUC mice from individual generations

	n	DUhTP_SB	DUhTP_SPF	*P*	DUC_SB	DUC_SPF	*P*	*P* (DUhTP_SB versus DUC_SB)	*P* (DUhTP_SPF versus DUC_SPF)
Body mass (g)	> 24	30.14 ± 0.60	32.61 ± 0.30	**0.00111**	33.93 ± 0.54	40.52 ± 0.63	< **0.00001**	**0.00002**	< **0.00001**
M. rectus femoris (g)	> 24	0.41 ± 0.01	0.38 ± 0.01	0.10401	0.39 ± 0.01	0.49 ± 0.01	< **0.00001**	0.69878	< **0.00001**
Liver mass (g)	> 24	1.73 ± 0.05	1.74 ± 0.02	0.99655	1.96 ± 0.05	1.97 ± 0.04	0.99983	**0.00143**	**0.00084**
Subcutaneous fat (g)	> 10	0.36 ± 0.03	0.45 ± 0.02	0.44078	0.20 ± 0.01	0.68 ± 0.06	< **0.00001**	**0.00003**	**0.00006**
Epidymal fat (g)	> 21	0.43 ± 0.02	0.24 ± 0.01	< **0.00001**	0.29 ± 0.02	0.38 ± 0.03	0.06680	**0.00043**	**0.00004**
Food consumption (g)	> 8	124.52 ± 7.54	116.79 ± 2.91	0.7332	142.01 ± 9.99	127.85 ± 3.01	0.25107	0.22265	0.22284
RW activity (rounds/3 weeks)	> 19	91,760.5 ± 9292.9	85,651.1 ± 6134.6	0.9578	101,535.9 ± 10,343.6	94,520.4 ± 8245.3	0.94397	0.89926	0.8239

Voluntary running wheel activity and food consumption of DUhTP and DUC mice of individual generations were determined from day 49 to 70. Mice were kept in semi-barrier (SB) and SPF condition. All values are means ± SE; *P* values as indicated; significant differences are printed in bold typeface

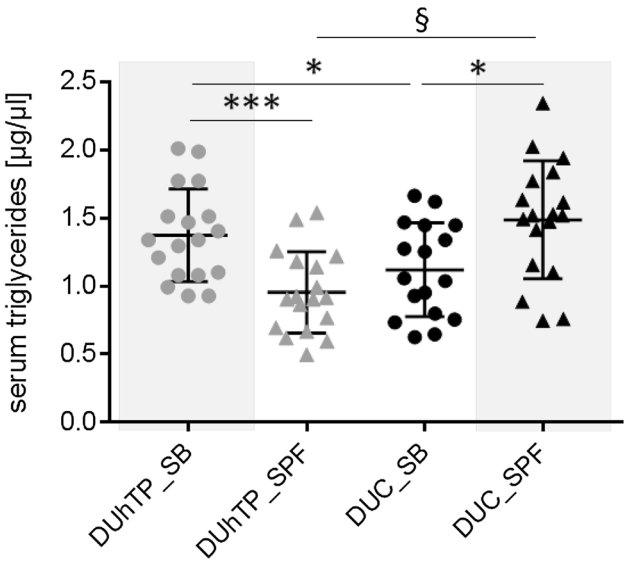

Fig. 4 Concentrations of triglycerides in serum of 70-day-old male DUhTP (grey data points) and DUC mice (black data points). Mice were kept in a semi-barrier (SB; dots) or in an SPF facility (triangles). Data are presented as means ± SE (*$P < 0.05$, ***$P < 0.0005$, § $P < 0.0001$)

Effects of animal husbandry on the IGF system

With respect to the differential effects of animal husbandry on body weight, we assessed serum concentrations of IGF-1 and IGFBPs in both mouse lines maintained under semi-barrier and SPF conditions. However, no significant differences of IGF-1 or IGFBP-2, -3, and -4 could be observed (Table 3). In all conditions assessed, serum concentrations of IGF-1 and IGFBPs were highly variable in both mouse lines.

Effects of animal husbandry on running performance, physical activity, and food consumption

SPF husbandry significantly increased submaximal running performance activity in both mouse lines ($P < 0.0001$) if compared to the semi-barrier (Fig. 5). In DUC_{SPF} or $DUhTP_{SPF}$ mice, an almost 100 or 40% increase was observed, respectively. In absolute terms, the increase of submaximal running performance in $DUhTP_{SPF}$ mice was almost twofold if compared to DUC_{SPF} mice ($DUhTP_{SPF}$ + 1620 m; DUC_{SPF} + 836 m). Thus, $DUhTP_{SPF}$ mice were able to maintain their prominent phenotype of higher running capacities if compared to unselected control mice also under conditions of SPF husbandry ($P < 0.00001$). Voluntary physical activity in running wheels and food consumption, examined at an age between 49 and 70 days during semi-barrier and SPF husbandry in both mouse facilities, were similar in all experimental groups (Table 2).

Effect of food on the body weights

Feeding semi-barrier diet (Altromin) under SPF conditions for two generations in a subpopulation resulted in significantly reduced body weight in DUC_{SPF} mice ($P < 0.0001$) and as a tendency also in $DUhTP_{SPF}$ mice (not significant) at an age of 21 days compared to the Ssniff diet (Fig. 6). While Ssniff-fed DUC mice had a mean body mass of 14.3 g corresponding to the weights of animals in SPF husbandry (15.28 ± 0.18 g), body weights of Altromin-receiving mice were decreased to an average mass of 11.98 g. Therefore, the body weights correspond to those of former animals in semi-barrier husbandry ($DUhTP_{SB}$ 11.25 ± 0.22 g; generation 149). Altromin diet in DUhTP mice increased TG, whereas

Table 3 Serum concentrations of IGF-1, IGFBP-3, IGFBP-2, IGFBP-4 and the ratio between IGFBP-3/IGFBP-2 in 70-day-old DUhTP and DUC mice

	n	DUhTP_SB	DUhTP_SPF	*P*	DUC_SB	DUC_SPF	*P*	*P* (DUhTP_SB versus DUC_SB)	*P* (DUhTP_SPF versus DUC_SPF)
IGF1 (ng/ml)	> 16	308.66 ± 70.58	168.38 ± 49.91	0.12603	192.92 ± 57.10	268.55 ± 74.75	0.44114	0.22510	0.36204
IGFBP-3 (ng/ml)	> 16	1171.43 ± 248.59	769.28 ± 168.81	0.20437	683.12 ± 141.18	875.99 ± 167.67	0.39937	0.10963	0.68958
IGFBP-2 (ng/ml)	> 16	435.76 ± 79.02	344.10 ± 67.90	0.40100	383.36 ± 68.08	367.25 ± 61.6	0.86575	0.62908	0.70329
IGFBP-4 (ng/ml)	> 16	193.35 ± 30.42	200.62 ± 28.29	0.86884	165.33 ± 24.43	258.49 ± 51.32	0.12853	0.49974	0.40422
IGFBP-3/IGFBP-2	> 16	2.90 ± 0.44	2.44 ± 0.48	0.50454	1.89 ± 0.33	3.61 ± 1.05	0.12490	0.08496	0.37222

Animals were kept in semi-barrier (SB) and SPF husbandry, respectively. All values are means ± SE. *P* values as indicated

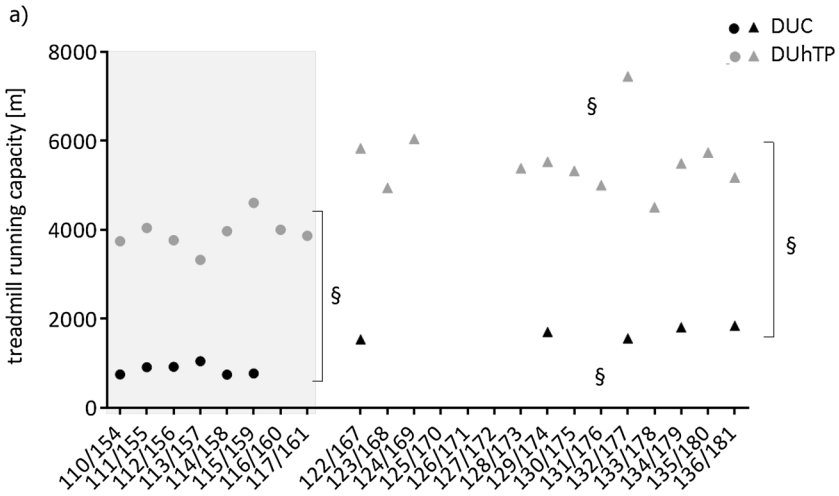

Fig. 5 Long-term assessment of submaximal running capacity in male DUhTP (grey) and DUC mice (black) at an age of 70 days. Between generation 110 and 117 for line DUhTP or between generation 154 and 159 for line DUC, respectively, the animals were kept in semi-barrier conditions (dots). Running performance of DUhTP mice after generation 120 or of DUC mice after 165 generations was assessed in mice maintained under SPF conditions (triangles). Data are presented as means ± SE (§ $P < 0.0001$)

in DUC mice the same diet reduced the concentrations of TG in serum if compared to autoclaved Ssniff diet (Fig. 7).

Discussion

The Dummerstorf high treadmill performance mouse model DUhTP established by long-term selection for high treadmill performance is characterized by highly efficient fat mobilization (Brenmoehl et al. 2015), increased fat cell browning, and higher surface temperature (Brenmoehl et al. 2016) if compared to DUC mice deriving from the identical genetic background at the beginning of the selection experiment. Under conditions of Altromin1314 diet in the semi-barrier, DUhTP mice had a significant lower body mass than controls at day 70 but not at day 49 of age (Brenmoehl et al. 2013, 2015). After hygienic reorganization and establishing of Dummerstorf mouse lines in a new building, defined by the SPF status, we observed line-specific effects of the new environment. Due to the huge dimensions of the selection experiment—spanning more than 35 years now—and concerning the non-inbred structure of the genetic background—maintained by inclusion of up to 100 families per litter—the current phenotype of the mouse model requires an update and a discussion of potential effects due to the relocation or SPF husbandry in DUhTP versus DUC mice.

Body and organ weights

As a major effect of relocation or SPF husbandry, body weights and lengths were increased in DUC_{SPF} mice to a significantly higher dimension if compared to $DUhTP_{SPF}$ mice. The stronger effects of SPF husbandry were evident in mice older than 5 days, when DUC_{SPF} mice have higher body weights due to an increased body weight gain than $DUhTP_{SPF}$ mice. It could be assumed that the higher living weight of the DUC mothers offers a better rearing capacity

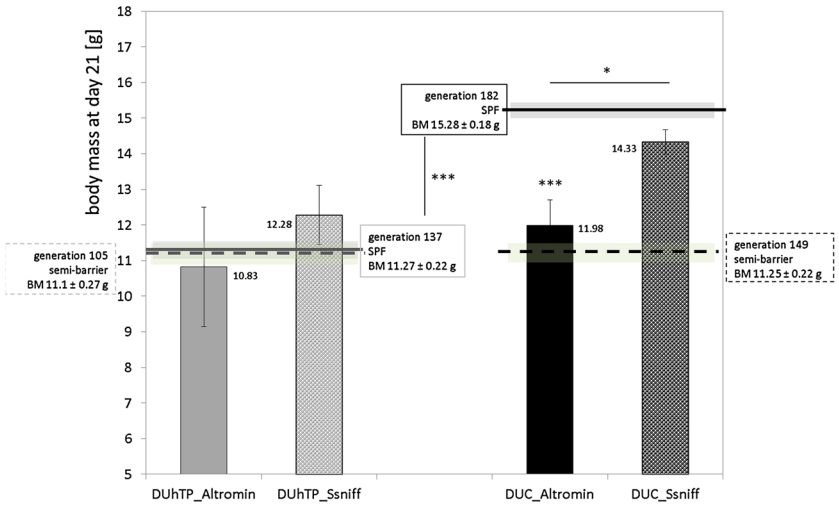

Fig. 6 Effect of diet on body mass in male DUhTP mice (grey bars) and unselected controls (DUC; black bars) maintained under SPF conditions at an age of 21 days. For the experiment, mice of both lines were kept in the quarantine station and either received Altromin diet fed in the semi-barrier or autoclaved Ssniff® diet fed in the SPF facility. The dashed line indicates body weights under conditions of semi-barrier husbandry (DUhTP: generation 105; DUC: generation 149). The continuous line displays body weights monitored within the SPF facility (DUhTP: generation 137; DUC: generation 182). Data are presented as means ± SE (*$P < 0.05$, ***$P < 0.0005$)

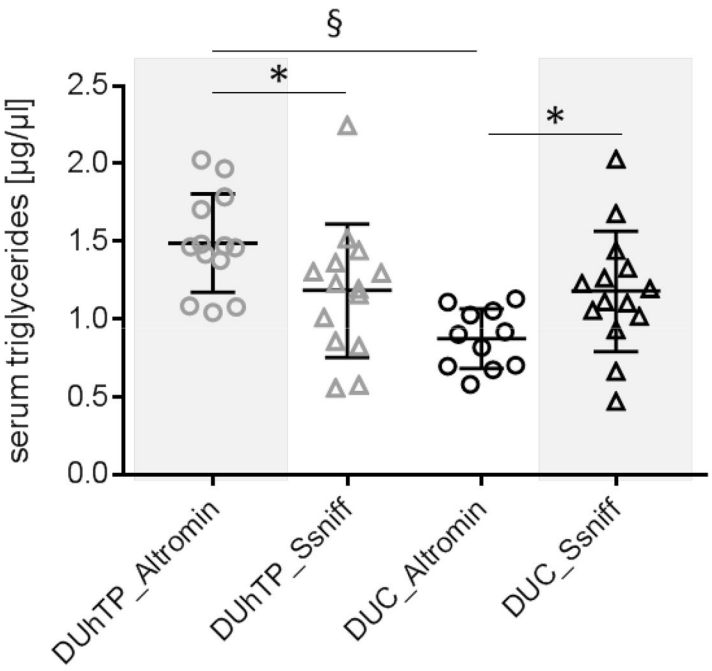

Fig. 7 Effect of diet on concentrations of triglycerides in serum obtained from male DUhTP (grey) and DUC mice (black data points) at an age of 70 days. Mice were kept in the quarantine station under SPF conditions and received SB (Altromin, open dots) and autoclaved SPF diet (Ssniff, open triangles), respectively. Data are presented as means ± SE (*$P < 0.05$, § $P < 0.0001$)

with a better milk supply for the offspring. At an age of 21 and 42 days, DUC_{SPF} mice have significantly increased body weights also if compared to DUC_{SB} mice maintained under semi-barrier conditions. In addition, SPF husbandry differentially affected the accretion of adipose and muscular tissues in both mouse lines. Accordingly, exclusively in DUC_{SPF} mice, muscle mass as well as the amounts of subcutaneous or epididymal fat were increased by SPF husbandry. By contrast, epididymal fat mass was decreased in $DUhTP_{SPF}$ mice if compared to $DUhTP_{SB}$ mice. The differential effects of animal husbandry on fat mass in both mouse lines were reflected also on the level of serum triglycerides, which were decreased by SPF in DUhTP but increased in DUC mice maintained under SPF conditions. For the increase of body weight in both mouse lines, we thus have to consider dietary factors such as food intake and macronutrient composition (Hall and Guo 2017). More generally, food intake or the input of metabolizable energy

were similar in both genetic lines and in both treatment groups at an age of 70 days ($DUhTP_{SB}$ 831.3 ± 89.0 kcal, $DUhTP_{SPF}$ 787.9 ± 42.9 kcal and DUC_{SB} 858.9 ± 36.5 kcal, DUC_{SPF} 812.7 ± 99.8 kcal). However, Ssniff diet contained more metabolizable energy from protein than Altromin (Tabel 2; Ssniff 36%; Altromin 27%). Accordingly, the expense of energy metabolizable from fat (Ssniff 11%; Altromin 13%) or of carbohydrates (Ssniff 53%; Altromin 60%) was higher in Altromin food. In adult mice, the use of high-protein diets can promote weight loss via reduction of fat accretion (Petzke et al. 2014). In the growth period, amino acids have been provided to highly efficient support growth rates in rats (Rogers and Harper 1965). In rats, direct comparison of a high versus low protein diet during pregnancy and lactation revealed higher growth rates in the offspring in a sex-specific manner (Thone-Reineke et al. 2006). The protein-to-energy ratio also was demonstrated in non-rodent animals as an important determinant of weight gain (Garling and Wilson 1976; Dong et al. 2017). An excess of protein intake in mice by means of a 40% protein diet, impaired postnatal growth (Kucia et al. 2011), supporting a major effect of macronutrient composition also in mice. In addition to diet under SPF husbandry, also an improved animal health status due to the absence of defined pathogens has to be considered. To specifically address the effects of Ssniff versus Altromin diet, we applied both diets under SPF conditions over a period of two generations in a subpopulation. In fact, Altromin diet significantly reduced body weight in DUC mice in the absence of specific pathogens under conditions of SPF husbandry. Accordingly, body weights in DUC mice were no longer different if both treatments were compared identifying diet as the causative factor for the prominent weight increases and not the improved health status. In addition, feeding Altromin diet under SPF conditions reversed TG levels in both mouse lines resulting in a relative increase in DUhTP mice but in a decrease in DUC mice. Interestingly, increased protein intake by use of the earlier mentioned high-protein diet impaired liver weights (Kucia et al. 2011) and regulated hepatic expression of the GH/IGF pathway in the perinatal period in mice (Vanselow et al. 2011). In DUC_{SPF} mice, liver weights were unaffected by husbandry in both mouse lines. Because liver is a sensitive target for the effects of growth hormone (GH) (Bates et al. 1964), we may assume that accelerated growth in DUC mice in response to SPF husbandry is not related to altered GH. This assumption is further supported by similar serum concentrations of IGF-1 and IGFBP-3 in all experimental conditions. Both IGF-I and IGFBP-3 represent established biomarkers for GH secretion (Blum et al. 1993). Also, the serum levels of IGFBP-2 were similar in both mouse lines and during semi-barrier or SPF husbandry. Because IGFBP-2 is potently suppressed by GH, IGFBP-2 represents an indirect marker of GH secretion (Kirsch et al. 2007). Finally, the ratio of IGFBP-3/IGFBP-2 as the most sensitive marker of GH secretion (Mesotten 2008) was unaffected by genotype or treatment, which further did not support effects of diet on GH secretion in our experimental system.

The accretion of muscle mass or body fat is related to physical activity or food consumption. However, both parameters also were similar both in DUC mice and in DUhTP mice independent of husbandry.

Litter size and birth weight

Relocation of DUC and DUhTP mice from the semi-barrier to the SPF facility increased the average litter size in DUC_{SPF} mice but not in $DUhTP_{SPF}$ mice. Litter size is a function of inbreeding (Falconer 1960), and inbreeding negatively affects litter size. Two arguments do not support an effect of inbreeding on the increase of litter size in DUC_{SPF} mice. On one hand, during relocation not all DUC families could be transferred resulting in a reduction of genetic complexity in DUC mice. In addition, the increase in litter size in DUC mice was sudden and appears to be stable, which also may argue against a long-term effect of outbreeding. Due to the high number of founder animals in DUC with 110 and in DUhTP with 46 mice during relocation process in both mouse strains, we included a sufficient genetic background for phenotypic variation in different selection traits. The inbreeding level which could affect the fertility traits like litter size (Holt et al. 2004) has increased during the long selection period in both environments (DUC 0.175 and DUhTP 0.592, respectively). But no abrupt rise of the average inbreeding level could be observed after changing to the new mouse facility with SPF hygienic standard. Thus, we suppose the heavier body mass of DUC_{SPF} mothers as a substantial factor or the increasing average number of born pups per litter. Those positive correlation between female body mass at mating and litter size were described by Holt et al. (2004). In addition, diets may have effects on reproductive performance including litter size (Ghosh et al. 2016) and an interaction between diet and genotype has been described in growth selected mice (Corva et al. 2004). Notably, diets with positive effects on body weight also increased reproductive performance in mice (Hoover-Plow et al. 1988), suggesting that the increases of body weight and litter size in DUC_{SPF} mice are connected. Also, in other mammalian species, dietary factors have been identified with an effect on litter size (Gado et al. 2016; Li et al. 2015). Under field conditions, a link between food quality and reproductive performance could not be observed in mice (Ylonen et al. 2003).

Probably due to increased litter size, DUC_{SPF} mice had lower body weights at birth than $DUhTP_{SPF}$ mice. Between days 1 and days 21 after birth, DUC_{SPF} mice were

characterized by significantly increased weight gain if compared to $DUhTP_{SPF}$ mice resulting in higher body weights in DUC mice elder than 5 days if compared to DUhTP mice. The increased growth rate of DUC_{SPF} mice in the perinatal period may thus be due to accelerated compensatory growth or due to SPF husbandry. Very clearly, also in mice neonatal catch-up growth shortly after birth is associated with visceral obesity later in life (Isganaitis et al. 2009). Thus, reduced birth weight in fact may trigger catch-up growth and visceral obesity, and therefore contribute at least in part to the markedly increased body weights in DUC_{SPF} mice. However, in DUC_{SPF} mice also muscle weight was increased if compared to DUC_{SB} mice which is not explained by reduced birth weights or catch-up growth in the perinatal period because low birth weight was associated with increased fat mass but reduced lean mass in mice (Ju et al. 2016). Therefore, also an effect of maternal diet has to be considered which is well documented in the literature, e.g., by the postnatal control of growth or litter performance in suckling pigs (He et al. 2016). Finally, litter size is also a function of fetal mortality (Falconer 1960) and reproductive performance. In rats, the absence of pathogens under SPF conditions significantly increased litter size if compared to a conventional barrier, which was discussed in a context of higher numbers of corpora lutea and decreased post implantation losses of embryos or fetuses (Wakafuji et al. 1984).

Effects of cryopreservation

For the efficient resettlement and establishment of the new and empty mouse facility, embryos from DUC_{SB} mice were cryoconserved by vitrification and transferred into pseudopregnant Crl:CD1(ICR) fosters defined by the SPF status. These generated DUC_{SPF} mice were used for initial stocking of the new SPF facility in Dummerstorf. Additionally, fresh embryos from line DUC_{SB} were transferred to pseudopregnant CD1 and DUC_{SFP} foster mothers. By contrast, fresh embryos from $DUhTP_{SB}$ mice were used for transfer without cryopreservation. Therefore, we cannot exclude that cryoconservation in DUC_{SPF} mice is related to differential phenotype effects of SPF husbandry. In fact, higher body weights have been observed in cryopreserved mice if compared to controls (Dulioust et al. 1995). However, the increases in body weight were described as a long-term effect in adult mice only (Dulioust et al. 1995). Because growth activities were evident early after birth in DUC_{SPF} mice, cryopreservation seems not to account for the differential growth response of DUC versus DUhTP mice during SPF husbandry. Cryopreservation in human embryos explicitly did not affect growth during infancy and early childhood (Wennerholm et al. 1998) also not arguing for an effect of cryoconservation in young DUC_{SPF} mice. In general, it can be doubted that potential epigenetic modification established during handling of the embryo is transmitted to the offspring at all, because in cloned mice altered growth and obesity were found only in the born animal but not in the offspring of cloned mice (Tamashiro et al. 2002). In DUC_{SPF} mice, the phenotype of elevated growth is observed over 15 generations now, not supporting reversible effects of epigenetic modifications.

Effects on running capacity

Animal husbandry in SPF conditions increased absolute weights of body, muscle, and different fat depots in DUC but not in DUhTP mice. These specific effects were not reflected by differential effects on running capacities in DUhTP mice versus DUC mice. Instead, SPF husbandry significantly elevated running capacities in both lines ($P < 0.0001$). Therefore, we may assume that the positive effects of husbandry on endurance exercise are related to improved animal health, due to the lack of specific pathogens and/or to the diet fed in the new SPF facility. Some pathogens (e.g., Helicobacter spp. or Pasteurellaceae) included in hygiene monitoring according to the FELASA guidelines (Mahler Convenor et al. 2014) are less clinically apparent. Under conditions of stress or in the presence of coinfections, clinical signs may become more prominent. Infections with mouse hepatitis virus (MHV) or the presence of endo- and ectoparasites severely can impact on animal health and result in life-threatening tissue damage during acute infection (Baker 2003). Because latent infections form various pathogens could be present under conditions of semi-barrier husbandry, it is conceivable that exercise capacity was limited in DUC_{SB} and $DUhTP_{SB}$ mice by coinfection with different pathogens.

Summary and conclusion

Here, we present a very rare direct comparison of different husbandry conditions on physiological parameters in animal models. The small number of comparative analyses, that can be found in the literature, relates to questions on health status in pigs (Clapperton et al. 2009), effects on immune state in mice (Beura et al. 2016), decontamination of mice (Wiese et al. 2007), or enzyme activity of alkaline phosphatase (Pickering and Pickering 1984). In the present comparative analysis, we demonstrate that both improved health and diet used under SPF conditions have multiple effects in the DUC/DUhTP mouse model. DUC_{SPF} mice have higher body weights at an age of more than 5 days and this effect is almost exclusively an effect of diet. The increased litter size might be an effect both of body weight and improved health and could be responsible for reduced birth weights in DUC_{SPF} mice. The strong increases of running capacities observed in both mouse lines could represent a benefit of

improved health status in both mouse lines due to the lack of pathogens. However, very clearly we provide evidence that DUC and DUhTP mice differentially respond to environmental factors including improved health and an adjusted diet. From the differential increase or decrease of body fat, we may assume that energy metabolism is involved in the differential response of both mouse lines to environmental factors. Our results therefore strongly support the interaction of genomes with the environment, which may inspire the inclusion of environmental factors in phenotype analysis performed in animal models.

Acknowledgements The authors want to thank Luong Chau, Dr. Daniela Ohde, Zianka Meyer and Sabine Hinrichs, Sabine Maibohm, Benita Lucht, Karin Ullerich, Sonja Alm, Dr. Ulla Renne, Erika Wytrwat, and Ines Müntzel for excellent technical assistance. The publication of this article was funded by the Open Access Fund of the Leibniz Institute for Farm Animal Biology (FBN).

Compliance with ethical standards

Conflict of interest All authors declare no conflicts of interest.

References

Baker DG (2003) Natural pathogens of laboratory animals: their effects on research. ASM Press, Washington, DC

Bates RW, Milkovic S, Garrison MM (1964) Effects of prolactin, growth hormone and acth, alone and in combination, upon organ weights and adrenal function in normal rats. Endocrinology 74:714–723

Beura LK et al (2016) Normalizing the environment recapitulates adult human immune traits in laboratory mice. Nature 532(7600):512–516

Blum WF et al (1993) Serum levels of insulin-like growth factor I (IGF-I) and IGF binding protein 3 reflect spontaneous growth hormone secretion. J Clin Endocrinol Metab 76(6):1610–1616

Brenmoehl J et al (2013) Metabolic adaptations in the liver of born long-distance running mice. Med Sci Sports Exerc 45(5):841–850

Brenmoehl J et al (2015) Dynamics of fat mass in duhtp mice selected for running performance—fat mobilization in a walk. Obes Facts 8(6):373–385

Brenmoehl J et al (2016) Browning of subcutaneous fat and higher surface temperature in response to phenotype selection for advanced endurance exercise performance in male DUhTP mice. J Comp Physiol B 187:361–373

Clapperton M et al (2009) Traits associated with innate and adaptive immunity in pigs: heritability and associations with performance under different health status conditions. Genet Sel Evol 41:54

Corva PM et al (2004) Diet effects on female reproduction in high growth (hg/hg) mice that are deficient in the Socs-2 gene. Reprod Nutr Dev 44(4):303–312

Dietl G, Langhammer M, Renne U (2004) Model simulations for genetic random drift in the outbred strain Fzt:DU. Arch Tierzucht 47:595–604

Dong LF et al (2017) Feeding different dietary protein to energy ratios to Holstein heifers: effects on growth performance, blood metabolites and rumen fermentation parameters. J Anim Physiol Anim Nutr (Berl) 101(1):30–37

Dulioust E et al (1995) Long-term effects of embryo freezing in mice. Proc Natl Acad Sci USA 92(2):589–593

Falconer DS (1960) The genetics of litter size in mice. J Cell Comp Physiol 56(Suppl 1):153–167

Falkenberg H, Langhammer M, Renne U (2000) Comparison of biochemical blood traits after long-term selection on high or low locomotory activity in mice. Arch Tierzucht 43:513–522

Gado HM et al (2016) Fertility, mortality, milk output, and body thermoregulation of growing Hy-Plus rabbits fed on diets supplemented with multi-enzymes preparation. Trop Anim Health Prod 48(7):1375–1380

Garling DL Jr, Wilson RP (1976) Optimum dietary protein to energy ratio for channel catfish fingerlings, Ictalurus punctatus. J Nutr 106(9):1368–1375

Ghosh S et al (2016) Severe but Not moderate vitamin B12 deficiency impairs lipid profile, induces adiposity, and leads to adverse gestational outcome in female C57BL/6 mice. Front Nutr 3:1

Hall KD, Guo J (2017) Obesity energetics: body weight regulation and the effects of diet composition. Gastroenterology 152:1718–1727

He B et al (2016) Effects of sodium butyrate supplementation on reproductive performance and colostrum composition in gilts. Animal 10(10):1722–1727

Holt M, Vangen O, Farstad W (2004) Components of litter size in mice after 110 generations of selection. Reproduction 127(5):587 –592

Hoover-Plow J, Elliott P, Moynier B (1988) Reproductive performance in C57BL and I strain mice. Lab Anim Sci 38(5):595–602

Isganaitis E et al (2009) Accelerated postnatal growth increases lipogenic gene expression and adipocyte size in low-birth weight mice. Diabetes 58(5):1192–1200

Ju L et al (2016) Endurance exercise ameliorates low birthweight developed catch-up growth related metabolic dysfunctions in a mouse model. Endocr J 63(3):275–285

Kirsch S et al (2007) Development of an absolute quantification method targeting growth hormone biomarkers using liquid chromatography coupled to isotope dilution mass spectrometry. J Chromatogr A 1153(1–2):300–306

Kucia M et al (2011) High-protein diet during gestation and lactation affects mammary gland mRNA abundance, milk composition and pre-weaning litter growth in mice. Animal 5(2):268–277

Li J et al (2015) Effects of arginine supplementation during early gestation (day 1 to 30) on litter size and plasma metabolites in gilts and sows. J Anim Sci 93(11):5291–5303

Mahler Convenor M et al (2014) FELASA recommendations for the health monitoring of mouse, rat, hamster, guinea pig and rabbit colonies in breeding and experimental units. Lab Anim 48(3):178–192

Mesotten G (2008) Changes within the GH/IGF-I/IGFBP axis in critical illness. In: Berghe GVD (ed) Contemporary endocrinology: acute cause to consequence. Humana Press, New York, pp 181–199

Petzke KJ, Freudenberg A, Klaus S (2014) Beyond the role of dietary protein and amino acids in the prevention of diet-induced obesity. Int J Mol Sci 15(1):1374–1391

Pickering CE, Pickering RG (1984) Alkaline phosphatase activity of the mouse. Comp Biochem Physiol C 79(2):417–424

Rogers QR, Harper AE (1965) Amino acid diets and maximal growth in the rat. J Nutr 87(3):267–273

Tamashiro KL et al (2002) Cloned mice have an obese phenotype not transmitted to their offspring. Nat Med 8(3):262–267

Thone-Reineke C et al (2006) High-protein nutrition during pregnancy and lactation programs blood pressure, food efficiency, and body weight of the offspring in a sex-dependent manner. Am J Physiol Regul Integr Comp Physiol 291(4):R1025–R1030

Vanselow J et al (2011) Hepatic expression of the GH/JAK/STAT/IGF pathway, acute-phase response signalling and complement system are affected in mouse offspring by prenatal and early postnatal exposure to maternal high-protein diet. Eur J Nutr 50(8):611–623

Wakafuji Y et al (1984) Increase in litter size and decrease of post-implantation loss of fetuses observed in an SPF colony of Wistar-Imamichi rats. Jikken Dobutsu 33(2):165–171

Wennerholm UB et al (1998) Postnatal growth and health in children born after cryopreservation as embryos. Lancet 351(9109):1085–1090

Wiese E et al (2007) Decontamination of a barrier facility using microisolator cages and provisional partitioning. Lab Anim (NY) 36(7):31–35

Wirthgen E et al (2016) Quantitative Western ligand blotting reveals common patterns and differential features of IGFBP-fingerprints in domestic ruminant breeds and species. Growth Horm IGF Res 26:42–49

Ylonen H et al (2003) Is reproduction of the Australian house mouse (*Mus domesticus*) constrained by food? A large-scale field experiment. Oecologia 135(3):372–377

5.2 Publikationen zum Einfluss von moderater freiwilliger Bewegung

i) **Brenmoehl, J.**, Ohde, D., Walz, C., Schultz, J., Tuchscherer, A., Rieder, F., Renne, U., Hoeflich, A. (2015). Dynamics of Fat Mass in DUhTP Mice Selected for Running Performance - Fat Mobilization in a Walk. *Obes Facts., 8:373-85. doi: 10.1159/000442399.*

Geleisteter Eigenanteil: Projekt- und Tierversuchsplanung, Phänotypische Erhebungen (Ermittlung des freiwilligen Laufvermögens, Sektion, Gewebeentnahme und –wiegung), Auswertung und Darstellung der Daten sowie Schreiben des Manuskriptes.

ii) **Brenmoehl, J.**, Albrecht, E., Komolka, K., Schering, L., Langhammer, M., Hoeflich, A., Maak, S. (2014). Irisin is elevated in skeletal muscle and serum of mice immediately after acute exercise. *Int J Biol Sci., 10:338-49. doi: 10.7150/ijbs.7972.*

Geleisteter Eigenanteil: Tierversuchsplanung, Phänotypische Erhebungen (Sektion, Gewinnung von Gewebe und Serum), Labortätigkeiten (Western Blots), Schreiben von Manuskriptteilen.

iii) **Brenmoehl, J.**, Ohde, D., Albrecht, E., Walz, C., Langhammer, M., Schultz, J., Hoeflich, A. (2017). Browning of subcutaneous fat and higher surface temperature in response to phenotype selection for advanced endurance exercise performance in male DUhTP mice. *J Comp Physiol B., 187:361-373. doi: 10.1007/s00360-016-1036-7.*

Geleisteter Eigenanteil: Projekt- und Tierversuchsplanung, Phänotypische Erhebungen (Sektion, Gewinnung von Gewebe und Serum), Koordinierung der Wärmebildaufnahmen, Labortätigkeiten (qRT-PCR, Western Blots), Auswertung und Darstellung der Daten sowie Schreiben des Manuskriptes.

iv) **Brenmoehl, J.**, Ohde, D., Walz, C., Tuchscherer, A., Hoeflich, A. (2020). Analysis of Activity-Dependent Energy Metabolism in Mice Reveals Regulation of Mitochondrial Fission and Fusion mRNA by Voluntary Physical Exercise in Subcutaneous Fat from Male Marathon Mice (DUhTP). *Cells, 9:2697. doi: 10.3390/cells9122697.*

Geleisteter Eigenanteil: Projekt- und Tierversuchsplanung, Phänotypische Erhebungen (Sektion, Gewinnung von Gewebe und Serum), Auswertung und Darstellung der Daten sowie Schreiben des Manuskriptes.

Obesity Facts
The European Journal of Obesity

Obes Facts 2015;8:373–385
DOI: 10.1159/000442399
Received: July 6, 2015
Accepted: October 8, 2015
Published online: December 3, 2015

1662–4033/15/0086–0373$39.50/0
www.karger.com/ofa

Karger Open access

Original Article

Dynamics of Fat Mass in DUhTP Mice Selected for Running Performance – Fat Mobilization in a Walk

Julia Brenmoehl[a, b] Daniela Ohde[a] Christina Walz[a, b] Julia Schultz[c]
Armin Tuchscherer[d] Florian Rieder[e] Ulla Renne[b] Andreas Hoeflich[a, b]

[a]Cell Signaling Unit from the Institute for Genome Biology, Leibniz-Institute for Farm Animal Biology (FBN), Dummerstorf, Germany; [b]Laboratory for Mouse Genetics, Institute for Genetics & Biometry, Leibniz Institute for Farm Animal Biology (FBN), Dummerstorf, Germany; [c]Institute of Medical Biochemistry and Molecular Biology, University of Rostock, Rostock, Germany; [d]Livestock Genetics and Breeding Unit, Institute for Genetics & Biometry, Leibniz-Institute for Farm Animal Biology (FBN), Dummerstorf, Germany; [e]Department of Pathobiology, Lerner Research Institute, Cleveland Clinic Foundation, Cleveland, OH, USA

Key Words
Adipose tissue · Subcutaneous adipose tissue · Fat loss · Mitochondrial biogenesis · Physical activity

Abstract
Objective: Reduction of body fat can be achieved by dietary programs and/or aerobic exercise training. More convenient methods to rid the body of excess fat are needed. However, it is unclear whether it is possible to more easily lose body weight at all. ***Methods:*** DUhTP mice bred through phenotype selection for high treadmill performance and unselected controls were voluntarily physically active in a running wheel over a period of 3 weeks. Phenotypical data were collected, and subcutaneous fat was analyzed for expression of mitochondria-relevant proteins. ***Results:*** Voluntary physical activity over 3 weeks exclusively in DUhTP mice severely reduced subcutaneous (–38%; $p < 0.05$) and epididymal (–32%; $p < 0.05$) fat. Following mild physical activity, subcutaneous fat derived from DUhTP mice showed increased levels of long chain acyl dehydrogenase (LCAD; +230%; $p < 0.05$) and peroxisome proliferator-activated receptor gamma coactivator 1-alpha (PGC1-α; $p < 0.01$). Mitochondrial transcription factor A (Tfam) expression was similar in both sedentary genotypes but physical activity in-

Julia Brenmoehl and Daniela Ohde contributed equally to the paper.

Dr. Andreas Hoeflich
Cell Signaling Unit from the Institute for Genome Biology
Leibniz-Institute for Farm Animal Biology (FBN)
Wilhelm-Stahl-Allee 2, 18196 Dummerstorf, Germany
hoeflich@fbn-dummerstorf.de

Obes Facts 2015;8:373–385
DOI: 10.1159/000442399

creased Tfam levels exclusively in DUhTP ($p < 0.05$). ***Conclusion:*** Our findings indicate that the mitochondrial mass is highly active in DUhTP mice and responsive even to mild physical activity. While genetic predisposition could not prevent fat accretion in DUhTP mice, voluntary activity was sufficient to reduce excess body fat almost completely.

Introduction

Surplus energy is stored in the form of lipids in white adipose tissue (WAT). Hence WAT mass can be used as a marker of positive energy balance in a given organism [1]. Under conditions of negative energy balance, e.g. during physical exercise, elevated lipolytic activity in WAT results in an increase of non-esterified ('free' or unsaturated) fatty acids in the circulation, which serve as the main energy source of the muscle [2]. With increasing energy demands, for example during high-intensity physical exercise, fat and glycogen from the muscle get recruited for energy production [3, 4]. Utilization of energy from fat stores can be augmented by distinct resistance exercise training protocols [5, 6]. Lipolytic activity in WAT can be induced or blocked by growth hormone, cortisol, interleukin-6, β-adrenergic signaling or insulin [2, 4]. Different pharmacological approaches have been tested concerning their potential to induce fat degradation, e.g., L-carnithin, polyphenols, and others [7].

An increase of WAT mass was also observed in our mouse model, generated by long-term selection for high treadmill performance (DUhTP mice [8]). As shown previously, DUhTP mice have the same voluntary activity if running wheels (RWs) were included in their home cages [8]. Thus obesity in DUhTP mice seems not being related to altered physical activity. DUhTP mice are characterized by about fourfold increased endurance running capacity, increased hepatic lipogenesis, hyperlipidemia, and massive accumulation of body fat in external fat depots compared to unselected control mice [8]. Their fat depots contain high amounts of energy, exceeding the requirements of even ultra-long distance runs or extreme resistance training.

While control of exercise-related energy metabolism has been intensively studied in muscle, adipose tissue has received only limited attention [9]. In rat muscles, endurance training leads to increases of tricarboxylic acid cycle activity, β-oxidation, and oxidative phosphorylation [10–12]. Specific enzyme activity providing β-oxidation, such as palmityl CoA dehydrogenase and carnithine palmitoyltransferase (CPT1), increases in response to exercise [12]. In women, prolonged physical activity resulted in an increase of medium and very long chain acyl CoA (MCAD) dehydrogenase in skeletal muscles [13]. However, glycerol release from muscle is small, compared to release from subcutaneous adipose tissue during moderate- and high-intensity exercise [14]. Both, physical activity and exercise can induce metabolic activity and mitochondrial biogenesis also in adipose tissues. Specifically, citrate synthase activity [15], mRNA expression of peroxisome proliferator-activated receptor gamma coactivator 1-alpha (PGC1-α) as well as cytochrome c oxidase and mitochondrial content have been found to be regulated by exercise in adipose tissues [16, 17]. Exercise-related induction of mitochondrial biogenesis and glucose uptake in subcutaneous fat tissues are dependent on endothelial nitric-oxide synthase (eNOS) as described previously [16].

Key regulators of lipid oxidation (MCAD, CPT1) are increased in muscle through an increase in PGC1-α [18, 19] as shown in muscles of exercising DUhTP mice [20]. PGC1-α is a known inducer of mitochondrial mass and increases the amounts of mitochondrial DNA (mtDNA) [19, 21, 22]. Furthermore, PGC1-α coordinately induces expression of the mitochondrial transcription factor (Tfam) enhancing the replication of mtDNA and transcription of mitochondria-encoded genes [23]. In response to exercise, expression of Tfam or of mitochondria- and nucleus-encoded mitochondrial proteins was increased in muscles and adipose

Obes Facts 2015;8:373–385
DOI: 10.1159/000442399

tissue of rats, mice, and humans [15, 24–26]. We thus hypothesized that energy metabolism in WAT is altered in DUhTP mice in a manner improving muscle supply with energy, in particular fatty acids. In order to test the hypothesis of an increased energy-metabolic activity in WAT of DUhTP mice, we studied expression of lipid metabolic key enzymes and mitochondrial biogenesis in the presence and absence of RWs. By means of long-term selection in DUhTP mice, we demonstrate that it is possible to metabolize excess body fat in a walk.

Material and Methods

Animals

All in vivo experiments were performed in accordance with national and international guidelines and were approved by our internal institutional review board. In this study, we used a mouse model that has been generated by selection over 90 generations for high treadmill performance (marathon mice: DUhTP) and random selection (control mice: DUC). Both mouse lines were bred from the identical base population [8] avoiding inbreeding. In the original base population, 4 different outbred (NMRI orig., Han:NMRI, CFW, CF1) and 4 different inbred mouse lines (CBA/Bln, AB/Bln, C57BL/Bln, XVII/Bln) were included. The animals were housed in Makrolon cages Type II (EBECO, Castrop-Rauxel, Germany) under controlled environmental conditions in a semi-barrier system. Mice received fresh tap water and fixed formula food ad libitum (Altromin® 1314, Altromin GmbH, Lage, Germany). Body composition was quantified by dual energy X-ray absorptiometry (Lunar PIXImus II, GE Medical Systems, Solingen, Germany).

Running Wheel Performance

Physical activity was assessed over a period of 3 weeks in 49- to 70-day-old male DUhTP mice and controls by including RWs (diameter = 33.4 cm; Tecniplast, Hohenpeißenberg, Germany) in their home cages. A control group of mice was kept in cages without RWs. Mice were fasted overnight, killed by decapitation (N = 10), and serum samples were collected. Tissues were weighted, snap-frozen in liquid nitrogen, and stored at –70 °C for subsequent analysis.

Analysis of Triglycerides and Cholesterol

Triglycerides (TG) and cholesterol were assayed in serum and liver samples by using commercial kits (triglycerides: No. LT-TR 0015, total cholesterol: No. LT-CH 0031; both Labor & Technik Eberhard Lehmann, Berlin, Germany) as described previously [8].

Quantitative Real Time-PCR (qPCR)

Expression of PGC1-α mRNA transcripts in subcutaneous fat samples (N = 7) was analyzed as described previously [20] and primers used are summarized in table 1. Different housekeeping genes (HKGs; *Hprt1*, *Rplp2*, and *β-actin*) were tested, identifying the HKGs with comparable Crossing point (Cp) values (Cp_{Rplp2}: DUhTP mice = 24.45 ± 1.17; DUC mice = 25.80 ± 1.03) to normalize expression of PGC1-α. Mitochondrial DNA (mtDNA) was determined by comparison of gene expression levels of cytochrome B mtDNA and large ribosomal protein p0 (36B4).

Immunoblotting

Western immunoblotting was performed as described previously [20]. Equal loading of the gels and proper transfer of the proteins to the membranes were verified by Coomassie blue staining. We analyzed the expression of PGC1-α, fatty acid synthase (FAS), long chain acyldehydrogenase (LCAD), Tfam, sirtuin 3 (SIRT3), and NADH-ubiquinone oxidoreductase alpha subunit 9 (NDUFA9) of complex I by using specific antibodies (table 2).

Mitochondrial Morphology in Adipose Tissue

Mitochondrial staining was performed on 5 µm thick frozen tissue sections using MitoTracker® Deep Red (Molecular Probes®; Invitrogen, Darmstadt, Germany) for 30 min at 37 °C. Tissues were fixed in ice-cold acetone (–20 °C) for 10 min [27]. All sections were counterstained with Dapi (Vector Laboratories, Burlingame, CA, USA), and mitochondrial morphology was observed using a confocal laser-scanning microscope Fluoview FV10i (Olympus, Hamburg, Germany).

Obes Facts 2015;8:373–385
DOI: 10.1159/000442399

Table 1. Sequences of primer sets used for amplification of specific cDNA

Name	5′ → 3′	To detect
PGC1-α1-forw PGC1-α1-rev	ggacatgtgcagccaagactct cacttcaatccacccagaaagct	PGC-1a isoform 1, inducer of browning
Hprt1-forw Hprt1-rev	tcctcctcagaccgctttt cctggttcatcatcgctaatc	hypoxanthine guanine phosphoribosyl transferase 1
Rplp2-forw Rplp2-rev	cagtctagagctcctggaaggt tgtggaaaacagcaggttagc	ribosomal protein, large P2
CytB-forw CytB-rev	cttcgctttccacttcatcttacc ttgggttgtttgatcctgtttcg	cytochrome B
36B4-forw 36B4-rev	aggatatgggattcggtctcttc tcatcctcctgcttaagtgaacaaact	large ribosomal protein p0
beta-actin-forw beta-actin-rev	tgacaggatgcagaaggaga cgctcaggaggagcaatg	actin, beta, cytoplasmatic

Table 2. Primary antibodies used for western immunoblotting

Name	Catalogue number	Company
PGC1-α	sc-13067	Santa Cruz Biotechnology
FAS	sc-20140	Santa Cruz Biotechnology
LCAD	sc-82466	Santa Cruz Biotechnology
Tfam	sc-23588	Santa Cruz Biotechnology
ND-1	sc-20493	Santa Cruz Biotechnology
NDUFA9	sc-58392	Santa Cruz Biotechnology
SIRT3	sc-99143	Santa Cruz Biotechnology

Statistical Analysis

The data analysis was performed using SAS software (Version 9.4 for Windows, SAS Institute Inc., Cary, NC, USA). Descriptive statistics and tests for normality were calculated with the UNIVARIATE procedure of Base SAS software (Base SAS® 9.4 Procedures Guide, 2nd ed; SAS Institute Inc.). Data considered as approximately normal were analyzed by ANOVA using the GLIMMIX procedure of SAS/STAT software (SAS/STAT® 13.1 User's Guide; SAS Institute Inc.). The ANOVA model for the 70-day data contained the fixed factors line (levels: DUC, DUhTP), group (levels: control, RW), and the interaction line × group. The model for the variables rel_subcutaneous_fat, rel_epididymal_fat, rel_perinephric_fat, and rel_brown_fat included the fixed effects line (levels: DUC, DUhTP), group (levels: 49 days, 70 days, 70 days + RWs), and the interaction line × group. Homogeneity of covariance parameters across groups was tested for all ANOVA models. In addition, least-squares means (LSM) and their standard errors (SE) were computed for each fixed effect in the models, and all pairwise differences of LS means were tested by the Tukey-Kramer procedure. Effects and differences were considered significant if $p < 0.05$.

Results

Physical Changes in DUhTP Mice in Response to Moderate Physical Activity

DUhTP mice accomplished 3,935 ± 1,719 revolutions per day (r/day) at an age of 70 days, which was comparable to control mice (3,913 ± 1,181 r/day). Table 3 shows the phenotypical alterations in our mouse lines in the presence and absence of RWs. Although body weights were different in both mouse lines, liver and muscle mass (M. quadriceps femoris) were

Obes Facts 2015;8:373–385
DOI: 10.1159/000442399

Table 3. Phenotypical traits of male mice long-term selected for high treadmill performance (DUhTP) and unselected controls (DUC) at an age of 70 days[a]

	n	DUhTP			DUC			p value	
		co	RW	p value	co	RW	p value	DUhTP-co vs. DUC-co	DUhTP-RW vs. DUC-RW
Body mass, g	10	32.18 ± 1.02	31.25 ± 0.87	0.4925	35.18 ± 0.67	34.65 ± 0.79	0.6125	0.0191	0.0066
Lean body mass, g	10	20.89 ± 0.59	20.49 ± 0.59	0.6314	23.56 ± 0.48	23.45 ± 0.54	0.8693	0.0012	0.0007
Body length, cm	10	10.04 1 0.12	9.93 1 0.11	0.4907	10.44 ± 0.10	10.42 1 0.09	0.8845	0.0135	0.0014
Musculus rectus femoris, g	10	0.37 ± 0.01	0.38 ± 0.01	0.2969	0.39 ± 0.01	0.36 ± 0.01	0.0795	0.1378	0.1767
Liver mass, g	10	1.81 ± 0.07	1.76 ± 0.08	0.6301	1.94± 0.06	1.82 ± 0.06	0.1513	0.1571	0.5192
Subcutaneous fat, g	10	0.36 ± 0.03	0.22 ± 0.03	0.0012	0.20 ± 0.01	0.18 ± 0.02	0.4910	0.00003	0.2448
Epidymal fat, g	10	0.33 ± 0.03	0.23 ± 0.03	0.0145	0.28 ± 0.03	0.20 ± 0.02	0.0183	0.2122	0.2718
Perinephric fat, g	10	0.16 ± 0.02	0.08 ± 0.01	0.0020	0.09 ± 0.01	0.06 ± 0.01	0.0086	0.0035	0.2327
Brown fat, g	10	0.09 ± 0.01	0.07 ± 0.00	0.0191	0.06 ± 0.00	0.06 ± 0.00	0.7512	0.0006	0.1189
Serum triglyceride, mg/ml	>7	1.37 ± 0.12	0.96 ± 0.08	0.0079	1.15 ± 0.12	0.90 ± 0.06	0.0694	0.1999	0.5438
Serum cholesterol, µg/ml	>7	1.97 ± 0.09	1.95 ± 0.07	0.8103	1.58 ± 0.04	1.63 ± 0.07	0.5841	0.0003	0.0039
Liver triglyceride, µg/mg	>7	13.09 ± 1.74	6.43 ± 0.33	0.0049	6.25 ± 0.32	7.10 ± 0.33	0.1003	0.0042	0.1840
Liver cholesterol, µg/mg	>7	3.72 ± 0.24	2.51 ± 0.22	0.0007	3.38 ± 0.18	3.61 ± 0.20	0.3937	0.2710	0.0007

[a] Mice were kept in cages without (co) and with running wheels (RW). Physical activity was studied in RW for a period of 3 weeks in 7- to 10-week male mice of both lines. Total body lean mass was analyzed by dual energy X-ray absorptiometry. Vales are presented as mean ± SE. Significances like indicated.

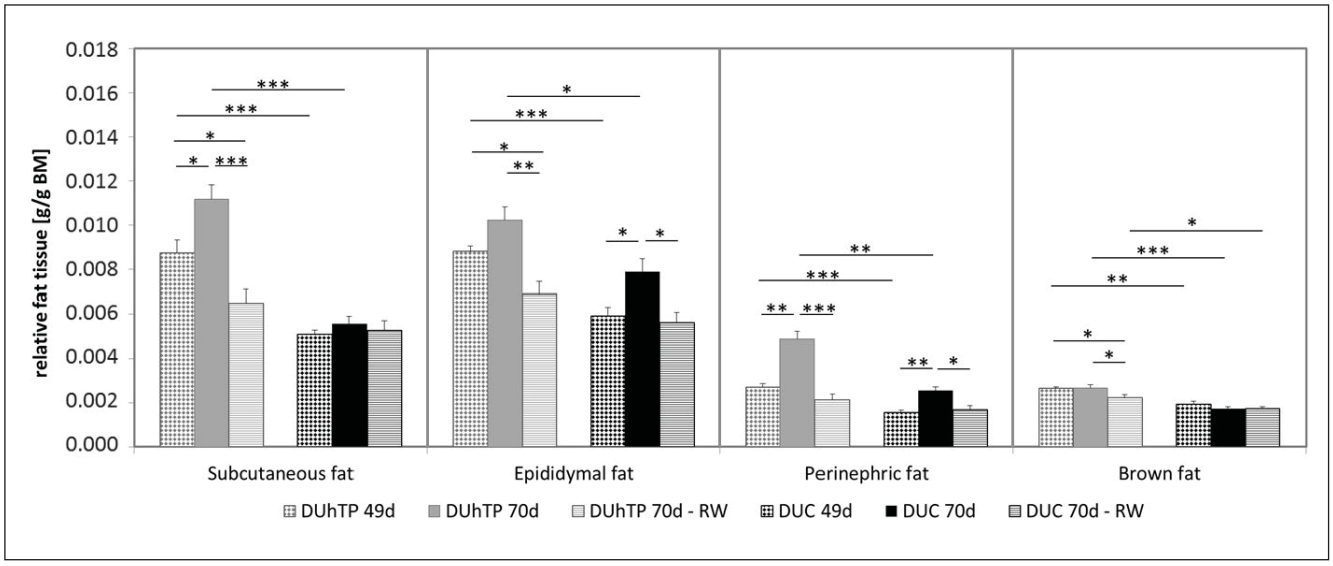

Fig. 1. Weights of subcutaneous, epididymal, perinephric, and brown fat depots normalized to body weight in 7- and 10-week-old male DUhTP (grew bars) and DUC mice (black bars) (n = 10). At an age of 7 weeks mice were kept in cages with (striped bars) or without RWs (filled bars) for a period of 3 weeks. Values are means ± SE; *p < 0.05, **p < 0.005, ***p < 0.0005.

similar in all experimental groups. In DUhTP mice serum, cholesterol concentrations were 1.3-fold ($p < 0.05$) higher compared with controls. In the liver of DUhTP mice levels of TG were 2.1-fold higher than in DUC mice ($p < 0.01$). In response to physical RW activity over a period of 3 weeks, exclusively DUhTP mice showed reduced concentrations of serum TG ($p < 0.01$) and lower levels of hepatic TG or hepatic cholesterol ($p < 0.05$). Liver TG and cholesterol were lower in DUhTP mice having access to RWs compared with DUC ($p < 0.001$). At an age

Obes Facts 2015;8:373–385
DOI: 10.1159/000442399

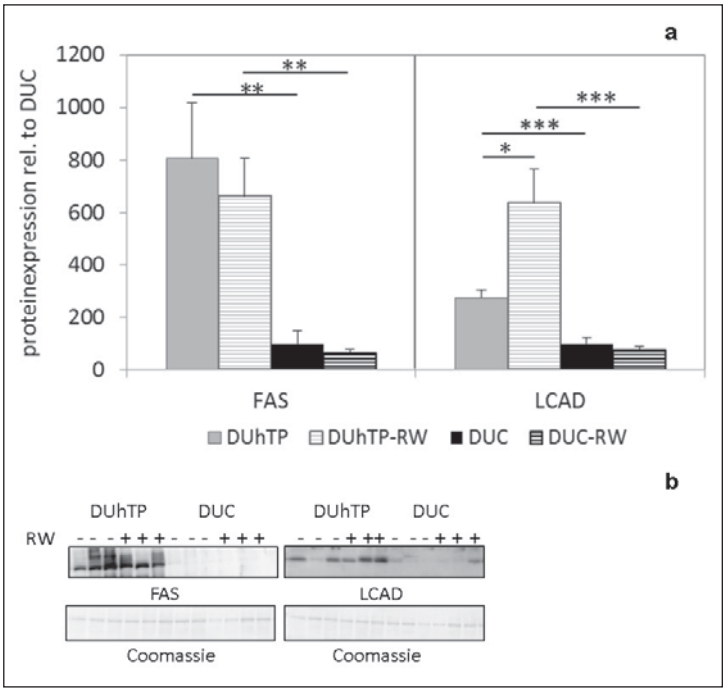

Fig. 2. a Effect of voluntary physical activity in RWs on protein expression of FAS (left panel) and LCAD (right panel) in subcutaneous fat tissue of 10-week-old male DUhTP and DUC mice. **b** The analysis was performed by Western immunoblotting. Protein expression was quantified by densitometry and normalized for the Coomassie blue signal. Data are presented as means and SE and are expressed relative to the expression level of control mice from line DUC (lower panel). Significant differences are indicated: *p < 0.05, **p < 0.005.

of 49 days, DUhTP mice were characterized by increased amounts of fat present in different fat depots (subcutaneous, epididymal, perinephric, and brown fat mass) compared with DUC mice. Highest differences of relative fat mass were observed for the subcutaneous and perinephric fat (≈ 70% increase; fig. 1). The marked increases in fat mass were even more pronounced at an age of 70 days in DUhTP mice (subcutaneous fat: +100%, perinephric fat +91%; $p < 0.005$). Also for epididymal and brown fat tissues significant increases were present in 70-day-old DUhTP when compared to DUC mice (>30%; $p < 0.05$). Interestingly, voluntary physical activity in 70-day-old DUhTP mice significantly reduced absolute weights of all fat depots assessed compared with their sedentary 70-day-old littermates (table 2). If normalized for body mass, reductions were most obvious in perinephric fat (–56%; $p < 0.0005$; fig. 1) and subcutaneous fat (–38%; $p < 0.0005$) followed by epididymal and brown fat (–32% and –17%, respectively; $p < 0.05$). Voluntary physical activity also reduced fat mass in control DUC mice compared to sedentary littermates in the epididymal (–28%) and perinephric fat depots (–34%), while brown and subcutaneous fat depots remained unchanged. In subcutaneous and perinephric fat, we were able to observe age-related increases of fat accumulation between 49 days and 70 days of age (+29% and +80%, respectively; $p < 0.05$). Moreover, physical activity reduced fat masses in subcutaneous, epididymal and brown fat (–20%, –21% and –15% respectively; $p < 0.05$) in 70-day-old DUhTP mice not only when compared to sedentary littermates but also if compared to 49-day-old mice of the same line. Taken together, voluntary physical activity was able to eliminate the mouse line-specific accumulation of body fat in subcutaneous, epididymal, and perinephric tissues in DUhTP mice. Exclusively in subcutaneous fat, we were able to observe both a block of age-related fat increase as well as active degradation of existing body fat at an age of 49 days. We therefore focused on the control of energy metabolism in subcutaneous fat tissue in this subgroup.

Expression of Fat-Producing and -Degrading Enzymes in Subcutaneous Fat

At an age of 70 days subcutaneous fat tissue from DUhTP mice was characterized by massive expression of FAS in both experimental groups (fig. 2, left panel). In sedentary mice,

Obes Facts 2015;8:373–385
DOI: 10.1159/000442399

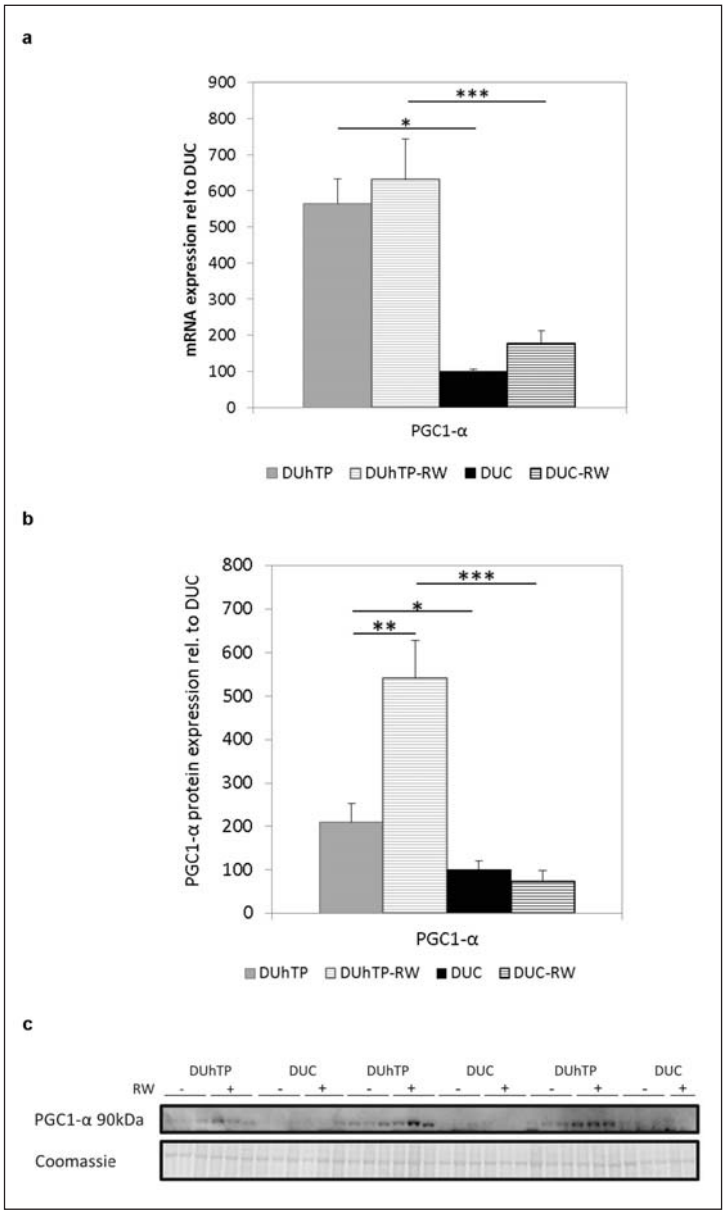

Fig. 3. Effect of voluntary physical activity in RWs on relative mRNA (**a**) and protein (**b**) levels of PGC-1a in subcutaneous adipose tissue from DUhTP and DUC. Analysis of mRNA expression was performed by qPCR and normalized to expression of HKG Rplp2. **c** Protein analysis was performed by Western immunoblotting. Protein expression was quantified by densitometry and normalized for the Coomassie blue signal. All data are expressed relative to the expression level of sedentary unselected controls (DUC) with no access to RW (lower panel). Values are means ± SE; *p < 0.05, **p < 0.005, ***p < 0.0005.

FAS expression in DUhTP animals was about eightfold ($p < 0.005$) higher compared to DUC mice, indicating higher lipid synthesis in subcutaneous fat. In the presence of RWs, the high level of FAS expression was maintained in DUhTP mice, and voluntary physical activity did not have any effect on FAS expression in both mouse lines. Furthermore, expression of the lipid-degrading enzyme LCAD was elevated in sedentary DUhTP versus DUC mice (threefold; $p < 0.0005$). Physical activity over a period of 3 weeks further increased LCAD expression (2.3-fold; $p < 0.05$) in subcutaneous fat tissue of DUhTP, but not of DUC mice (fig. 2, right panel).

Mitochondrial Biogenesis in Subcutaneous Fat

The more than twofold increase of LCAD expression in subcutaneous fat in response to physical activity led us to investigate PGC1-α-mediated mitochondrial biogenesis in our system. PGC1-α mRNA expression was significantly increased in DUhTP mice (5.6-fold; $p < 0.0005$) compared to controls. Physical activity as a trend increased mRNA expression of PGC1-α in

Obes Facts 2015;8:373–385
DOI: 10.1159/000442399

subcutaneous fat of both mouse lines (12% or 77%). The transcription data was confirmed via immunoblot by higher expression of the PGC1-α isoform 1 in sedentary DUhTP mice (2.1-fold; $p < 0.05$; fig. 3b). Interestingly, physical activity significantly increased protein levels of PGC1-α (+157%; $p < 0.0005$) in DUhTP, but not in DUC mice. To further address PGC1-α-mediated induction of mitochondrial biogenesis, we investigated protein expression of Tfam, mitochondria-encoded subunit ND-1 of respiratory chain complex I, NDUFA9 as well as mitochondrial SIRT3 (fig. 4). In total subcutaneous fat tissue extracts, two isoforms of Tfam (fig. 4a) were detected (mitochondrial Tfam: ~29 kDa; nuclear Tfam: ~25 kDa; Uni-Prot P40630). DUhTP mice as a trend showed increased levels of mitochondrial Tfam (+41%), whereas protein levels of nuclear Tfam were similar in both mouse lines. Mitochondrial and nuclear Tfam was significantly elevated in response to physical activity in DUhTP mice only (+40% and +75%, respectively; $p < 0.05$). Tfam-related expression of ND-1 in mitochondria (fig. 4a) was also significantly increased in DUhTP compared with control mice (+76%; $p < 0.05$). In the presence of RWs, protein expression of ND-1 was elevated as a trend by 31% (DUhTP) and 25% (DUC). In sedentary DUhTP mice, protein levels of complex I subunit NDUFA-9 and SIRT3 (fig. 4b) were increased if compared to DUC mice. In mitochondria, physical activity significantly increased protein levels exclusively in DUhTP mice (NDUFA9: 1.5-fold, $p < 0.05$; SIRT3: about 2.3-fold, $p < 0.05$). Furthermore, in subcutaneous fat of DUhTP mice, a 16-fold increase of mtDNA content was observed when compared to DUC mice ($p < 0.0001$; fig. 4c). Physical activity over a period of 3 weeks further increased mtDNA content in DUhTP and DUC mice (7.8-fold and 7.7-fold, respectively; $p < 0.05$). Interestingly, in contrast to subcutaneous fat of controls, that of DUhTP mice has less clustering of mitochondria around the nucleus and mitochondrial fragmentation (fig. 4c). In response to RW activity more mitochondrial mass is detectable in subcutaneous fat of both genotypes. In controls, formation of elongated mitochondria appears in combination with mitochondrial clustering in the cell because of alterations in mitochondrial fission. Only in DUhTP mice a homogenous mitochondrial network structure was found across the cell.

Discussion

We have previously described a novel genetic mouse model (DUhTP) established by long-term selection for high treadmill performance that is characterized by genetically fixed elevated running capacity, increased hepatic lipogenesis, and peripheral obesity compared to control mice (DUC) [8]. We now examined energy metabolism and mitochondrial biogenesis in our mouse model with and without voluntary physical activity. As expected and observed in other studies in mice [28, 29] or humans [24], voluntary physical activity efficiently blocked the accumulation of body fat in peripheral fat depots from both genetic groups if compared to sedentary controls. In addition, prominent reductions of existing fat mass were found in perinephric and subcutaneous fat tissues exclusively in DUhTP mice in response to mild physical exercise over a period of 3 weeks. This was surprising, because the extent of voluntary physical activity in the RWs is similar in DUhTP mice and controls as described before [8]. In particular, physical activity is thought to exert beneficial effects on health through induction of lipolytic activity within adipose tissues [30]. In Osborne-Mendel rats, Zachwieja and colleagues [31] detected reduced fat masses in inguinal, epididymal, retroperitoneal, and perirenal fat pads in response to exercise for 7 weeks. Vieira et al. [32] could demonstrate a negative effect of physical activity (40 min/day over 12 weeks) on epididymal fat mass and hepatic TG levels. In DUhTP mice, we detected reduced hepatic cholesterol and TG content and serum TG levels by voluntary physical activity. While other studies have applied specific exercise training protocols over a period of 6–12 weeks [32], in our experiment merely 3 weeks of voluntary physical activity were sufficient to reduce hepatic TG and cholesterol in

Obes Facts 2015;8:373–385
DOI: 10.1159/000442399

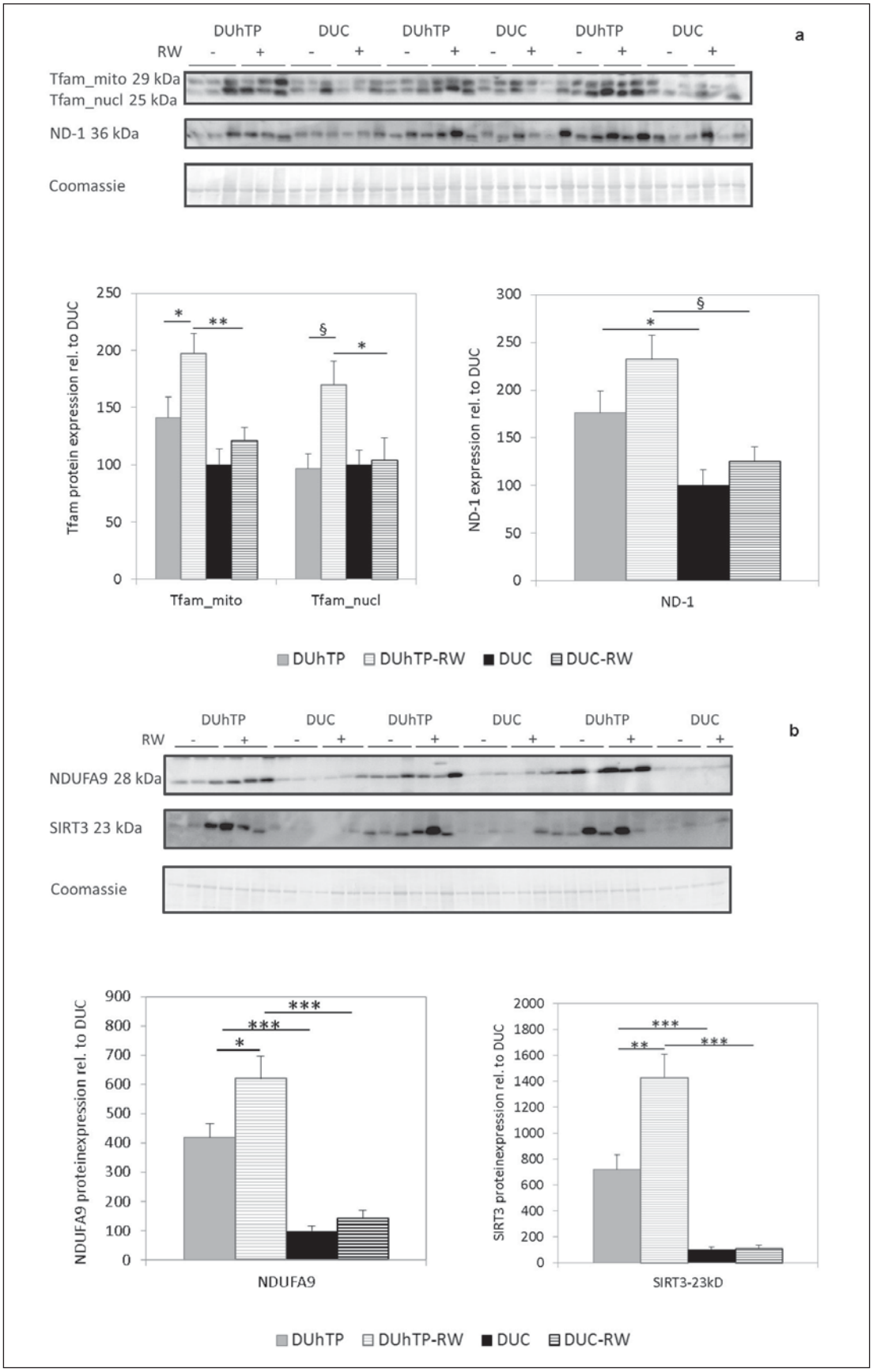

4

(For legend see next page.)

Obes Facts 2015;8:373–385
DOI: 10.1159/000442399

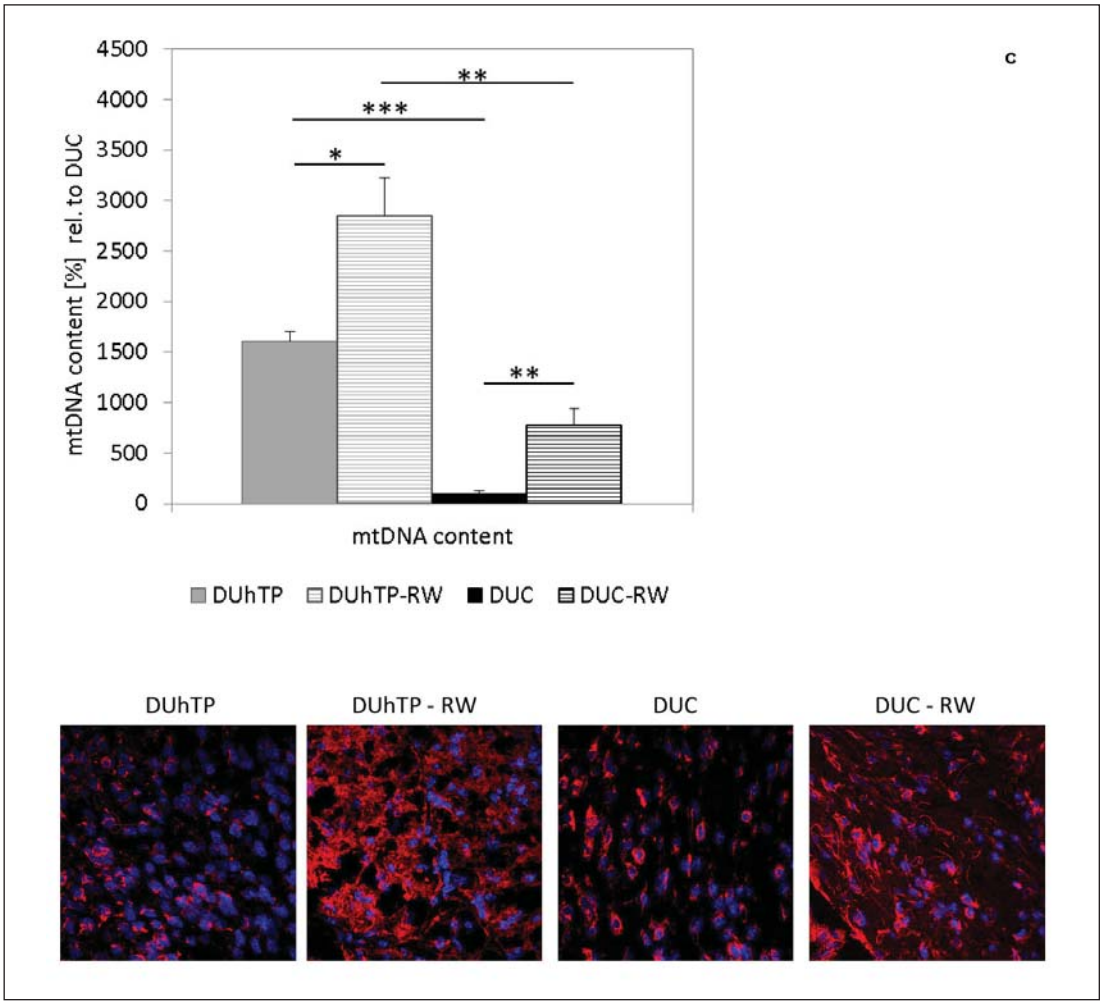

Fig. 4. Effect of voluntary physical activity in RWs on the expression of mitochondrial transcription factor A (Tfam) and mitochondria-encoded complex I subunit ND-1 (**a**) and mitochondrial proteins complex I subunit NDUFA9 and SIRT3 (**b**) as well as mtDNA content and mitochondrial biogenesis (**c**) in subcutaneous fat tissue of 10-week male DUhTP and DUC. Mitochondrial staining was achieved using Mitotracker Deep Red in fixed tissues as described in 'Material and Methods'. The analysis was performed by Western immunoblotting. Protein expression was quantified by densitometry and normalized for the Coomassie blue signal. Data are expressed relative to the expression level of the sedentary unselected controls (DUC). Vales are presented as mean ± SE. Significances are indicated; *$p < 0.05$, §$p < 0.01$, **$p < 0.005$, ***$p < 0.0005$.

DUhTP mice. In addition, the previous study was focused on the analysis of endpoints in divergently selected rats, whereas we have studied control of fat metabolism in different age groups in the presence or absence of RWs in DUhTP mice.

Expression of FAS and LCAD was higher in subcutaneous fat from DUhTP mice than in that of control mice, and expression of LCAD was further increased by physical activity in DUhTP mice. Also in human muscles, gene expression of LCAD increased after 8 h in response to 30 min single bout of exercise [25], and in muscle of rats, already in 1971, Mole and colleagues [12] could detect a twofold increased oxidation of long-chain fatty acids like oleate or linoleate in response to exercise on a treadmill over 12 weeks. In our model increased expression of LCAD in response to physical activity might correlate with increased β-oxidation

Obes Facts 2015;8:373–385
DOI: 10.1159/000442399

in mitochondria on the one hand and a reduction of fat mass on the other. Thus we may assume a higher mitochondrial mass established by increased mitochondrial biogenesis in DUhTP in response to RW activity. In fact very recent work provided evidence for exercise-induced mitochondrial biogenesis in subcutaneous fat in mice [16]. Exercise-induced mitochondrial biogenesis in adipose tissues so far has been considered only by a comparably small number of studies. In muscle or adipose tissues, higher concentrations of PGC1-α, a potent effector of mitochondrial biogenesis, were found in response to exercise training [15, 16, 22]. In murine preadipocytes, PGC1-α and PPARα induce gene expression of LCAD involved in mitochondrial fatty acid oxidation [33]. PGC1-α stimulates mitochondrial biogenesis in terms of higher mtDNA content and modulates regulators of mitochondrial replication and transcription in myotubes [22]. PGC1-α controls mitochondria- and nucleus-encoded genes involved in mitochondrial respiration and oxidative phosphorylation in cardiac myocytes and muscle cells [22, 34]. Most interestingly DUhTP mice synthesize severalfold higher levels of PGC1-α in their subcutaneous fat, if compared to controls. Expression of PGC1-α was further increased by physical activity only in DUhTP mice. Surprisingly, in contrast to muscle [20, 35] or heart [35] only one form of PGC1-α (90 kDa) was observed in subcutaneous fat corresponding to PGC1-α isoform 1.

Transcription of mitochondrial-encoded genes is mediated by Tfam in HeLa cells and Tfam expression again is induced in nucleus by PGC1-α via NRF-1, which identifies the latter two as bi-genomic coordinators of respiratory subunit expression [36]. Tfam is imported into mitochondrial subcompartments inducing transcription of 13 mtDNA-encoded protein subunits, which are essential components of the mitochondrial electron transport chain [37]. In sedentary DUhTP and control mice, mitochondrial or nuclear Tfam protein levels were on a comparable level. Nevertheless, voluntary physical activity significantly increased levels of both mitochondrial and nuclear Tfam in DUhTP, but not in DUC mice. In epididymal and retroperitoneal fat patches of male Wistar rats [15] or in subcutaneous fat of mice [16], an increase in mitochondrial biogenesis accompanied by higher PGC1-α and Tfam mRNA levels was found after 4 or 6 weeks of exercise swim training. Directly after an acute 2-hour bout of swimming only *PGC1-α* gene expression was increased in WAT, whereas mRNA concentration of Tfam was unchanged [15]. PGC1-α has been shown to induce expression of proteins encoded by the mitochondria such as ND-1 to ND-4 and ND-6 as markers of mitochondrial biogenesis and compounds of the respiratory chain in human and murine muscles, in the hippocampus and Corpus striatum regions of rat brain, and in rat kidneys [24, 25]. Both in the presence and absence of RWs, protein expression of ND-1 was higher in DUhTP mice than in controls. In response to physical activity, ND-1 expression increased slightly in both genotypes but the increase did not reach statistical significance.

In addition, nucleus-encoded mitochondrial proteins SIRT3 and NDUFA9 were examined to support the hypothesis of elevated mitochondrial biogenesis in DUhTP mice. Both proteins are expressed in a PGC1-α-dependent and Tfam-independent fashion [38]. In fact, in subcutaneous fat of sedentary DUhTP mice, higher protein levels of SIRT3 and NDUFA9 were detected when compared to controls. Again only in DUhTP mice voluntary activity further increased expression of SIRT3 and NDUFA9. It is known that PGC1-α induces gene expression of SIRT3 [38] while inhibition of SIRT3 expression blocked PGC1-α-mediated mitochondrial biogenesis [38], potentially since SIRT3 is required for the activation of NDUFA9 by deacetylation [39]. In addition, an increased content of mitochondrial DNA was found in DUhTP mice. In response to RW activity, mtDNA levels were elevated in DUhTP and DUC mice. In subcutaneous fat of DUhTP mice, physical activity coincides with the presence of a homogenous mitochondrial network distributed across the cell, maintaining cellular function and respiratory capacity. These dynamic networks continuously undergo fusion and fission events that allow damaged mitochondria to recover its activity and maintain metabolic functions, whereas

Obes Facts 2015;8:373–385
DOI: 10.1159/000442399

dysfunctional mitochondria get removed from the network by autophagy. The correct balance between fusion and fission of mitochondria is required for normal tubular morphology. An imbalance of this process results in fragmentation, elongation, or clustering of mitochondria [40] and a lack of mitophagy [41]. Future studies are designed also to address CO_2 consumption and body temperature in our mouse model.

Conclusions

To summarize, we provide direct evidence that subcutaneous fat from DUhTP mice is characterized by elevated expression of LCAD, PGC1-α, ND-1, NDUFA9, SIRT3 and increased mtDNA, which per se are not sufficient to induce subcutaneous fat mobilization. By contrast, in DUhTP mice even voluntary physical activity on RWs is sufficient to induce efficient lipolytic activity, which is reflected by a substantial loss of fat mass in different depots. Moderate physical activity further increased levels of LCAD, PGC1-α, Tfam, NDUFA9, and SIRT3 as well as mitochondrial biogenesis in subcutaneous fat from DUhTP mice, but not from controls. We hypothesize that during long-term selection DUhTP mice have acquired a set of energy-metabolic adaptations in order to fuel the high energy demands during physical activity. These adaptations confer the capacities to burn down existing fat mass even during comparably mild voluntary physical activity.

Acknowledgements

The authors want to thank Luong Chau, Sabine Hinrichs, Sabine Geist, Benita Lucht, Karin Ullerich, Sonja Alm and Magdalene Bülau for excellent technical assistance and Gordon Lynch for help with the manuscript. This study was supported by the Deutsche Forschungsgemeinschaft (DFG HO 2003/6-1).

Disclosure Statement

The authors declare no conflict of interest.

References

1 Feng B, Zhang T, Xu H: Human adipose dynamics and metabolic health. Ann N Y Acad Sci 2013;1281:160–177.
2 Frayn KN: Fat as a fuel: emerging understanding of the adipose tissue-skeletal muscle axis. Acta Physiol (Oxf) 2010;199:509–518.
3 Melzer K: Carbohydrate and fat utilization during rest and physical activity. e-SPEN 2011;6:e45–e52.
4 Romijn JA, Coyle EF, Sidossis LS, et al: Regulation of endogenous fat and carbohydrate metabolism in relation to exercise intensity and duration. Am J Physiol 1993;265:E380–E391.
5 Goto K, Ishii N, Sugihara S, Yoshioka T, Takamatsu K: Effects of resistance exercise on lipolysis during subsequent submaximal exercise. Med Sci Sports Exerc 2007;39:308–315.
6 Kang J, Rashti SL, Tranchina CP, Ratamess NA, Faigenbaum AD, Hoffman JR: Effect of preceding resistance exercise on metabolism during subsequent aerobic session. Eur J Appl Physiol 2009;107:43–50.
7 Wang S, Moustaid-Moussa N, Chen L, et al: Novel insights of dietary polyphenols and obesity. J Nutr Biochem 2014;25:1–18.
8 Brenmoehl J, Walz C, Renne U, et al: Metabolic adaptations in the liver of born long-distance running mice. Med Sci Sports Exerc 2013;45:841–850.
9 Wright DC: Exercise- and resveratrol-mediated alterations in adipose tissue metabolism. Appl Physiol Nutr Metab 2014;39:109–116.
10 Holloszy JO: Biochemical adaptations in muscle. Effects of exercise on mitochondrial oxygen uptake and respiratory enzyme activity in skeletal muscle. J Biol Chem 1967;242:2278–2282.
11 Holloszy JO, Oscai LB, Don IJ, Mole PA. Mitochondrial citric acid cycle and related enzymes: adaptive response to exercise. Biochem Biophys Res Commun. 1970;40(6):1368–1373.

Obes Facts 2015;8:373–385
DOI: 10.1159/000442399

12 Mole PA, Oscai LB, Holloszy JO: Adaptation of muscle to exercise. Increase in levels of palmityl Coa synthetase, carnitine palmityltransferase, and palmityl Coa dehydrogenase, and in the capacity to oxidize fatty acids. J Clin Invest 1971;50:2323–2330.
13 Horowitz JF, Leone TC, Feng W, Kelly DP, Klein S: Effect of endurance training on lipid metabolism in women: a potential role for PPARalpha in the metabolic response to training. Am J Physiol Endocrinol Metab 2000; 279:E348–E355.
14 Jeppesen J, Kiens B: Regulation and limitations to fatty acid oxidation during exercise. J Physiol 2012;590: 1059–1068.
15 Sutherland LN, Bomhof MR, Capozzi LC, Basaraba SA, Wright DC: Exercise and adrenaline increase PGC-1{alpha} mRNA expression in rat adipose tissue. J Physiol 2009;587:1607–1617.
16 Trevellin E, Scorzeto M, Olivieri M, et al: Exercise training induces mitochondrial biogenesis and glucose uptake in subcutaneous adipose tissue through eNOS-dependent mechanisms. Diabetes. 2014;63:2800–2811.
17 Hashimoto T, Sato K, Iemitsu M: Exercise-inducible factors to activate lipolysis in adipocytes. J Appl Physiol 2013;115:260–267.
18 Summermatter S, Handschin C: PGC-1alpha and exercise in the control of body weight. Int J Obes (Lond) 2012; 36:1428–1435.
19 Summermatter S, Troxler H, Santos G, Handschin C: Coordinated balancing of muscle oxidative metabolism through PGC-1alpha increases metabolic flexibility and preserves insulin sensitivity. Biochem Biophys Res Commun 2011;408:180–185.
20 Brenmoehl J, Albrecht E, Komolka K, et al: Irisin is elevated in skeletal muscle and serum of mice immediately after acute exercise. Int J Biol Sci 2014;10:338–349.
21 Evans MJ, Scarpulla RC: NRF-1:a trans-activator of nuclear-encoded respiratory genes in animal cells. Genes Dev 1990;4:1023–1034.
22 Wu Z, Puigserver P, Andersson U, et al: Mechanisms controlling mitochondrial biogenesis and respiration through the thermogenic coactivator PGC-1. Cell 1999;98:115–124.
23 Ryan MT, Hoogenraad NJ: Mitochondrial-nuclear communications. Annu Rev Biochem 2007;76:701–722.
24 Short KR, Vittone JL, Bigelow ML, et al: Impact of aerobic exercise training on age-related changes in insulin sensitivity and muscle oxidative capacity. Diabetes 2003;52:1888–1896.
25 Fluck M: Functional, structural and molecular plasticity of mammalian skeletal muscle in response to exercise stimuli. J Exp Biol 2006;209:2239–2248.
26 Safdar A, Little JP, Stokl AJ, Hettinga BP, Akhtar M, Tarnopolsky MA: Exercise increases mitochondrial PGC-1alpha content and promotes nuclear-mitochondrial cross-talk to coordinate mitochondrial biogenesis. J Biol Chem 2011;286:10605–10617.
27 Hofmeister-Brix A, Kollmann K, Langer S, Schultz J, Lenzen S, Baltrusch S: Identification of the ubiquitin-like domain of midnolin as a new glucokinase interaction partner. J Biol Chem 2013;288:35824–35839.
28 Colman RJ, Nam G, Huchthausen L, Mulligan JD, Saupe KW: Energy restriction-induced changes in body composition are age specific in mice. J Nutr 2007;137:2247–2251.
29 Leamy LJ, Kelly SA, Hua K, Pomp D: Exercise and diet affect quantitative trait loci for body weight and composition traits in an advanced intercross population of mice. Physiol Genomics 2012;44:1141–1153.
30 Stephenson EJ, Lessard SJ, Rivas DA, et al: Exercise training enhances white adipose tissue metabolism in rats selectively bred for low- or high-endurance running capacity. Am J Physiol Endocrinol Metab 2013;305:E429–E438.
31 Zachwieja JJ, Hendry SL, Smith SR, Harris RB: Voluntary wheel running decreases adipose tissue mass and expression of leptin mRNA in Osborne-Mendel rats. Diabetes 1997;46:1159–1166.
32 Vieira VJ, Valentine RJ, Wilund KR, Antao N, Baynard T, Woods JA: Effects of exercise and low-fat diet on adipose tissue inflammation and metabolic complications in obese mice. Am J Physiol Endocrinol Metab 2009; 296:E1164–E1171.
33 Vega RB, Huss JM, Kelly DP: The coactivator PGC-1 cooperates with peroxisome proliferator-activated receptor alpha in transcriptional control of nuclear genes encoding mitochondrial fatty acid oxidation enzymes. Mol Cell Biol 2000;20:1868–1876.
34 Lehman JJ, Barger PM, Kovacs A, Saffitz JE, Medeiros DM, Kelly DP: Peroxisome proliferator-activated receptor gamma coactivator-1 promotes cardiac mitochondrial biogenesis. J Clin Invest 2000;106:847–856.
35 Ruas JL, White JP, Rao RR, et al: A PGC-1alpha isoform induced by resistance training regulates skeletal muscle hypertrophy. Cell 2012;151:1319–1331.
36 Virbasius JV, Scarpulla RC: Activation of the human mitochondrial transcription factor A gene by nuclear respiratory factors: a potential regulatory link between nuclear and mitochondrial gene expression in organelle biogenesis. Proc Natl Acad Sci U S A 1994;91:1309–1313.
37 Menzies KJ, Hood DA: The role of SirT1 in muscle mitochondrial turnover. Mitochondrion 2012;12:5–13.
38 Kong X, Wang R, Xue Y, et al: Sirtuin 3, a new target of PGC-1alpha, plays an important role in the suppression of ROS and mitochondrial biogenesis. PLoS One 2010;5:e11707.
39 Ahn BH, Kim HS, Song S, et al: A role for the mitochondrial deacetylase Sirt3 in regulating energy homeostasis. Proc Natl Acad Sci U S A. 2008;105:14447–14452.
40 Huang P, Yu T, Yoon Y: Mitochondrial clustering induced by overexpression of the mitochondrial fusion protein Mfn2 causes mitochondrial dysfunction and cell death. Eur J Cell Biol 2007;86:289–302.
41 Mouli PK, Twig G, Shirihai OS: Frequency and selectivity of mitochondrial fusion are key to its quality maintenance function. Biophys J 2009;96:3509–3518.

IVYSPRING INTERNATIONAL PUBLISHER

International Journal of Biological Sciences

2014; 10(3): 338-349. doi: 10.7150/ijbs.7972

Research Paper

Irisin Is Elevated in Skeletal Muscle and Serum of Mice Immediately after Acute Exercise

Julia Brenmoehl[1], Elke Albrecht[2]✉, Katrin Komolka[2], Lisa Schering[2], Martina Langhammer[3], Andreas Hoeflich[1], Steffen Maak[2]

1. Institute for Genome Biology, Leibniz Institute for Farm Animal Biology (FBN), Dummerstorf, Germany;
2. Institute for Muscle Biology and Growth, Leibniz Institute for Farm Animal Biology (FBN), Dummerstorf, Germany;
3. Institute for Genetics and Biometry, Leibniz Institute for Farm Animal Biology (FBN), Dummerstorf, Germany.

✉ Corresponding author: Dr. Elke Albrecht, Institute for Muscle Biology and Growth, Leibniz Institute for Farm Animal Biology. Wilhelm-Stahl-Allee 2, 18196 Dummerstorf, Germany. Tel: +49 38208 68858, Fax: +49 38208 68852 E-mail: elke.albrecht@fbn-dummerstorf.de.

Received: 2013.10.24; Accepted: 2014.02.24; Published: 2014.03.11

Abstract

Recent findings regarding the response of fibronectin type III domain-containing protein 5 (Fndc5) and irisin to exercise are partly controversial. While the 25 kDa form of Fndc5 can be observed in muscle and serum of different species, the ~12 kDa irisin band was not detectable up to now. The present study aimed to clarify whether irisin exists in its theoretical size of ~12 kDa in mice and if it is affected by exercise. Male mice were randomly assigned to a sedentary control group (CO), a group with free access to running wheels (RW), and a treadmill group (TM). Blood and leg muscles were collected to investigate the regulatory cascade including peroxisome proliferator-activated receptor gamma co-activator 1-alpha (Ppargc1a) and Fndc5. In western blot analysis, antibodies were used capable of differentiation between full-length Fndc5 and irisin. This enabled us to demonstrate that irisin exists in muscle and serum of mice independent of exercise and that it is increased immediately after acute exercise. Different transcripts of Ppargc1a mRNA, but not Fndc5 mRNA, were up-regulated in the TM group. Furthermore, neither Fndc5 (25 kDa) nor Ppargc1a protein was elevated in muscle tissue. The Ppargc1a-Fndc5/irisin pathway did not clearly respond to mild exercise in the RW group. Our results provide evidence for the existence of irisin and for its immediate response to acute exercise in mice.

Key words: endurance exercise, Fndc5, irisin, myokine, Ppargc1a.

Introduction

Two years ago, Boström et al. (3) characterized irisin as a new myokine originating from cleavage of the transmembrane protein fibronectin type III domain-containing protein 5 (Fndc5). Mice overexpressing peroxisome proliferator-activated receptor gamma coactivator 1-alpha (Ppargc1a, also known as PGC1-α) in muscle responded with an increase in Fndc5 mRNA. This increase could also be induced by physical exercise. It was demonstrated that recombinant Fndc5 induced a thermogenic program in white adipose tissue thus linking exercise with browning of adipose tissue indirectly (3). Cleavage and modification of Fndc5 was proposed as prerequisite for this action. However, cleavage of the extracellular part of Fndc5 and release of the resulting peptide irisin was only demonstrated in transfected HEK293 cells (3). Furthermore, Boström et al. (3) as well as subsequent studies employing western blot in tissues and serum of mice, rats, and humans (24,28,32) failed to demonstrate a peptide of the size expected for irisin (12 kDa), but analyzed proteins between 22 to 28 kDa which corresponded to the size of full-length Fndc5.

Since the initial description of irisin, more than 25 ELISA (enzyme-linked immunosorbent assay)

based studies were conducted in humans, mice, and pigs to elucidate either effects of exercise on circulating irisin (9,13,17,18,20) or relationships between irisin level, body composition, type II diabetes and further diseases [reviewed by Novelle et al. (19)]. The results of these studies were controversial which may in part be caused by unspecific bindings of the capture antibody. Importantly, Erickson (8) stated that antibodies used in these ELISA kits must be validated by quantitative western blot to prove their specificity. Consequently, there is still no direct evidence for circulating irisin in any species (8).

The inducer of Fndc5/irisin – Ppargc1a – was subjected to a detailed analysis recently (25). Expression of 4 different Ppargc1a transcripts (Ppargc1a1 to 4) was shown in a variety of murine tissues including skeletal muscle. Interestingly, specific expression of Ppargc1a4 in primary myotubes did not induce several classic Ppargc1a1 targets but stimulated insulin-like growth factor 1 (Igf1) expression and suppressed expression of myostatin (25). The authors concluded from a series of subsequent experiments that forced Ppargc1a4 expression in muscle – either by transgenesis or by resistance training – may result in functional hypertrophy. The role of Ppargc1a transcripts 2 and 3 was not further investigated in this study, however (25).

Against this background, we aimed to provide evidence for circulation of 12 kDa irisin peptide in mice. Furthermore, we investigated effects of voluntary and acute exercise on circulating irisin, on expression of its precursor Fndc5, and on expression of different transcripts of its potential activator Ppargc1a.

Material and Methods

Animals and husbandry

All procedures were done in accordance to national and international guidelines and approved by our own institutional board (Animal Protection Board from the Leibniz Institute for Farm Animal Biology) as well as by the national Animal Protection Board Mecklenburg-Western Pomerania (file number: LVL-MV/TSD/7221.3-1.1-013/12).

We used the outbred mouse line DUhTP (Dummerstorf high treadmill performance) generated by selection for high treadmill performance for 117 generations as described elsewhere (4,10), because mice are able to run long distances either in a treadmill or running wheel with sufficient variation. The animals were housed in Makrolon-cages Type II (EBECO, Castrop-Rauxel, Germany) in a semi-barrier system under environmentally controlled conditions with a 12 h light / 12 h dark cycle (room temperature 22.5 ± 0.2 °C, humidity 50–60 %). Fresh tap water and fixed formula food for laboratory mice were supplied ad libitum (ssniff V1124: protein, 22 %; fat, 4.5 %; raw fiber, 3.9 %; ash, 6.8 %; ssniff Spezialdiäten, Soest, Germany).

Running wheel and treadmill performance

Three groups of mice were randomly assigned, each consisting of 11 to 12 70-days-old male DUhTP mice with 32.6 ± 6.1 g mean body weight. One group (RW) was kept in cages including running wheels (d = 33.4 cm) equipped with wheel counters (Tecniplast, Hohenpeissenberg, Germany) for a period of 3 weeks from the 49th to the 70th day of age. Another group of 70-days-old male mice (TM) was undertaken a submaximal test on a computer controlled treadmill. Details of the test were described elsewhere (10). Briefly, a special test program with increasing speed (start speed: 15 m/min, final speed: 38 m/min) was applied. The test stopped as soon as the mice remained at the stimulating equipment. Coeval mice without access to running wheels were used as control group (CO).

Animals were sacrificed by decapitation at day 70 of age, TM mice immediately after the test, and serum samples were prepared according to standard procedures. Femoral muscles (*quadriceps femoris*), representative for a single, highly active leg muscle, and crus muscles (incl. *soleus, extensor digitorum longus*, and *gastrocnemius*), a group of heterogeneous muscles, were flash frozen within 15 min after death and stored in liquid nitrogen for subsequent analyses.

Quantitative PCR (qPCR)

Muscle tissue of 12 TM mice, 8 RW mice, and 8 CO mice was homogenized using the Xiril Dispomix (Xiril, Hombrechtikon, Switzerland) and Qiazol Lysis Reagent (Qiagen, Hilden, Germany) as described by the manufacturer. The RNA was isolated and purified with NucleoSpin Extract II reagent (Macherey-Nagel, Dueren, Germany) according to manufacturer's guidelines. RNA was quantified with a NanoDrop ND-1000 spectrophotometer (Peqlab, Erlangen, Germany). The RNA integrity was determined with an Experion RNA StdSens analysis chip (BioRad, Munich, Germany). All RNA samples had RQI numbers between 8.0 and 9.5. First strand cDNA was synthesized from 100 ng total RNA in 20 µl reaction volume using iScript cDNA Synthesis Kit (BioRad) according to the provided protocol.

The iCycler MyiQ 2 with iQ detection system (BioRad) was used for qPCR as described in (1). Gene expression measurements were performed in duplicates in 10 µl reaction volumes containing 10 ng cDNA templates, 2 µM of the respective forward and

reverse primers, and 5 µl SYBR Green Supermix (BioRad). The primers listed in Table 1 were selected from recent publications as indicated or designed with Primer 3 (Version 0.4.0., http://frodo.wi.mit.edu/primer3/) and synthesized by Sigma-Aldrich (Munich, Germany). The amplification involved a denaturation step (95 °C for 3 min) followed by 45 cycles (95 °C for 10 s, 60 °C for 30 s, 70 °C for 45 s). For amplification of Ppargc1a transcripts 2 and 4, the annealing temperature was adapted to 62 °C and 58 °C, respectively. The specificity of the amplicons was analyzed by melting curve analysis. Crossing point (C_p) values were determined automatically by iQ5 software (Version 2.1.97.1001, BioRad). For each qPCR, the amplification efficiency was calculated from a standard curve derived from six serial dilutions (1:1, 1:10, 1:50, 1:100, 1:500, 1:1,000) as $E = 10^{-1/\text{slope of standard curve}} - 1$. The identity of the products was confirmed by sequencing (ABI PRISM 310 Genetic Analyzer; Applied Biosystems, Darmstadt, Germany). Results are expressed as fold-changes in experimental groups compared to a CO group (mice without running treatment). The expression values were normalized to beta-2-microglobulin [B2m, (1)] and hypoxanthin-phosphoribosyl-transferase 1 [Hprt1, (6)]. The significance of expression differences was calculated with the REST algorithm as described by Pfaffl [(22); REST 2009, Version 2.0.13, QIAGEN].

Western immunoblotting

Proteins were extracted from femoral muscles of 12 TM mice, 12 RW mice, and 11 CO mice and crus muscles from 12 TM mice, 8 RW mice and 8 CO mice (app. 60 mg, each). Muscle tissue was homogenized in CelLytic MT lysis buffer (Sigma-Aldrich) supplemented with protease inhibitor cocktail (P8340, Sigma-Aldrich) using the Dispomix (Xiril). After centrifugation (14,000 rpm, 15 min, 4 °C) and elimination of cell debris, protein content of the tissue lysate was quantified using the BSA mode of Nanodrop 1000 (Peqlab). Serum samples were measured directly by Nanodrop technology.

Twenty micrograms of muscle protein or 30 µg protein of serum samples, respectively, diluted in Laemmli buffer with ß-mercaptoethanol were separated on 15 % sulfate–polyacrylamide gel electrophoresis gels and transferred to polyvinylidene difluoride (PVDF) membranes (Carl Roth, Karlsruhe, Germany). Equal loading of the gels and proper transfer of the proteins to the membranes were verified by Coomassie Blue staining according to standard procedures. We analyzed the protein expression of Ppargc1a, Fndc5, and irisin by using respective antibodies as follows. Membranes were blocked for 1 h in either 5 % non-fat dry milk in Tris-buffered saline (TBS), for Fndc5 and Ppargc1a, or 1× Roti-Block (Carl Roth), for detection of irisin. Membranes were incubated with primary antibodies over night at 4 °C. Horseradish peroxidase–conjugated goat anti rabbit IgG secondary antibody (Cell Signaling Technology, New England Biolabs, Frankfurt/Main, Germany) was diluted 1: 5,000 and incubated for 1 h. Protein abundance was detected by enhanced chemiluminescence (TMA-100, Lumigen technology, Bioquote Limited, York, UK) using Kodak Image Station 4000 MM (Raytest, Straubenhardt, Germany). LabImage 1D software (Kapelan Bio-Imaging, Leipzig, Germany) was used to quantify intensity of specific bands. To verify the results, each blot, i.e. sample, was repeated 2 to 4 times. After exposure, the antibody was stripped from the membrane with stripping solution (Restore Plus Western Blot Stripping Buffer, Thermo Fisher Scientific, Schwerte, Germany) for 20 min at room temperature.

Table 1: Sequences of primer sets used for amplification of specific cDNA.

Locus	Primer	bp	Sequence 5'- 3'	Accession No.	Position
B2m	forward	175	CCTGGTCTTTCTGGTGCTTG	NM_009735	69-89
(reference)	reverse		TTTCCCGTTCTTCAGCATTT		224-243
Hprt1	forward	90	TCCTCCTCAGACCGCTTTT	NM_013556	104-122
(reference)	reverse		CCTGGTTCATCATCGCTAATC		173-193
Fndc5	forward	162	CAACGAGCCCAATAACAACA	NM_027402.3	553-574
	reverse		AGAAGGTCCTCTCGCATTCTC		694-714
Ppargc1a	forward	156	GGACATGTGCAGCCAAGACTCT	NM_008904.2	148-169
transcript 1[A]	reverse		CACTTCAATCCACCCAGAAAGCT		281-303
Ppargc1a	forward	109	CCACCAGAATGAGTGACATGGA	JX866946.1	19-40
transcript 2[A, B]	reverse		GTTCAGCAAGATCTGGGCAAA		107-127
Ppargc1a	forward	103	AAGTGAGTAACCGGAGGCATTC	JX866947	94-115
transcript 3[A]	reverse		TTCAGGAAGATCTGGGCAAAG A		175-196
Ppargc1a	forward	172	TCACACCAAACCCACAGAAA	JX866948	687-706
transcript 4[A]	reverse		CTGGAAGATATGGCACAT		841-858

[A] Ruas et al. (25), [B] co-amplifies transcripts 2, 3, and 4.

Primary antibody for Ppargc1a, (1: 1,000; sc-13067, Santa Cruz Biotechnology, Heidelberg, Germany) is supposed to detect isoform 1 and 4 with higher affinity and isoform 2 and 3 with lower affinity according to sequence homology. The Fndc5 antibody (1: 1,000; AP8746b, BioCat, Heidelberg, Germany) binds to the C-terminus of Fndc5 (amino acids [aa] 149-178, human) and detects a band of about 25 kDa, which is in the range of the calculated molecular weight for the protein. The specificity of binding was tested in parallel blots which were incubated with either the antibody or with the antibody previously blocked with the respective blocking peptide. The irisin antibody (1: 3,000; A00170-01-100, Biotrend, Cologne, Germany) was developed using full-length recombinant irisin and detects a ~12 kDa band of irisin and several additional bands of larger size. As a control for specific binding of the irisin antibody, again two membranes were processed in parallel, which were incubated with either the irisin antibody or with the irisin antibody previously blocked by incubation with full-length recombinant irisin (aa 32-143). The ~12 kDa band was blocked exclusively in that case.

Immunohistochemical analysis

Femoral muscle samples were cryo-sectioned (8 µm thick) using a Leica CM3050 S (Leica, Bensheim, Germany) cryostat microtome. Tissue sections were fixed with 4 % paraformaldehyde and washed with PBS. Unspecific binding of the secondary antibody was blocked using 10 % goat serum in PBS for 15 min. Sections were incubated with the primary antibody against either irisin (1: 100) for 1 h at room temperature or Fndc5 (1: 100) at 4 °C overnight in a humidity chamber. Specific binding of primary antibody was detected with the respective goat anti rabbit IgG secondary antibody labeled with MFP 488 (MoBiTec, Goettingen, Germany). Nuclei were counterstained with 1 µg/ml Hoechst 33258 (Sigma-Aldrich). Slides were covered using Mowiol mounting medium including 1,4-diazabicyclo[2.2.2]octan (DABCO, Carl Roth) and appropriate cover-slips. Negative controls were incubated either omitting the primary antibody or blocking the primary antibody with the respective peptide. No unspecific binding of the secondary antibody and only minimal unspecific binding of the primary antibody was detected. Disturbing auto-fluorescence was reduced by including a step of Sudan black (0.1 % in 70 % ethanol) staining for 30 min prior to the blocking step. Immunofluorescence was visualized with a Nikon Microphot SA fluorescence microscope (Nikon, Duesseldorf, Germany) and an image analysis system equipped with CELL^F software and a CC-12 high resolution color camera (OSIS, Muenster, Germany).

Statistical analysis

Statistical analysis was performed using the SAS statistical software (Version 9.2, SAS Inst., Cary, USA). Data were analyzed by ANOVA using the MIXED procedure with fixed factor group (treatment) and random animal. Values of different blots for the same tissue and antibody were included as repeated measurements. The t-test was used as post-hoc test with $P \leq 0.05$ as threshold for significant differences.

Relationships between traits were calculated within groups as Pearson's-correlation coefficients using the CORR procedure of SAS.

Results

Running performance of DUhTP mice

Basic phenotypical and physiological parameters of the outbred line DUhTP were described elsewhere (4). Mice of the RW group, which had free access to the running wheel, ran on average 4.7 ± 2.6 km per day during 3 weeks of voluntary endurance training. The body weight gain during this time was not significantly different (P = 0.11) from that of the CO group. However, running distance and body weight gain were negatively correlated (r = -0.67, P = 0.02) in the RW group. Mice subjected to a single submaximal test on a treadmill (TM group) ran 5.1 ± 1.8 km. They lost on average 2.0 ± 1.3 g body mass during this test.

Irisin is abundant in murine muscle and serum and is elevated after acute exercise

To clarify whether the secreted cleavage product of Fndc5 exists in mice, we used western blot analysis with an antibody specific to irisin. This antibody detects full-length recombinant irisin at about 12 kDa (lane 6 in Fig. 1A, left) and also a ~12 kDa band in mouse serum and muscle tissue (lanes 2 to 5 in Fig. 1A, left). In serum samples, this band usually appeared as a doublet band. To test whether the slightly larger band was glycosylated irisin, PNGase treatment was applied to serum samples. The second band disappeared after this treatment (Fig. 1B). Several additional bands were still observed in muscle and serum. Therefore, recombinant irisin was used to block the specific binding of the antibody and to discriminate between specific and unspecific bands. The strong band of recombinant irisin disappeared when the antibody was blocked in advance. Accordingly, the bands of similar size detected in mouse serum (lanes 2 and 3 in Fig. 1A, right) and muscle (lanes 4 and 5) could also be blocked. Further bands of different sizes were considered as unspecific, because

they were still detected by the primary antibody after blocking with recombinant irisin. Consequently, the chemiluminescence intensity of the ~12 kDa band was measured to elucidate the effect of acute or voluntary exercise on irisin level in serum and muscle of mice. Samples for comparison of irisin abundance were not treated with PNGase prior to analysis and the volume of the doublet band was measured.

Figure 2A shows a representative western blot of serum from each 3 mice of the 3 groups and the results of quantification for all mice. Mice of the TM group had higher serum irisin levels ($P < 0.01$) than CO or RW group mice. This was accompanied by higher irisin levels in homogenates of femoral ($P < 0.01$) but not of crus muscles ($P > 0.05$, Fig. 2B). There was no difference in irisin levels between CO and RW group ($P > 0.5$) neither in serum nor in muscle tissues. Using a serial dilution of recombinant irisin as a standard (7 dilutions 1:2, from 40 ng to 0.625 ng), we estimated the basal concentration of irisin in serum to 1.4 µg/ml and the concentration after treadmill exercise to 2.7 µg/ml. This corresponded to a 1.9-fold increase of circulating irisin.

To test whether the irisin abundance in serum is directly related to the distance covered during the test, Pearson correlation coefficients were calculated. Neither irisin abundance in serum nor in muscle was directly associated with the running distance of either acute or voluntary exercise (data not shown).

Expression of Fndc5 is not altered immediately after exercise

Next we analyzed the irisin precursor Fndc5 at mRNA and protein level. The mRNA expression of Fndc5 was not different between CO, RW, and TM mice, neither in femoral nor in crus muscle tissue (Fig. 3A).

Fndc5 protein was analyzed using an anti-Fndc5 antibody directed against the C-terminal end of the protein (corresponds to the murine Fndc5 aa 147-175), thus excluding the irisin peptide. This antibody recognized Fndc5 at the expected size of ~25 kDa in muscle (Fig. 3B, left). Specificity was confirmed by blocking the antibody with the respective peptide prior to incubation (Fig. 3B, right). In serum samples, Fndc5 was detected only in rare cases (data not shown). Therefore, Fndc5 was analyzed in muscle tissue only, separately for femoral and crus muscles. The protein abundance of Fndc5 was not altered by any type of exercise ($P = 0.29$) neither in femoral muscles nor in crus muscles (Fig. 3C).

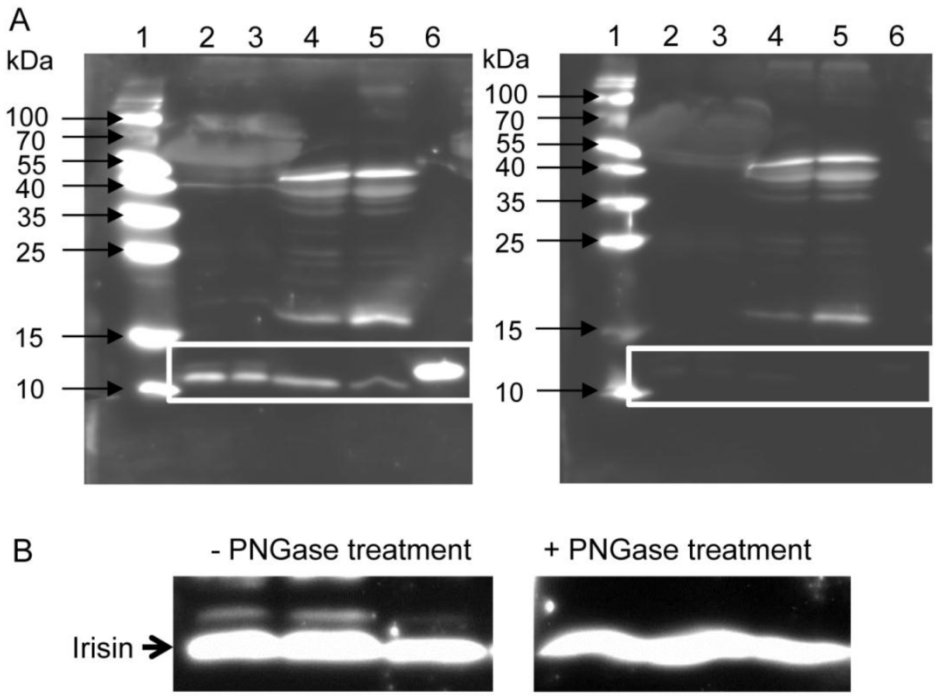

Figure 1: Detection of irisin in mouse serum and muscle. (A) Western Blot of each 2 mouse serum (lane 2 and 3) and muscle samples (lane 4 and 5) and recombinant irisin (lane 6) incubated with either (left) antibody directed against irisin (aa 32-143) or (right) antibody against irisin previously blocked with the recombinant protein. A specific band was detected at approximately ~12 kDa in serum and muscle tissue as indicated by the white frame. Images were identically enhanced in contrast. (B) Irisin band of mouse serum (left) without or (right) with PNGase treatment indicating that circulating irisin was partly glycosylated. Images were identically enhanced in contrast and cropped to the specific ~12 kDa band.

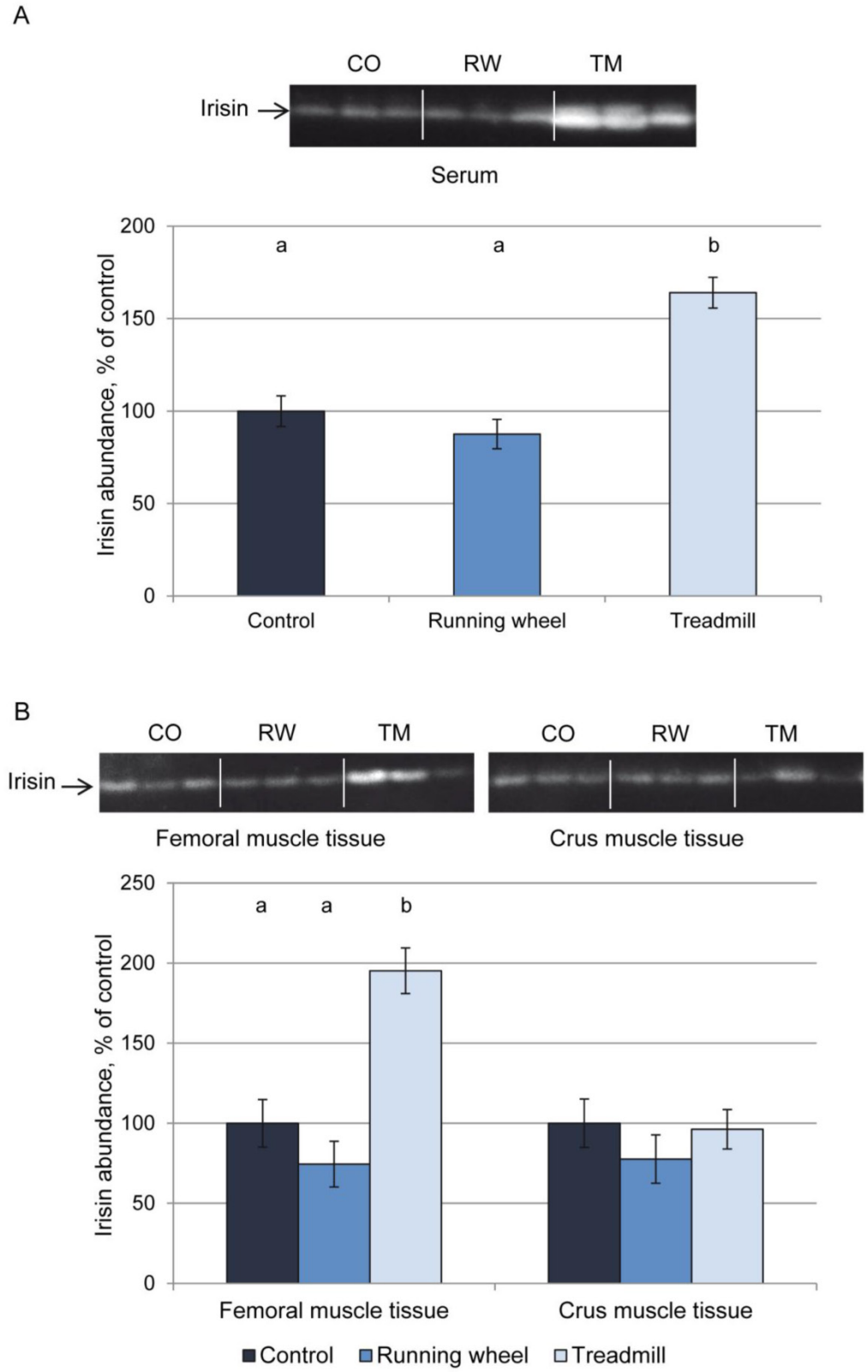

Figure 2: Protein abundance of irisin in (A) serum and (B) muscle tissue of mice after 3 weeks of voluntary exercise in a running wheel (serum and FM: n = 12, CM: n = 8) or one bout of treadmill exercise (serum, FM, and CM: n = 12) relative to a sedentary control (serum and FM: n = 11, CM: n = 8). Representative parts of the respective western blots for determination of irisin protein expression are shown above the graphs. Different letters indicate significant differences between groups ($P < 0.05$). CO – control group, RW – running wheel group, TM – treadmill group.

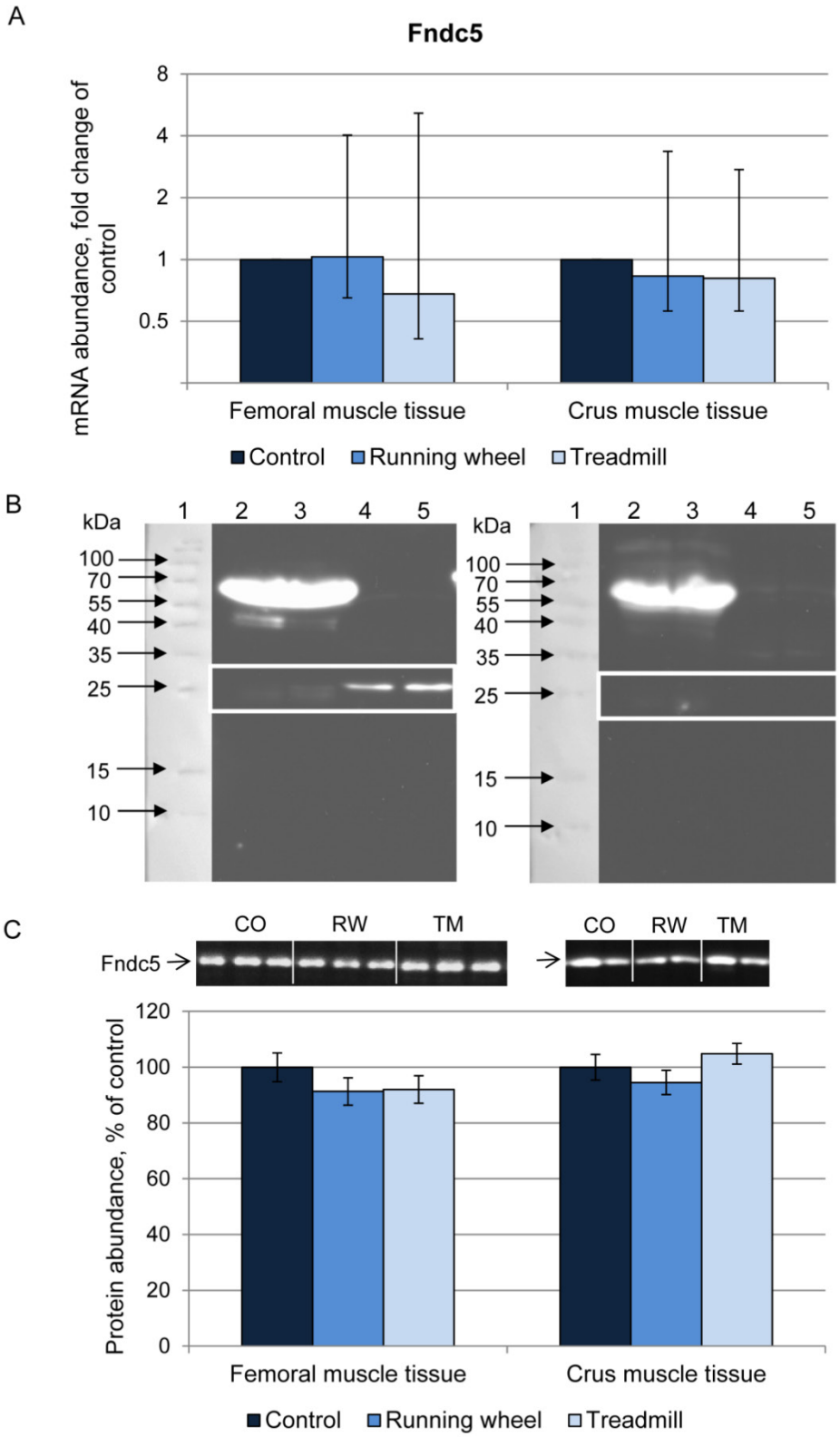

Figure 3: Abundance of Fndc5 mRNA and protein in femoral (FM) and crus muscle (CM) tissue of mice after 3 weeks of voluntary exercise in a running wheel (FM: n = 12, CM: n = 8) or one bout of treadmill exercise (FM and CM: n = 12) relative to a sedentary control (FM: n = 11, CM: n = 8). (A) mRNA abundance normalized to B2m and Hprt1. Bars represent means of fold changes compared to control group with 95 % confidence intervals marked as vertical lines. (B) Western blot of each 2 mouse serum (lane 2 and 3) and muscle samples (lane 4 and 5) incubated with either (left) antibody directed against Fndc5 (aa 149-178) or (right) the antibody against Fndc5 previously blocked with the corresponding blocking peptide. The marker lane is laid on the image to determine the protein size. A specific band was detected at ~25 kDa exclusively in muscle tissue as indicated by the white frame. Images were identically enhanced in contrast. (C) Protein abundance of Fndc5 determined by quantitative western blot analysis. Representative parts of respective western blots are shown above the graph. CO – control group, RW – running wheel group, TM – treadmill group.

Immunohistochemical detection of irisin in muscle tissue indicates extracellular localization

The cellular localization of irisin and its precursor Fndc5 was visualized and studied in femoral muscle tissue. Fndc5 was detected at the sarcolemma as expected for a transmembrane protein and additionally in the sarcoplasm showing a punctate signal, but not in the intercellular space between muscle fibers (Fig. 4A). Additionally, few cells located in connective tissue showed immunohistochemical Fndc5 staining at the cell membrane. This observation was also made in mice from CO and RW groups (data not shown).

Irisin-related immunofluorescence was detected as weak, diffuse signal across muscle fibers and was more intense at muscle fiber membranes and between muscle fibers (Fig. 4B) in TM mice. Weaker but similarly located signals for irisin were observed in CO and RW mice (data not shown).

Ppargc1a mRNA but not protein increases immediately after acute exercise

To elucidate the proposed induction of Fndc5/irisin by Pparga1a, we then investigated mRNA and protein expression of different transcripts and isotypes of Ppargc1a in skeletal muscle. Using primers published by Ruas et al. (25), 3 of 4 transcripts could be analyzed separately (transcripts 1, 3, and 4). The primers for transcript 2 described by Ruas et al. (25) co-amplified transcripts 3 and/or 4 as indicated by double peaks in the melting curve analysis resulting from different amplicon lengths. An *in silico*-analysis of all described transcripts revealed that a separate analysis of transcript 2 with standard qPCR techniques is precluded by its identity to transcript 3. It differs from transcript 2 only by a 70 bp longer exon 1. Consequently, Ppargc1a2 could not be considered further in the present study.

The abundance of transcript 4 was 9- and 6-fold higher in the TM compared to the CO group in femoral and crus muscles, respectively (Fig. 5A, B). There was a positive relationship ($r = 0.63$ and 0.69, $P < 0.05$) between Ppargc1a4 mRNA abundance and running performance in the TM group (Fig. 5C) in femoral and crus muscles, respectively. Surprisingly, the strongest increase in mRNA abundance after treadmill exercise was measured for transcript 3. Mice of the TM group had 33- and 10-fold higher Ppargc1a3 mRNA expression than the sedentary CO group in femoral and crus muscles, respectively (Fig. 5A, B). In contrast to transcript 4, there were no significant relationships between individual increase in mRNA abundance and running distance. Voluntary exercise in a running wheel (RW group) had no effect on Ppargc1a3 and 4 mRNA abundances in both muscle groups. Transcript 1 of Ppargc1a was slightly but significantly up-regulated in TM mice (1.6- and 1.9-fold, in femoral and crus muscles, respectively, $P < 0.01$) and also in femoral muscle of RW group (1.5-fold, $P = 0.025$).

Next, the consequences of exercise on protein abundance of Ppargc1a were investigated. The antibody against Ppargc1a is supposed to detect different isoforms. Western blot analysis revealed bands of different size, usually larger than the predicted sizes of the respective isoforms (Ppargc1a1: ~90 kDa; Ppargc1a2 and 3: ~41 kDa; Ppargca1a4: ~29 kDa, Uni-Prot O70343). Separate analysis of each band revealed similar protein amounts ($P > 0.05$) between CO and treatment groups, in both femoral and crus muscles. The results for isoform 4 are exemplarily shown in Figure 6.

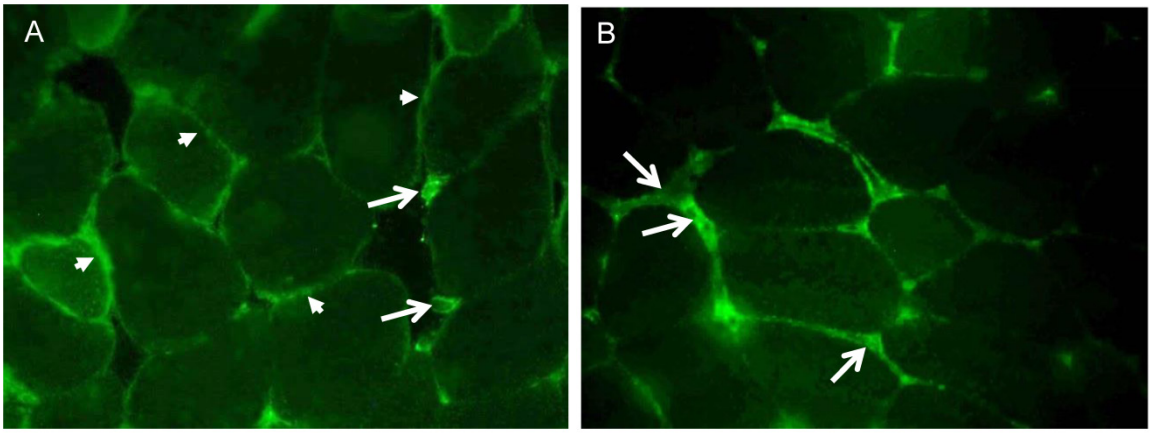

Figure 4: Cellular localization of (A) Fndc5 and (B) irisin in muscle cross sections of rectus femoris of a treadmill exercised mouse. Cryo-sections were immunostained with anti-Fndc5 and irisin primary antibodies and a MFP488 labeled goat anti-rabbit IgG secondary antibody. Fndc5 immunoreactivity was detected at the muscle fiber membrane (A, arrowheads) and punctuate in the cytoplasm, as well as in additional cells in the connective tissue (A, arrows). Irisin was mainly located in the intercellular space (B, arrows).

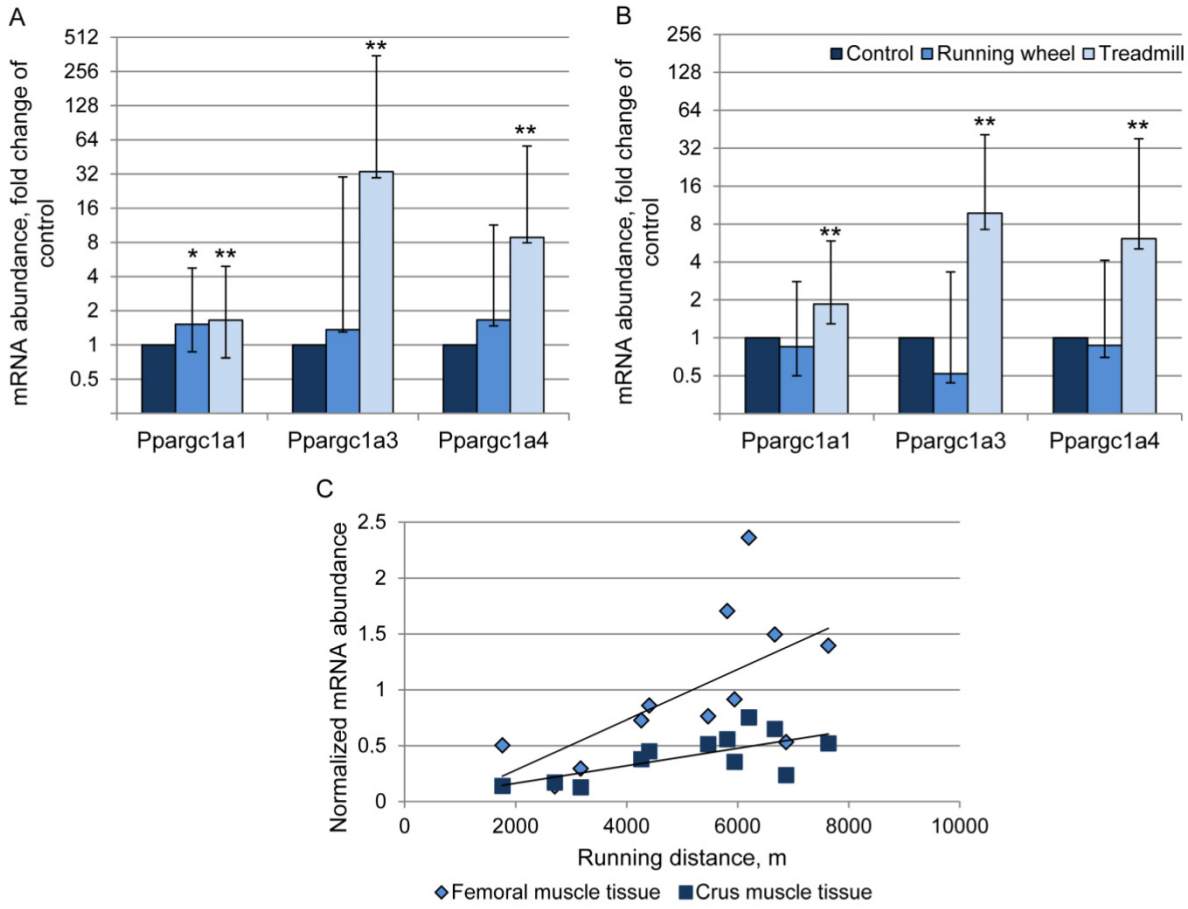

Figure 5: Relative mRNA expression of Ppargc1a transcripts 1, 3, and 4 in femoral (A) and crus (B) muscle tissue of mice after 3 weeks of voluntary exercise in a running wheel (n = 8) or one bout of treadmill exercise (n = 12) compared to a sedentary control (n = 8). The values were normalized to B2m and Hprt1. Bars represent means of fold changes compared to control group with 95 % confidence intervals marked as vertical lines. Asterisks indicate significant differences to control (*$P < 0.05$, **$P < 0.01$). (C) Relationship between Ppargc1a4 mRNA abundance, normalized to Hprt1 ($2^{-\Delta C_P}$), in femoral and crus muscles of mice and running distance during one bout of treadmill exercise ($r = 0.63$ and 0.69, respectively, $P < 0.05$).

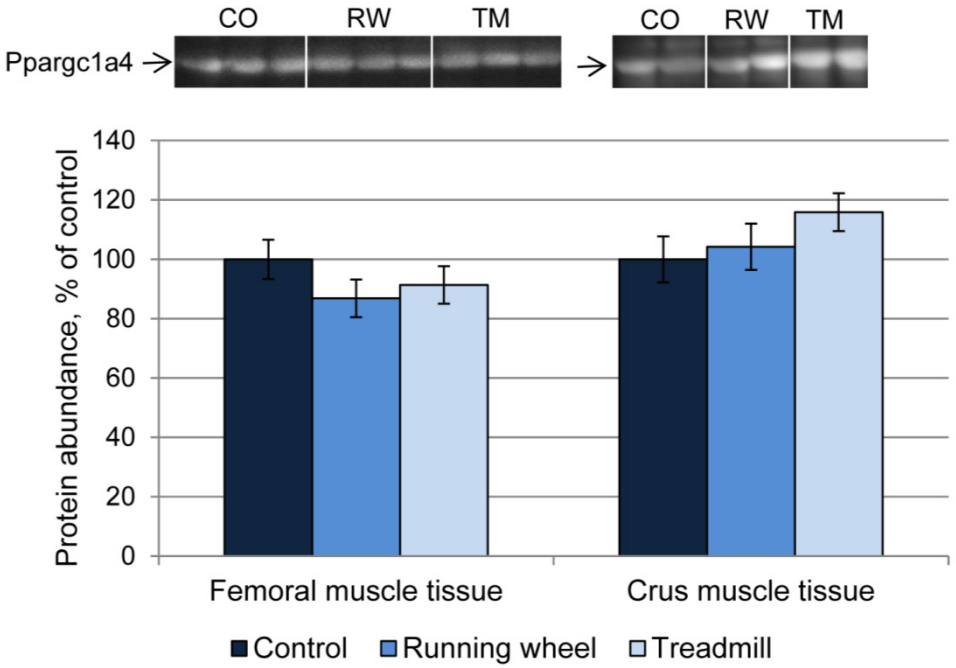

Figure 6: Protein abundance of Ppargc1a4 in femoral (FM) and crus muscle (CM) tissue of mice after 3 weeks of voluntary exercise in a running wheel (FM: n = 12, CM: n = 8) or one bout of treadmill exercise (FM and CM: n = 12) relative to a sedentary control (FM: n = 11, CM: n = 8). Representative parts of respective western blots are shown above the graph. CO – control group, RW – running wheel group, TM – treadmill group.

Discussion

In the present study, we investigated the Ppargc1a-Fndc5/irisin response in mice long-term selected for high treadmill performance (DUhTP) after a single bout of treadmill exercise or 3 weeks of voluntary exercise in a running wheel compared to a sedentary control. Mice of this line were selected because of their improved running capabilities with sufficient variation in running distances. The genetically fixed high running capacity of these mice was not achieved by training and the voluntary exercise activity of DUhTP mice was not distinct from that in unselected control mice (4).

In this mouse model, we demonstrated that irisin, the cleavage product of Fndc5, was present in skeletal muscle tissue and serum under resting conditions. Immunohistochemical analysis confirmed presence of irisin in murine skeletal muscle tissue. Its predominant location in the extracellular space between muscle cells is in agreement with the proposed mechanism of cleavage of the extracellular domain of transmembrane protein Fndc5 (3).

This is the first study that detected irisin by western blot at its predicted size of ~12 kDa and quantified exercise induced changes of this peptide in mice. Irisin responded with a significant, immediate increase to acute but not to repeated voluntary exercise in femoral muscle and in circulation. A similar reaction of irisin was observed in unselected mice (unpublished data) thus excluding a restriction of the results to the model used here. The increase of irisin in femoral but not in crus muscles after treadmill running may correspond to higher exposure of femoral muscles. Likewise, force measurements have shown that e.g. the gastrocnemius muscle, which is contained in crus muscle tissue, is activated only with increasing speed (18).

Our results of the blocking experiment provided evidence for the specific detection of irisin at ~12 kDa. The used antibody is directed against aa 32-142 of human Fndc5 thus covering the irisin peptide completely. In contrast, Roca-Rivada et al. (24) failed to detect a quantifiable 12 kDa irisin band in the secretome of rat skeletal muscle using an antibody recognizing aa 42-112 of human Fndc5. Obviously, binding to all amino acids of irisin is crucial for an efficient detection of the peptide. Numerous further studies employing western blot to detect Fndc5 and/or irisin used antibodies recognizing aa 149-178 of the human protein (3,27-30,33). Importantly, this antibody cannot detect irisin per se as it is directed against the C-terminus of Fndc5 which does not include any sequence from the irisin peptide (8,23,24). Accordingly, full length Fndc5 protein was detected at ~25 kDa with this antibody in our study.

Irisin appeared in serum as two bands at ~12 and ~13 kDa corresponding to the native and the glycosylated peptide, respectively, as confirmed by PNGase treatment. This is in contrast to a study on recombinant irisin which was detected as bands of 15 kDa (native), 22 kDa (one site glycosylated) and 25 kDa (two sites glycosylated) as predominant form in a specific yeast expression system (33). It remains to be investigated whether the size discrepancy for glycosylated irisin is due to different experimental settings in both studies.

To elucidate the background of the exercise induced irisin increase we investigated the proposed upstream factors, Ppargc1a and Fndc5 (3,27), in the same mice at mRNA and protein level. Additionally, recent findings on expression of Ppargc1a isoforms in skeletal muscle were considered (25). A transcript specific analysis of Ppargc1a mRNA abundance revealed a significant induction of transcripts 1, 3, and 4 by acute exercise in murine femoral and crus muscle tissue. In contrast, voluntary wheel running did only result in a 1.5-fold increase of transcript 1 in femoral muscle. Boström et al. (3) observed a ~2-fold up-regulation of total Ppargc1a mRNA in response to wheel running. This was likely caused by transcript 1 according to our data. Transcript 4 increased 6- to 9-fold in skeletal muscle of TM mice, whereas Ruas et al. (25) noticed a 3-fold increase in human Ppargc1a4 only when resistance and endurance training were combined. In our experiment Ppargc1a3 mRNA responded with the largest increase to acute exercise in femoral and crus muscles (33- and 10-fold up-regulation, respectively). Chinsomboon et al. (5) reported a 125-fold increase of a Ppargc1a transcript resulting from an alternative promoter in exercised mice. This promoter however, is responsible for transcription of Ppargc1a2, 3, and 4 as was shown later (25). Consequently, our results provide evidence that transcript 3 contributes a large proportion to the exercise-induced increase in total Ppargc1a mRNA. The role of transcript 2 remains to be investigated. Importantly, transcripts 1, 3, and 4 regulate different gene programs (25). Transcript 1 affects numerous classical Ppargc1a targets whereas transcript 4 exerts effects on IGF1 and myostatin signaling. The observed correlation between Ppargc1a4 mRNA abundance and individual running distance may thus indicate a link between physical activity and IGF1/myostatin signaling. Ppargc1a transcript 3 was shown to affect 69 genes which await further investigation (25). Collectively, our results support the notion that Ppargc1a transcripts are inducible by exercise to a different extent. Whether the slight increase of transcript 1 after both types of exercise mediates long term effects of

exercise in general and the strong up-regulation of transcripts 3 and 4 immediately after acute exercise is responsible for fast reaction of skeletal muscle to exercise, remains to be addressed in further studies. In support of this assumption, Perry et al. (21) described a "saw tooth-shaped" Ppargc1a mRNA increase with peaks immediately after single training bouts in humans using primers supposed to amplify all human transcripts. In contrast, Ppargc1a protein was elevated with several hours delay and accumulated with increasing number of exercise bouts. This may explain our observation of unchanged Ppargc1a protein in mice immediately after acute exercise.

Boström et al. (3) demonstrated that Fndc5 mRNA was induced by overexpression of Ppargc1a and that this increase in Fndc5 could also be observed after physical exercise in human and mouse. The positive effect of exercise on Fndc5 expression was confirmed in a number of studies at mRNA (11,15,18,24) and protein level (24,29) in different experimental settings in rats and humans. We detected Fndc5 at 25 kDa in femoral as well as in crus muscles with western blot and localized the protein immunohistochemically, in accordance with Dun et al. (7), mainly at muscle cell membranes as expected for a transmembrane protein. In our experiment however, Fndc5 mRNA as well as protein remained unchanged in both muscle tissues after voluntary and immediately after acute exercise. This is in line with several studies which did not find a clear response of Fndc5 mRNA and/or protein to physical exercise in humans and pigs (2,9,14,20,31) or exercise mimetics in cell cultures (26). Studies in rats, however, support the notion that there is a relationship between the abundance of Fndc5 and the oxidative capacity of muscle. Stephenson et al. (29) reported on elevated Fndc5 associated with higher oxidative capacity in glycolytic muscle of rats with higher running ability. Roca-Rivada et al. (24) described a 40 % higher Fndc5 secretion from oxidative compared to glycolytic muscle under basal conditions and a significant increase after 3 weeks of voluntary wheel running in both muscles. Beside glycolytic *m. quadriceps femoris* from upper hind leg, we have analyzed crus muscles from lower hind leg comprising different muscles with different metabolic fiber types. Given the equal sampling of all mice in the experimental groups and the results obtained in rat muscles, we would have been able to detect changes in Fndc5 protein if present even in this heterogeneous muscle preparation.

In contrast to other studies, we observed Fndc5 protein only in single cases in serum of mice. In humans, Huh et al. (11) reported high levels of circulating Fndc5 (25 kDa) in a subpopulation of young athletes and hypothesized that this might have resulted from muscle damage rather than being a physiological response. In conclusion, the reaction of Fndc5 to physical exercise remains controversial. Time series analyses with defined exercise regimens on defined muscles could resolve the controversies.

We analyzed the proposed Ppargc1a – Fndc5 – irisin signaling chain (3,27) at mRNA and protein level in response to acute exercise. The finding that only the first (Ppargc1a mRNA) and the last (circulating irisin peptide) chain link were elevated in acute response to exercise indicates that additional, unknown mechanisms for irisin secretion from muscle may exist. Nevertheless, fast induction of Ppargc1a mRNA upon exercise may start a process of recovering muscle irisin and its precursor Fndc5. The relatively high basal level of irisin suggests that irisin cleavage and secretion is a continuous, physiological process in mice. This is remarkably different from observations in other species. A recent study provided evidence for a different genetic make-up of the human Fndc5 locus resulting in drastically reduced expression of the full-length protein *in vitro*. Consequently, it was supposed that irisin cannot be produced by cleavage of Fndc5 and seems not to exist in humans at all (23). Own results in cattle demonstrated that full-length Fndc5 is abundant in skeletal muscle but irisin is neither detectable in muscle nor in circulation under resting conditions (12). Since direct evidence for existence of irisin was not yet provided in any species except in mice of this study, it is necessary to target possible species specificities in further investigations.

Conclusions

For the first time, our study provides evidence for the existence of irisin as ~12 kDa peptide in muscle tissue and for its circulation in mice under basal conditions. Muscle and circulating irisin increased immediately after acute but not after repeated voluntary exercise. Since this increase was not paralleled by an induction of Ppargc1a protein and Fndc5 mRNA and protein it is likely that the acute irisin response is mediated by additional, unknown factors. The elevated mRNA abundance of different Ppargc1a transcripts after acute exercise however, may indicate that Ppargc1a induces recovery of muscular Fndc5 and irisin. The mRNA abundance of Ppargc1a4 was positively related to running distance and may thus be a marker for exercise capacity. Collectively, these new findings extend the knowledge on irisin and may provide a basis to revisit the Ppargc1a-Fndc5/irisin signaling pathway under consideration of species specificities.

Abbreviations

aa: amino acid; B2M: beta-2-microglobulin; CO: control; C_p: crossing point; DUhTP: Dummerstorf high treadmill performance; ELISA: enzyme-linked immunosorbent assay; Fndc5: fibronectin type III domain-containing protein 5; Hprt1: hypoxanthin-phosphoribosyl-transferase 1; IGF1: insulin-like growth factor 1; Ppargc1a: peroxisome proliferator-activated receptor gamma coactivator 1-alpha; qPCR: quantitative polymerase chain reaction; RW: running wheel; TBS: Tris-buffered saline; TM: treadmill.

Acknowledgement

We are grateful to L. Chau, S. Hinrichs, E. Schwitulla, S. Foß, S. Geist, B. Lucht, S. Alm, and K. Ullerich for expert technical assistance and animal care.

This work was supported in part by grants of the Leibniz Association (grant no. SAW-2013-FBN-3) and the Deutsche Forschungsgemeinschaft (grant no. DFG H0 2003/6-1).

Competing Interests

The authors have declared that no competing interest exists.

References

1. Albrecht E, Komolka K, Kuzinski J, Maak S. Agouti revisited: Transcript quantification of the ASIP gene in bovine tissues related to protein expression and localization. PLoS One. 2012; 7: e35282.
2. Besse-Patin A, Montastier E, Vinel C, Castan-Laurell I, Louche K, Dray C, Daviaud D, Mir L, Marques MA, Thalamas C, Valet P, Langin D, Moro C, Viguerie N. Effect of endurance training on skeletal muscle myokine expression in obese men: identification of apelin as a novel myokine. Int J Obes (Lond). 2013; doi: 10.1038/ijo.2013.158.
3. Boström P, Wu J, Jedrychowski MP Korde A, Ye L, Lo JC, Rasbach KA, Boström EA, Choi JH, Long JZ, Kajimura S, Zingaretti MC, Vind BF, Tu H, Cinti S, Højlund K, Gygi SP, Spiegelman BM. A PGC1-α-dependent myokine that drives brown-fat-like development of white fat and thermogenesis. Nature. 2012; 481: 463-468.
4. Brenmoehl J, Walz C, Renne U, Ponsuksili S, Wolf C, Langhammer M, Schwerin M, Hoeflich A. Metabolic adaptations in the liver of born long-distance running mice. Med Sci Sports Exerc. 2013; 45: 841-850.
5. Chinsomboon J, Ruas J, Gupta RK, Thom R, Shoag J, Rowe GC, Sawada N, Raghuram S, Arany Z. The transcriptional coactivator PGC-1alpha mediates exercise-induced angiogenesis in skeletal muscle. Proc Natl Acad Sci U S A. 2009; 106: 21401-21406.
6. de Kok JB, Roelofs RW, Giesendorf BA, Pennings JL, Waas ET, Feuth T, Swinkels DW, Span PN. Normalization of gene expression measurements in tumor tissues: comparison of 13 endogenous control genes. Lab Invest. 2005; 85: 154-159.
7. Dun SL, Lyu RM, Chen YH, Chang JK, Luo JJ, Dun NJ. Irisin-immunoreactivity in neural and non-neural cells of the rodent. Neurosci. 2013; 240: 155-162.
8. Erickson HP. Irisin and FNDC5 in retrospect: An exercise hormone or a transmembrane receptor? Adipocyte. 2013; 2: 289-293.
9. Fain JN, Company JM, Booth FW, Laughlin MH, Padilla J, Jenkins NT, Bahouth SW, Sacks HS. Exercise training does not increase muscle FNDC5 protein or mRNA expression in pigs. Metabolism. 2013; 62: 1503-1511.
10. Falkenberg H, Langhammer M, Renne U. Comparison of biochemical blood traits after long-term selection on high or low locomotory activity in mice. Arch Tierz. 2000; 43: 513-522.
11. Huh JY, Panagiotou G, Mougios V, Brinkoetter M, Vamvini MT, Schneider BE, Mantzoros CS. FNDC5 and irisin in humans, I. Predictors of circulating concentrations in serum and plasma and II. mRNA expression and circulating concentrations in response to weight loss and exercise. Metabolism. 2012; 61: 1725-1738.
12. Komolka K, Albrecht E, Schering L, Brenmoehl J, Hoeflich A, Maak S. Locus characterization and gene expression of bovine FNDC5: Is the myokine irisin relevant in cattle? PLoS One. 2014; 9: e88060.
13. Kraemer RR, Shockett P, Webb ND, Shah U, Castracane VD. A Transient Elevated Irisin Blood Concentration in Response to Prolonged, Moderate Aerobic Exercise in Young Men and Women. Horm Metab Res. 2014; 46: 150-154.
14. Kurdiova T, Balaz M, Vician M, Maderova D, Vlcek M, Valkovic L, Srbecky M, Imrich R, Kyselovicova O, Belan V, Jelok I, Wolfrum C, Klimes I, Krssak M, Zemkova E, Gasperikova D, Ukropec J, Ukropcova B. Are Skeletal Muscle & Adipose Tissue Fndc5 Gene Expression and Irisin Release Affected by Obesity, Diabetes and Exercise? In vivo & in vitro studies. J Physiol. 2014; doi: 10.1113/jphysiol.2013.264655.
15. Lecker SH, Zavin A, Cao P, Arena R, Allsup K, Daniels KM, Joseph J, Schulze PC, Forman DE. Expression of the irisin precursor FNDC5 in skeletal muscle correlates with aerobic exercise performance in patients with heart failure. Circ Heart Fail. 2012; 5: 812-818.
16. Lieber RR. Skeletal muscle structure, function, and plasticity; 2nd Ed. The physiological basis of rehabilitation. MD, USA: Lippincott Williams & Wilkins, Baltimore. 2002.
17. Moraes C, Leal VO, Marinho SM, Barroso SG, Rocha GS, Boaventura GT, Mafra D. Resistance exercise training does not affect plasma irisin levels of hemodialysis patients. Horm Metab Res. 2013; 45: 900-904.
18. Norheim F, Langleite TM, Hjorth M, Holen T, Kielland A, Stadheim HK, Gulseth HL, Birkeland KI, Jensen J, Drevon CA. The effects of acute and chronic exercise on PGC-1α, irisin and browning of subcutaneous adipose tissue in humans. FEBS J. 2014; 281: 739-749.
19. Novelle MG, Contreras C, Romero-Picó A, López M, Diéguez C. Irisin, two years later. Int J Endocrinol. 2013; 2013: 746281.
20. Pekkala S, Wiklund PK, Hulmi JJ, Ahtiainen JP, Horttanainen M, Pöllänen E, Mäkelä KA, Kainulainen H, Häkkinen K, Nyman K, Alén M, Herzig KH, Cheng S. Are skeletal muscle FNDC5 gene expression and irisin release regulated by exercise and related to health? J Physiol. 2013; 59: 5393-5400.
21. Perry CGR, Lally J, Holloway GP, Heigenhauser GJF, Bonen A, Spriet LL. Repeated transient mRNA bursts precede increases in transcriptional and mitochondrial proteins during training in human skeletal muscle. J Physiol 2010; 588: 4795-4810.
22. Pfaffl MW, Horgan GW, Dempfle L. Relative expression software tool (REST) for group-wise comparison and statistical analysis of relative expression results in real-time PCR. Nucleic Acids Res. 2002; 30: e36.
23. Raschke S, Elsen M, Gassenhuber H, Sommerfeld M, Schwahn U, Brockmann B, Jung R, Wisløff U, Tjønna AE, Raastad T, Hallén J, Norheim F, Drevon CA, Romacho T, Eckardt K, Eckel J. Evidence against a beneficial effect of irisin in humans. PLoS One. 2013; 8: e73680.
24. Roca-Rivada A, Castelao C, Senin LL, Landrove MO, Baltar J, Belén Crujeiras A, Seoane LM, Casanueva FF, Pardo M. FNDC5/irisin is not only a myokine but also an adipokine. PLoS One. 2013; 8: e60563.
25. Ruas JL, White JP, Rao RR et al. A PGC-1α isoform induced by resistance training regulates skeletal muscle hypertrophy. Cell. 2012; 151: 1319-1331.
26. Sánchez J, Nozhenko Y, Palou A, Rodríguez AM. Free fatty acid effects on myokine production in combination with exercise mimetics. Mol Nutr Food Res. 2013; 57: 1456-1467.
27. Shan T, Liang X, Bi P, Kuang S. Myostatin knockout drives browning of white adipose tissue through activating the AMPK-PGC1α-Fndc5 pathway in muscle. FASEB J. 2013; 27: 1981-1989.
28. Sharma N, Castorena CM, Cartee GD. Greater insulin sensitivity in calorie restricted rats occurs with unaltered circulating levels of several important myokines and cytokines. Nutr Metab (Lond). 2012; 9: 90.
29. Stephenson EJ, Stepto NK, Koch LG, Britton SL, Hawley JA. Divergent skeletal muscle respiratory capacities in rats artificially selected for high and low running ability: a role for Nor1? J Appl Physiol. 2012; 113: 1403-1412.
30. Swick AG, Orena S, O'Connor A. Irisin levels correlate with energy expenditure in a subgroup of humans with energy expenditure greater than predicted by fat free mass. Metabolism. 2013; 62: 1070-1073.
31. Timmons JA, Baar K, Davidsen PK, Atherton PJ. Is irisin a human exercise gene? Nature. 2012; 488: E9-10.
32. Wen MS, Wang CY, Lin SL, Hung KC. Decrease in irisin in patients with chronic kidney disease. PLoS One. 2013; 8: e64025.
33. Zhang Y, Li R, Meng Y, Li S, Donelan W, Zhao Y, Qi L, Zhang M, Wang X, Cui T, Yang LJ, Tang D. Irisin Stimulates Browning of White Adipocytes through Mitogen-Activated Protein Kinase p38 MAP Kinase and ERK MAP Kinase Signaling. Diabetes. 2013;: DB_131106.

J Comp Physiol B
DOI 10.1007/s00360-016-1036-7

ORIGINAL PAPER

Browning of subcutaneous fat and higher surface temperature in response to phenotype selection for advanced endurance exercise performance in male DUhTP mice

J. Brenmoehl[1] · D. Ohde[1] · E. Albrecht[2] · C. Walz[1] · A. Tuchscherer[3] · A. Hoeflich[1]

Received: 28 January 2016 / Revised: 12 September 2016 / Accepted: 20 September 2016

Abstract For the assessment of genetic or conditional factors of fat cell browning, novel and polygenic animal models are required. Therefore, the long-term selected polygenic mouse line DUhTP originally established in Dummerstorf for high treadmill performance is used. DUhTP mice are characterized by increased fat accumulation in the sedentary condition and elevated fat mobilization during mild voluntary physical activity. In the present study, the phenotype of fat cell browning of subcutaneous fat and a potential effect on oral glucose tolerance, an indicator of metabolic health, were addressed in DUhTP mice. Analysis of peripheral fat pads revealed increased brite (brown-in-white) subcutaneous adipose tissues and in subcutaneous fat from DUhTP mice higher levels of irisin and different markers of fat cell browning like T-box transcription factor (Tbx1), PPARα, and uncoupling protein (UCP1) ($P < 0.05$) when compared to unselected controls. UCP1 was further increased in subcutaneous fat from DUhTP mice in response to mild exercise (fourfold, $P < 0.05$). In addition, surface temperature of DUhTP mice was increased when compared to controls indicating a physiological effect of increased UCP1 expression. The present study suggests that DUhTP mice exhibit different markers of mitochondrial biogenesis and fat browning without external stimuli. At an age of 43 days, sedentary DUhTP mice have improved metabolic health as judged from lower levels of blood glucose after an oral glucose tolerance test. Consequently, the non-inbred mouse model DUhTP represents a novel model for the identification of fat cell browning mechanisms in white adipose tissues.

Keywords Selection · Browning · Irisin · Subcutaneous fat · Uncoupling protein

Introduction

The Dummerstorf marathon mouse model DUhTP has been selected over 90 generations for high treadmill performance (Falkenberg et al. 2000) and thus represents a unique model for the study of energy metabolism. In the liver of DUhTP mice increased lipid synthesis has been postulated based on the analysis of hepatic metabolome by current mass spectrometry (Brenmoehl et al. 2013). In the sedentary condition, marathon mice accumulate high amounts of body fat in external depots indicating physiological relevance of lipids for superior endurance exercise performance in DUhTP mice. In fact, recent work revealed that external fat mass in DUhTP mice is highly responsive to physical activity because voluntary exercise in running wheels completely abolished the obese phenotype of DUhTP mice (Brenmoehl et al. 2015). In subcutaneous fat from DUhTP mice, PGC1-α and mitochondrial DNA content were increased and it was speculated that fat cell browning may occur in subcutaneous white adipocytes (Brenmoehl et al. 2015). It is known that brite

Communicated by G. Heldmaier.

✉ A. Hoeflich
hoeflich@fbn-dummerstorf.de

[1] Institute for Genome Biology, Leibniz-Institute for Farm Animal Biology (FBN), Wilhelm-Stahl-Allee 2, 18196 Dummerstorf, Germany

[2] Institute for Muscle Biology and Growth, Leibniz-Institute for Farm Animal Biology (FBN), Wilhelm-Stahl-Allee 2, 18196 Dummerstorf, Germany

[3] Institute for Biometry and Genetics, Leibniz-Institute for Farm Animal Biology (FBN), Wilhelm-Stahl-Allee 2, 18196 Dummerstorf, Germany

Published online: 30 September 2016

adipocytes, converted from white adipocytes, exhibit properties of brown adipocytes like expression of UCP1 and a proposed mechanism for the induction of browning in WAT may occur by irisin derived from muscle after contraction (Bostrom et al. 2012) or from the fat independent of physical exercise (Roca-Rivada et al. 2013). A number of studies has demonstrated that the addition of exogenous irisin or irisin precursors (FNDC5) induced browning of white fat cells both in rodent (Zhang et al. 2014; Bostrom et al. 2012) and in human white fat cells (Zhang et al. 2016; Huh et al. 2014; Lee et al. 2014). Fat cell browning in response to irisin treatment further induced cellular thermogenesis in mature human white fat cells (Zhang et al. 2016). Because irisin may represent an early marker of fat cell browning and thermogenesis, it may have the potential as a novel anti-obesity drug (Bostrom et al. 2012) or in a more general view could be seen as an attractive tool for the manipulation of energy metabolism in vivo.

Interestingly, after acute exercise, higher levels of irisin have been found in muscle extracts and in serum of marathon mice (DUhTP) long-term selected for endurance exercise (Brenmoehl et al. 2014) supporting the idea that irisin may act as an endogenous effector of energy metabolism.

The aim of the present work is to determine if the marathon mouse model DUhTP is a natural model for the analysis of adipose browning in the presence of elevated FNDC5/irisin expression. To accomplish this, we measured FNDC5/irisin expression and content of selected tissues, UCP1 content, and skin temperature as a surrogate for core temperature both in DUhTP mice and in unselected controls.

Materials and methods

Animals

All in vivo experiments were performed in accordance with national and international guidelines and were approved by our internal institutional review board. In this study, on one hand, a non-inbred mouse line that has been generated by selection over 90 generations for high treadmill performance (DUhTP) (Falkenberg et al. 2000) and on the other control mice (DUC) that had been generated from the identical base population without phenotype selection was used (Dietl et al. 2004). The males were housed under controlled environmental conditions in a semi-barrier system with a 12-h light–12-h dark cycle (room temperature = 22.5 ± 0.2 °C, humidity = 50–60 %) as described in (Brenmoehl et al. 2013). At an age of 49 days, DUhTP mice and controls were kept either in home cages with running wheels (RW) (d = 33.4 cm; Tecniplast, Hohenpeißenberg, Germany) to assess physical activity over a period of 3 weeks (n = 10 per group) or in cages without RW as controls (n = 10 per group). At 70 days of age, mice were fasted overnight and killed by decapitation to collect serum samples. Tissues were weighted (summary in Table 1), snap-frozen in liquid nitrogen, and stored at −70 °C for subsequent analysis. In parallel, mice (n = 9 per group) were analyzed under temperature conditions of husbandry at 22 °C for surface temperature using an infrared camera (Testo 881; Testo AG, Lenzkirch, Germany).

Oral glucose tolerance test

Oral glucose tolerance tests (oGTT) were performed in mice at an age of 43 and 71 days, essentially as described before (Renne et al. 2013). In brief, glucose was applied to overnight fasted mice (43 days: n = 20; 71 days: $n > 5$ per group) in an oral dose of 1 g glucose/kg body weight dissolved in tap water and concentrations of blood glucose were assessed before and 10, 30, 60, and 120 min after the oral glucose bolus. Glucose concentrations were analyzed using a glucometer (Roche, Penzberg, Germany).

Quantitative real-time PCR

Expression of different mRNA transcripts in subcutaneous fat samples (n = 7) was analyzed in triplicates as described previously (Brenmoehl et al. 2014, 2015). Primers used are mTbx1-forw: ggcaggcagacgaatgttc, mTbx1-rev: ttgtcatctacgggcacaaag, UCP1-forw: ggcctctacgactcagtcca, UCP1-rev: taagccggctgagatcttgt, Tcf21-forw: cattcaccagtcaacctga, Tcf21-rev: ttccttcaggtcattctctgg, Fndc5-forw: caacgagcccaataacaaca, Fndc5-rev: agaaggtcctctcgcattctc. Different housekeeping genes (Brenmoehl et al. 2015) were tested to identify the HKG with comparable Crossing point (Cp)-values (Cp_{Rplp2}: DUhTP: 24.45 ± 1.17; DUC: 25.80 ± 1.03) to normalize expression of *Tbx1* and *Ucp1*.

Immunoblotting

Western immunoblotting was performed as described previously (Brenmoehl et al. 2014). Equal loading of the gels and proper transfer of the proteins to the membranes were verified by Coomassie Blue staining according to standard procedures (Taylor et al. 2013). Expression of UCP1 (sc-6529, Santa Cruz, Heidelberg, Germany), irisin (A00170-01-100; Bio Trend, Cologne, Germany), and FNDC5 (AP8746b; Abgent, San Diego, CA, USA) in all ten animals per group were studied by Western immunoblotting. Western immunoblots were repeated at least three times. Thereby, samples were determined in different order to avoid position effects while blotting.

Table 1 Body and tissue weights of male mice long-term selected for high treadmill performance (DUhTP) and unselected controls (DUC) at an age of 70 days as published before (Brenmoehl et al. 2015)

	n	DUhTP	DUhTP-RW	*P*	DUC	DUC-RW	*P*	*P* (DUhTP vs DUC)	*P* (DUhTP-RW vs DUC-RW)
Body mass (g)	10	32.18 ± 1.02	31.25 ± 0.87	0.4925	35.18 ± 0.67	34.65 ± 0.79	0.6125	**0.0191**	**0.0066**
Lean body mass (g)	10	20.89 ± 1.76	20.5 ± 1.78	0.7529	23.56 ± 1.44	23.45 ± 1.61	0.8702	**0.0025**	**0.0007**
Body length (cm)	10	10.04 ± 0.12	9.93 ± 0.11	0.4907	10.44 ± 0.10	10.42 ± 0.09	0.8845	**0.0135**	**0.0014**
Musculus rectus femoris (g)	10	0.37 ± 0.01	0.38 ± 0.01	0.2969	0.39 ± 0.01	0.36 ± 0.01	0.0795	0.1378	0.1767
Musculus rectus femoris (%)	10	0.0114 ± 0.00	0.0122 ± 0.00	**0.0372**	0.0111 ± 0.00	0.0104 ± 0.00	0.0862	0.3829	**0.0004**
Liver mass (g)	10	1.81 ± 0.07	1.76 ± 0.08	0.6301	1.94 ± 0.06	1.82 ± 0.06	0.1513	0.1571	0.5192
Liver mass (%)	10	0.0561 ± 0.00	0.0561 ± 0.00	0.9855	0.0552 ± 0.00	0.0525 ± 0.00	0.1388	0.5363	0.0758
Subcutaneous fat (g)	10	0.36 ± 0.03	0.22 ± 0.03	**0.0012**	0.20 ± 0.01	0.18 ± 0.02	0.4910	**0.00003**	0.2448
Subcutaneous fat (%)	10	0.0112 ± 0.00	0.0065 ± 0.00	**0.0002**	0.0056 ± 0.00	0.0053 ± 0.00	0.6095	**0.00001**	0.1495
Epidymal fat (g)	10	0.33 ± 0.03	0.23 ± 0.03	**0.0145**	0.28 ± 0.03	0.20 ± 0.02	**0.0183**	0.2122	0.2718
Epidymal fat (%)	10	0.0102 ± 0.00	169 ± 0.00	**0.0025**	179 ± 0.00	156 ± 0.00	**0.0195**	**0.0320**	0.1383
Perinephric fat (g)	10	0.16 ± 0.02	0.08 ± 0.01	**0.0020**	0.09 ± 0.01	0.06 ± 0.01	**0.0086**	**0.0035**	0.2327
Perinephric fat (%)	10	0.0049 ± 0.00	0.0021 ± 0.00	**0.0002**	0.0025 ± 0.00	0.0017 ± 0.00	**0.0083**	**0.0003**	0.2122
Brown fat (g)	10	0.09 ± 0.01	0.07 ± 0.00	**0.0191**	0.06 ± 0.00	0.06 ± 0.00	0.7512	**0.0006**	0.1189
Brown fat (%)	10	0.0027 ± 0.00	0.0022 ± 0.00	**0.0361**	0.0017 ± 0.00	0.0017 ± 0.00	0.8656	**0.00005**	**0.0103**

Mice were kept in cages with running wheels (RW) or without. Total body lean mass was analyzed by dual energy X-ray absorptiometry. Values are presented as mean ± SE. Significant group effects (*P*) are indicated in bold letters (%: normalized by body weight)

Immunohistochemical staining in adipose tissue

In addition to standard hematoxylin/eosin (H/E) staining, immunohistochemistry was applied for UCP1 and C/EBPβ detection on 12 µm thick frozen tissue sections (2–3 randomly selected mice per group) using antibodies against either UCP1 (1:100, sc-6529, Santa Cruz) for 1 h at room temperature or C/EBPβ (1:100, sc-150, Santa Cruz) for 2 h at room temperature in a humidity chamber similar to previously described procedure (Albrecht et al. 2015a). Specific binding was detected with fluorescence-labeled secondary antibodies (MFP 488 rabbit anti- goat IgG for UCP1 and MFP 590 goat anti-rabbit IgG for C/EBPβ, MoBiTec, Goettingen, Germany). All sections were counterstained with 1 µg/ml Hoechst 33258 (Sigma-Aldrich, Munich, Germany). Immunofluorescence was visualized with a Nikon Microphot SA fluorescence microscope (Nikon Instruments Europe B.V., The Netherlands) and an image analysis system equipped with CELL^F image analysis software and a CCD-12 high resolution color camera (OSIS, Münster, Germany). The selected H/E images are representative in any case for a region of typical unilocular white adipocytes and a region of multilocular adipocytes. Fluorescence images represent a region of multilocular cells to illustrate protein expression typical for either heat producing or differentiating adipocytes. Subcutaneous fat samples were cryosectioned (25 µm thick) using a Leica CM3050 S (Leica, Bensheim, Germany) cryostat microtome. Sections were stained with hematoxylin/eosin (H/E; hematoxylin: Dako, Glostrup, DK; eosin: Chroma Gesellschaft, Münster, Germany) and embedded with Roti-Histokit (Roth, Karlsruhe, Germany). Adipocyte size was measured using the interactive measurement module of an image analysis system equipped with an Olympus BX43 microscope (Olympus, Hamburg, Germany), an UC30 color camera (Olympus) and CELL^D image analysis software (OSIS, Munster, Germany). About 300 adipocytes per sample were randomly selected and measured, after following the contour using the interpolating polygon function.

Statistical analysis

The data analysis was performed using SAS software (Version 9.4 for Windows, SAS Institute Inc., Cary, NC, USA). Descriptive statistics and tests for normality were calculated with the UNIVARIATE procedure of Base SAS software (SAS Institute Inc. 2013. Base SAS® 9.4 Procedures Guide, Second Edition. Cary, NC: SAS Institute Inc.). Data considered approximately normal were analyzed by ANOVA using the GLIMMIX procedure of SAS/STAT

software (SAS Institute Inc. 2013. SAS/STAT® 13.1 User's Guide. Cary, NC: SAS Institute Inc.). The ANOVA model for the 70 days data included the fixed factors line (levels: DUC, DUhTP), group (levels: co, RW), and the interaction line × group. Homogeneity of covariance parameters across groups was tested for all ANOVA models. In addition, least-squares means (LSM) and their standard errors (SE) were computed for each fixed effect in the models, and all pairwise differences of LS-means were tested by the Tukey–Kramer procedure. Effects and differences were considered significant if $P < 0.05$. Glucose levels in response to oral glucose application were further analyzed by repeated measurements ANOVA provided by the BASE SAS software package.

Results

Irisin in subcutaneous adipose tissue

Previously, expression of FNDC5 protein in muscles and abundance of irisin in serum of DUhTP mice was demonstrated (Brenmoehl et al. 2014). Now expression of irisin and FNDC5 was analyzed in active and sedentary DUhTP and control mice. Both mouse lines voluntarily used running wheels present in their home cages to a similar extent (DUhTP: 3935 ± 1719; DUC 3913 ± 1181 m/day). A comparison of FNDC5 and irisin between both sedentary mouse lines revealed abundant but unchanged levels of muscular FNDC5 (Fig. 1a) but higher levels of irisin (Fig. 1b) in serum of DUhTP mice (~fourfold, $P < 0.05$). Physical activity had no influence on FNDC5 or irisin levels. Indeed, very high concentrations of irisin were detected in subcutaneous adipose tissue of DUhTP mice (Fig. 1c). In contrast to controls, sedentary and active DUhTP mice showed over twofold increased irisin levels; FNDC5 protein was barely detectable in subcutaneous adipose tissue and showed no clear differences.

Elevated browning in subcutaneous fat from DUhTP mice

Subcutaneous fat dissected from DUhTP mice of both treatment groups appeared darker when compared to unselected control mice, which suggested differential browning in DUhTP and DUC mice. Histological examination revealed clustered formation of smaller multilocular adipocytes (brite fat cell) and larger unilocular adipocytes (white fat cell) in tissue sections from subcutaneous fat of both mouse lines at an age of 10 weeks (Fig. 2). Clustered appearance of white and brite fat cells was also observed in 90-day-old mice of both genetic groups. Examination of the tissue sections indicated larger areas covered by brite fat cells in DUhTP versus DUC mice. In white adipocytes, histological parameters (area, diameter, and Feret diameter) were unaffected by genetic group of voluntary physical activity (data not shown). To describe the differential phenotype of fat cell browning, biomarkers of brown, white, and brite fat cells were assessed in subcutaneous fat (Fig. 3a). Tbx1 mRNA expression was significantly increased in DUhTP mice (56 %; $P < 0.05$) compared to unselected controls. Physical activity in DUhTP had no significant effect on mRNA expression of the brite adipose tissue marker Tbx1 (22 %, n.s.). As expected, white adipose tissue marker transcription factor 21 (Tcf21) was barely expressed in sedentary DUhTP mice when compared to control mice but the differences between both mouse lines reached no statistical significance because of high individual variability. Transcription factor PPARα was also elevated in the subcutaneous fat of active and sedentary DUhTP mice in contrast to control animals (17-fold; $P < 0.005$ and 21-fold; $P < 0.05$, respectively). Downstream expression of BAT-marker Ucp1 was increased in subcutaneous fat of DUhTP mice as well (50-fold; $P < 0.005$). In response to activity, expression of Ucp1 further increased threefold ($P < 0.05$). In controls, expression of Tbx1, PPARα, and Ucp1 were unaffected by physical activity.

Higher expression of UCP1 in DUhTP mice in subcutaneous fat was present also on the protein level as demonstrated by Western immunoblotting (Fig. 3b). Compared to sedentary DUC mice, UCP1 was 7.3-fold increased in sedentary DUhTP mice. Moderate voluntary activity for 3 weeks resulted in a further 4.2-fold higher protein expression in subcutaneous fat of DUhTP mice when compared to non-exercised controls. Higher protein levels of UCP1 were further demonstrated by immunohistochemistry. Cryostat sections of subcutaneous adipose tissue of sedentary and physical active DUhTP mice displayed areas of multilocular adipocytes. These areas stained massively for UCP1, while in comparable sections of control mice, only weak UCP1 protein expression was detectable (Fig. 3c). Multilocular adipocytes in control mice could be confirmed as differentiating adipocytes with positive staining for CCAAT/enhancer-binding protein beta (C/EBPβ). Only few C/EBPβ-positive adipocytes were observed in UCP1-stained regions of DUhTP mice.

UCP1 is known to uncouple ATP production leading to enhanced energy production, allowing small animals to better tolerate cold (Himms-Hagen 1970). As an indirect and noninvasive method to determine UCP1 activity, heat production indicated by change in surface temperature was measured in both mouse lines using an infrared camera. It was asked if the increased UCP1 expression in subcutaneous fat correlates with an elevated surface temperature at 22 °C room temperature. In fact, DUhTP mice showed a significantly higher surface temperature (+1 °C; $P < 0.005$)

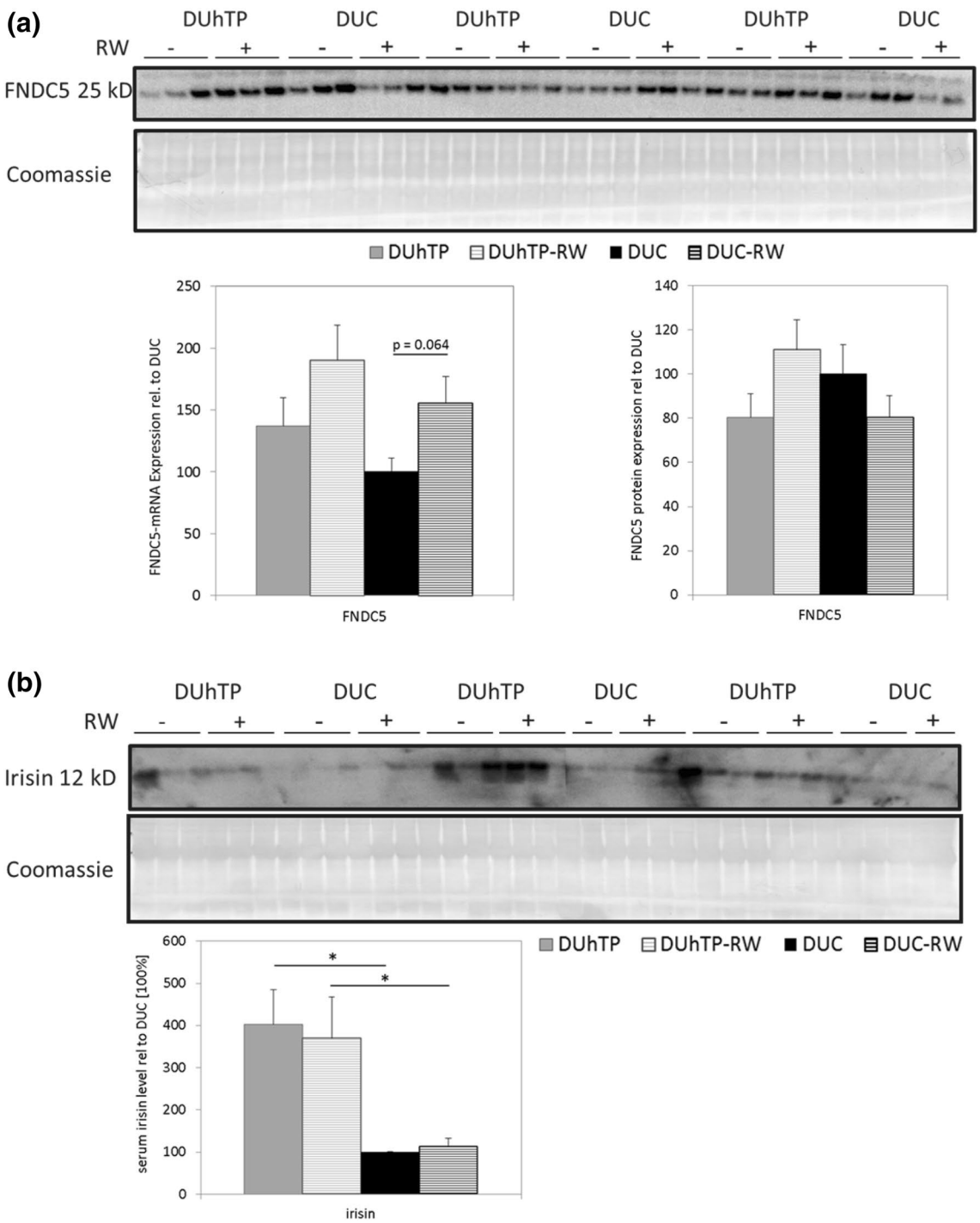

Fig. 1 Effect of voluntary physical activity (RW) on levels of **a** FNDC5 in muscles, **b** irisin in serum and **c** FNDC5 and irisin in subcutaneous adipose tissue from DUhTP and DUC mice. Analysis of FNDC5-mRNA expression was performed by quantitative real-time PCR and normalized to expression of HKG Rplp2. Protein analysis was performed by Western immunoblotting. Protein expression was quantified by densitometry and normalized for the Coomassie blue signal. All data are expressed in relation to the expression level of sedentary unselected controls (DUC) with no access to RW. Values are mean ± SE; $*P < 0.05$, $**P < 0.005$

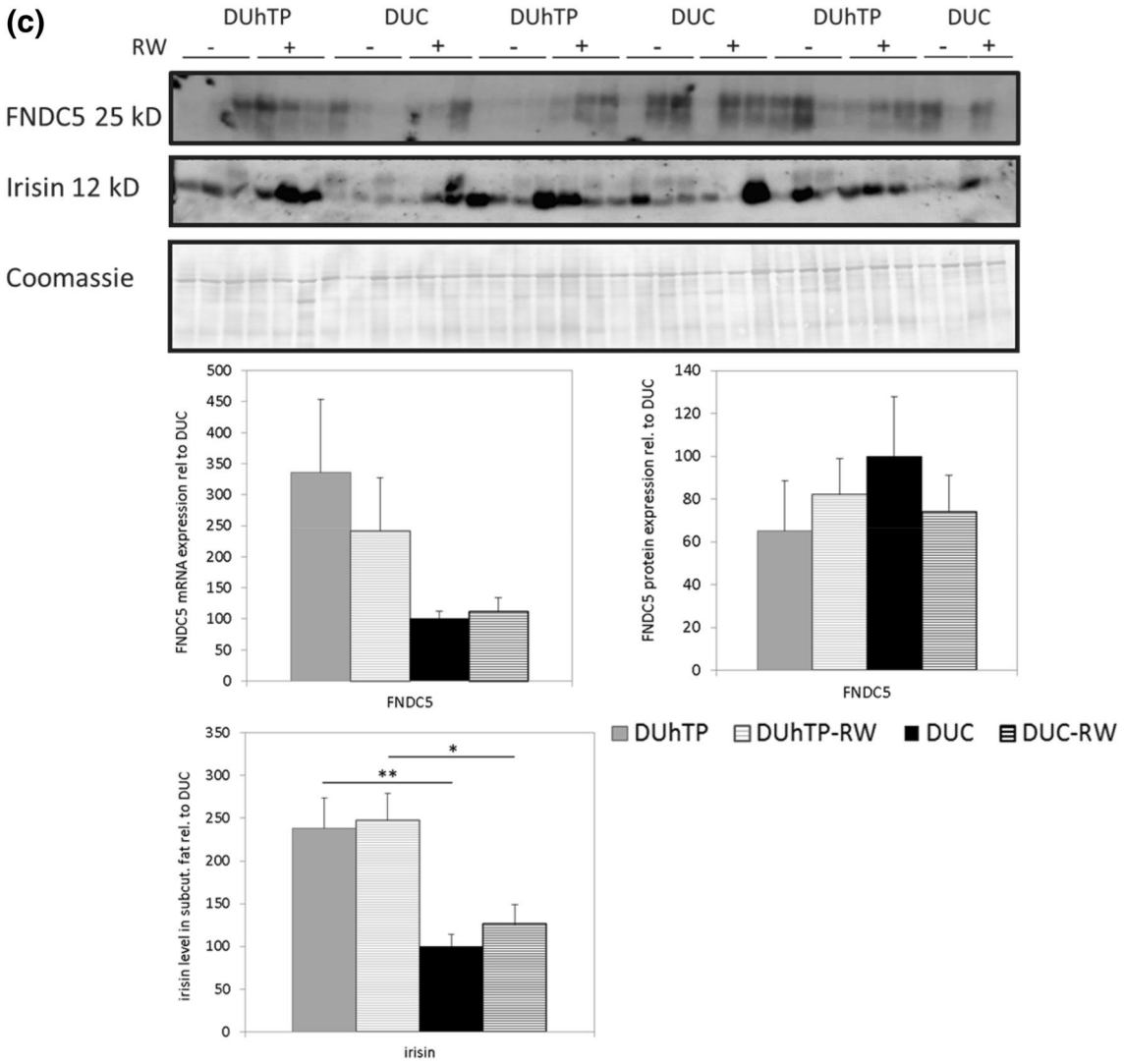

Fig. 1 continued

than control mice (Fig. 4), but differences between active and sedentary littermates were not found.

Better oral glucose tolerance in DUhTP mice

At an age of 43 days, male DUhTP mice had lower blood glucose levels before and after oral application of glucose (Fig. 5a) at all time points assessed ($P < 0.01$). Lower blood glucose levels were not found in elder DUhTP mice at an age of 71 days (Fig. 5b). However, voluntary physical activity over a period of 3 weeks in DUhTP mice significantly reduced blood glucose ($P < 0.05$). The areas under curve of oral glucose levels after oral glucose tolerance tests in DUhTP mice and unselected controls were statistically not significantly different (data not shown). However, repeated measurement ANOVA revealed a significant interaction between the time of glucose testing and mouse line ($P < 0.05$).

Discussion

Irisin has been identified as an effector of fat cell browning and thermogenesis by the induction of UCP1 (Bostrom et al. 2012). In addition, irisin effects on carbohydrate and lipid metabolism also have been provided for the liver (Mo et al. 2016) suggesting broader effects on energy metabolism. Our marathon mouse model DUhTP, established by long-term selection for high treadmill performance, is characterized by increased hepatic lipogenesis on one hand and peripheral obesity on the other, if compared to unselected control mice (DUC) (Brenmoehl et al. 2013). For the sake of clarity, we included Table 1 in our manuscript providing published data on increased fat accretion in DUhTP mice (Brenmoehl et al. 2015). Notably, in DUhTP also irisin concentrations were found being increased in skeletal muscle and plasma (Brenmoehl et al. 2014). To establish

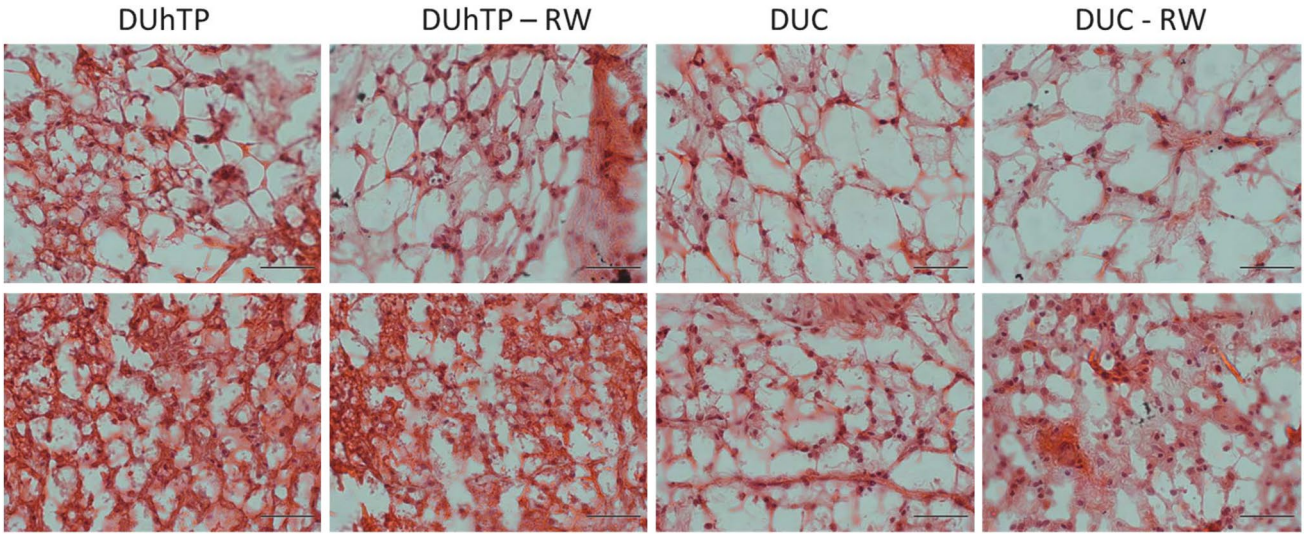

Fig. 2 Hematoxylin/Eosin staining of subcutaneous adipose tissue from sedentary and physical active (−RW) male DUhTP and DUC mice, respectively. *Upper set* of *pictures* displays areas of white adipocytes and *lower pictures* show area with clusters of brite adipocytes. *Scale bar* 50 µm

DUhTP mice as an in vivo-relevant and polygenic model of irisin actions, we tested current hypotheses in DUhTP mice. We therefore assessed known effects of irisin in subcutaneous fat and investigated fat cell morphology, browning, UCP1 expression, and thermogenesis in our experimental system. Finally we asked if higher irisin expression in DUhTP also correlated with improved metabolic health.

Adipose tissue of DUhTP mice showed more multilocular adipocytes than DUC mice, with no obvious effect on white adipocyte histology. Real-time PCR and immunohistochemical analyses revealed lower expression of markers associated with white (C/EBP; Tcf21), brite (Tbx1) and brown adipose tissue (UCP1, PPARα) (Escher et al. 2001; Wu et al. 2012) arguing for elevated abundance of brite adipocytes in this fat depot of DUhTP mice already under sedentary conditions. In response to 3 weeks of voluntary exercise, UCP1-expression was further increased in DUhTP mice, whereas in controls, no changes were detectable. High UCP1 abundance in DUhTP and weak expression in control mice were confirmed by immunohistochemistry. Especially UCP1, a known regulator of BAT-dependent thermogenesis (Argyropoulos and Harper 2002) with low-level expression in WAT (Wu et al. 2012), indicates the presence of brite cells in subcutaneous fat. Fat cell browning or enhancement of mitochondrial biogenesis in WAT, respectively, is part of the thermogenic program and is induced and activated by the transcriptional regulator PGC1-α leading to increased expression of FNDC5 and after cleavage of FNDC5 higher circulating levels of irisin (Bostrom et al. 2012; Handschin and Spiegelman 2008). Recently, a study on PGC1-α in muscles of DUhTP mice after endurance exercise on a treadmill provided increased expression of PGC1-α isoforms 1, 3, and 4 on mRNA level (Brenmoehl et al. 2014). Voluntarily exercised mice only showed alterations of PGC1-α isoform 1 mRNA when compared to sedentary littermates (Brenmoehl et al. 2014). These observations nicely agree with those of Ruas et al., who linked PGC1-α isoform 1 mRNA to endurance performance but isoform 4 to resistance training (Ruas et al. 2012). FNDC5 is highly abundant in muscle, rectum, heart, and pericardium but present also in fat, brain, kidney, and liver, however, with lower abundance (Huh et al. 2012). Here, we assessed FNDC5 and irisin in muscle, serum, and subcutaneous fat of both mouse lines. The existence of FNDC5 in muscle and irisin in serum of DUhTP mice had originally been described using an antibody that was able to detect the irisin band of 12 kDa by Western immunoblotting (Brenmoehl et al. 2014). Also in the present work, this antibody was used. As far as we know, this antiserum is the only one that recognizes recombinant irisin with its correct molecular weight of 12 kDa (Albrecht et al. 2015b). Currently, this antiserum is not available because production and distribution have been halted. As discussed recently, different antibodies or antisera used for western immunoblotting or in ELISA studies revealed a number of bands but none of them corresponded to the correct size of irisin at ~12 kDa (Albrecht et al. 2015b). Instead only FNDC5 was identified by different antisera assessed in the study

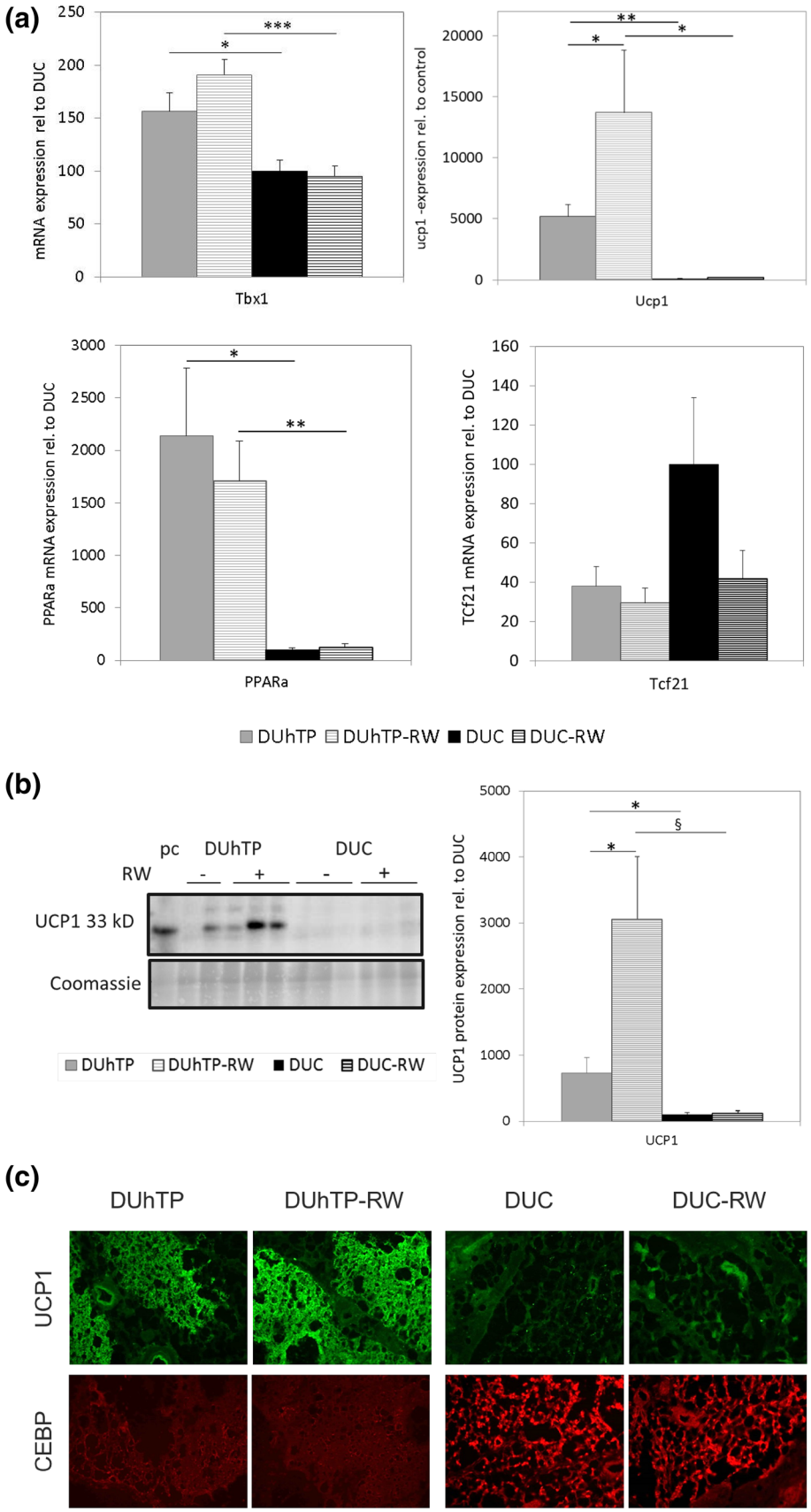

Fig. 3 Effect of voluntary physical activity (RW) on mRNA expression (**a**) of brite adipose tissue marker Tbx1 (*upper left panel*), brown adipose tissue marker UCP1 (*upper right panel*) as well as PPARα (*lower left panel*) and white adipose tissue marker Tcf21 (*lower right panel*) in subcutaneous fat tissue of 10-week male DUhTP and DUC mice ($n = 7$ per group). Analysis of mRNA expression was performed by quantitative real-time PCR and normalized to expression of HKG Rplp2. The analysis was performed by Western immunoblotting. Protein expression of UCP1 (**b**) was quantified by densitometry and normalized for the Coomassie blue signal. UCP1 (*green*) and C/EBPβ protein (*red*) were also analyzed by immunohistochemistry (**c**) in subcutaneous adipose tissue of 10-week male DUhTP and DUC mice. Cryosections of running wheel (RW) exercised and sedentary mice were immunostained with anti-UCP1 and C/EBPβ primary antibodies and MFP 488 rabbit anti- goat IgG secondary antibody for UCP1 and MFP 590 goat anti-rabbit IgG for C/EBPβ. Data are presented as mean ± SE and are expressed relative to the expression level of control mice from line DUC. Significant differences are indicated: $^{*}P < 0.05$, $^{**}P < 0.005$; $^{***}P < 0.0005$; $^{\S}P < 0.01$ (C/EBPβ CCAAT enhancer-binding protein beta, Tbx1 T-box transcription factor 1, UCP1 uncoupling protein 1, PPARα, pc positive control) (color figure online)

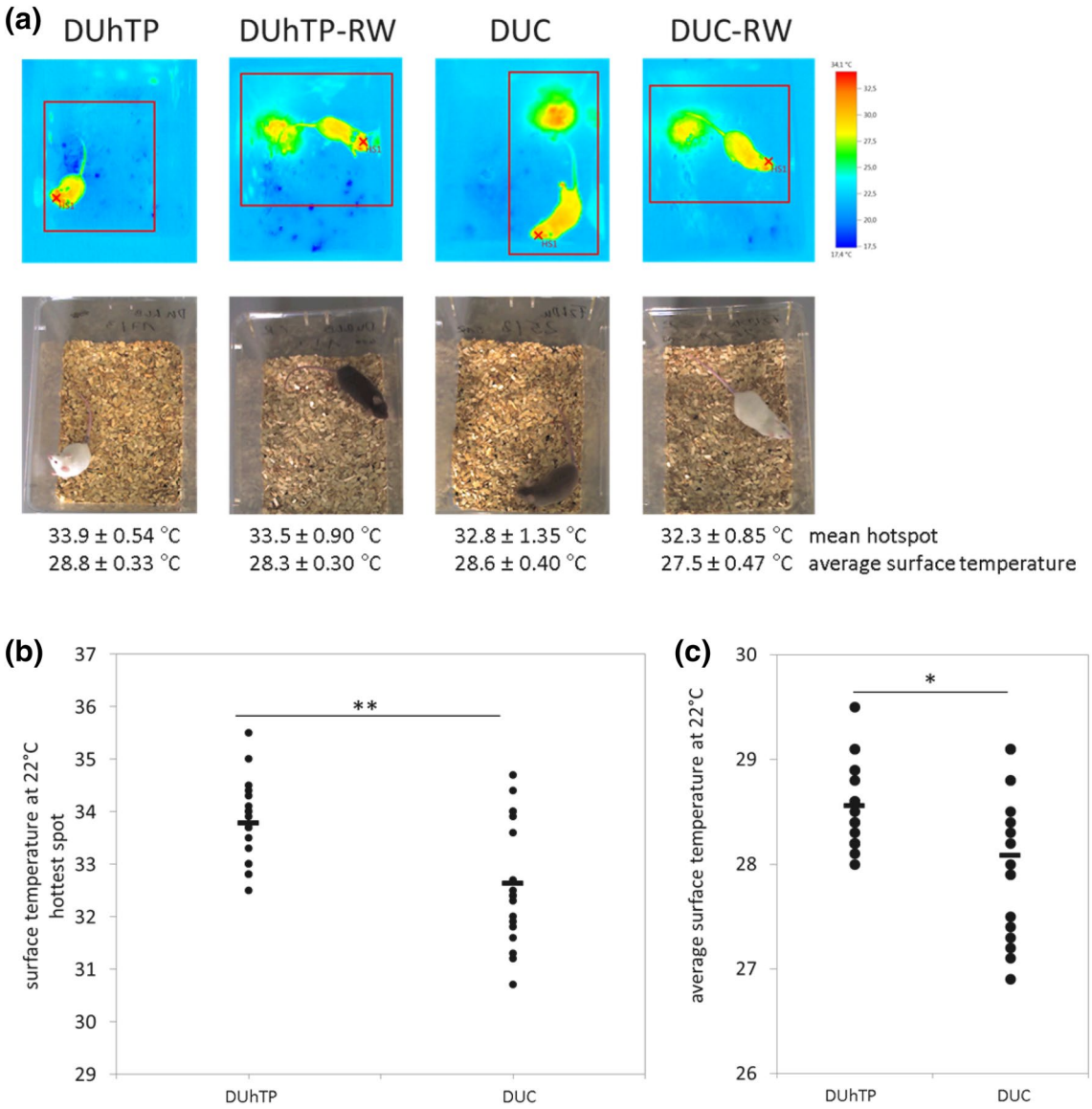

Fig. 4 Analysis of surface temperature of physical active and sedentary DUhTP and DUC mice ($n = 9$ per group). Mice were photographed at 22 °C using infrared technology (**a**). *Normal photos* were taken in parallel. Testo software determined the hottest spot (**b**) and the average surface temperature (**c**) of the mouse. The displayed mouse with according surface temperature is representable for each group-average. Significant differences are indicated: $*P < 0.05$; $**P < 0.005$

of Albrecht and coauthors. Barja-Fernandez et al. (2016) could detect a 15 kDa band stained by an irisin antibody that contains indeed no specific peptide signature for irisin. In the present study, higher levels of irisin were observed in serum and subcutaneous adipose tissue of DUhTP mice when compared with controls. However, expression of FNDC5 did not vary between both genotypes in muscle and in subcutaneous fat. Low abundance of FNDC5 protein in subcutaneous fat in contrast to muscular FNDC5 protein is also observed in human studies. Thus, higher local irisin concentrations in subcutaneous fat may be due to transport of muscular-derived irisin to adipose tissue via the blood stream or to enhanced release from other tissues like liver, heart, rectum or brain (Huh et al. 2012). We further cannot exclude the possibility that increased irisin levels arise from enhanced proteolytic cleavage of FNDC5. In response to voluntary activity, changes in FNDC5 expression and irisin levels were not observed in serum or subcutaneous fat when compared to sedentary littermates. Alterations of irisin levels independent of physical activity were only detectable in serum and muscle of our mouse line DUhTP passing a submaximal running test on a treadmill (Brenmoehl et al. 2014). It seems that voluntary physical activity has no influence on irisin level in serum and subcutaneous

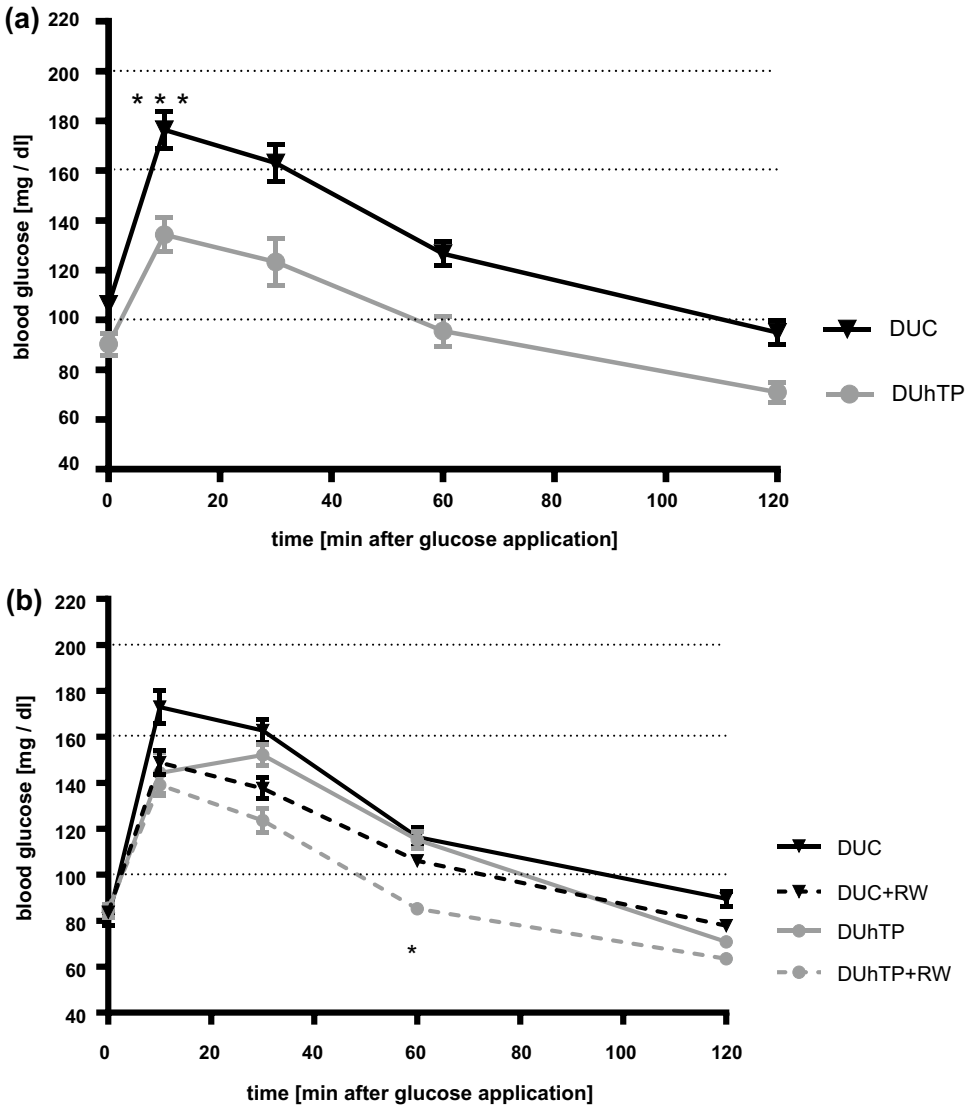

Fig. 5 Oral glucose tolerance tests (oGTT) in male DUhTP and DUC mice under standard chow at an age of 43 days (**a**; $n = 20$) and at an age of 71 days (**b**; $n > 5$). At an age of 43 days for all pairwise comparisons, significant differences were found between DUhTP mice and controls fed standard diet ($P < 0.01$). At an age of 71 days in the presence of running wheels (RW), reduced blood glucose were measured in DUhTP mice if compared to other groups ($^*P < 0.05$)

fat in either mouse line but browning of subcutaneous fat as a potential effect of irisin was increased after 3 weeks of moderate exercise.

In cultured skeletal muscle cells, irisin administration results in increased oxidative metabolism and elevated energy expenditure by induction of metabolic genes like PGC1-α, Tfam, GLUT4 or UCP3 (Vaughan et al. 2014). In primary cultured rat adipocytes from subcutaneous fat pads a direct administration of recombinant irisin significantly increased gene expression of UCP1 and PGC1-α (Zhang et al. 2014). Daily treatment of normal and obese mice with injection of recombinant irisin for 2 weeks led to elevated levels of Ucp1, Pgc1-α, and Pparα mRNA in subcutaneous fat (Zhang et al. 2014). In mice that were injected with FNDC5-expressing adenovirus, subcutaneous fat pads expressed high levels of Pgc1-α mRNA as well as UCP1 mRNA and protein (Bostrom et al. 2012).

Otherwise, irisin is thought to increase expression of PGC1-α in adipose tissue (Bostrom et al. 2012). We could detect high levels of transcription cofactor PGC1-α mRNA and protein in subcutaneous fat of DUhTP mice compared to unselected controls (Brenmoehl et al. 2015). Additional voluntary exercise resulted in an increase of PGC1-α protein levels. The requirement of PGC1-α to induce acute exercise-mediated Ucp1 mRNA expression in WAT was demonstrated by Ringholm et al. (Ringholm et al. 2013). They found in PGC1-α KO mice no changes in expression of UCP1 protein in response to exercise training. PGC1-α acts in muscle and adipose tissue as an inducer of mitochondrial biogenesis leading to elevated mitochondrial mass, proteins, and capacity (Lin et al. 2002; Puigserver and Spiegelman 2003; Olesen et al. 2010). DUhTP mice also express high amounts of Tfam, complex I subunits ND1 and NDUFA9, and SIRT3. Voluntary activity

increased nuclear encoded proteins NDUFA9 and SIRT3 (Brenmoehl et al. 2015), thus implicating higher mitochondrial biogenesis in subcutaneous fat from DUhTP mice associated with higher potential of energy supply.

Detection of substantial irisin levels in subcutaneous fat of DUhTP mice further inspired characterization of adipose tissue of sedentary DUhTP and DUC mice. PPARα, induced by irisin (Huh et al. 2014), is known to induce transcription of UCP1 in adipose tissue (Puigserver 2005) and correlates with the levels of UCP1 (Xue et al. 2005). In the present investigations, high expression levels of both PPARα and UCP1 in DUhTP mice were identified. Interestingly, positive correlations between Pparα and Ucp1 mRNA expression ($R^2 = 0.73$) and PPARα mRNA and UCP1 protein expression ($R^2 = 0.61$) were only identified following voluntary activity in DUhTP mice (data not shown). In DUhTP mice, moderate voluntary activity further increased UCP1 levels, which, however, were not reflected by alterations of local irisin concentrations. Thus, we cannot exclude that other mechanisms may contribute to activity-related increases of UCP1 in subcutaneous fat. Precisely, because mitochondrial protein UCP1 uncouples the electron transport chain from energy production, resulting in heat release (Aquila et al. 1985; Argyropoulos and Harper 2002), the surface temperature of both mouse lines was investigated at retained husbandry temperature of 22 °C without any cold stress. The surface temperature was increased by 1 °C in DUhTP mice compared to controls. Noninvasive detection of surface temperature by infrared camera identified brown adipose tissue as "hottest spot" of heat production. From the present experiments, it is not clear if core temperature also is increased in DUhTP mice, which can be seen as a limitation of the present study. Subcutaneous fat seems to contribute to higher thermogenesis in DUhTP mice since UCP1 production in brown adipose tissue does not differ between both mouse lines (data not shown). Interestingly, endurance exercise in inbred mice over a period of 6 weeks produced a similar phenotype but in the muscle (Morton et al. 2013). Endurance exercised mice fed a high fat diet were characterized by higher FNDC5, PGC1-α, and UCP1 expression and fat cell browning in muscle tissues was discussed in a context of adaptive response to endurance exercise (Morton et al. 2013). While browning in muscle with mitochondrial biogenesis can be interpreted in a context of higher production of energy equivalents, browning and UCP1 production in subcutaneous fat is less clear. On one hand, the activity of UCP1 can be considered as an energy-consuming or even -wasting process. On the other hand, higher surface temperature may also increase biochemical reaction-kinetics associated with endurance performance. To support this idea, again core temperature would have to be assessed in separate studies. The contribution of UCP1 activation and increased surface temperature to physical endurance performance of DUhTP mice needs to be addressed in future studies. At an age of 43 days, DUhTP mice have improved glucose tolerance if fed a normal diet, which is in line with current concepts of metabolic health associated with brown adipose tissues (Stanford et al. 2015). With advanced age improved glucose tolerance is progressively lost in DUhTP mice. Nevertheless, voluntary physical activity maintained improved glucose tolerance at an age of 71 days in DUhTP mice. The reason for the additional increase of UCP1 expression in subcutaneous fat from DUhTP in the presence of running wheels and its specific function for metabolic health is certainly worth of a follow-up study in the future.

To summarize and conclude, the present findings indicate that subcutaneous adipose tissue in DUhTP mice is characterized by increased irisin levels and a substantial browning phenotype if compared to unselected controls. Browning of subcutaneous fat in DUhTP mice includes increased levels of Tbx1, PPARα, UCP1, and heat production and correlates with improved oral glucose tolerance at an age of 43 days. While other animal models or humans may exhibit fat cell browning and mitochondrial biogenesis particularly in subcutaneous fat for instance after long and repeated training (Stanford et al. 2015), DUhTP mice have acquired energetic and metabolic adaptations since birth and thus can display fat cell browning in sedentary conditions. Thus, this study demonstrates that the mouse model DUhTP may represent a unique polygenic model for the analysis of mechanism of fat cell browning without previous training, cold exposure or calorie restriction.

Acknowledgments The authors want to thank Luong Chau, Sabine Hinrichs, Stefanie Foß, Dr. Martina Langhammer, Sabine Maibohm, Benita Lucht, Karin Ullerich, Sonja Alm and Magdalene Bülau for excellent technical assistance. Special thanks to Felix Brenmoehl helping us to take infrared photos of our mice using the infrared camera. Andreas Hoeflich and Daniela Ohde were supported by grants from the Deutsche Forschungsgemeinschaft (DFG HO 2003/6-1) and the H. Wilhelm Schaumann Stiftung, respectively. The publication of this article was funded by the Open Access fund of the Leibniz Institute for Farm Animal Biology (FBN).

Compliance with ethical standards

Conflict of interest All other authors declare no conflicts of interest.

References

Albrecht E, Kuzinski J, Komolka K, Gotoh T, Maak S (2015a) Localization and abundance of early markers of fat cell differentiation in the skeletal muscle of cattle during growth–are DLK1-positive cells the origin of marbling flecks? Meat Sci 100:237–245. doi:10.1016/j.meatsci.2014.10.012

Albrecht E, Norheim F, Thiede B, Holen T, Ohashi T, Schering L, Lee S, Brenmoehl J, Thomas S, Drevon CA, Erickson HP, Maak S (2015b) Irisin—a myth rather than an exercise-inducible myokine. Sci Rep 5:8889. doi:10.1038/srep08889

Aquila H, Link TA, Klingenberg M (1985) The uncoupling protein from brown fat mitochondria is related to the mitochondrial ADP/ATP carrier. Analysis of sequence homologies and of folding of the protein in the membrane. EMBO J 4(9):2369–2376

Argyropoulos G, Harper ME (2002) Uncoupling proteins and thermoregulation. J Appl Physiol (1985) 92(5):2187–2198. doi:10.1152/japplphysiol.00994.2001

Barja-Fernandez S, Folgueira C, Castelao C, Al-Massadi O, Bravo SB, Garcia-Caballero T, Leis R, Pardo M, Casanueva FF, Seoane LM (2016) FNDC5 is produced in the stomach and associated to body composition. Sci Rep 6:23067. doi:10.1038/srep23067

Bostrom P, Wu J, Jedrychowski MP, Korde A, Ye L, Lo JC, Rasbach KA, Bostrom EA, Choi JH, Long JZ, Kajimura S, Zingaretti MC, Vind BF, Tu H, Cinti S, Hojlund K, Gygi SP, Spiegelman BM (2012) A PGC1-alpha-dependent myokine that drives brown-fat-like development of white fat and thermogenesis. Nature 481(7382):463–468. doi:10.1038/nature10777

Brenmoehl J, Walz C, Renne U, Ponsuksili S, Wolf C, Langhammer M, Schwerin M, Hoeflich A (2013) Metabolic adaptations in the liver of born long-distance running mice. Med Sci Sports Exerc 45(5):841–850. doi:10.1249/MSS.0b013e31827e0fca

Brenmoehl J, Albrecht E, Komolka K, Schering L, Langhammer M, Hoeflich A, Maak S (2014) Irisin is elevated in skeletal muscle and serum of mice immediately after acute exercise. Int J Biol Sci 10(3):338–349. doi:10.7150/ijbs.7972

Brenmoehl J, Ohde D, Walz C, Schultz J, Tuchscherer A, Rieder F, Renne U, Hoeflich A (2015) Dynamics of fat mass in DUhTP mice selected for running performance—fat mobilization in a walk. Obes Facts 8(6):373-385. doi:10.1159/000442399

Dietl G, Langhammer M, Renne U (2004) Model simulations for genetic random drift in the outbred strain Fzt:DU. Arch Tierzucht 47:595–604

Escher P, Braissant O, Basu-Modak S, Michalik L, Wahli W, Desvergne B (2001) Rat PPARs: quantitative analysis in adult rat tissues and regulation in fasting and refeeding. Endocrinology 142(10):4195–4202. doi:10.1210/endo.142.10.8458

Falkenberg H, Langhammer M, Renne U (2000) Comparison of biochemical blood traits after long-term selection on high or low locomotory activity in mice. Arch Tierzucht 43:513–522

Handschin C, Spiegelman BM (2008) The role of exercise and PGC1alpha in inflammation and chronic disease. Nature 454(7203):463–469. doi:10.1038/nature07206

Himms-Hagen J (1970) Regulation of metabolic processes in brown adipose tissue in relation to nonshivering thermogenesis. Adv Enzyme Regul 8:131–151

Huh JY, Panagiotou G, Mougios V, Brinkoetter M, Vamvini MT, Schneider BE, Mantzoros CS (2012) FNDC5 and irisin in humans: I. Predictors of circulating concentrations in serum and plasma and II. mRNA expression and circulating concentrations in response to weight loss and exercise. Metabolism 61(12):1725–1738. doi:10.1016/j.metabol.2012.09.002

Huh JY, Dincer F, Mesfum E, Mantzoros CS (2014) Irisin stimulates muscle growth-related genes and regulates adipocyte differentiation and metabolism in humans. Int J Obes (2005) 38(12):1538–1544. doi:10.1038/ijo.2014.42

Lee P, Linderman JD, Smith S, Brychta RJ, Wang J, Idelson C, Perron RM, Werner CD, Phan GQ, Kammula US, Kebebew E, Pacak K, Chen KY, Celi FS (2014) Irisin and FGF21 are cold-induced endocrine activators of brown fat function in humans. Cell Metab 19(2):302–309. doi:10.1016/j.cmet.2013.12.017

Lin J, Wu H, Tarr PT, Zhang CY, Wu Z, Boss O, Michael LF, Puigserver P, Isotani E, Olson EN, Lowell BB, Bassel-Duby R, Spiegelman BM (2002) Transcriptional co-activator PGC-1 alpha drives the formation of slow-twitch muscle fibres. Nature 418(6899):797–801. doi:10.1038/nature00904

Mo L, Shen J, Liu Q, Zhang Y, Kuang J, Pu S, Cheng S, Zou M, Jiang W, Jiang C, Qu A, He J (2016) Irisin is regulated by CAR in liver and is a mediator of hepatic glucose and lipid metabolism. Mol Endocrinol (Baltim, Md) 30(5):533–542. doi:10.1210/me.2015-1292

Morton TL, Styner M, Rubin JE (2013) Running increases and alters intramyocellular lipid phenotype. Paper presented at the annual meeting of the Endocrine Society, San Francisco

Olesen J, Kiilerich K, Pilegaard H (2010) PGC-1alpha-mediated adaptations in skeletal muscle. Pflugers Arch 460(1):153–162. doi:10.1007/s00424-010-0834-0

Puigserver P (2005) Tissue-specific regulation of metabolic pathways through the transcriptional coactivator PGC1-alpha. Int J Obes (Lond) 29(Suppl 1):S5–S9. doi:10.1038/sj.ijo.0802905

Puigserver P, Spiegelman BM (2003) Peroxisome proliferator-activated receptor-gamma coactivator 1 alpha (PGC-1 alpha): transcriptional coactivator and metabolic regulator. Endocr Rev 24(1):78–90. doi:10.1210/er.2002-0012

Renne U, Langhammer M, Brenmoehl J, Walz C, Zeissler A, Tuchscherer A, Piechotta M, Wiesner RJ, Bielohuby M, Hoeflich A (2013) Lifelong obesity in a polygenic mouse model prevents age- and diet-induced glucose intolerance- obesity is no road to late-onset diabetes in mice. PLoS One 8(11):e79788. doi:10.1371/journal.pone.0079788

Ringholm S, Grunnet KJ, Leick L, Lundgaard A, Munk NM, Pilegaard H (2013) PGC-1alpha is required for exercise- and exercise training-induced UCP1 up-regulation in mouse white adipose tissue. PLoS One 8(5):e64123. doi:10.1371/journal.pone.0064123

Roca-Rivada A, Castelao C, Senin LL, Landrove MO, Baltar J, Belen Crujeiras A, Seoane LM, Casanueva FF, Pardo M (2013) FNDC5/irisin is not only a myokine but also an adipokine. PLoS One 8(4):e60563. doi:10.1371/journal.pone.0060563

Ruas JL, White JP, Rao RR, Kleiner S, Brannan KT, Harrison BC, Greene NP, Wu J, Estall JL, Irving BA, Lanza IR, Rasbach KA, Okutsu M, Nair KS, Yan Z, Leinwand LA, Spiegelman BM (2012) A PGC-1alpha isoform induced by resistance training regulates skeletal muscle hypertrophy. Cell 151(6):1319–1331. doi:10.1016/j.cell.2012.10.050

Stanford KI, Middelbeek RJ, Goodyear LJ (2015) Exercise effects on white adipose tissue: beiging and metabolic adaptations. Diabetes 64(7):2361–2368. doi:10.2337/db15-0227

Taylor SC, Berkelman T, Yadav G, Hammond M (2013) A defined methodology for reliable quantification of Western blot data. Mol Biotechnol 55(3):217–226. doi:10.1007/s12033-013-9672-6

Vaughan RA, Gannon NP, Barberena MA, Garcia-Smith R, Bisoffi M, Mermier CM, Conn CA, Trujillo KA (2014) Characterization of the metabolic effects of irisin on skeletal muscle in vitro. Diabetes Obes Metab 16(8):711–718. doi:10.1111/dom.12268

Wu J, Bostrom P, Sparks LM, Ye L, Choi JH, Giang AH, Khandekar M, Virtanen KA, Nuutila P, Schaart G, Huang K, Tu H, van Marken Lichtenbelt WD, Hoeks J, Enerback S, Schrauwen P, Spiegelman BM (2012) Beige adipocytes are a distinct type of thermogenic fat cell in mouse and human. Cell 150(2):366–376. doi:10.1016/j.cell.2012.05.016

Xue B, Coulter A, Rim JS, Koza RA, Kozak LP (2005) Transcriptional synergy and the regulation of Ucp1 during brown adipocyte induction in white fat depots. Mol Cell Biol 25(18):8311–8322. doi:10.1128/MCB.25.18.8311-8322.2005

Zhang Y, Li R, Meng Y, Li S, Donelan W, Zhao Y, Qi L, Zhang M, Wang X, Cui T, Yang LJ, Tang D (2014) Irisin stimulates browning of white adipocytes through mitogen-activated protein kinase p38 MAP kinase and ERK MAP kinase signaling. Diabetes 63(2):514–525. doi:10.2337/db13-1106

Zhang Y, Xie C, Wang H, Foss RM, Clare M, George EV, Li S, Katz A, Cheng H, Ding Y, Tang D, Reeves WH, Yang LJ (2016) Irisin exerts dual effects on browning and adipogenesis of human white adipocytes. Am J Physiol Endocrinol Metab 311(2):E530–E541. doi:10.1152/ajpendo.00094.2016

cells

MDPI

Article

Analysis of Activity-Dependent Energy Metabolism in Mice Reveals Regulation of Mitochondrial Fission and Fusion mRNA by Voluntary Physical Exercise in Subcutaneous Fat from Male Marathon Mice (DUhTP)

Julia Brenmoehl [1], Daniela Ohde [1], Christina Walz [1], Martina Langhammer [2], Julia Schultz [3] and Andreas Hoeflich [1,*]

[1] Institute for Genome Biology, Leibniz-Institute for Farm Animal Biology (FBN), Wilhelm-Stahl-Allee 2, 18196 Dummerstorf, Germany; brenmoehl@fbn-dummerstorf.de (J.B.); ohde@fbn-dummerstorf.de (D.O.); walz@fbn-dummerstorf.de (C.W.)

[2] Lab Animal Facility, Leibniz-Institute for Farm Animal Biology (FBN), Wilhelm-Stahl-Allee 2, 18196 Dummerstorf, Germany; martina.langhammer@fbn-dummerstorf.de

[3] Institute of Medical Biochemistry and Molecular Biology, University of Rostock, Schillingallee 70, 18057 Rostock, Germany; julia.schultz@med.uni-rostock.de

* Correspondence: hoeflich@fbn-dummerstorf.de; Tel.: +49(0)38208-68-744

Received: 11 November 2020; Accepted: 12 December 2020; Published: 16 December 2020

Abstract: Physical inactivity is considered as one of the main causes of obesity in modern civilizations, and it has been demonstrated that resistance training programs can be used to reduce fat mass. The effects of voluntary exercise on energy metabolism are less clear in adipose tissue. Therefore, the effects of three different voluntary exercise programs on the control of energy metabolism in subcutaneous fat were tested in two different mouse lines. In a cross-over study design, male mice were kept for three or six weeks in the presence or absence of running wheels. For the experiment, mice with increased running capacity (DUhTP) were used and compared to controls (DUC). Body and organ weight, feed intake, and voluntary running wheel activity were recorded. In subcutaneous fat, gene expression of browning markers and mitochondrial energy metabolism were analyzed. Exercise increased heart weight in control mice ($p < 0.05$) but significantly decreased subcutaneous, epididymal, perinephric, and brown fat mass in both genetic groups ($p < 0.05$). Gene expression analysis revealed higher expression of browning markers and individual complex subunits present in the electron transport chain in subcutaneous fat of DUhTP mice compared to controls (DUC; $p < 0.01$), independent of physical activity. While in control mice, voluntary exercise had no effect on markers of mitochondrial fission or fusion, in DUhTP mice, reduced mitochondrial DNA, transcription factor Nrf1, fission- (Dnm1), and fusion-relevant transcripts (Mfn1 and 2) were observed in response to voluntary physical activity ($p < 0.05$). Our findings indicate that the superior running abilities in DUhTP mice, on one hand, are connected to elevated expression of genetic markers for browning and oxidative phosphorylation in subcutaneous fat. In subcutaneous fat from DUhTP but not in unselected control mice, we further demonstrate reduced expression of genes for mitochondrial fission and fusion in response to voluntary physical activity.

Keywords: mitochondrial fission and fusion; voluntary activity; subcutaneous fat; DUhTP mice

1. Introduction

Physical exercise can have positive effects on health by reducing body or fat mass. On the cellular or molecular level in fat cells, even moderate or voluntary mild exercise may induce specific adaptations

inducing the formation of beige fat, thermogenesis, or fat mobilization with the consecutive reduction of body fat [1–3]. Beige adipose tissue is characterized by increased mitochondrial biogenesis induced by peroxisome-proliferator-activated receptor-gamma-coactivator-1-alpha (PGC1-α) in muscle and fat, leading to an increase in mitochondrial mass, proteins, and capacity [4]. Elevated protein and mRNA levels of PGC1-α can be observed in various tissues of mice and rats in response to physical activity, particularly after endurance training [5–7]. In addition, Pgc1-α expression was induced by voluntary running wheel activity in subcutaneous fat [8,9] or in brown adipose tissue [1]. In subcutaneous fat, voluntary physical activity resulted in elevated mRNA expression of genes involved in PGC1-α-related pathways, including transcription factors nuclear respiratory factor 1 (Nrf1) and mitochondrial transcription factor A (Tfam) [9], inducing the transcription of mitochondrial genes. That, in turn, led to an induction of browning/beiging, and mitochondrial biogenesis [3,9] or an improved mitochondrial network [8].

It is known that mitochondria undergo dynamics that include biogenesis, fission, fusion, depolarization, and autophagy [10–12] to ensure the exchange of organelle content and meet the energy demand of the tissue [13]. Mitochondrial fusion is mainly induced by mitofusin 1 (MFN1) and mitofusin 2 (MFN2) for outer mitochondrial membrane fusion and the optical protein atrophy 1 (OPA1) protein for inner mitochondrial membrane fusion. On the contrary, mitochondrial fission 1 protein (FIS1) and dynamin-related protein 1 (DNM1) play a decisive role in mitochondrial fission [14,15]. Since muscle PGC1-α regulates the expression of Mfn1 and 2 [16] and mitophagy in response to acute stress [17], a direct relationship was assumed between the transcriptional regulation of mitochondrial biogenesis and mitochondrial dynamics in the muscle [10]. In response to acute stress, mitochondrial fission appears to be favored in skeletal muscle [18], as reduced muscular mitofusin1 protein expression and fission-related FIS1 protein increase were detected in rats up to 48 h after the last exercise bout [19,20], and DRP1 activation was induced in mice [21]. Whereas increased mitochondrial fusion appears to predominate as a result of prolonged training in muscle [22]. For example, C57BL/6J mice active in the running wheel for 30 days exhibited similar levels of proteins involved in mitochondrial fusion and fission but had elevated levels of phosphorylated dynamin-related protein 1 (DRP1; gene *Dnm1*), which reduced its translocation and thus mitochondrial fission [23]. In subcutaneous fat, mitochondrial dynamics especially in response to voluntary activity, have been less well studied, to date.

The mouse model DUhTP (Dummerstorf mice selected for high treadmill performance) is characterized by beige subcutaneous fat already in a sedentary condition due to long-term selection for high treadmill performance [8,24,25]. Since the selection was based on a single submaximal run with males after mating, a selection line was generated, exhibiting genetically high running ability without any previous training. Interestingly, the extraordinary endurance performance of the DUhTP animals did not correlate with elevated voluntary running wheel activity, which was not significantly different from the unselected controls (DUC mice) [8,24,26]. DUhTP mice have selection-related adaptations that indicate the efficient use of lipids for superior endurance performance. The increased fat storage under sedentary conditions, associated with increased hepatic lipid production [24], is efficiently reduced by voluntary physical activity, which could be attributed to both reduced deposition of additional fat (subcutaneous, epididymal, perinephric, and brown fat) and mobilization of existing fat [8].

Since we had observed strong effects of voluntary physical activity on lipid metabolism in subcutaneous fat from DUhTP mice [8,27], we wanted to test the effects of voluntary exercise on the control of energy metabolism in this tissue on the molecular level. Therefore, we tested the effects of three different exercise programs in a cross-over study design on energy metabolism in subcutaneous fat from marathon mice (DUhTP) and unselected controls (DUC). In particular, we analyzed the expression of browning markers, genes from the oxidative phosphorylation pathway, and the expression of genes regulating mitochondrial fission and fusion in response to voluntary exercise protocols in DUhTP and DUC mice. In the present manuscript, we discuss the effects of genetic selection and the effects of exercise on the control of mitochondrial energy metabolism in subcutaneous fat.

2. Materials and Methods

2.1. Animals and Cross-Over Study Design

All in vivo experiments were conducted according to national and international guidelines and approved by our internal institutional review board. This study used mice selected from a broad genetic base population for high treadmill performance (DUhTP) over 140 generations [24,25] and unselected controls (DUC). Both mouse lines represent non-inbred lines, maintained by avoiding inbreeding. The animals were kept in H-Temp Polysulfon cages with a floor area of 370 cm^2 (Eurostandard Type II, Tecniplast, Hohenpeißenberg, Germany) under controlled, specified pathogen-free (SPF) conditions. The mice were given fresh tap water and were fed autoclaved Ssniff® M-Z feed (Ssniff-Spezialdiäten GmbH, Soest, Germany) ad libitum. Weekly feed intake and body weight development were monitored for 42 days in 7- to 13-week-old mice as described [24]. For the study, male full-sib animals kept in single cages from day 21 were divided into four groups (n = 8) at the age of 48 days and assigned to an individual voluntary exercise program (Figure 1). The animals of the sedentary control group were kept in individual cages for six weeks without any treatment (sed/sed). Whereas, the exercising control group had six weeks of access to a running wheel (Conventional Activity Wheel, diameter = 33.4 cm, equipped with a counter that recognized every quarter rotation; Tecniplast) in their cages (ex/ex). In a cross-over study design, the wheels were removed from one experimental group (ex/sed) after three weeks and placed in the cages of another experimental group that spent three weeks sedentary (sed/ex). Accordingly, groups sed/ex and ex/sed were sedentary in the first or in the second half of the six-week study period. The animals could use the wheel at will, and voluntary physical activity was determined based on running wheel activity (quarter rounds per day). The individual activity was monitored, whereby one complete rotation of the wheel (diameter = 33.4 cm) corresponded to a running distance of 1 m.

At the age of 13 weeks, mice were sacrificed, and serum samples were taken. Tissues were weighed, shock frozen in liquid nitrogen, and stored at −70 °C for subsequent analysis.

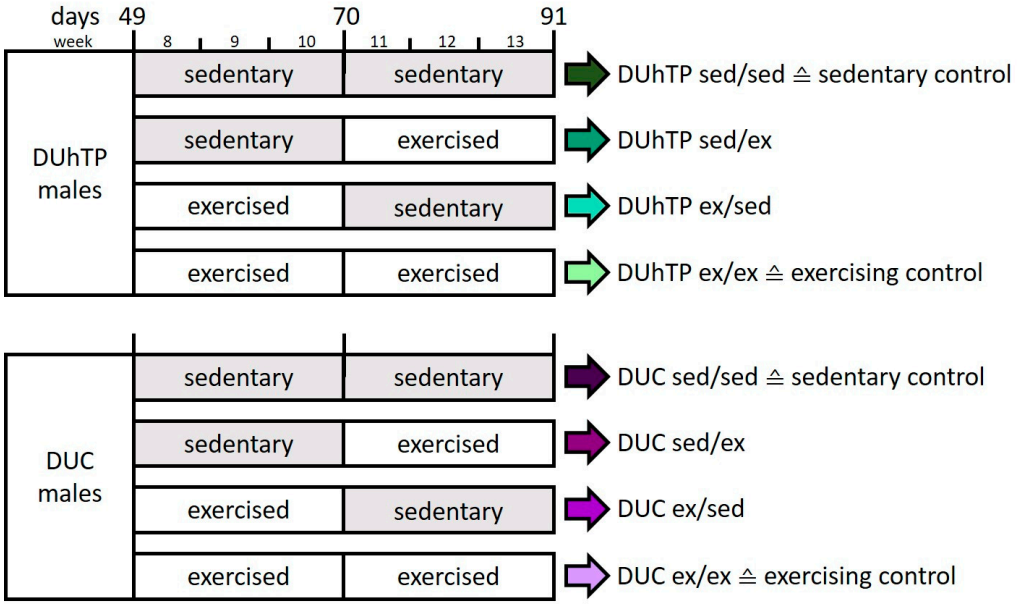

Figure 1. Voluntary exercise program for each experimental group. Male mice of the DUhTP and DUC lines were kept in individual cages without (sed) or with (ex) running wheel from 8 to 13 weeks of age (n = 8).

2.2. Analysis of Triglycerides in Serum Samples

Total triglyceride concentration was determined in serum samples using commercial kits (triglycerides: No. LT-TR 0015; Labor & Technik Eberhard Lehmann, Berlin, Germany) [24]. Serum was used undiluted and analyzed for triglyceride content according to the manufacturer's recommendations.

2.3. mRNA Expression in Subcutaneous Fat

The complete inguinal subcutaneous fat was ground in liquid nitrogen. Total RNA was isolated using Trizol as described before [28]. cDNA synthesis followed the manufacturer's protocol of the used commercial kit (GoScript™ Reverse Transcription System, Promega, Walldorf, Germany). Transcript abundance was measured in 96well format on LightCycler 480® (Roche, Mannheim, Germany) using GoTaq® qPCR Master Mix (Promega) with BRYT Green® Dye according to manufacturers' instructions. Primers used are listed in Table 1. A serial dilution of the cDNA pool was used for relative quantification. Recalculation and normalization were done using software DAG [29].

Table 1. List of primers used for mRNA expression analysis in the subcutaneous tissue.

Gene	Forward 5′-3′	Reverse 5′-3′
Nrf1	ACAGATAGTCCTGTCTGGGGAAA	TGGTACATGCTCACAGGGATCT
Tfam	AAGACCTCGTTCAGCATATAACATT	TTTTCCAAGCCTCATTTACAAGC
Atp5b	CGTGAGGGCAATGATTTATACCAT	TCCTGGTCTCTGAAGTATTCAGCAA
Cyc	ATAGGGGCATGTCACCTCAAAC	GTGGTTAGCCATGACCTGAAAG
Cox4i1	TGGGACTATGACAAGAATGAGTGG	TTAGCATGGACCATTGGATACGG
18S	CTGCCCTATCAACTTTCGATGGTAG	CCGTTTCTCAGGCTCCCTCTC
Cyb	CTTCGCTTTCCACTTCATCTTACC	TTGGGTTGTTTGATCCTGTTTCG
36B4	AGGATATGGGATTCGGTCTCTTC	TCATCCTGCTTAAGTGAACAAACT
Ucp1	GGCCTCTACGACTCAGTCCA	TAAGCCGGCTGAGATCTTGT
Pgargc1a	CTGCATGAGTGTGTGCTGTG	GGAAGATCTGGGCAAAGAGG
Tbx1	GGCAGGCAGACGAATGTTC	TTGTCATCTACGGGCACAAAG
Cidea	GTACTCGGTGTCCTACGACATC	TCATCTGTGCAGCATAGGACATA
Dnm1	CGGTTAGACAGTGCACCAAG	GGATGTGGGTGGTCACAAT
Fis1	GCCCCTGCTACTGGACCAT	CCCTGAAAGCCTCACACTAAGG
Mfn1	AGCCAAGGAAGTTCTCAACTC	GCTCTGATAGTGTGCTGTTCA
Mfn2	GCCAGCTTCCTTGAAGACAC	GCAGAACTTTGTCCCAGAGC
Opa1	TGACAAACTTAAGGAGGCTGTG	CATTGTGCTGAATAACCCTCAA
Rpl19	CAATGCCAACTCCCGTCAGC	TCTTGGATTCCCGGTATCTC
Pgk1	CAGTCTAGAGCTCCTGGAAGGT	GCCACTAGCTGAATCTTGCG
Actb	TGACAGGATGCAGAAGGAGA	CGCTCAGGAGGAGCAATG
Rplp2	GACGATGATCGGCTCAACAAG	ACCCTGAGCGATGACATCCT
Sdha	CAAATTCTCTCTTGGACCTTGTAGT	CCTTAATTGAAGGAACTTTATCTCCA

Nrf1, nuclear respiratory factor 1; *Tfam*, mitochrondrial transcription factor A; *Atp5b*, ATP synthase subunit beta; *Cyc*, cytochrome C; *Cox4i1*, cytochrome c oxidase subunit 4 isoform 1; *Cyb*, cytochrome B; *Ucp1*, uncoupling protein 1; *Ppargc1a*, peroxisome-proliferator-activated receptor-gamma-coactivator-1-alpha; *Tbx1*, T-box protein 1; *Cidea*, cell death activator; *Dnm1*, dynamin related protein 1; *Fis1*, mitochondrial fission 1 protein; *Mfn1*, mitofusin 1; *Mfn2*, mitofusin 2; *Opa1*, optic atrophy protein 1; *Rpl19*, 60S ribosomal protein L19; *Pgk1*, phosphoglycerate kinase 1; *Actb*, actin beta; *Rplp2*, 60S acidic ribosomal protein P2; *Sdha*, succinate dehydrogenase.

2.4. Mitochondrial Morphology in Adipose Tissue

Mitochondrial staining was performed as previously described [8,30]. Frozen tissue sections (5 µm) were stained with MitoTracker® Deep Red (Molecular Probes® Invitrogen, Darmstadt, Germany) for 30 min at 37 °C before fixation in ice-cold acetone (−20 °C) for 10 min and DAPI counterstaining (Vector Laboratories, Burlingame, CA, USA). Mitochondrial morphology was demonstrated using a confocal laser-scanning microscope Fluoview FV10i (Olympus, Hamburg, Germany).

2.5. Statistical Analysis

Data analysis and graphical representations were performed using GraphPad Prism 8.2.1 (GraphPad Software, San Diego, CA, USA). The data could be considered as approximately normally distributed; outliers identified by the statistical analysis package from GraphPad Prism 8.2.1 were removed from the data set. All data concerning running activity, feed intake, phenotypic data, and serum triglycerides were analyzed by one-way ANOVA, multiple comparisons. Body weights between the groups within a line and bodyweight development within the group as well as mRNA expression data were compared by two-way ANOVA, multiple comparisons. The effect of selection or physical exercise on mRNA expression was evaluated for statistical significance by unpaired t-test or one-way ANOVA, respectively. All results were displayed as means with their standard errors of the mean (SEM).

Pearson correlation coefficients were calculated to determine the relations between the expression of browning markers and different mitochondrial genes. The effects and differences were considered significant if $p < 0.05$.

3. Results

3.1. Running Wheel Performance and Food Consumption in Response to Differential Exercise Programs

The voluntary activity of each animal was recorded daily, and the average physical activity of the active groups was determined. The animals' age and voluntary physical activity duration did not influence weekly or 3-weeks running performance (data not shown). However, line-specific differences were visible. While the groups DUhTP sed/ex, ex/sed, and ex/ex covered 4340 ± 737, 4877 ± 729, and 4530 ± 565 m per day, respectively, DUC sed/ex, ex/sed, and ex/ex mice ran 6002 ± 673, 5869 ± 745, 6051 ± 950 m per day (Figure 2). Accordingly, the DUC mice were characterized by a significantly higher voluntary running activity than the DUhTP mice ($p < 0.005$).

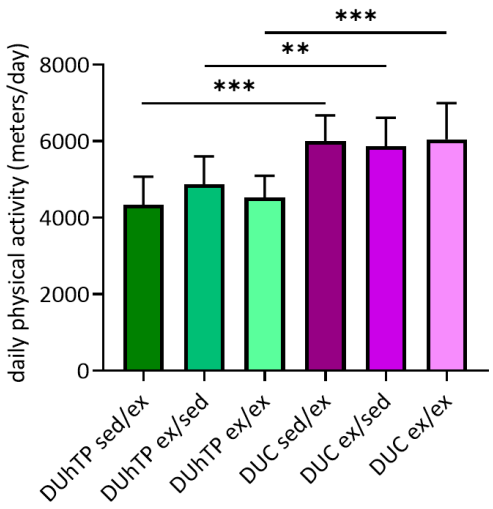

Figure 2. Voluntary physical activity of DUhTP and DUC males. The mice were kept from week 8 to 13, either in cages with or without included running wheels. Shown is the daily voluntary activity in meters for the respective running groups with the standard error of the mean ± SEM, n = 8. Significant differences were calculated by GraphPad, one-way ANOVA: ** $p < 0.005$, *** $p < 0.0005$.

After six weeks of voluntary activity, feed intake increased by 11% (not significant) in DUhTP animals and by 4.6% (not significant) in DUC animals, compared to their respective sedentary control group (DUhTP ex/ex: 299.3 ± 11.2 g, DUhTP sed/sed: 264.8 ± 6.5 g; DUC ex/ex: 280.5 ± 11.2 g, DUC sed/sed: 268.2 ± 6.3 g). Also a 3-week comparison revealed no significant effect of physical activity on feed intake neither in DUhTP nor in DUC mice (Figure 3).

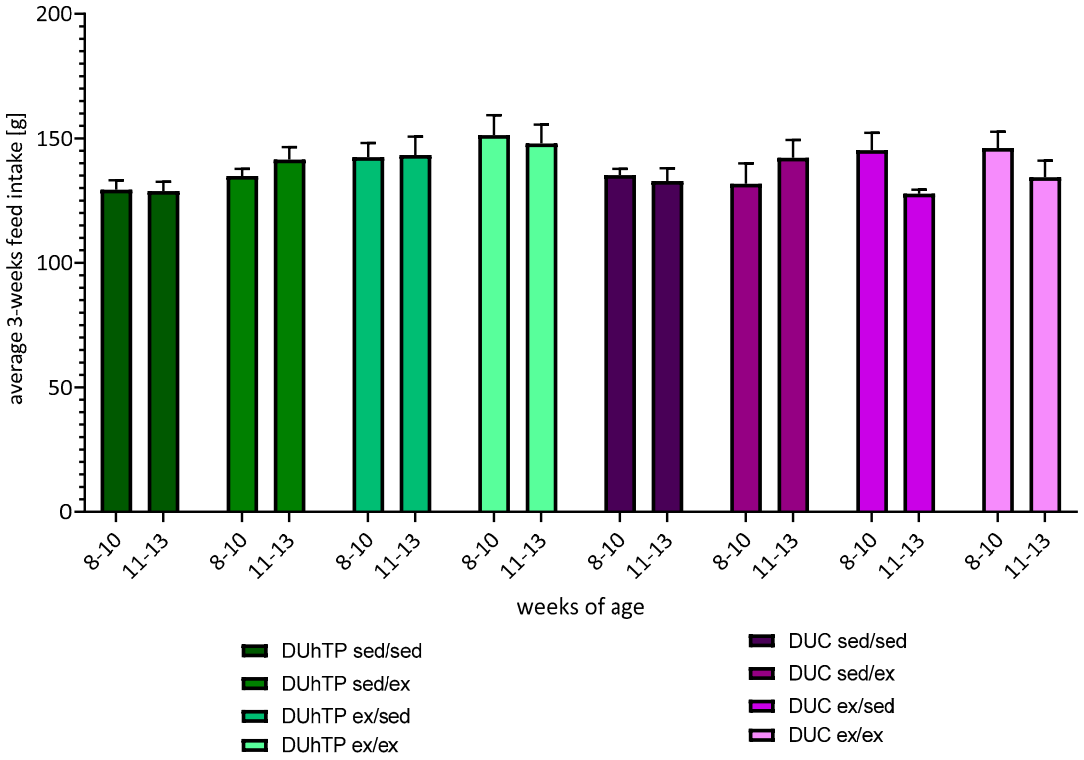

Figure 3. Feed intake of DUhTP and DUC mice from week 8 to 10 and 11 to 13. The food consumption was calculated by subtracting the remaining food from the weighed diet and displayed as average 3-weeks feed intake in grams ± SEM.

3.2. Effects of Three Different Exercise Programs on Body Weight, Serum Triglyceride Levels, and Fat Deposition

The experimental groups of both genetic groups did not start with identical body weights in the beginnings of the study at day 49 (not significant; Figure 4). Body weights in DUC mice were approximately 33% higher than those of the DUhTP animals (DUhTP: 29.2 ± 2.7 g, DUC: 38.9 ± 2.1 g, $p < 0.0001$).

Within the first three weeks of the study, the body weights of sedentary DUhTP and DUC animals (sed/sed and sed/ex) increased to a greater extent than those of the animals, which had the opportunity to be physically active in a running wheel (ex/sed and ex/ex). A steady increase in body weight of about 3% per week was observed in the DUC sedentary controls. In contrast, the DUhTP sedentary controls increased significantly in weight, especially in the first two weeks (sed/sed: week 7–8: +9.9%, $p < 0.0001$; week 8–9: +5.9%, $p < 0.05$). After that, weight increased less from week to week but differed significantly between the beginning and the end of the 3-week interval ($p < 0.005$).

Interestingly, the body weight of the sedentary control (sed/sed) or exercising control (ex/ex) DUhTP mice increased steadily in the same manner with a weight difference of about 2–3 g, which were not significant due to individual variations within the exercise groups (Figure 5A). Instead, in the DUC exercising control group, mice gained weight more slowly than sedentary controls, resulting in significantly different body weights at week 13. Thus, permanent exercise slowed down body weight gain in DUC mice (Figure 4).

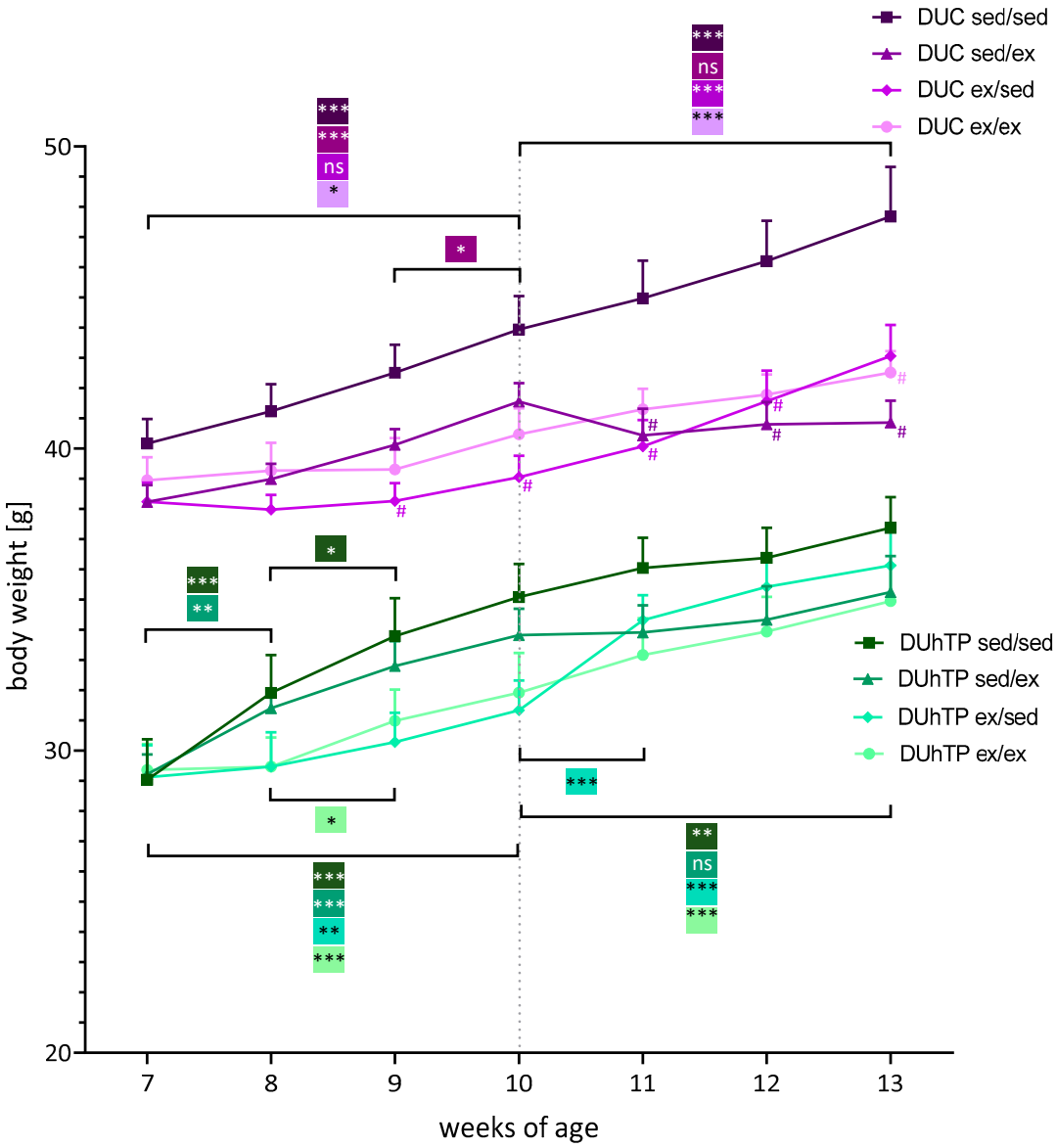

Figure 4. Effects of different exercise programs on body mass in DUhTP and DUC mice. Both lines' animals were randomly attributed to four groups and individually kept with (ex) or without running wheel (sed) from week 8 to 10 or 11 to 13. The animals were weighed weekly, and the mean body mass ± SEM from eight animals per group are provided. Statistical analysis was performed by two-way ANOVA. Significance between two age points within one exercise group is depicted by a bracket, * $p < 0.05$, ** $p < 0.005$, *** $p < 0.0005$, ns, not significant; # $p < 0.05$ relative to respective sed/sed group at the same age.

However, DUhTP ex/sed animals were characterized by a substantial increase in body weight (week 10–13: +15.3%, $p < 0.0001$), especially during the first week of inactivity (Figure 4; week 11: +3 g, $p < 0.0001$). Initially sedentary and then active DUhTP mice (sed/ex) showed a reduced body weight development from week 10 to 11 compared to the sedentary control DUhTP (sed/sed;) and then a weight development parallel to the sedentary control (Figure 5A).

DUC ex/sed mice also gained weight (+10.9%, $p < 0.0005$) due to inactivity in the second activity interval, although to a lower extent than the other line's ex/sed animals. Thus, at week 13, no significant difference between the body weight of the DUC ex/sed and that of the DUC sedentary controls was found. Instead, it was observed that mice voluntarily active in the second interval (sed/ex) showed no

increase in body weight (Figure 4, week 10–13: −0.7 g, n.s.). In relation to DUC sedentary controls, they exhibited a significantly diminished body weight development similar to the exercising control mice (Figure 5B).

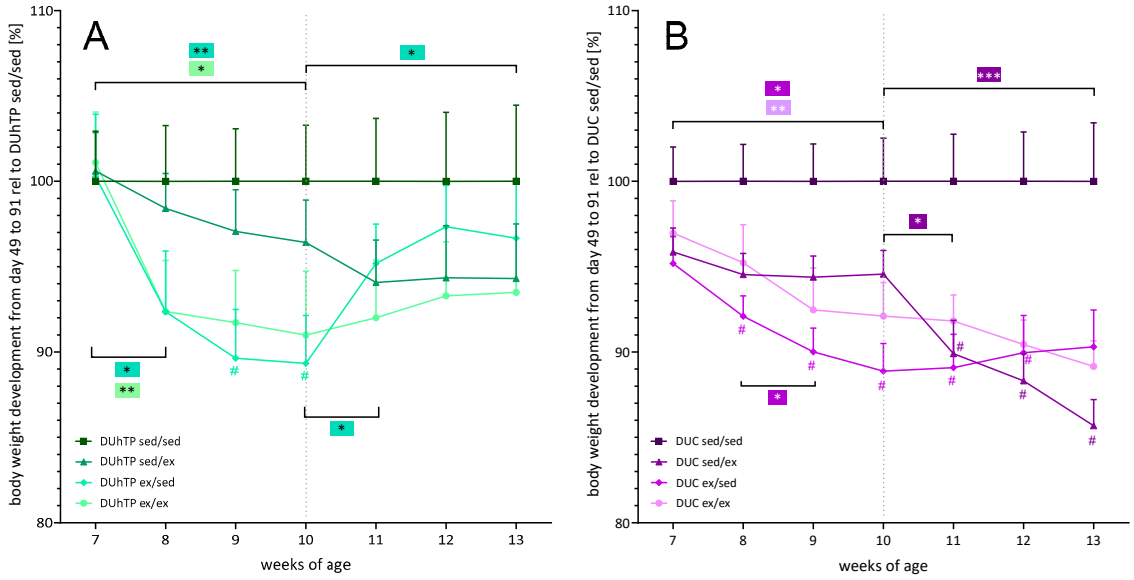

Figure 5. The relative weekly body weight developments of (**A**) DUhTP and (**B**) DUC animals with (ex) or without running wheels (sed) in the cage from week 8 to 10 or 11 to 13, by relating the body masses of the inactive control animals 100% and the determined body masses of the other groups. The body weights from eight animals per group ± SEM are provided. Statistical analysis was performed by two-way ANOVA. Significant differences between two age points within one exercise groups are depicted by brackets and color codes; * $p < 0.05$, ** $p < 0.005$, *** $p < 0.0005$; # $p < 0.05$ relative to the respective sed/sed group at the same age.

At the age of 13 weeks, the animals were phenotypically examined in more detail. The liver, heart, and muscle mass (M. quadriceps femoris) were similar in all experimental groups of the respective mouse line (Figure 6A–C). However, it was shown that exercise, in general, had a positive effect on heart weight in DUC mice compared to sedentary control littermates (Figure 6B).

Robust effects of voluntary activity were observed on the fat depot weights (Figure 6D–G). In both genetic groups, voluntary activity, as a rule, decreased the weights of all fat depots examined ($p < 0.05$). In subcutaneous fat from DUhTP mice, six weeks of voluntary exercise led to reductions of 35% (ex/ex, $p < 0.05$), and three weeks of exercise in the second activity period resulted in a reduction of fat mass by 32% (sed/ex, $p < 0.05$) compared to the sedentary control group (sed/sed). Similar effects of physical activity were found in DUC mice with reductions of 30.9% (ex/ex, $p < 0.05$) and 33.6% (sed/ex, $p < 0.05$; Figure 6D). Also, significant effects were observed in epididymal, perinephric, and brown fat depots (Figure 6E–G), where voluntary physical activity decreased fat mass by up to 75%. In response to physical activity, serum concentrations of triglycerides were also decreased in both lines, however, to a significant extent only after six weeks of voluntary exercise ($p < 0.05$, Figure 7). In general, exercise significantly affected serum triglyceride levels in both lines ($p < 0.0005$).

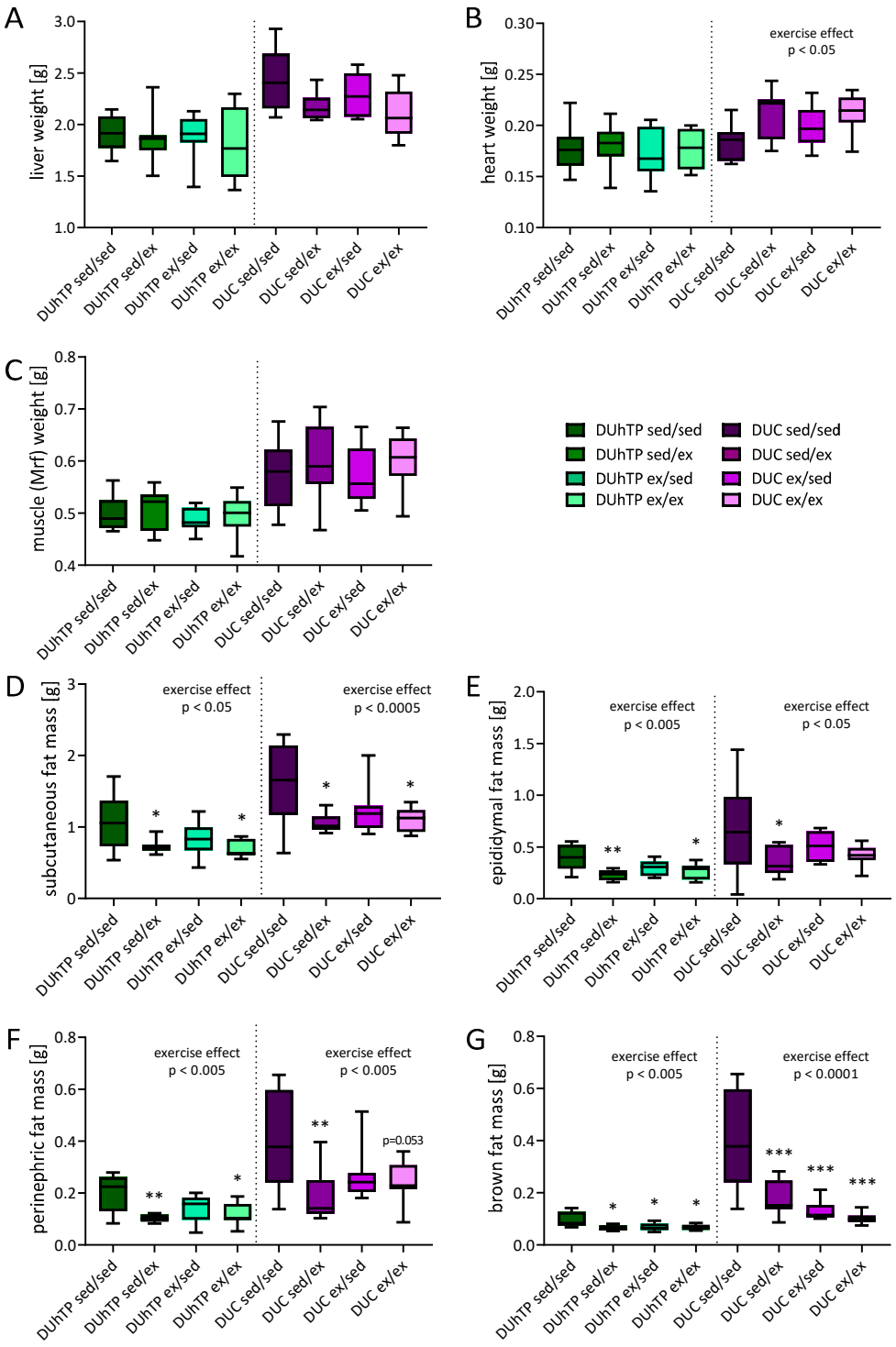

Figure 6. Absolute organ and tissue weights at week 13 of age in DUhTP and DUC mice in response to different activity programs. Both lines' animals were attributed to four groups and individually kept from week 8 to 10 or 11 to 13, either with or without a running wheel. The absolut weights from (**A**) liver, (**B**) heart, and (**C**) muscle, as well as (**D**) subcutaneous, (**E**) epididymal, (**F**) perinephric, and (**G**) brown fat are presented as means ± SEM from eight animals per group. Statistical analysis was performed by two-way ANOVA. Significant effects of activity compared to the respective sedentary control as marked; * $p < 0.05$, ** $p < 0.005$, *** $p < 0.0005$. The overall effects of exercise are also stated.

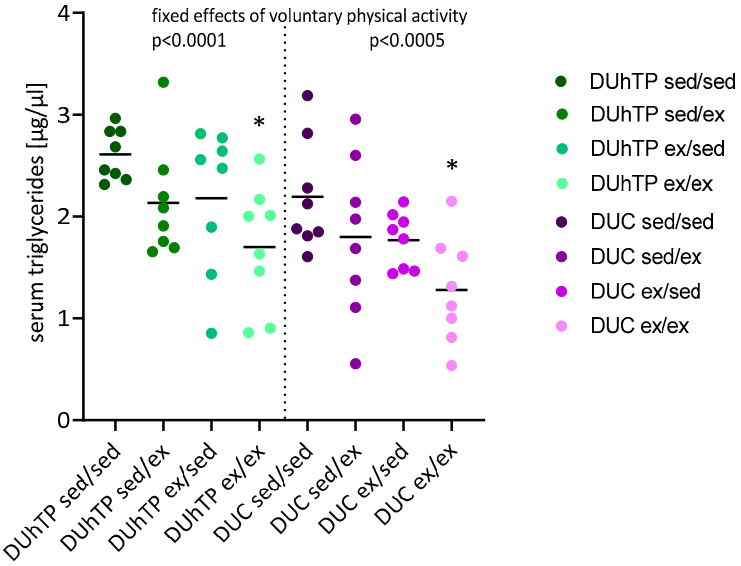

Figure 7. Serum triglyceride levels in 13-week-old exercised and sedentary DUhTP and DUC mice (n = 8). The mice were individually kept from week 8 to 10 or 11 to 13, either with or without a running wheel. Values are means of three technical replicates. Significant effects of six weeks of voluntary physical activity (ex/ex) compared to six weeks in sedentary conditions (sed/sed): * $p < 0.05$ (one-way ANOVA). The fixed effect of physical activity in general, as stated: $p < 0.0005$.

3.3. Effects of Three Different Exercise Programs on the Expression of Browning Markers and Mitochondrial Genes

Before we started an in-depth molecular analysis of genetic markers for mitochondrial functions in subcutaneous adipose tissue in our experimental system, we conducted a preceding cross-sectional pilot study via a screening approach. We asked whether different conditions of the mitochondrial network can generally be assumed, or whether the mitochondrial network is identical in all experimental groups, which in the latter case would less strongly support further studies of energy metabolism in our study. Therefore, we chose one cryogenic section per experimental group and assessed the morphology of the mitochondrial networks, provided as supplementary material (Figure S1). These initial mitochondrial stainings revealed different conditions ranging from networks defined by a well-branched network of mitochondria in different groups to the presence of a mitochondrial network accompanied by massive clustering, fragmentation, and elongation of the mitochondria in one group. Since this pilot study, in fact, suggested the presence of different conditions of the mitochondrial network in different experimental groups, we next performed a detailed study of mitochondrial energy metabolism on the level of gene expression.

Therefore, we first investigated the expression of browning markers in the context of the different exercise programs (Figure 8A). As a main effect of the genetic group and independent of physical activity, subcutaneous adipose tissue of DUhTP mice was characterized by elevated mRNA levels for Cidea, Tbx1, and Ucp1 ($p < 0.0001$) compared to unselected DUC mice. By comparing distinct treatment groups, sedentary control DUhTP mice had higher levels of Cidea mRNA transcripts in fat depots compared to DUC mice ($p < 0.005$). Besides, in DUhTP mice, six weeks of voluntary activity increased mRNA levels of Ucp1 in subcutaneous fat depots ($p < 0.05$) compared to the DUC mice from the identical treatment group. The three exercise interventions had no significant impact on Cidea, Tbx1, Ppargc1a, and Ucp1 mRNA expression. However, both lines showed a strong correlation between Cidea and Ucp1 expression, with no statistical significance for long-term active DUhTP (ex/ex) and short-term active DUC mice (sed/ex) (Table 2).

Since browning of adipose tissue is associated with mitochondrial biogenesis, we also studied mtDNA (ratio cytB/36B4) and the transcription factors Nrf1 and Tfam expression. Mitochondrial DNA

expression was increased in the subcutaneous fat samples of sedentary control DUhTP mice compared to the DUC line (Figure 8B; $p < 0.05$). Interestingly, in DUhTP sed/ex mice, mtDNA expression was decreased ($p < 0.05$). Expression of the transcription factors Nrf1 and Tfam was also reduced in response to voluntary physical activity from week 10 to 13 (Figure 8C,D), although only the Nrf1 expression was significantly lower (Figure 8C; $p < 0.005$). DUC sed/ex mice expressed more subcutaneous fat Nrf1 transcripts than DUhTP mice ($p < 0.005$). Nevertheless, only for Tfam and Ppargc1a, a positive correlation could be shown in all exercised DUhTP animals and DUC sed/ex (Table 2).

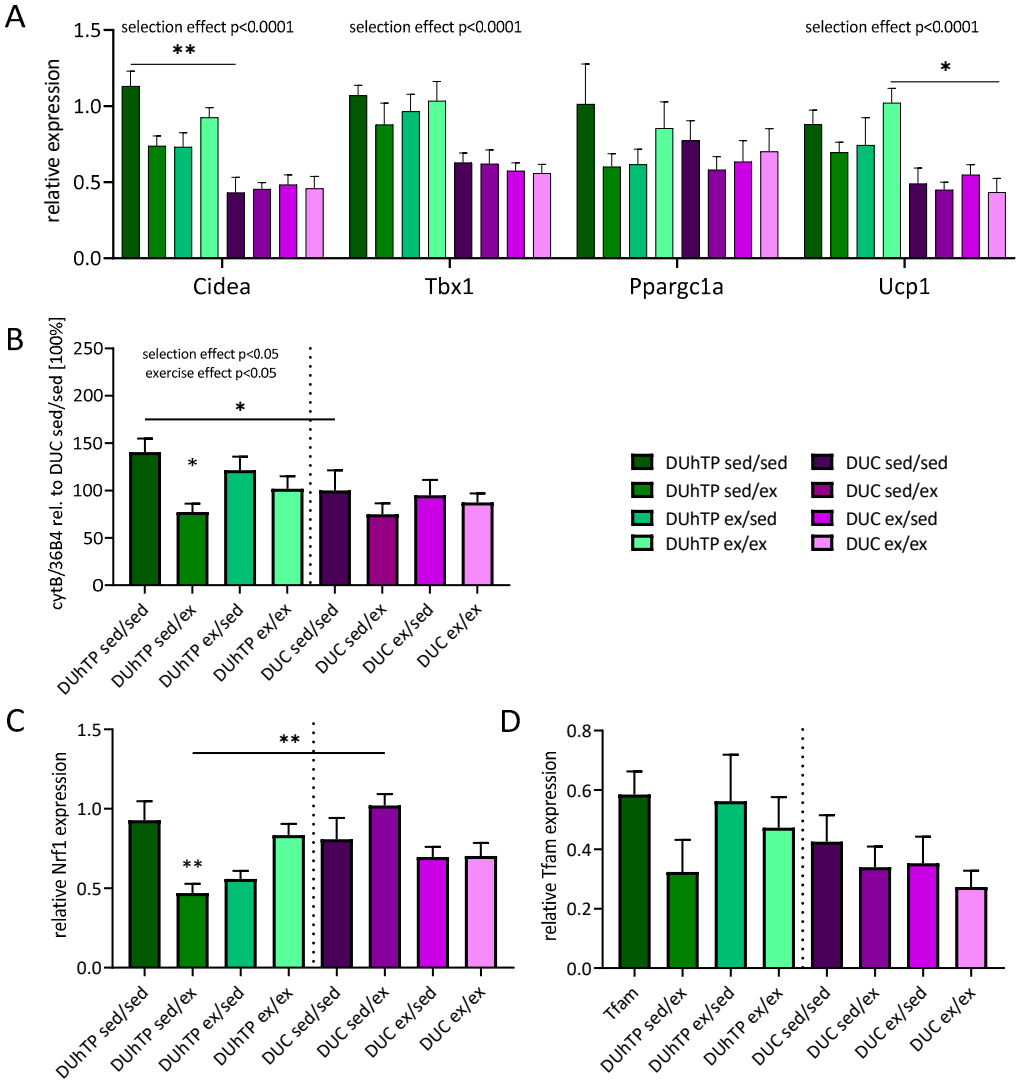

Figure 8. Analysis of mRNA expression in subcutaneous fat determined by quantitative real-time PCR in 13-weeks-old DUhTP and DUC mice after absolving different activity programs. The expression is normalized to housekeeping gene expression. Graphs show the relative expression of (**A**) browning markers, (**B**) ratio of mitochondrial to genomic DNA, and transcription factors (**C**) Nrf1 and (**D**) Tfam. Statistical analysis was performed by two-way ANOVA. Graphs show means (n = 8) with SEM. Significant effect of exercise compared to the respective sedentary line control as indicated by * $p < 0.05$, ** $p < 0.005$. Significant differences between the same exercise groups of both mouse lines are indicated by a line drawn over the bars and * $p < 0.05$ or ** $p < 0.005$. Overall effects of selection or exercise are also provided with the graphs.

Surprisingly, gene expression of mitochondrial complex subunits showed no exercise-related changes (Figure 9A). However, an effect of selection was found for the complex subunits Cox4i1 ($p < 0.0001$) and Cytb ($p < 0.05$) as well as a positive correlation between Ppargc1a and Cytb and Cyc (Table 2).

Under the conditions of this experiment, an effect of selection could not be identified for any of the five genetic markers (Dnm1, Fis1, Mfn1, Mfn2, or Opa1) controlling mitochondrial fission or fusion in subcutaneous adipose tissue (Figure 9B). Instead, a main effect of voluntary exercise could be observed in DUhTP mice for Dnm1 and Mfn2 ($p < 0.05$). Significant effects of the exercise were also demonstrated if distinct experimental groups were compared with sedentary DUhTP mice ($p < 0.05$).

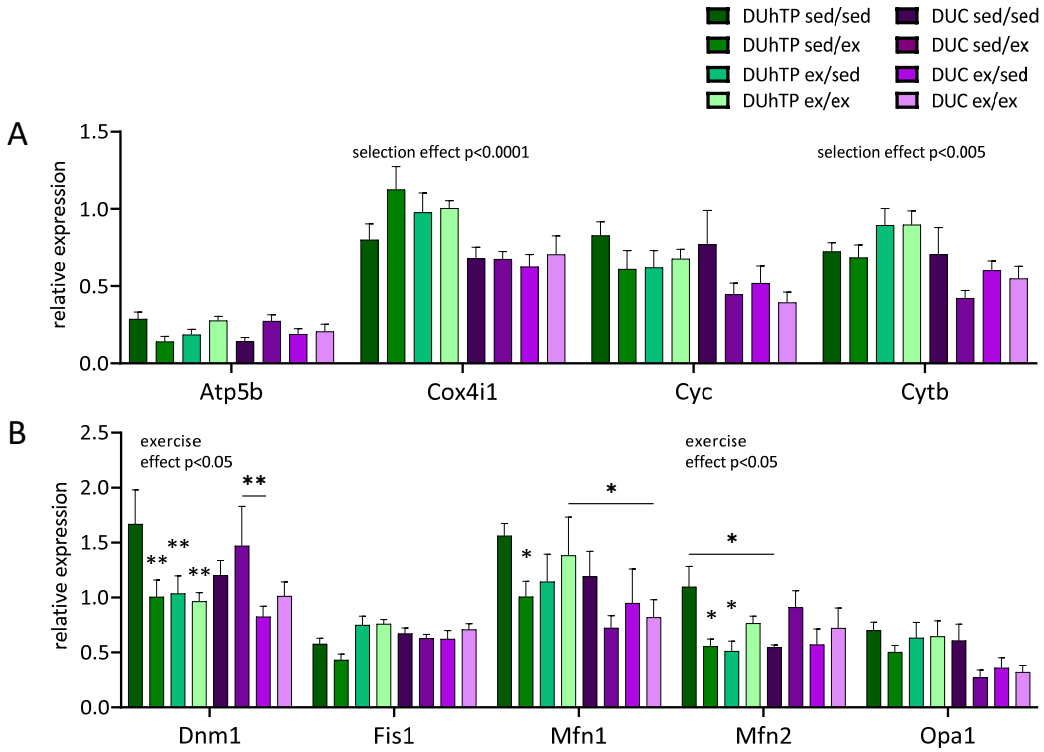

Figure 9. Analysis of mRNA expression in subcutaneous fat of 13-week-old DUhTP and DUC mice in response to different activity programs, determined by quantitative real-time PCR. The graphs show the relative expression (relative to the expression of the measured household genes) of genes related to (**A**) oxidative phosphorylation and (**B**) mitochondrial dynamics (fusion and cleavage). Statistical analysis was performed by two-way ANOVA. The graphs show the mean values (n = 8) with SEM. Significant effects of voluntary activity compared to the respective sedentary control, indicated by * $p < 0.05$, ** $p < 0.005$. Significant differences between two groups are indicated by a line over the bars and * $p < 0.05$ or ** $p < 0.005$. The main effects of selection and exercise in DUhTP are also shown in the graphs.

Notably, mRNA expression of three different fission or fusion markers was reduced by voluntary physical activity in subcutaneous fat samples of DUhTP mice ($p < 0.05$). An inhibitory effect of physical activity was not observed in control mice.

Besides, correlation studies revealed a strong association between Ppargc1a and Opa1 and Mfn1 in exercised DUhTP mice and only sporadically in DUC mice (Table 2). The strong relationship between Mfn1 and Opa1 could be shown for both lines.

Table 2. Correlation studies between the expression of transcription factors and genes related to oxidative phosphorylation and mitochondrial fusion (n = 8).

		DUhTP				DUC			
Correlation		**sed/sed**	**sed/ex**	**ex/sed**	**ex/ex**	**sed/sed**	**sed/ex**	**ex/sed**	**ex/ex**
Ucp1/Cidea	r	**0.754**	**0.785**	**0.935**	0.48	**0.968**	0.664	**0.865**	**0.793**
	p	*	*	**	ns	***	ns	**	*
Ppargc1a/Nrf1	r	0.375	0.379	−0.266	0.334	0.098	−0.237	−0.444	0.057
	p	ns	ns	ns	ns	ns	ns	ns	ns
Ppargc1a/Tfam	r	−0.000	**0.867**	**0.828**	**0.850**	0.211	0.753	0.008	0.424
	p	ns	**	*	**	ns	*	ns	ns
Ppargc1a/Cyc	r	−0.102	**0.733**	**0.836**	**0.843**	0.275	0.501	0.210	0.021
	p	ns	*	*	**	ns	ns	ns	ns
Ppargc1a/Cytb	r	0.067	0.632	**0.731**	**0.854**	0.406	0.495	0.653	0.211
	p	ns	ns	*	**	ns	ns	ns	ns
Ppargc1a/Mfn1	r	−0.401	**0.866**	**0.925**	**0.945**	0.285	0.626	**0.745**	0.315
	p	ns	**	**	***	ns	ns	*	ns
Ppargc1a/Opa1	r	0.363	**0.943**	**0.788**	**0.899**	0.196	**0.694**	0.414	0.310
	p	ns	***	*	**	ns	*	ns	ns
Mfn1/Opa1	r	0.464	**0.963**	**0.938**	**0.936**	**0.899**	**0.990**	**0.830**	**0.914**
	p	ns	***	**	***	***	***	*	**

Significant correlations were calculated by Pearson correlation, are expressed in bold letters and indicated with two-tailed p-value * $p < 0.05$; ** $p < 0.005$; *** $p < 0.0005$. r, Pearson correlation coefficient; ns, not significant; Ucp1, uncoupling protein 1; Cidea, cell death activator; Ppargc1a, peroxisome-proliferator-activated receptor-gamma-coactivator-1-alpha; Nrf1, nuclear respiratory factor 1; Cyc, cytochrome C; Cytb, Cytochrome B; Mfn1, Mitofusin 1; Opa 1, optic atrophy protein 1; Tfam, mitochondrial transcription factor A.

4. Discussion

Beige fat thermogenesis plays an essential role in the regulation of body weight. The conversion of white to beige adipose tissue (called browning) is typically induced by cold exposure [31] or training [2]. Due to long-term selection for high submaximal treadmill running over 140 generations, DUhTP mice have beige subcutaneous fat even in sedentary conditions and without external induction [24].

In previous studies, we demonstrated that three weeks of voluntary running wheel exercise significantly reduced fat mass and increased browning markers and the mitochondrial network in subcutaneous fat, particularly in DUhTP mice [8,27]. Considering the prominent effects of voluntary physical activity in the previous study [8], we now investigated three different voluntary exercise programs on gene expression related to energy metabolism in DUhTP mice and DUC controls.

Unexpectedly, the physical activity of DUhTP mice was significantly lower compared to unselected controls. This result was different from our previous study in animals of earlier generations under conditions of a semi-barrier animal facility [8,24], where no significant difference of voluntary activity was described in the DUhTP and DUC mice. Meanwhile, the mice were brought to an SPF facility, and several genotype/environment interactions have been identified [26]. In particular, the new environment had a significant effect on growth and reproduction traits. At the time of the present study, voluntary physical activity in our model also seemed to be affected by the new environmental effects. We can therefore assume that voluntary physical activity is a dynamic trait in our model, which is currently being investigated in a separate study. Overall, the observed dynamic traits are related to the mouse model's complex genetic background, initially composed of four different inbred and four different outbred mouse strains [32]. Moreover, as an effort to maintain genetic diversity in our mouse lines, inbreeding was avoided during the selection experiment. Within each line, voluntary physical activity was similar at all time points tested. This observation is different from a study by Davidson and

colleagues [33]. They demonstrated increased running activity over time, although the running activity in DUhTP and DUC mice were on higher levels compared to the referenced study.

Voluntary physical activity blocked the age-related weight gain in both genetic groups in the first period of the 3-week segments compared to both sedentary control groups. However, the negative effects of exercise on body weight gain were no longer present after three weeks of physical inactivity, especially in DUhTP mice. When the sedentary mice of both genetic groups were allowed to use a running wheel in the second half of the study (sed/ex), weight gain between weeks 10 and 11 decreased in both genetic groups as well. While this effect persisted in the DUC animals until the end of the experiment, similar weight gain was observed in the DUhTP sed/ex animals from week 11 onwards as in the sedentary control siblings. The body weight differences of the sedentary controls compared to partially and long-term exercised animals were more pronounced in the DUC animals and reached statistical significance for animals that ran until the end of the experiment (sed/ex, ex/ex). Physical activity affected DUC animals much more strongly in the second half of the experiment resulting in the lowest bodyweight of this line. On the other hand, the DUhTP animals increased in weight due to forced inactivity during the second part of the experiment and hardly differed from sedentary control animals.

Comparable results were described in rats that stopped training four weeks earlier than their littermates, which trained for a total of 12 weeks [34]. After the resting period, these animals were also characterized by an increase in body weight, and their final body weight corresponded to the body mass of sedentary subjects. While food consumption was not investigated in this study [34], Tokuyama and colleagues demonstrated that physical activity correlates with increased feed intake compared to sedentary controls [35]. This finding was not confirmed using our experimental design.

However, it was clearly shown that under our experimental conditions, substantial reductions in body fat were present in response to voluntary physical activity, as described in a previous, slightly different experimental design with only a 3-week-exercise interval [8]. In the current study, we identified significant reductions in all examined fat depots in DUhTP and unselected controls, which voluntarily ran until the experiment's end. Voluntary exercise, which started later, showed a more significant effect on fat depots in mice of both lines. The animals of this group were characterized by lower epididymal and perinephric fat depots than exercising control animals. Lean aged mice that underwent a 10-weeks voluntary exercise intervention also showed a better decrease in epididymal fat mass and average adipocyte area than half aged animals [36]. Lehnig et al. also showed significant reductions in five (interscapular and perirenal brown as well as interscapular, perigonadal, and inguinal white adipose tissue) of 14 investigated fat depots in older animals by voluntary 3-week running wheel activity [9]. With the chosen study design of 10-week-old animals and 3-week voluntary wheel activity, these animals corresponded to the experimental group sed/ex from our cross-over study, as they were also physically active between 10 and 13 weeks of age.

No significant changes in subcutaneous, perinephric, and epididymal fat depot mass were detected in the animals of both lines that stopped exercising in the second part of our experiment. Sertie et al. made similar observations with rats undergoing 12 weeks of treadmill training [34]. Early discontinuation of training after eight weeks followed by 4-weeks of sedentary caging resulted in subcutaneous and retroperitoneal fat mass weights similar to those of entirely untrained animals, while those of permanently trained siblings were reduced. Another trial with rats applied the so-called wheel-lock model, which provides a one-week blocking of the running wheels after three weeks of voluntary exercise. During the last week, a dramatic increase in fat mass, especially visceral and perirenal fat, was observed in rats with wheel-lock, in contrast to permanently active [37] or permanently active and sedentary rats [38]. Noteworthy, the authors of this study were able to stop this increase in body fat by administering AICAR, a pharmacological agent that activates the AMP kinase and, therefore, energy metabolism [38].

Brown fat depots were reduced in both lines under the influence of voluntary physical activity. The reduction of this thermogenic tissue and its thermogenic capacity was also observed in other

exercise trials in rodent models [8,9,39]. These reductions are assumed to be an adaptation to regular, chronic physical activity to counteract the training-mediated increase in muscular heat production [39]. This seems to be a longer-lasting adaptation since a cessation of voluntary exercise in our animals did not regain brown adipose tissue mass. According to Aldiss and colleagues, the exercise-induced reduction and browning of subcutaneous fat could be an adaptive mechanism that increases the thermal potential of the reduced brown but also subcutaneous fat mass and thus may compensate for the elevated sensation of cold [40].

Serum triglyceride levels were reduced by voluntary physical activity in both lines, and significant differences were observed after six weeks of physical activity. When quantified directly after three weeks of voluntary physical activity at the age of 10 weeks, a significant reduction of serum triglyceride concentration was identified in the DUhTP mouse model [8]. Thus, three weeks of physical inactivity could have normalized serum triglyceride levels in DUhTP mice at the age of 13 weeks in the present study. Since three weeks of voluntary physical activity between 10 and 13 weeks of age had no effect on serum triglycerides, we may argue that the effects of physical activity on serum triglycerides may depend on age. In fact, the triglyceride levels in serum from sedentary animals in both lines at the age of 13 weeks were twice as high if compared to 10 weeks of age and similar (DUC) or almost similar (DUhTP) to mice at the age of 7 weeks [24]. Since lipid metabolism, without a doubt, is required for aerobic energy metabolism during exercise in mice [41], the age-dependency of serum triglycerides in DUhTP mice deserves a separate study in the future.

Already under sedentary conditions, beige subcutaneous fat tissue is present in the DUhTP mouse model [8], which indicates a larger mitochondrial mass and increased mitochondrial biogenesis in this tissue, further enhanced by training [8,27]. The exercise-induced browning of adipose tissue is associated with increased expression of genes, which are regarded as markers for beige fat as T-box protein 1 (Tbx1), cell death activator (Cidea), or uncoupling protein 1 (Ucp1) [42]. Although physical activity clearly had an effect on fat mass and partly on serum triglycerides in our mouse lines, browning markers were not significantly affected by exercise in the present study. However, an impact of phenotype selection was identified on mRNA expression for Cidea, Tbx1, and Ucp1 by elevated expression in the subcutaneous fat of DUhTP mice. Jash and colleagues described a strong association between CIDEA and *UCP1* in human fat samples [43], which we could also confirm in subcutaneous fat samples from both lines. Surprisingly, *Ppargc1a* (gene for PGC1-α) transcription was unaffected by exercise or selection in the subcutaneous fat depot of DUhTP mice. In previous studies in younger animals, we could detect an increase in the expression of Ppargc1a [8] and Ucp1 [27] in the subcutaneous fat of DUhTP mice. Other studies also demonstrated increased Ppargc1a mRNA expression in subcutaneous fat in response to physical activity [3,5–7,9]. However, our previous results were also obtained from animals of an earlier generation under semi-barrier conditions before re-establishing the animals in the current SPF facility [23]. We also cannot exclude the influence of age since the previous experiments were performed with 10-week-old mice and not with 13-week-old ones. Nevertheless, we could clearly demonstrate the prominent role of PGC1-α in the DUhTP line in response to exercise due to the strong correlation between Ppargc1a expression and various other measured mitochondrial-relevant mRNA transcripts.

In muscle samples of healthy, trained human subjects, a strong correlation between Ppargc1a and Nrf1 or Tfam was demonstrated [44]. The authors also could demonstrate a positive correlation between Ppargc1a and mitochondrial creatine kinase, CoxI, CoxXVb, citrate synthase, and the regulators of mitochondrial dynamics.

In our study, a positive correlation between Ppargc1a and Cyc and Cytb, subunits of the respiratory chain complexes, was detectable in DUhTP animals in response to exercise, with a stronger correlation in mice that exercised until the end of the experiment. Nevertheless, no altered gene expression of the investigated complex subunits could be shown in response to any exercise program. By contrast, a selection-mediated increase in Cytb and Cox4i1 gene expression was identified, which was also visible in elevated mitochondrial DNA in DUhTP compared to DUC mice. Three weeks of exercise

reduced the mitochondrial DNA (ratio Cytb/36B4) content in DUhTP sed/ex mice. Notably, this reduced mitochondrial DNA was accompanied by decreased gene expression of the transcription factor Nrf1, which allowed direct identification of possible mediators of the negative effects of physical activity on subcutaneous fat energy expenditure. NRF1 induces the transcription of mitochondrial genes encoded in the nucleus and the transcription factor Tfam, which in turn is responsible for the expression of mitochondria-encoded genes [45,46]. NRF1 binds to the promoter of *Cyc* but not to the promoter of the *Cox4i1* gene [47]. Its transcription is induced by NRF2 binding, which we have not investigated in this study. While Nrf1 expression did not correlate with either Ppargc1a, Tfam, or Cyc expression in either line, a positive correlation between Ppargc1a and Tfam was observed in exercised DUhTP animals. Accordingly, neither reduced Nrf1 expression nor reduced mitochondrial DNA levels were correlated with the altered expression of respiratory chain subunits.

In response to exercise, reduced expression of known regulators of mitochondrial fusion and fission was observed in the subcutaneous fat from only DUhTP mice. In comparison to the DUC mice, the reduction found in DUhTP mice can be interpreted as normalization of previously elevated levels, which was significant for Mfn2 in the sedentary condition. Accordingly, a negative effect of exercise on Dnm1 and Mfn2 expression was demonstrated in the DUhTP but not DUC mice. While Dnm1, which mediates GTP-dependent mitochondrial fission [48], was reduced by each exercise intervention in the subcutaneous fat of DUhTP mice, fusion-relevant Mfn2 was reduced in DUhTP mice exercised for three weeks and Mfn1 only in DUhTP sed/ex mice. Interestingly, only the double knockout of muscular *Mfn1* and *2* significantly reduced running performance [49]. Optic atrophy protein 1 (OPA1), which is involved in inner mitochondrial membrane fusion, positively affects exercise performance as provided in Opa1 transgenic mice [50]. Its expression did not vary in response to physical activity in either DUhTP or DUC mice. In comparison, the overexpression of mitofusin-2 in rats did not reveal insights into mitochondrial energy metabolism by using primary skeletal muscle cells [51]. The muscular overexpression of Drp1, instead, reduced muscle growth and attenuated long-term low-intensity running as well as a short-term high-intensity exercise in mice [52]. The overexpression of Fis1 resulted in elevated mitochondrial fragmentation and the simultaneous blocking of fusion [53,54].

In mouse muscle, 30-days wheel running did not change the levels of proteins involved in mitochondrial fusion and fission [23]. Instead, the authors demonstrated that exercise increased phosphorylation at Ser637 of DRP1 (gene Dnm1), inhibiting its translocation to the mitochondria and, thus, reducing mitochondrial fission [23,55]. In male cyclists, reduced mitochondrial fission in response to physical exercise was also concluded based on the increased expression of Ppargc1a, Mfn1 and 2, and Nrf2 in muscle biopsies [56]. However, the muscular expression of genes for mitochondrial fission and fusion may also be related to repair and adaptation after exercise. Accordingly, in rats, 24 h after exercise, a decreased muscular MFN1 protein, increased Fis1 mRNA and protein expression were observed [19,20], and, in mice, a DRP1 activation was induced [21].

This prevailing fission was discussed in the context of degradation of damaged mitochondria before the synthesis of new mitochondria can occur during recovery, which finally leads to an improved mitochondrial quality [18]. Trewin and colleagues recently discussed partially controversial results of mitochondrial dynamics after diverse exercise interventions [22]. Although different energy metabolic responses in the muscle might be attributed to distinct experimental design (intensity, training status, species, sex, age, etc.), there was substantial evidence for an increase of fusion proteins in response to prolonged exercise. The concept of mitochondrial repair and replacement clearly suggests the impact of training intensity and duration on mitochondrial fission and fusion as well as the relevance of the time points when these genes are assessed. The principles of mitochondrial dynamics in muscle might also be relevant for subcutaneous fat, which to our knowledge, has not been studied in this context before.

In fact, in subcutaneous fat, higher mitochondrial fusion in DUhTP mice can be hypothesized due to the reduced expression of the cleavage-relevant Dnm1 in response to long-term physical activity. This assumption would confirm the concept of Trewin et al. [22] now in subcutaneous fat. Although it is impossible to identify the specific functions of the effects of physical exercise on mitochondrial fission

and fusion at present, our first mRNA-based results suggest imbalanced mitochondrial dynamics in the subcutaneous fat from our marathon mouse model. Future studies will have to assess the regulation of mitochondrial fission and fusion at the protein level and additional time points to establish a more comprehensive picture of mitochondrial dynamics in subcutaneous fat from DUhTP mice. Another issue for a future study is to test mitochondrial dynamics in subcutaneous fat in response to higher exercise intensities such as forced training.

Nevertheless, the reduced amount of mitochondrial DNA in DUhTP mice due to physical exertion compared to unselected controls can also be interpreted as the normalization of mitochondrial content in subcutaneous fat. Similarly, reduced gene expression associated with mitochondrial fission and fusion could be considered as a normalization with respect to unselected controls.

Furthermore, the substantially reduced subcutaneous fat mass due to physical activity in both mouse lines indicates significant reconstruction activities due to physical activity. However, sedentary DUhTP mice are characterized by elevated levels of energy metabolism in this tissue, which was associated with higher surface temperatures [27]. An explanatory approach for why energy metabolism is increased in subcutaneous fat from marathon mice was not available at that time. The new insights from the present study, with longer durations of the physical activity and later time points of biomarker assessment, may suggest normalization of energy metabolism in subcutaneous fat and support current concepts of interaction between muscle and fat in DUhTP vs. DUC mice [57]. This may fuel the idea that elevated energy metabolism in the subcutaneous fat from sedentary DUhTP mice is related to physical inactivity. This newly established concept will have to be investigated in the future by longitudinal studies addressing the effects of higher training intensities and longitudinal observations. The present study has several limitations. First, the assessment of mitochondrial energy metabolism was performed on mRNA level only and needs to be compared with protein levels and morphology in the future. Also, the timing of adaptive response in subcutaneous fat and the duration of physical activity were predefined by the experimental design. Accordingly, it will be of particular interest for the development of the animal model to study the prolonged effects of physical activity on mitochondrial biogenesis in adipose tissues.

5. Conclusions

The present study was performed in order to study the effects and interactions of genotype and voluntary physical activity on the control of energy metabolism in subcutaneous fat from mice. It was possible to confirm previous results showing significant differences in genetic markers for browning and oxidative phosphorylation in DUhTP mice in response to selection. These selection-derived genetic markers were not further induced by the exercise duration and intensity chosen in the current study. Instead, fat mass reductions, accompanied by reduced mitochondrial content, the reduced expression of Nrf1 mRNA, and the reduced expression of mRNA coding for DNM1, MFN1, and MFN2, were observed in response to physical activity. On the level of gene expression, our results demonstrate that the mitochondrial energy metabolism can be triggered by voluntary physical activity in subcutaneous fat from marathon mice but not in unselected controls. This animal model thereby may provide unique opportunities for the study of voluntary activity on adipose tissues.

Supplementary Materials: The following are available online at http://www.mdpi.com/2073-4409/9/12/2697/s1, Figure S1: Effect of different exercise protocols on the mitochondrial network in subcutaneous adipose tissue of DUhTP (upper row) and DUC mice (lower row).

Author Contributions: Conceptualization, J.B. and A.H.; methodology, D.O., C.W., J.S. and J.B; software, D.O. and J.B.; validation, D.O. and J.B.; formal analysis, J.B. and A.H.; investigation, M.L., D.O., C.W., J.S. and J.B; writing—original draft preparation, J.B. and A.H.; writing—review and editing, J.B., D.O., M.L, C.W., J.S. and A.H. All authors have read and agreed to the published version of the manuscript.

Funding: This article's publication was funded by the Open Access Fund of the Leibniz Institute for Farm Animal Biology (FBN).

Acknowledgments: The authors want to thank Luong Chau, Sabine Hinrichs, Julian Buchholz, and the Lab Animal Facility technicians for excellent animal care and technical assistance.

Conflicts of Interest: The authors declare no conflict of interest.

References

1. Cao, L.; Choi, E.Y.; Liu, X.; Martin, A.; Wang, C.; Xu, X.; During, M.J. White to brown fat phenotypic switch induced by genetic and environmental activation of a hypothalamic-adipocyte axis. *Cell Metab.* **2011**, *14*, 324–338. [CrossRef] [PubMed]
2. Bostrom, P.; Wu, J.; Jedrychowski, M.P.; Korde, A.; Ye, L.; Lo, J.C.; Rasbach, K.A.; Bostrom, E.A.; Choi, J.H.; Long, J.Z.; et al. A PGC1-alpha-dependent myokine that drives brown-fat-like development of white fat and thermogenesis. *Nature* **2012**, *481*, 463–468. [CrossRef] [PubMed]
3. Stanford, K.I.; Middelbeek, R.J.; Goodyear, L.J. Exercise Effects on White Adipose Tissue: Beiging and Metabolic Adaptations. *Diabetes* **2015**, *64*, 2361–2368. [CrossRef]
4. Puigserver, P.; Spiegelman, B.M. Peroxisome proliferator-activated receptor-gamma coactivator 1 alpha (PGC-1 alpha): Transcriptional coactivator and metabolic regulator. *Endocr. Rev.* **2003**, *24*, 78–90. [CrossRef] [PubMed]
5. Little, J.P.; Safdar, A.; Bishop, D.; Tarnopolsky, M.A.; Gibala, M.J. An acute bout of high-intensity interval training increases the nuclear abundance of PGC-1α and activates mitochondrial biogenesis in human skeletal muscle. *Am. J. Physiol. Regul. Integr. Comp. Physiol.* **2011**, *300*, 1303–1310. [CrossRef]
6. Trevellin, E.; Scorzeto, M.; Olivieri, M.; Granzotto, M.; Valerio, A.; Tedesco, L.; Fabris, R.; Serra, R.; Quarta, M.; Reggiani, C.; et al. Exercise training induces mitochondrial biogenesis and glucose uptake in subcutaneous adipose tissue through eNOS-dependent mechanisms. *Diabetes* **2014**, *63*, 2800–2811. [CrossRef]
7. Sutherland, L.N.; Bomhof, M.R.; Capozzi, L.C.; Basaraba, S.A.; Wright, D.C. Exercise and adrenaline increase PGC-1{alpha} mRNA expression in rat adipose tissue. *J. Physiol.* **2009**, *587*, 1607–1617. [CrossRef]
8. Brenmoehl, J.; Ohde, D.; Walz, C.; Schultz, J.; Tuchscherer, A.; Rieder, F.; Renne, U.; Hoeflich, A. Dynamics of Fat Mass in DUhTP Mice Selected for Running Performance—Fat Mobilization in a Walk. *Obes. Facts* **2015**, *8*, 373–385. [CrossRef]
9. Lehnig, A.C.; Dewal, R.S.; Baer, L.A.; Kitching, K.M.; Munoz, V.R.; Arts, P.J.; Sindeldecker, D.A.; May, F.J.; Lauritzen, H.; Goodyear, L.J.; et al. Exercise Training Induces Depot-Specific Adaptations to White and Brown Adipose Tissue. *iScience* **2019**, *11*, 425–439. [CrossRef]
10. Tanaka, T.; Nishimura, A.; Nishiyama, K.; Goto, T.; Numaga-Tomita, T.; Nishida, M. Mitochondrial dynamics in exercise physiology. *Pflug. Arch.* **2019**. [CrossRef]
11. Hyde, B.B.; Twig, G.; Shirihai, O.S. Organellar vs cellular control of mitochondrial dynamics. *Semin. Cell Dev. Biol.* **2010**, *21*, 575–581. [CrossRef] [PubMed]
12. Van der Bliek, A.M.; Shen, Q.; Kawajiri, S. Mechanisms of mitochondrial fission and fusion. *Cold Spring Harb. Perspect. Biol.* **2013**, *5*. [CrossRef] [PubMed]
13. Gan, Z.; Fu, T.; Kelly, D.P.; Vega, R.B. Skeletal muscle mitochondrial remodeling in exercise and diseases. *Cell Res.* **2018**, *28*, 969–980. [CrossRef] [PubMed]
14. Chan, D.C. Mitochondrial fusion and fission in mammals. *Annu Rev. Cell Dev. Biol.* **2006**, *22*, 79–99. [CrossRef]
15. Chen, H.; Chan, D.C. Emerging functions of mammalian mitochondrial fusion and fission. *Hum. Mol. Genet.* **2005**, *14*, R283–R289. [CrossRef]
16. Martin, O.J.; Lai, L.; Soundarapandian, M.M.; Leone, T.C.; Zorzano, A.; Keller, M.P.; Attie, A.D.; Muoio, D.M.; Kelly, D.P. A Role for PGC-1 Coactivators in the Control of Mitochondrial Dynamics during Postnatal Cardiac Growth. *Circ. Res.* **2014**, *114*, 626–636. [CrossRef]
17. Vainshtein, A.; Tryon, L.D.; Pauly, M.; Hood, D.A. Role of PGC-1α during acute exercise-induced autophagy and mitophagy in skeletal muscle. *Am. J. Physiol. Cell Physiol.* **2015**, *308*, C710–C719. [CrossRef]
18. Drake, J.C.; Wilson, R.J.; Yan, Z. Molecular mechanisms for mitochondrial adaptation to exercise training in skeletal muscle. *FASEB J.* **2016**, *30*, 13–22. [CrossRef]
19. Ding, H.; Jiang, N.; Liu, H.; Liu, X.; Liu, D.; Zhao, F.; Wen, L.; Liu, S.; Ji, L.L.; Zhang, Y. Response of mitochondrial fusion and fission protein gene expression to exercise in rat skeletal muscle. *Biochim. Biophys. Acta* **2010**, *1800*, 250–256. [CrossRef]
20. Marton, O.; Koltai, E.; Takeda, M.; Koch, L.G.; Britton, S.L.; Davies, K.J.A.; Boldogh, I.; Radak, Z. Mitochondrial biogenesis-associated factors underlie the magnitude of response to aerobic endurance training in rats. *Pflug. Arch. Eur. J. Physiol.* **2015**, *467*, 779–788. [CrossRef]

21. Pagano, A.F.; Py, G.; Bernardi, H.; Candau, R.B.; Sanchez, A.M. Autophagy and protein turnover signaling in slow-twitch muscle during exercise. *Med. Sci. Sports Exerc.* **2014**, *46*, 1314–1325. [CrossRef] [PubMed]
22. Trewin, A.J.; Berry, B.J.; Wojtovich, A.P. Exercise and Mitochondrial Dynamics: Keeping in Shape with ROS and AMPK. *Antioxidant (Basel)* **2018**, *7*, 7. [CrossRef] [PubMed]
23. Moore, T.M.; Zhou, Z.; Cohn, W.; Norheim, F.; Lin, A.J.; Kalajian, N.; Strumwasser, A.R.; Cory, K.; Whitney, K.; Ho, T.; et al. The impact of exercise on mitochondrial dynamics and the role of Drp1 in exercise performance and training adaptations in skeletal muscle. *Mol. Metab.* **2019**, *21*, 51–67. [CrossRef] [PubMed]
24. Brenmoehl, J.; Walz, C.; Renne, U.; Ponsuksili, S.; Wolf, C.; Langhammer, M.; Schwerin, M.; Hoeflich, A. Metabolic adaptations in the liver of born long-distance running mice. *Med. Sci. Sports Exerc.* **2013**, *45*, 841–850. [CrossRef]
25. Falkenberg, H.; Langhammer, M.; Renne, U. Comparison of biochemical blood traits after long-term selection on high or low locomotory activity in mice. *Arch. Tierz.* **2000**, *43*, 513–522. [CrossRef]
26. Brenmoehl, J.; Walz, C.; Spitschak, M.; Wirthgen, E.; Walz, M.; Langhammer, M.; Tuchscherer, A.; Naumann, R.; Hoeflich, A. Partial phenotype conversion and differential trait response to conditions of husbandry in mice. *J. Comp. Physiol. B* **2018**, *188*, 527–539. [CrossRef]
27. Brenmoehl, J.; Ohde, D.; Albrecht, E.; Walz, C.; Tuchscherer, A.; Hoeflich, A. Browning of subcutaneous fat and higher surface temperature in response to phenotype selection for advanced endurance exercise performance in male DUhTP mice. *J. Comp. Physiol. B* **2017**, *187*, 361–373. [CrossRef]
28. Ohde, D.; Brenmoehl, J.; Walz, C.; Tuchscherer, A.; Wirthgen, E.; Hoeflich, A. Comparative analysis of hepatic miRNA levels in male marathon mice reveals a link between obesity and endurance exercise capacities. *J. Comp. Physiol. B* **2016**, *186*, 1067–1078. [CrossRef]
29. Ballester, M.; Cordón, R.; Folch, J.M. DAG expression: High-throughput gene expression analysis of real-time PCR data using standard curves for relative quantification. *PLoS ONE* **2013**, *8*, e80385. [CrossRef]
30. Hofmeister-Brix, A.; Kollmann, K.; Langer, S.; Schultz, J.; Lenzen, S.; Baltrusch, S. Identification of the ubiquitin-like domain of midnolin as a new glucokinase interaction partner. *J. Biol. Chem.* **2013**, *288*, 35824–35839. [CrossRef]
31. Barbatelli, G.; Murano, I.; Madsen, L.; Hao, Q.; Jimenez, M.; Kristiansen, K.; Giacobino, J.P.; De Matteis, R.; Cinti, S. The emergence of cold-induced brown adipocytes in mouse white fat depots is determined predominantly by white to brown adipocyte transdifferentiation. *Am. J. Physiol. Endocrinol. Metab.* **2010**, *298*, E1244–E1253. [CrossRef] [PubMed]
32. Dietl, G.; Langhammer, M.; Renne, U. Model simulations for genetic random drift in the outbred strain Fzt:DU. *Arch. Tierz.* **2004**, *47*, 595–604. [CrossRef]
33. Davidson, S.R.; Burnett, M.; Hoffman-Goetz, L. Training effects in mice after long-term voluntary exercise. *Med. Sci. Sports Exerc.* **2006**, *38*, 250–255. [CrossRef] [PubMed]
34. Sertie, R.A.L.; Curi, R.; Oliveira, A.C.; Andreotti, S.; Caminhotto, R.O.; de Lima, T.M.; Proenca, A.R.G.; Reis, G.B.; Lima, F.B. The mechanisms involved in the increased adiposity induced by interruption of regular physical exercise practice. *Life Sci.* **2019**, *222*, 103–111. [CrossRef]
35. Tokuyama, K.; Saito, M.; Okuda, H. Effects of wheel running on food intake and weight gain of male and female rats. *Physiol. Behav.* **1982**, *28*, 899–903. [CrossRef]
36. Ziegler, A.K.; Damgaard, A.; Mackey, A.L.; Schjerling, P.; Magnusson, P.; Olesen, A.T.; Kjaer, M.; Scheele, C. An anti-inflammatory phenotype in visceral adipose tissue of old lean mice, augmented by exercise. *Sci Rep.* **2019**, *9*, 12069. [CrossRef]
37. Ruegsegger, G.N.; Company, J.M.; Toedebusch, R.G.; Roberts, C.K.; Roberts, M.D.; Booth, F.W. Rapid Alterations in Perirenal Adipose Tissue Transcriptomic Networks with Cessation of Voluntary Running. *PLoS ONE* **2015**, *10*, e0145229. [CrossRef]
38. Ruegsegger, G.N.; Sevage, J.A.; Childs, T.E.; Grigsby, K.B.; Booth, F.W. 5-Aminoimidazole-4-carboxamide ribonucleotide prevents fat gain following the cessation of voluntary physical activity. *Exp. Physiol.* **2017**, *102*, 1474–1485. [CrossRef]
39. Wu, M.V.; Bikopoulos, G.; Hung, S.; Ceddia, R.B. Thermogenic capacity is antagonistically regulated in classical brown and white subcutaneous fat depots by high fat diet and endurance training in rats: Impact on whole-body energy expenditure. *J. Biol. Chem.* **2014**, *289*, 34129–34140. [CrossRef]
40. Aldiss, P.; Betts, J.; Sale, C.; Pope, M.; Budge, H.; Symonds, M.E. Exercise-induced 'browning' of adipose tissues. *Metabolism* **2018**, *81*, 63–70. [CrossRef]

41. Templeman, N.M.; Schutz, H.; Garland, T., Jr.; McClelland, G.B. Do mice bred selectively for high locomotor activity have a greater reliance on lipids to power submaximal aerobic exercise? *Am. J. Physiol. Regul. Integr. Comp. Physiol.* **2012**, *303*, R101–R111. [CrossRef]
42. Wu, J.; Bostrom, P.; Sparks, L.M.; Ye, L.; Choi, J.H.; Giang, A.H.; Khandekar, M.; Virtanen, K.A.; Nuutila, P.; Schaart, G.; et al. Beige adipocytes are a distinct type of thermogenic fat cell in mouse and human. *Cell* **2012**, *150*, 366–376. [CrossRef]
43. Jash, S.; Banerjee, S.; Lee, M.-J.; Farmer, S.R.; Puri, V. CIDEA Transcriptionally Regulates UCP1 for Britening and Thermogenesis in Human Fat Cells. *iScience* **2019**, *20*, 73–89. [CrossRef] [PubMed]
44. Garnier, A.; Fortin, D.; Zoll, J.; N'Guessan, B.; Mettauer, B.; Lampert, E.; Veksler, V.; Ventura-Clapier, R. Coordinated changes in mitochondrial function and biogenesis in healthy and diseased human skeletal muscle. *FASEB J.* **2005**, *19*, 43–52. [CrossRef] [PubMed]
45. Wu, Z.; Puigserver, P.; Andersson, U.; Zhang, C.; Adelmant, G.; Mootha, V.; Troy, A.; Cinti, S.; Lowell, B.; Scarpulla, R.C.; et al. Mechanisms controlling mitochondrial biogenesis and respiration through the thermogenic coactivator PGC-1. *Cell* **1999**, *98*, 115–124. [CrossRef]
46. Virbasius, J.V.; Scarpulla, R.C. Activation of the human mitochondrial transcription factor A gene by nuclear respiratory factors: A potential regulatory link between nuclear and mitochondrial gene expression in organelle biogenesis. *Proc. Natl. Acad. Sci. USA* **1994**, *91*, 1309–1313. [CrossRef] [PubMed]
47. Wright, D.C.; Han, D.H.; Garcia-Roves, P.M.; Geiger, P.C.; Jones, T.E.; Holloszy, J.O. Exercise-induced mitochondrial biogenesis begins before the increase in muscle PGC-1alpha expression. *J. Biol. Chem.* **2007**, *282*, 194–199. [CrossRef] [PubMed]
48. Chang, C.R.; Blackstone, C. Dynamic regulation of mitochondrial fission through modification of the dynamin-related protein Drp1. *Ann. N. Y. Acad. Sci.* **2010**, *1201*, 34–39. [CrossRef] [PubMed]
49. Bell, M.B.; Bush, Z.; McGinnis, G.R.; Rowe, G.C. Adult skeletal muscle deletion of Mitofusin 1 and 2 impedes exercise performance and training capacity. *J. Appl. Physiol. (1985)* **2019**, *126*, 341–353. [CrossRef] [PubMed]
50. Civiletto, G.; Varanita, T.; Cerutti, R.; Gorletta, T.; Barbaro, S.; Marchet, S.; Lamperti, C.; Viscomi, C.; Scorrano, L.; Zeviani, M. Opa1 overexpression ameliorates the phenotype of two mitochondrial disease mouse models. *Cell Metab.* **2015**, *21*, 845–854. [CrossRef] [PubMed]
51. Lally, J.S.; Herbst, E.A.; Matravadia, S.; Maher, A.C.; Perry, C.G.; Ventura-Clapier, R.; Holloway, G.P. Over-expressing mitofusin-2 in healthy mature mammalian skeletal muscle does not alter mitochondrial bioenergetics. *PLoS ONE* **2013**, *8*, e55660. [CrossRef] [PubMed]
52. Touvier, T.; De Palma, C.; Rigamonti, E.; Scagliola, A.; Incerti, E.; Mazelin, L.; Thomas, J.L.; D'Antonio, M.; Politi, L.; Schaeffer, L.; et al. Muscle-specific Drp1 overexpression impairs skeletal muscle growth via translational attenuation. *Cell Death Dis.* **2015**, *6*, e1663. [CrossRef] [PubMed]
53. Liesa, M.; Van der Bliek, A.; Shirihai, O.S. To Fis or not to Fuse? This is the question! *EMBO J.* **2019**, *38*. [CrossRef]
54. Yu, R.; Jin, S.B.; Lendahl, U.; Nister, M.; Zhao, J. Human Fis1 regulates mitochondrial dynamics through inhibition of the fusion machinery. *EMBO J.* **2019**, *38*. [CrossRef]
55. Cereghetti, G.M.; Stangherlin, A.; de Brito, O.M.; Chang, C.R.; Blackstone, C.; Bernardi, P.; Scorrano, L. Dephosphorylation by calcineurin regulates translocation of Drp1 to mitochondria. *Proc. Natl. Acad. Sci. USA* **2008**, *105*, 15803–15808. [CrossRef]
56. Cartoni, R.; Leger, B.; Hock, M.B.; Praz, M.; Crettenand, A.; Pich, S.; Ziltener, J.L.; Luthi, F.; Deriaz, O.; Zorzano, A.; et al. Mitofusins 1/2 and ERRalpha expression are increased in human skeletal muscle after physical exercise. *J. Physiol.* **2005**, *567*, 349–358. [CrossRef]
57. Rodríguez, A.; Becerril, S.; Ezquerro, S.; Méndez-Giménez, L.; Frühbeck, G. Crosstalk between adipokines and myokines in fat browning. *Acta Physiol. (Oxf.)* **2017**, *219*, 362–381. [CrossRef]

5.3 Publikationen zum Einfluss von gezielter, erzwungener Bewegung

i) Walz, C., **Brenmoehl, J.**, Trakooljul, N., Noce, A., Caffier, C., Ohde, D., Langhammer, M., Wimmers, K., Ponsuksili, S; Hoeflich, A. (2021). Control of Protein and Energy Metabolism in the Pituitary Gland in Response to Three-Week Running Training in Adult Male Mice. *Cells, 10:736. doi: 10.3390/cells10040736.*

Geleisteter Eigenanteil: Projekt- und Tierversuchsplanung, Schreiben des Tierversuchantrages, Phänotypische Erhebungen (Sektion, Gewinnung von Gewebe und Serum), Auswertung und Darstellung der Daten sowie Schreiben des Manuskriptes.

ii) **Brenmoehl, J.**, Walz, C., Caffier, C., Brosig, E., Walz, M., Ohde, D., Trakooljul, N., Langhammer, M., Ponsuksili, S; Wimmers, K., Zettl, U.K., Hoeflich, A. (2021). Central Suppression of the GH/IGF Axis and Abrogation of Exercise-Related mTORC1/2 Activation in the Muscle of Phenotype-Selected Male Marathon Mice (DUhTP). *Cells, 10:3418. doi: 10.3390/cells10123418.*

Geleisteter Eigenanteil: Projekt- und Tierversuchsplanung, Schreiben des Tierversuchantrages, Phänotypische Erhebungen (Sektion, Gewinnung von Gewebe und Serum), Auswertung und Darstellung der Daten sowie Schreiben des Manuskriptes.

iii) **Brenmoehl, J.**, Brosig, E., Trakooljul, N., Walz, C., Ohde, D., Noce, A., Walz, M., Langhammer, M., Petkov, S., Röntgen, M., Maak, S., Galuska, C.E., Fuchs, B., Kuhla, B., Ponsuksili, S; Wimmers, K., Hoeflich, A. (2023). Metabolic Pathway Modeling in Muscle of Male Marathon Mice (DUhTP) and Controls (DUC)-A Possible Role of Lactate Dehydrogenase in Metabolic Flexibility. *Cells, 12:1925. doi: 10.3390/cells12151925.*

Geleisteter Eigenanteil: Projekt- und Tierversuchsplanung, Schreiben des Tierversuchsantrages, Phänotypische Erhebungen (Sektion, Gewinnung von Gewebe und Serum), Koordinierung der Kollaborationen, KEGG-Pathway-Analysen, Auswertung und Darstellung der Daten sowie Schreiben des Manuskriptes.

cells

MDPI

Article

Control of Protein and Energy Metabolism in the Pituitary Gland in Response to Three-Week Running Training in Adult Male Mice

Christina Walz §, Julia Brenmoehl *,§, Nares Trakooljul, Antonia Noce, Caroline Caffier, Daniela Ohde, Martina Langhammer ‡, Klaus Wimmers, Siriluck Ponsuksili and Andreas Hoeflich *

Institute for Genome Biology, Lab Animal Facility, Institute for Genetics and Biometry, Leibniz Institute for Farm Animal Biology (FBN), Wilhelm-Stahl-Allee 2, 18196 Dummerstorf, Germany; walz@fbn-dummerstorf.de (C.W.); trakooljul@fbn-dummerstorf.de (N.T.); noce@fbn-dummerstorf.de (A.N.); caro.caffier@yahoo.de (C.C.); ohde@fbn-dummerstorf.de (D.O.); martina.langhammer@fbn-dummerstorf.de (M.L.); wimmers@fbn-dummerstorf.de (K.W.); ponsuksili@fbn-dummerstorf.de (S.P.)

* Correspondence: brenmoehl@fbn-dummerstorf.de (J.B.); hoeflich@fbn-dummerstorf.de (A.H.); Tel.: +49(0)38208-68-937 (J.B.); +49(0)38208-68-744 (A.H.)

‡ Lab Animal Facility, Institute for Genetics and Biometry, 18196 Dummerstorf, Germany.

§ The authors contributed equally.

Abstract: It is assumed that crosstalk of central and peripheral tissues plays a role in the adaptive response to physical activity and exercise. Here, we wanted to study the effects of training and genetic predisposition in a marathon mouse model on mRNA expression in the pituitary gland. Therefore, we used a mouse model developed by phenotype selection for superior running performance (DUhTP) and non-inbred control mice (DUC). Both mouse lines underwent treadmill training for three weeks or were kept in a sedentary condition. In all groups, total RNA was isolated from the pituitary gland and sequenced. Molecular pathway analysis was performed by ingenuity pathway analysis (IPA). Training induced differential expression of 637 genes (DEGs) in DUC but only 50 DEGs in DUhTP mice. Genetic selection for enhanced running performance strongly affected gene expression in the pituitary gland and identified 1732 DEGs in sedentary DUC versus DUhTP mice. Training appeared to have an even stronger effect on gene expression in both lines and comparatively revealed 3828 DEGs in the pituitary gland. From the list of DEGs in all experimental groups, candidate genes were extracted by comparison with published genomic regions with significant effects on training responses in mice. Bioinformatic modeling revealed induction and coordinated expression of the pathways for ribosome synthesis and oxidative phosphorylation in DUC mice. By contrast, DUhTP mice were resistant to the positive effects of three-week training on protein and energy metabolism in the pituitary gland.

Keywords: pituitary gland; treadmill training; DUhTP mice; pathway analysis; ribosome synthesis; oxidative phosphorylation; miR-124

Citation: Walz, C.; Brenmoehl, J.; Trakooljul, N.; Noce, A.; Caffier, C.; Ohde, D.; Langhammer, M.; Wimmers, K.; Ponsuksili, S.; Hoeflich, A. Control of Protein and Energy Metabolism in the Pituitary Gland in Response to Three-Week Running Training in Adult Male Mice. *Cells* **2021**, *10*, 736. https://doi.org/10.3390/cells10040736

Academic Editor: Robert Wessells

Received: 16 February 2021
Accepted: 20 March 2021
Published: 26 March 2021

1. Introduction

The pituitary gland is located on the lower side of the brain and, under hypothalamic control, regulates growth, reproductive development, stress response, and energy metabolism. Complex endocrine control by the anterior pituitary gland is achieved by the presence of different types and subtypes of cells with distinct gene expression patterns [1,2]. It produces growth hormone (GH), reproductive hormones such as luteinizing hormone (LH) and follicle-stimulating hormone (FSH), adrenocorticotrophic hormone (ACTH), or thyroid-stimulating hormone (TSH), and thus can influence growth and metabolism in multiple tissues. In addition, pituitary glands contribute to energy homeostasis in concert with the hypothalamus, which integrates peripheral and central stimuli in the arcuate nucleus [3]. Due to its central position in hormone production, pituitary glands can also

mediate adaptive or even benefitting effects of physical activity. Accordingly, the secretion of growth hormone (GH) is increased in response to resistance training in humans [4]. Notably, exercise induced the secretion of GH to a significantly higher extent than pharmacological stimulation [4]. On the histological level in rats, physical activity induced specific adaptations in somatotropic cells, including increased cell size and the production of larger secretory granules [5]. Exercise in different experimental settings also affected the pituitary–gonadal [6], pituitary–adrenal [7], and pituitary–thyroid [8] hormone axes.

Because the pituitary gland is highly responsive to the effects of physical activity, we postulated that physical activity also induces organ-wide molecular pathways in the pituitary gland not directly related to distinct hormonal axes or distinct cell types. In order to test this hypothesis at the genetic level, we used mice long-term selected for high running performance (DUhTP mice) and unselected controls (DUC) and asked whether we can use bulk RNA-sequencing (RNA-seq) to identify different transcriptional patterns in the pituitary gland in marathon mice and controls. To identify the impact of physical activity, we tested the effects of three-week training in both mouse models. Finally, we asked whether the genetically fixed molecular pathways in pituitary glands of marathon mice (DUhTP) can also be induced by three weeks of training in unselected control mice (DUC). By this approach, we aimed to identify and test transcriptional signatures of physical activity in pituitary glands.

2. Materials and Methods

2.1. Animals and Study Design

All in vivo experiments were performed according to national and international guidelines and were approved by the internal institutional audit committee and by the State of Mecklenburg–Western Pomerania (State Office for Agriculture, Food Safety, and Fisheries; AZ 7221.3-1-014/17, date of approval: 25/04/2017). In this study, we used a long-term selected mouse line (DUhTP), selected for high running endurance, and the corresponding unselected control line DUC [9,10]. The mice were kept under controlled, specified pathogen-free (SPF) conditions in H-Temp Polysulfon cages with a floor area of 370 cm^2 (Eurostandard Type II, Tecniplast, Hohenpeißenberg, Germany). The animals received fresh drinking water and autoclaved Ssniff® M-Z food (Ssniff-Spezialdiäten GmbH, Soest, Germany) *ad libitum*. Male animals were individually kept in cages from day 21, divided into two groups at 48 days of age, and assigned to a training program (Figure 1; DUC trained (tr.), DUhTP tr.; n = 10).

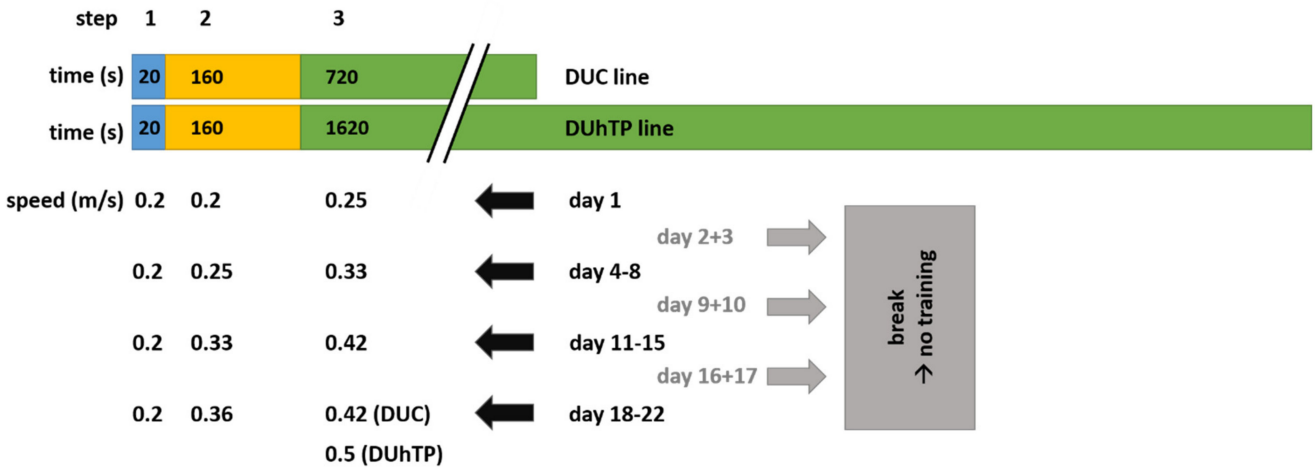

Figure 1. Three-week training program for high running performance (DUhTP) and unselected control (DUC) mice. From day 49, the animals passed a training program on a computer-controlled treadmill for 30 min (DUhTP) and 15 min (DUC) for five days per week, respectively. The duration of running corresponds to 22.56% of their last tested submaximal running performance. The final running speed of a half meter per second was stepwise increased.

Mice from the sedentary group (n = 10) were individually kept in cages for three weeks without any treatment (DUC sedentary (sed.); DUhTP sed.). Both experimental groups from the mouse lines DUC and DUhTP were trained on a treadmill (TSE, Germany) for three weeks. Because DUhTP and DUC mice had different running capacities, DUhTP and DUC were trained for 30 and 15 min per day, respectively. These training intensities correspond to 22.6% of the submaximal treadmill running capabilities in both mouse lines, determined in previous generations ([11], DUhTP: 2 h 13 min; DUC: 1 h 6 min). At the age of 49 days, the training program started with an initial run by animals of both lines for 15 and 30 min. After a break of 2 days, regular training was started for a total duration of three weeks (5 days training with a break over the weekend). For this purpose, the mice performed a run on a treadmill with an initial speed of 0.2 m/s for 30 m, 0.25 m/s for 50 m, and a final speed of 0.33 m/min. The final distance/speed was increased in weekly intervals up to a final speed of 0.5 m/min (Figure 1). Only the control mice could not manage the final speed of 0.5 m/s, so they completed the last week of training with a final speed of 0.42 m/s. After completing the final run, the mice were sacrificed, and tissue and serum samples were collected. The tissues were weighed, shock-frozen in liquid nitrogen, and stored at −70 °C for subsequent analysis.

2.2. Generation of DNA Library

The entire pituitary gland of each animal was homogenized in 1 mL of TRIzol reagent (Invitrogen, Karlsruhe, Germany). Total RNA was extracted in accordance with the manufacturing instructions. The extracted RNA was additionally treated with DNase I using the RNase-free DNase kit (Base-Zero DNase, Biozym, Hessisch Oldendorf, Germany) and with the Zymo® RNA Clean&Concentrator kit (Zymo Research, Irvine, CA, USA). The RNA quality was assessed using an Agilent RNA 6000 Nano kit and 2100 Bioanalyzer (Agilent, Waldbronn, Germany). Samples with RNA integrity numbers (RIN) >8 [12] were used to generate a DNA library using a TruSeq Stranded mRNA Sample Preparation kit in accordance with the manufacture's protocol (Illumina, Berlin, Germany). Essentially, polyadenylated mRNA molecules were enriched from 2 µg of total RNA using poly-T oligo-coated magnetic beads and chemically fragmented under elevated temperature conditions. The fragmented RNA was then reverse-transcribed into cDNA using random hexamers and Superscript II reverse transcriptase and ligated with TruSeq RNA adapters containing a unique DNA sequencing index to enable multiplexing. The DNA libraries were quality-control assessed for fragment-size distribution using an Agilent Technologies 2100 Bioanalyzer and Agilent DNA-1000 Chip kit.

2.3. Next-Generation Sequencing (NGS)

DNA library concentration was quantified using a KAPA qPCR Library Quantification kit (KAPA-Biosystems, Wilmington, MA, USA). Normalized multiplexed DNA libraries with the 0.5% spiked-in PhiX control were clonally cluster amplified using the cBot system and paired-end sequenced for 2 × 101 bp using the high-output mode on a HiSeq2500 (Illumina) at our sequencing facility of the Genome Biology Institute, Leibniz Institute for Farm Animal Biology (FBN), Dummerstorf, Germany.

2.4. Differential Gene Expression Analysis

The raw sequencing reads (fastq) were quality-assessed using FastQC (version 0.11.5) (access date: 11/04/2019; http://www.bioinformatics.babraham.ac.uk/projects/fastqc/) and pre-processed by filtering out low-quality reads with a mean Q-score < 30 and read length shorter than 30 bp and trimming adapter-like sequences. High-quality paired-end reads were then aligned to the Ensembl reference mouse genome (GRCm38.p6) using Hisat2 version 2.1.0 [13,14]. The number of reads uniquely mapped to each gene was extracted from the HISAT2 mapping results using HTSeq version 0.8.0 [15].

2.5. Data Processing and Evaluation

The resulting gene count data were further analyzed for differently expressed genes (DEGs) using EdgeR [16] and R dependency packages. Genes with lower read values (count per million, cpm) were filtered out to obtain only genes with >0.5 cpm. These had to be present in at least four libraries. EdgeR standard parameters were applied with the trimmed mean of M values (TMM) option considering library size and composition bias and the estimateGLMRobustDisp option to estimate interlibrary variation [16]. The glmFit and glmLRT functions implemented in EdgeR were used for statistical testing of DEGs. The RNA-seq data were then evaluated using the following pipeline: The list contained a cpm value for each analyzed individual and each identified transcript. The average reads cpm values of each transcript were compared between groups in pairs. Line and training comparisons were performed (DUC tr. vs. sed., DUhTP tr. vs. sed., DUhTP sed. vs. DUC sed., DUhTP tr. vs. DUC tr.). The data sets of the four comparison groups then contained a gene identification (Gen-ID), the fold change ($\log_2$FC), the p-value, and the false discovery rate (FDR; Supplementary Table S1). In all analyses, the FDR was defined as the significance level of $\leq$0.05. For bioinformatic analyses, the DEGs data obtained from the group comparisons were used. For the Venn diagram, the free Venny website (access date: 08/03/2021; https://bioinfogp.cnb.csic.es/tools/venny/) was used [17].

2.6. Manhattan Plot

The "ggplot2" R packages [18] were used to perform the mirrored Manhattan plots where only the significant (FDR $\leq$ 0.05) DEGs in each group comparison were visualized with their genomic position. In these plots, each point represented a gene; the x-axis reported the chromosome number, and the y-axis showed the DEGs as $\log_2$FC values. The y-axis gray line, referring to the null $\log_2$FC value, was positioned in the middle of each plot to recognize the upregulated genes as those points shown above that line and the downregulated genes as those points shown under that line.

2.7. Validation by Fluidigm

The RNASeq data were validated by 2-step reverse transcription-quantitative PCR (RT-qPCR) using the Fluidigm technique [19]. Thirteen DEGs of isolated pathways were selected to validate if the reads' cpm was >1 in more than 50% of the samples. Specific primers (Supplementary Table S2) were identified with PrimerBank [20] and blasted using the blastn® software [21] against mouse genome and transcript databases for their suitability in the mouse. mRNA (250–1000 ng) was reverse-transcribed with GOScript™ Reverse Transcriptase kit (Promega). The primers were quality checked with Roche LightCycler® 480 (Roche) using a cDNA dilution of 25 ng to 0.025 ng per reaction. For validation, specific target amplification was performed with the final primer setup and TaqMan PreAmp Mastermix in accordance with the manufacturer's recommendations. All samples were treated with exonuclease I and diluted. The sample and primer setup followed the instructions for a 48 × 48 array, performing a fast PCR program with a melting curve. Run data were imported and analyzed by data analysis gene (DAG) expression; [22]. For qPCR normalization step, three housekeeping genes were selected within a total of five through the DAG tool Gene Stability Measurement, and the relative expression was calculated for each sample-primer combination. Outliers were identified (Q = 0.1%) and removed using the ROUT method GraphPad Prism V 8.4.2. Group independent correlation analysis was performed for each gene between RNA sequencing signals (cpm) and relative qPCR expression ($2^{-\Delta\Delta Ct}$). The Pearson correlation coefficient and p-value were calculated and displayed with GraphPad Prism. Group means and $\log_2$FC calculations were calculated according to RNASeq data.

2.8. Pathway Analysis

Ingenuity® Pathway Analysis (IPA®, Qiagen, Germantown, MD, USA) was used for the bioinformatic analysis of the holistic data, linking the contents of large data sets from

RNA sequencing with the current literature, organizing, linking, and visualizing them [23]. The bioinformatic interpretation was performed with the core analysis of IPA® below the limit of FDR at 0.05. Pathway analysis was performed with the comparison groups and used with the default settings of the program. To indicate significant up- or downregulation pathways, only those with a—log (p-value) $\geq$ 1.3 and a $|$z-score$|$ $\geq$ 2 were considered for further interpretation. In addition, we used the freely accessible Pathview website (access date: 08/03/2021; https://pathview.uncc.edu) to visualize KEGG (Kyoto Encyclopedia of Genes and Genomes) paths. The definitions of the options were: for gene data, the DEGs (FDR $\leq$0.05) loaded with Gen-ID (ENSEMBL) and $\log_2$FC; as species restricted to *Mus musculus*. The DEGs were manually matched with the KEGG pathways "ribosome" and "oxidative phosphorylation" for all comparison groups.

2.9. Localization of DEGs in Published Quantitative Trait Locus (QTLs) Associated with Training Response

Masset and colleagues [24] identified several QTL regions associated with training response in mice after genotyping through a specific single nucleotide polymorphism (SNP) panel [25,26]. We used this information to explore the genome regions around the most important SNPs reported [24] for pre-training, post-training, and change-work in the mouse. We therefore asked if the DEGs identified in the present study were located in the genomic regions described by Masset et al. [24]. To this end, we selected the genome region of 1 megabase (Mb) around the SNPs reported (0.5 Mb upstream and downstream of each SNP). We extracted reference genes present in these regions from the Mouse Genome Database through the search tool "Gene & Markers Query" [27] and compared them with the significant DEGs in each of our group comparisons. The presence of DEGs in genomic regions of previously identified QTLs may add an additional argument for the biomarker content of potential candidate genes identified here.

3. Results

3.1. RNA-Sequencing Data and Validation by RT-qPCR

Using RNA-seq, an average of 39.3 $\pm$ 7.5 million reads per sample were generated in the pituitary gland of DUC mice and 30.7 $\pm$ 4.9 million reads per sample in the pituitary gland of DUhTP mice. Around 96% were successfully mapped to the mouse reference genome (GRCm38.p6), and we only selected the mapped reads corresponding to exonic regions, which were approximately 88%. After considering genetic and training comparison, we detected a total of 17,429 expressed genes (data not shown) in the mice's pituitary gland; 6188 DEGs of them showed a significant (FDR $\geq$0.05) difference in their expression level between groups (Table 1).

Table 1. Overview of differentially expressed genes (DEGs) in the pituitary glands from trained and sedentary DUhTP and DUC mice with a false discovery rate (FDR) $\leq$0.05.

Comparison	Number of DEGs (FDR $\leq$ 0.05)		
	Total	Up	Down
DUC tr. vs. DUC sed.	637	428	209
DUhTP tr. vs. DUhTP sed.	50	38	12
DUhTP sed. vs. DUC sed.	1732	890	842
DUhTP tr. vs. DUC tr.	3828	1617	2211

Numbers of differentially expressed transcripts are shown in black: total genes, in red: upregulated, and in green: downregulated DEGs. Abbreviations: sed. = sedentary, tr. = trained, vs. = versus.

Single DEGs identified by RNA-seq were cross-validated through Fluidigm assays (Supplementary Table S3). The significant Pearson correlation coefficients ranging from 0.5630 ($p \leq 0.01$) to 0.9850 ($p \leq 0.001$) (Figure 2) confirmed a good concordance between RNA-seq and RT-qPCR results for the pituitary gland.

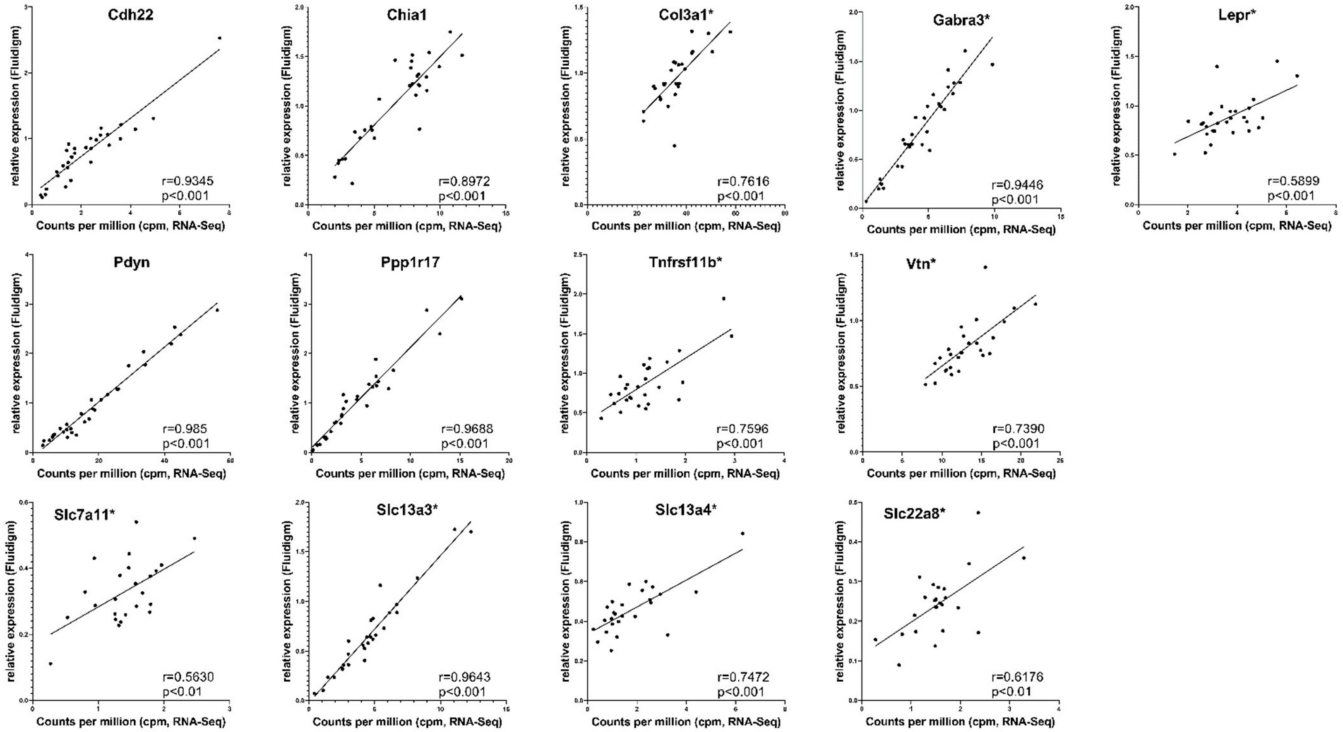

Figure 2. Validation of RNA-seq data by the Fluidigm technique for 13 differentially expressed genes (DEGs) from selected pathways in the pituitary gland. For each gene, the total reads (count per million, cpm) obtained by RNA-seq were plotted on the *x*-axis and RT-qPCR data ($2^{-\Delta\Delta Ct}$) on the *y*-axis. Stars at the gene name indicate that outliers were removed during processing, as described in Materials and Methods. Corresponding correlation coefficients (r) and *p*-values are shown.

3.2. Global Effects of Training and Phenotype Selection on Gene Expression in the Pituitary Gland

As an effect of training, 637 and 50 genes were differentially expressed between the trained and sedentary groups in DUC or DUhTP mice, respectively (Table 1). As an effect of genetic selection, 1732 genes were differentially expressed in sedentary DUhTP versus DUC mice, and 3828 genes were differentially expressed in the trained DUhTP versus DUC mice.

The Venn diagram provides the number of common and differently expressed genes in all experimental groups (Figure 3). Training had a clear effect on gene expression in DUC mice's pituitary glands since 637 transcripts were characterized by altered abundance in response to training. By contrast, in DUhTP mice, only 50 transcripts indicated an effect of training on gene expression in pituitary glands. Notably, from these 50 transcripts, only two transcripts were also regulated in unselected control mice. Furthermore, 465 transcripts regulated by training in DUC mice overlapped with genetic selection for high running performance in untrained and trained DUhTP mice. However, most transcripts identified in DUhTP mice (4152) revealed no overlap with training effects on gene expression identified in unselected control mice. Therefore, the effect of training on gene expression is clear in DUC mice, whereas in DUhTP mice, most of the transcripts affected by training in DUC mice are genetically fixed in DUhTP mice. Almost 90% of the differentially expressed genes in sedentary and trained DUhTP mice versus DUC mice, respectively, had no overlap with the effects observed in trained versus sedentary DUC mice.

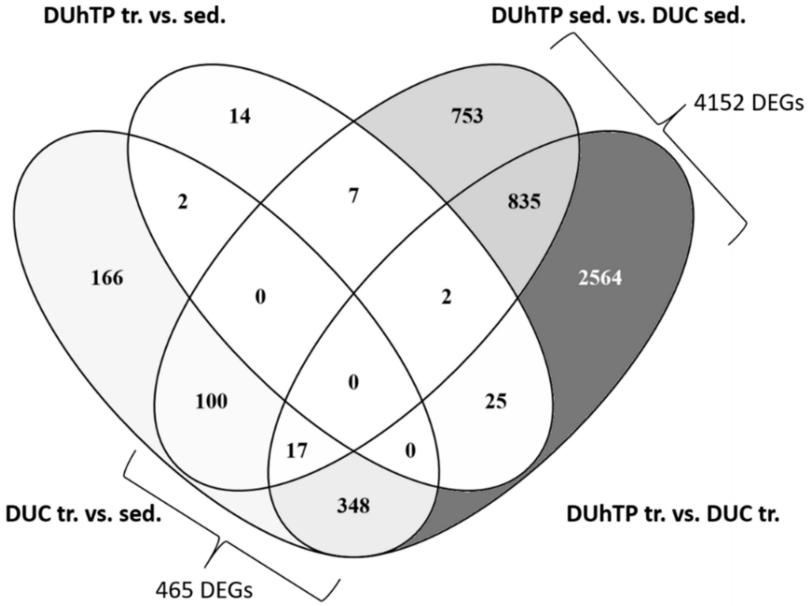

Figure 3. Venn diagram of differentially expressed genes (DEGs) in all comparison groups (FDR $\leq$ 0.05, sed. = sedentary, tr. = trained, vs. = versus).

3.3. Identification of TOP5 Regulated mRNA Transcripts

Table 2 provides the TOP5 up- and downregulated genes in all experimental groups. In response to training, all TOP5 genes differed between the two genetic groups. Accordingly, training had effects on transcripts associated with calcium sensitivity (Syt2, Vsnl1), Mg2+ transport (Cldn19), regulation of post-synaptic actin cytoskeleton modification (Camkv), and glutamate uptake (Grm4) in DUC mice. At the same time, transcripts for ion channels (Kcnj13, Slc6A20, Slc6A12, and Slc22A6) were substantially suppressed in DUC mice in response to training. In DUhTP mice, genes linked with RNA transcription (Rn7sk, Ciart), sodium ion transport (Asic2), blood pressure (Corin), and circulatory regulation (Ciart, Per2) were the most strongly induced ones by training. In addition, training inhibited the abundance of genes associated with oxidative stress (Gstp3) and detoxification (Aldh3b2) as well as receptor binding (Rpsa-ps10, Rxfp1, Cd72) in DUhTP compared to sedentary littermates.

In the Venn diagram, 835 DEGs overlapped in the genetic model (DUhTP vs. DUC sed. and DUhTP vs. DUC tr.). Remarkably, the same TOP5 upregulated genes could be found in both genetic groups (DUhTP vs. DUC sed. and DUhTP vs. DUC tr.). Accordingly, TOP DEGs identified ribosomal proteins 2 and 26, double homoeobox B-like 1, complement component 1 R, and glyceraldehyde-3P-dehydrogenase to be particularly induced in the pituitary gland of DUhTP mice compared to DUC mice. In contrast, transcription for the ribosomal protein L26 and chromobox 3, histone H2a protein type 1, and ATP synthase pseudogene was substantially decreased in trained or sedentary DUhTP mice compared to corresponding unselected controls.

Although several markedly regulated genes (TOP5) were located on chromosome 14 (genetic effect) and chromosome 3 (effect of training; Table 2), the global comparison revealed the contribution of all chromosomes to the differential gene expression in response to phenotype selection or training (Figure 4a–d, Table S1).

Table 2. TOP5 up- and downregulated genes in all comparison groups. The five most upregulated and five most downregulated genes are listed with the corresponding regulation intensity and chromosome localization. Abbreviation: sed. = sedentary, tr. = trained, vs. = versus.

Comparison	Gen-ID	Regulation (log_2FC)	Description	Chromosome
DUC tr. vs. sed.	Syt2	4.1	Synaptotagmin 2	1
	Camkv	3.5	CaM kinase, vesicle-associated	9
	Cldn19	3.4	Claudin 19	4
	Vsnl1	3.3	Visinin-like 1	12
	Grm4	3.2	Metabotropic glutamate receptor 4	17
	Kcnj13	−4.0	Potassium channel protein	1
	Slc6a20	−3.7	Na^+- and Cl^--dependent transporter	9
	Slc6a12	−3.6	Na^+/Cl^--dependent betaine/GABA transporter	6
	Gm15387	−3.6	High-mobility group 1 protein (pseudogene)	15
	Slc22a6	−3.4	Na^+-dependent transporter	19
DUhTP tr. vs. sed.	Rn7sk	3.1	snRNA (transcription regulation)	9
	Ciart	2.2	Circadian-associated repressor of transcription	3
	Asic2	1.6	Neuronal sodium channel 1, acid sensitive ion channel 2	11
	Corin	1.4	Serine peptidase, neuronal natriuretic peptide convertase	5
	Per2	1.4	Periodic circadian regulator 2 in neuronal pacemaker	1
	Gstp3	−4.7	Glutathione S-transferase; oxidative stress	19
	Rpsa-ps10	−3.9	Ribosomal protein SA (pseudogene), cell surface receptor	3
	Rxfp1	−3.0	Peptide receptor 1 of the relaxin/insulin-like family	3
	Aldh3b2	−2.9	Aldehyde dehydrogenase	19
	Cd72	−1.3	Lymphocyte receptor	4
DUhTP sed. vs. DUC sed.	Rps2-ps13	6.6	Ribosomal protein2 (pseudogene)	X
	Rps26-ps1	6.2	Ribosomal protein26 (pseudogene)	8
	Duxbl1	5.3	Double homeobox B-like 1	14
	C1r	5.1	Complement component 1 R	6
	Gm4804	4.6	Glyceraldehyd-3P-dehydrogenase (pseudogene)	12
	Gm8104	−8.5	Unknown	14
	Gm7233	−7.7	Unknown	14
	Cbx3-ps7	−7.7	Chromobox 3 (pseudogene)	1
	Gm6356	−7.3	Unknown	14
	Gm15772	−7.3	Ribosomal protein L26 (pseudogene)	5
DUhTP tr. vs. DUC tr.	Rps2-ps13	6.4	Ribosomal protein2 (pseudogene)	X
	Rps26-ps1	6.4	Ribosomal protein26 (pseudogene)	8
	C1r	5.7	Complement component 1 R	6
	Gm4804	5.2	Glyceraldehyd-3P-dehydrogenase (pseudogene)	12
	Duxbl1	5.2	Double homeobox B-like 1	14
	Gm42743	−8.9	Unknown	3
	Hist1h2al	−8.5	Histone H2a-protein type 1, core protein	13
	Gm16440	−7.7	Unknown	14
	Gm10039	−7.5	ATP synthase (pseudogene)	11
	Gm7233	−7.4	Unknown	14

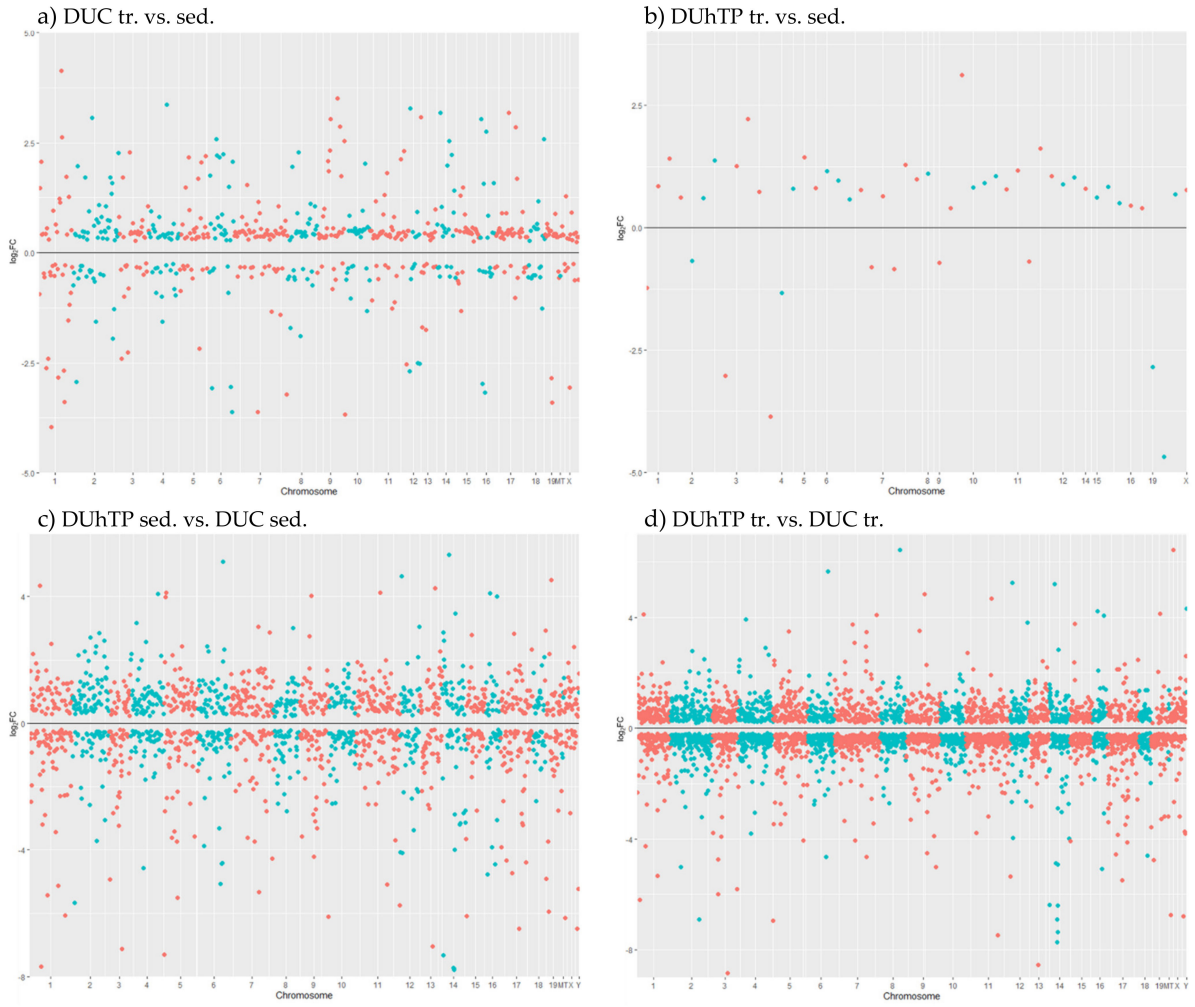

Figure 4. Mirrored Manhattan plots of the significant (FDR $\leq$ 0.05) differently expressed genes (DEGs) concerning the chromosome location in all comparison groups. Each point represents one gene in its genomic position. The chromosome numbers are reported in the x-axis, the level of expression in the y-axis as log2FC values. The maximum and minimum limits of the y-axis represent the range of log2FC values of each comparison. The gray line in the middle corresponds to log2FC = 0. All points visualized above the line belong to upregulated genes, while all the points visualized under the line are downregulated genes. The comparison groups are shown as (**a**) DUC tr. vs. sed., (**b**) DUhTP tr. vs. sed., (**c**) DUhTP sed. vs. DUC sed., and (**d**) DUhTP tr. vs. DUC tr. Abbreviation: sed. = sedentary, tr. = trained, vs. = versus.

3.4. Functional Analysis of DEGs

In order to study the potential interaction of genes and pathways related to physical activity and running performance in mice, we compared genes and pathways regulated by both training and phenotype selection. Functional analyses were performed by IPA, including all DEGs, to identify canonical pathways in the experimental groups (Table 3). In response to training, two pathways were activated (EIF2 signaling, oxidative phosphorylation), and four canonical pathways were inhibited (GP6 signaling, cardiogenesis promoting factors, basal cell carcinoma signaling, liver fibrosis signaling) in the pituitary gland from DUC mice. The effect of training on protein metabolism and the oxidative phosphorylation (OXPHOS) pathway was exclusively observed in DUC mice. In fact, training did not affect molecular or metabolic pathways in the pituitary gland of the DUhTP mice at all. In addition, the direct comparison between sedentary DUhTP mice and sedentary DUC mice revealed no effect either on protein metabolism or on the OXPHOS pathway. Instead, two different canonical pathways were significantly inhibited (unfolded protein response and LXR/RXR activation).

Table 3. Significantly, enriched canonical pathways (Fisher's exact test adjusted p-value ≤ 0.05) were deduced from DEGs of the pituitary gland in all comparison groups.

Group	Canonical Pathway	z-Score	Molecules
DUC tr. vs. sed.	EIF2 signaling	4.7	Eif3g, Eif3i, Fau, Hras, Rpl10, Rpl11, Rpl12, Rpl13, Rpl18, Rpl18a, Rpl19, Rpl26, Rpl27, Rpl27a, Rpl28, Rpl30, Rpl31, Rpl35, Rpl36a, Rpl37, Rpl37a, Rpl38, Rpl41, Rpl6, Rpl8, Rpl9, Rplp2, Rps10, Rps12, Rps13, Rps14, Rps15, Rps16, Rps17, Rps19, Rps20, Rps21, Rps23, Rps25, Rps27a, Rps28, Rps29, Rps3, Rps5, Rps6, Rps8, Rps9, Rpsa, Sos2
	Oxidative phosphorylation	4.5	Atp5f1d, Atp5mc2, Atp5mf, Atp5pd, Atp5po, Cox4i1, Cox6a1, Cox6b1, Cox7a2l, Cox8a, Mt-Nd5, Ndufa1, Ndufa11, Ndufa13, Ndufa2, Ndufa7, Ndufb10, Ndufb11, Ndufb4, Ndufb7, Ndufb8, Ndufs7, Uqcr10, Uqcr11
	GP6 signaling pathway	−3.2	Cert1, Col3a1, Col4a1, Col4a2, Col4a3, Col4a4, Col5a1, Lamc3, Prkca, Prkce
	Factors promoting cardiogenesis in vertebrates	−2.5	Bmp6, Bmp7, Camk2a,Crebbp, Prkca, Prkce, Tcf4, Tcf7l2, Tgfbr2, Wnt6
	Basal cell carcinoma signaling	−2.0	Bmp6, Bmp7, Dvl3, Tcf4, Tcf7l2, Wnt6
	Hepatic fibrosis signaling pathway	−2.2	Col3a1, Crebbp, Dvl3, Fth1, Ftl, Hras, Lepr, Pdgfrb, Prkca, Prkce, Rhobtb2, Sos2, Tcf4, Tcf7l2, Tgfbr2, Tnfrsf11b, Wnt6
DUhTP tr. vs. sed.	None		
DUhTP sed. vs. DUC sed.	Unfolded protein response	−2.1	Calr, Cebpg, Cebpz, Dnajc3, Edem1, Hspa1b, Os9, P4hb, Ubxn4
	LXR/RXR activation	−2.5	Abcg4, Alb, Apoa2, Arg2, Ccl2, Cd36, Gc, Hpx, Il1r2, Il33, Ncor2, Serpina1, Tnfrsf11b, Ttr, Vtn
DUhTP tr. vs. DUC tr.	Oxidative phosphorylation	−7.6	Atp5e, Atp5f1a, Atp5f1b, Atp5f1d, Atp5mc1, Atp5mc2, Atp5mc3, Atp5mf, Atp5mg, Atp5pb, Atp5pd, Atp5pf, Atp5po, Cox10, Cox4i1, Cox5a, Cox6a1, Cox6b1, Cox6c, Cox7a2, Cox7a2l, Cox7b, Cox8a, Cyc1, Cycs, Mt-Co2, Mt-Co3, Mt-Nd4l, Ndufa1, Ndufa10, Ndufa11, Ndufa12, Ndufa13, Ndufa2, Ndufa3, Ndufa4, Ndufa5, Ndufa6, Ndufa7, Ndufa8, Ndufa9, Ndufab1, Ndufb10, Ndufb11, Ndufb2, Ndufb3, Ndufb4, Ndufb5, Ndufb6, Ndufb7, Ndufb8, Ndufb9, Ndufs2, Ndufs3, Ndufs4, Ndufs6, Ndufs7, Ndufs8, Ndufv1, Ndufv2, Ndufv3, Sdhc, Sdhd, Uqcr10, Uqcr11, Uqcrb, Uqcrc1, Uqcrfs1, Uqcrq
	EIF2 signaling	−5.0	Acta1, Akt1, Atf3, Atf4, Atf5, Eif2ak2, Eif2b1, Eif2b3, Eif2b5, Eif3d, Eif3g, Eif3h, Eif3i, Eif3k, Eif3l, Eif4a1, Eif4e, Fau, Hras, Hspa5, Map2k2, Mt-Rnr1, Myc, Pik3cg,Pik3r2, Ppp1ca, Rpl10, Rpl10a, Rpl11, Rpl12, Rpl13, Rpl14, Rpl15, Rpl17, Rpl18, Rpl18a, Rpl19, Rpl23, Rpl27, Rpl27a, Rpl28, Rpl31, Rpl35, Rpl36a, Rpl36al, Rpl37, Rpl37a, Rpl38, Rpl4, Rpl41, Rpl5, Rpl6, Rpl7, Rpl7a, Rpl7l1, Rpl8, Rpl9, Rplp0, Rplp2, Rps10, Rps11, Rps12, Rps13, Rps14, Rps15, Rps15a, Rps16, Rps17, Rps18, Rps19, Rps2, Rps20, Rps21, Rps23, Rps24, Rps25, Rps26, Rps27a, Rps27l, Rps28, Rps29, Rps3, Rps4y1, Rps5, Rps6, Rps8, Rps9, Rpsa
	Synaptogenesis signaling pathway	−2.1	Adcy1, Adcy3, Adcy5, Akt1, Ap1g2,Ap2a1, Ap2a2, Ap2m1, Ap2s1, Arpc2, Arpc3, Arpc4, Arpc5l, Atf2,Atf4, Bad, Bet1l, Calm1 (Includes Others), Camk2b, Cdh1, Cdh12,Cdh24, Cdh6, Cdh8, Cdk5, Cfl1, Clasp2, Cplx3, Creb3, Crebbp,Efna3, Epha6, Gosr2, Grin2c, Grin3a,Grina, Grm4, Hras, Hspa8, Itsn2, Kalrn, Lrrtm2, Map1b, Nap1l1,Nap1l4, Napa, Nlgn2, Nlgn3, Nrxn1, Pik3cg, Pik3r2, Plcg2, Prkag1, Prkar1b, Rab3a, Rab5c, Rac1, Rasgrp1, Reln, Shf, Sncb, Syn3,Syt1,Syt12, Syt14,Syt2, Syt6, Thbs3, Vti1b
	TCA cycle II (eukaryotic)	−2.7	Aco2, Dhtkd1, Fh, Idh3a, Mdh1, Mdh2, Ogdhl, Sdhaf4, Sdhc, Sdhd, Suclg1
	Estrogen receptor signaling	−2.9	Adcy1, Adcy3, Adcy5, Agt, Akt1, Arg2, Atf2, Atf4, Atp5f1a, Atp5f1d, Atp5mc1, Atp5pb, Bad, Cfl1, Creb3, Crebbp,Cyc1, Egfr,Eif2b1, Eif2b3, Eif2b5, Eif4e, Ep300,Esr2, Foxo6, Gna14,Gnal, Gnat2, Gng11, Gng5, Hras, Map2k2, Mdk, Med12,Med21, Mmp14,Mmp17, Mmp19, Mmp20, Mmp7, Myc, Myl12a, Myl6, Myl6b, Myl9, Ncoa1, Ncoa2,Nos3, Pcna, Pdia3, Pgf, Pik3cg,Pik3r2, Plcb2, Plce1, Plcg2, Plch1, Prkaa2, Prkag1, Prkar1b, Prkcg,Sdhc, Sdhd, Shf, Sra1, Thrap3, Uqcrfs1, Vegfd
	Pentose phosphate pathway	−2.4	G6pd, H6pd, Pgd, Rpe, Taldo1, Tkt
	Dolichyl diphospho-oligosaccharide biosynthesis	−2.4	Alg1, Alg3, Alg8, Dpagt1, Dpm2, Dpm3
	tRNA charging	−2.1	Farsb, Hars1, Iars2,Kars1, Lars2, Mars1, Nars1, Rars1, Sars1, Tars1, Wars2
	Endocannabinoid neuronal synapse pathway	2.2	Adcy1, Adcy3, Adcy5, Cacna1h, Cacna2d4, Cacnb2, Cacng5, Cacng6, Faah, Gna14, Gnal, Gng11, Gng5, Grin2c, Grin3a,Grina, Kcnj9, Mapk13, Ndufs2, Pdia3, Plcb2, Plce1, Plcg2, Plch1,Prkag1, Prkar1b
	Integrin signaling	−2.1	Acta1, Actn1, Akt1, Arf1, Arf4, Arf5, Arhgap26,Arpc2, Arpc3, Arpc4, Arpc5l, Capn10, Capn5,Capn8, Hras, Itga11, Itga7, Itga8,Itgal, Itgb3,Itgb5, Itgb6,Map2k2, Myl12a, Myl9, Parva, Pfn1, Pik3cg, Pik3r2, Plcg2,Ptk2, Rac1, Rhob, Rhobtb2, Rhof, Rhog, Rnd2, Tnk2, Tspan5, Zyx

Pathways with a |z-score| $\geq$2 were considered as significantly activated and inhibited in the pituitary of the corresponding group, respectively. Font color of the gene symbol indicates lower expression (green) and higher expression (red) concerning the control for each comparison (unselected or untrained). Abbreviation: sed. = sedentary, tr. = trained, vs. = versus.

However, the comparison of trained DUhTP mice to trained DUC mice demonstrated robust activation of protein metabolism and OXPHOS in trained DUC mice since all, except a few members of both pathways, were significantly inhibited in the pituitary gland of DUhTP animals compared with trained DUC mice. Interestingly, considering

genetic selection and running performance enhances the selection-dependent differences between the lines and revealed the significant regulation of additional canonical pathways by training. In trained DUhTP mice, nine canonical pathways were inhibited compared to trained DUC mice. Only the endocannabinoid neuronal synapse pathway was upregulated in trained DUhTP mice vs. trained unselected controls.

By examining genomic regions in the proximity of 11 SNPs previously reported by Masset et al. [24] to be related to training adaptation, we identified which genes changed their expression levels in response to training (DUC tr. vs. sed. and DUhTP tr. vs. sed.), genetic selection (DUhTP sed. vs. DUC sed.), or both together (DUhTP tr. vs. DUC tr.).

The comparisons demonstrated that the selected line activated only one gene (Dnah9) in response to training, which was not present in the unselected line, located on chromosome 11 close to the variant reported for the change-work in Masset et al. [24]. Importantly, no DEGs were found in the selected line in response to activity for pre- or post-training variants, underlining the high performance of this mouse line obtained by long-term genetic selection. In turn, the unselected line activated three genes close to pre-training variants on chromosomes 2 and 8 and one gene close to a post-training variant on chromosomes 14. The Ces1d gene, located on chromosome 8, was found overexpressed in DUhTP mice when comparing both lines in sedentary conditions. Interestingly, in response to training, DUC mice showed an expression increase higher (log_2FC 0.67) than sedentary DUhTP mice compared to sedentary controls (log_2FC 0.59). MiR-124a-1hg, identified within the post-training chromosome 14 variants [24], was overexpressed in trained DUC mice compared to sedentary DUC (log_2FC 2.54) and trained DUhTP mice (log_2FC 2.03). In DUhTP animals, training did not alter miR124a-1hg expression.

Regarding the response to genetic selection, we found seven genes (including Ces1d mentioned above) distributed on chromosomes 1, 2, 8, and 19 and differentially expressed only in sedentary DUhTP pituitary glands.

Finally, ten DEGs (including Dnah9 and Mir124a-1hg) were found distributed on chromosomes 1, 4, 11, 14, and 19 in response to genetic selection along with training. The genes found on chromosome 2 (Accs) and 19 (Avpi1, Crtac1) were also observed in sedentary DUhTP mice. Table 4 provides information on all DEGs identified in the present study and which are located in the direct neighborhood of known QTLs with an effect on training response in mice [24].

Table 4. Identification of DEGs, located in the direct neighborhood (0.5 Mb up and downstream) of previously published genetic markers and residing in Quantitative Trait Locus (QTL) regions with significant effects (marked with an asterisk) on training response in mice [24].

			Response to Exercise		Response to Genetic Selection	Response to Genetic Selection with Exercise
Condition	**SNPs**	**Chromosome: Position (bp)**	**DUC tr. vs. sed.**	**DUhTP tr. vs. sed.**	**DUhTP sed. vs. DUC sed.**	**DUhTP tr. vs. DUC tr.**
Pre-training	rs4222922	1: 193,272,691	NA	NA	Traf3ip3	Gm37691, Irf6, Hsd11b1, Syt14
	rs4223268	2: 93,419,862	Alx4, Tspan18	NA	Accs	Accs
	rs368717 *	3: 120,768,827	NA	NA	NA	NA
	rs3089148	8: 92,941,850	Ces1d	NA	Ces1d	NA
	rs3689508 *	14: 9,760,330	NA	NA	NA	Fhit
	rs3679049 *	19: 42,060,307	NA	NA	Avpi1, Crtac1, Marveld1	Avpi1, Crtac1, Exosc1, Rrp12
Post-training	rs368717 *	3: 120,768,827	NA	NA	NA	NA
	rs3667625	4: 54,194,913	NA	NA	NA	Rps15a-ps8
	rs3660830 *	14: 64,812,463	Mir124a-1hg	NA	NA	Mir124a-1hg
	rs3023460	17: 93,199,618	NA	NA	NA	NA
	rs3023517	19: 59,969,286	NA	NA	Fam204a	NA
Change	rs3023267	11: 65,710,376	NA	Dnah9	NA	Dnah9
	rs3660830 *	14: 64,812,463	Mir124a-1hg	NA	NA	Mir124a-1hg

The table provides information on chromosomal localization and regulation by phenotype selection (genetic effect), training (exercise), and phenotype selection with training. Font color of the gene symbol indicates lower expression (green) and higher expression (red) with respect to the control for each comparison (unselected or untrained). Underlined genes are considered as affected only by genetic effect because of no change of expression (log_2FC) between phenotype selection and phenotype selection with training comparison. QTL regions with significant effect are marked with an *. Abbreviation: sed. = sedentary, tr. = trained, vs. = versus, NA = not available, SNP = single nucleotide polymorphism, bp = base pairs.

3.5. Pathway Analysis

Because the protein metabolic and OXPHOS pathways were consistently elevated in DUC in response to training, both KEGG paths were visualized using Pathview in more detail. Figure 5 shows the training- and line-related effects on gene expression of ribosomal transcripts in the ribosomal pathway called EIF2 signaling. Accordingly, fractions from both the small and large ribosomal subunits were increased by training in DUC mice (Figure 5A). Intriguingly, 49 out of a total of approximately 80 ribosomal proteins were increased, and no inhibitory effect of training on gene expression of the EIF2 pathway was identified in DUC mice. In DUhTP mice, training did not affect gene expression of ribosomal proteins (Figure 5B). Direct comparison of trained DUC and trained DUhTP mice (Figure 5D) revealed a significant increase in RNA transcripts coding ribosomal proteins in the pituitary gland of trained DUC mice compared with trained DUhTP mice, caused by significant transcript upregulation in DUC mice in response to training. Even more, this comparison identified several additional ribosomal proteins regulated by training or by genetic selection for running performance. Accordingly, the present study identified 72 transcripts coding for ribosomal proteins, which are regulated exclusively in control mice in response to training. An effect of training in DUhTP mice was completely absent (Figure 5B).

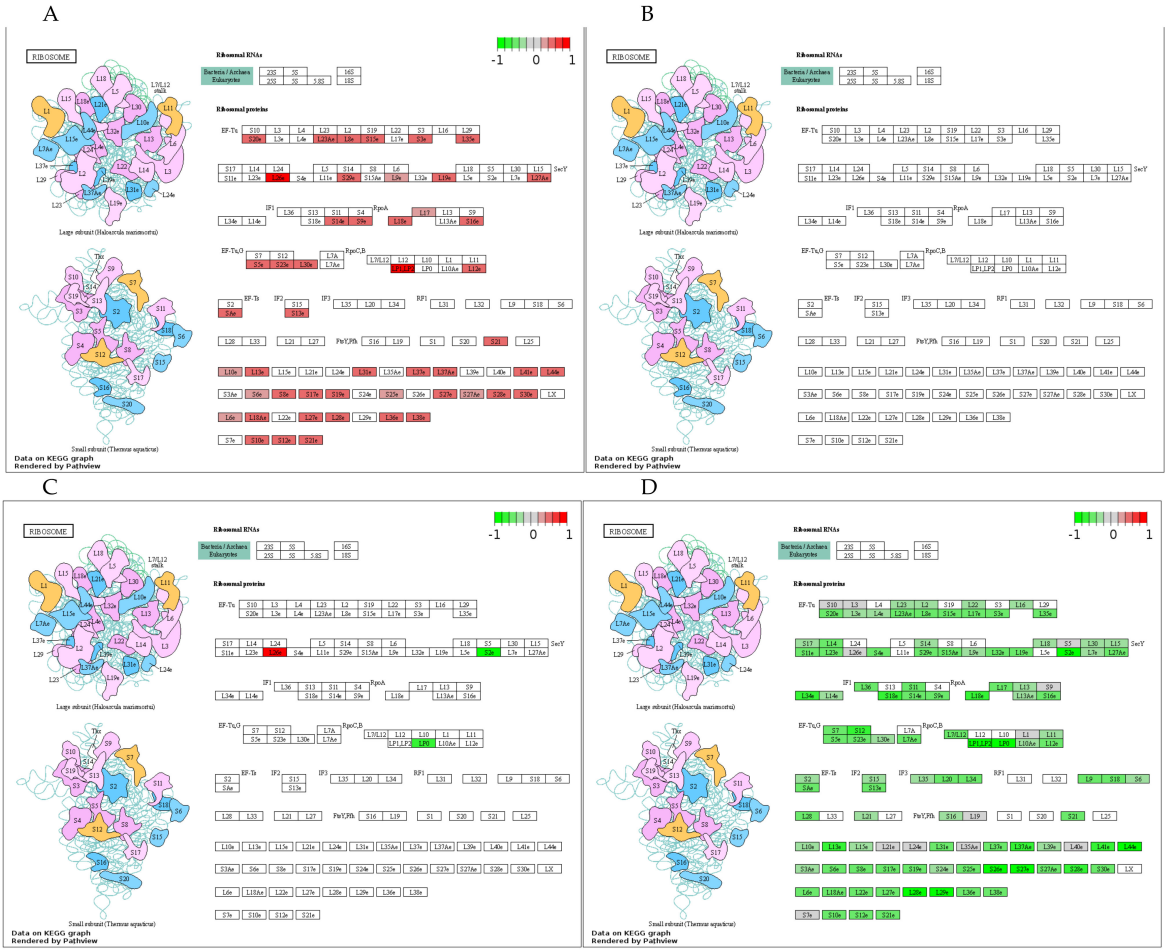

Figure 5. Regulation of ribosome expression in the pituitary gland and the influence of training. KEGG (Kyoto Encyclopedia of Genes and Genomes) pathway analyses of DEGs (FDR $\leq$ 0.05) in all comparison groups ((**A**): DUC tr. vs. sed.; (**B**): DUhTP tr. vs. sed.; (**C**): DUhTP sed. vs. DUC sed.; (**D**): DUhTP tr. vs. DUC tr.) via https://pathview.uncc.edu (access date: 08/03/2021). Abbreviation: sed. = sedentary, tr. = trained, vs. = versus.

As the second canonical pathway significantly activated by training, oxidative phosphorylation was identified in DUC (Figure 6A) but not in DUhTP mice (Figure 6B). In

DUC mice, training increased the expression of 34 transcripts coding for OXPHOS proteins, summarized in Figure 6A. Collectively, the activation of these OXPHOS members indicated activation of complexes I, III, IV, and V in DUC mice's pituitary gland in response to training (Figure 6A). Similar to the protein metabolic pathway, also by comparison of trained DUC vs. trained DUhTP mice, almost all transcripts were significantly higher in unselected controls. Again, several additional transcripts from the OXPHOS pathway were identified by comparing the interaction of training and genetic selection for running performance. Eighty-six transcripts were significantly higher in trained DUC mice than in trained DUhTP mice, and only seven OXPHOS subunits were higher in trained DUhTP vs. trained DUC mice (Table 3 and Figure 6D). Three of the upregulated transcripts belong to the mitochondria-encoded subunits ND3, ND4L, and ND5 of complex I (Figure 6D). Considering the DEGs of the untrained animals of both lines (Figure 6C), a total of 12 OXPHOS transcripts (six up- and six downregulated) were affected. Ten of these transcripts were also regulated by training, whereby two transcripts changed their relative direction of expression. These transcripts were encoding NADH dehydrogenase (7.1.1.2) and cytochrome C oxidase (7.1.1.9).

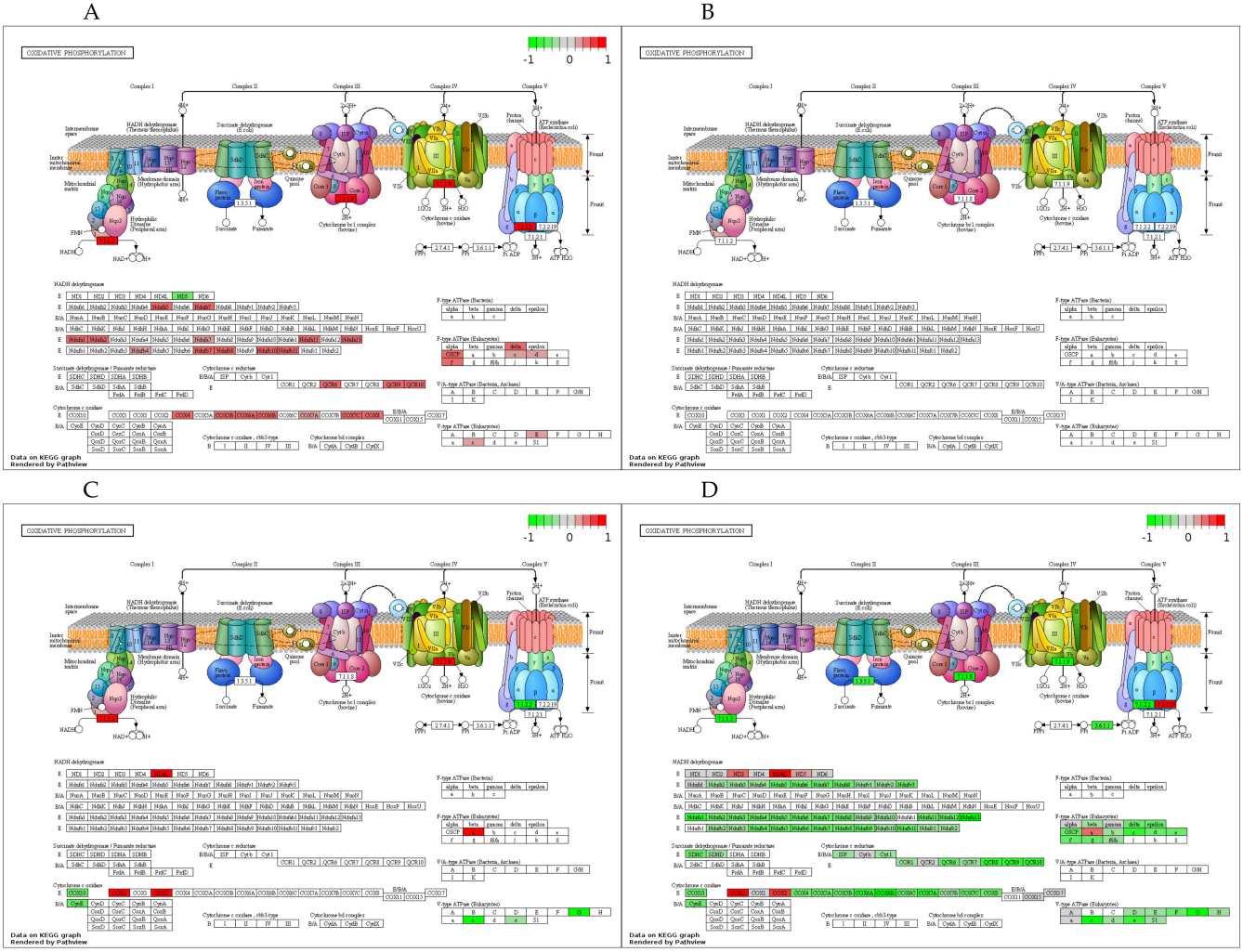

Figure 6. Regulation of oxidative phosphorylation in the pituitary gland influenced by selection and training. The KEGG pathway analyses were obtained by using the DEGs (FDR ≤ 0.05) of all comparison groups ((**A**): DUC tr. vs. sed.; (**B**): DUhTP tr. vs. sed.; (**C**): DUhTP sed. vs. DUC sed.; (**D**): DUhTP tr. vs. DUC tr.) via https://pathview.uncc.edu (access date: 08/03/2021). Abbreviation: sed. = sedentary, tr. = trained, vs. = versus.

4. Discussion

This study's original motivation was based on a unique mouse model DUhTP, which has been selected for superior performance for over nearly 35 years [9,10,28]. The advanced running capacities were due to phenotype selection only, and interaction with physical activity was excluded during the selection experiment because running wheels were not offered in the cages. In fact, voluntary physical activity is not elevated in DUhTP compared to unselected controls (DUC) [29]. Because pituitary glands hold a central position in the endocrine control of energy metabolism, we asked whether canonical pathways in this tissue were affected by repeated physical exercise (training) or long-term selection for running performance. In particular, we sought to determine whether phenotype selection for endurance exercise regulates the identical pathways activated by training. In the present study, we addressed tissue-wide adaptations in the pituitary gland and, therefore, studied transcriptome in bulk RNA.

The transcriptome in pituitary glands from phenotype-selected marathon mice (DUhTP) and unselected controls (DUC) was sequenced using an NGS method, and the effects of genotype (DUhTP vs. DUC) and physical activity (trained vs. sedentary) were investigated through comparison of animals from four groups (DUC trained vs. sedentary, DUhTP trained vs. sedentary, DUhTP sedentary vs. DUC sedentary, DUhTP trained vs. DUC trained). Validation by the Fluidigm® technique revealed a significant correlation between RNA sequencing and RT-qPCR results for the tested genes. The total number of pituitary transcripts with more than 17,000 identifications was comparable to 16,654 genes identified before in the same tissue from mice [30], 16,009 genes in cattle breeds [31] but lower than 24,873 genes obtained in laying hens [32]. Notably, on a cellular level, only 4506 different genes were expressed in the pituitary gland from human embryos on average, as demonstrated by single-cell transcriptomics, which is related to the cellular heterogeneity in the pituitary gland and/or due to the developmental status of the tissues [2].

If compared to phenotype selection, training had a moderate effect on gene expression in the pituitary gland. Interestingly, in DUhTP mice, training had almost no effect on gene expression since less than 0.3% of all DEGs were affected by physical activity. Thus, we may conclude that phenotype selection genetically fixed the training-induced metabolic responses in DUhTP mice by direct or indirect mechanisms. In fact, 465 from a total of 637 genes in DUC regulated by training were genetically fixed by phenotype selection in DUhTP mice. This may further imply that although these 465 genes affected by phenotype selection in DUhTP mice have an association with physical activity, the majority of all DEGs in DUhTP vs. DUC mice (n = 5560 DEGs) could not directly be linked to physical activity by the present approach. In other words, since the present study may only explain 8.4% of all DEGs in DUhTP mice vs. DUC mice, we may assume that more than 90% of all DEGs are related to longer-term or shorter-term effects or have no function for physical activity.

Nevertheless, the comparison of DEGs in pituitary glands from marathon mice and unselected controls demonstrated that marathon mice are less responsive to training. This may further suggest that specific adaptations in DUC mice in response to training have already resulted from the genetic selection in DUhTP mice. As discussed further down, we may argue that training was perceived on a different level by DUhTP and DUC mice and that endocrine or metabolic feedbacks between peripheral tissues and the pituitary gland were different in both mouse lines. Nevertheless, in DUC mice, the pituitary gland was responsive to the effects of physical exercise.

4.1. Genomic Effects and Identification of Candidate Genes

We next addressed the question of whether the DEGs identified by RNA-seq were overrepresented in distinct chromosomes. This question was related to the particular roles postulated for chromosomes 3, 6, 19, and 14 in the adaptive response to exercise in mice [24,33]. Five of the candidate genes present in the TOP5 of the up- and downregulated transcripts in DUhTP vs. DUC mice were located on chromosome 14 (line-associated). Notably, Duxbl1 was the only candidate upregulated in DUhTP vs. DUC mice. Since

Duxbl1 is regulated by retinoic acid and involved in the transition of embryonic stem cells to the two-cell state [34], an effect of Duxbl1 on embryonic stem cell reprogramming was discussed. Notably, the retinoic acid pathway was activated in muscle from human subjects in response to resistance training, and thus activation of developmental processes has been debated [35]. Retinoic acids are regulators of growth and development and are required for the adaptive immune response [36]. The retinoic acid pathway was further involved in developmental neurogenesis [37]. Exercise-related neurogenesis was demonstrated in the absence of retinoic acid receptor activation in mice [38]. In addition, chromosomes 3 and 6 were identified by the presence of one DEG per chromosome in DUhTP mice vs. DUC mice. Therefore, we selected the genomic regions close to 11 SNPs reported by Massett et al. (2009) as associated with pre-training, post-training, and work-change in mice. We asked whether DEGs identified by the present study may map to the genomic regions involved in training responses, according to Masset et al. [24]. By this comparison, Dnah9 was identified as a candidate gene in DUhTP mice affected by training. Dnah9 has a role in the proper development of motile monocilia, and loss-of-function mutants are characterized by laterality defects and subtle respiratory ciliary-beating defects in human subjects [39]. A potential effect of Dnah9 for DUhTP mice is not directly evident. Moreover, we identified the Ces1d gene on chromosome 8, overexpressed in sedentary DUhTP and trained DUC mice, suggesting that this gene is genetically fixed in sedentary DUhTP mice related to the selection for high running performance. Ces1d encodes a carboxylesterase in mice and humans and is involved in lipid metabolism [40]. It has been demonstrated that Ces1d has a key role for establishment or maintenance of cytosolic lipid droplets (CLDs) and energy metabolism by regulating lipid transfer rate during development [41,42]. In the context of our study, this would imply that years of selection resulted in increased expression of Ces1d, which is associated with increased formation of cytosolic energy stores in the pituitary gland. As a result of training, Ces1d transcription was further increased in unselected controls, hypothetically leading to increased cytosolic lipid droplets' formation.

Regarding the variants reported as significant by Masset et al., 2009, we further identified Fhit (fragile histidine triad protein), located close to rs3689508 in chromosome 14, by the comparison of trained DUhTP vs. DUC mice. Fhit represents a tumor repressor [43] and regulates blood pressure in men and mice [44]. Finally, Mir124a-1hg, localized near the SNP rs3660830 on chromosome 14, could be detected with elevated expression in trained DUC but not in trained DUhTP. This marker has a significant effect on post-training effects and training capacity [24]. The gene product, miR-124, plays a role in neurogenesis in the developing [45] and mature brain [46]. In the hippocampus of singly housed mice, exercise reduced miR-124 levels and has been discussed concerning stress resilience [47]. MicroRNAs are further discussed as mediators of beneficial exercise effects on peripheral organs such as the heart [48]. In rats, swimming reduced miR-124 levels and has been discussed in a synergistic relationship with AKT/mTOR signaling, as PI3-K is a target of miR-124 [49]. Therefore, altered miR-124 may have adaptive central and peripheral effects in our experimental system, which opens an interesting field for future studies.

4.2. Molecular Pathway Analysis

Long-term selection for high treadmill performance, as a rule, had an inhibitory effect on molecular or metabolic pathways in the pituitary gland. Accordingly, the direct comparison of untrained DUhTP and DUC mice suggested inhibition of the LXR/RXR and the unfolded protein response (UPR) pathway. The UPR pathway is activated in response to cellular stress and is required to control protein quality during protein translation [50]. In the pituitary gland, the UPR pathway was discussed in the context of hormone secretion under the control of selenoprotein T [51]. By contrast, the LXR/RXR pathway seems to play a role in controlling the metabolism and inflammatory response in pituitary glands [52]. In addition, control of the RXR pathway was discussed earlier based on the elevated expression of Duxbl1 in trained DUhTP vs. controls.

In line with the high number of DEGs in trained DUhTP vs. trained DUC mice, several different canonical pathways were affected by the interaction of genetic group and physical activity. The pathway analysis collectively suggested the inhibition of carbon-, lipid-, and protein-metabolism, steroid-signaling, synaptic signaling, and appetite regulation in trained DUhTP vs. trained DUC mice. Integrin signaling was also identified, indicating differential effects on intracellular signaling pathways in trained DUhTP mice vs. unselected controls. Notably, in the liver of untrained DUhTP mice, activation of carbohydrate-, lipid-, and steroid metabolism was described compared to DUC mice [53].

Because EIF2 signaling and the OXPHOS pathways appeared as the only two pathways activated by physical activity, we now discuss potential roles during adaptive response to exercise, respectively. First of all, neither pathway was activated in the pituitary glands of DUhTP mice, suggesting that other adaptations are present that prevent or eliminate activation of both pathways. While this assumption cannot be answered here, we can identify both pathways as the first line of adaptive response in untrained control animals. From approximately 80 ribosomal proteins, 49 members were increased by training in DUC mice. In addition, in response to training, but in human muscle, the EIF2 pathway was identified by IPA [35]. However, a negative effect was found, resulting in the downregulation of 70 rRNA transcripts. In this study, the training period lasted for 20 weeks, resulting in part in a marked hypertrophic response. Accordingly, the different regulation directions could be related to different species, tissues, and training parameters. Accordingly, our study supports regulation of protein synthesis in response to physical activity, initially provided by Phillips et al. [35]. Interestingly, in this study in human muscle, EIF2 signaling was negatively correlated with mTOR pathway activation and lean mass [35]. Ribosome synthesis is a highly coordinated process, and the interaction of different ribosomal proteins establishes two principal functions, namely t-RNA decoding and protein translation [54]. Both functions are separated into two different subunits. Since training had a positive effect on gene expression coding for ribosomal proteins from both subunits, we assumed a coordinated adaptive response in DUC mice resulting in a coordinated increase of both ribosomal subunits resulting in an increased capacity of protein translation in response to training.

Training induced mRNA expression of several oxidative phosphorylation chain subunits, except Mt-Nd5, in unselected controls. Accordingly, gene set enrichment analysis in trained versus untrained control mice identified significant activation of oxidative phosphorylation in pituitary glands. From a significant increase in total oxidative phosphorylation, an increase in energy production could be assumed since this pathway is also associated with pituitary adenoma [55]. Notably, the enhanced energy production could be linked to the elevated demands of protein translation, as discussed earlier. Accordingly, both pathways could be interpreted as a common signature of exercise-related adaptation to increase the pituitary gland's secretory capacity, whose protective effects could be associated with an improved pituitary function [56].

Notably, the effects of training on both metabolic pathways were not observed in pituitary glands from marathon mice. Instead, trained DUhTP mice were characterized by similar OXPHOS subunits' expression as untrained controls but by lower expression than trained control mice. This clearly demonstrates that pituitary glands can respond to training by different mechanisms: In untrained DUC mice, molecular pathways of protein synthesis and energy metabolism were increased by training. In DUhTP mice with high endurance exercise performance, these pathways were unaffected by training. Instead, many different transcripts were increased in response to training, suggesting specific effects in different cell populations from the pituitary gland. In addition, the high number of DEGs in untrained DUhTP mice compared to untrained controls may point to a plethora of cell-type-specific adaptations during the long history of phenotype selection in DUhTP mice. Therefore, and as a limitation of the present study, future investigations will have to address these specific effects using single-cell transcriptomics. Nevertheless, the differential response to training in marathon mice and controls could be due to different

metabolites in the two mouse lines' circulation. For example, lactate [57] or butyrate [58] were demonstrated to control GH-secretion by pituitary cells from rats and, therefore, were discussed as potential metabolic effectors of exercise on neuroendocrine responses. As a general limitation, phenotype selection cannot be used for the differentiation of direct versus indirect effects. In order to identify direct or indirect effects on gene expression of the pituitary gland from our animal model, we would have to perform metabolomics studies to identify candidate metabolites, which then could be tested using ex vivo assessment in pituitary explants. However, and as an advantage, results in phenotype-selected models may contain a higher degree of physiological relevance since genotype-based models may not always provide effects that, in fact, play a role under physiological conditions. Finally, non-inbred mice used in the present manuscript have a higher phenotypic variance than inbred mice, which are often used as genotype-based mouse models for functional genome analysis. Accordingly, elevated phenotypic variability could have prevented the detection of hormonal pathways in cellular subpopulations from the pituitary gland. To cope with the issue of sensitivity, other methods like single-cell/nucleus RNA sequencing may be useful, as described earlier in this manuscript. However, since higher phenotypic variance is a function of higher genetic variability due to the non-inbred genetic background present in the animal model used here, it can also be perceived as an advantage due to a better representation of broader populations.

5. Summary and Conclusions

An effect of training on the regulation of molecular pathways in the pituitary gland was observed in control mice (DUC) but not in mice long-term selected for high treadmill performance (DUhTP). In particular, two metabolic pathways involved in protein translation and energy metabolism were induced by training in DUC mice. Since both pathways were defined by increased mRNA transcript abundance in response to training and also in comparison to DUhTP mice, we assumed increased protein synthesis and elevated energy supply in DUC mice in response to training. Comparative analysis of DEGs with the literature supported the role of miR-124 for adaptive training responses. Accordingly, miR-124 was decreased by phenotype selection in marathon mice or by exercise in rats [49] and located in the close neighborhood to a QTL region associated with training responses in mice [24]. Accordingly, the role of miR-124, which targets the AKT/mTOR pathway, appears as an interesting subject for subsequent studies in our experimental mouse model.

Supplementary Materials: The following are available online at https://www.mdpi.com/article/10.3390/cells10040736/s1, Table S1: List of significant (FDR $\leq$ 0.05) DEGs found in each group by comparing the corresponding chromosome, $\log_2$FC, and FDR. The group comparisons are reported in the following sequence: (**a**) DUC tr. vs. sed., (**b**) DUhTP tr. vs. sed., (**c**) DUhTP vs. DUC sed., (**d**) DUhTP vs. DUC tr. Table S2: List of DEGs and housekeeping genes selected for RT-qPCR validation with corresponding forward and reverse primers. Table S3: Comparison of $\log_2$FC of mRNA abundance measured with RNA-sequencing (NGS) and quantitative real-time PCR for selected genes; significant *p*-value in bold. Abbreviation: sed. = sedentary, tr. = trained, vs. = versus.

Author Contributions: Conceptualization, C.W., J.B., N.T., S.P., K.W., and A.H.; methodology, C.W., J.B., N.T., A.N., and D.O.; software, C.W., N.T., A.N., and C.C.; validation, C.W. and D.O.; formal analysis, C.W., N.T., and A.N.; investigation, C.W., J.B., N.T., A.N., C.C., and D.O.; resources, M.L.; writing—original draft preparation, C.W., J.B., A.N., and A.H.; writing—review and editing, all authors. All authors have read and agreed to the published version of the manuscript.

Funding: This article's publication was funded by the Open Access Fund of the Leibniz Institute for Farm Animal Biology (FBN).

Institutional Review Board Statement: The animal study was approved by the Animal Protection Board Mecklenburg–Western Pomerania (State Office for Agriculture, Food Safety, and Fisheries; AZ 7221.3-1-014/17, date of approval: 25/04/2017).

Data Availability Statement: Data are contained within the article or Supplementary Material.

Acknowledgments: The authors want to thank Luong Chau, Annette Jugert, and the Lab Animal Facility technicians for their excellent support.

Conflicts of Interest: The authors declare no conflict of interest.

References

1. Yeung, C.M.; Chan, C.B.; Leung, P.S.; Cheng, C.H. Cells of the anterior pituitary. *Int. J. Biochem. Cell Biol.* **2006**, *38*, 1441–1449. [CrossRef]
2. Zhang, S.; Cui, Y.; Ma, X.; Yong, J.; Yan, L.; Yang, M.; Ren, J.; Tang, F.; Wen, L.; Qiao, J. Single-cell transcriptomics identifies divergent developmental lineage trajectories during human pituitary development. *Nat. Commun.* **2020**, *11*, 5275. [CrossRef] [PubMed]
3. Flier, J.; Maratos-Flier, E. Energy homeostasis and body weight. *Curr. Biol.* **2000**, *10*, R215–R217. [CrossRef]
4. Sutton, J.; Lazarus, L. Growth hormone in exercise: Comparison of physiological and pharmacological stimuli. *J. Appl. Physiol.* **1976**, *41*, 523–527. [CrossRef] [PubMed]
5. Kraemer, W.J.; Flanagan, S.D.; Volek, J.S.; Nindl, B.C.; Vingren, J.L.; Dunn-Lewis, C.; Comstock, B.A.; Hooper, D.R.; Szivak, T.K.; Looney, D.P.; et al. Resistance exercise induces region-specific adaptations in anterior pituitary gland structure and function in rats. *J. Appl. Physiol.* **2013**, *115*, 1641–1647. [CrossRef] [PubMed]
6. Khajehnasiri, N.; Khazali, H.; Sheikhzadeh, F. Various responses of male pituitary-gonadal axis to different intensities of long-term exercise: Role of expression of KNDYrelated genes. *J. Biosci.* **2018**, *43*, 569–574. [CrossRef]
7. Sze, Y.; Gill, A.C.; Brunton, P.J. Sex-dependent changes in neuroactive steroid concentrations in the rat brain following acute swim stress. *J. Neuroendocrinol.* **2018**, *30*, e12644. [CrossRef]
8. Uribe, R.M.; Jaimes-Hoy, L.; Ramírez-Martínez, C.; García-Vázquez, A.; Romero, F.; Cisneros, M.; Cote-Vélez, A.; Charli, J.L.; Joseph-Bravo, P. Voluntary exercise adapts the hypothalamus-pituitary-thyroid axis in male rats. *Endocrinology* **2014**, *155*, 2020–2030. [CrossRef]
9. Brenmoehl, J.; Walz, C.; Renne, U.; Ponsuksili, S.; Wolf, C.; Langhammer, M.; Schwerin, M.; Hoeflich, A. Metabolic adaptations in the liver of born long-distance running mice. *Med. Sci. Sports Exerc.* **2013**, *45*, 841–850. [CrossRef]
10. Falkenberg, H.; Langhammer, M.; Renne, U. Comparison of biochemical blood traits after long-term selection on high or low locomotory activity in mice. *Arch. Anim. Breed.* **2000**, *43*, 513–522. [CrossRef]
11. Brenmoehl, J.; Walz, C.; Spitschak, M.; Wirthgen, E.; Walz, M.; Langhammer, M.; Tuchscherer, A.; Naumann, R.; Hoeflich, A. Partial phenotype conversion and differential trait response to conditions of husbandry in mice. *J. Comp. Physiol. B* **2018**, *188*, 527–539. [CrossRef] [PubMed]
12. Schroeder, A.; Mueller, O.; Stocker, S.; Salowsky, R.; Leiber, M.; Gassmann, M.; Lightfoot, S.; Menzel, W.; Granzow, M.; Ragg, T. The RIN: An RNA integrity number for assigning integrity values to RNA measurements. *BMC Mol. Biol.* **2006**, *7*, 1–14. [CrossRef] [PubMed]
13. Kim, D.; Langmead, B.; Salzberg, S.L. HISAT: A fast spliced aligner with low memory requirements. *Nat. Methods* **2015**, *12*, 357–360. [CrossRef] [PubMed]
14. Pertea, M.; Kim, D.; Pertea, G.M.; Leek, J.T.; Salzberg, S.L. Transcript-level expression analysis of RNA-seq experiments with HISAT, StringTie and Ballgown. *Nat. Protoc.* **2016**, *11*, 1650–1667. [CrossRef]
15. Anders, S.; Pyl, P.T.; Huber, W. HTSeq—A Python framework to work with high-throughput sequencing data. *Bioinformatics* **2015**, *31*, 166–169. [CrossRef]
16. Robinson, M.D.; McCarthy, D.J.; Smyth, G.K. edgeR: A Bioconductor package for differential expression analysis of digital gene expression data. *Bioinformatics* **2010**, *26*, 139–140. [CrossRef]
17. Oliveros, J.C. VENNY. An Interactive Tool for Comparing Lists with Venn Diagrams. 2007. Available online: http://bioinfogp.cnb.csic.es/tools/venny/index.html (accessed on 8 March 2021).
18. Wickham, H. ggplot2. *WIREs Comput. Stat.* **2011**, *3*, 180–185. [CrossRef]
19. Spurgeon, S.L.; Jones, R.C.; Ramakrishnan, R. High throughput gene expression measurement with real time PCR in a microfluidic dynamic array. *PLoS ONE* **2008**, *3*, e1662. [CrossRef]
20. Wang, X.; Spandidos, A.; Wang, H.; Seed, B. PrimerBank: A PCR primer database for quantitative gene expression analysis, 2012 update. *Nucleic Acids Res.* **2012**, *40*, D1144–D1149. [CrossRef]
21. Altschul, S.F.; Madden, T.L.; Schäffer, A.A.; Zhang, J.; Zhang, Z.; Miller, W.; Lipman, D.J. Gapped BLAST and PSI-BLAST: A new generation of protein database search programs. *Nucleic Acids Res.* **1997**, *25*, 3389–3402. [CrossRef]
22. Ballester, M.; Cordón, R.; Folch, J.M. DAG expression: High-throughput gene expression analysis of real-time PCR data using standard curves for relative quantification. *PLoS ONE* **2013**, *8*, e80385. [CrossRef]
23. Krämer, A.; Green, J.; Pollard Jr, J.; Tugendreich, S. Causal analysis approaches in ingenuity pathway analysis. *Bioinformatics* **2014**, *30*, 523–530. [CrossRef]
24. Massett, M.P.; Fan, R.; Berk, B.C. Quantitative trait loci for exercise training responses in FVB/NJ and C57BL/6J mice. *Physiol. Genom.* **2009**, *40*, 15–22. [CrossRef] [PubMed]
25. Petkov, P.M.; Ding, Y.; Cassell, M.A.; Zhang, W.; Wagner, G.; Sargent, E.E.; Asquith, S.; Crew, V.; Johnson, K.A.; Robinson, P.; et al. An efficient SNP system for mouse genome scanning and elucidating strain relationships. *Genome Res.* **2004**, *14*, 1806–1811. [CrossRef] [PubMed]

26. Petkov, P.M.; Cassell, M.A.; Sargent, E.E.; Donnelly, C.J.; Robinson, P.; Crew, V.; Asquith, S.; Haar, R.V.; Wiles, M.V. Development of a SNP genotyping panel for genetic monitoring of the laboratory mouse. *Genomics* **2004**, *83*, 902–911. [CrossRef] [PubMed]
27. Bult, C.J.; Blake, J.A.; Smith, C.L.; Kadin, J.A.; Richardson, J.E. Mouse Genome Database (MGD) 2019. *Nucleic Acids Res.* **2019**, *47*, D801–D806. [CrossRef]
28. Dietl, G.; Langhammer, M.; Renne, U. Model simulations for genetic random drift in the outbred strain Fzt:DU. *Arch. Anim. Breed.* **2004**, *47*, 595–604. [CrossRef]
29. Brenmoehl, J.; Ohde, D.; Walz, C.; Langhammer, M.; Schultz, J.; Hoeflich, A. Analysis of Activity-Dependent Energy Metabolism in Mice Reveals Regulation of Mitochondrial Fission and Fusion mRNA by Voluntary Physical Exercise in Subcutaneous Fat from Male Marathon Mice (DUhTP). *Cells* **2020**, *9*, 2697. [CrossRef]
30. Liu, X.; Fang, Z.; Pan, Z.; Lu, W.; Wu, Z.; Liang, C.; Zhang, Y. Pituitary transcriptome profile of liver cancer mice with different syndromes reveals the relevance of pituitary to the cancer and syndromes. *J. Tradit. Chin. Med.* **2014**, *34*, 691–698. [CrossRef]
31. Lu, X.; Arbab, A.A.I.; Zhang, Z.; Fan, Y.; Han, Z.; Gao, Q.; Sun, Y.; Yang, Z. Comparative Transcriptomic Analysis of the Pituitary Gland between Cattle Breeds Differing in Growth: Yunling Cattle and Leiqiong Cattle. *Animals* **2020**, *10*, 1271. [CrossRef]
32. Wang, C.; Ma, W. Hypothalamic and pituitary transcriptome profiling using RNA-sequencing in high-yielding and low-yielding laying hens. *Sci. Rep.* **2019**, *9*, 1–11. [CrossRef]
33. Courtney, S.M.; Massett, M.P. Effect of chromosome substitution on intrinsic exercise capacity in mice. *F1000Res* **2014**, *3*, 9. [CrossRef]
34. Tagliaferri, D.; Mazzone, P.; Noviello, T.M.R.; Addeo, M.; Angrisano, T.; Del Vecchio, L.; Visconte, F.; Ruggieri, V.; Russi, S.; Caivano, A.; et al. Retinoic Acid Induces Embryonic Stem Cells (ESCs) Transition to 2 Cell-Like State Through a Coordinated Expression of Dux and Duxbl1. *Front. Cell Dev. Biol.* **2019**, *7*, 385. [CrossRef] [PubMed]
35. Phillips, B.E.; Williams, J.P.; Gustafsson, T.; Bouchard, C.; Rankinen, T.; Knudsen, S.; Smith, K.; Timmons, J.A.; Atherton, P.J. Molecular networks of human muscle adaptation to exercise and age. *PLoS Genet.* **2013**, *9*, e1003389. [CrossRef]
36. Oliveira, L.M.; Teixeira, F.M.E.; Sato, M.N. Impact of Retinoic Acid on Immune Cells and Inflammatory Diseases. *Mediators Inflamm.* **2018**, *2018*, 3067126. [CrossRef]
37. Zieger, E.; Candiani, S.; Garbarino, G.; Croce, J.C.; Schubert, M. Roles of Retinoic Acid Signaling in Shaping the Neuronal Architecture of the Developing Amphioxus Nervous System. *Mol. Neurobiol.* **2018**, *55*, 5210–5229. [CrossRef]
38. Aberg, E.; Perlmann, T.; Olson, L.; Brené, S. Running increases neurogenesis without retinoic acid receptor activation in the adult mouse dentate gyrus. *Hippocampus* **2008**, *18*, 785–792. [CrossRef]
39. Loges, N.T.; Antony, D.; Maver, A.; Deardorff, M.A.; Güleç, E.Y.; Gezdirici, A.; Nöthe-Menchen, T.; Höben, I.M.; Jelten, L.; Frank, D.; et al. Recessive DNAH9 Loss-of-Function Mutations Cause Laterality Defects and Subtle Respiratory Ciliary-Beating Defects. *Am. J. Hum. Genet.* **2018**, *103*, 995–1008. [CrossRef]
40. Lian, J.; Nelson, R.; Lehner, R. Carboxylesterases in lipid metabolism: From mouse to human. *Protein Cell* **2018**, *9*, 178–195. [CrossRef]
41. Wang, H.; Wei, E.; Quiroga, A.D.; Sun, X.; Touret, N.; Lehner, R. Altered lipid droplet dynamics in hepatocytes lacking triacylglycerol hydrolase expression. *Mol. Biol. Cell* **2010**, *21*, 1991–2000. [CrossRef] [PubMed]
42. Lian, J.; Wei, E.; Wang, S.P.; Quiroga, A.D.; Li, L.; Di Pardo, A.; van der Veen, J.; Sipione, S.; Mitchell, G.A.; Lehner, R. Liver specific inactivation of carboxylesterase 3/triacylglycerol hydrolase decreases blood lipids without causing severe steatosis in mice. *Hepatology* **2012**, *56*, 2154–2162. [CrossRef]
43. Zanesi, N.; Mancini, R.; Sevignani, C.; Vecchione, A.; Kaou, M.; Valtieri, M.; Calin, G.A.; Pekarsky, Y.; Gnarra, J.R.; Croce, C.M.; et al. Lung cancer susceptibility in Fhit-deficient mice is increased by Vhl haploinsufficiency. *Cancer Res.* **2005**, *65*, 6576–6582. [CrossRef]
44. Zambrowicz, B.P.; Abuin, A.; Ramirez-Solis, R.; Richter, L.J.; Piggott, J.; BeltrandelRio, H.; Buxton, E.C.; Edwards, J.; Finch, R.A.; Friddle, C.J.; et al. Wnk1 kinase deficiency lowers blood pressure in mice: A gene-trap screen to identify potential targets for therapeutic intervention. *Proc. Natl. Acad. Sci.USA* **2003**, *100*, 14109–14114. [CrossRef] [PubMed]
45. Visvanathan, J.; Lee, S.; Lee, B.; Lee, J.W.; Lee, S.K. The microRNA miR-124 antagonizes the anti-neural REST/SCP1 pathway during embryonic CNS development. *Genes Dev.* **2007**, *21*, 744–749. [CrossRef] [PubMed]
46. Cheng, L.C.; Pastrana, E.; Tavazoie, M.; Doetsch, F. miR-124 regulates adult neurogenesis in the subventricular zone stem cell niche. *Nat. Neurosci.* **2009**, *12*, 399–408. [CrossRef]
47. Pan-Vazquez, A.; Rye, N.; Ameri, M.; McSparron, B.; Smallwood, G.; Bickerdyke, J.; Rathbone, A.; Dajas-Bailador, F.; Toledo-Rodriguez, M. Impact of voluntary exercise and housing conditions on hippocampal glucocorticoid receptor, miR-124 and anxiety. *Mol. Brain* **2015**, *8*, 1–12. [CrossRef] [PubMed]
48. Schüttler, D.; Clauss, S.; Weckbach, L.T.; Brunner, S. Molecular Mechanisms of Cardiac Remodeling and Regeneration in Physical Exercise. *Cells* **2019**, *8*, 1128. [CrossRef]
49. Ma, Z.; Qi, J.; Meng, S.; Wen, B.; Zhang, J. Swimming exercise training-induced left ventricular hypertrophy involves microRNAs and synergistic regulation of the PI3K/AKT/mTOR signaling pathway. *Eur. J. Appl. Physiol.* **2013**, *113*, 2473–2486. [CrossRef]
50. Khetchoumian, K.; Balsalobre, A.; Mayran, A.; Christian, H.; Chénard, V.; St-Pierre, J.; Drouin, J. Pituitary cell translation and secretory capacities are enhanced cell autonomously by the transcription factor Creb3l2. *Nat. Commun.* **2019**, *10*, 1–13. [CrossRef]
51. Hamieh, A.; Cartier, D.; Abid, H.; Calas, A.; Burel, C.; Bucharles, C.; Jehan, C.; Grumolato, L.; Landry, M.; Lerouge, P.; et al. Selenoprotein T is a novel OST subunit that regulates UPR signaling and hormone secretion. *EMBO Rep.* **2017**, *18*, 1935–1946. [CrossRef]

52. Ghaddab-Zroud, R.; Seugnet, I.; Steffensen, K.R.; Demeneix, B.A.; Clerget-Froidevaux, M.S. Liver X receptor regulation of thyrotropin-releasing hormone transcription in mouse hypothalamus is dependent on thyroid status. *PLoS One* **2014**, *9*, e106983. [CrossRef]
53. Ohde, D.; Moeller, M.; Brenmoehl, J.; Walz, C.; Ponsuksili, S.; Schwerin, M.; Fuellen, G.; Hoeflich, A. Advanced running performance by genetic predisposition in male dummerstorf marathon mice (DUhTP) reveals higher sterol regulatory element-binding protein (srebp) related mrna expression in the liver and higher serum levels of progesterone. *PLoS One* **2016**, *11*, e0146748. [CrossRef]
54. Peña, C.; Hurt, E.; Panse, V.G. Eukaryotic ribosome assembly, transport and quality control. *Nat. Struct. Mol. Biol.* **2017**, *24*, 689–699. [CrossRef] [PubMed]
55. Zhan, X.; Desiderio, D.M. Signaling pathway networks mined from human pituitary adenoma proteomics data. *BMC Med. Genom.* **2010**, *3*, 1–26. [CrossRef]
56. Strauss, K.I. Antiinflammatory and neuroprotective actions of COX2 inhibitors in the injured brain. *Brain Behav. Immun.* **2008**, *22*, 285–298. [CrossRef]
57. Salgueiro, R.B.; Peliciari-Garcia, R.A.; do Carmo Buonfiglio, D.; Peroni, C.N.; Nunes, M.T. Lactate activates the somatotropic axis in rats. *Growth Horm. IGF Res.* **2014**, *24*, 268–270. [CrossRef] [PubMed]
58. Miletta, M.C.; Petkovic, V.; Eblé, A.; Ammann, R.A.; Flück, C.E.; Mullis, P.E. Butyrate increases intracellular calcium levels and enhances growth hormone release from rat anterior pituitary cells via the g-protein-coupled receptors gpr41 and 43. *PLoS ONE* **2014**, *9*, e107388. [CrossRef]

cells

MDPI

Article

Central Suppression of the GH/IGF Axis and Abrogation of Exercise-Related mTORC1/2 Activation in the Muscle of Phenotype-Selected Male Marathon Mice (DUhTP)

Julia Brenmoehl [1,†], Christina Walz [1,†], Caroline Caffier [1,2], Elli Brosig [1,2], Michael Walz [1], Daniela Ohde [1], Nares Trakooljul [1], Martina Langhammer [3], Siriluck Ponsuksili [1], Klaus Wimmers [1], Uwe K. Zettl [2] and Andreas Hoeflich [1,*]

[1] Institute for Genome Biology, Research Institute for Farm Animal Biology (FBN), Wilhelm-Stahl-Allee 2, 18196 Dummerstorf, Germany; brenmoehl@fbn-dummerstorf.de (J.B.); walz@fbn-dummerstorf.de (C.W.); caro.caffier@yahoo.de (C.C.); e.brosig@web.de (E.B.); walz.michael@fbn-dummerstorf.de (M.W.); ohde@fbn-dummerstorf.de (D.O.); trakooljul@fbn-dummerstorf.de (N.T.); ponsuksili@fbn-dummerstorf.de (S.P.); wimmers@fbn-dummerstorf.de (K.W.)

[2] Department of Neurology, Neuroimmunological Section, University Medicine Rostock, Gehlsheimer Str. 20, 18147 Rostock, Germany; uwe.zettl@med.uni-rostock.de

[3] Lab Animal Facility, Research Institute for Genetics and Biometry, Institute for Farm Animal Biology (FBN), Wilhelm-Stahl-Allee 2, 18196 Dummerstorf, Germany; martina.langhammer@fbn-dummerstorf.de

* Correspondence: hoeflich@fbn-dummerstorf.de

† These authors contributed equally to this work.

Citation: Brenmoehl, J.; Walz, C.; Caffier, C.; Brosig, E.; Walz, M.; Ohde, D.; Trakooljul, N.; Langhammer, M.; Ponsuksili, S.; Wimmers, K.; et al. Central Suppression of the GH/IGF Axis and Abrogation of Exercise-Related mTORC1/2 Activation in the Muscle of Phenotype-Selected Male Marathon Mice (DUhTP). *Cells* **2021**, *10*, 3418. https://doi.org/10.3390/cells10123418

Academic Editor: Vera M. Chesnokova

Received: 10 November 2021
Accepted: 2 December 2021
Published: 4 December 2021

Abstract: The somatotropic axis is required for a number of biological processes, including growth, metabolism, and aging. Due to its central effects on growth and metabolism and with respect to its positive effects on muscle mass, regulation of the GH/IGF-system during endurance exercise is of particular interest. In order to study the control of gene expression and adaptation related to physical performance, we used a non-inbred mouse model, phenotype-selected for high running performance (DUhTP). Gene expression of the GH/IGF-system and related signaling cascades were studied in the pituitary gland and muscle of sedentary males of marathon and unselected control mice. In addition, the effects of three weeks of endurance exercise were assessed in both genetic groups. In pituitary glands from DUhTP mice, reduced expression of Pou1f1 ($p = 0.002$) was accompanied by non-significant reductions of Gh mRNA ($p = 0.066$). In addition, mRNA expression of Ghsr and Sstr2 were significantly reduced in the pituitary glands from DUhTP mice ($p \leq 0.05$). Central downregulation of Pou1f1 expression was accompanied by reduced serum concentrations of IGF1 and coordinated downregulation of multiple GH/IGF-signaling compounds in muscle (e.g., Ghr, Igf1, Igf1r, Igf2r, Irs1, Irs2, Akt3, Gskb, Pik3ca/b/a2, Pten, Rictor, Rptor, Tsc1, Mtor; $p \leq 0.05$). In response to exercise, the expression of Igfbp3, Igfbp 4, and Igfbp 6 and Stc2 mRNA was increased in the muscle of DUhTP mice ($p \leq 0.05$). Training-induced specific activation of AKT, S6K, and p38 MAPK was found in muscles from control mice but not in DUhTP mice ($p \leq 0.05$), indicating a lack of mTORC1 and mTORC2 activation in marathon mice in response to physical exercise. While hormone-dependent mTORC1 and mTORC2 pathways in marathon mice were repressed, robust increases of Ragulator complex compounds ($p \leq 0.001$) and elevated sirtuin 2 to 6 mRNA expression were observed in the DUhTP marathon mouse model ($p \leq 0.05$). Activation of AMPK was not observed under the experimental conditions of the present study. Our results describe coordinated downregulation of the somatotropic pathway in long-term selected marathon mice (DUhTP), possibly via the pituitary gland and muscle interaction. Our results, for the first time, demonstrate that GH/IGF effects are repressed in a context of superior running performance in mice.

Keywords: endurance exercise; energy metabolism; pituitary gland; muscle; growth hormone; insulin-like growth factor; mTORC; PTEN; Ragulator complex; sirtuins; mouse model

1. Introduction

As a neuroendocrine organ in the brain, the pituitary gland acts as a mediator of central signals to peripheral tissues. It is required for normal growth and development but also has adaptive functions. Already in 1963, it was demonstrated that the secretion of growth hormone (GH) could be induced by physical exercise [1]. However, the mechanisms and conditions related to GH secretion under resistance and aerobic exercise conditions are still debated [2]. Elevated secretion of GH in response to resistance exercise can be seen in the context of hypertrophic muscle growth, and the misuse of GH as an agent for muscle accretion has a long but inglorious tradition [3]. However, the role of GH in response to endurance exercise is not directly evident because endurance exercise is less a direct function of muscle mass but more related to energy-metabolic adaptation in muscle but also in the liver and fat depots.

Inside the cell, hormonal stimuli are mediated by signaling cascades, such as PI3K, controlling mTOR activity via S6K [4]. And although the direct connection between GH/IGF and hypertrophic muscle growth is plausible in general, direct activation of IGF-depending PI3K/mTOR/S6K by exercise so far cannot be proven. In addition, although a number of studies have demonstrated GH-secretion in response to physical activity, so far, elevated activity of free IGF1 in serum cannot be proven [5]. In fact, there is experimental evidence that mTOR/S6K-dependent hypertrophic muscle growth is induced by IGF-independent mechanisms [6,7], raising the question of the molecular function of the GH/IGF system in the adaptive response to physical exercise.

Concerning the fundamental question about the role of the GH/IGF axis in physical exercise, we asked if and how the somatotrophic axis is regulated in born marathon runners. We addressed this question in a mouse model (DUhTP) selected for more than 140 generations of high-endurance exercise on a treadmill. DUhTP mice acquired running capacities three to four times higher than unselected controls (DUC mice) during the selection experiment [8]. Importantly, DUhTP mice were kept in the absence of running wheels in their home cages; accordingly, the running capacities are based on genetic adaptation but not on self-training. Moreover, the selection experiment was performed starting from an outbred background while avoiding inbreeding during selection; therefore, we assume multiple genetic adaptations in response to the selection pressure in DUhTP mice.

In the present study, we compared marathon mice and unselected controls, but in addition, we investigated the effects of three weeks of endurance exercise on the somatotropic axis in both mouse lines. To do so, we compared a genetic model (DUhTP vs. DUC mice) and an experimental model (sedentary versus trained). We used two related RNAseq experiments, which studied mRNA expression in the pituitary gland [9] and muscle (Brenmoehl et al., submitted) by integrating the genetic model and training effects. Here, for the first time, we considered the interaction of two different tissues, the pituitary gland and muscle, with respect to phenotype selection and training. Finally, hypotheses derived from the interpretation of mRNA expression were tested on the protein level by analyzing intra-cellular signal transduction.

2. Materials and Methods

2.1. Animals, Study Design, and Sample Preparation

The present study is based on an animal experiment described previously [9]. All experiments adhered to national and international standards, guidelines, and laws and were approved by the internal institutional committee and the state of Mecklenburg-Vorpommern (State Office for Agriculture, Food Safety, and Fisheries; AZ 7221.3-1-014/17, date of approval: 25 April 2017 and AZ 7221.3-1-064/19, date of approval: 30 January 2020). Long-term selected mice of the Dummerstorf high treadmill line (DUhTP) were compared with their corresponding unselected control (DUC) without (sed) and with three weeks of treadmill training adapted to the performance capacity of the respective line (trained). According to the three-week training program, the mice were running five days per week (Monday to Friday) starting at the age of 49 days after birth [9]. All mice were sacrificed

at day 70 of life, and different tissues were collected, including the pituitary gland and *Musculus rectus femoris* (Mrf). Furthermore, serum and plasma samples were produced from fresh blood samples. For the generation of serum, the samples were centrifuged for 10 min at 1500× *g* at room temperature after incubation at room temperature for 30 min, and the supernatants were transferred to fresh 1.5 mL vials and finally centrifuged for 5 min at 1500× *g* at room temperature. The supernatants were then stored in fresh 1.5 mL vials at −20 °C. For plasma production, fresh blood was collected in a 1.5 mL vial containing 5 µL 500 mM ethylenediaminetetraacetic acid (EDTA). The samples were mixed and centrifuged at 5000× *g* for 10 min at 8 °C before the supernatants were stored at −20 °C.

2.2. Next-Generation Sequencing (NGS), Differential Gene Expression Analysis, and Data Processing

Isolation of total RNA derived from pituitary glands and Mrf, the generation of the DNA-Library, and the NGS procedure were performed and validated as previously described [9,Brenmoehl et al., submitted]. The obtained data were analyzed by comparing gene expression in the genetic groups (DUhTP and DUC) as well as the treatment groups (sedentary and trained). The following comparisons were made: DUhTP sed vs. DUC sed, DUhTP trained vs. DUC trained, DUC trained vs. DUC sed, and DUhTP trained vs. DUhTP sed. The effects were expressed as logarithmic fold change ($\log_2$ FC) with associated false discovery rate (FDR) [9]. As significantly regulated, a threshold FDR of 0.1 was set, and accordingly, differentially expressed genes (DEGs) were marked in red for higher expression and green for lower expression. To visualize more stringent regulation (FDR $\leq$ 0.05), the significant effects on the levels of gene expression were marked in bold.

2.3. IGF1 Assay

IGF1 concentrations in mouse sera and muscle lysates were determined using commercial ELISA kits (Mediagnost, Reutlingen, Germany) for mouse/rat IGF1 according to the manufacturer's instructions. Serum was diluted at 1:100 with sample buffer (Mediagnost) before the determination. The Mrf tissue (≈50 mg) was combined with 10× (*w*/*v*) TE buffer (100 mM tris(hydroxymethyl)aminomethane, 10 mM EDTA, set to pH 7.5–8.0 with sodium dodecyl sulfate) and mechanically homogenized (6000 rpm, 2 min) in a vial with ceramic beads in the Precellys®24 (Peqlab Biotechnologie, Erlangen, Germany) and centrifuged (21,000× *g*) for 2 min at 4 °C after cooling on ice. The supernatant was diluted 1:2 with sample buffer and used in ELISA according to the manufacturer's instructions. The concentration of IGF1 in muscle lysate is expressed concerning total protein concentration, determined by the bicinchoninic acid method (BCA Test Kit, SERVA Electrophoresis GmbH, Heidelberg, Germany).

2.4. Protein Isolation and SDS-PAGE

Again, ≈50 mg of muscle tissue were mechanically homogenized (6000 rpm for 2 × 30 s) in 1 × CST Cell Lysis Buffer (Cell Signaling, Frankfurt am Main, Germany) using Precellys ceramic beads. Samples were incubated on ice for 20 min and diluted 1:2 with 2× Laemmli (31.25 mM tris(hydroxymethyl)aminomethane, 1% sodium dodecyl sulfate, 5% glycerol). After denaturation (10 min, 94 °C) and centrifugation (2 min, 21,000× *g*, 4 °C), the protein concentration was also determined using the bicinchoninic acid method described earlier. The protein concentrations were then adjusted to 1 mg/mL with 1 × Laemmli, and beta-mercaptoethanol was added (to 0.4% finally). The samples (20 µg total protein) were separated by SDS-PAGE (Bio-Rad TGX Stain-Free FastCast Acrylamide kit; Bio-Rad Laboratories GmbH, Munich, Germany). After electrophoresis, proteins were transferred to a polyvinylidene fluoride (PVDF) membrane by semi-dry blotting (60 min, current 80 mA/gel).

2.5. Analysis of Signal Transduction by Western Immunoblotting (WIB)

For WIB, membranes were incubated in 3% dry milk in TBST (Tris-buffered saline with Tween20) for 1 h to block free binding sites of the membrane. After three washing

steps, the membranes were incubated overnight at 4 °C with primary antibodies purchased from Cell Signaling Technology (CST, Danvers, MA, USA). Antibodies detecting total S6K (CST: #2708S) or phosphorylated S6K (CST: #9234S) were used at a dilution of 1:1000 in 3% bovine serum albumin (BSA). After five washing steps in TBST, the membranes were incubated for 2 h with the secondary antibody (anti-rabbit IgG HRP, #7074, dilution 1:2000, CST). The bands were visualized using Lumigen ECL Ultra (Lumigen Inc., Southfield, MI, USA) under a Bio-Rad station (Bio-Rad Chemi-Doc MP System, Bio-Rad Laboratories GmbH, Hercules, USA) with UV light and appropriate instrument software (Image Lab Ver. 6.0.1, Bio-Rad). In the relative calculation, the protein quantity of the samples was normalized to the total protein quantity.

2.6. Analysis of Signal Transduction by Capillary Immuno-Electrophoresis (WES^{TM})

For WES^{TM}-analyses, protein samples were mixed with Fluorescent Master Mix (Protein Simple, San Jose, USA) and denatured for 5 min at 94 °C. The signal transduction analysis was performed with the WES^{TM} device from Protein Simple (San Jose, CA, USA) according to the manufacturer's manual and as described before [10]. To perform the analysis, the following components were used: WES separation kit for 12–230 kDa with 8 × 25 capillary cartridges (#SM-W004-1), the affiliated standard pack (#PS-ST05-8), and an anti-rabbit detection module (DM-001). All devices and chemicals were purchased from Protein Simple. The analysis was performed with the software package Compass for Simple Western (Protein Simple). For the individual proteins, the following antibodies from CST were used (Danvers, Massachusetts, USA) with specific dilutions: Akt (CST: #9272; 1:50), phosphorylated Akt (CST: #9271; 1:20), p38 MAPK (CST: #9212; 1:50), phosphorylated p38 MAPK (CST: #4511; 1:20), PTEN (CST: #9188; 1:50), phosphorylated PTEN (CST: #9551; 1:3), and phosphorylated AMPKa (CST: #2535; 1:50). For AMPKa1/2 detection, the antibody sc-25792 from Santa Cruz Biotechnology (Dallas, TX, USA) was used with a dilution of 1:10. For analyses of phosphorylated PTEN, AMPKa1/2, and phosphorylated AMPKa, a sample dilution of 2 mg/mL and for the other analyses of 1 mg/mL were used according to the manufacturer's protocol.

2.7. Statistical Analysis

All statistical analyses were performed using GraphPad Prism (version 9.0; GraphPad Software, San Diego, CA, USA). A linear balance line of known protein standard concentrations was used to calculate the measured protein concentrations. ANOVA for mixed models was used for significance testing, and pairwise comparisons were performed using the Tukey-Kramer method.

3. Results

3.1. Effects of Phenotype Selection and Running on the GH/IGF Axis in the Pituitary Gland and Muscle Tissue

To investigate effects of phenotype selection and treadmill running on somatic growth control and signal transduction, expression of respective candidate genes was assessed in the pituitary gland and muscle (Mrf) from marathon mice (DUhTP) and controls (DUC, Table 1).

Table 1. Effects of phenotype selection and exercise training on the GH/IGF system. List of comparative gene expression (Gene ID) as logarithmic fold change (log2FC) with corresponding false discovery rate (FDR) in the pituitary gland and skeletal muscle in the four comparison groups. Significant effects below a threshold of FDR $\leq$ 0.1 are marked in red (upregulated) or green (downregulated) and below an FDR $\leq$ 0.05 in bold.

Signaling Pathway	Gene ID	Comparison Parameters	Expression in the Pituitary Gland				Expression in Skeletal Muscle			
			DUhTP vs. DUC		DUC	DUhTP	DUhTP vs. DUC		DUC	DUhTP
			Sed	Trained	Trained vs. Sed		Sed	Trained	Trained vs. Sed	
GH axis	Pou1f1	log2FC	**−0.378**	−0.067	**−0.339**	−0.028				
		FDR	**0.002**	0.650	**0.027**	1.000				
	Gh	log2FC	−0.440	**−0.724**	0.378	0.095				
		FDR	0.066	**0.000**	0.158	1.000				
	Ghsr	log2FC	**−0.813**	−0.134	−0.683	−0.004				
		FDR	**0.016**	0.744	0.082	1.000				
	Sstr1	log2FC	0.676	−0.084	0.862	0.102				
		FDR	0.107	0.861	0.053	1.000				
	Sstr2	log2FC	**−1.367**	**−1.653**	−0.287	−0.573				
		FDR	**0.004**	**0.000**	0.668	1.000				
	Ghrhr	log2FC	−0.144	**0.493**	−0.176	0.462				
		FDR	0.545	**0.002**	0.427	0.087				
	Ghr	log2FC	−0.014	0.397	−0.190	0.221	**−0.291**	**−0.557**	−0.097	**−0.363**
		FDR	0.977	0.073	0.526	1.000	**0.034**	**0.000**	0.859	**0.025**
IGF system	Igf1	log2FC	−0.075	0.299	−0.563	−0.189	**−0.882**	**−1.722**	0.098	**−0.742**
		FDR	0.906	0.426	0.179	1.000	**0.000**	**0.000**	0.914	**0.002**
	Igf2	log2FC	**−4.277**	−0.280	**−3.217**	0.780	−0.332	−0.711	1.017	0.638
		FDR	**0.000**	0.843	**0.021**	1.000	0.569	0.138	0.303	0.363
	Igf1r	log2FC	−0.302	0.117	−0.209	0.211	**−0.480**	**−0.279**	−0.173	0.029
		FDR	0.069	0.487	0.267	0.989	**0.000**	**0.046**	0.670	0.913
	Igf2r	log2FC	−0.249	0.109	**−0.307**	0.050	**−0.717**	**−0.625**	0.013	0.105
		FDR	0.086	0.450	**0.049**	1.000	**0.000**	**0.000**	0.987	0.565
	Irs1	log2FC	0.164	0.394	−0.207	0.022	**−0.826**	**−1.161**	−0.021	−0.357
		FDR	0.579	0.054	0.445	1.000	**0.000**	**0.000**	0.985	0.091
	Irs2	log2FC	−0.334	−0.132	−0.068	0.134	**−1.119**	−0.331	−0.236	0.552
		FDR	0.271	0.648	0.868	1.000	**0.037**	0.562	0.920	0.474
	Insr	log2FC	−0.157	0.208	−0.204	0.161	**−0.604**	**−0.724**	−0.114	−0.235
		FDR	0.389	0.147	0.242	1.000	**0.000**	**0.000**	0.740	0.080
	Igfbp2	log2FC	**−1.494**	**−0.943**	−0.678	−0.127				
		FDR	**0.001**	**0.032**	0.220	1.000				
	Igfbp3	log2FC	−0.204	−0.106	−0.133	−0.035	0.364	**0.495**	−0.394	−0.263
		FDR	0.318	0.570	0.547	1.000	0.053	**0.006**	0.302	0.295
	Igfbp4	log2FC	0.368	−0.238	0.527	−0.079	0.211	**0.459**	0.066	**0.314**
		FDR	0.220	0.378	0.080	1.000	0.094	**0.000**	0.899	**0.030**
	Igfbp5	log2FC	−0.194	0.000	−0.175	0.019	−0.215	−0.107	−0.326	−0.218
		FDR	0.305	1.000	0.367	1.000	0.273	0.589	0.419	0.399
	Igfbp6	log2FC	−0.565	−0.525	−0.149	−0.109	0.174	**0.582**	−0.041	**0.367**
		FDR	0.395	0.344	0.859	1.000	0.289	**0.000**	0.955	**0.043**
	Igfbp7	log2FC	−0.153	**−0.577**	0.233	−0.191	0.179	**0.307**	0.015	0.142
		FDR	0.479	**0.000**	0.236	1.000	0.141	**0.006**	0.985	0.387
	Pappa2	log2FC	**−0.759**	**−0.566**	−0.090	0.103	−0.233	−0.341	0.560	0.453
		FDR	**0.000**	**0.006**	0.792	1.000	0.660	0.470	0.659	0.493
	Stc1	log2FC	−0.247	−0.003	−0.481	−0.237	−0.810	−0.627	−0.308	−0.124
		FDR	0.536	0.993	0.173	1.000	0.059	0.153	0.850	0.877

Table 1. *Cont.*

Signaling Pathway	Gene ID	Comparison Parameters	Expression in the Pituitary Gland				Expression in Skeletal Muscle			
			DUhTP vs. DUC		DUC	DUhTP	DUhTP vs. DUC		DUC	DUhTP
			Sed	Trained	Trained vs. Sed		Sed	Trained	Trained vs. Sed	
	Stc2	log2FC	0.511	0.667	0.289	0.445	0.550	**0.595**	0.240	0.285
		FDR	0.256	0.064	0.566	1.000	0.088	**0.049**	0.850	0.525
	Slc2a4	log2FC	0.178	−0.129	0.276	−0.031	**0.227**	**0.362**	0.134	**0.268**
		FDR	0.732	0.751	0.530	1.000	**0.033**	**0.000**	0.654	**0.033**

Abbreviations: GH: growth hormone; IGF: insulin-like growth factor; DUhTP: mouse line selected for high treadmill performance; DUC: unselected control mouse line; sed: sedentary; vs: versus; Pou1f1: POU class 1 homeobox 1; Ghsr: growth hormone secretagogue receptor; Sstr: somatostatin receptor; Ghrhr: growth-hormone-releasing hormone receptor; Ghr: growth hormone receptor; Igf1/2r: insulin-like growth factor receptor 1/2; Irs: insulin receptor substrate; Insr: insulin receptor; Igfbp: insulin-like growth factor binding protein; Pappa2: pappalysin-2; Stc: stanniocalcin; Slc2a4: glucose transporter type 4.

In the pituitary gland of sedentary DUhTP mice, gene expression of the transcription factor for GH (Pou1f1, also known as Pit1), GH secretagogue receptor (Ghsr), Igf2, Igfbp2, and Pappa2 was reduced compared to sedentary DUC mice ($p \leq 0.05$). Interestingly, gene expression of Pou1f1 and Igf2 was also reduced in DUC mice in response to exercise ($p \leq 0.05$). In the pituitary gland, gene expression of growth hormone was reduced in sedentary DUhTP mice compared to sedentary DUC mice only with borderline significance ($p = 0.066$), whereas in trained DUhTP mice, the reduction of Gh mRNA expression was highly significant ($p \leq 0.001$). In pituitary glands, expression of growth hormone-releasing hormone receptor (Ghrhr) mRNA was significantly increased in response to training in DUhTP versus DUC mice ($p \leq 0.005$). In plasma samples from sedentary DUhTP mice, reduced concentrations of IGF1 were found compared to DUC mice (Figure 1; $p \leq 0.05$).

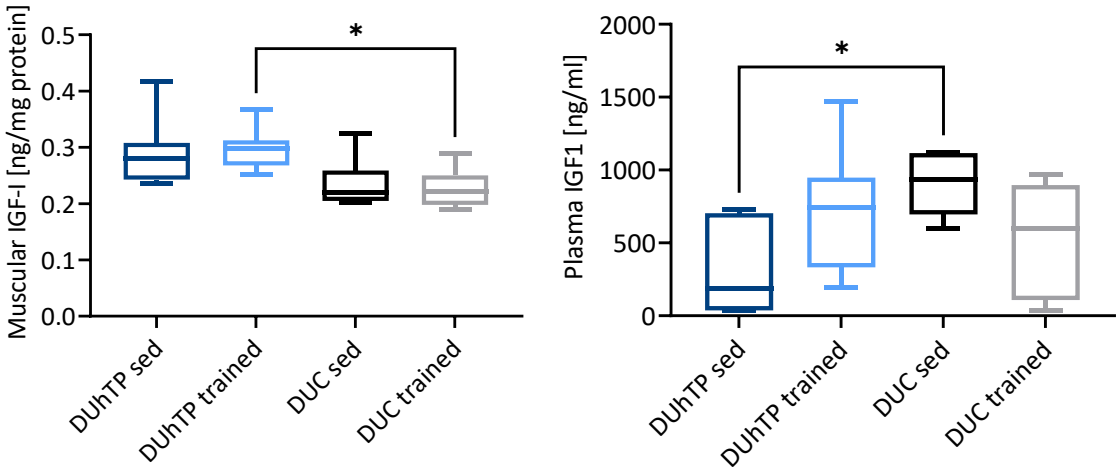

Figure 1. Effects of phenotype selection and three-week endurance exercise training on the concentrations of IGF1 in lysates from *Musculus rectus femoris* (**left**) and plasma (**right**). The concentrations of IGF1 in both matrices were determined by ELISA as described in the Materials and Methods. Results are presented as box plots. Statistical analysis was performed using one-way ANOVA. Significant differences are marked with an asterisk (* $p < 0.05$). Abbreviations are defined in Table 1.

In the femoral skeletal muscle, several members of the GH/IGF-system were affected in terms of the level of mRNA expression (Table 1). Notably, in addition to Igf1, mRNA expression for several receptors from the GH/IGF-system (Ghr, Igf1r, Igf2r) was reduced in both experimental DUhTP groups ($p \leq 0.05$). In addition, the insulin receptor (Insr) and insulin receptor substrate 1 (Irs1) were reduced in both experimental DUhTP groups compared to their unselected control groups ($p < 0.001$). Instead, the expression of several IGFBPs was elevated in trained DUhTP mice ($p \leq 0.01$). Contrasting the significantly reduced expression of IGF1 mRNA in muscle, protein levels of IGF1 in muscle tissue were higher in trained DUhTP mice compared to trained DUC mice ($p \leq 0.05$; Figure 1).

3.2. Effects of Phenotype Selection and Endurance Exercise on mRNA Expression of Intracellular Signaling Compounds in the Pituitary Gland and Muscle

Hormonal signals from the pituitary gland can regulate intracellular signal transduction by autocrine or endocrine mechanisms. On the level of GH, IGFs, IGF-receptors, and IGFBPs, mainly inhibitory effects of phenotype selection have been observed so far in the present study. Therefore, we analyzed the gene expression of IGF-dependent intracellular signaling pathways in the pituitary gland and muscle (Mrf). Except for Tsc2 ($p \leq 0.01$, Table 2), no significant effect of long-term selection on intracellular signaling was identified in the pituitary from sedentary DUhTP mice. By contrast, long-term selection in muscle tissue affected several DEGs involved in mTORC1 and mTORC2 pathways. Notably, the abundance of several mRNA transcripts coding for proteins mediating hormonal signals related to mTORC1 or mTORC2 activation or signaling was significantly suppressed ($p \leq 0.05$) in sedentary DUhTP versus DUC mice, including Akt3, Gsk3b, Mtor, Clock, Pdpk1, Tsc1, Pten, Rictor, Rptor, Deptor, Rps6kp1 Foxo3, and Ei4einif1. Only the expression of Mlst8 as a part of the mTORC1/mTORC2 complex was increased in direct comparison and unremarkable after training. Notably, a known inhibitor of mTORC1 was significantly increased in DUhTP versus DUC mice (Akt1s1, $p \leq 0.001$). In addition, mRNA expression of an inhibitor of protein translation (Eif4ebp1) and of Rps6 was significantly increased ($p \leq 0.001$) in muscle of DUhTP compared to DUC mice.

Table 2. Effects of phenotype selection and endurance exercise training on mRNA expression of components from hormone-dependent intracellular signaling cascades in the pituitary gland and muscle. The effects of selection or exercise are presented as logarithmic fold change (log2FC) with corresponding false discovery rate (FDR) in both tissues in four comparison groups. Significant effects below a threshold of FDR ≤ 0.1 are marked in red (upregulated) or green (downregulated) and below an FDR ≤ 0.05 in bold.

Functional Group	Gene ID	Comparison Parameters	Expression in the Pituitary Gland				Expression in Skeletal Muscle			
			DUhTP vs. DUC		DUC	DUhTP	DUhTP vs. DUC		DUC	DUhTP
			Sed	Trained	Trained vs. Sed		Sed	Trained	Trained vs. Sed	
Hormonal control of mTORC activity	Akt1	log2FC	−0.033	**−0.180**	0.088	−0.059	0.125	0.199	0.082	0.156
		FDR	0.834	**0.049**	0.476	1.000	0.368	0.116	0.877	0.384
	Akt2	log2FC	−0.113	−0.138	−0.016	−0.042	0.079	**0.254**	−0.028	0.146
		FDR	0.395	0.190	0.929	1.000	0.496	**0.010**	0.954	0.292
	Akt3	log2FC	−0.005	0.227	−0.070	0.162	**−0.668**	**−0.467**	−0.076	0.124
		FDR	0.983	0.060	0.695	1.000	**0.000**	**0.000**	0.881	0.508
	Gsk3b	log2FC	−0.239	0.002	−0.267	−0.026	**−0.684**	**−0.642**	−0.189	−0.147
		FDR	0.157	0.991	0.133	1.000	**0.000**	**0.000**	0.506	0.383
	Bmal1	log2FC	0.332	−0.064	−0.444	**−0.840**	−0.165	−0.650	−0.755	**−1.240**
		FDR	0.288	0.845	0.153	**0.012**	0.684	0.055	0.269	**0.001**
	Clock	log2FC	−0.093	0.153	−0.350	−0.105	**−0.539**	**−1.026**	**−0.509**	**−0.997**
		FDR	0.713	0.386	0.074	1.000	**0.000**	**0.000**	**0.012**	**0.000**
	Mtor	log2FC	−0.106	0.159	−0.207	0.058	**−0.330**	0.010	−0.142	0.198
		FDR	0.556	0.233	0.189	1.000	**0.005**	0.944	0.687	0.205
	Pik3ca	log2FC	−0.140	0.123	−0.203	0.060	**−0.532**	**−0.618**	−0.303	**−0.389**
		FDR	0.378	0.355	0.180	1.000	**0.000**	**0.000**	0.111	**0.003**
	Pik3cb	log2FC	−0.092	0.034	−0.086	0.041	**−0.400**	**−0.527**	−0.005	−0.133
		FDR	0.704	0.867	0.706	1.000	**0.011**	**0.000**	0.994	0.589
	Pik3c2a	log2FC	−0.131	0.156	−0.296	−0.009	**−0.986**	**−1.328**	−0.240	**−0.582**
		FDR	0.604	0.413	0.168	1.000	**0.000**	**0.000**	0.678	**0.020**
	Pdpk1	log2FC	−0.140	0.072	−0.163	0.049	**−0.797**	**−0.771**	−0.016	0.010
		FDR	0.508	0.700	0.413	1.000	**0.000**	**0.000**	0.980	0.968
	Tsc1	log2FC	0.019	**0.279**	−0.163	0.097	**−0.557**	**−0.447**	0.008	0.119
		FDR	0.946	**0.038**	0.352	1.000	**0.000**	**0.000**	0.991	0.441

Table 2. *Cont.*

Functional Group	Gene ID	Comparison Parameters	Expression in the Pituitary Gland				Expression in Skeletal Muscle			
			DUhTP vs. DUC		DUC	DUhTP	DUhTP vs. DUC		DUC	DUhTP
			Sed	Trained	Trained vs. Sed		Sed	Trained	Trained vs. Sed	
Hormonal control of mTORC activity	Akt1	log2FC	−0.033	**−0.180**	0.088	−0.059	0.125	0.199	0.082	0.156
	Tsc2	log2FC	**−0.254**	−0.046	−0.143	0.065	−0.182	0.047	0.048	**0.277**
		FDR	**0.008**	0.688	0.223	1.000	0.091	0.691	0.919	**0.025**
	Rheb	log2FC	−0.054	**−0.304**	0.198	−0.052	0.094	−0.028	0.061	−0.061
		FDR	0.710	**0.000**	0.077	1.000	0.388	0.805	0.881	0.701
	Pten	log2FC	−0.186	0.243	−0.361	0.069	**−0.678**	**−1.056**	0.017	**−0.361**
		FDR	0.404	0.166	0.083	1.000	**0.000**	**0.000**	0.981	**0.009**
	Rictor	log2FC	0.008	**0.347**	−0.227	0.112	**−0.550**	**−0.772**	−0.257	**−0.478**
		FDR	0.980	**0.015**	0.215	1.000	**0.004**	**0.000**	0.630	**0.044**
	Rptor	log2FC	−0.127	−0.011	−0.072	0.044	**−0.264**	−0.058	0.047	**0.252**
		FDR	0.283	0.932	0.585	1.000	**0.008**	0.599	0.919	**0.036**
	Deptor	log2FC	0.178	**0.582**	−0.122	0.281	−0.120	**−0.529**	0.150	−0.258
		FDR	0.576	**0.006**	0.709	1.000	0.501	**0.000**	0.783	0.217
	Rps6kb1	log2FC	−0.113	0.151	−0.184	0.080	**−0.341**	**−0.786**	−0.033	**−0.479**
		FDR	0.583	0.325	0.308	1.000	**0.013**	**0.000**	0.962	**0.002**
	Rps6	log2FC	−0.088	**−0.451**	**0.375**	0.011	**0.368**	**0.529**	0.048	0.209
		FDR	0.696	**0.001**	**0.034**	1.000	**0.000**	**0.000**	0.908	0.069
	Mlst8	log2FC	−0.002	−0.200	0.076	−0.122	**0.274**	0.169	0.104	−0.001
		FDR	0.994	0.090	0.645	1.000	**0.020**	0.154	0.808	0.996
	Mapkap1	log2FC	−0.008	−0.196	0.063	−0.126	0.095	0.155	0.074	0.135
		FDR	0.976	0.096	0.714	1.000	0.334	0.080	0.823	0.259
	Akt1s1	log2FC	−0.035	−0.225	0.232	0.042	**0.406**	**0.629**	−0.101	0.122
		FDR	0.900	0.145	0.215	1.000	**0.000**	**0.000**	0.813	0.472
	Telo2	log2FC	−0.230	**−0.352**	−0.009	−0.131	0.043	−0.054	0.088	−0.010
		FDR	0.085	**0.002**	0.971	1.000	0.805	0.738	0.883	0.973
	Eif4ebp1	log2FC	−0.194	−0.213	0.199	0.180	**0.563**	**0.862**	−0.048	0.251
		FDR	0.651	0.506	0.615	1.000	**0.000**	**0.000**	0.944	0.186
	Eif4enif1	log2FC	−0.004	0.086	−0.083	0.007	**−0.219**	−0.099	−0.065	0.056
		FDR	0.982	0.390	0.493	1.000	**0.021**	0.318	0.866	0.722
	Foxo3	log2FC	−0.018	0.194	−0.142	0.070	**−0.388**	0.209	−0.015	**0.582**
		FDR	0.952	0.195	0.460	1.000	**0.002**	0.093	0.987	**0.000**

Abbreviations: DUhTP: mouse line selected for high treadmill performance; DUC: unselected control mouse line; sed: sedentary; vs: versus; Akt: protein kinase B; Gsk3b: glycogen synthase kinase 3 beta; Bmal1: brain and muscle ARNT-like 1; Clock: circadian locomotor output cycles kaput; Mtor: mechanistic target of rapamycin; Pik3c: phosphatidylinositol 3-kinase subunits; Pdpk1: phosphoinositide-dependent kinase-1; Tsc: tuberous sclerosis complex; Rheb: Ras homolog enriched in brain; Pten: phosphatase and tensin homolog; Rictor: rapamycin-insensitive companion of mammalian target of rapamycin; Rptor: regulatory-associated protein of mTOR; Deptor: DEP domain-containing mTOR-interacting protein; Rps6kb1: ribosomal protein S6 kinase beta-1; Rps6: ribosomal protein S6; Mlst8: target of rapamycin complex subunit LST8; Mapkap1: target of rapamycin complex 2 subunit; Akt1s1: proline-rich AKT1 substrate 1; Telo2: telomere length regulation protein TEL2 homolog; Eif4ebp1: eukaryotic translation initiation factor 4E-binding protein 1; Eif4enif1: eukaryotic translation initiation factor 4E transporter; Foxo3: forkhead box O3.

In contrast to these hormone-sensitive signaling members, nutrient-sensitive mTORC1 signaling components were characterized by elevated mRNA expression in DUhTP versus DUC mice. Accordingly, mRNA expression of four components from the pentameric Ragulator complex (Lamtor1, 2, 4, and 5) was significantly increased in the muscle of sedentary DUhTP mice compared to controls ($p \leq 0.001$; Table 3). In muscles of trained DUhTP mice, all members of the Lamtor family (Lamtor 1 to 5) were increased compared to trained DUC mice ($p \leq 0.05$). Similarly, several members (sirtuin 2, 3, 4, 5, or 6) of the sirtuin family, a second nutrient-sensing protein family, were elevated in muscles from sedentary or trained DUhTP mice compared to their respective control group ($p \leq 0.05$, Table 3). By contrast, mRNA expression encoding sirtuin1 was reduced in both DUhTP groups compared to DUC mice ($p \leq 0.001$). In addition, four AMPK subunits were differentially

regulated in both DUhTP groups compared to corresponding unselected control groups, respectively. Accordingly, mRNA expression of catalytic subunits Prkaa1 and -2 was reduced, whereas expression of Prkab1 and Prkag1 was elevated in the muscle of DUhTP mice ($p < 0.05$).

Table 3. Effects of phenotype selection and endurance exercise on mRNA expression coding for proteins and protein-complex subunits related to metabolic cell signaling in the pituitary gland and muscle. The effects of selection and exercise are presented as logarithmic fold change (log2FC) with corresponding false discovery rate (FDR) in the pituitary gland and skeletal muscle in four comparison groups. Significant regulations below a threshold of FDR ≤ 0.1 are marked in red (upregulated) or green (downregulated) and below an FDR ≤ 0.05 in bold.

Signaling Pathway Members	Gene ID	Comparison Parameters	Expression in the Pituitary Gland				Expression in Skeletal Muscle			
			DUhTP vs. DUC		DUC	DUhTP	DUhTP vs. DUC		DUC	DUhTP
			Sed	Trained	Trained vs. Sed		Sed	Trained	Trained vs. Sed	
Lamtors	Lamtor1	log2FC	0.035	**−0.265**	0.237	−0.063	**0.470**	**0.525**	0.131	0.186
		FDR	0.887	**0.049**	0.159	1.000	**0.000**	**0.000**	0.593	0.109
	Lamtor2	log2FC	−0.097	**−0.640**	**0.427**	−0.116	**0.377**	**0.331**	−0.029	−0.076
		FDR	0.710	**0.000**	**0.033**	1.000	**0.000**	**0.000**	0.951	0.611
	Lamtor3	log2FC	0.086	−0.049	0.022	−0.112	0.191	**0.238**	−0.077	−0.030
		FDR	0.571	0.708	0.904	1.000	0.068	**0.017**	0.850	0.868
	Lamtor4	log2FC	0.090	**−0.395**	0.416	−0.069	**0.490**	**0.486**	0.014	0.010
		FDR	0.751	**0.021**	0.050	1.000	**0.000**	**0.000**	0.983	0.959
	Lamtor5	log2FC	0.019	−0.097	0.199	0.084	**0.446**	**0.399**	0.069	0.023
		FDR	0.955	0.609	0.329	1.000	**0.000**	**0.000**	0.876	0.905
Sirtuins	Sirt1	log2FC	−0.247	0.060	−0.258	0.049	**−0.554**	**−0.899**	0.040	−0.305
		FDR	0.216	0.771	0.207	1.000	**0.000**	**0.000**	0.956	0.128
	Sirt2	log2FC	0.021	0.002	0.043	0.024	**0.260**	**0.384**	0.011	0.134
		FDR	0.896	0.988	0.739	1.000	**0.002**	**0.000**	0.986	0.249
	Sirt3	log2FC	0.205	0.074	0.166	0.034	**0.480**	**0.454**	0.106	0.080
		FDR	0.105	0.567	0.228	1.000	**0.000**	**0.000**	0.839	0.718
	Sirt4	log2FC	−0.098	−0.028	−0.025	0.045	**0.297**	0.134	0.191	0.029
		FDR	0.567	0.858	0.904	1.000	**0.028**	0.333	0.591	0.905
	Sirt5	log2FC	0.064	0.239	0.044	0.219	**0.570**	**1.177**	−0.093	**0.514**
		FDR	0.836	0.196	0.884	1.000	**0.001**	**0.000**	0.909	**0.012**
	Sirt6	log2FC	0.041	−0.136	0.084	−0.092	**0.337**	0.285	0.035	−0.017
		FDR	0.876	0.395	0.692	1.000	**0.041**	0.078	0.968	0.959
	Sirt7	log2FC	−0.227	**−0.339**	0.097	−0.016	−0.047	0.104	0.025	0.177
		FDR	0.090	**0.002**	0.549	1.000	0.810	0.541	0.978	0.437
AMPK subunits	Prkaa1	log2FC	−0.046	0.133	−0.202	−0.024	**−0.680**	**−0.844**	−0.105	−0.269
		FDR	0.842	0.364	0.224	1.000	**0.000**	**0.000**	0.818	0.099
	Prkaa2	log2FC	0.051	**0.351**	−0.203	0.096	**−0.672**	**−0.885**	−0.084	−0.297
		FDR	0.872	**0.046**	0.372	1.000	**0.000**	**0.000**	0.881	0.080
	Prkab1	log2FC	0.066	0.028	0.083	0.045	**0.355**	**0.315**	−0.037	−0.077
		FDR	0.720	0.852	0.610	1.000	**0.010**	**0.021**	0.957	0.736
	Prkab2	log2FC	0.077	0.277	−0.121	0.079	−0.111	−0.101	0.031	0.041
		FDR	0.762	0.077	0.575	1.000	0.577	0.592	0.974	0.897
	Prkag1	log2FC	−0.091	**−0.286**	0.186	−0.009	**0.437**	**0.527**	0.026	0.115
		FDR	0.569	**0.007**	0.177	1.000	**0.000**	**0.000**	0.960	0.434
	Prkag2	log2FC	0.029	0.099	−0.186	−0.115	0.244	0.217	0.077	0.049
		FDR	0.883	0.405	0.167	1.000	0.150	0.188	0.917	0.864
	Prkag3	log2FC					0.297	−0.043	0.330	−0.010
		FDR					0.163	0.856	0.498	0.981

Abbreviations: DUhTP: mouse line selected for high treadmill performance; DUC: unselected control mouse line; sed: sedentary; vs: versus; mTORC1: mechanistic target of rapamycin complex 1; Lamtor: Ragulator-Rag complex; Sirt: sirtuin; AMPK: 5′-AMP-activated protein kinase; Prka: 5′-AMP-activated protein kinase subunits.

Results from Tables 1–3 are summarized in Figure 2. Additional effects of phenotypic selection and training on gene expression of growth factors or growth factor signaling are listed in Supplemental Table S1.

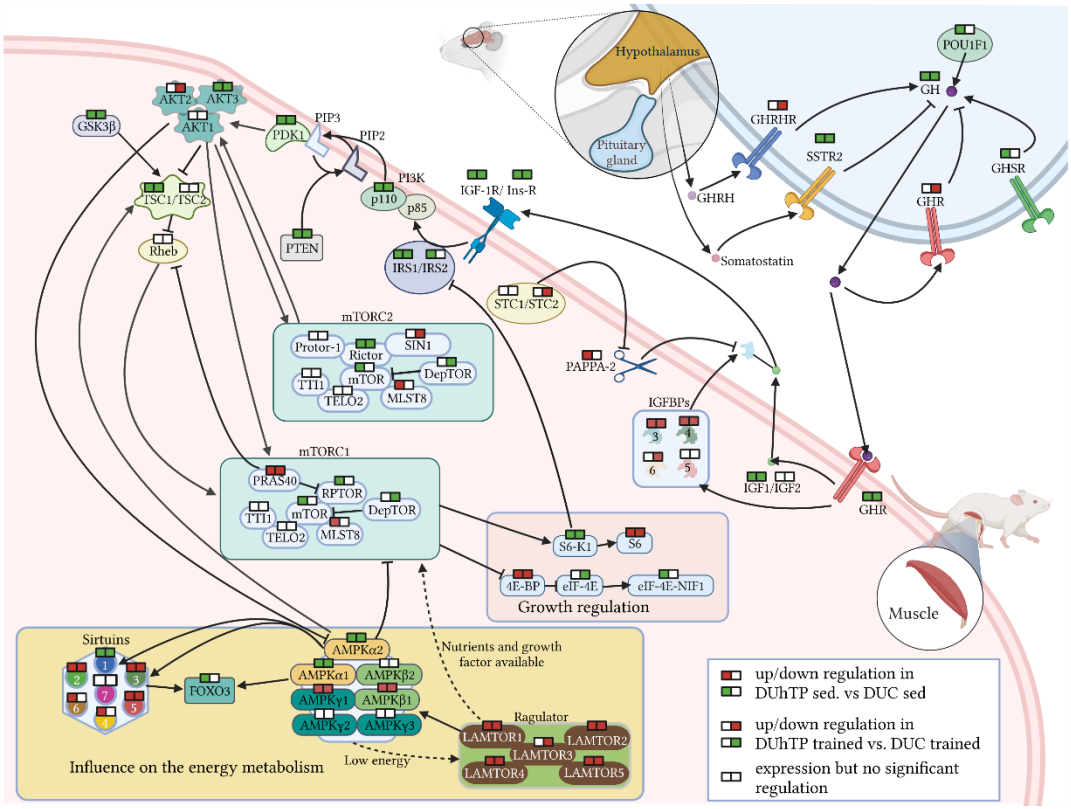

Figure 2. Gene expression of GH/IGF-related signaling cascades in the pituitary gland and muscle of phenotype-selected marathon mice (DUhTP) and unselected controls (DUC). The schematic summary presents results from Tables 1–3. The double boxes indicate regulation of mRNA expression when sedentary groups (left half of the box) or trained groups (right half of the box) were compared (red/green color: higher/lower gene expression in DUhTP versus DUC mice at $p < 0.05$; white boxes indicate no significant effects of genotype). Blunted arrows indicate inhibition, and dotted lines indicate indirect interactions between signaling compounds. Created on BioRender.com (accessed on 23/09/2021). Abbreviations are mentioned in Tables 1–3.

3.3. Effects of Phenotype Selection and Training on Intracellular Signal Transduction in the Muscle

In order to test the hypothesis of GH/IGF suppression in marathon mice, or whether reduced mRNA expression of signaling components also affects protein levels and activation, we performed a signal transduction study examining protein expression and phosphorylation in muscles from all four experimental groups. Expression of AKT protein was higher in muscles from trained DUhTP mice than trained DUC mice ($p \leq 0.05$; Figure 3a). Training increased the absolute levels of phosphorylated AKT in both genetic groups compared to their sedentary control groups ($p \leq 0.05$). Specific activation of AKT, however, was only observed in DUC but not in DUhTP mice ($p \leq 0.01$). Accordingly, the specific activity was lower in muscles from DUhTP versus DUC mice ($p \leq 0.01$). By contrast, the expression of PTEN was higher in sedentary DUhTP than in sedentary DUC mice ($p \leq 0.05$; Figure 4a). Based on the higher ratios of unphosphorylated PTEN to phosphorylated PTEN, higher levels of active PTEN can be assumed in sedentary DUhTP mice compared to trained littermates ($p \leq 0.05$) or sedentary controls ($p \leq 0.01$). In addition, specific activation of p38 MAPK was found only in trained DUC ($p \leq 0.05$; Figure 3b) but not in trained DUhTP mice. Expression and phosphorylation of AMPK were highly variable in different experimental groups (Figure 3c). Selection or training had no significant effect on

AMPK expression or activation. In muscle extracts from trained DUC mice, higher levels of phosphorylated S6K were found compared to sedentary DUC littermates or trained DUhTP mice ($p \leq 0.001$; Figure 4b). Also, the specific activity of S6K (ratio of phosphorylated to total protein) was higher in trained DUC mice than in both control groups ($p \leq 0.05$).

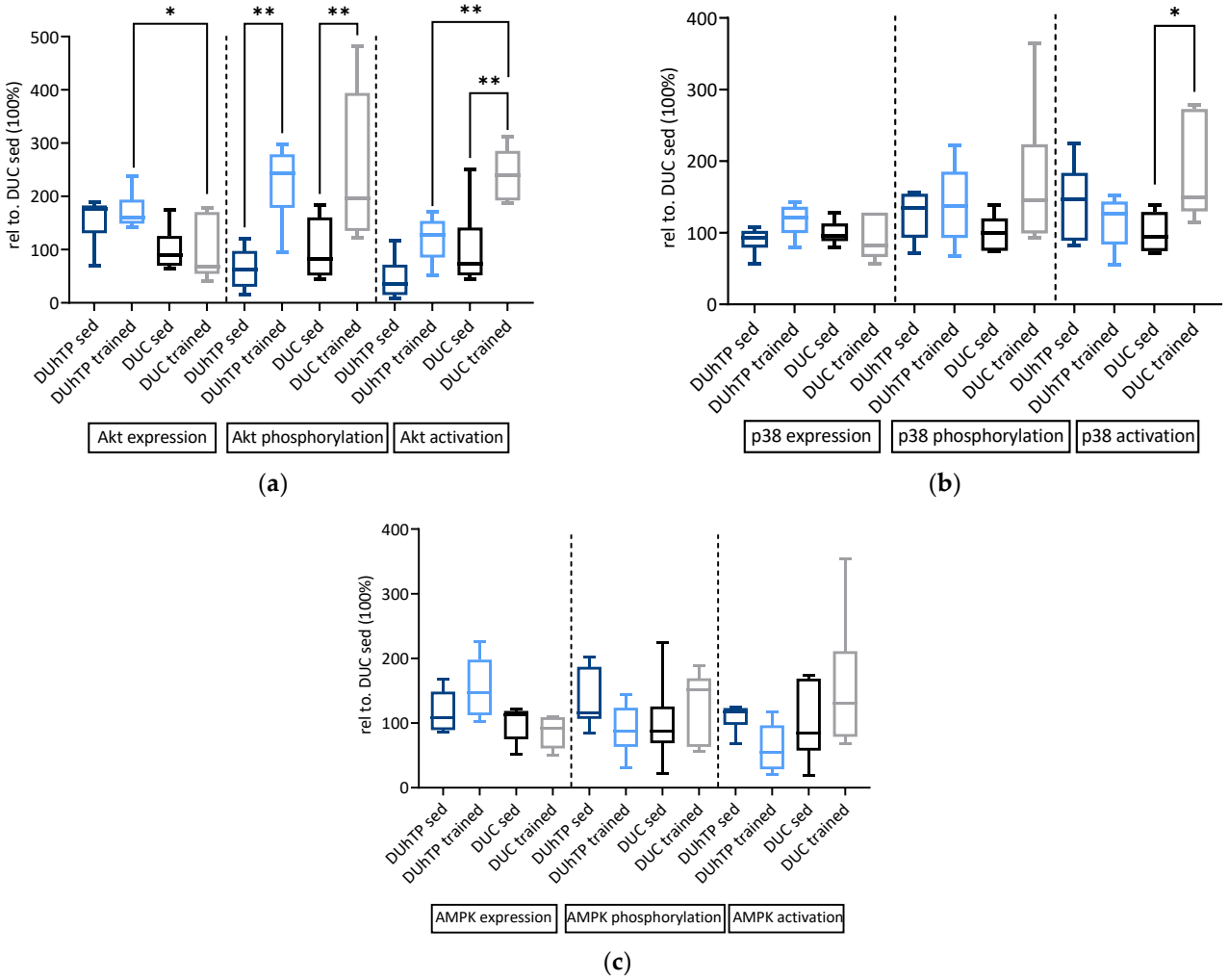

Figure 3. Effects of phenotype selection and endurance exercise on protein expression, phosphorylation, and specific activation of (**a**) AKT, (**b**) p38 MAPK, and (**c**) AMPK in *Musculus rectus femoris*. The analysis was performed by capillary immuno-electrophoresis (WES). Representative WES histograms created by Protein Simple Software are shown in Supplemental Figure S1. Data are presented as box plots and relative to sedentary DUC control mice, set to 100%. As an indicator of protein activation, the ratios were formed between protein phosphorylation and total protein expression. Statistical analysis was performed using one-way ANOVA. Significant differences are marked with asterisks (* $p < 0.05$, ** $p < 0.01$; $n = 6$). Abbreviations are defined in Tables 1–3.

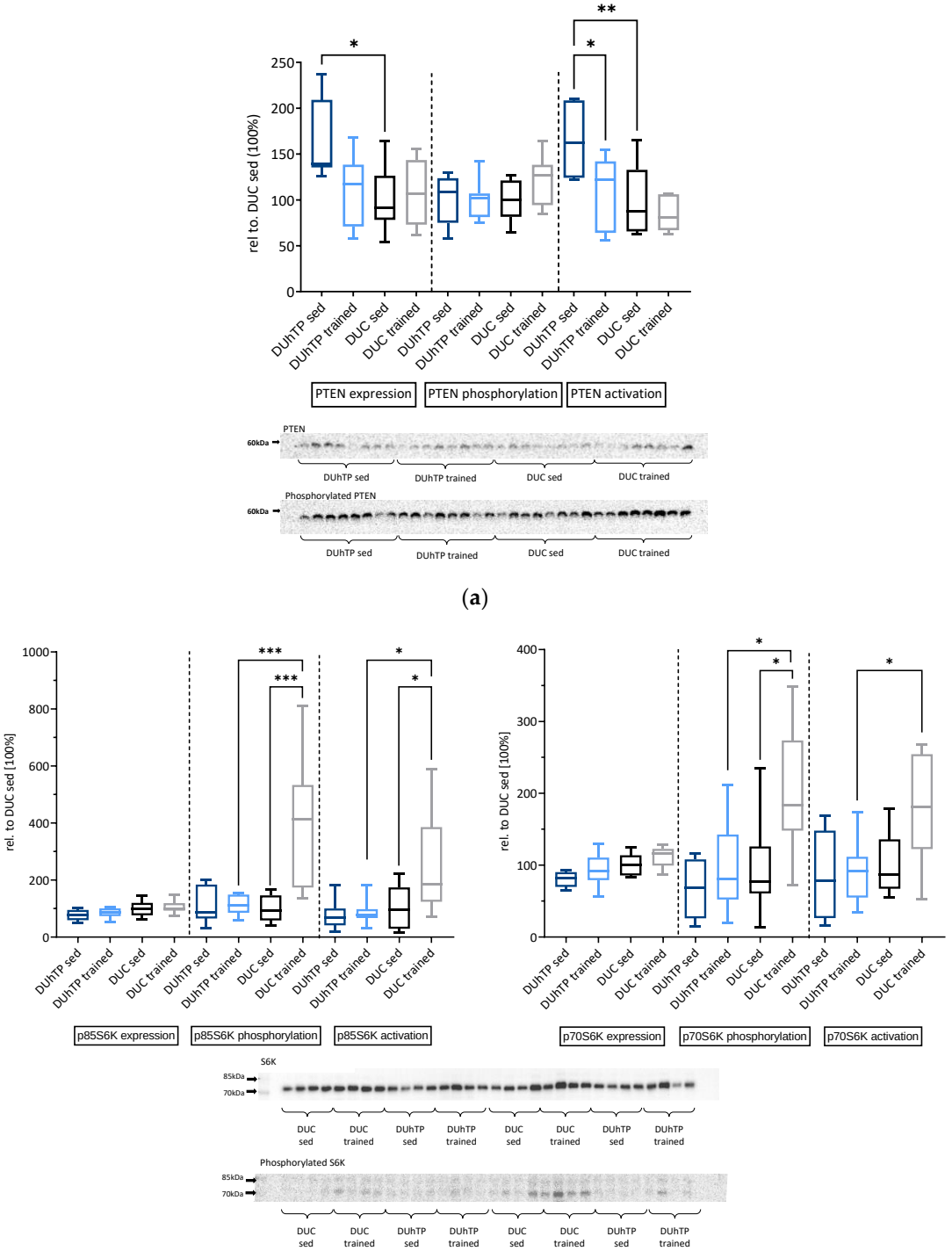

Figure 4. Effects of phenotype selection and endurance exercise on protein expression, phosphorylation, and specific activation of (**a**) PTEN and (**b**) p85S6K (left panel) and p70S6K (right panel) by Western immunoblot analysis in *Musculus rectus femoris*. The protein abundances in trained and untrained DUhTP (light/dark blue) and DUC mice (gray/black) were calculated relative to DUC sed (100%). Results are shown as box plots. Statistical analysis was performed using one-way ANOVA. Significant differences are marked with: * $p < 0.05$, ** $p < 0.01$, *** $p < 0.001$. Abbreviation: sed = sedentary.

4. Discussion

Preliminary work demonstrated that long-term selection for elevated endurance exercise capacities negatively affected body mass and muscle weight in male DUhTP

marathon mice compared to unselected controls (Brenmoehl et al., submitted). Notably, exercise further reduced body mass and muscle weight in DUhTP mice but had no negative effect in unselected controls (DUC) (Brenmoehl et al., submitted). Therefore, we aimed to investigate the molecular basis of somatic and organ growth inhibition in DUhTP mice by comparing gene expression in the pituitary gland and femoral muscle tissue between phenotype-selected mice and unselected controls with and without previous training using RNAseq. This manuscript discusses endocrine signals from the pituitary gland for their potential effects on signal transduction in the muscle. The discussion is supported by an analysis of signal transduction on the protein level guided by predictions and models derived from RNA expression analysis.

4.1. Regulation of the Somatotropic Axis

In our non-inbred marathon mouse model DUhTP, characterized by superior running performance, expression of Pou1f1 was significantly reduced in pituitary glands, and notably, Pou1f1 expression was also suppressed by training in the pituitary gland of unselected control mice. These results may thus support the notion that reduced Pou1f1 expression in DUhTP, genetically fixed by several decades of phenotype selection, may be related to running performance in a physiological context. Pou1f1 represents a central pituitary transcription factor required for growth and development of the pituitary gland and expression of growth hormone (GH), thyrotropin, and prolactin (Prl) [11,12]. In fact, Gh expression was also suppressed in the pituitary gland of DUhTP mice, indicating physiological relevance of reduced Pou1f1 expression in DUhTP mice. Similar to Pou1f1, Ghsr was reduced in sedentary DUhTP versus DUC mice and with borderline significance also in trained versus sedentary DUC mice, suggesting not only reduced expression but also reduced secretion of GH from the pituitary gland in response to peripheral or metabolic signals [13]. Since serum levels of IGF1 were also reduced in sedentary DUhTP mice, central suppression of the GH/IGF axis can be assumed to result from phenotype selection. Reduced levels of IGF1 in DUhTP versus control mice were also found in a previous study [8], although the IGF1 concentrations described in the present study were on a lower level by factor 2. The reason for this discrepancy can be related to the high phenotypical variability of our model, which was described in detail before [8].

The GH/IGF-axis is centrally involved in growth and metabolism and regulated by physical activity. Therefore, it is tempting to speculate that exercise-related activation of GH expression in the pituitary gland, which is frequently described [14], would correlate with elevated circulating concentrations of IGF1, which might act as a potent mediator of GH-dependent muscle growth. However, a clear correlation of GH expression and elevated circulating IGF1 concentrations appears not to be present in response to exercise [5]. In his review, Frystyk discussed the discrepancy between pituitary GH-secretion, which is increased in response to exercise, and the lack of elevated circulating levels of free or bioactive IGF1 [5]. The lack of an exercise effect on the concentration of free IGF1 was confirmed more recently by a meta-analysis including 21 reports from the literature. However, this identified a positive effect of endurance and resistance exercise on absolute serum concentrations of IGF1 [15]. It was argued [5] that local production of IGF1 could be induced by GH-independent mechanisms, as suggested by Zanconato et al. [6]. In fact, in our study, local IGF1 was also elevated in the muscle of trained DUhTP mice compared to trained DUC mice, and muscle IGF1 thus contrasted and reduced GH mRNA expression in the pituitary gland of trained DUhTP mice.

However, the increases of muscle IGF1 on protein level were only weak and exclusively found in trained DUhTP mice, and we do not have evidence from our results that higher protein levels of IGF1 in muscle were functional for a number of reasons. First of all, in addition to the Ghr, several components from the PI3 signaling cascades were expressed at lower levels of mRNA, including Igf1, Igf1r, Insr, Irs1, Pten, Akt3, Gsk3b, Pdk, Tsc1, Rictor, and Rps6kb1 in both experimental DUhTP groups. By contrast, mRNA expression of Igfbp3 and Igfbp 4 was elevated in DUhTP mice. This finding clearly suggests

coordinated inactivation of hormonal mTORC1 signaling, as discussed comprehensively by Philp et al. [16]. In this review, several studies collectively suggested adaptive muscle hypertrophy in the absence of IGF1R [7] or PI3K [17,18] signaling. While this evidence only supports the notion that hormone-dependent activation is not required for controlling muscle growth and metabolism in response to exercise, the present study identifies active downregulation of GH/IGF-related control of PI3K activation in the course of the selection experiment in DUhTP mice. The reductions of the GH/IGF system in the pituitary gland with coordinated downregulation of the PI3K in muscle may explain the reduced body and muscle mass in the DUhTP marathon mouse model (Brenmoehl et al., submitted). Collectively, downregulation of GH/IGF expression or signaling in DUhTP mice, characterized by the lower body and muscle mass than unselected controls, may suggest that body and muscle mass reductions may provide benefits for superior running performance. In fact, at least in a warm and humid environment, human runners with smaller body masses produced less heat than heavier runners and were able to run longer times and distances before a predefined rectal temperature was reached [19]. Since smaller runners are characterized by lower heat production, the authors stated that "smallness is an asset of distance running" [19]. Since marathon mice are characterized by massive fat cell browning and higher uncoupling protein 1 levels in fat tissues, including subcutaneous fat, correlating with elevated surface temperature [20], heat tolerance may be of critical importance to these mice. Accordingly, metabolic activity and heat tolerance could be related to central or peripheral somatotrophic growth inhibition in DUhTP marathon mice. The apparently successful management of heat stress in DUhTP mice, proven by the superior running capacities in this model, is highly relevant for heat stress management in farm animals and humans, which has never been more urgent than now given the increasing ambient temperatures during the climate crisis. Perhaps DUhTP mice can reveal novel mechanisms for heat stress defense in future studies.

4.2. Exercise-Related Activation of mTORC1 and mTORC2 in Muscle of DUC but Not of DUhTP Mice

In unselected control mice, training specifically induced activation of S6K without affecting systemic IGF1 concentrations or local IGF1 expression, which agrees with a recent report describing IGF1/AKT-independent activation of mTORC1 in response to resistance exercise in AKT1 knockout mice [21]. Accordingly, we also lack evidence for hormone-related activation of mTORC1 in DUC mice. In response to training, activation of mTORC1 in DUC mice fits with current concepts of exercise-related activation [22]. In fact, mTORC1 is considered a critical component for the muscle [23] since muscle growth during resistance training [24] depends on ribosomal biogenesis [25] and protein translation [4,26,27]. Clearly, and contrasting our findings in unselected controls, exercise-related activation of S6K was absent in DUhTP mice. The lack of mTORC1 activation in marathon mice could be related to multiple reductions of permissive signaling compounds described on the level of mRNA expression or to reduced serum IGF1 concentrations. In addition, the lack of mTORC1 activation could be due to the elevated expression of inhibitory proteins. Accordingly, the specific inhibitor of mTOR in the complex mTORC1, PRAS40 (gene Akt1s1), is upregulated in sedentary and trained DUhTP mice. This inhibitor is displaced by activated AKT [28], which is lacking in trained DUhTP mice. Since the negative effects of PRAS40 on S6K phosphorylation and Rheb-mediated mTORC1 activation can be blocked by insulin [29], and Insr and Irs1 were also repressed in muscle of DUhTP mice, we cannot rule out the notion that effects of insulin on mTORC1 could be toned down in muscle of DUhTP mice. Accordingly, multiple levels of mTORC1 repression composed of the interaction of activators and inhibitors and different hormonal systems can be considered in DUhTP mice. Importantly, the presence of multiple levels of mTORC1 repression can be related to the non-inbred background of DUhTP mice and speaks against a permissive function of mTORC1 for superior running performance in DUhTP mice. Notably, inhibition of mTORC1 by rapamycin improved mitochondrial function in a mouse model for myopathy [30].

Similar to mTORC1, we also have evidence that mTORC2 is activated in response to training in DUC but not in DUhTP mice since AKT was specifically activated in trained DUC mice compared to sedentary DUC mice or exercised DUhTP mice, and activation of AKT at serine 473 is a marker of mTORC2 activity [31]. Activation of mTORC2, in turn, is required for AKT/c-myc-dependent hypertrophic muscle growth in response to physical exercise [32]. However, we have no reason to postulate hormone-dependent activation of mTORC2 in DUC in response to exercise because local or systemic IGF1 concentrations were not increased in trained DUC mice. Accordingly, we have to assume, so far, unknown factors are involved in exercise-related mTORC2 activation. Notably, in sedentary DUhTP mice, elevated expression and higher levels of active PTEN, both in terms of total expression and reduced inactivation by protein phosphorylation of PTEN, could be related to the lack of mTORC2 activation in DUhTP mice in response to training. Inhibition of PTEN improved muscle function in Duchenne muscular dystrophy [33], and aerobic exercise had a negative effect on the expression of PTEN in mice [34]. Just recently, moderate training in rats was shown to block expression of PTEN, and it was discussed that thereby an age-related loss of muscle mass might be blocked on the level of the PI3K pathway [35,36]. Training also activated the p38 MAPK in the muscle of rats [36]. We identified activation of both PI3K and p38 MAPK in trained DUC mice but not in trained DUhTP mice, although we did not observe altered expression or activity of PTEN in response to exercise in our experimental system. While PI3K is thought to be related to hypertrophic growth and protein translation, as discussed earlier, p38 MAPK is a mediator of energy metabolic adaptation in response to exercise [37]. Accordingly, p38 MAPK can activate PGC1α on the protein level by direct interaction [38]. Furthermore, p38 MAPK can induce gene expression of PGC1α and GLUT4 by indirect mechanisms, e.g., via MEF2 on the level of mRNA expression [39,40].

Additional candidate genes were identified in the muscle of unselected control mice controlled by exercise (Clock, Ncam1, Fgfr4, and Hbegf). For these candidates, specific roles have been suggested with respect to metabolic adaptation [41], muscle innervation [42], training responses [43], or muscle cell differentiation [44]. It is possible that decades of selection under avoidance of inbreeding have enriched multiple mechanisms related to superior running performance in DUhTP mice, which might also warrant separate studies in the future.

4.3. Effects of Phenotype-Selection on mRNA Expression Related to Metabolic Cell Signaling

Neither exercise-related activation of signal transduction (AKT, S6K, and p38 MAPK) nor expression of Clock, Ncam1, or other candidate genes described in control mice were identified in the muscle of DUhTP mice. Accordingly, we must assume other pathways and mechanisms genetically fixed by long-term selection in the marathon mouse model. In fact, in muscle, the coordinated downregulation of GH/IGF-signaling was accompanied by substantially increased mRNA expression of pentameric Ragulator complex components, and except for Sirt1, also of several sirtuin family members. Notably, both protein families are regulated by signals related to energy metabolism but not by endocrine growth factors. The Ragulator complex is composed of Lamtor 1 to 5 and is required for leucine-dependent activation of mTORC1 [45]. Intriguingly, the Ragulator complex also activates AMPK, and therefore, has been identified as a molecular "switch between anabolism and catabolism" [46]. Under high energy conditions, the Ragulator complex activates anabolic mTORC1 signaling, whereas, under conditions of low energy availability, catabolic AMPK is activated [46]. In DUC mice, AMPK was not activated in response to training in contrast to mTORC1 and mTORC2. Since we observed abrogated anabolic signaling by coordinated reduction of hormone-induced signal transduction and a lack of exercise-induced activation of mTORC1 in the muscle of DUhTP mice, we might interpret massive induction of Ragulator complex expression in a context of AMPK-related metabolic control in the muscle of DUhTP mice. However, the coordinated induction of gene expression for the pentameric Ragulator complex in the muscle of DUhTP mice did not correlate with elevated phospho-

rylation of AMPK under the experimental conditions of the present study. Both catalytic subunits (Prkaa1/2) from the AMPK protein complex were reduced, whereas one beta and one gamma subunit were increased (Prkab1, Prkag1) in DUhTP mice. Effects on exercise tolerance [47], glucose uptake [47], glycogen content [48], mitochondrial mass [47], fat oxidation [49], and intracellular lipid content [50] have been described for the alpha, beta, and gamma subunits of the AMPK complex. Based on the differential control of AMPK subunits in DUhTP mice, we may assume multiple effects on metabolic control in their muscle. However, the classical concept of mutual anabolic versus metabolic control cannot be described or confirmed in marathon mice. In future experiments, the potential effect of elevated Ragulator complex expression on AMPK activation could be studied under more strict energy restriction conditions because the selection experiment was characterized by higher running intensities compared to the training units applied here.

From the strong effects on the expression of sirtuins in muscle, we may assume adaptive responses on the level of energy metabolism and protein acetylation. Sirtuins are a group of deacetylases and ADP-ribosylases with multiple effects on the level of DNA, RNA, protein, or metabolites in different cellular compartments [51]. In elderly men, resistance exercise training increased serum levels of Sirt1, 3, and 6 [52]. Since this increase was associated with elevated serum levels of telomerase and PGC-1α, beneficial effects of exercise were discussed in a context with sirtuins and PGC-1α [52]. In muscles from DUhTP mice, sirtuin 1 expression was abrogated, not directly supporting a joint effect of Sirt1 and 3 on mitochondrial biogenesis as discussed in our review [53]. Instead, multiple effects of Sirt2 to 6 may be assumed in the muscle of DUhTP mice in response to long-term phenotype selection characterized by multiple repeats of selection originating from a genetic outbred background.

This study has several limitations. First of all, we were unable to assess the effects of selection and training in both sexes. This is related to the fact that male mice were used when the phenotype selection experiment started decades ago. Nevertheless, the hypothesis should also be tested in females in future studies. Future studies will also examine in-depth metabolic control by the insulin receptor and glucose metabolism in our model.

5. Conclusions

To conclude, we have identified centrally reduced Pou1f1 and Gh mRNA expression in the pituitary gland of marathon mice, which correlated with reduced IGF1 serum concentrations in sedentary DUhTP mice. In muscle of DUhTP, but not in unselected control mice, coordinate downregulation of multiple components from the mTORC1 and -2 pathways was observed, whereas expression of IGFBPs was elevated in muscle. Downregulation of hormone-dependent signaling pathways in DUhTP mice, as demonstrated on the level of mRNA expression, coincided with abrogated activation of mTORC2 (AKT) and mTORC1 (S6K), which was well-observed in control mice in response to training. Accordingly, results on the level of protein appear to support results from pathway analysis on the level of mRNA expression. Therefore, we may conclude that central downregulation of the somatotropic axis and local downregulation of hormone-dependent mTORC activity represent adaptations as a response to long-term selection for high running performance in DUhTP mice. The downregulation of the somatotropic axis in DUhTP mice suggests not only that the somatotropic axis is not required for improved running performance but that it even needs to be suppressed for improved running performance in mice.

Supplementary Materials: The following are available online at https://www.mdpi.com/article/10.3390/cells10123418/s1, Table S1: Effects of phenotype selection and endurance exercise on mRNA expression of other growth factors and receptors in the pituitary gland and muscle. Figure S1: Capillary immuno-electrophoresis (WES) spectra.

Author Contributions: Conceptualization, J.B., C.W. and A.H.; methodology, C.W. and N.T.; software, C.W. and N.T.; validation, C.W., D.O., C.C. and E.B.; formal analysis, C.W., C.C., E.B., M.W. and N.T.;

investigation, J.B.; resources, M.L., S.P., K.W. and U.K.Z.; data curation, C.W.; writing—original draft preparation, J.B., C.W. and A.H.; writing—review and editing, all authors; visualization, J.B., C.W. and M.W.; supervision, A.H.; project administration, J.B., C.W. and A.H. All authors have read and agreed to the published version of the manuscript.

Funding: This research received no external funding.

Institutional Review Board Statement: The study was conducted according to the guidelines of the Declaration of Helsinki, and approved by the Institutional Review Board of the Research Institute for Farm Animal Biology and by the State of Mecklenburg-Western Pomerania (State Office for Agriculture, Food Safety, and Fisheries; AZ 7221.3-1-014/17 (25 April 2017) and AZ 7221.3-1-064/19 (30 January 2020)).

Informed Consent Statement: Not applicable.

Data Availability Statement: All data are available in the present manuscript, in the Supplement, in referenced manuscripts [9], or upon the request from the corresponding author.

Acknowledgments: The authors want to thank Luong Chau, Annette Jugert, and the Lab Animal Facility technicians for their excellent support. We further express our gratitude to Anne-Marie Galow for support with Figure 2, developed using BioRender software.

Conflicts of Interest: The authors declare no conflict of interest.

References

1. Roth, J.; Glick, S.M.; Yalow, R.S.; Berson, S.A. Secretion of human growth hormone: Physiologic and experimental modification. *Metabolism* **1963**, *12*, 577–579.
2. Wideman, L.; Weltman, J.Y.; Hartman, M.L.; Veldhuis, J.D.; Weltman, A. Growth hormone release during acute and chronic aerobic and resistance exercise: Recent findings. *Sports Med.* **2002**, *32*, 987–1004. [CrossRef]
3. Liu, W.; Bretz, F.; Böhning, D.; Holt, R.; Böhning, W.; Guha, N.; Sönksen, P.; Cowan, D. Comparison of normal distribution-based and nonparametric decision limits on the GH-2000 score for detecting growth hormone misuse (doping) in sport. *Biom. J.* **2021**, *63*, 187–200. [CrossRef]
4. Holz, M.K.; Ballif, B.A.; Gygi, S.P.; Blenis, J. mTOR and S6K1 Mediate Assembly of the Translation Preinitiation Complex through Dynamic Protein Interchange and Ordered Phosphorylation Events. *Cell* **2005**, *123*, 569–580. [CrossRef] [PubMed]
5. Frystyk, J. Exercise and the growth hormone-insulin-like growth factor axis. *Med. Sci. Sports Exerc.* **2010**, *42*, 58–66. [CrossRef] [PubMed]
6. Zanconato, S.; Moromisato, D.Y.; Moromisato, M.Y.; Woods, J.; Brasel, J.A.; Leroith, D.; Roberts, C.T., Jr.; Cooper, D.M. Effect of training and growth hormone suppression on insulin-like growth factor I mRNA in young rats. *J. Appl. Physiol.* **1994**, *76*, 2204–2209. [CrossRef] [PubMed]
7. Spangenburg, E.E.; Le Roith, D.; Ward, C.W.; Bodine, S.C. A functional insulin-like growth factor receptor is not necessary for load-induced skeletal muscle hypertrophy. *J. Physiol.* **2008**, *586*, 283–291. [CrossRef] [PubMed]
8. Brenmoehl, J.; Walz, C.; Spitschak, M.; Wirthgen, E.; Walz, M.; Langhammer, M.; Tuchscherer, A.; Naumann, R.; Hoeflich, A. Partial phenotype conversion and differential trait response to conditions of husbandry in mice. *J. Comp. Physiol. B* **2018**, *188*, 527–539. [CrossRef]
9. Walz, C.; Brenmoehl, J.; Trakooljul, N.; Noce, A.; Caffier, C.; Ohde, D.; Langhammer, M.; Wimmers, K.; Ponsuksili, S.; Hoeflich, A. Control of Protein and Energy Metabolism in the Pituitary Gland in Response to Three-Week Running Training in Adult Male Mice. *Cells* **2021**, *10*, 736. [CrossRef]
10. Walz, M.; Höflich, C.; Walz, C.; Ohde, D.; Brenmoehl, J.; Sawitzky, M.; Vernunft, A.; Zettl, U.K.; Holtze, S.; Hildebrandt, T.B.; et al. Development of a Sensitive Bioassay for the Analysis of IGF-Related Activation of AKT/mTOR Signaling in Biological Matrices. *Cells* **2021**, *10*, 482. [CrossRef]
11. Schaufele, F.; West, B.L.; Reudelhuber, T. Somatotroph- and lactotroph-specific interactions with the homeobox protein binding sites in the rat growth hormone gene promoter. *Nucleic Acids Res.* **1990**, *18*, 5235–5243. [CrossRef] [PubMed]
12. Cohen, L.E.; Wondisford, F.E.; Radovick, S. Role of Pit-1 in the gene expression of growth hormone, prolactin, and thyrotropin. *Endocrinol. Metab. Clin. North. Am.* **1996**, *25*, 523–540. [CrossRef]
13. Kojima, M.; Hosoda, H.; Date, Y.; Nakazato, M.; Matsuo, H.; Kangawa, K. Ghrelin is a growth-hormone-releasing acylated peptide from stomach. *Nature* **1999**, *402*, 656–660. [CrossRef] [PubMed]
14. Gibney, J.; Healy, M.L.; Sönksen, P.H. The growth hormone/insulin-like growth factor-I axis in exercise and sport. *Endocr. Rev.* **2007**, *28*, 603–624. [CrossRef]
15. de Alcantara Borba, D.; da Silva Alves, E.; Rosa, J.P.P.; Facundo, L.A.; Costa, C.M.A.; Silva, A.C.; Narciso, F.V.; Silva, A.; de Mello, M.T. Can IGF-1 Serum Levels Really be Changed by Acute Physical Exercise? A Systematic Review and Meta-Analysis. *J. Phys. Act. Health* **2020**, *17*, 575–584. [CrossRef]

16. Philp, A.; Hamilton, D.L.; Baar, K. Signals mediating skeletal muscle remodeling by resistance exercise: PI3-kinase independent activation of mTORC1. *J. Appl. Physiol.* **2011**, *110*, 561–568. [CrossRef]
17. Hornberger, T.A.; Stuppard, R.; Conley, K.E.; Fedele, M.J.; Fiorotto, M.L.; Chin, E.R.; Esser, K.A. Mechanical stimuli regulate rapamycin-sensitive signalling by a phosphoinositide 3-kinase-, protein kinase B- and growth factor-independent mechanism. *Biochem. J.* **2004**, *380*, 795–804. [CrossRef]
18. Hamilton, D.L.; Philp, A.; MacKenzie, M.G.; Baar, K. A limited role for PI(3,4,5)P3 regulation in controlling skeletal muscle mass in response to resistance exercise. *PLoS ONE* **2010**, *5*, e11624. [CrossRef] [PubMed]
19. Marino, F.E.; Mbambo, Z.; Kortekaas, E.; Wilson, G.; Lambert, M.I.; Noakes, T.D.; Dennis, S.C. Advantages of smaller body mass during distance running in warm, humid environments. *Pflug. Arch.* **2000**, *441*, 359–367. [CrossRef] [PubMed]
20. Brenmoehl, J.; Ohde, D.; Albrecht, E.; Walz, C.; Tuchscherer, A.; Hoeflich, A. Browning of subcutaneous fat and higher surface temperature in response to phenotype selection for advanced endurance exercise performance in male DUhTP mice. *J. Physiol. B* **2017**, *187*, 361–373. [CrossRef]
21. Miyazaki, M.; Moriya, N.; Takemasa, T. Transient activation of mTORC1 signaling in skeletal muscle is independent of Akt1 regulation. *Physiol. Rep.* **2020**, *8*, e14599. [CrossRef] [PubMed]
22. Kotani, T.; Takegaki, J.; Tamura, Y.; Kouzaki, K.; Nakazato, K.; Ishii, N. Repeated bouts of resistance exercise in rats alter mechanistic target of rapamycin complex 1 activity and ribosomal capacity but not muscle protein synthesis. *Exp. Physiol.* **2021**, *106*, 1950–1960. [CrossRef]
23. Solsona, R.; Pavlin, L.; Bernardi, H.; Sanchez, A.M. Molecular Regulation of Skeletal Muscle Growth and Organelle Biosynthesis: Practical Recommendations for Exercise Training. *Int. J. Mol. Sci.* **2021**, *22*, 2741. [CrossRef]
24. Schoenfeld, B.J.; Ogborn, D.; Krieger, J.W. Dose-response relationship between weekly resistance training volume and increases in muscle mass: A systematic review and meta-analysis. *J. Sports Sci.* **2017**, *35*, 1073–1082. [CrossRef] [PubMed]
25. Wen, Y.; Alimov, A.P.; McCarthy, J.J. Ribosome Biogenesis is Necessary for Skeletal Muscle Hypertrophy. *Exerc. Sport Sci. Rev.* **2016**, *44*, 110–115. [CrossRef]
26. West, D.W.; Baehr, L.M.; Marcotte, G.R.; Chason, C.M.; Tolento, L.; Gomes, A.V.; Bodine, S.C.; Baar, K. Acute resistance exercise activates rapamycin-sensitive and -insensitive mechanisms that control translational activity and capacity in skeletal muscle. *J. Physiol.* **2016**, *594*, 453–468. [CrossRef]
27. Csibi, A.; Cornille, K.; Leibovitch, M.P.; Poupon, A.; Tintignac, L.A.; Sanchez, A.M.; Leibovitch, S.A. The translation regulatory subunit eIF3f controls the kinase-dependent mTOR signaling required for muscle differentiation and hypertrophy in mouse. *PLoS ONE* **2010**, *5*, e8994. [CrossRef] [PubMed]
28. Wang, L.; Harris, T.E.; Roth, R.A.; Lawrence, J.C., Jr. PRAS40 regulates mTORC1 kinase activity by functioning as a direct inhibitor of substrate binding. *J. Biol. Chem.* **2007**, *282*, 20036–20044. [CrossRef] [PubMed]
29. Sancak, Y.; Thoreen, C.C.; Peterson, T.R.; Lindquist, R.A.; Kang, S.A.; Spooner, E.; Carr, S.A.; Sabatini, D.M. PRAS40 is an insulin-regulated inhibitor of the mTORC1 protein kinase. *Mol. Cell* **2007**, *25*, 903–915. [CrossRef] [PubMed]
30. Civiletto, G.; Dogan, S.A.; Cerutti, R.; Fagiolari, G.; Moggio, M.; Lamperti, C.; Benincá, C.; Viscomi, C.; Zeviani, M. Rapamycin rescues mitochondrial myopathy via coordinated activation of autophagy and lysosomal biogenesis. *EMBO Mol. Med.* **2018**, *10*. [CrossRef]
31. Hresko, R.C.; Mueckler, M. mTOR.RICTOR is the Ser473 kinase for Akt/protein kinase B in 3T3-L1 adipocytes. *J. Biol. Chem.* **2005**, *280*, 40406–40416. [CrossRef] [PubMed]
32. Ogasawara, R.; Fujita, S.; Hornberger, T.A.; Kitaoka, Y.; Makanae, Y.; Nakazato, K.; Naokata, I. The role of mTOR signalling in the regulation of skeletal muscle mass in a rodent model of resistance exercise. *Sci. Rep.* **2016**, *6*, 31142. [CrossRef] [PubMed]
33. Yue, F.; Song, C.; Huang, D.; Narayanan, N.; Qiu, J.; Jia, Z.; Yuan, Z.; Oprescu, S.N.; Roseguini, B.T.; Deng, M.; et al. PTEN Inhibition Ameliorates Muscle Degeneration and Improves Muscle Function in a Mouse Model of Duchenne Muscular Dystrophy. *Mol. Ther.* **2021**, *29*, 132–148. [CrossRef] [PubMed]
34. Wang, D.; Wang, Y.; Ma, J.; Wang, W.; Sun, B.; Zheng, T.; Wei, M.; Sun, Y. MicroRNA-20a participates in the aerobic exercise-based prevention of coronary artery disease by targeting PTEN. *Biomed. Pharmacother.* **2017**, *95*, 756–763. [CrossRef]
35. Gao, H.E.; Wu, D.S.; Sun, L.; Yang, L.D.; Qiao, Y.B.; Ma, S.; Wu, Z.J.; Ruan, L.; Li, F.H. Effects of lifelong exercise on age-related body composition, oxidative stress, inflammatory cytokines, and skeletal muscle proteome in rats. *Mech. Ageing Dev.* **2020**, *189*, 111262. [CrossRef]
36. Gao, H.E.; Li, F.H.; Xie, T.; Ma, S.; Qiao, Y.B.; Wu, D.S.; Sun, L. Lifelong Exercise in Age Rats Improves Skeletal Muscle Function and MicroRNA Profile. *Med. Sci. Sports Exerc.* **2021**, *53*, 1873–1882. [CrossRef] [PubMed]
37. Bengal, E.; Aviram, S.; Hayek, T. p38 MAPK in Glucose Metabolism of Skeletal Muscle: Beneficial or Harmful? *Int. J. Mol. Sci.* **2020**, *21*, 6480. [CrossRef] [PubMed]
38. Fan, M.; Rhee, J.; St-Pierre, J.; Handschin, C.; Puigserver, P.; Lin, J.; Jäeger, S.; Erdjument-Bromage, H.; Tempst, P.; Spiegelman, B.M. Suppression of mitochondrial respiration through recruitment of p160 myb binding protein to PGC-1alpha: Modulation by p38 MAPK. *Genes Dev.* **2004**, *18*, 278–289. [CrossRef]
39. Michael, L.F.; Wu, Z.; Cheatham, R.B.; Puigserver, P.; Adelmant, G.; Lehman, J.J.; Kelly, D.P.; Spiegelman, B.M. Restoration of insulin-sensitive glucose transporter (GLUT4) gene expression in muscle cells by the transcriptional coactivator PGC-1. *Proc. Natl. Acad. Sci. USA* **2001**, *98*, 3820–3825. [CrossRef] [PubMed]

40. Zhao, M.; New, L.; Kravchenko, V.V.; Kato, Y.; Gram, H.; di Padova, F.; Olson, E.N.; Ulevitch, R.J.; Han, J. Regulation of the MEF2 family of transcription factors by p38. *Mol. Cell Biol.* **1999**, *19*, 21–30. [CrossRef]
41. Fukatsu, Y.; Noguchi, T.; Hosooka, T.; Ogura, T.; Kotani, K.; Abe, T.; Shibakusa, T.; Inoue, K.; Sakai, M.; Tobimatsu, K.; et al. Muscle-specific overexpression of heparin-binding epidermal growth factor-like growth factor increases peripheral glucose disposal and insulin sensitivity. *Endocrinology* **2009**, *150*, 2683–2691. [CrossRef]
42. Messi, M.L.; Li, T.; Wang, Z.M.; Marsh, A.P.; Nicklas, B.; Delbono, O. Resistance Training Enhances Skeletal Muscle Innervation without Modifying the Number of Satellite Cells or their Myofiber Association in Obese Older Adults. *J. Gerontol. A Biol. Sci. Med. Sci.* **2016**, *71*, 1273–1280. [CrossRef]
43. Adamovich, Y.; Dandavate, V.; Ezagouri, S.; Manella, G.; Zwighaft, Z.; Sobel, J.; Kuperman, Y.; Golik, M.; Auerbach, A.; Itkin, M.; et al. Clock proteins and training modify exercise capacity in a daytime-dependent manner. *Proc. Natl. Acad. Sci. USA* **2021**, *118*. [CrossRef]
44. Zhang, W.; Xu, Y.; Zhang, L.; Wang, S.; Yin, B.; Zhao, S.; Li, X. Synergistic effects of TGFβ2, WNT9a, and FGFR4 signals attenuate satellite cell differentiation during skeletal muscle development. *Aging Cell* **2018**, *17*, e12788. [CrossRef]
45. Bar-Peled, L.; Schweitzer, L.D.; Zoncu, R.; Sabatini, D.M. Ragulator Is a GEF for the Rag GTPases that Signal Amino Acid Levels to mTORC1. *Cell* **2012**, *150*, 1196–1208. [CrossRef]
46. Zhang, C.S.; Jiang, B.; Li, M.; Zhu, M.; Peng, Y.; Zhang, Y.L.; Wu, Y.Q.; Li, T.Y.; Liang, Y.; Lu, Z.; et al. The lysosomal v-ATPase-Ragulator complex is a common activator for AMPK and mTORC1, acting as a switch between catabolism and anabolism. *Cell Metab.* **2014**, *20*, 526–540. [CrossRef]
47. O'Neill, H.M.; Maarbjerg, S.J.; Crane, J.D.; Jeppesen, J.; Jørgensen, S.B.; Schertzer, J.D.; Shyroka, O.; Kiens, B.; van Denderen, B.J.; Tarnopolsky, M.A.; et al. AMP-activated protein kinase (AMPK) beta1beta2 muscle null mice reveal an essential role for AMPK in maintaining mitochondrial content and glucose uptake during exercise. *Proc. Natl. Acad. Sci. USA* **2011**, *108*, 16092–16097. [CrossRef] [PubMed]
48. Costford, S.R.; Kavaslar, N.; Ahituv, N.; Chaudhry, S.N.; Schackwitz, W.S.; Dent, R.; Pennacchio, L.A.; McPherson, R.; Harper, M.E. Gain-of-function R225W mutation in human AMPKgamma(3) causing increased glycogen and decreased triglyceride in skeletal muscle. *PLoS ONE* **2007**, *2*, e903. [CrossRef] [PubMed]
49. Steinberg, G.R.; Michell, B.J.; van Denderen, B.J.; Watt, M.J.; Carey, A.L.; Fam, B.C.; Andrikopoulos, S.; Proietto, J.; Görgün, C.Z.; Carling, D.; et al. Tumor necrosis factor alpha-induced skeletal muscle insulin resistance involves suppression of AMP-kinase signaling. *Cell Metab.* **2006**, *4*, 465–474. [CrossRef]
50. Wu, W.; Xu, Z.; Zhang, L.; Liu, J.; Feng, J.; Wang, X.; Shan, T.; Wang, Y. Muscle-specific deletion of Prkaa1 enhances skeletal muscle lipid accumulation in mice fed a high-fat diet. *J. Physiol. Biochem.* **2018**, *74*, 195–205. [CrossRef] [PubMed]
51. Dali-Youcef, N.; Lagouge, M.; Froelich, S.; Koehl, C.; Schoonjans, K.; Auwerx, J. Sirtuins: The 'magnificent seven', function, metabolism and longevity. *Ann. Med.* **2007**, *39*, 335–345. [CrossRef] [PubMed]
52. Hooshmand-Moghadam, B.; Eskandari, M.; Golestani, F.; Rezae, S.; Mahmoudi, N.; Gaeini, A.A. The effect of 12-week resistance exercise training on serum levels of cellular aging process parameters in elderly men. *Exp. Gerontol.* **2020**, *141*, 111090. [CrossRef] [PubMed]
53. Brenmoehl, J.; Hoeflich, A. Dual control of mitochondrial biogenesis by sirtuin 1 and sirtuin 3. *Mitochondrion* **2013**, *13*, 755–761. [CrossRef] [PubMed]

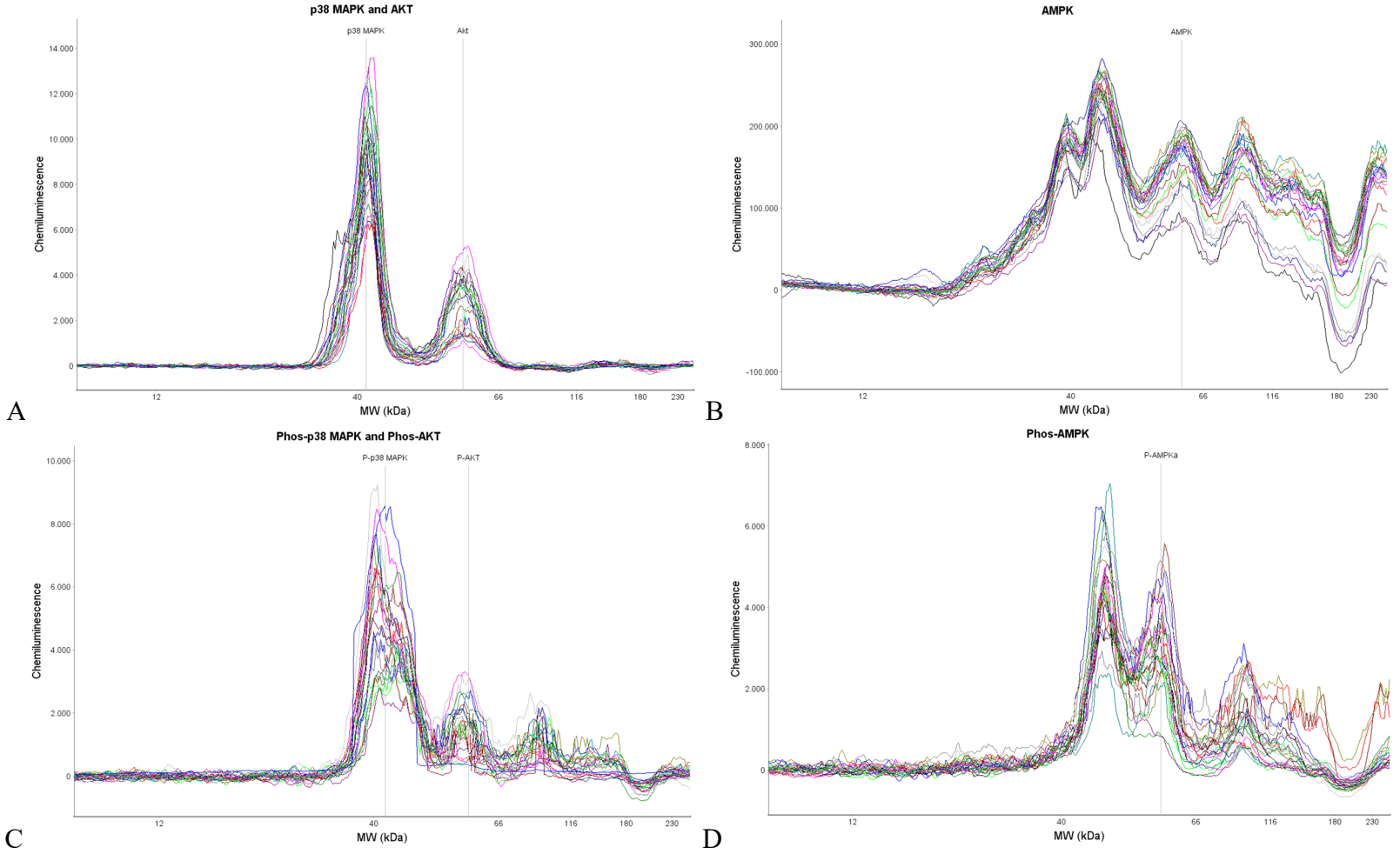

Supplement Figure 1 Effects of phenotype selection and endurance exercise on protein expression and phosphorylation (Phos) of AKT and p38 MAPK (A and C), as well as AMPK (B and D) in Musculus rectus femoris. The analysis was performed by capillary immuno-electrophoresis (WES). The WES spectra were created by Protein Simple Software Compass and show the chemiluminescence for every single capillary. Analysis and peak finding was performed in the software Compass with the following settings for peak finding: For AKT and p38 (phosphorylated and total): Threshold 10.0, Width 9.0, area calculation by Gaussian Fit; for AMPK (phosphorylated and total): Threshold 10.0, Width 6.0, area calculation by Dropped Lines. The results of spectra evaluations are shown in Figure 3. Abbreviations are mentioned in Tables 1-3.

Supplemental Table1. Effects of phenotype selection and endurance exercise on mRNA expression of other growth factors and receptors in the pituitary gland and muscle. The selection and exercise-mediated effects are presented as logarithmic fold change (log2FC) with corresponding false discovery rate (FDR) in the pituitary gland (left) and skeletal muscle (right) in four comparison groups. Significant regulations below a threshold of FDR ≤ 0.1 are marked in red (upregulated) or green (downregulated) and below an FDR ≤ 0.05 in bold.

	Gene ID		Expression in the pituitary gland				Expression in skeletal muscle			
			DUhTP vs DUC		DUC	DUhTP	DUhTP vs DUC		DUC	DUhTP
			sed	trained	trained vs sed		sed	trained	trained vs sed	
Growth factors and associated genes	Gap43	log2FC	**0.856**	0.232	0.637	0.013				
		FDR	**0.017**	0.553	0.134	1.000				
	Sp1	log2FC	-0.074	0.221	-0.185	0.110	**-0.448**	**-0.575**	-0.225	**-0.352**
		FDR	0.733	0.112	0.283	1.000	**0.000**	**0.000**	0.429	**0.021**
	Atg13	log2FC	-0.113	-0.130	0.018	0.001	**-0.257**	-0.172	0.012	0.097
		FDR	0.482	0.305	0.931	1.000	**0.011**	0.089	0.986	0.523
	Eif4e3	log2FC	-0.260	-0.151	-0.113	-0.004	-0.005	**-0.250**	0.148	-0.097
		FDR	0.069	0.270	0.514	1.000	0.976	**0.041**	0.691	0.616
	Foxo1	log2FC	0.090	0.134	-0.098	-0.054	-0.339	**0.602**	0.000	**0.941**
		FDR	0.719	0.450	0.673	1.000	0.223	**0.017**	1.000	**0.001**
	Ulk1	log2FC	-0.068	-0.003	-0.062	0.003	**-0.230**	-0.021	-0.101	0.107
		FDR	0.724	0.987	0.733	1.000	**0.044**	0.872	0.801	0.524
	Il18	log2FC	0.336	**0.357**	-0.042	-0.021	0.403	0.293	0.083	-0.027
		FDR	0.095	**0.044**	0.890	1.000	0.320	0.460	0.968	0.971
	Il18r1	log2FC	**1.641**	**1.492**	-0.035	-0.184				
		FDR	**0.000**	**0.000**	0.973	1.000				
	Cxcl1	log2FC	**-2.160**	**-1.971**	0.413	0.602				
		FDR	**0.011**	**0.010**	0.708	1.000				
	Cxcl13	log2FC	**-1.062**	**-0.894**	-0.111	0.058	-0.155	-0.082	0.888	0.960
		FDR	**0.010**	**0.023**	0.863	1.000	0.820	0.888	0.461	0.154
	Cxcl14	log2FC	-0.249	**-0.488**	0.086	-0.154	0.289	0.224	0.218	0.153
		FDR	0.207	**0.002**	0.725	1.000	0.086	0.177	0.627	0.530
	Nrtn	log2FC	0.212	**-0.923**	**0.929**	-0.206	**0.785**	0.436	0.278	-0.071
		FDR	0.728	**0.012**	**0.043**	1.000	**0.013**	0.168	0.819	0.897
	Ret	log2FC	**-0.756**	**-1.004**	0.378	0.130	**-0.610**	-0.215	0.010	0.405
		FDR	**0.016**	**0.000**	0.317	1.000	**0.001**	0.287	0.993	0.104
	Ncam1	log2FC	-0.103	**0.463**	-0.175	**0.392**	-0.564	**-1.360**	**1.307**	0.511
		FDR	0.580	**0.000**	0.284	**0.030**	0.121	**0.000**	**0.006**	0.280
	Muc15	log2FC	**2.720**	**2.788**	-0.400	-0.333				
		FDR	**0.000**	**0.000**	0.720	1.000				
	Npy	log2FC	**2.440**	0.779	**2.212**	0.551				
		FDR	**0.011**	0.401	**0.050**	1.000				
	Stat5a	log2FC	-0.173	**-0.566**	-0.003	-0.396	**0.342**	**0.337**	-0.180	-0.185
		FDR	0.480	**0.001**	0.994	0.353	**0.019**	**0.019**	0.683	0.365
	Fgf15	log2FC	-0.767	**1.439**	-0.629	1.577				
		FDR	0.351	**0.014**	0.444	0.161				
	Fgf22	log2FC	**0.863**	0.650	-0.004	-0.218				
		FDR	**0.038**	0.107	0.995	1.000				
	Fgf23	log2FC	1.161	**1.238**	0.012	0.088				
		FDR	0.070	**0.028**	0.993	1.000				
	Fgf13	log2FC	-0.069	0.238	0.020	0.327	-0.182	**-0.502**	0.118	-0.202
		FDR	0.892	0.441	0.972	1.000	0.092	**0.000**	0.717	0.136
	Fgf20	log2FC	0.442	-0.661	0.544	-0.560	0.652	**1.107**	-0.769	-0.314
		FDR	0.481	0.173	0.347	1.000	0.146	**0.012**	0.488	0.632
	Fgf6	log2FC					-0.384	**-0.446**	0.044	-0.018
		FDR					0.086	**0.036**	0.969	0.970
	Fgfbp1	log2FC	**-2.349**	-0.049	-2.033	0.267	**2.175**	**2.751**	-0.892	-0.316
		FDR	**0.018**	0.969	0.075	1.000	**0.001**	**0.000**	0.643	0.759
	Fgfr2	log2FC	0.145	0.316	-0.028	0.143	0.177	**0.842**	-0.380	0.285
		FDR	0.713	0.228	0.951	1.000	0.709	**0.032**	0.800	0.628

	Fgfr4	log2FC	**1.241**	0.559	0.965	0.283	**1.001**	-0.228	**1.097**	-0.132
		FDR	**0.004**	0.179	0.070	1.000	**0.001**	0.481	**0.012**	0.800
	Fgfrl1	log2FC	**0.416**	-0.019	0.346	-0.089	**0.437**	**0.341**	0.042	-0.053
		FDR	**0.040**	0.941	0.133	1.000	**0.002**	**0.015**	0.953	0.832
	Fgfr1op2	log2FC	**-0.194**	-0.041	-0.070	0.083	**-0.242**	**-0.410**	-0.123	**-0.291**
		FDR	**0.043**	0.701	0.565	1.000	**0.028**	**0.000**	0.718	**0.026**
	Egfr	log2FC	-0.035	**0.407**	-0.363	0.080	**-0.548**	-0.271	-0.041	0.236
		FDR	0.914	**0.013**	0.080	1.000	**0.002**	0.129	0.962	0.342
	Egflam	log2FC	0.128	**0.713**	**-0.468**	0.116	**0.419**	**0.424**	0.141	0.146
		FDR	0.625	**0.000**	**0.033**	1.000	**0.002**	**0.001**	0.761	0.464
	Megf10	log2FC	**-1.463**	**-1.023**	-0.585	-0.145	-0.526	**-1.918**	0.731	-0.661
		FDR	**0.000**	**0.000**	0.123	1.000	0.285	**0.000**	0.488	0.304
	Hbegf	log2FC	-0.206	**-0.727**	0.423	-0.097	0.350	-0.041	**0.956**	**0.566**
		FDR	0.624	**0.008**	0.220	1.000	0.091	0.859	**0.000**	**0.014**
Estrogen receptors	Esr1	log2FC	**-0.317**	0.190	**-0.454**	0.053	-0.175	-0.080	-0.138	-0.043
		FDR	**0.022**	0.159	**0.008**	1.000	0.279	0.628	0.794	0.875
	Esr2	log2FC	-1.295	**-2.302**	0.657	-0.351				
		FDR	0.096	**0.000**	0.368	1.000				

Abbreviations: DUhTP: mouse line selected for high treadmill performance; DUC: unselected control mouse line; sed: sedentary; vs: versus; Gap43: Growth associated protein; Sp1: Transcription factor Sp1; Atg13: Autophagy-related protein; Eif4e3: Eukaryotic translation initiation factor 4e-3; Foxo1: Forkhead box protein O1; Ulk1: Serin/threonine-protein kinase ULK1; Il18: Interleukin-18; Il18r1: Il18 receptor 1; Cxcl: C-X-C motif chemokine; Nrtn: Neurturin; Ret: Proto-oncogene tyrosine-protein kinase receptor Ret; Ncam1: Neural cell adhesion molecule 1; Muc15: Mucin-15; Npy: Neuropeptide Y; Stat5a: Signal transducer and activator of transcription 5a; Fgf: Fibroblast growth factor; Fgfbp: Fgf binding protein; Fgfr: Fgf receptor; Fgfrl: Fgf receptor-like; Fgfr1op2: Fgfr1 oncogene partner 2; Egfr: Epidermal growth factor receptor; Egflam: Pikachurin; Megf10: Multiple epidermal growth factor-like domains protein 10; Hbegf: Heparin-binding Egf-like growth factor; Esr: estrogen receptor

cells

MDPI

Article

Metabolic Pathway Modeling in Muscle of Male Marathon Mice (DUhTP) and Controls (DUC)—A Possible Role of Lactate Dehydrogenase in Metabolic Flexibility

Julia Brenmoehl [1,*], Elli Brosig [1,2], Nares Trakooljul [1], Christina Walz [1], Daniela Ohde [1], Antonia Noce [1,3], Michael Walz [1], Martina Langhammer [4], Stefan Petkov [5], Monika Röntgen [5], Steffen Maak [5], Christina E. Galuska [6], Beate Fuchs [6], Björn Kuhla [7], Siriluck Ponsuksili [1], Klaus Wimmers [1] and Andreas Hoeflich [1,*]

1 Institute of Genome Biology, Research Institute for Farm Animal Biology (FBN), Wilhelm-Stahl-Allee 2, 18196 Dummerstorf, Germany
2 Department of Neurology, Neuroimmunological Section, University Medicine Rostock, Gehlsheimer Str. 20, 18147 Rostock, Germany
3 Department of Animal Genomics, Centre for Research in Agricultural Genomics (CRAG), Campus de la Universitat Autònoma de Barcelona, 08193 Cerdanyola, Spain
4 Lab Animal Facility, Institute of Genetics and Biometry, Research Institute for Farm Animal Biology (FBN), Wilhelm-Stahl-Allee 2, 18196 Dummerstorf, Germany
5 Institute of Muscle Biology and Growth, Research Institute for Farm Animal Biology (FBN), Wilhelm-Stahl-Allee 2, 18196 Dummerstorf, Germany
6 Core Facility Metabolomics, Research Institute for Farm Animal Biology (FBN), Wilhelm-Stahl-Allee 2, 18196 Dummerstorf, Germany
7 Institute of Nutrition, Research Institute for Farm Animal Biology (FBN), Wilhelm-Stahl-Allee 2, 18196 Dummerstorf, Germany
* Correspondence: brenmoehl@fbn-dummerstorf.de (J.B.); hoeflich@fbn-dummerstorf.de (A.H.)

check for updates

Citation: Brenmoehl, J.; Brosig, E.; Trakooljul, N.; Walz, C.; Ohde, D.; Noce, A.; Walz, M.; Langhammer, M.; Petkov, S.; Röntgen, M.; et al. Metabolic Pathway Modeling in Muscle of Male Marathon Mice (DUhTP) and Controls (DUC)—A Possible Role of Lactate Dehydrogenase in Metabolic Flexibility. *Cells* **2023**, *12*, 1925. https://doi.org/10.3390/cells12151925

Academic Editor: Michael Deschenes

Received: 13 June 2023
Revised: 18 July 2023
Accepted: 21 July 2023
Published: 25 July 2023

Abstract: In contracting muscles, carbohydrates and fatty acids serve as energy substrates; the predominant utilization depends on the workload. Here, we investigated the contribution of non-mitochondrial and mitochondrial metabolic pathways in response to repeated training in a polygenic, paternally selected marathon mouse model (DUhTP), characterized by exceptional running performance and an unselected control (DUC), with both lines descended from the same genetic background. Both lines underwent three weeks of high-speed treadmill training or were sedentary. Both lines' muscles and plasma were analyzed. Muscle RNA was sequenced, and KEGG pathway analysis was performed. Analyses of muscle revealed no significant selection-related differences in muscle structure. However, in response to physical exercise, glucose and fatty acid oxidation were stimulated, lactate dehydrogenase activity was reduced, and lactate formation was inhibited in the marathon mice compared with trained control mice. The lack of lactate formation in response to exercise appears to be associated with increased lipid mobilization from peripheral adipose tissue in DUhTP mice, suggesting a specific benefit of lactate avoidance. Thus, results from the analysis of muscle metabolism in born marathon mice, shaped by 35 years (140 generations) of phenotype selection for superior running performance, suggest increased metabolic flexibility in male marathon mice toward lipid catabolism regulated by lactate dehydrogenase.

Keywords: glycogen; lactate; pathway analysis; skeletal muscle; treadmill training

1. Introduction

Energy supply during physical exercise relies on the involvement of phosphagen, glycolytic, and oxidative energy pathways. Whether energy (ATP) is generated more through oxygen- and mitochondria-independent anaerobic or oxidative energy fluxes depends on the intensity and duration of physical activity, training status, nutrition, sex,

age, and ambient conditions [1]. Strength training with short bursts of maximal work, such as supramaximal sprinting or field sports, relies primarily on phosphocreatine and glycogen catabolism associated with anaerobic glycolysis since these processes have high ATP production rates [2]. In contrast, continuous endurance activities, such as running, cycling, or swimming, rely primarily on oxidative (aerobic) phosphorylation of carbohydrates and fatty acids, providing a higher ATP production capacity [2]. During the early stages of aerobic exercise, muscle glycogen and intramuscular fatty acids are oxidized, and, with prolonged duration, peripheral glucose and fatty acids are taken up and metabolized [3].

Thus, substrates for anaerobic and aerobic glycolytic metabolism can be glycogen, the glucose reservoir stored in muscle fibers, or glucose circulating in the blood, taken up by muscle via constitutive glucose transporters 1 (GLUT1) or GLUT4 transporters, which are mobilized from intracellular storage vesicles to the plasma membrane after insulin stimulation. The anaerobic glycolysis product lactate, converted from pyruvate by lactate dehydrogenase, oxidizing NADH, is produced primarily in glycolytic fibers [4] and is increasingly exported from cells with the onset of muscle contraction [5]. According to the cell–cell lactate shuttle concept [6], lactate serves as a primary energy substrate for oxidative muscle fibers within a working muscle [7] or other lactate-consuming organs such as the heart, brain, liver, kidneys, and adipose tissue [8]. Lactate uptake occurs when lactate has been metabolized in the cell, and the lactate breakdown rate exceeds the rate of lactate production [9]. Thus, the blood lactate level reflects the balance between lactate production and degradation.

Lactate export and import are accomplished by specific bidirectional monocarboxylate transporters (MCTs) in symport with protons [10], with MCT4 responsible for lactate export from glycolytic fibers [11] and MCT1 for the import into type I fibers, enabling the lactate uptake for glycolytic oxidation [12]. In this process, lactate is first converted to pyruvate by cytosolic lactate dehydrogenase, which is then transported into the mitochondria by mitochondrial pyruvate carriers 1 (MPC1) and 2 (MPC2) [13]. It has also been described that lactate can be transported directly into mitochondria via mitochondrial MCT1 transporters and then converted by mitochondrial lactate dehydrogenase to pyruvate [14], which is then further metabolized and fed into the TCA cycle and respiratory chain to generate ATP for muscle contractions. However, this concept of intracellular lactate shuttling [6] is controversially discussed due to methodological discrepancies in proteolytic tissue processing, according to Cruz et al. [15].

Quantitatively more ATP molecules are produced during fatty acid oxidation (FAO). Fatty acids originate from intramuscular and peripheral fat depots. Transport of fatty acids into the muscle cell occurs by diffusion or is facilitated by inducible CD36 together with fatty-acid-binding proteins (FABPs) or the fatty acid transport protein FATP [16]. Fatty acids are activated in the muscle cell cytosol before being transported into mitochondria for complete oxidation.

Exercise intensity at the muscle level defines the substrate source for energy production [1,17]. During continuous cycling with a workload of 30% maximal oxygen uptake, glucose and free fatty acids contribute to substrate utilization. Glucose oxidation predominates for up to 90 min and is then surpassed by FAO [18]. Fatty acid oxidation is increased during low- and moderate-intensity endurance exercise, whereas carbohydrate oxidation is also preferred during marathons [19]. Maximum fat oxidation occurs at 64% maximal oxygen uptake [20], whereas during exercise above 80% maximal oxygen uptake, fat oxidation decreases, and plasma glucose and muscle glycogen utilization predominate [17]. The physiological adaptability to respond appropriately to increasing energy demands and fuel availability (e.g., in response to exercise or fasting) at the level of substrate recognition, transport, utilization, and storage level is indicative of high metabolic flexibility [21,22]. Training-associated metabolic flexibility is regulated by transcription factors involved in the transcription of metabolic genes relevant to oxidative phosphorylation, glucose and lipid transport, or mitochondrial biogenesis [22]. A targeted and timely switch to the oxidative

degradation of energy-rich fatty acids could not only contribute to the long-term energy supply of the muscle, but also positively affect the mobilization of storage lipids.

The marathon mouse model DUhTP, generated by long-term paternal selection for high treadmill performance [23], is characterized by superior forced running performance but also by increased lipid accumulation. In response to voluntary moderate physical activity, increased lipid turnover has been observed in the liver [24,25] and adipose tissue [26], particularly subcutaneous fat [26,27], suggesting greater metabolic flexibility toward lipid metabolism in this mouse model. In this work, we used the marathon mice and a control strain, both derived from the same genetic background, to perform three weeks of treadmill training at an intensive speed that favors glycolytic utilization. We hypothesized that the marathon mice rely on a lipid-based metabolism despite the high speed and investigated the differences in energy metabolism in the muscles of both strains at the molecular and biochemical levels. Muscle energy metabolism was compared between marathon mice and unselected controls (genetic model), between physically active and sedentary animals of one strain (experimental model), and between trained animals of both strains (genetic × experimental model), respectively, to identify selection-related adaptations in carbohydrate- and especially lipid-based energy metabolism and to further relate them to the increased lipid turnover in subcutaneous fat observed in marathon mice. The present study discusses the results of molecular pathway modeling in muscle concerning systemic or global biomarkers of energy metabolism.

2. Materials and Methods

2.1. Animals and Experimental Design and Sample Collection

All animal experiments were performed in the mouse facility of the Research Institute for Farm Animal Biology in Dummerstorf, Germany. The experiments were approved by our internal institutional review board and were conducted following national and international animal welfare guidelines (Animal Welfare Act (TierSchG); AZ 7221.3.1.014/17 and AZ 7221.3-1-064/19). We used the non-inbred mouse line DUC, generated in the 1970s from a polygenic base population without phenotype selection [28], and the selection line DUhTP [23]. This line was paternally selected for high treadmill performance starting eleven years later from the unselected control line for about 140 generations and is now maintained as a conservation line. A recently published study describes the selection procedure in more detail [29]. Nevertheless, in brief, in each generation, males completed a submaximal run after mating, avoiding inbreeding, to identify the best runners and select their offspring as the next generation's parents. This generated a non-inbred mouse line characterized by exceptional running ability without prior training. After around 140 generations, the DUhTP line showed a 3–4 times longer running distance than the unselected control.

Male animals of generations 141 and 151 (DUhTP) and 185 and 196 (DUC) were used in this study. The animals were housed in the SPF barrier unit in polysulfone cages of 267 × 207 × 140 mm (H-Temp PSU, Type II, Eurostandard Tecniplast, Hohenpeißenberg, Germany) in compliance with hygiene management and health surveillance according to FELASA recommendations. The housing conditions of the mice were defined by a 12 hlight-dark cycle (room temperature = 22.5 °C ± 0.2 °C, humidity = 45–60%), and the animals had free access to autoclaved Ssniff® M-Z food (12 kJ% fat, 27 kJ% protein, 61 kJ% carbohydrates; gross energy 16.7 MJ/kg; Ssniff-Spezialdiäten GmbH, Soest, Germany) and water.

After weaning, males of both lines were kept in pairs in one cage until 48 days of age, when they were randomly divided into two groups and housed in individual cages. From 49 to 70 days of age, a part (n = 16 per generation) of the animals completed a fixed 3-week exercise program ("trained") [30] on a computer-controlled treadmill (TSE company), while the remaining animals (n = 10) remained in their cages and served as a control group ("sedentary", "sed"). Food consumption and body weights of the mice during this experiment are summarized in the supplement (Table S1). Since the mice are

characterized by a different running performance [31], we adapted the training duration to the running capacity of each strain in order to challenge the animals equally. We based this on the completed submaximal temporal running performance of previous generations (DUhTP: 133 min, DUC: 66 min) [31]. We chose approximately 23% of the previous average submaximal running duration as the training duration and accordingly estimated 30 min and 15 min per training session for the DUhTP and control males, respectively. The training was conducted during the light phase between 8 and 9 am, five days per week for three weeks. After an initial run and a two-day rest, regular training (5× per week, 15/30 min, 0% incline) was started. For this, the mice were exposed to an initial speed of 0.2 m/s for 20 s, then to a speed of 0.36 m/s for 160 s, followed by a final speed period. The final speed up to 0.5 m/s (DUhTP) and 0.42 m/s (DUC) was reached after a series of gradual weekly increases over time (detailed study design published in [30]). If an animal did not perform on the motorized treadmill, the run was stopped for that animal. If the same animal also did not perform the next day, it was excluded from the experiment. Animals with possible injuries were also excluded from the experiment.

At 70 days of age, the animals were sacrificed by decapitation either after the last running session or in a sedentary state. Thus, we ensured that the influence of the current treadmill run with the background of three weeks of training could be investigated. Plasma or serum was collected from the trunk blood and stored at −20 °C. Tissues (liver, rectus femoris muscle, pituitary gland, epididymal, and posterior subcutaneous fat) were removed, weighed, shock-frozen in liquid nitrogen, and stored at −70 °C for subsequent analysis.

2.2. Immunohistochemical Evaluation of Musculus rectus femoris

Immunohistochemistry was performed on the *Musculus rectus femoris* (Mrf) of seven (DUC sed) to eight animals per group (DUhTP sed, DUhTP trained, DUC trained), as described by Rehfeldt et al. [32]. Briefly, 10 µm cross-sections were cut at the end of the proximal origin tendon, and the metabolic fiber types (red, intermediate, white) were stained using NADH-tetrazolium reductase. The muscular cross-sectional area (CSA), and the fibers over an area of 3.316 mm^2 (approximately 32% of the total CSA) were determined separately by image analysis (TEMA v1.00, Scan Beam APS, Hadsund, Denmark). In these analyzed areas, a total of four fields of view (representative images for one animal per group are shown in Figure S2c), 100–150 muscle fibers each in the light (superficial) and dark (profound) areas were evaluated for the distribution and CSA of the red, intermediate, and white fibers. Fat content was analyzed by using Oil Red O (Sigma-Aldrich, Taufkirchen, Germany). Therefore, the 10 µm cross-sections were fixed in 4% formal calcium fixative for 5 min, washed in aqua dest. for another 5 min, incubated with Oil Red O (0.5% wt/vol dissolved in 99% isopropanol and diluted with 4/6 parts H_2O before use), and washed in aqua dest., both for another 15 min.

2.3. RNA Isolation, Next-Generation Sequencing (NGS), and Differential Gene Expression Analysis

Total RNA was extracted from Mrf tissue samples using Trizol (Sigma-Aldrich) and treated with DNase I to eliminate DNA contamination. Testing of RNA quality, enrichment and fragmentation of RNA, reverse transcription into cDNA, and DNA library generation were performed as previously described [30]. The normalized multiplexed DNA libraries with a 0.5% PhiX control were amplified clonally clustered with the cBot system and then sequenced at 2 × 101 bp in high-performance mode on a HiSeq2500 (Illumina, San Diego, CA, USA) in our sequencing facility at the Research Institute of Farm Animal Biology (FBN). Raw sequencing reads (fastq) were processed and mapped using Hisat2 and the mouse reference genome (GRCm38) as previously published [30]. The resulting gene count data (ArrayExpress accession E-MTAB-12072) were further analyzed for differentially expressed genes (DEGs; Table S3) using edgeR and R dependency packages. Genes with low readings (count per million (cpm)) were excluded to obtain only genes with >0.5 cpm in at least four libraries. The edgeR standard parameters were applied with the option

trimmed mean of M values (TMM) considering library size and composition bias and the option estrimateGLMRobustDisp to estimate interlibrary variation. The glmFit and glmLRT functions implemented in edgeR were used for statistical testing of DEGs.

2.4. Validation by Fluidigm

RNASeq data were validated by 2-step reverse transcription-quantitative PCR using the Fluidigm technique [33] described in Walz et al., 2021 [30] with the following modifications. Nine DEGs with different read counts (cpm) were selected for this purpose; the primers used are listed in Table S2. For reverse transcription, 800 ng of RNA were used, and the cDNA concentration in the PCR to check primer quality ranged from 25 to 0.0125 ng. We calculated the relative expression of each primer-template combination and related it to four housekeeping genes (Actb, Pgk1, Rplp2, Rpl26) using Data Analysis Gene (DAG) expression software [34]. Group-independent correlation analysis was performed for each gene between RNA sequencing signals (cpm) and relative qPCR expression ($2^{-\Delta\Delta Ct}$) (Figure S1) after checking for outliers (ROUT method, Q = 0.1%) in GraphPad Prism V 9.4.1. Pearson's correlation coefficient and *p*-value were calculated and displayed.

2.5. Pathway Analysis

Significantly upregulated and downregulated DEGs (FDR < 0.05, Table S3) of the comparison groups DUhTP sed versus (vs.) DUC sed, DUhTP trained vs. DUC trained, DUhTP trained vs. DUhTP sed, and DUC trained vs. DUC sed were bioinformatically analyzed as previously described [30]. In order to understand which pathways were activated or silenced, enrichment analysis was performed separately for up- and downregulated genes of the DUhTP trained vs. DUC trained comparison (FDR < 0.05). For this purpose, the DAVID V6.8 software [35] was used with default threshold filters (EASE = 0.1, minimum gene count = 2; access date: 25 November 2022). To ensure stringency, the results of the enrichment analysis (KEGG pathways) were subjected to a multiple testing correction (adjusted *p*-value Benjamini < 0.05). The obtained list of KEGG pathways for the upregulated and downregulated DEGs is summarized in Table S4b, including the minimum gene number for each KEGG pathway. Since 423 significantly upregulated DEGs (Table S4b) are involved in the regulation of metabolic pathways, the significant DEGs (FDR < 0.05) from all comparison groups were entered into the Pathview software [36] to obtain graphical visualization of their regulation in the glycolysis, beta-oxidation, TCA cycle, and oxidative phosphorylation pathways (access date: 1 December 2022).

2.6. Determination of Enzyme Activities

Frozen muscle tissue samples (100 mg/per mouse) were powdered under liquid N_2 using a mortar and pestle. All powders were homogenized in a 1:20 (weight/volume) dilution of 0.01 M potassium phosphate buffer containing 150 mM potassium chloride, 5.8 mM monopotassium phosphate, 4.2 mM dipotassium phosphate, and 1 mM EDTA (pH = 6.9) and centrifuged (14,000× *g*, 15 min, 4 °C). The supernatants were used for further analysis. Creatine kinase (EC 2.7.3.2.) activity was measured at 37 °C in 1:400 diluted muscle homogenates using a commercial kit (CK-NAC-Hit kit, IFCC method, BIOMED Labordiagnostik GmbH, Oberschleißheim, Germany) according to the manufacturer's instructions. Enzyme activity of lactate dehydrogenase (LDH; EC 1.1.1.28) and isocitrate dehydrogenase (IDH; EC 1.1.1.42) was determined by using 0.19 mM NADH and 0.757 mM sodium pyruvate or 4 mM isocitrate, 3.3 mM $MnSO_4$, and 0.35 mM NADP, respectively, according to an adapted protocol (http://www.sigmaaldrich.com/life-science/metabolomics/enzyme-explorer/learning-center/assay-library.html, accessed on 25 September 2019). The protein suspension was used 1:20 diluted (LDH) or undiluted (IDH), respectively. All enzyme activities were determined on a Spectramax Plus384 spectrophotometer/plate reader (Molecular Devices Corporation, Sunnyvale, CA, USA) in technical triplicates per animal.

Furthermore, pyruvate dehydrogenase activity was evaluated using a kit from Abcam (ab109902, Cambridge, UK). For this purpose, protein lysates were isolated from 50 to

100 mg Mrf tissue powder according to the manufacturer's instructions, which were uniformly adjusted to 8 µg/µL muscle protein concentration in deviation from the instructions. Proteins were extracted by adding the detergent solution at a final dilution of 1/20. For each sample, 250 µg protein per well was added to the plate and incubated for three hours at room temperature. After recording the linear kinetics by the increase in absorbance in 30 min, the rate between the two time points (according to the instructions) was calculated and used to determine the PDH activity relative to the DUC sed rate (100%).

2.7. Determination of Plasma Glucose, Insulin, and Lactate

Glucose and insulin were determined in plasma using commercial kits (Glucose GOD-PAP:LT-GL 0251, Labor&Technik Eberhard Lehmann, Berlin, Germany; Ultra Sensitive Mouse Insulin ELISA Kit, Crystal Chem, Zaandam, The Netherlands) according to the manufacturer's protocol, with a reduced total approach for glucose. Plasma lactate levels were analyzed spectrophotometrically using a semi-automated analyzer (Abx Pentra 400, Horiba, Kyoto, Japan) and a commercial kit for L-lactate concentrations (A11A01721, Horiba).

2.8. Untargeted LC-MS/MS Analysis of Lipids and Fatty Acids in Serum

A total of 30 µL of serum was mixed with 120 µL of isopropanol for lipid extraction and 120 µL of methanol for small metabolite extraction, vortexed for 15 s, and centrifuged for 15 min at 4 °C and 15,800× *g*. The supernatant was transferred to an appropriate sample vial for further analysis. A QC pool was created from all extracted serum samples. After equilibration of the system with the QC samples, the samples were randomly analyzed using an ultra-high-performance liquid chromatography-tandem mass spectrometry (UHPLC-MS/MS) system (Vanquish UHPLC-system with heated electrospray ionization (HESI) QExactive plus Orbitrap mass spectrometer (Thermo Scientific, Waltham, MA, USA)) in the positive and negative ionization modes. MS data were acquired over a scan range of 100–1200 *m*/*z* with a full MS resolution of 70,000 and a data-dependent MS2 resolution of 17,500. Chromatographic separation of the lipids was performed on a reversed-phase column (Accucore Polar Premium 100 × 2.1 mm (2.6 µm) with guard column: Accucore Polar Premium 10 × 2.1 mm (2.6 µm); Thermo Scientific). The autosampler temperature was set to 10 °C and maintained throughout the measurements. Mobile phase A consisted of 60% acetonitrile, 10 mM ammonium formate, and 0.1% formic acid in ultrapure water, and mobile phase B consisted of 90% isopropanol, 10 mM ammonium formate, and 0.1% formic acid in ultrapure water. The gradient was 20–100% B in 8.5 min over a total run time of 15 min. The flow rate employed was 0.4 mL/min, and the column temperature was 55 °C. Chromatographic separation of the small metabolites was performed on a reversed-phase column (Accucore Polar Premium 100 × 2.1 mm (2.6 µm) with guard column: Hypercarb 10 × 2.1 mm; Thermo Scientific) at 45 °C. The temperature of the autosampler was 6 °C. Mobile phase A was 0.1% formic acid in ultrapure water, and mobile phase B was 0.1% formic acid in methanol. The components were separated at a 0.5 mL/min flow rate using the following gradient: 1–99% B in 12 min. Annotation and relative quantification of individual metabolic and lipid species were performed by Compound Discoverer 3.1 (Thermo Scientific) and Lipid Data Analyzer software from the University of Graz (Austria).

2.9. Determination of Muscular Glycogen Content

The quantitative muscle glycogen determination is based on Hassid and Abraham [37] and measures glucose, as reduced sugar, colorimetrically at 680 nm. For this purpose, 25–50 mg of muscle tissue were boiled for 20 min in 800 mL 30% KOH, cooled on ice, mixed with 1 mL 95% ethanol, brought to boiling, cooled again, and centrifuged for 15 min (750× *g*). The resulting pellet was dissolved in 1 mL H_2O, mixed with 1 mL ethanol, and centrifuged again. The pellet was then dissolved in 500 mL H_2O and 1 mL 0.2% anthrone reagent (0.2 g anthrone/100 mL 95% sulfuric acid) and boiled (10 min). After cooling, the solution was measured at 680 nm. Four determinations were performed per animal (n = 8) of each group, and the values were recalculated using a glucose standard series between

2–100 µg/mL or 10–500 mg/g sample weight. Glycogen content is expressed as mg/g wet tissue.

2.10. Statistical Analysis

Data analysis and graphs were performed using GraphPad Prism 9.4.1 (GraphPad Software, San Diego, CA, USA). The data could be considered as approximately normally distributed; outlier identification was performed using the GraphPad Prism 9.4.1 statistical analysis package. Different animal numbers were used for each analysis. Therefore, the sample number is noted in the figure legend for the respective result. All data were analyzed using two-way ANOVA with multiple comparisons, considering the two different mouse strains (DUhTP, DUC) and the two different treatments (sed, trained). The distribution of fiber types or areas of fiber types in the superficial and deep regions of mice's Mrfs were statistically evaluated using the linear model (lm in R) followed by the TukeyHSD post hoc test (TukeyHSD in R) to test the dependence between phenotype and the interaction of strain × treatment × muscle fiber type. The effect of training was calculated using the unpaired *t*-test with Welch correction. Data were presented as scatter plots with mean and standard deviation. Pearson correlation coefficients were calculated using GraphPad Prism 9.4.1 to determine the relationships between muscle mass and cross-sectional area (CSA). The effects and differences were considered significant at $p < 0.05$.

3. Results

3.1. Reduced Body and Muscle Weight in Response to Selection and Training in Marathon Mice

At 70 days of age, DUhTP mice had a significantly lower body weight than control mice, independent of training ($p < 0.0001$; Figure 1a). Physical activity decreased body weight ($p < 0.01$), as well as fat mass ($p < 0.005$), in particular epididymal (Figure 1b; $p < 0.05$) and posterior subcutaneous fat ($p < 0.06$), exclusively in DUhTP mice. Femoral muscle weights were significantly lower in sedentary DUhTP than in DUC mice ($p < 0.01$; Figure 1c). After three weeks of training, femoral muscle weight was reduced in DUhTP but not in DUC mice (Figure 1c, −10.8%, $p < 0.05$). As a result, femoral muscle weight differed by approximately 28% ($p < 0.0001$) between trained animals of both lines. However, the relative femoral muscle weight to body mass was approximately 1.28% in all groups.

In sedentary conditions, the cross-sectional area (CSA) of the Mrf was similar between the two lines, whereas in trained DUhTP mice, the CSA of the Mrf was smaller than in trained DUC mice (Figure 1d, −17%, $p < 0.05$). Interestingly, muscle mass and CSA were positively correlated in DUC (sed: Pearson coefficient r = 0.9; trained: r = 0.83, $p < 0.005$) but not in DUhTP mice. The number of fibers per mm^2 analyzed muscle region (see Method part) was not significantly different in sedentary mice of both lines (Figure 1e, DUhTP: 428.7 fibers/mm^2; DUC: 360.6 fibers/mm^2; $p = 0.087$). In contrast, trained DUhTP mice had significantly higher fiber numbers per mm^2 than trained DUC animals (434.7 fibers/mm^2 vs. 349.8 fibers/mm^2; $p < 0.05$; Figure 1e). Interestingly, regardless of the training status, the Mrfs of DUhTP mice appeared macroscopically darker (Figure S2a) and had significantly more mitochondria-rich fibers, i.e., more red and intermediate fibers, per mm^2 analyzed muscle region than DUC mice ($p < 0.01$; Figure 1f). In trained DUhTP's Mrfs, significantly more mitochondria-rich fibers were found than in trained DUC mice ($p < 0.05$). Intramuscular fat content in Mrf was not significantly different between sedentary and trained DUhTP and DUC mice (Figure S2b). However, an exercise-induced reduction in intramuscular fat content was observed in both lines ($p < 0.05$). The distribution of oxidative (red), glycolytic (white), and hybrid (intermediate) fibers in both superficial and profound areas of the Mrf (Figure S2c) was examined in all experimental groups. In both lines, significantly more glycolytic than intermediate or red fibers were detected in the superficial muscle region ($p < 0.0001$; Figure S2d). In the deep muscle region, more red (approximately 41%) than intermediate (approximately 29%) or white fibers (approximately 30%) were found in sedentary and trained DUhTP and sedentary DUC mice, respectively ($p < 0.05$; Figure S2d). In trained DUC mice, the fiber type percentage was similar (red: 36.3%, intermediate:

30.3%, white: 33.4%). In trained and sedentary animals of both lines, the average glycolytic fiber area was significantly larger than the intermediate or red fiber area in superficial and profound muscle regions ($p \leq 0.05$; Figure S2e). Control animals had a higher mean glycolytic fiber area than DUhTP animals in both training conditions in the deep muscle region ($p < 0.01$; Figure S2e).

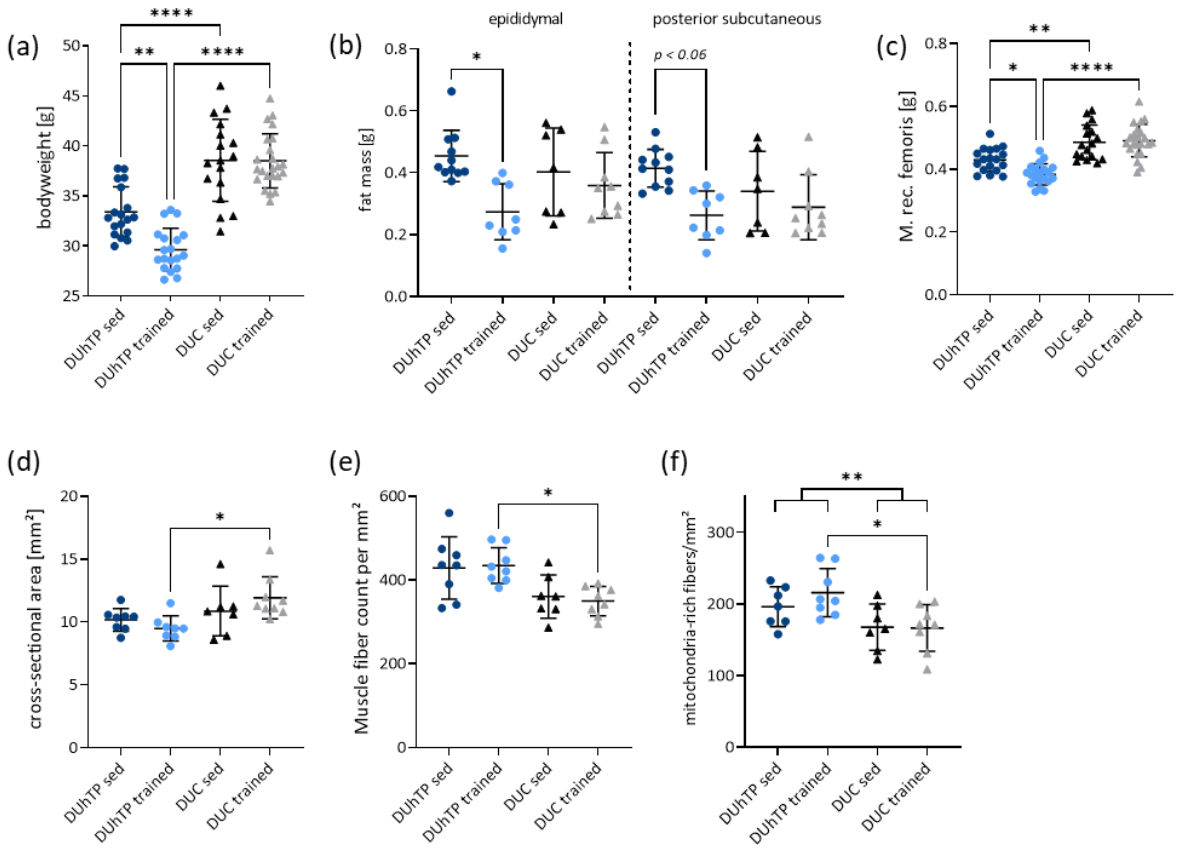

Figure 1. (**a**) Body weight (n ≥ 17), (**b**) epididymal (left panel, n ≥ 7) and posterior subcutaneous fat (right panel, n ≥ 7), and (**c**–**f**) detailed analysis of the muscle in trained and sedentary DUhTP and DUC mice at 70 days of age. (**c**) The dissected *Musculus rectus femoris* (Mrf) were weighted (n ≥ 17), and the (**d**) cross-sectional area (CSA, n ≥ 7), as well as (**e**) muscle fiber count and (**f**) mitochondria-rich fibers per mm^2 analyzed muscle region (see Method part) were determined. The color used corresponds to the mouse groups (dark blue: DUhTP sed, light blue: DUhTP trained, black: DUC sed, gray: DUC trained). Data are presented as scatter plots with means and standard deviations. Statistical analysis was performed using two-way ANOVA. Significant differences are indicated: * $p < 0.05$, ** $p < 0.01$, **** $p < 0.0001$.

Thus, the results show that long-term selection for high treadmill performance results in a phenotype with lower body and muscle mass weight, which under training conditions is further characterized by lower Mrf muscle cross-sectional areas, higher muscle fiber number per mm^2, and more mitochondria-rich muscle fibers. Exclusively in the DUhTP mice, a decrease in fat depots was also observed by training, consistent with the hypothesis of a predominant role of lipids in muscle metabolism.

3.2. Analysis of mRNA Indicates Induction of Glycolysis, Beta-Oxidation, TCA-Cycle, and Oxidative Phosphorylation in Muscles from DUhTP Mice

To investigate muscle gene expression and metabolic pathways in response to selection and physical activity, we performed NGS using total RNA preparations isolated from trained and sedentary DUhTP and DUC Mrfs. Differentially expressed genes (DEGs) in different experimental groups were characterized by a false discovery rate (FDR) of <0.05.

Accordingly, 13,982 DEGs were identified and quantified in muscle from the different experimental groups (data set NGS = Table S3). Direct mouse strain comparison (DUhTP sed vs. DUC sed) identified 5916 transcripts differentially regulated due to long-term selection for high-endurance exercise (Table S4a). These transcripts were upregulated and downregulated to a similar extent. After three weeks of training, the total number of altered muscle transcripts between the two lines increased to 7042, with 460 more downregulated than upregulated transcripts. Based on the number of DEGs, exercise had a stronger effect on gene expression in DUhTP (DUhTP trained vs. DUhTP sed: 1606 DEGs) than in DUC mice (DUC trained vs. DUC sed: 130 DEGs). The comparison between trained DUhTP and trained DUC muscle transcripts revealed that several signaling pathways were silenced or less activated (Table S4b, downregulated), whereby multiple metabolic pathways were highly activated (Table S4b, upregulated).

Therefore, all DEGs identified in DUhTP sed vs. DUC sed, DUhTP trained vs. DUC trained, DUhTP trained vs. sed, and DUC trained vs. sed were implemented into Pathview to obtain their visualization (Figure S3a–d) in some metabolic KEGG pathways enriched by DAVID. Pathway analysis suggested higher glycolysis activity in sedentary DUhTP mice than in sedentary DUC mice. Indeed, several enzyme transcripts catalyzing the conversion of glucose-6-phosphate to pyruvate and further to acetyl-CoA were increased (Figure S3a, Table 1). However, the gene expression of hexokinase (2.7.1.1), the initial enzyme of glycolysis, was lower in DUhTP than in DUC mice. The expression of glucokinase (2.7.1.2), which plays a role in the blood glucose sensing system, was also lower in marathon mice. Training increased hexokinase transcription in both DUhTP and DUC animals such that significant differences in hexokinase transcription between the two exercised strains could no longer be detected. However, the reduction in glucokinase expression persisted in trained DUhTP mice compared with trained control animals. In addition, fewer transcripts of ADP-dependent glucokinase (2.7.1.147) were also found in the muscles of trained DUhTP animals (FDR < 0.0007). In DUhTP mice, physical activity increased the transcript levels of glyceraldehyde-3-phosphate dehydrogenase (1.2.1.12). Interestingly, transcripts encoding glycogen-degrading enzymes were also significantly decreased (FDR < 0.05) in DUhTP compared with control muscles (Table 1). Transcripts for phosphorylase b kinase, glycogen debranching enzyme, and phosphoglucomutase-2 were decreased in muscles of sedentary and trained DUhTP compared with the corresponding DUC mice (FDR < 0.05). In addition, lower transcript levels of UTP-glucose-1-phosphate uridylyltransferase (FDR < 0.015) but higher glycogen phosphorylase (FDR < 0.002) and glycogen synthase transcripts (FDR < 0.03) were detected in DUhTP muscles compared with control muscles after training. For fatty acid degradation, more enzyme transcripts (FDR < 0.05) were found in the Mrf of DUhTP compared with control animals (Figure S3b, Table 1). High abundances of Cpt2 (FDR < 0.004), acyl-CoA dehydrogenases (1.3.8.7, 1.3.8.9, FDR < 0.002), enoyl-CoA hydratase (4.2.1.17, FDR < 0.04), 3-hydroxyacyl-CoA dehydrogenase (1.1.1.35, FDR < 0.0001), and 3-ketoacyl-CoA thiolase (2.3.1.16, FDR < 0.0002) were detectable in marathon mice (Table 1). In response to treadmill running, the expression of these genes was further increased. Furthermore, increased expressions of another acyl-CoA dehydrogenase (1.3.8.8, FDR < 0.0001) and an acyl-CoA oxidase (1.3.3.6, FDR < 0.05) were detected in trained DUhTP muscles compared with those of controls. Transcripts of the long-chain fatty acid CoA ligase (6.2.1.3) were lower in DUhTP mice's muscles than in controls (FDR < 0.0001), independent of exercise. The number of transcripts corresponding to citrate cycle enzymes was significantly higher in Mrf of DUhTP than in control mice (FDR < 0.05), independent of training status (Figure S3c, Table 1). However, physical activity enhanced these significant differences, although no significant expression differences were detected within either line. Substantial expression differences were found for the enzymes isocitrate dehydrogenase (1.1.1.41; 1.1.1.42, FDR < 0.002), succinate-CoA ligase (6.2.1.4; 6.2.1.5, FDR < 0.009), succinate dehydrogenase (1.3.5.1, FDR < 0.0007), and malate dehydrogenase (1.1.1.37, FDR < 0.0001) (Table 1). The increase in the expression of alpha-ketoglutarate dehydrogenase was significant after the last training session (FDR < 0.0001).

In addition, many oxidative phosphorylation pathway genes were upregulated in DUhTP mice compared with controls, independent of physical activity (Figure S3d). When compared with sedentary animals, many transcripts of subunits of complexes I, II, III, IV, and V were upregulated in DUhTP muscles. Interestingly, after three weeks of training, the mitochondria-encoded subunits of complex I (ND1, ND2, ND3, ND4L) were significantly reduced between trained DUhTP and DUC mice (FDR < 0.008, Table S1). While no changes were detected in DUC mice after physical activity (DUC trained vs. DUC sed), DUhTP animals showed significant downregulation of mitochondria-encoded complex I subunit transcripts (DUhTP trained vs. DUhTP sed, FDR < 0.03).

Thus, the muscle transcriptome of the marathon mice, in contrast to that of the controls, shows upregulation of gene expression of glycolysis, FAO, TCA cycle, and respiratory chain enzymes but downregulation of glycogen degrading enzymes, indicating higher metabolic activity in the muscle of the selection line.

3.3. Plasma Levels of Energy Metabolites in Response to Phenotype Selection and Physical Activity

To challenge the bioinformatics pathway analysis predictions, we assessed selected plasma levels of energy metabolites in all experimental groups. Sedentary DUhTP and DUC mice had similar plasma levels of glucose (Figure 2a), lactate (Figure 2b), and insulin (Figure 2c). In response to exercise after three weeks of training, plasma glucose and plasma lactate levels were increased in DUC mice ($p < 0.05$). Insulin levels were not significantly altered by exercise in either strain. However, an exercise-induced decrease in plasma insulin levels was observed ($p < 0.01$; Figure 2c). Whereas exercise had no effect on plasma glucose or lactate concentrations in trained DUhTP mice, trained DUC mice were characterized by higher glucose and lactate levels than trained DUhTP mice ($p < 0.05$).

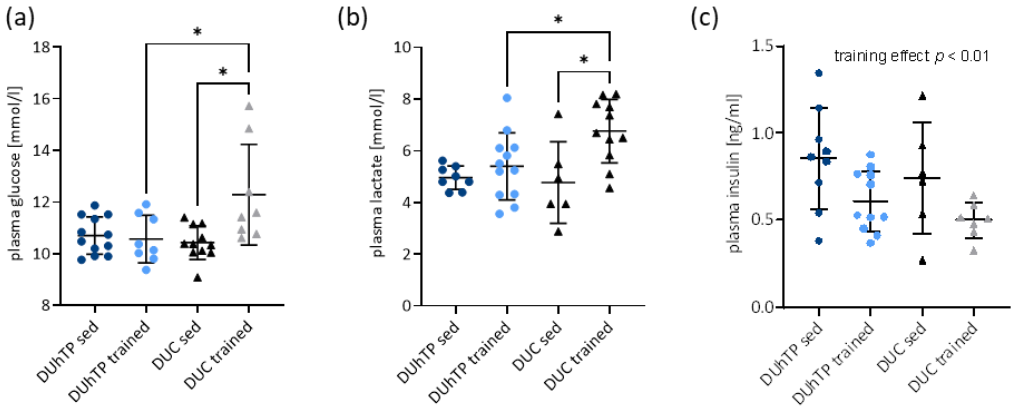

Figure 2. Analysis of metabolites in the circulation. (**a**) Blood glucose ($n \geq 8$), (**b**) plasma lactate ($n \geq 6$), and (**c**) plasma insulin ($n \geq 6$) in trained and sedentary DUhTP (light/dark blue) and DUC mice (gray/black). All results are presented as scatter plots with mean and standard deviations. Statistical analysis was performed using two-way ANOVA. The training-mediated effect on plasma insulin level was statistically evaluated by using an unpaired *t*-test with Welch correction. Significant differences as indicated: * $p < 0.05$.

Interestingly to note, three days after treadmill training, serum lactate levels were significantly reduced in the DUhTP animals (2.78 ± 0.42 mmol/L) compared with sedentary DUhTP mice (4.96 ± 0.45 mmol/L, $p < 0.04$). In contrast, in DUC mice, lactate levels three days after exercise were similar (4.76 ± 0.90 mmol/L) to those in sedentary DUC mice (4.77 ± 1.58 mmol/L).

Table 1. List of upregulated (red) and downregulated (green) DEGs involved in metabolic pathways in the four comparison groups extracted from the list of all DEGs (Table S3). Significant differences as indicated: * FDR < 0.05, ** FDR < 0.01, *** FDR < 0.001, **** FDR < 0.0001, gray cells: comparable gene expression, n = 7–8 animals per group.

Pathway	Involved Genes	Gene Name	DUhTP Sed vs. DUC Sed		DUhTP Trained vs. DUC Trained		DUhTP Trained vs. DUhTP Sed		DUC Trained vs. DUC Sed	
			logFC	FDR	logFC	FDR	logFC	FDR	logFC	FDR
Glycogen metabolism	Phosphorylase b kinase	Phkb	−0.41	**	−0.38	*				
	Glycogen phosphorylase	Pygm			0.44	**				
	Glycogen debranching enzyme	Agl	−0.48	**	−0.35	*				
	Glycogenin	Gyg			0.28	**				
	UTP-glucose-1-phosphate uridylyltransferase	Ugp2			−0.28	*				
	Glycogen synthase	Gys1			0.23	*				
Glycolysis	Glucose transporter Glut1	Slc2a1								
	Glucose transporter Glut4	Slc2a4	0.23	*	0.36	****	0.27	*		
	Hexokinase	Hk2	−0.50	***			0.75	***	0.41	*
	Phosphoglucoisomerase	Gpi1	0.38	***	0.58	****	0.26	0.057		
	Phosphofructokinase	Pfkm			0.30	*				
	Aldolase	Aldoa	0.36	**	0.51	****				
	Phosphotriose isomerase	Tpi1	0.45	****	0.53	****				
	Glyceraldehyde 3-P dehydrogenase	Gapdh	0.66	****	0.84	****	0.39	*		
	Phosphoglycerate kinase	Pgk1	0.29	*	0.27	*				
	Phosphoglycerate mutase	Pgam1			0.73	*				
		Pgam2	0.52	****	0.61	****				
	Enolase	Eno3	0.62	****	0.55	****				
	Pyruvate kinase	Pkm	0.30	*	0.39	***				
	Lactate dehydrogenase	Ldha	0.41	***	0.40	***				
		Ldhd	0.26	*	0.25	*				
	Pyruvate Transporter	Mpc1	0.43	****	0.59	****				
		Mpc2	0.47	****	0.29	**				
	Lactate transporter MCT1	Slc16a1			−0.43	*				
	Lactate transporter MCT2	Slc16a3	0.40	*	0.40	*				

Table 1. *Cont.*

Pathway	Involved Genes	Gene Name	DUhTP Sed vs. DUC Sed		DUhTP Trained vs. DUC Trained		DUhTP Trained vs. DUhTP Sed		DUC Trained vs. DUC Sed	
			logFC	FDR	logFC	FDR	logFC	FDR	logFC	FDR
Fatty acid (FA) oxidation	FA transporter CD36	Cd36								
	FA transportprotein 1	Slc27a1	0.58	**	1.03	****				
	FA transportprotein 4	Slc27a4			0.39	***	0.32	*		
	FA binding protein 3	Fabp3	0.54	*	1.14	****				
	Carnitine-O-palmitoyltransferase 2	Cpt2	0.45	**	0.63	****				
	Acyl-CoA dehydrogenase	Acads	0.62	****	0.77	****				
		Acadm	0.52	**	0.53	**				
		Acadl			0.83	****				
		Acadvl	0.57	***	0.84	****				
	Enoyl-CoA hydratase	Hadha	0.32	*	0.68	****				
	Hydroxy acyl-CoA dehydrogenase	Hsd17b10	0.58	****	0.75	****				
	Ketoacyl-CoA thiolase	Acaa2	0.77	****	1.05	****				
TCA cycle	Citrate synthase	Cs	0.43	***	0.50	****				
	Aconitate hydratase	Aco2	0.38	**	0.64	****				
	Isocitrate dehydrogenase	Idh2	0.86	**	1.35	****				
	Isocitrate dehydrogenase	Idh3b	0.42	****	0.55	****				
	Isocitrate dehydrogenase	Idh3g	0.45	****	0.59	****				
	a-ketoglutarate dehydrogenase	Ogdh			0.43	****	0.24	0.062		
	Succinyl-CoA synthetase	Suclg1	0.45	****	0.50	****				
		Suclg2	0.31	**	0.28	**				
		Sucla2	0.27	**						
	Succinate dehydrogenase	Sdhc	0.63	****	0.53	****				
		Sdhd	0.45	****	0.46	****				
		Sdhb	0.47	**	0.72	****				
		Sdha			0.38	***				
	Fumarase	Fh1	0.45	****	0.52	****				
	Malate dehydrogenase	Mdh2	0.53	****	0.83	****				

Since lactate is an effector of lipolysis, we performed a detailed analysis of lipids in mouse blood samples. Serum from trained and sedentary DUhTP mice was characterized by significantly increased concentrations of specific circulating lipid species (acylcarnitines, di/triglycerides, and fatty acids derivates) compared with corresponding control mice (Figure 3, top left and right panel, Table S5). In particular, increased levels of acylcarnitines, phospholipids, and fatty acid derivatives were found in trained DUhTP mice compared with sedentary DUhTP mice (Figure 3, lower left panel, Table S5). In addition, during exercise, the levels of certain phospholipids that act as signaling molecules increased in DUhTP and control mice, but with more pronounced increases in DUhTP mice. For example, the platelet-activating factor was significantly increased in trained DUhTP compared with sedentary mice and, in contrast, not changed in control mice (Table S5). Other phospholipids with signaling functions, such as lysophosphatidylcholines, were increased during physical activity in both mouse groups.

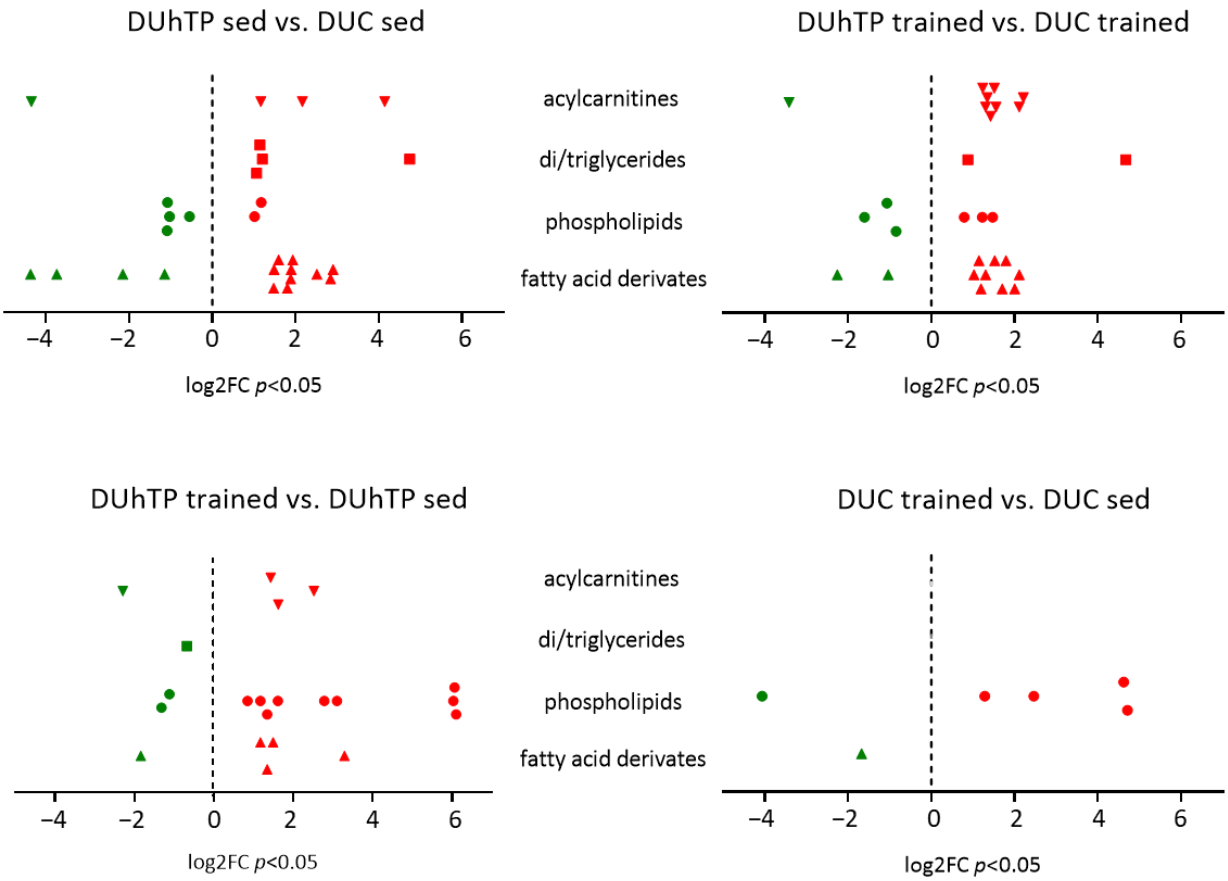

Figure 3. Significantly upregulated (red-colored) and downregulated (green-colored) levels of various acylcarnitines (triangles, tip down), di-/triglycerides (squares), phospholipids (circles), and fatty acid derivates (triangles, tip up) in the serum samples of sedentary or trained DUhTP mice (n = 10) and controls (n = 10) analyzed by untargeted metabolomics using high-resolution LC-MS/MS. Significant ($p < 0.05$) increases or decreases are labeled in red or green. Differences are shown as log2FC.

Altogether, there were more lipids in the circulation of trained marathon mice and more glucose and lactate in that of trained control mice, suggesting oxidative lipid metabolism in the muscles of DUhTP and carbohydrate-based metabolism in the muscle of control mice.

3.4. Treadmill Running Results in Higher Glycogen Levels and Reduced Lactate Dehydrogenase Activity in Muscle from DUhTP Mice

Higher glycogen content was found in the Mrf of trained DUhTP mice than in the Mrf of sedentary littermates or trained DUC mice ($p < 0.05$; Figure 4a). We further demonstrated

that DUhTP mice showed a reduction in lactate dehydrogenase (LDH) activity in response to repeated physical activity ($p < 0.0001$; Figure 4b), whereas treadmill running did not induce any changes in controls. However, the activity of muscle LDH differed by 20% ($p < 0.0001$) between trained animals of both lines. Pyruvate dehydrogenase (PDH) activity, instead, was significantly increased in sedentary DUhTP mice compared with controls ($p < 0.005$; Figure 4c). After treadmill training, a 70% higher PDH activity was observed in DUhTP mice ($p < 0.05$), while DUC mice only showed a 44% increase (not significant). Therefore, PDH enzyme activity differed by 117% between both trained lines ($p = 0.0001$). The enzyme activity of IDH was increased in sedentary and trained DUhTP compared with the groups of controls (Figure S4a, $p < 0.01$). CK activity was decreased in trained DUhTP muscles compared with those of trained DUC ($p < 0.05$; Figure S4b) and sedentary DUhTP mice ($p < 0.01$).

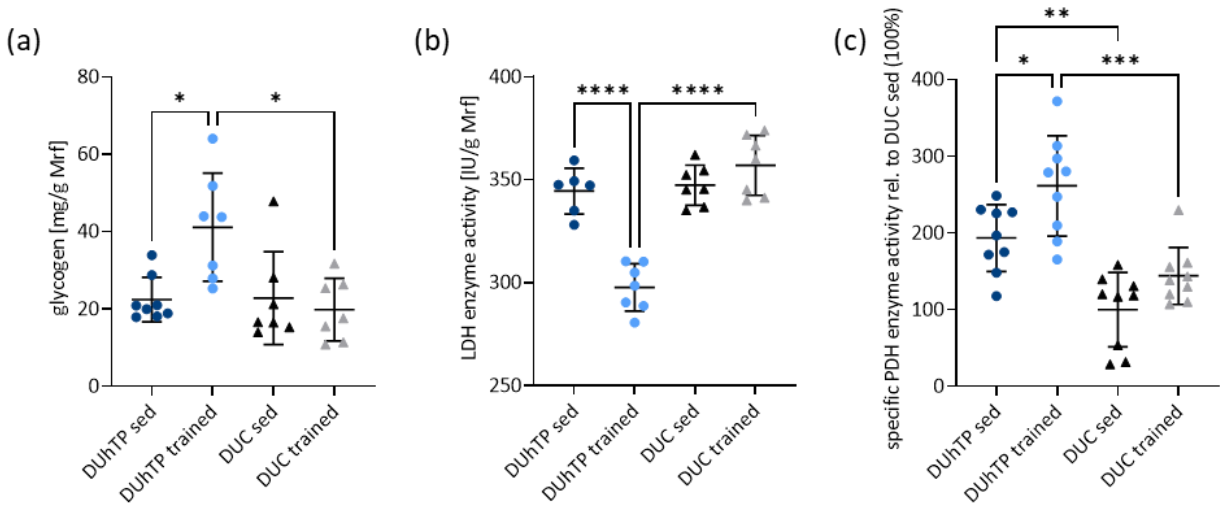

Figure 4. Analysis of metabolites and metabolic enzymes in muscle tissue of trained and sedentary DUhTP (light/dark blue) and DUC mice (gray/black). (**a**) Muscle glycogen content and (**b**) the lactate dehydrogenase (LDH) enzyme activity were determined per gram of *Musculus rectus femoris* (Mrf, n $\geq$ 6 per group). (**c**) Pyruvate dehydrogenase activity was measured over a duration of 30 min (Mrf, n = 9) and displayed as changes relative to DUC sed. All results are presented as scatter plots with mean and standard deviations. Statistical analysis was performed using two-way ANOVA. Significant differences as indicated: * $p < 0.05$, ** $p < 0.01$, *** $p < 0.001$, **** $p < 0.0001$.

Thus, the results clearly argue against anaerobic glycolysis (increased glycogen stores as well as reduced LDH activity) and energy supply by CK in the muscle of trained DUhTP mice compared with trained controls; instead, the results suggest increased substrate oxidation shown by increased PDH and IDH activities.

4. Discussion

The primary objective of the present study was to identify control mechanisms of lipid-based energy metabolism in the muscle of the non-inbred marathon mouse model (DUhTP) related to their superior running performance in contrast to an unselected control line (DUC), originally derived from the same genetic background. To this purpose, we investigated the interactions between long-term phenotype selection for high treadmill performance (indirect effects) and repeated high-speed treadmill training (direct effects) on muscle metabolism and asked which metabolic mechanisms and adaptations manifested in the muscle through phenotype selection to ensure the exceptional endurance capabilities of DUhTP mice after 140 generations of selection. Data from the current study indicate (i) that long-term selection resulted in metabolic adaptations in the DUhTP mouse line and (ii) that three weeks of treadmill training at intensive speed directly favors energy expenditure

from glycolytic utilization in DUC but appears more to rely on lipid-based metabolism in DUhTP mice, with substrate flux controlled by specific enzyme activities.

Phenotype selection resulted in reduced body mass and muscle weight of DUhTP compared with control mice but no significant structural changes in Mrf. Since both muscle mass and body weight were reduced during selection, the ratio of muscle to body mass was the same as in the unselected controls, indicating a general reduction in the size of the DUhTP animals. Based on the significantly increased gene expression of metabolic enzymes involved in glycolysis, the TCA cycle, oxidative phosphorylation, and FAO in the Mrf of marathon mice compared with controls, metabolic adaptations can be assumed as a consequence of phenotypic selection, since these animals have never trained. In particular, the transcript abundance of enzymes related to beta-oxidation and the TCA cycle was, on average, 50% higher (logFC $\approx$ 0.5) in DUhTP mice than in controls. Consistent with the increased transcript levels of Pdhb, Idh2, and Idh3, both PDH and IDH enzyme activities are increased in the DUhTP mice, suggesting a stronger oxidative metabolic potential of the muscles of the DUhTP mice.

In response to physical activity, significant differences were found between the muscles of both lines and partially between trained and sedentary DUhTP mice. The body and muscle weights of trained DUhTP mice were even lower than those of sedentary littermates. Concomitantly, the CSA of the muscles from trained DUhTP mice was also reduced. Because the Mrfs of the trained DUhTP mice simultaneously had a significantly higher number of muscle fibers per square millimeter of CSA than the Mrfs of trained DUC mice, it is reasonable to speculate that the higher number per square millimeter of CSA is related to the decrease in the cross-sectional area of muscle fibers, particularly the decrease in the area of white muscle fiber area. Thus, in the counted areas in the trained DUhTP mice, and only in them, the number of white fibers correlated negatively with their fiber area, whereas the number of intermediate fibers correlated positively with their area. Overall, more mitochondria-rich fibers, i.e., intermediate and red fibers, were detected per square millimeter of counted area in trained marathon mice, which are generally characterized by smaller diameters than fast glycolytic fibers [38]. Similar observations have been made in mice after six weeks of voluntary running wheel use [39] or in guinea pigs after eight weeks of treadmill training [40]. Thus directly after three weeks of exercise, treadmill running induced a greater shift toward the oxidative fiber type in DUhTP versus DUC mice, which may be associated with a stronger preference toward fat-dependent metabolism and may indicate improved metabolic flexibility [22,41,42] in marathon mice than in unselected control mice in response to running training.

Although metabolic flexibility was not explicitly examined in this study, RNA transcript levels suggest increased oxidation of glucose and lipids through increased glycolysis, beta-oxidation, TCA cycle, and respiratory chain transcripts in the Mrfs of trained DUhTP mice. In particular, transcript levels of hexokinase 2, the initial enzyme of glycolysis and, therefore, an essential player in metabolic flexibility, were induced in both lines by exercise. Notably, increased hexokinase-2 transcript levels in trained mouse skeletal muscle have also been described in a recent review of endurance-associated gain-of-function and loss-of-function genes [43]. In C57BL6 mice running to exhaustion, threefold hexokinase 2 overexpression results in improved endurance performance, and 50% knockout results in decreased endurance performance compared with wild-type mice [44]. Muscle glycogen is not spared in partial knockout animals. During high-intensity exercise, muscle glycogen generally becomes more critical [45], although glycogen-sparing animals have also been reported to have high levels of free fatty acids circulating in their plasma [46]. In particular, with increasing training intensity, glycogen stores are depleted [17] as in Wistar rats by up to 87% in the red vastus lateralis muscle after thirty minutes of treadmill training at 25 m/min [47] or in BALB/c mice by 33% in gastrocnemius muscle after five days of thirty minutes of treadmill training at 25 m/min [48]. Although the treadmill speed in the last week of training was 30 m/min in DUhTP mice, there was no depletion of glycogen stores. This may be due to decreased expression of glycogen-degrading enzymes (Phkb, Agl) and

increased expression of glycogen-synthesizing enzymes (Gyg, Gys1). On the other hand, it can be assumed that energy production from plasma glucose occurs without glycogen utilization in contrast to control mice. In trained control mice, blood glucose levels were elevated compared with trained DUhTP mice, the same as blood lactate levels.

Blood lactate levels, as a product and substrate of LDH, were not affected by treadmill running in DUhTP mice and were similar to those of sedentary littermates. Lactate is produced primarily by glycolytic fibers [4,7], although oxidative fibers also produce lactate [49]. It can be assessed as a measure of the anaerobic glycolytic contribution to exercise as a function of exercise intensity, duration, and type of physical activity. For example, peak blood lactate concentrations were observed after a supramaximal 400 m sprint and were thus higher than in long-distance runners or sedentary subjects [50]. Blood lactate concentrations of approximately 6–8 mmol/L, as measured in DUC mice, correspond to moderately elevated lactate levels during exercise and indicate that the DUC animals are not overloaded with the selected training volume in this study. High exercise intensity with predominant anaerobic glycolysis results in levels of 10–15 mmol/L and higher [51]. The lack of increased lactate production in the muscles of trained DUhTP mice may be related to the observed decreased LDH enzyme activity, which we confirmed by lower lactate levels three days after three weeks of treadmill training in DUhTP, but not in DUC mice. Consequently, we assumed that reduced LDH activity abolishes anaerobic glycolysis with concomitant lactate formation and instead drives glucose oxidation in the muscle of trained DUhTP mice. Evidence for this is provided by decreased transcript levels of the mitochondrial lactate transporter Slc16a1 [14], increased PDH enzyme activity, increased transcript levels encoding the mitochondrial pyruvate transporters Mpc1 and 2 [13], enzymes of the TCA cycle and oxidative phosphorylation, and the increased activity of IDH, responsible for the conversion of isocitrate to α-ketoglutarate in the TCA cycle, in DUhTP compared with DUC muscles (Figure 5). Increased PDH and IDH activities in contrast to decreased LDH and CK activities in active DUhTP mice compared with sedentary littermates or physically active DUC mice support this hypothesis of increased oxidative metabolism in physically active DUhTP mice. Since PDH controls the influx of pyruvate derived from carbohydrates into mitochondria, it is thought to play a critical role in metabolic flexibility in muscle [52].

The shift from the glycolytic to the oxidative muscle fiber type not only increases the ability to utilize glucose oxidatively but also increases the ability to burn fat as fuel [41]. During fat oxidation, white adipose tissue, particularly subcutaneous abdominal fat [53], plays a key role in the flexibility of lipid supply and serves as a buffer for lipid flux [54]. Fatty acids, stored as triglycerides in adipose tissue, are transported via the blood circulation to cells with increased energy demand and are taken up by diffusion, fatty acid transport protein (FATP1, Slc27a1), or CD36, which requires the induction of their translocation to the cell membrane [16]. Increased blood concentrations of specific circulating triglycerides (especially TAG 62:16), acylcarnitines, phospholipids, and fatty acid derivatives were found in trained DUhTP mice compared with sedentary littermates as well as trained DUC mice. Circulating fatty acid levels increase during endurance exercise, promoting lipid uptake into muscle and muscle oxidation [45,55]. Therefore, Fernández-Verdejo et al. suggested that elevated lipid availability and increased lipid oxidation during exercise are true measures of metabolic flexibility toward lipids [55]. Consistent with increased fat mobilization, trained DUhTP animals have lower epididymal and posterior subcutaneous fat depots than sedentary ones. While muscular Cd36 transcripts did not differ between trained strains, a higher expression of Slc27a1 was observed in trained DUhTP mice.

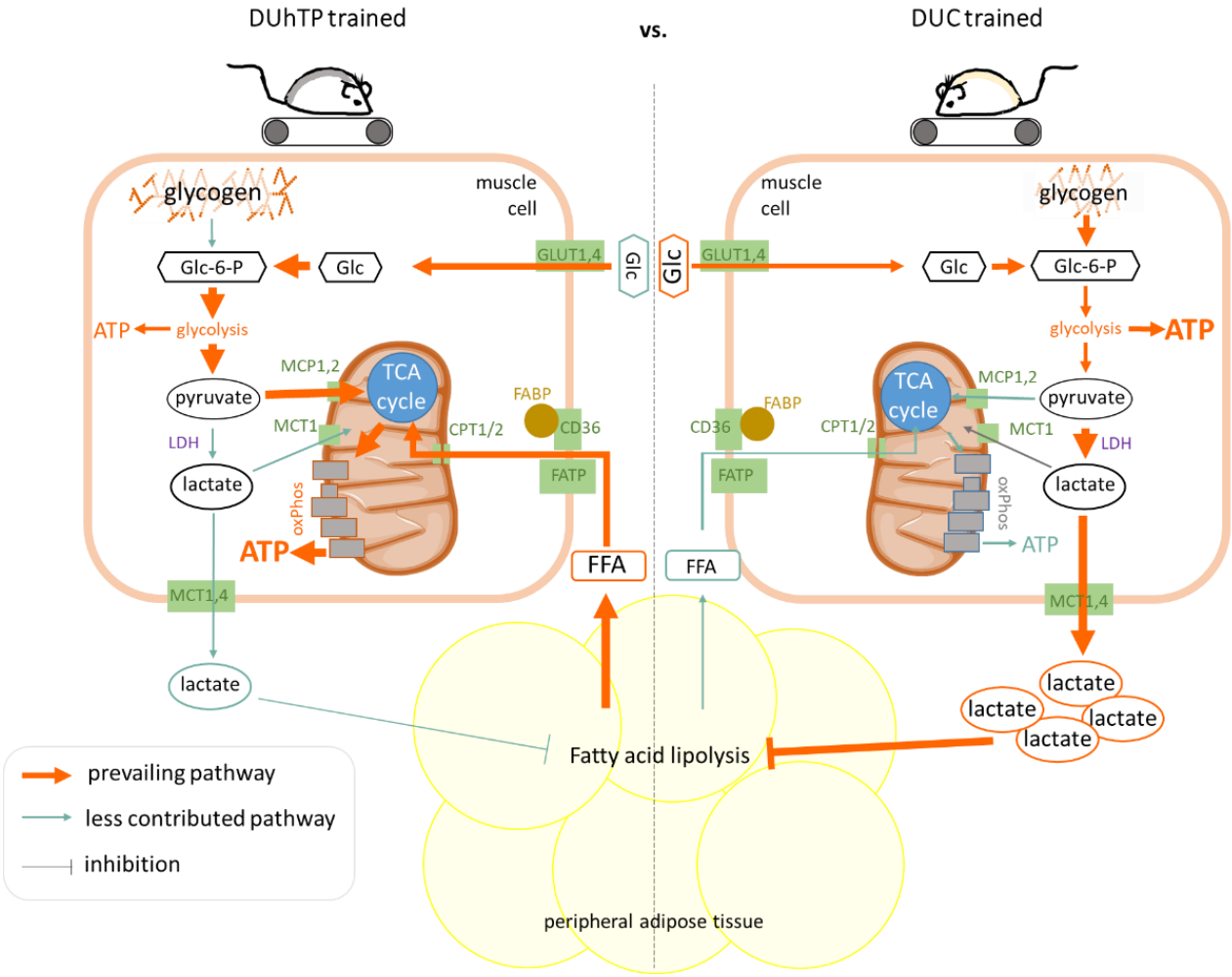

Figure 5. Pathway modeling in *Musculus rectus femoris* (Mrf) of trained DUhTP mice (left) vs. trained DUC mice (right). The underlying data were obtained by NGS, enzyme activity assays, and muscle and plasma levels determination. Dominant pathways are shown in orange, and less-dominant ones are shown in blue-green. Thicker arrows correspond to a higher prevalence. The specific relationships are summarized in the discussion.

It has been shown that cellular uptake of long-chain fatty acids from blood across the endothelial-cell layer via the fatty acid transport proteins FATP3 and FATP4 is induced by VEGF-B and coregulated with mitochondrial genes [56]. Muoio postulated that by high VEGF-B production, fatty-acid-utilizing muscle cells communicate their substrate preference to local vessels to be supplied with these nutrients [57]. This facilitates a shift in energy metabolism towards a reliance on lipids. For example, repeated physical activity activates PGC1α and mitochondrial biogenesis and increases oxidative fat catabolism in muscle. Accordingly, we found significantly increased Slc27a4 (FATP4) and Vegfb expression in DUhTP compared with DUC mice, with higher expression after training. Ppargc1a mRNA expression was also increased in trained DUhTP mice compared with sedentary littermates. Interestingly, Storlien et al. hypothesized that induction of PGC1α (due to exercise) and associated increased mitochondrial biogenesis and insulin sensitivity might enhance the metabolic flexibility of muscle cells to effectively switch between carbohydrate and lipid fuel sources [41].

Mitochondrial uptake of activated fatty acids is mediated by carnitine palmitoyltransferase (Cpt) 1 and 2, and muscular CPTI overexpression results in increased FAO and decreased intramuscular fatty acid esterification [58]. The increased Cpt2 transcripts and increased gene expression of FAO enzymes detected in DUhTP mice indicate increased

uptake of fatty acids into mitochondria for β-oxidation and explain the decreased intramuscular triacylglycerol storage in trained animals of both lines. The decreased intramuscular triacylglycerol storage may also be related to reduced plasma insulin levels caused by physical activity in both lines, as insulin promotes muscle lipid uptake and intramuscular fat accumulation. However, the inconspicuous intramuscular lipid storage, combined with the increased gene expression of FAO, TCA cycle, and oxidative phosphorylation enzymes observed here, and the increased activity of IDH, a TCA cycle enzyme, in the trained DUhTP animals, suggests increased mitochondrial fatty acid uptake and subsequent oxidative energy production in these mice (Figure 5).

Despite the adaptation of running time and speed in the training design of this study to the capabilities of the mice, anaerobic glucose utilization plays a more important role in energy supply in the control line than in our marathon mouse model in response to physical activity, as evidenced by higher muscular CK activity, higher LDH activity and elevated plasma lactate levels in DUC than DUhTP mice. High circulating plasma lactate levels suppress the need for lipolysis because glucose and glycogen are abundant [8]. In this context, plasma lactate acts directly as a signal to adipose tissue by binding to the highly expressed receptor GPR81 in adipose tissue and leading to a dose-dependent inhibition of glycerol and FFA release via inhibition of adenylyl cyclase [59,60]. In contrast, GPR81-deficient mice do not show an antilipolytic response to lactate [60]. In marathon mice, the anti-lipolytic signal is absent during exercise due to low plasma lactate levels resulting from reduced LDH activity (Figure 5). Instead, increased fat mobilization from peripheral adipose tissues occurs alongside glucose oxidation without glycogen breakdown contribution, resulting in decreased fat depots (epididymal and posterior subcutaneous).

The present study has several limitations. First, the study was evaluated only for genotype × exercise interactions. To test the concept of enhanced energy metabolism developed by long-term selection for high treadmill running performance in DUhTP mice in the future, we need to consider additional interactions, such as age, sex, or nutrition. Furthermore, additional exercise programs, preferably with defined maximal oxygen consumption, could be used to test the state when the exclusively aerobic glucose metabolism is abandoned. Finally, in this study, we exclusively tested effects directly after a three-week training program. However, examining the animals at different time points during the experiment and at later time points after the last training session may be interesting to study intermediate or chronic training effects.

5. Conclusions

Compared with the control model, the results of this manuscript impressively demonstrate that three weeks of treadmill training in long-term-selected marathon mice result in hardly any histological (muscle fiber types) but much more metabolic changes. Paternal selection for high running performance has conferred greater metabolic flexibility to the muscle, allowing simultaneous oxidative utilization of glucose and fatty acids during high-speed exercise. We propose that LDH plays a critical role in this process, as its downregulated activity prevents increased lactate production during endurance exercise and thus selectively provides peripheral energy from fat depots. Acute downregulation of LDH in muscle may play a specific role in improving metabolic flexibility in the muscle of marathon mice or may be required to meet the high energy demands during endurance exercise.

Supplementary Materials: The following supporting information can be downloaded at: https://www.mdpi.com/article/10.3390/cells12151925/s1, Table S1: Body weight, weight gain, and food consumption of all mice during the 3-week experiment starting from day 49 and ending at day 70. Table S2: Primer sequences for quantitative real-time PCR for selected genes. Table S3: List of all differentially expressed genes (DEGs) in the four different comparison groups; Table S4: Identification of differentially expressed genes (DEGs) in the four different comparison groups; Table S5: List of significantly upregulated and downregulated levels of various acylcarnitines, di/triglycerides, phospholipids, and fatty acid derivates in serum samples of the four comparison groups; Figure S1: Validation of RNA-seq data by the Fluidigm technique for nine differentially expressed genes (DEGs).

Figure S2: Immunohistochemical evaluation of *Musculus rectus femoris* (Mrf) of trained and sedentary (sed) DUhTP and DUC mice at the age of 70 days; Figure S3: Graphical visualization of gene regulation in (a) glycolysis, (b) fatty acid degradation, (c) TCA cycle, (d) oxidative phosphorylation KEGG pathways for the four comparison groups; Figure S4: Analysis of isocitrate dehydrogenase enzyme activity and creatine kinase enzyme activity per gram *Musculus rectus femoris* of trained and sedentary DUhTP and DUC mice.

Author Contributions: Conceptualization, J.B., S.P. (Siriluck Ponsuksili), K.W. and A.H.; methodology, E.B., N.T., C.W., D.O., M.L., S.P. (Stefan Petkov), M.R., S.M., C.E.G., B.F., B.K., M.W. and J.B.; resources: M.L.; software, C.W., N.T., A.N., E.B., C.E.G., B.F. and J.B.; formal analysis, J.B., E.B., C.W., N.T. and A.N.; writing—original draft preparation, J.B. and A.H.; writing—review and editing, all authors. All authors have read and agreed to the published version of the manuscript.

Funding: This research received no external funding.

Institutional Review Board Statement: The study was approved by our internal institutional review board (Research Institute for Farm Animal Biology in Dummerstorf, Germany) and was conducted following international (Declaration of Helsinki) and national animal welfare guidelines (Animal Welfare Act (TierSchG); AZ 7221.3.1.014/17 and AZ 7221.3-1-064/19).

Informed Consent Statement: Not applicable.

Data Availability Statement: All raw data were generated at the FBN Dummerstorf. Derived data supporting the findings of this study are available on request from the corresponding author.

Acknowledgments: The authors are very grateful to Luong Chau, Annette Jugert, Angela Steinborn, Marie Jugert-Lund, and Rico Fürstenberg for their excellent technical support. The authors would also like to thank the Lab Animal Facility technicians for excellent animal care and technical support in handling the treadmill training. We further thank Henry Reyer for helping with statistical questions.

Conflicts of Interest: The authors declare no conflict of interest.

References

1. Hargreaves, M.; Spriet, L.L. Skeletal muscle energy metabolism during exercise. *Nat. Metab.* **2020**, *2*, 817–828. [CrossRef] [PubMed]
2. Sahlin, K.; Tonkonogi, M.; Soderlund, K. Energy supply and muscle fatigue in humans. *Acta Physiol. Scand.* **1998**, *162*, 261–266. [CrossRef] [PubMed]
3. Watt, M.J.; Heigenhauser, G.J.; Dyck, D.J.; Spriet, L.L. Intramuscular triacylglycerol, glycogen and acetyl group metabolism during 4 h of moderate exercise in man. *J. Physiol.* **2002**, *541*, 969–978. [CrossRef] [PubMed]
4. Brooks, G.A. Lactate: Glycolytic End Product and Oxidative Substrate During Sustained Exercise in Mammals—The "Lactate Shuttle". In *Proceedings of Circulation, Respiration, and Metabolism*; Springer: Berlin/Heidelberg, Germany, 1985; pp. 208–218.
5. Stanley, W.C.; Gertz, E.W.; Wisneski, J.A.; Neese, R.A.; Morris, D.L.; Brooks, G.A. Lactate extraction during net lactate release in legs of humans during exercise. *J. Appl. Physiol.* **1986**, *60*, 1116–1120. [CrossRef]
6. Brooks, G.A. Lactate shuttles in nature. *Biochem. Soc. Trans.* **2002**, *30*, 258–264. [CrossRef]
7. Kitaoka, Y.; Hoshino, D.; Hatta, H. Monocarboxylate transporter and lactate metabolism. *J. Phys. Fit. Sports Med.* **2012**, *1*, 247–252. [CrossRef]
8. Brooks, G.A. Lactate as a fulcrum of metabolism. *Redox Biol.* **2020**, *35*, 101454. [CrossRef]
9. Brooks, G.A. The Science and Translation of Lactate Shuttle Theory. *Cell Metab.* **2018**, *27*, 757–785. [CrossRef]
10. Adijanto, J.; Philp, N.J. The SLC16A family of monocarboxylate transporters (MCTs)—Physiology and function in cellular metabolism, pH homeostasis, and fluid transport. *Curr. Top. Membr.* **2012**, *70*, 275–311. [CrossRef]
11. Fishbein, W.N.; Merezhinskaya, N.; Foellmer, J.W. Relative distribution of three major lactate transporters in frozen human tissues and their localization in unfixed skeletal muscle. *Muscle Nerve* **2002**, *26*, 101–112. [CrossRef]
12. Hashimoto, T.; Masuda, S.; Taguchi, S.; Brooks, G.A. Immunohistochemical analysis of MCT1, MCT2 and MCT4 expression in rat plantaris muscle. *J. Physiol.* **2005**, *567*, 121–129. [CrossRef]
13. Herzig, S.; Raemy, E.; Montessuit, S.; Veuthey, J.L.; Zamboni, N.; Westermann, B.; Kunji, E.R.; Martinou, J.C. Identification and functional expression of the mitochondrial pyruvate carrier. *Science* **2012**, *337*, 93–96. [CrossRef]
14. Dubouchaud, H.; Butterfield, G.E.; Wolfel, E.E.; Bergman, B.C.; Brooks, G.A. Endurance training, expression, and physiology of LDH, MCT1, and MCT4 in human skeletal muscle. *Am. J. Physiol. Endocrinol. Metab.* **2000**, *278*, E571–E579. [CrossRef]
15. Cruz, R.S.; de Aguiar, R.A.; Turnes, T.; Dos Santos, R.P.; de Oliveira, M.F.; Caputo, F. Intracellular shuttle: The lactate aerobic metabolism. *ScientificWorldJournal* **2012**, *2012*, 420984. [CrossRef]
16. Koonen, D.P.; Glatz, J.F.; Bonen, A.; Luiken, J.J. Long-chain fatty acid uptake and FAT/CD36 translocation in heart and skeletal muscle. *Biochim. Biophys. Acta* **2005**, *1736*, 163–180. [CrossRef]

17. Jeukendrup, A.E. Regulation of fat metabolism in skeletal muscle. *Ann. N. Y. Acad. Sci.* **2002**, *967*, 217–235. [CrossRef]
18. Ahlborg, G.; Felig, P.; Hagenfeldt, L.; Hendler, R.; Wahren, J. Substrate Turnover during Prolonged Exercise in Man: Splanchnic and leg metabolism of glucose, free fatty acids, and amino acids. *J. Clin. Investig.* **1974**, *53*, 1080–1090. [CrossRef]
19. O'Brien, M.J.; Viguie, C.A.; Mazzeo, R.S.; Brooks, G.A. Carbohydrate dependence during marathon running. *Med. Sci. Sports Exerc.* **1993**, *25*, 1009–1017.
20. Achten, J.; Gleeson, M.; Jeukendrup, A.E. Determination of the exercise intensity that elicits maximal fat oxidation. *Med. Sci. Sports Exerc.* **2002**, *34*, 92–97. [CrossRef]
21. Goodpaster, B.H.; Sparks, L.M. Metabolic Flexibility in Health and Disease. *Cell Metab.* **2017**, *25*, 1027–1036. [CrossRef]
22. Smith, R.L.; Soeters, M.R.; Wüst, R.C.I.; Houtkooper, R.H. Metabolic Flexibility as an Adaptation to Energy Resources and Requirements in Health and Disease. *Endocr. Rev.* **2018**, *39*, 489–517. [CrossRef] [PubMed]
23. Falkenberg, H.; Langhammer, M.; Renne, U. Comparison of biochemical blood traits after long-term selection on high or low locomotory activity in mice. *Arch. Anim. Breed.* **2000**, *43*, 513–522. [CrossRef]
24. Brenmoehl, J.; Walz, C.; Renne, U.; Ponsuksili, S.; Wolf, C.; Langhammer, M.; Schwerin, M.; Hoeflich, A. Metabolic adaptations in the liver of born long-distance running mice. *Med. Sci. Sports Exerc.* **2013**, *45*, 841–850. [CrossRef] [PubMed]
25. Ohde, D.; Moeller, M.; Brenmoehl, J.; Walz, C.; Ponsuksili, S.; Schwerin, M.; Fuellen, G.; Hoeflich, A. Advanced Running Performance by Genetic Predisposition in Male Dummerstorf Marathon Mice (DUhTP) Reveals Higher Sterol Regulatory Element-Binding Protein (SREBP) Related mRNA Expression in the Liver and Higher Serum Levels of Progesterone. *PLoS ONE* **2016**, *11*, e0146748. [CrossRef] [PubMed]
26. Brenmoehl, J.; Ohde, D.; Walz, C.; Schultz, J.; Tuchscherer, A.; Rieder, F.; Renne, U.; Hoeflich, A. Dynamics of Fat Mass in DUhTP Mice Selected for Running Performance—Fat Mobilization in a Walk. *Obes. Facts* **2015**, *8*, 373–385. [CrossRef] [PubMed]
27. Brenmoehl, J.; Ohde, D.; Albrecht, E.; Walz, C.; Tuchscherer, A.; Hoeflich, A. Browning of subcutaneous fat and higher surface temperature in response to phenotype selection for advanced endurance exercise performance in male DUhTP mice. *J. Comp. Physiol. B* **2017**, *187*, 361–373. [CrossRef]
28. Dietl, G.; Langhammer, M.; Renne, U. Model simulations for genetic random drift in the outbred strain Fzt: DU. *Arch. Fur Tierz. Arch. Anim. Breed.* **2004**, *47*, 595–604. [CrossRef]
29. Petkov, S.; Brenmoehl, J.; Langhammer, M.; Hoeflich, A.; Röntgen, M. Myogenic Precursor Cells Show Faster Activation and Enhanced Differentiation in a Male Mouse Model Selected for Advanced Endurance Exercise Performance. *Cells* **2022**, *11*, 1001. [CrossRef]
30. Walz, C.; Brenmoehl, J.; Trakooljul, N.; Noce, A.; Caffier, C.; Ohde, D.; Langhammer, M.; Wimmers, K.; Ponsuksili, S.; Hoeflich, A. Control of Protein and Energy Metabolism in the Pituitary Gland in Response to Three-Week Running Training in Adult Male Mice. *Cells* **2021**, *10*, 736. [CrossRef]
31. Brenmoehl, J.; Walz, C.; Spitschak, M.; Wirthgen, E.; Walz, M.; Langhammer, M.; Tuchscherer, A.; Naumann, R.; Hoeflich, A. Partial phenotype conversion and differential trait response to conditions of husbandry in mice. *J. Comp. Physiol. B* **2018**, *188*, 527–539. [CrossRef]
32. Rehfeldt, C.; Ott, G.; Gerrard, D.; Varga, L.; Schlote, W.; Williams, J.L.; Renne, U.; Bunger, L. Effects of the Compact mutant myostatin allele Mstn(Cmpt-dl1Abc) introgressed into a high growth mouse line on skeletal muscle cellularity. *J. Muscle Res. Cell Motil.* **2005**, *26*, 103–112. [CrossRef]
33. Spurgeon, S.L.; Jones, R.C.; Ramakrishnan, R. High Throughput Gene Expression Measurement with Real Time PCR in a Microfluidic Dynamic Array. *PLoS ONE* **2008**, *3*, e1662. [CrossRef]
34. Ballester, M.; Cordón, R.; Folch, J.M. DAG Expression: High-Throughput Gene Expression Analysis of Real-Time PCR Data Using Standard Curves for Relative Quantification. *PLoS ONE* **2013**, *8*, e80385. [CrossRef] [PubMed]
35. Huang, D.W.; Sherman, B.T.; Lempicki, R.A. Bioinformatics enrichment tools: Paths toward the comprehensive functional analysis of large gene lists. *Nucleic Acids Res.* **2009**, *37*, 1–13. [CrossRef] [PubMed]
36. Luo, W.; Pant, G.; Bhavnasi, Y.K.; Blanchard, S.G., Jr.; Brouwer, C. Pathview Web: User friendly pathway visualization and data integration. *Nucleic Acids Res.* **2017**, *45*, W501–W508. [CrossRef] [PubMed]
37. Hassid, W.Z.; Abraham, S. [7] Chemical procedures for analysis of polysaccharides. In *Methods in Enzymology*; Academic Press: Cambridge, MA, USA, 1957; Volume 3, pp. 34–50.
38. Nakatani, T.; Nakashima, T.; Kita, T.; Hirofuji, C.; Itoh, K.; Itoh, M.; Ishihara, A. Cell size and oxidative enzyme activity of different types of fibers in different regions of the rat plantaris and tibialis anterior muscles. *Jpn. J. Physiol.* **2000**, *50*, 413–418. [CrossRef]
39. Soffe, Z.; Radley-Crabb, H.G.; McMahon, C.; Grounds, M.D.; Shavlakadze, T. Effects of loaded voluntary wheel exercise on performance and muscle hypertrophy in young and old male C57Bl/6J mice. *Scand. J. Med. Sci. Sports* **2016**, *26*, 172–188. [CrossRef]
40. Faulkner, J.A.; Maxwell, L.C.; Lieberman, D.A. Histochemical characteristics of muscle fibers from trained and detrained guinea pigs. *Am. J. Physiol.* **1972**, *222*, 836–840. [CrossRef]
41. Storlien, L.; Oakes, N.D.; Kelley, D.E. Metabolic flexibility. *Proc. Nutr. Soc.* **2004**, *63*, 363–368. [CrossRef]
42. Wilson, J.M.; Loenneke, J.P.; Jo, E.; Wilson, G.J.; Zourdos, M.C.; Kim, J.-S. The Effects of Endurance, Strength, and Power Training on Muscle Fiber Type Shifting. *J. Strength. Cond. Res.* **2012**, *26*, 1724–1729. [CrossRef]

43. Yaghoob Nezhad, F.; Verbrugge, S.A.J.; Schonfelder, M.; Becker, L.; de Angelis, M.H.; Wackerhage, H. Genes Whose Gain or Loss-of-Function Increases Endurance Performance in Mice: A Systematic Literature Review. *Front. Physiol.* **2019**, *10*, 262. [CrossRef] [PubMed]
44. Fueger, P.T.; Shearer, J.; Krueger, T.M.; Posey, K.A.; Bracy, D.P.; Heikkinen, S.; Laakso, M.; Rottman, J.N.; Wasserman, D.H. Hexokinase II protein content is a determinant of exercise endurance capacity in the mouse. *J. Physiol.* **2005**, *566*, 533–541. [CrossRef]
45. Romijn, J.A.; Coyle, E.F.; Sidossis, L.S.; Gastaldelli, A.; Horowitz, J.F.; Endert, E.; Wolfe, R.R. Regulation of endogenous fat and carbohydrate metabolism in relation to exercise intensity and duration. *Am. J. Physiol.* **1993**, *265*, E380–E391. [CrossRef]
46. Dyck, D.J.; Peters, S.J.; Wendling, P.S.; Chesley, A.; Hultman, E.; Spriet, L.L. Regulation of muscle glycogen phosphorylase activity during intense aerobic cycling with elevated FFA. *Am. J. Physiol. Endocrinol. Metab.* **1996**, *270*, E116–E125. [CrossRef]
47. Green, H.J.; Ball-Burnett, M.E.; Morrissey, M.A.; Spalding, M.J.; Hughson, R.L.; Fraser, I.G. Fiber type specific glycogen utilization in rat diaphragm during treadmill exercise. *J. Appl. Physiol.* **1987**, *63*, 75–83. [CrossRef]
48. Murase, T.; Haramizu, S.; Shimotoyodome, A.; Tokimitsu, I.; Hase, T. Green tea extract improves running endurance in mice by stimulating lipid utilization during exercise. *Am. J. Physiol. Regul. Integr. Comp. Physiol.* **2006**, *290*, R1550–R1556. [CrossRef]
49. Gladden, L.B. Muscle as a consumer of lactate. *Med. Sci. Sports Exerc.* **2000**, *32*, 764–771. [CrossRef]
50. Ohkuwa, T.; Kato, Y.; Katsumata, K.; Nakao, T.; Miyamura, M. Blood lactate and glycerol after 400-m and 3,000-m runs in sprint and long distance runners. *Eur. J. Appl. Physiol. Occup. Physiol.* **1984**, *53*, 213–218. [CrossRef]
51. Fujitsuka, N.; Yamamoto, T.; Ohkuwa, T.; Saito, M.; Miyamura, M. Peak blood lactate after short periods of maximal treadmill running. *Eur. J. Appl. Physiol. Occup. Physiol.* **1982**, *48*, 289–296. [CrossRef]
52. Zhang, S.; Hulver, M.W.; McMillan, R.P.; Cline, M.A.; Gilbert, E.R. The pivotal role of pyruvate dehydrogenase kinases in metabolic flexibility. *Nutr. Metab.* **2014**, *11*, 10. [CrossRef] [PubMed]
53. Arner, P.; Kriegholm, E.; Engfeldt, P.; Bolinder, J. Adrenergic regulation of lipolysis in situ at rest and during exercise. *J. Clin. Investig.* **1990**, *85*, 893–898. [CrossRef]
54. Frayn, K.N. Adipose tissue as a buffer for daily lipid flux. *Diabetologia* **2002**, *45*, 1201–1210. [CrossRef] [PubMed]
55. Fernández-Verdejo, R.; Bajpeyi, S.; Ravussin, E.; Galgani, J.E. Metabolic flexibility to lipid availability during exercise is enhanced in individuals with high insulin sensitivity. *Am. J. Physiol. Endocrinol. Metab.* **2018**, *315*, E715–E722. [CrossRef]
56. Hagberg, C.E.; Falkevall, A.; Wang, X.; Larsson, E.; Huusko, J.; Nilsson, I.; van Meeteren, L.A.; Samen, E.; Lu, L.; Vanwildemeersch, M.; et al. Vascular endothelial growth factor B controls endothelial fatty acid uptake. *Nature* **2010**, *464*, 917–921. [CrossRef]
57. Muoio, D.M. Metabolism and vascular fatty acid transport. *N. Engl. J. Med.* **2010**, *363*, 291–293. [CrossRef]
58. Bruce, C.R.; Brolin, C.; Turner, N.; Cleasby, M.E.; van der Leij, F.R.; Cooney, G.J.; Kraegen, E.W. Overexpression of carnitine palmitoyltransferase I in skeletal muscle in vivo increases fatty acid oxidation and reduces triacylglycerol esterification. *Am. J. Physiol. Endocrinol. Metab.* **2007**, *292*, E1231–E1237. [CrossRef]
59. Ahmed, K.; Tunaru, S.; Tang, C.; Muller, M.; Gille, A.; Sassmann, A.; Hanson, J.; Offermanns, S. An autocrine lactate loop mediates insulin-dependent inhibition of lipolysis through GPR81. *Cell Metab.* **2010**, *11*, 311–319. [CrossRef] [PubMed]
60. Liu, C.; Wu, J.; Zhu, J.; Kuei, C.; Yu, J.; Shelton, J.; Sutton, S.W.; Li, X.; Yun, S.J.; Mirzadegan, T.; et al. Lactate inhibits lipolysis in fat cells through activation of an orphan G-protein-coupled receptor, GPR81. *J. Biol. Chem.* **2009**, *284*, 2811–2822. [CrossRef]

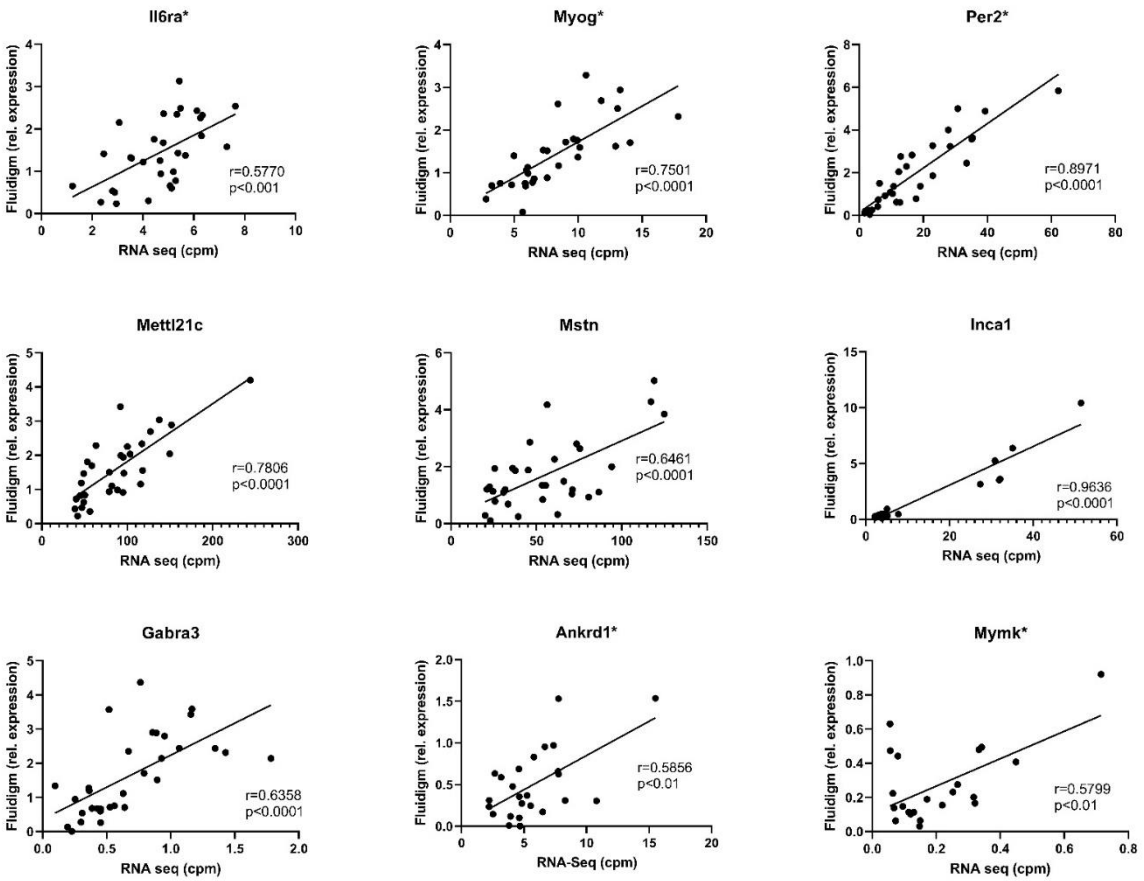

Fig. S1: Validation of RNA-seq data by the Fluidigm technique for nine differentially expressed genes (DEGs). For each gene, the total reads (count per million, cpm) obtained by RNA-seq were plotted on the x-axis and RT-qPCR data ($2^{-\Delta\Delta Ct}$) on the y-axis. Stars at the gene name indicate that outliers were removed during processing, as described in Materials and Methods. Corresponding correlation coefficients (r) and p-values are shown. Abbreviations: Ankrd1 – Ankyrin repeat domain-containing protein 1, Gabra3 – Gamma-aminobutyric acid A receptor subunit alpha 3, Il6ra – Interleukin 6 receptor alpha, Inca1 – Inhibitor of CDK, Cyclin A1 interacting protein 1, Mettl21c – methyltransferase like 21C, Mstn – myostatin, Mymk – myomaker, MyoG – myogenin, Per2 – period circadian clock 2.

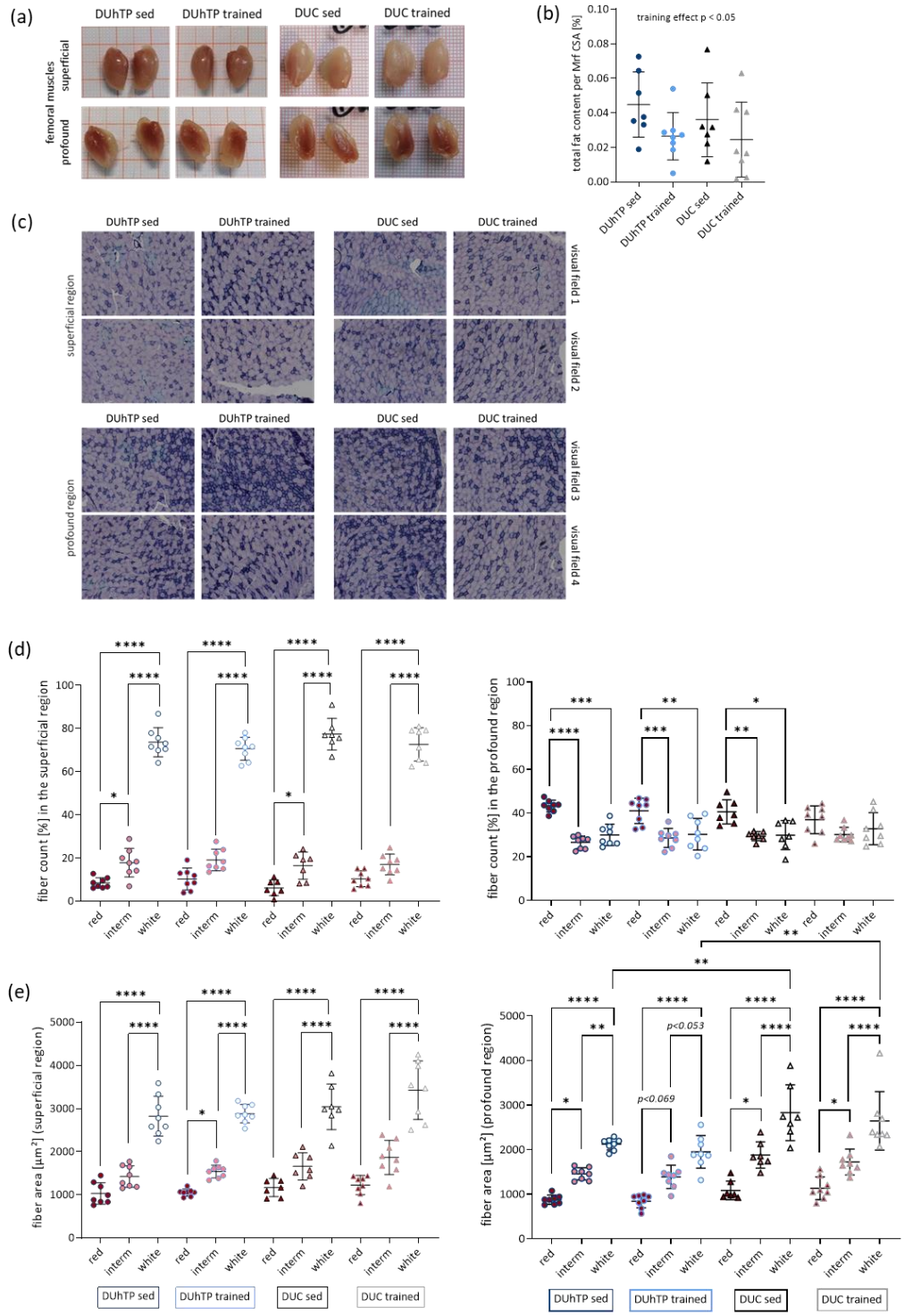

Fig. S2: Immunohistochemical evaluation of *Musculus rectus femoris* (Mrf) of trained and sedentary (sed) DUhTP and DUC mice at the age of 70 days (n = 7-8 animals). **a)** Representative dissected Mrfs showing superficial region (upper panel) and profound (lower panel) region of sedentary and trained DUhTP (left) and DUC mice (right). **b)** Percentage of total fat per cross-sectional area (CSA) in the four groups. The training-mediated effect was statistically evaluated by using the unpaired t-test with Welch correction. **c)** Representative histological images of 10 µm Mrf cryosections stained with NADH-tetrazolium reductase to determine red (dark blue), intermediate (mid blue), and white (light blue) fibers in sedentary and trained DUhTP (left) and DUC (right) mice. Shown are two images, each from the superficial and profound regions from a mouse of each group. **d)** Percentage muscle fiber count and **e)** muscle fiber area per µm² analyzed muscle region (see Method part) of red (dark red), intermediate (light red), and white fibers (white) in trained and sedentary DUhTP (light/dark blue) and DUC (gray/black) mice were measured and calculated by using by image analysis. Data are shown as scatter plots with means and standard derivations. Statistical analysis was performed using the linear model followed by TukeyHSD post hoc test to test the dependence between phenotype and the interaction of line x treatment x muscle fiber type. Significant differences as indicated: * $p < 0.05$, ** $p < 0.01$, *** $p < 0.001$, **** $p < 0.0001$. Borderline significances as indicated.

(a) DUhTP sedentary vs DUC sedentary

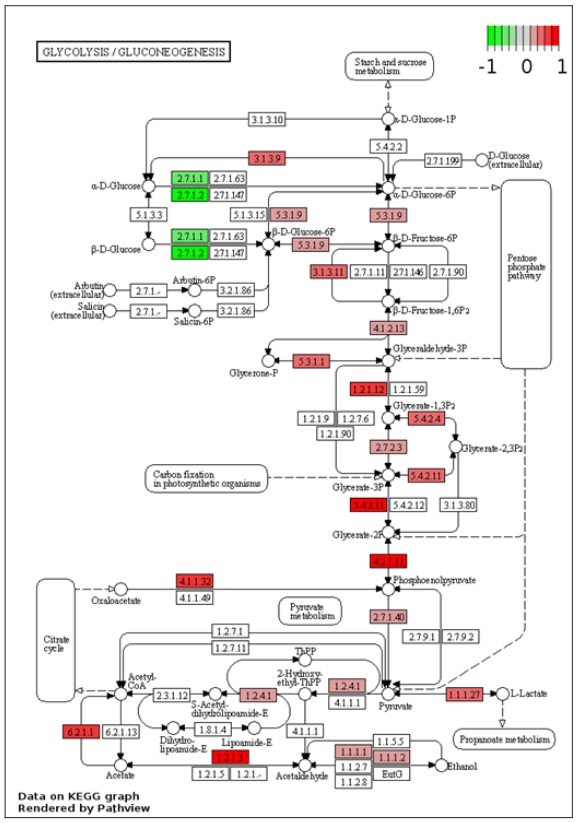

DUhTP trained vs DUC trained

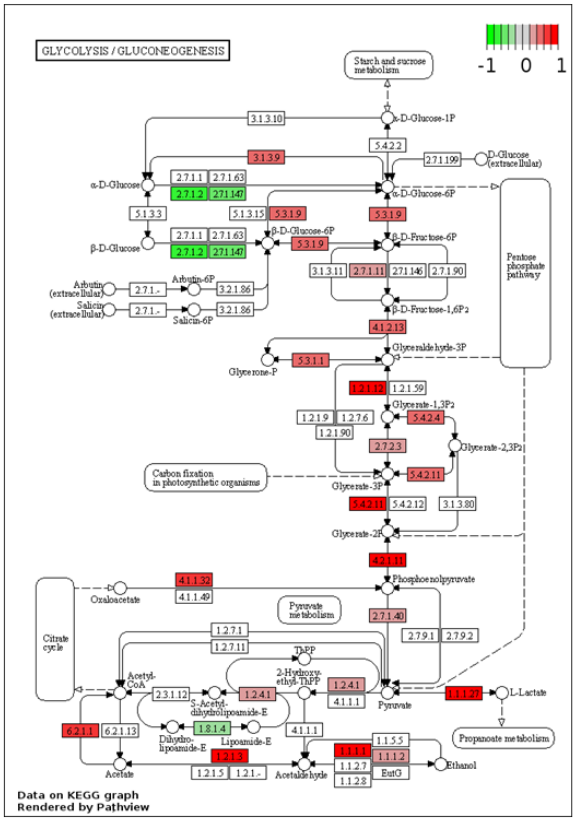

DUhTP trained vs sedentary

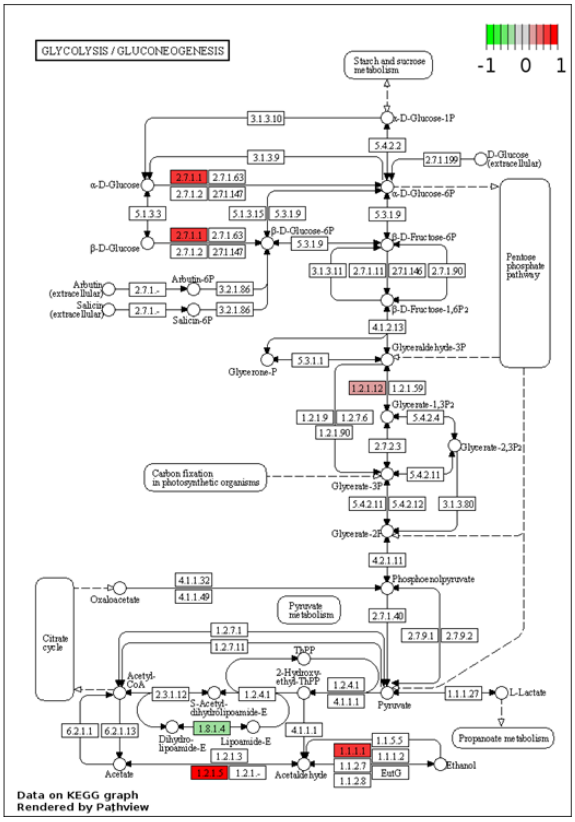

DUC trained vs sedentary

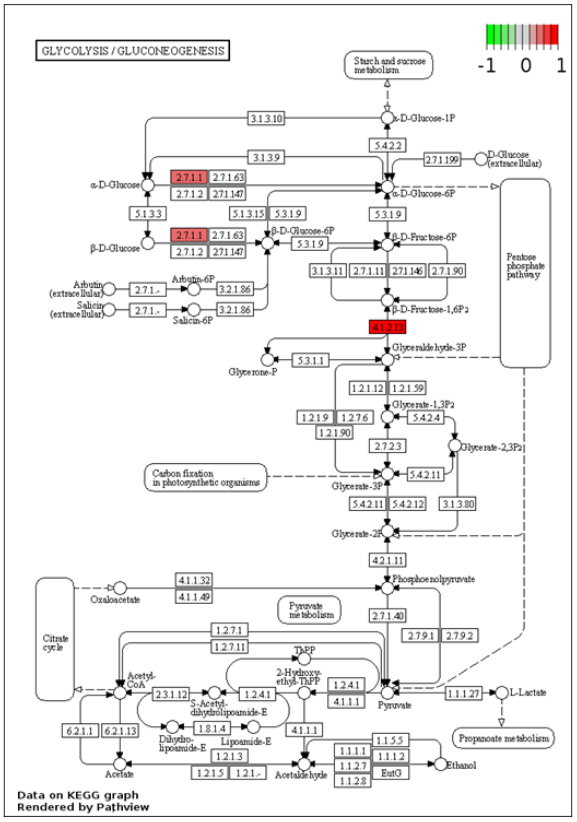

(b) DUhTP sedentary vs DUC sedentary

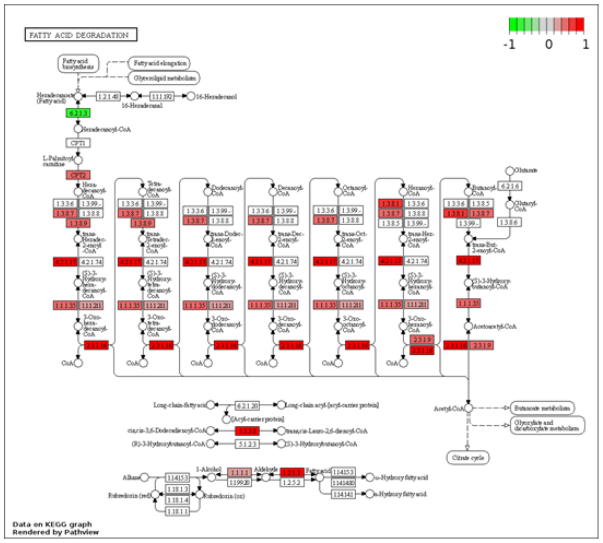

DUhTP trained vs DUC trained

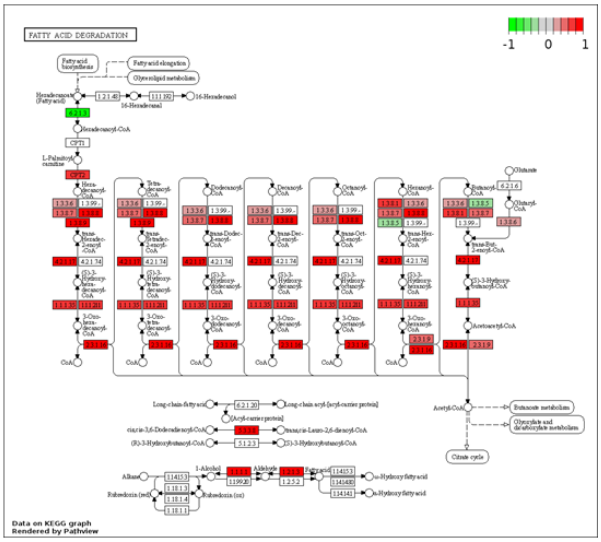

DUhTP trained vs sedentary

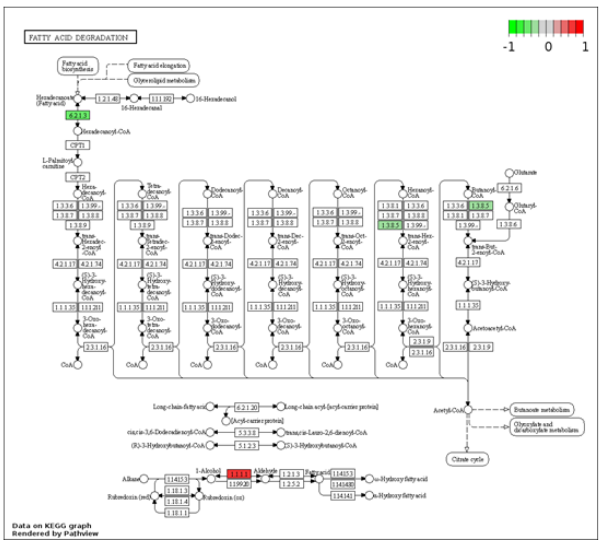

DUC trained vs sedentary

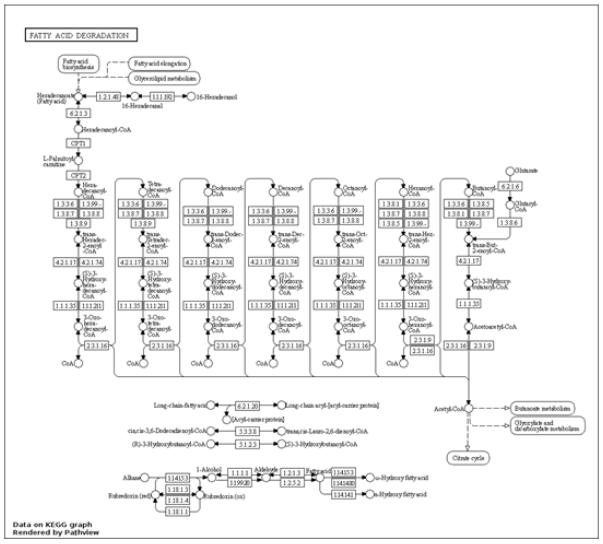

(c) DUhTP sedentary vs DUC sedentary

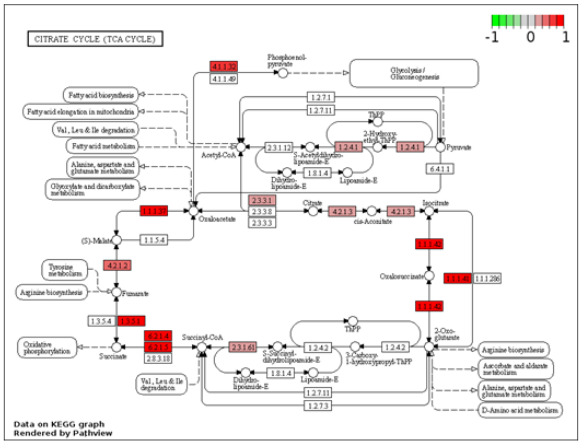

DUhTP trained vs DUC trained

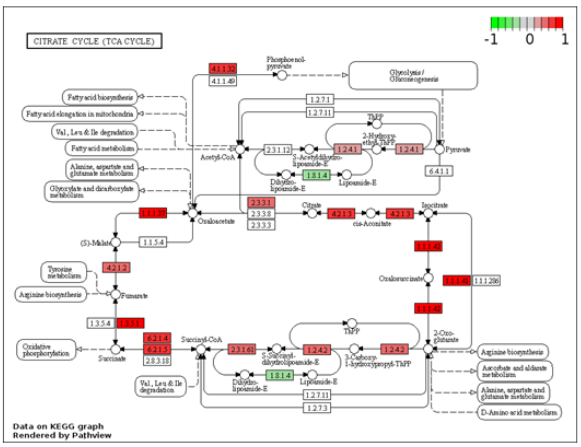

DUhTP trained vs sedentary

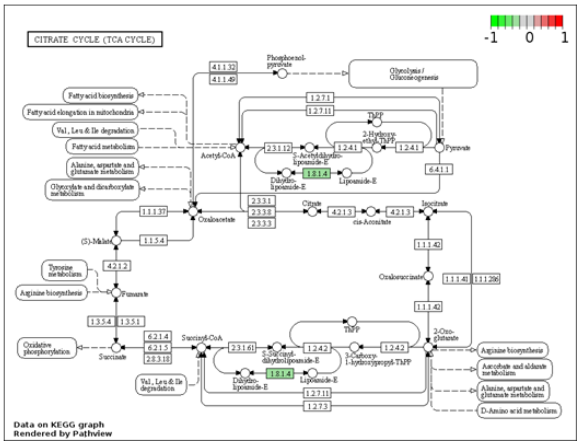

DUC trained vs sedentary

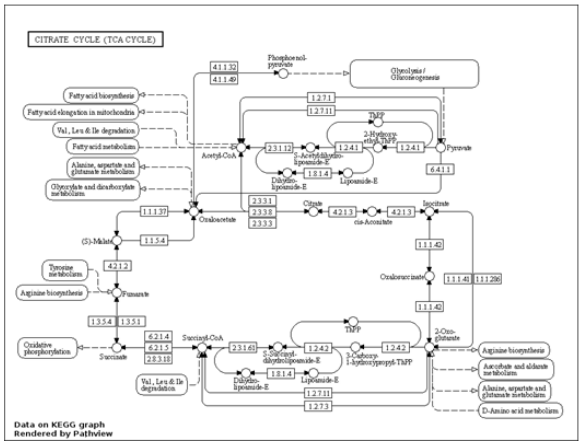

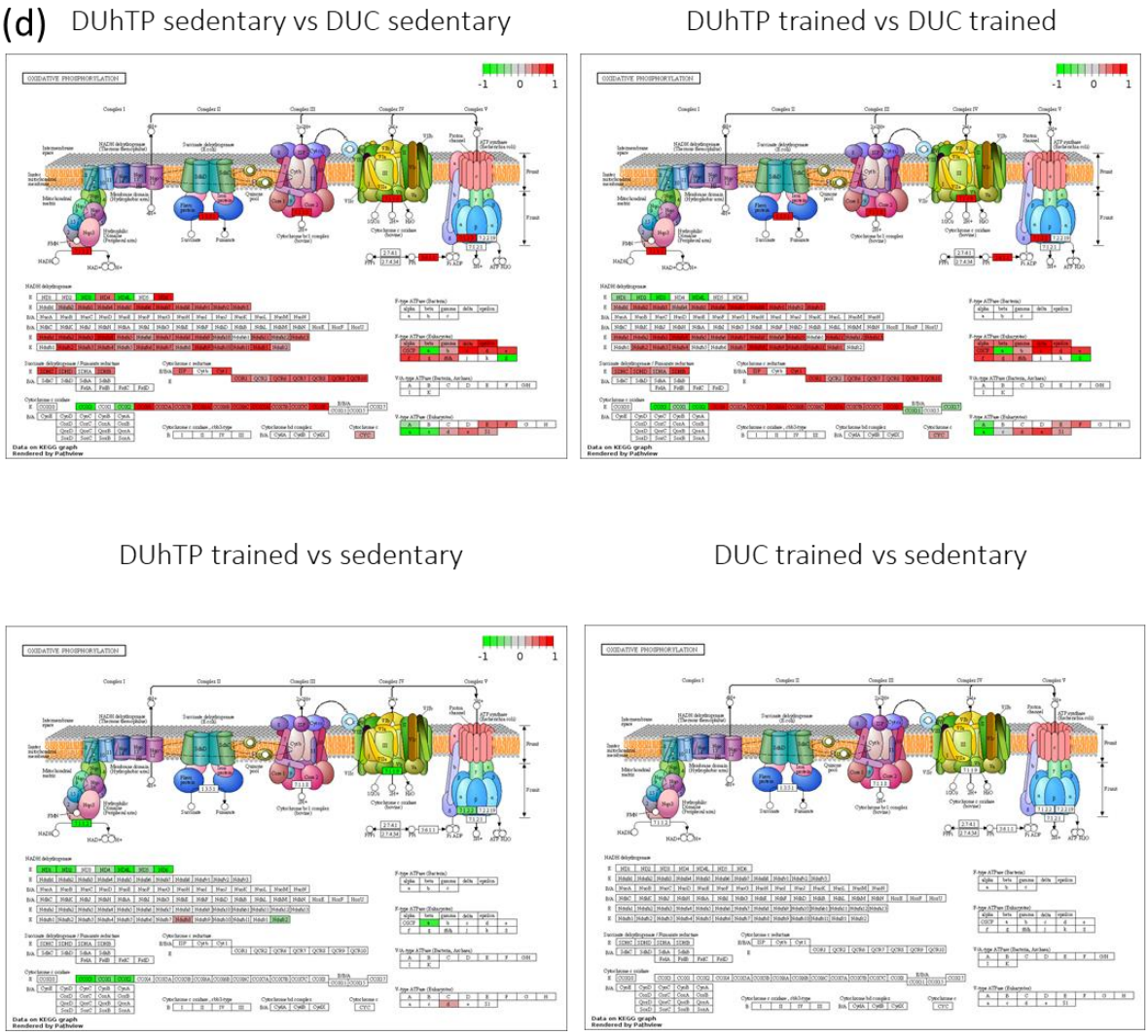

Fig. S3: Graphical visualization of gene regulation in a) glycolysis, b) fatty acid degradation, c) TCA cycle, and d) oxidative phosphorylation KEGG pathways for the four comparison groups. The KEGG Pathway analyses were obtained by using the DEGs (FDR < 0.05) of all comparison groups (DUhTP sedentary vs DUC sedentary, DUhTP trained vs DUC trained, DUhTP trained vs. sedentary, DUC trained vs. sedentary) via https://pathview.uncc.edu (access date: : 12/01/2022). Abbreviation: DEGs = differential expressed genes, vs = versus

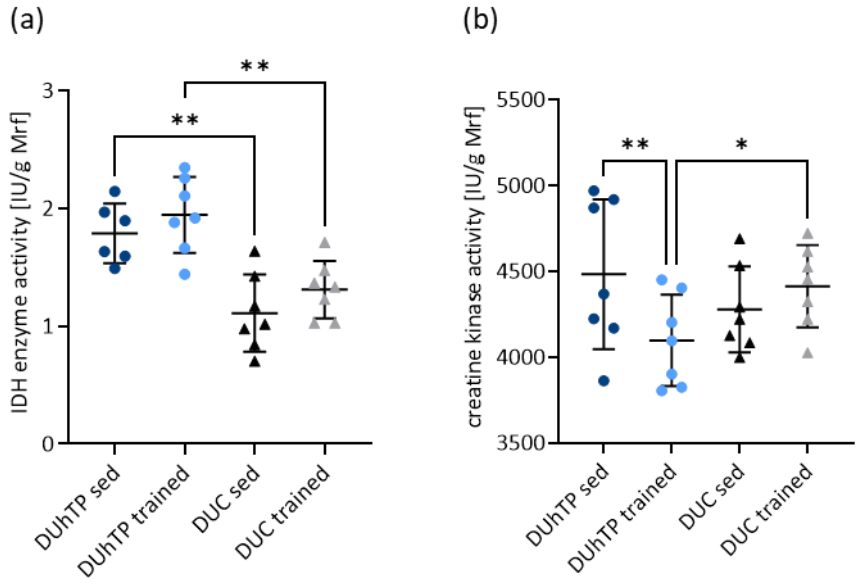

Fig. S4: Analysis of a) isocitrate dehydrogenase (IDH) enzyme activity and b) creatine kinase enzyme activity per gram *Musculus rectus femoris* of trained and sedentary DUhTP (light/dark blue) and DUC mice (gray/black). Results are shown as scatter plots with mean and standard derivations. Statistical analysis was performed using two-way ANOVA. Significant differences are marked with: * $p < 0.05$, ** $p < 0.01$, **** $p < 0.0001$.

Table S1: Body weight, weight gain, and food consumption of all mice during the 3-week experiment, starting from day 49 and ending at day 70. All data are means with standard deviations and were statistically analyzed using two-way ANOVA with GraphPad. Different letters denote significant age-related differences ($p < 0.05$). Hashtags mark significant differences compared to sedentary or trained control mice DUC ($p < 0.05$), and paragraph symbols mark significant differences compared to sedentary littermates of the respective line ($p < 0.05$).

	Experiment time	DUhTP sed n = 19	DUhTP trained n = 19	DUC sed n = 17	DUC trained n = 23
Body weight [g]	day 49	30.67 ± 2.31[a]#	30.07 ± 2.86[a]#	35.47 ± 4.37[a]	37.07 ± 2.66[a]
	day 56	31.90 ± 2.61[b]#	30.23 ± 3.04[a]#	36.99 ± 4.14[b]	37.78 ± 2.66[b]
	day 63	32.83 ± 2.77[c]#	30.92 ± 3.03[b]#	38.48 ± 4.39[c]	38.69 ± 2.67[c]
	day 70	34.21 ± 2.60[d]#	31.04 ± 2.73[b]#§	39.35 ± 4.44[d]	39.18 ± 2.94[c]
Weight gain [g]	week 1	1.24 ± 0.90	0.29 ± 0.95§	1.52 ± 0.80[a]	0.70 ± 0.69§
	week 2	0.93 ± 0.84	0.58 ± 0.54	1.50 ± 0.55[a]	0.91 ± 0.70§
	week 3	1.37 ± 0.97	0.09 ± 1.14§	0.86 ± 0.58[b]	0.49 ± 1.10
weekly feed intake [g]	week 1	35.23 ± 2.90[a]#	36.48 ± 3.21[a]#	51.15 ± 10.19	45.03 ± 7.90
	week 2	38.01 ±3.55[b]#	39.83 ± 3.64[b]#	47.57 ± 4.53	44.80 ± 5.21
	week 3	36.65 ± 4.04[a]#	38.96 ± 7.62[a,b]#	49.48 ± 6.01	45.87 ± 6.85

Table S2: Primer sequences for quantitative real-time PCR for selected genes.

Gene	forward primer 5′→3′	reverse primer 5′→3′
Actb	TGACAGGATGCAGAAGGAGA	CGCTCAGGAGGAGCAATG
Ankrd1	GCTGGTAACAGGCAAAAAGAAC	CCTCTCGCAGTTTCTCGCT
Gabra3	CTCTCTGCTTCGGGGAAGTG	CTTGGCTAGTGGTTCCAGGG
Il6ra	CCTGAGACTCAAGCAGAAATGG	AGAAGGAAGGTCGGCTTCAGT
Inca1	ATGCCTCAGCCGTATGGAGAT	GCCCTCAGAATTGGTGGAATGTA
Mettl21c	ACTCTCGGGGACTCCACAG	GCTCTTGTGTGTAGCTGGCATA
Mstn	AGTGGATCTAAATGAGGGCAGT	GTTTCCAGGCGCAGCTTAC
Mymk	TTCCTCCCGACAGTGAGCAT	GCACAGCACAGACAAACCAG
MyoG	AGTGAATGCAACTCCCACA	CTGGGAAGGCAACAGACATA
Per2	CAGAGGAGAAGACTCCGCAC	TTGCTGTCGCTGGATGATGT
Pgk1	CAGTCTAGAGCTCCTGGAAGGT	AGGAGCACAGGAACCAAAGG
Rplp2	GACGATGATCGGCTCAACAAG	ACCCTGAGCGATGACATCCT
Rpl26	GAACCGCAAACGGCATTTCA	TAGTGTCCGCGAACAACCTG

Abbreviations: Actb – actin β, Ankrd1 – Ankyrin repeat domain-containing protein 1, Gabra3 – Gamma-aminobutyric acid A receptor subunit alpha 3, Il6ra – Interleukin 6 receptor alpha, Inca1 – Inhibitor of CDK, Cyclin A1 interacting protein 1, Mettl21c – methyltransferase like 21C, Mstn – myostatin, Mymk – myomaker, MyoG – myogenin, Per2 – period circadian clock 2, Pgk1 – phosphoglycerate kinase 1, Rplp2 – ribosomal protein, large P2, Rpl26 – ribosomal protein L26. The housekeeping genes are underlined.

Table S3: List of all differentially expressed genes (DEGs) in the four different comparison groups, each group consisting of 8 animals, by RNAseq. Abbreviations: trained – 3-weeks treadmill training, sed – sedentary, FDR – false discovery rate

As an extra file

https://hotcloud.fbn-dummerstorf.de/owncloud/index.php/s/dSNtF3Kisj2BrH0

Table S4: Identification of differentially expressed genes (DEGs; FDR < 0.05) in the four different comparison groups, each group consisting of eight animals, by RNAseq, providing a) the number of total, up- and downregulated transcripts. The percentage of up- or down-regulated transcripts is noted in parentheses. b) List of enriched pathways for upregulated (upper part) or downregulated (lower part) genes in the comparison between trained DUhTP and DUC mice (DUhTP trained vs. DUC trained), ordered by the count of involved genes. The level of enrichment is reported as p-value and gene count. Abbreviations: trained – 3-weeks treadmill training, sed – sedentary

(a)

comparison group	DEGs	downregulated DEGs	upregulated DEGs
DUhTP sed vs. DUC sed	5916	3077 (52%)	2839 (48%)
DUhTP trained vs. DUC trained	7042	3751 (53%)	3291 (47%)
DUhTP trained vs. DUhTP sed	1606	1037 (65%)	569 (35%)
DUC trained vs. DUC sed	130	27 (21%)	103 (79%)

(b)

KEGG_PATHWAY	Count	Benjamini
upregulated		
Metabolic pathways	423	3,90E-27
Pathways of neurodegeneration - multiple diseases	172	8,00E-26
Amyotrophic lateral sclerosis	146	8,40E-26
Alzheimer disease	146	6,70E-24
Huntington disease	139	3,10E-32
Parkinson disease	134	3,20E-36
Prion disease	124	4,80E-29
Thermogenesis	116	5,10E-31
Chemical carcinogenesis - reactive oxygen species	109	3,70E-28
Diabetic cardiomyopathy	108	9,20E-30
Ribosome	106	3,20E-36
Oxidative phosphorylation	87	1,80E-33
Coronavirus disease - COVID-19	87	2,10E-11
Non-alcoholic fatty liver disease	78	1,30E-20
Salmonella infection	58	4,80E-02
Spliceosome	57	4,40E-11
Retrograde endocannabinoid signaling	54	1,20E-07
Carbon metabolism	51	1,10E-09
Spinocerebellar ataxia	45	1,20E-04
Biosynthesis of cofactors	42	6,20E-03
Fluid shear stress and atherosclerosis	38	3,30E-02
Autophagy - animal	37	3,30E-02
Peroxisome	35	4,00E-06
Cardiac muscle contraction	34	1,70E-05

Biosynthesis of amino acids	31	4,70E-05
Insulin resistance	30	4,00E-02
Proteasome	28	3,50E-09
Valine, leucine and isoleucine degradation	25	5,30E-05
Nucleotide metabolism	25	3,00E-02
Aminoacyl-tRNA biosynthesis	24	2,40E-03
Glycolysis / Gluconeogenesis	24	2,90E-03
Glutathione metabolism	24	8,00E-03
Mitophagy - animal	23	8,20E-03
Fatty acid metabolism	22	6,10E-03
Pyruvate metabolism	21	8,10E-05
Fatty acid degradation	21	1,40E-03
Citrate cycle (TCA cycle)	18	3,20E-05
Arginine and proline metabolism	18	3,50E-02
RNA polymerase	17	1,40E-04
Glyoxylate and dicarboxylate metabolism	15	2,80E-03
Glycine, serine and threonine metabolism	15	2,90E-02
Propanoate metabolism	14	6,60E-03
Fatty acid elongation	12	3,50E-02
2-Oxocarboxylic acid metabolism	10	2,30E-02
Sulfur relay system	7	4,40E-03
downregulated		
Herpes simplex virus 1 infection	142	2,50E-13
Pathways in cancer	128	1,40E-04
PI3K-Akt signaling pathway	83	4,20E-03
Human papillomavirus infection	83	4,80E-03
MAPK signaling pathway	74	9,40E-04
Endocytosis	69	1,20E-03
Salmonella infection	66	8,70E-04
Focal adhesion	62	1,40E-05
Regulation of actin cytoskeleton	60	6,80E-04
Lipid and atherosclerosis	59	6,80E-04
Proteoglycans in cancer	58	3,50E-04
Hepatitis B	56	1,50E-06
Rap1 signaling pathway	55	3,60E-03
Ras signaling pathway	54	3,00E-02
Autophagy - animal	51	1,50E-06
Transcriptional misregulation in cancer	51	4,30E-02

FoxO signaling pathway	49	1,20E-06
Protein processing in endoplasmic reticulum	49	9,00E-04
mTOR signaling pathway	46	8,70E-04
Signaling pathways regulating pluripotency of stem cells	45	1,40E-04
Axon guidance	45	1,60E-02
Cellular senescence	44	3,30E-02
Ubiquitin mediated proteolysis	42	2,30E-03
Insulin signaling pathway	41	1,40E-03
Hepatitis C	40	3,80E-02
Measles	39	9,00E-03
Growth hormone synthesis, secretion and action	38	5,30E-04
Yersinia infection	38	4,80E-03
Cell cycle	37	2,60E-03
Gastric cancer	37	3,90E-02
Prostate cancer	35	1,90E-04
Thyroid hormone signaling pathway	35	4,50E-03
Neurotrophin signaling pathway	35	4,80E-03
Sphingolipid signaling pathway	35	6,60E-03
Small cell lung cancer	34	1,40E-04
Nucleocytoplasmic transport	34	4,90E-03
Chronic myeloid leukemia	33	3,70E-06
Endocrine resistance	32	6,80E-04
TGF-beta signaling pathway	32	8,70E-04
Colorectal cancer	30	1,00E-03
Phosphatidylinositol signaling system	30	3,80E-03
mRNA surveillance pathway	30	9,00E-03
Toxoplasmosis	30	2,20E-02
AGE-RAGE signaling pathway in diabetic complications	29	1,30E-02
ErbB signaling pathway	28	2,30E-03
Longevity regulating pathway	28	5,20E-03
Lysine degradation	27	1,10E-04
EGFR tyrosine kinase inhibitor resistance	27	2,10E-03
PD-L1 expression and PD-1 checkpoint pathway in cancer	27	7,60E-03
ECM-receptor interaction	26	1,50E-02
Progesterone-mediated oocyte maturation	26	2,60E-02
Renal cell carcinoma	25	1,20E-03
Non-small cell lung cancer	25	2,60E-03
Pancreatic cancer	25	4,80E-03

Bacterial invasion of epithelial cells	25	4,80E-03
p53 signaling pathway	24	4,90E-03
Glioma	24	6,90E-03
Adherens junction	23	8,90E-03
Prolactin signaling pathway	23	1,50E-02
Viral life cycle - HIV-1	22	3,60E-03
Melanoma	22	2,20E-02
Long-term depression	21	5,70E-03
Longevity regulating pathway - multiple species	20	1,90E-02
Endometrial cancer	19	2,00E-02
Notch signaling pathway	19	2,80E-02
Hedgehog signaling pathway	18	4,20E-02

Table S5: List of significantly up- and downregulated levels of various acylcarnitines, di/triglycerides, phospholipids, and fatty acid derivates in serum samples of the four comparison groups (DUhTP sed vs. DUC sed, DUhTP trained vs. DUC trained, DUhTP trained vs. DUhTP sed, and DUC trained vs. DUC sed; each n = 9) shown as log2FC ($p < 0.05$). Metabolites were analyzed by high-resolution LC-MS/MS.

metabolite name	log2FC	p-Value	metabolite class
DUhTP sed vs. DUC sed			
Traumatic Acid	-4.37	0.000	Dicarboxylic Acid/ Fatty acid derivate (prostaglandin synthesis intermediate)
11-Aminoundecanoic acid	-3.74	0.000	Fatty acid/ Amine
Octatrienal	-2.15	0.000	Fatty aldehyde
7-Mercaptoheptanoylthreonine	-1.15	0.014	Fatty acid derivate
3-Hydroxytetradecanoic acid	1.47	0.022	Hydroxy fatty acid
10-Nitrooleate	1.48	0.019	Nitrated Fatty acid
9S,13R-12-Oxophytodienoic acid	1.59	0.033	Fatty acid derivate (lipoxygenase metabolite of linolenic acid)
5-Hydroxydecanoic acid	1.80	0.000	Hydroxy fatty acid
12-Oxododecanoic acid	1.88	0.008	Oxo fatty acid
3-oxopalmitic acid	1.89	0.048	Oxo fatty acid
12-Hydroxylauric acid	1.93	0.004	Hydroxy fatty acid
(2Z)-3,7-Dimethyl-2,6-octadien-1-yl 3-oxobutanoate	2.51	0.006	Fatty alcohol ester
2,3-Dinor-6-oxoprostaglandin F1alpha	2.84	0.000	Eicosanoide/ Prostaglandine/ arachidonic acid metabolite
3-Oxotetradecanoic acid	2.90	0.005	Oxo fatty acid
P-PE 41:6	-1.09	0.001	Phospholipid
SM 29:2 / sphingomyeline 29:2	-1.08	0.019	Phospholipid
PS 42:3 / phosphatidylserine 42:3	-1.03	0.000	Phospholipid
PC 37:2	-0.55	0.011	Phospholipid
PE 40:9	1.01	0.007	Phospholipid
1-[(9Z)-hexadecenoyl]-sn-glycero-3-phosphocholine (PC 18:1/20:3)	1.17	0.047	Phospholipid
TAG 48:2	1.06	0.006	Triglyceride
TAG 47:6	1.14	0.000	Triglyceride
(2S)-1-(Docosanoyloxy)-3-hydroxy-2-propanyl (7Z,10Z,13Z,16Z)-7,10,13,16-docosatetraenoate (DAG 22:0/22:5)	1.20	0.021	Diglyceride
TAG 62:16	4.74	0.003	Triglyceride
3-[(3-Hydroxydecanoyl)oxy]-4-(trimethylammonio)butanoate (3-hydroxydecanoyl carnitine)	1.16	0.027	Acylcarnitine
3-hydroxydodecanoylcarnitine	2.16	0.016	Acylcarnitine

9,12-Hexadecadienoylcarnitine	4.14	0.000	Acylcarnitine
DUhTP trained vs DUC trained			
7-Mercaptoheptanoylthreonine	-2.26	0.000	Hydroxy fatty acid
11-Aminoundecanoic acid	-1.04	0.034	Fatty acid/ Amine
5-Hydroxydecanoic acid	1.02	0.003	Hydroxy fatty acid
12-Oxododecanoic acid	1.14	0.003	Oxo fatty acid
Brassylic acid	1.19	0.013	Dicarboxylic acid
12-Hydroxylauric acid	1.30	0.002	Hydroxy fatty acid
3-Hydroxytetradecanoic acid	1.52	0.001	Hydroxy fatty acid
3-oxopalmitic acid	1.70	0.050	Oxo fatty acid
DL-α-Aminocaprylic acid	1.79	0.000	Fatty acid/ Amine
(2Z)-3,7-Dimethyl-2,6-octadien-1-yl 3-oxobutanoate	2.00	0.004	fatty alcohol esters
3-Oxotetradecanoic acid	2.11	0.001	Oxo fatty acid
P-PE 38:1	-1.61	0.026	Phospholipid
PC 37:2	-1.07	0.000	Phospholipid
PS 42:3 / phosphatidylserine 42:3	-0.85	0.000	Phospholipid
PS 40:0 /phosphatidylserine 40:0	0.79	0.049	Phospholipid
1-hexadecanoyl-2-(4Z,7Z,10Z,13Z,16Z,19Z-docosahexaenoyl)-sn-glycero-3-phosphocholine (PC (16:0/22:6))	1.22	0.025	Phospholipid
1-[(9Z)-hexadecenoyl]-sn-glycero-3-phosphocholine (LPC 16:1)	1.47	0.011	Phospholipid
TAG 48:2	0.88	0.027	Triglyceride
TAG 62:16	4.67	0.000	Triglyceride
2-Hexenoylcarnitine	-3.42	0.000	Acylcarnitine
Tiglylcarnitine	1.23	0.020	Acylcarnitine
Decanoylcarnitine	1.30	0.046	Acylcarnitine
3-[(3-Hydroxydecanoyl)oxy]-4-(trimethylammonio)butanoate (3-hydroxydecanoyl carnitine)	1.34	0.029	Acylcarnitine
Oleoylcarnitine	1.42	0.017	Acylcarnitine
3-hydroxydodecanoylcarnitine	1.51	0.014	Acylcarnitine
(2E)-hexadecenoylcarnitine	1.55	0.008	Acylcarnitine
3-Hydroxy-5, 8-tetradecadiencarnitine	2.11	0.014	Acylcarnitine
9,12-Hexadecadienoylcarnitine	2.21	0.044	Acylcarnitine
DUhTP trained vs DUhTP sed			
2,3-Dinor-6-oxoprostaglandin F1alpha	-1.84	0.002	Eicosanoide/ Prostaglandine/ arachidonic acid metabolite
DL-α-Aminocaprylic acid	1.17	0.002	Fatty acid/ Amine

Icosanedioic acid	1.34	0.040	Fatty acid derivate dicarboxylic acid
Icosatetraenoic acid	1.49	0.025	Fatty acid
11-Aminoundecanoic acid	3.29	0.000	Fatty acid/ Amine
Cer 17:4 /ceramide 17:4	-1.32	0.033	Ceramide
P-PE 40:8	-1.12	0.041	Phospholipid
P-PE 41:6	0.85	0.049	Phospholipid
PS 45:9 / phosphatidylserine 45:9	1.17	0.002	Phospholipid
PS 40:0 /phosphatidylserine 40:0	1.34	0.004	Phospholipid
1-octadecanoyl-2-(7Z,10Z,13Z,16Z)-docosatetraenoyl-sn-glycero-3-phosphoethanolamine	1.61	0.035	Phospholipid
1-hexadecanoyl-2-(4Z,7Z,10Z,13Z,16Z,19Z-docosahexaenoyl)-sn-glycero-3-phosphocholine	2.78	0.013	Phospholipid
1-[(9Z)-octadecenoyl]-2-[(4Z,7Z,10Z,13Z,16Z,19Z)-docosa-hexaenoyl]-sn-glycero-3-phosphocholine	3.10	0.007	Phospholipid
Platelet-activating factor	6.03	0.015	Phospholipid
1-Linoleoyl-sn-glycero-3-phosphocholine	6.06	0.007	Phospholipid
1-arachidonoyl-sn-glycero-3-phosphocholine	6.10	0.011	Phospholipid
TAG 47:6	-0.68	0.014	Triglyceride
9,12-Hexadecadienoylcarnitine	-2.29	0.002	Acylcarnitine
2-Hexenoylcarnitine	1.43	0.007	Acylcarnitine
stearoylcarnitine	1.62	0.046	Acylcarnitine
3-hydroxydodecanoylcarnitine	2.52	0.014	Acylcarnitine
DUC trained vs DUC sed			
Octatrienal	-1.68	0.000	fatty aldehyde
1-arachidonoyl-sn-glycero-3-phosphocholine	-4.07	0.039	Phospholipid
1-[(1Z,9Z)-octadecadienyl]-sn-glycero-3-phosphocholine	1.28	0.004	Phospholipid
1-(1Z-hexadecenyl)-sn-glycero-3-phosphocholine	2.46	0.021	Phospholipid
1-[(9Z)-hexadecenoyl]-sn-glycero-3-phosphocholine	4.62	0.006	Phospholipid
Docosanoyl-lysophosphatidylethanolamine	4.71	0.048	Phospholipid

Danksagung

Mein großer Dank gilt Herrn PD Dr. Andreas Höflich, der mich damals in sein Team aufgenommen und mich in meiner wissenschaftlichen Arbeit stets gefördert hat. Ohne seine tatkräftige Unterstützung und Hilfe wären die Manuskripte, die als Grundlagen für diese Habilitationsschrift dienen, gar nicht möglich gewesen.

Prof. Dr. Tom Goldammer danke ich für die Bereitschaft, mich in meinem Habilitationswunsch zu unterstützen, sowie für seine Gespräche.

Ein sehr großes Dankeschön geht an alle Mitarbeiter des FBN, besonders jedoch an meine jetzigen und ehemaligen Kolleginnen und Kollegen: Dr. Christina Walz, Dr. Daniela Ohde, Dr. Anne-Marie Galow, Zianka Meyer, PD Dr. Monika Röntgen, Dr. Nares Trakooljul, Dr. Eduard Murani, Dr. Henry Reyer, Dr. Ronald Brunner, Erika Wytrwat, Dr. Elke Albrecht, Dr. Antonia Noce, Dr. Ulla Renne, Sabine Hinrichs, Vanessa Caton, Dr. Caroline Caffier, Dr. Elli Brosig, Martin Kunze, Dr. Michael Walz, Dr. Mandy Sawitzky, Anja Reyer, Stefan Petkov und Dr. Martina Langhammer.

Besonderen Dank möchte ich explizit Christina für die vielen Gespräche, den fachlichen Austausch und ihre Begeisterung für „unsere Marathonmaus-Forschung“, Daniela für die Unterstützung bei den PCRs und den schnellen Austausch von Schreibtisch zu Schreibtisch sowie Luong für Ihre große Hilfe im Labor und die Umsetzung meiner Ideen aussprechen. Zudem danke ich Herrn Prof. Steffen Maak für seine Bereitschaft, meine Arbeit Korrektur zu lesen.

Des Weiteren danke ich all meinen Koautoren sowie den Mitarbeiterinnen der Maustierhaltung für die erfolgreiche Zusammenarbeit.

Ich danke meinen Freundinnen Katja und Angi für unser jährliches Highlight sowie meinen Eltern und meinem Bruder plus Familie sowie der Restfamilie für ihre treue Unterstützung.

Ein besonders großes Dankeschön haben meine Töchter und mein Mann verdient! Ihnen danke ich für alles, was sie getan haben und natürlich tun. Für all unsere schönen Momente, Erinnerungen aber auch das Drama, das Teenagertöchter so mit sich bringen, bin ich unendlich froh und dankbar.

DANKE!

Eidesstattliche Erklärung

Hiermit erkläre ich eidesstattlich, dass ich die Habilitationsschrift selbstständig und ohne fremde Hilfe verfasst und keine anderen als die angegebenen Quellen und Hilfsmittel benutzt habe.

Des Weiteren versichere ich, dass diese Arbeit nicht vorher und auch nicht gleichzeitig bei einer anderen als der Mathematisch-Naturwissenschaftlichen Fakultät der Universität Rostock zur Eröffnung eines Habilitationsverfahrens eingereicht worden ist.

Außerdem erkläre ich, dass mir die Habilitationsordnung bekannt ist und ich sie anerkenne.

_____

Julia Brenmoehl

Lebenslauf

Name:	Dr. rer. nat. Julia Brenmoehl
Geburtsdatum:	06.01.1979
Geburtsort:	Rostock

Schulische Ausbildung:

1997	Abitur am Gymnasium Sanitz

Berufliche Ausbildung:

10/97 - 04/02	Fachhochschule Jena, Diplomstudiengang: Medizintechnik – Vertiefungsrichtung Biotechnologie; Abschlussnote: 2,1
10/03 - 12/04	Aufbaustudium Biologie, Universität Regensburg; Erhalt der Eignung zur Promotion
01/05 - 05/07	Promotion (Dr. rer. nat.); Abschlussnote: magna cum laude

Berufliche Stationen:

03/01 - 12/01	Diplomandin, Creatogen AG, Augsburg
04/02 - 06/02	wissenschaftliche Hilfskraft, Klinik und Poliklinik für Innere Medizin, Abteilung Gastroenterologie, Universität Rostock
07/02 - 12/06	wissenschaftliche Mitarbeiterin und Doktorandin, Klinik und Poliklinik für Innere Medizin I, Abteilung Gastroenterologie, Universität Regensburg
01/07 – 08/09	PostDoc/wissenschaftliche Mitarbeiterin/Laborleiterin, Klinik für Innere Medizin II, Abteilung für Gastroenterologie, Hepatologie und Infektiologie, Universitätsklinikum der FSU Jena
Seit 17.08.2009	wissenschaftliche Mitarbeiterin, Forschungsinstitut für Nutztierbiologie (FBN)

Berufliche Qualifikationen:

2015	Qualifikation FELASA B
2021	Qualifikation FELASA C